BINARY GAS ADSORPTION ON MOLECULAR SIEVES

Experimental data for the adsorption of oxygen, nitrogen and oxygen-nitrogen mixtures on five molecular sieve adsorbents at various temperatures and pressures and a comparison with theoretical models.

A THESIS PRESENTED FOR THE AWARD OF DEGREE OF

DOCTOR OF PHILOSOPHY

BY

George Ayad Sorial, B.Sc.(Hons.), M.Sc.

Postgraduate School of Studies in Chemical Engineering

University of Bradford

Bradford, West Yorkshire, BD7 1DP

March 1982

ABSTRACT

A study of adsorption equilibria of oxygen, nitrogen and oxygen-nitrogen mixtures on types 4A, 5A, 13X and Na-Mordenite molecular sieve pellets has been made.

Pure component isotherms, using a volumetric apparatus, have been measured for each gas on each adsorbent at pressures up to 9 bar and for temperatures of 278.15, 293.15 and 303.15 K.

Curve fitting of the pure component isotherms has been attempted using the kinetic model of Gonzalez and Holland, the vacancy solution model, the statistical thermodynamic model and a mathematical equation similar to the Hill-de Boer model. With the exception of the kinetic model, good curve fitting was obtained.

Binary equilibria data have been measured, using a constant volume method, for mixtures of oxygen and nitrogen at pressures of 1.7 and 4.4 bar and at temperatures of 278.15, 293.15 and 303.15 K for each of the adsorbents. These results have been presented graphically as equilibrium phase compositions and corresponding total adsorption loadings.

The binary experimental equilibria data have been examined against values predicted by mixture models (kinetic model, the extended vacancy solution model, the statistical thermodynamic model, the Cook and Basmadjian model, and the ideal adsorbed solution theory) using regression parameters obtained from the pure component isotherms. The statistical thermodynamic model and the ideal adsorbed solution theory gave the best representation of the experimental data.

The activity coefficients of the adsorbed phase for the binary experimental data have been calculated and the results showed no appreciable deviation of the adsorbed phase from ideality.

DEDICATIONS

"To my wife,

Elpis,

and my son,

Timothy"

ACKNOWLEDGEMENTS

I wish to thank Dr. W.H. Granville for his supervision and assistance throughout the duration of this research work and in the preparation of the thesis.

I also wish to thank Dr. W.O. Daly for his assistance during this research.

I wish to express my gratitude to Mr. J. Keighley and Mr. D. Steele for their assistance in constructing the experimental apparatus.

I am indebted to the British Council and the University of Gezira (Sudan) for their financial support to this research.

A profound gratitude is due to my parents, whose continuous encouragement was invaluable.

I would like to express my appreciation to Mrs. J.E. Steele and Miss J.A. Squires for their superb help in typing the manuscript.

CONTENTS

LIST OF FIGURES

LIST OF TABLES

NOMENCLATURE

		Units
A	Total surface area of adsorbent	m^2/kg pellet
A_o	Pre-exponential factor for Henry's law constant	bar
A''_o	Pre-exponential factor for Henry's law constant	bar/mol/kg
B	Dubinin's coefficient of affinity	
C	Constant in BET equation	
E	Polanyi adsorption potential	J
F	Helmoltz free energy of adsorbed phase	J/mol
G	Gibbs free energy of adsorbed phase	J/mol
ΔG_i^o	Standard state molar Gibbs free energy of adsorption of pure i	J/mol
H	Enthalpy of an adsorbed phase	J/mol
K	Henry's law constant	bar
K'	Henry's law constant	bar^{-1}
K''	Henry's law constant	bar/mol/kg
$\overline{K}$	Henry's law constant	molecule/cavity bar
K_j	Adsorption equilibrium constant in layer j in the kinetic model of Gonzalez and Holland	bar^{-1}
L	Ratio of adsorption pressure to vapour pressure in BET equation	
LRC	Loading ratio correlation	
M	Saturation limit in statistical thermodynamic model	molecule/cavity
P	Gas-phase pressure	bar
P_{A_1}	Equilibrium pressure from previous addition	bar
P_{A_2}	Equilibrium pressure	bar
P_c	Critical pressure	bar
P_D	Dosing pressure	bar
P_s	Saturated vapour pressure of liquid at adsorption temperature	bar

		Units
P_i^o	Equilibrium pressure of pure component i in absence of other components	bar
$P_i^o(\pi)$	Equilibrium pressure of pure component i at the spreading pressure of mixture	bar
R	Gas constant = 8.314	J/mol K
S	Entropy of adsorbed phase	J/mol K
T	Temperature	K
T_c	Critical temperature	K
T_B	Bath temperature	K
T^o	Boiling temperature of pure liquid	K
U	Internal energy of adsorbed phase	J/mol
U_o	Adsorption potential of adsorbed phase	J/mol
$\overline{U}_o$	Average adsorption potential of a heterogeneous adsorbent surface	J/mol
V	Volume of adsorbate	m^3/mol
V_A	Dead volume in adsorption vessel	ml
V_D	Circulation volume	ml
V_L	Volume of adsorbate as a saturated liquid at temperature of adsorption	m^3/mol
$\overline{V}_L$	Volume of adsorbate as a saturated liquid at adsorption pressure	m^3/mol
W_1	Amount adsorbed in previous addition	mol
W_2	Amount adsorbed	mol
W_A	Mass of adsorbent	kg
W_{O1}	Amount of oxygen adsorbed from previous addition	mol
W_{O2}	Amount of oxygen adsorbed	mol
W_{N1}	Amount of nitrogen adsorbed from previous addition	mol
W_{N2}	Amount of nitrogen adsorbed	mol
a	Molar area of adsorbate, reciprocal of moles adsorbed per unit surface area of adsorbent	m^2/mol

		Units
$a_i^o(\pi)$	Molar surface area of pure adsorbate i at the spreading pressure of mixture	m^2/mol
$\bar{a}_i$	Partial molar surface area	m^2/mol
b	Henry's law constant	mol/kg bar
f	Fugacity of an adsorbed phase	N/m
f^g	Fugacity of gas phase	N/m^2
f_s	Fugacity of saturated liquid at adsorption temperature	N/m^2
g^E	Total excess Gibbs free energy	J
i,j	Integers	
k	Constant in Equation (2.29)	
m	Number of layers in BET equation	
n	Amount adsorbed	mol/kg or molecule/cavity
n_{m_i}	Monolayer capacity of component i or maximum number of moles of component i in adsorbed phase	mol/kg
$n_i^o(\pi)$	Amount adsorbed of pure i at spreading pressure of mixture	mol/kg
$n_i^o(P)$	Amount adsorbed of pure i at total pressure of mixture	mol/kg
n_o	Maximum attainable loading for molecular sieves	mol/kg
q_{ST}	Isosteric heat of adsorption	J/mol
s	Parameter indicating the surface heterogeneity of adsorbent surface	
$s_{1,2}$	Selectivity coefficient	
v_1^o	Molar volume of pure liquid at boiling point	m^3/mol
v	Volume of zeolite cavity	A^3
x_i	Mole fraction of component i in adsorbed phase	
x_i^s	Mole fraction of component i in adsorbed phase vacancy solution	

		Units
y_i	Mole fraction of i in gas phase	
y_D	Dosing oxygen concentration in gas phase (mole fraction)	
y_{A1}	Equilibrium oxygen concentration in gas phase from previous addition (mole fraction)	
y_{A2}	Equilibrium oxygen concentration in gas phase (mole fraction)	
z	Coordination number	
α	Constant in a 2-D equation of state indicating inter-molecular forces	
α_p	Polarizability	
$\alpha_{1,2}$	Relative volatility	
$\alpha_{m_{1,2}}$	Mean relative volatility	
β	Constant in a 2-D equation of state indicating molecular size of adsorbate at monolayer capacity	m^2/mol
$\bar{\beta}$	Effective molecular volume of adsorbate	A^3/molecule
γ_i	Activity coefficient of component i	
θ	Ratio of equilibrium constant in consecutive layers in Gonzalez and Holland model	
λ_{ii}	Energy of interaction between two i molecules	J/mol
λ_{ij}	Energy of interaction between molecule i and molecule j	J/mol
$\Lambda_{12}, \Lambda_{21}$	Wilson's parameters for molecular interaction between 1 and 2	
$\Lambda_{13}, \Lambda_{31}$	Wilson's parameters for surface interaction between 1 and 3	
μ_i	Chemical potential, i.e. partial Gibbs free energy of component i in adsorbed phase	J/mol
μ_i^g	Chemical potential of i in gas phase	J/mol
π	Spreading pressure of adsorbed phase	N/m
ϕ	Fraction monolayer coverage n/n_m or β/a	

		Units
ω_{13}	Interaction coefficients in Margule's equation	
Ω	Surface potential	
Ω_r	Reduced surface potential	
Ω_s	Surface potential at saturation	

Superscripts

a or s	Adsorbed phase value
o	Standard state value
g	Gas phase value

Subscripts

i,j	Component i,j
T	Total number of components
1,2	Component 1,2
3	Vacancy

CHAPTER 1

INTRODUCTION

CHAPTER 1

INTRODUCTION

Adsorption has become an important unit operation which is employed commercially for the separation of a wide variety of gases. The adsorption of gaseous solutes from air in fixed beds is a basic operation in process technology and is used for purifying air by removing undesirable components, and may also be used for separation of components as in oxygen enrichment.

There are fundamentally two types of gas adsorption processes, which can be differentiated by the way in which adsorbed species are desorbed. In one type the adsorbed species are removed by raising the temperature of the adsorbent and in the other type the total pressure of the system is reduced to affect desorption. The first type is used when the solute constitutes only a small portion of the feed gas, while for bulk separation pressure reduction is the preferred mode of separation.

In this Chapter an introduction to pressure swing adsorption (PSA) is presented, some of the characteristics of the zeolite molecular sieves are described and finally the objectives of the present work are outlined.

1.1 Pressure Swing Adsorption (PSA)

Pressure swing adsorption (PSA), which is a short time cycle adsorption/desorption process in fixed beds of adsorbent using gas pressure variation as the principal operating parameter, is becoming increasingly popular for air separation[1,2,3]. Up to 95 per cent pure oxygen may be produced[3]. Since many of the applications of oxygen do not require the high purity of oxygen produced by cryogenic processes, PSA processes using zeolite adsorbents may be advantageous.

Although the technique of separation by PSA has been known for at least twenty years with patents dating from 1960[4,5,6], it is regarded as a rather complex process. It includes separate adsorption, depressurization, desorption (regeneration) and repressurization steps. The regeneration step relies on contacting the adsorbent with a gas stream containing the adsorbate at a significantly lower pressure than the minimum level obtained during the adsorption part of the cycle. In practice, this is achieved by using part of the product stream from the adsorption period as a purge at a reduced total pressure. A typical two bed PSA process is shown in Figure 1.1. Commercially, in order to accommodate a steady flow of feed and product, several beds, usually three or more in parallel, are used[1].

The design and optimization of PSA processes require basic experimental equilibria and rate data on the effect of temperature and pressure for each of the gases involved and their mixtures. Pure gas adsorption has been studied quite extensively[7-22]. An abundance of pure gas equilibria and rate data exist in the literature and good success has been achieved in the correlation of these data. By comparison, however, gas mixture data are extremely scarce and there is little published work on adsorption on zeolite molecular sieves.

The development and commercial manufacture of zeolite molecular sieves have provided the primary impetus for the expanded industrial utilization of adsorptive processing in process cycles such as PSA. Numerous references detail their industrial scope[23] and their physical characteristics[24-27]. However, a brief review will be of value here.

1.2 Characteristics of Zeolite Molecular Sieves

Zeolites are crystalline hydrated alumina silicates of sodium, potassium, magnesium, calcium, strontium and barium[24]. When the water of hydration is driven off the crystal does not collapse or

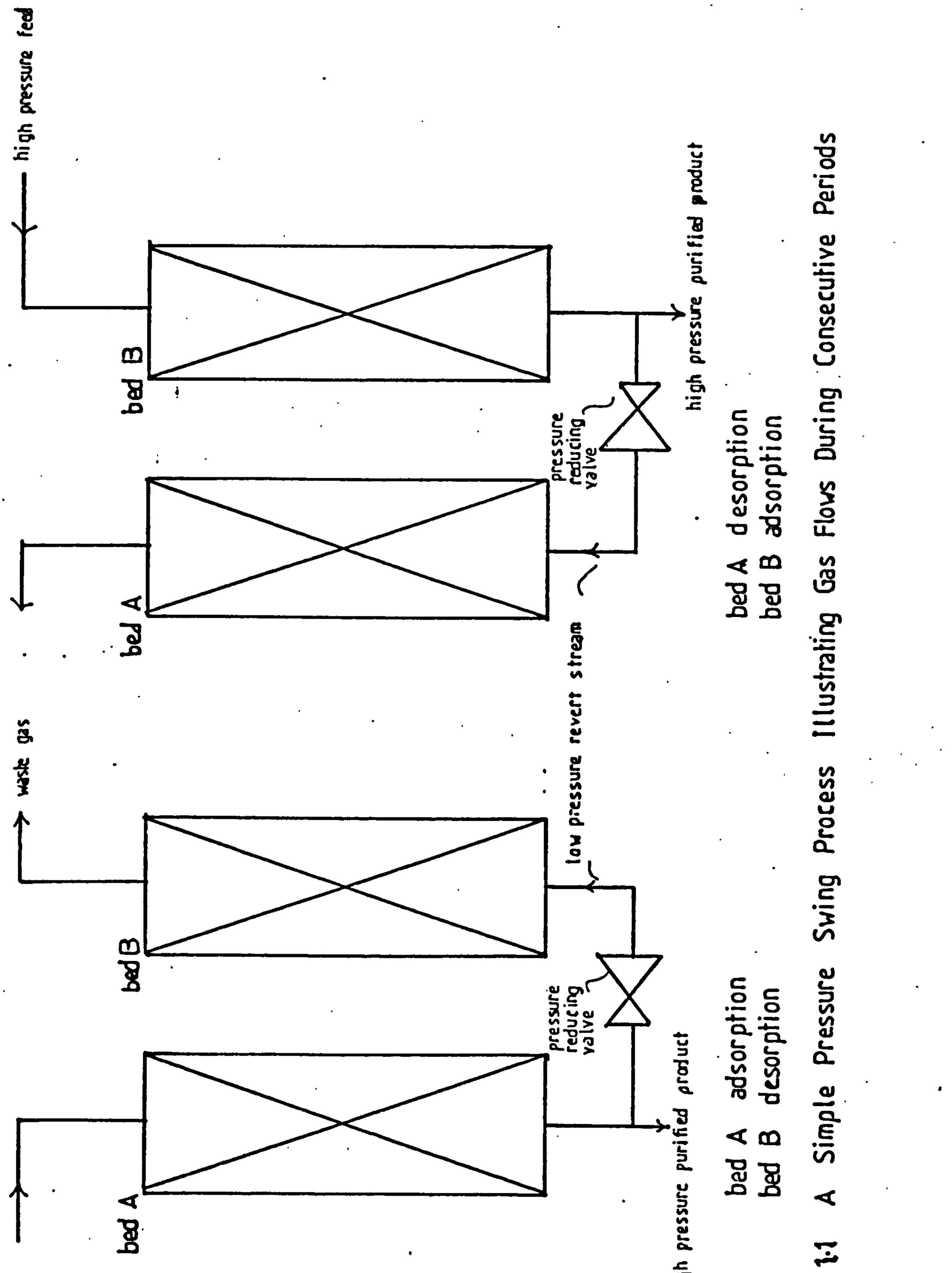

Figure 1.1 A Simple Pressure Swing Process

rearrange but rather gives cavities which are interconnected by empty pores of fixed and uniform dimension varying from about 3-10 Angstrom units in diameter.

Structurally the zeolites are "framework" alumino-silicates which are based on an infinitely extending three dimensional network of AlO_4 and SiO_4 tetrahedra linked to each other by sharing oxygen atoms. Generally they are represented by the following empirical formula:

$$M_{2/n}O.Al_2O_3.xSiO_2.yH_2O$$

where M is the cation, n is the cation valency and x is generally equal to or greater than 2.

The molecular sieving properties of zeolites are uniquely determined by their pore diameters, the magnitude of which determines what size molecules are totally excluded from the interior of the zeolite. Quite apart from their molecular sieving effects zeolites are also effective in selectively adsorbing particular components from a mixture of molecules capable of penetrating the entire zeolite. This is caused by the interaction of the zeolite with certain molecular parameters such as the dipole moments[27]. One selective adsorption that is being practised is the separation of oxygen from air by the preferred adsorption of nitrogen. Another is the selective adsorption of sulphur compounds from natural gas. A third is the selective adsorption of aromatics from hydrocarbon mixtures.

Compared with other adsorbents such as silica gel, activated alumina and activated carbon molecular sieve adsorbents can offer higher adsorption design loadings, resistance to fouling and coking, more complete impurity removal from the process stream and unique selective adsorption based on molecular size. In commercial operations these properties may lead to reduced adsorbent requirements, lower

pressure drop, greater operating flexibility, elimination or reduction of product loss due to co-adsorption, longer adsorbent life and more reliable and uniform performance[23].

The molecular sieves which are of interest to air separation are type A, type X and mordenite-type. For types A and X, they are normally produced as types 4A (NaA) and 13X (NaX) in which sodium is the alkali metal. Through an ion exchange mechanism about 75 per cent of the sodium ions are replaced by calcium ions thus producing types 5A (CaA) and 10X (CaX). The effective pore diameters of all of these types are shown in Table 1.1 and the kinetic diameters for various gases are given in Table 1.2.

In order to utilize the adsorption characteristics of zeolites in separation processes, commercial molecular sieve adsorbents are prepared as pelleted agglomerates containing a high percentage of the crystalline zeolite together with the necessary amount of an inert binder amounting to about 20 per cent of the total weight of the pellet.

Adsorption equilibrium in molecular sieves has been extensively studied and the behaviour of single systems involving a single adsorbable component is now fairly well understood. However, the practical applications of zeolites as selective adsorbents generally involve the adsorption of multicomponent mixtures. Available experimental data for such systems are very limited. This is true in adsorption involving binary gas mixtures of oxygen and nitrogen. Only three reported works appear in the literature[28,29,55], one of which[29] has been carried out at a low temperature (-129°C) which would be uneconomical on a commercial scale for separating air compared to other methods[27]. In the other two works, very limited data are presented on type 5A molecular sieve[28,55] and the mordenite type[55].

A number of techniques for predicting binary equilibria adsorption

TABLE 1.1

Nominal Pore Diameters for Different Zeolites[24]

Type	Nominal Pore Diameter A^{o}
4A	4
5A	5
13X	10
10X	8
Na-Mordenite	6.7

TABLE 1.2

Kinetic Diameters for Various Gases[24]

Gas	Kinetic Diameter A^{o}
He	2.6
H_2	2.89
Ar	3.4
O_2	3.46
N_2	3.64
CO	3.76
CO_2	3.3
SO_2	3.6
H_2S	3.6
CH_4	3.8
C_2H_2	3.3
C_2H_4	3.9
C_3H_8	4.3
Cyclopropane	4.23
Propylene	4.5
Benzene	5.85
Cyclohexane	6.0

from pure component isotherms have been published[30-43]. The lack of a comparative analysis of their merits due to lack of experimental data makes it difficult to choose between one method and another. Therefore the objects of the present investigation included a quantitative comparative analysis.

1.3 Objectives of Present Work

The objectives of the present work were:

1. Experimental

   (a) To measure oxygen and nitrogen isotherms on a variety of molecular sieve adsorbents at three temperatures, 278.15, 293.15 and 303.15 K with pressures up to 9 bar.

   (b) To measure binary equilibria of oxygen-nitrogen mixtures on the same variety of adsorbents at the same temperatures and two different pressures, namely 1.7 bar and 4.4 bar.

2. Theoretical

   (a) To analyse and correlate the isotherm data with recent models published in literature.

   (b) To evaluate the usefulness of the above models by predicting the binary equilibria data and comparing the results with the experimental data.

   (c) To measure the deviation of the binary system from ideal behaviour in the adsorbed phase by calculating the activity coefficients.

The adsorbents studied in this work were Laporte type 4A, 5A and 13X and two other samples provided by EKA (Sweden). In this work these two samples are referred to as EKA 5A and Na-Mordenite.

The oxygen and nitrogen gases used were BOC commercial grade.

CHAPTER 2

LITERATURE SURVEY

CHAPTER 2

LITERATURE SURVEY

In this Chapter a brief review is made of models correlating pure component isotherms and prediction theories for gas-mixture adsorption. The thermodynamics of adsorption are also described.

The phenomenon of adsorption of a solute on a solid surface may be a result of intermolecular forces of the van der Waal type between solid molecules and solute molecules colliding with the solid surface, or a result from a chemical interaction between the solid and the adsorbed component. The process in the first case is known as physical adsorption and the latter as chemisorption. The chemisorption process is of fundamental importance in the field of catalysis but is not normally of interest in relation to adsorption as a means of separation for it is commonly irreversible.

In physical adsorption the gas molecules will tend to attach themselves onto the surface of the adsorbent when the intermolecular forces between the solid and gas phase are greater than those between the gas molecules themselves. In general terms a dynamic equilibrium is established between the rate at which gas molecules condense on the surface and the rate at which they escape to the bulk gas phase. For a given system the position of this equilibrium is determined by the temperature of the system and the pressure of the gas. Physical adsorption is readily reversible and is accompanied by evolution of heat due to phase change.

The process of adsorption of a gas molecule from a flowing bulk gas stream by a commercial moleculer sieve pellet in a bed of adsorbent may be described by the following steps.

(a) Transfer of the adsorbate from the bulk stream across a fictitious film to the surface of the pellet.

(b) Transfer of the adsorbate through the macropore structure of the clay binder to the surface of the zeolite crystal.

(c) Adsorption of the gas molecule onto the surface of a zeolite crystal.

(d) Penetration by the adsorbate molecule into the intracrystalline cavity of the zeolite crystal.

(e) Heat release at the surface of crystal due to phase change.

(f) Transfer of the generated heat to the surface of the pellet by conduction.

(g) Transfer of the generated heat from the surface to the bulk gas stream.

(h) Transfer of the heat from the bulk gas stream into the wall of the container holding the molecular sieve pellets.

If all the heat transfer rates (items f-h) tend to infinity isothermal adsorption takes place.

2.1 Thermodynamics of Adsorption

The thermodynamics of physical adsorption equilibrium has been discussed by Hill[44], Myers and Prausnitz[36], and Van Ness[45]. The validity of thermodynamic equations to the adsorbed phase is based on the following assumptions.

(a) The adsorbent is assumed to be thermodynamically inert.

(b) The adsorbed phase (or the 2-D phase) is considered to be in thermal and mechanical equilibrium with the adsorbent solid and the gas phase (3-D phase) and the adsorbed phase is in phase equilibrium only with the gas phase.

(c) The adsorbent possesses a surface area which is an independent variable uninfluenced by temperature, pressure, compo-

sition or the amount of the material adsorbed. This assumption is not valid for a molecular sieve adsorbent because the area of adsorption depends on the molecule size. But later in this Chapter it will be shown how this can be overcome.

(d) The Gibbs definition of adsorption holds. This means a negligible adsorbed phase volume.

For a 3-D fluid phase the fundamental thermodynamic property is given by:

$$d(nU) = Td(nS) - Pd(nV) + \Sigma(\mu_i dn_i) \qquad (2.1)$$

The basic equation for the 2-D phase is analogous to Equation (2.1) with the pressure and volume terms replaced by the appropriate coordinates for a 2-D phase. Thus the pressure is replaced by the spreading pressure, π, and the molar volume by the molar area, a.

$$d(nU) = Td(nS) - \pi d(na) + \Sigma(\mu_i dn_i) \qquad (2.2)$$

Equation (2.2) is the fundamental property relation since all other equations interrelating thermodynamic properties such as enthalpy, H, Helmholtz-free energy, F, and Gibbs-free energy, G, of the 2-D phase are derived from it.

Expanding the differentials of Equation (2.2) and replacing n_i by nx_i gives:

$$n(dU - TdS + \pi da - \Sigma\mu_i dx_i) + dn(U - TS + \pi a - \Sigma\mu_i x_i) = 0 \qquad (2.3)$$

Since n and dn are independent and arbitrary the terms between the parentheses must separately be zero.

$$dU = TdS - \pi da + \Sigma\mu_i dx_i \qquad (2.4)$$

$$U = TS - \pi a + \Sigma \mu_i x_i \tag{2.5}$$

Equating the differential of U from Equation (2.5) to that of Equation (2.4) gives the Gibbs-Duhem equation for the 2-D phase:

$$-SdT + ad\pi - \Sigma x_i d\mu_i = 0 \tag{2.6}$$

Restricting Equation (2.6) for a constant temperature gives the Gibbs adsorption isotherm:

$$ad\pi - \Sigma x_i d\mu_i = 0 \quad \text{(constant T)} \tag{2.7}$$

When one uses the equilibrium criterion that the chemical potential of each species present is the same in both the adsorbate and gas phase and assuming ideal gas behaviour:

$$d\mu_i = d\mu_i^g = RT\ d\ \ell n\ y_i P \tag{2.8}$$

The Gibbs adsorption isotherm then becomes:

$$-ad\pi + RT\Sigma(x_i\ d\ \ell n\ y_i P) = 0 \quad \text{(constant T)} \tag{2.9}$$

For a binary gas mixture at constant temperature and pressure:

$$\frac{Ad\pi}{RT} = n_t \frac{x_1 - y_1}{y_1(1-y_1)} dy_1 \tag{2.10}$$

For a pure adsorbate, Equation (2.9) becomes:

$$-\frac{ad\pi}{RT} + d\ \ell n\ P = 0 \tag{2.11}$$

Equations (2.10) and (2.11) are the basic thermodynamic equations for a binary gas mixture and pure gas isotherm models respectively. It will be shown later in this Chapter how pure component isotherms or gas mixture models are derived from these equations.

A proposed model for the description of the equilibrium between the gas phase and the adsorbed phase is said to be thermodynamically consistent if it satisfies the Gibbs adsorption isotherm equation.

2.2 Pure Gas Adsorption Theories

Adsorption theories of pure gases on solids can be classified into the following groups.

(a) Kinetic models based on ideal localized adsorption. In this group falls the basic Langmuir equation and its extensions by other authors[46-52,31].

(b) Models based upon mobile monolayers. The basic theory is that the adsorbed phase may be characterized by a two-dimensional equation of state[7,54,56-63].

(c) Potential theory of Polanyi and its extensions by other authors[33,81,64,65].

(d) Statistical thermodynamics model by Ruthven and co-workers[67,68].

(e) The vacancy solution model by Suwanayuen and Danner[69].

2.2.1 Kinetic models

The first theoretical treatment of adsorption isotherms was done by Langmuir[46,47]. He applied both kinetic and thermodynamic considerations to a monolayer adsorption model in order to obtain the expression:

$$\frac{n}{n_m} = \frac{K'P}{1+K'P} \qquad (2.12)$$

Implicit in its development were the following assumptions.

1. The adsorbate in the bulk gas phase behaves as an ideal gas.
2. The amount adsorbed is confined to a monomolecular layer.
3. Every part of the surface has the same energy of adsorption.

4. Negligible adsorbate-adsorbate interaction.

5. The adsorbed molecules are localized, i.e. they have definite points of attachment to the surface.

Many workers[7,17,70-74] used the Langmuir model for correlation of adsorption isotherms or for developing models describing the rate of diffusion of gases into molecular sieves and it has been found to have limited applicability.

The Langmuir equation has provided a source for numerous modified equations[31,48-52,75]. The extension of Langmuir model for multilayer adsorption by Brunauer et al (BET theory) received more attention. The BET equations derived by Hill[52] using statistical mechanics are shown below for an infinite number of layers and also for m layers.

$$\frac{n}{n_m} = \frac{C\ P/P_s}{(1 - P/P_s)(1 - (1 - C)P/P_s)} \qquad (2.13)$$

$$\frac{n}{n_m} = \frac{C(P/P_s)}{1 - (P/P_s)} \cdot \frac{1 - (m + 1)(P/P_s)^m + m(P/P_s)^{m+1}}{1 + (C - 1)(P/P_s) - C(P/P_s)^{m+1}} \qquad (2.14)$$

Implicit in these equations is the assumption that the formation of the mth layer depends on the (m-1)th layer. The BET theory found great use in the field of determination of specific surface area of adsorbents[76].

In another modification of Langmuir's theory, Gonzalez and Holland[31,75] developed a kinetic model based on multilayer adsorption by assuming that the ratio of the adsorption equilibrium constants of consecutive adsorbed layers are equal and is the same for any gas over the same adsorbent. The expression so obtained for the amount of gas adsorbed in m layers is given by:

$$n = \left(\frac{n_m K_1 P}{1 + K_1 P}\right)\left(1 + \theta K_1 P + \theta^3 (K_1 P)^2 + ... + \theta^{\frac{(m-1)m}{2}} (K_1 P)^{m-1}\right) \qquad (2.15)$$

where:

$$\theta = \frac{K_2}{K_1} = \frac{K_3}{K_2} = ... = \frac{K_m}{K_{m-1}} \qquad (2.16)$$

The variations of n_m, θ and K_1 in Equation (2.15) with temperature is accounted for by use of expressions of the form:

$$n_m = C_1 e^{C_2/T}$$

For the data collected by Gonzalez and Holland[75] for the adsorption of hydrocarbons on activated carbon and silica gel they found that the contributions of the third and higher order layers were negligible and thus their equation was used for two layers.

In general the kinetic models have two major disadvantages:

(a) The experimental isotherms usually do not conform with the simple equations of these models due to the simplifying assumptions embedded in them. Their deficiency will be more pronounced when such models are used for prediction of multi-component adsorption.

(b) They are thermodynamically inconsistent, i.e. they do not satisfy the Gibbs adsorption isotherm (Equation (2.11)) unless the value of the monolayer coverage, n_m, is the same for each gas studied on the same adsorbent. This means that if such models are used to correlate the adsorption isotherms of say two gases on certain adsorbents, the curve fitting procedure of the experimental isotherms should be done simultaneously for obtaining the same value of n_m for each gas. This again will attribute to poor curve fitting if the affinities of two gases in the adsorbent vary widely.

2.2.2 Two-dimensional isotherm theories

Two-dimensional equations of state, relating spreading pressure (π), area (A), and temperature (T), have been used by many investigators[7,54,56-63] to obtain equations for expressing the amount of gas physically adsorbed as a function of pressure and temperature.

In the 3-D phase (gas phase) the equation of state describing the volumetric behaviour of the gas phase is represented in a general form by:

$$P = RT\, f(V,T) \qquad (2.17)$$

and:

$$\lim_{P \to 0} f(V,T) = \frac{1}{V}$$

Similarly for a 2-D phase (adsorbed phase) the equation of state describing its behaviour may be represented by:

$$\pi = RT\, g(a,T) \qquad (2.18)$$

and:

$$\lim_{\pi \to 0} g(a,T) = \frac{1}{a}$$

Introducing the concept of the fraction monolayer capacity of adsorbent which is expressed by:

$$\phi = \frac{n}{n_m} = \frac{\beta}{a}$$

where β is defined as the molar area of adsorbate at full monolayer capacity.

Equation (2.18) may thus be written as:

$$\pi = \frac{RT}{\beta}\, \overline{g}(\phi,T)$$

At constant temperature the total derivative of π is:

$$d\pi = \frac{RT}{\beta}\left(\frac{\partial \bar{g}(\phi,T)}{\partial \phi}\right)_T d\phi \qquad (2.19)$$

Substituting for a in Equation (2.11) and equating the differential of π with Equation (2.19) yields:

$$d \ln P = \left(\frac{\partial \bar{g}(\phi,T)}{\partial \phi}\right)_T \frac{d\phi}{\phi} \qquad (2.20)$$

Integrating:

$$\ln P = \int_0^{\phi} \left(\frac{\partial \bar{g}(\phi,T)}{\partial \phi}\right)_T d \ln \phi + \ln K(T)$$

where $\ln K(T)$ is an integration constant, hence the general isotherm equation may be written as:

$$P = K(T) \cdot G(\phi,T) \qquad (2.21)$$

The general restriction for the function G is:

$$\lim_{\phi \to 0} G(\phi,T) = \phi$$

If an ideal gas law is assumed to describe the two dimensional phase, a linear adsorption isotherm (Henry's law) is obtained.

Adsorption is characterized by two types of interaction. At very low coverage (Henry's law region) lateral interactions between adsorbed molecules are negligible and equilibrium data obtained in this region are directly dependent on the vertical interaction, that is, the interaction between the adsorbent and the adsorbing molecules. For a homogeneous surface, this interaction is uniform all over the surface. Lateral interactions are caused by the non-ideality of the

two-dimensional film that constitutes the adsorbed monolayer and the 2-D equation of state chosen must account for this non-ideality. Table (2.1) represents typical adsorption equations derived through the procedure outlined above. One of the most common used equations of state is the Hill De Boer[56-59]. This is based on the use of the 2-D analogue of the van der Waals equation of state:

$$\pi = \frac{RT}{\beta}\left[\frac{\phi}{1-\phi} - \frac{\alpha\,\phi^2}{RT\,\beta}\right] \qquad (2.22)$$

Several investigators[7,58,77,78] have applied the Hill De Boer equation for correlating their adsorption data. In the analysis and interpretation of equilibrium data for zeolitic adsorption this model has a limited applicability. Although an apparently satisfactory correlation of equilibrium data is obtained, the basic assumptions from which the model isotherm is derived is generally not fulfilled and it is therefore doubtful whether the parameters have a real physical significance.. The main defect has been attributed towards the heterogeneity of the adsorbent which is not accounted for by the model[7].

Ross and Olivier[56,57] developed a model to account for heterogeneity of adsorbents. The heterogeneous surface is visualized as a large collection of homogeneous patches each of which is characterized by a particular adsorption potential and the adsorption isotherm for each patch is given by the Hill De Boer equation. The distribution of the adsorption potential over the entire heterogeneous surface was selected to be according to the Gaussian distribution function:

$$F(U_{o_i}) = \frac{1}{s\sqrt{2\pi}} \exp\left[\frac{-(U_{o_i} - \bar{U}_o)^2}{2s^2}\right] \qquad (2.23)$$

The degree of surface coverage of the whole surface is obtained by

TABLE 2.1

Adsorption Isotherm Models for Homogeneous Adsorbents[56]

Model	2-D Equation of State	Adsorption Isotherm
Henry's Law	$\pi = \frac{RT}{\beta}\phi$	$P = K\phi$
Volmer's Isotherm	$\pi = \frac{RT}{\beta}\left(\frac{\phi}{1-\phi}\right)$	$P = K\frac{\phi}{1-\phi}\exp\left(\frac{\phi}{1-\phi}\right)$
Hill de Boer Isotherm	$\pi = \frac{RT}{\beta}\left(\frac{\phi}{1-\phi} - \frac{\alpha\phi^2}{RT\beta}\right)$	$P = K\frac{\phi}{1-\phi}\exp\left(\frac{\phi}{1-\phi} - \frac{2\alpha\phi}{RT\beta}\right)$
Redlich-Kwong Isotherm[7]	$\pi = \frac{RT}{\beta}\left(\frac{\phi}{1-\phi} - \psi\frac{\phi^2}{1+\phi}\right)$	$P = K\frac{\phi}{1-\phi}\left(\frac{1}{1+\phi}\right)^{\psi}\exp\left(\frac{\phi}{1-\phi} - \psi\frac{\phi}{1-\phi}\right)$

where $\psi = \frac{\alpha}{RT^{1.5}\beta}$

$K = A_o \exp\frac{-U_o}{RT}$

integrating ϕ_i over all the patches:

$$\overline{\phi} = \int_{\phi}^{\infty} \phi_i \, F(U_{o_i}) \, d \, U_o \qquad (2.24)$$

Although the model has the advantage of obtaining constants which are not affected by the surface heterogeneity of the adsorbent, its complexity prohibits its use for other applications such as kinetic modelling. When this model was extended for the prediction of gas mixture adsorption by Hoory and Prausnitz[32] it required a correlating parameter and therefore such a model will be a correlating model rather than a predictive one.

Other groups of investigators[60-63] applied virial-type adsorption equations truncated at an appropriate point for representing pure gas data. However when such models are used for the prediction of gas mixture equilibrium improved results are obtained by adding higher order terms. In this case the correlation becomes more empirical and the value of its parameters exhibit random behaviour[61,79,80].

2.2.3 Potential theory

Polanyi[81] defined the adsorption potential as the free energy change in transferring a gas molecule to the adsorbed phase. A characteristic curve which is the relationship between n, the moles adsorbed, and E, the potential, is formed using the Polanyi theory. The main assumption of the potential theory is that E is independent of temperature and is a function of the volume of the adsorbed phase. The familiar equation for this adsorption potential is:

$$E = n \, RT \, \ell n \frac{P_s}{P} \qquad (2.25)$$

In an extension of the Polanyi theory, Dubinin et al[65] suggested that similar types of adsorbates on a given adsorbent would have equal

adsorption potentials when equal amounts were adsorbed. The amount adsorbed was calculated as the moles adsorbed, n, times the molar volume of the adsorbate, V_L, measured as a saturated liquid at the temperature of adsorption. They arrived at the following equation:

$$\left.\frac{RT}{V_L} \ln\left(\frac{P_s}{P}\right)\right|_{\text{gas 1}} = \left.\frac{RT}{V_L} \ln\left(\frac{P_s}{P}\right)\right|_{\text{gas 2}} \qquad (2.26)$$

This means that if the amount adsorbed is plotted against:

$$\frac{RT}{V_L} \ln\left(\frac{P_s}{P}\right)$$

all points for similar adsorbates should fall on one curve.

Later Lewis et al[65] modified Equation (2.26) to allow its use for temperatures above the critical point and to correct for non-idealities in the gas phase at higher pressures. They proposed:

$$\left.\frac{RT}{\overline{V}_L} \ln\left(\frac{f_s}{f}\right)\right|_1 = \left.\frac{RT}{\overline{V}_L} \ln\left(\frac{f_s}{f}\right)\right|_2 \qquad (2.27)$$

where $\overline{V}_L$ is the molar volume of adsorbate as a saturated liquid at the adsorption pressure.

Maslan et al[34] found that the Lewis correlation gave separate lines for the adsorption of oxygen and nitrogen on carbon at -150°C. Grant and Manes[33] suggested the use of the molar volume of the adsorbate as a saturated liquid at the normal boiling point. They re-correlated Maslan et al results but still obtained two separate curves.

Dubinin[64] suggested that for different adsorbates the forces of attraction of the molecules to the surface of adsorbent are not the same and he then introduced the concept of the coefficient of affinity

B. He defined the coefficient of affinity to be the ratio of the adsorption potential of the adsorbates. According to the theory of dispersion interaction[81] the ratio of interactions of two adsorbates could be approximated by the ratio of the polarizability of their molecules. Hence:

$$B = \frac{E_1}{E_2} = \frac{\alpha_{P_1}}{\alpha_{P_2}} \qquad (2.28)$$

For molecular sieves Dubinin defined the equation of the characteristic curve to be of the form:

$$n = n_m \exp\ (-k\ E^2/B^2) \qquad (2.29)$$

It should be noted that n_m and k are the characteristics of the adsorbent and are not dependent on the adsorbate used.

Dubinin suggests the following approaches for defining both the adsorbed phase volume, V_L, and the saturation vapour pressure, P_s.

Adsorbed phase volume, V_L

(a) For temperatures below the normal boiling point the normal saturated liquid volume at the adsorption temperature is used.

(b) For temperatures between the normal boiling point and the critical temperature a linear interpolation between the molar volume at the normal boiling point and the van der Waal's co-volume, b, is used.

(c) For temperatures above the critical temperature the liquified volume of adsorbate, V_L, is taken to be equal to the van der Waal's co-volume, b.

Saturation vapour pressure, P_s

(a) For all temperatures below the critical temperature, T_c,

the saturation vapour pressure is taken from tabular data.

(b) Above the critical temperature the following expression is used:

$$E = RT \ln \left(\left(\frac{T}{T_c} \right)^2 \frac{P_c}{P} \right) \qquad (2.30)$$

Danner[74] correlated his adsorption data of oxygen, nitrogen and carbon monoxide on molecular sieves, type 5A and 10X, using Dubinin's interpretation of the potential theory but he obtained different values of k and n_m for each adsorbate.

In another modification of the potential theory Cook and Basmadjian[82] suggested that the adsorbed phase volume is estimated in terms of the saturated liquid properties.

$$V_L = v_1^o$$

for temperatures less than the boiling point.

$$V_L = v_1^o \left(\frac{T}{T^o} \right)^{\bar{m}}$$

for temperatures greater than the boiling point of the liquid. The values of v_1^o, T^o and $\bar{m}$ for oxygen and nitrogen are given below[7].

	T^o K	v_1^o m^3/mol	$\bar{m}$
oxygen	90.18	2.8176×10^{-5}	0.3844
nitrogen	77.35	3.5210×10^{-5}	0.00404

On comparing the values obtained for V_L for oxygen and nitrogen at the temperatures of this present work by the methods of Cook and Basmadjian and Dubinin, wide discrepancies were obtained.

The main advantage of the Polanyi theory is that isotherms of similar adsorbates can be predicted by knowing the characteristic curve of the adsorbent. However, this has to be balanced against the fact that no accurate correlation of isotherms could be obtained for some gases and investigators interpreted differently the choice of the molar volume of the adsorbate, V_L.

2.2.4 Statistical thermodynamic theory

Ruthven and co-workers[67,68] derived an isotherm model for adsorption on zeolites, based on statistical thermodynamics. The model isotherm is based on the following assumptions.

(a) The rate of interchange of adsorbate molecules between zeolite cavities is sufficiently low so that the system can be treated as if a given adsorbate molecule is confined to a particular cavity but not adsorbed at specific localized sites within the cavity.

(b) The molecular interaction between molecules in the same cavity is represented by a reduction in the free volume of the cavity due to the finite size of occluded molecules.

(c) The effect of adsorbate molecules in the neighbouring cavities are neglected.

(d) The adsorbate-adsorbent interaction is characterized by the Henry's law constant which may be determined experimentally from the limiting slope of the isotherm at low concentrations.

The equation for isotherms thus obtained was:

$$n = \frac{\bar{K}P + (\bar{K}P)^2(1 - 2\bar{\beta}/v)^2 + ... + \frac{(\bar{K}P)^M}{(M-1)!}(1 - M\bar{\beta}/v)^M}{1 + \bar{K}P + \frac{1}{2!}(\bar{K}P)^2(1 - 2\bar{\beta}/v)^2 + ... + \frac{(\bar{K}P)^M}{M!}(1 - M\bar{\beta}/v)^M} \qquad (2.31)$$

The saturation limit M (an integer) is determined by the condition $M \leq v/\overline{\beta}$ since the term $(1 - M\overline{\beta}/v)$ cannot be negative.

From the model isotherm it can be seen that for very low pressures higher orders of $\overline{K}P$ can be neglected and hence the equation reduces to the Langmuir model.

In the original development of the theory the adsorbate-adsorbate interaction has been accounted for but Ruthven and co-workers[68] found that it is generally small and can be neglected.

The isotherm model now contains only two adjustable parameters, the Henry's law constant, $\overline{K}$, and the effective co-volume of the adsorbate, $\overline{\beta}$. Ruthven and co-workers suggested that $\overline{\beta}$ can be estimated according to Dubinin's interpretation of the molar volume of adsorbate (see Section 2.2.3) and the Henry's law constant can be either estimated by the limiting slope of the isotherm at low concentrations or by curve fitting the theoretical isotherm to the experimental data.

The main difficulty in the application of this model seemed to be the accurate estimation of the co-volume of the adsorbate. In a later publication Ruthven[28] suggested that by matching the experimental data to a family of theoretical isotherm curves calculated for different values of the parameter $(v/\overline{\beta})$, the appropriate values of both $\overline{K}$ and $\overline{\beta}$ can be found.

This model has been successfully used to correlate single component equilibrium data for the light paraffins[68], olefins[14], oxygen, nitrogen and carbon monoxide[28] on type A zeolite and ethane and ethylene on type 13X zeolite[78]. However, the model was found to be unsatisfactory for high adsorbate loadings at a value of $n/M = 0.7$[68].

2.2.5 The vacancy solution model

Suwanayuen and Danner[69] developed an isotherm equation based on treating the adsorption equilibrium as an osmotic equilibrium between two vacancy solutions (gas phase and adsorbed phase) having different compositions. The vacancy solution is composed of the adsorbates and vacancies which are vacuum spaces acting as a solvent for the system. Using the equilibrium criterion that the chemical potential of both phases must be equal, they derived the following equation of state for the adsorbed phase:

$$\pi = \frac{-RT}{\bar{a}_3} \ln \gamma_3 \, x_3^{s} \qquad (2.32)$$

where $\bar{a}_3$ is the partial molar surface area of the vacancy and is given by:

$$\bar{a}_3 = \frac{A}{n_m} \qquad (2.33)$$

x_3^{s} is the mole fraction of the vacancy and is given by:

$$x_3^{s} = (1 - \phi)$$

The non-ideality of the adsorbed solution is accounted for by the activity coefficient γ_3 whose composition dependence could be expressed by a two-suffix Margules equation[83]:

$$\ln \gamma_3 = \frac{\omega_{13}}{RT} (x_1^{s})^2 \qquad (2.34)$$

or by Wilson's equation[83]:

$$\ln \gamma_3 = -\ln(x_3^{s} + \Lambda_{31} x_1^{s}) - x_1^{s}\left(\frac{\Lambda_{13}}{x_1^{s} + \Lambda_{13} x_3^{s}} - \frac{\Lambda_{31}}{x_3^{s} + \Lambda_{31} x_1^{s}}\right) \qquad (2.35)$$

In both equations x_1^{s} is the fraction coverage and is given by:

$$x_1^s = \frac{n_1}{n_m} = \phi \qquad (2.36)$$

The equation of state (Equation (2.32)) together with the Gibbs adsorption equation (Equation (2.11)) were used to develop the isotherm equation depending on the choice of the activity coefficient expression. For the 2-suffix Margules equation:

$$P = \frac{n_m}{b} \frac{\phi}{1-\phi} \exp \frac{-2\ \omega_{13}\ \phi}{RT} \qquad (2.37)$$

Whilst for Wilson's equation:

$$P = \frac{n_m}{b} \frac{\phi}{1-\phi} \left(\Lambda_{13} \frac{1 - (1 - \Lambda_{31})\ \phi}{\Lambda_{31} + (1 - \Lambda_{13})\ \phi} \right) \exp \left(- \frac{\Lambda_{31}\ (1 - \Lambda_{31})\ \phi}{1 - (1 - \Lambda_{31})\ \phi} - \frac{(1 - \Lambda_{13})\ \phi}{\Lambda_{13} + (1 - \Lambda_{13})\ \phi} \right) \qquad (2.38)$$

The integration constant, b, is defined so that there is agreement with Henry's law (see Table 2.1) as the pressure approaches zero.

From the isotherm equation it is seen that the Langmuir model will be approached if the non-ideality of the adsorbed phase is neglected, that is, if $\Lambda_{13} = \Lambda_{31} = 1$.

The isotherm model using Wilson's equation (Equation (2.38)) has been tested by the authors for the adsorption of oxygen, nitrogen, carbon monoxide on zeolite type 10X and hydrocarbons and carbon dioxide on activated carbon at different temperatures. They found the correlation was successful for both adsorbents.

2.3 Prediction Theories for Adsorption of Gaseous Mixtures

In the case of adsorption of gas mixtures at a given temperature and pressure a complete specification of the system is given by the total amount adsorbed and the compositions of both the gas and the adsorbed phase.

In a binary mixture, as in the case of vapour-liquid equilibrium, a relative volatility has been defined as:

$$\alpha_{1,2} = \frac{y_1/x_1}{y_2/x_2} \qquad (2.39a)$$

In adsorption work, a selectivity coefficient has been defined[36]:

$$S_{1,2} = \frac{x_1/y_1}{x_2/y_2} = \frac{1}{\alpha_{1,2}} \qquad (2.39b)$$

The selectivity coefficient, $S_{1,2}$, is greater than unity if component 1 is the more strongly adsorbed whilst the relative volatility, $\alpha_{1,2}$, is greater than unity if component one is less adsorbed.

Prediction theories for the adsorption of gaseous mixtures can be classified into the following groups:

(a) extensions of pure gas equations;

(b) extensions of the Polanyi Potential Theory;

(c) empirical methods;

(d) ideal adsorbed solution theory;

(e) real adsorbed solution theory.

2.3.1 Extensions of pure gas equations

In this group the gas-mixture adsorption equilibrium is derived in terms of parameters of the pure gas isotherm equations. The derivation can be classified into the following sections.

(i) Derivations based on ideal localized adsorption. In

this group comes the various extensions of the Langmuir theory for gaseous mixtures[31,53,75,84-86].

(ii) Derivations based on mixed mobile adsorption. This is an extension of the two-dimensional equation of state developed for the pure component system[7,32].

(iii) Extension of the statistical thermodynamics model for gaseous mixtures[42].

2.3.1.1 Extensions of Langmuir theory

Markham and Benton[84] were the first to extend the Langmuir model for the adsorption of gaseous mixtures. They considered the kinetics of simultaneous adsorption to derive the following equation for a binary mixture for the adsorption of component one:

$$\frac{n_1}{n_{m_1}} = \frac{K_1' P_1}{1 + K_1' P_1 + K_2' P_2} \qquad (2.40)$$

Later Kemball et al[85] pointed out that Markam extensions for Langmuir theory is thermodynamically inconsistent if different values of n_m are used, because according to the Gibbs adsorption formula it is stated that the area of each site is a fixed quantity determined solely by the geometry of the surface. Postulating separate n_m values also makes the correct derivation algebraically impossible since the fraction of the surface uncovered with the gas is now given by the term:

$$\left(1 - \frac{n_1}{n_{m_1}} - \frac{n_2}{n_{m_2}}\right)$$

a quantity which has no limiting meaning unless $n_{m_1} = n_{m_2}$.

By use of statistical thermodynamics Kemball et al surmounted the problem of using different values of n_m and arrived at exactly the same

equation but with a constant value of n_m for both components. The use of a constant value of n_m yields equations in term of adsorbed phase composition in which the term n_m no longer exists:

$$x_1 = \frac{(K_1'/K_2')\ y_1}{1 + ((K_1'/K_2') - 1)\ y_1} \qquad (2.41)$$

The extended Langmuir model has been used by Danner[74] for predicting binary equilibrium of O_2-N_2, N_2-Co, Co-O_2 on zeolite molecular sieves, type 5A and 10X, but poor predictions were obtained.

Hill[53] extended the multilayer BET theory to gaseous mixtures and arrived at a complex equation which has been simplified by Arnold[86] by assuming that Raoult's law was applicable. Thus Arnold showed that:

$$\frac{n_1}{n_m} = \frac{C_1 L_1\left(1 - (1 - \bar{C}/C_1)\bar{L}\right)}{(1 - \bar{L})(1 - (1 - \bar{C})\ \bar{L})} \qquad (2.42)$$

where:

$$L_1 = P_1/P_{s_1} \quad , \quad \bar{L} = \sum_{j=1}^{r} L_j \quad , \quad \bar{C} = \sum_{j=1}^{r} C_j\ L_j/\bar{L}$$

The extended BET theory has been tested by White and Schneider[87] for the adsorption of binary mixtures of O_2-N_2 and O_2-Ar on chromic oxide gel, by Arnold[86] for the adsorption of O_2-N_2 on Anatase and by Danner[74] for the adsorption of O_2-N_2, N_2-Co and O_2-Co on zeolite molecular sieves, types 5A and 10X. All the three investigators have found great deviations from the experimental and the predicted values. However, Mason and Cooke[88] applied the BET theory for the adsorption of hydrocarbon mixtures on silica gel and their experimental data were predicted reasonably good.

The bi-molecular kinetic model of Gonzalez and Holland[31,75] for a gaseous mixture is given by:

$$n_1 = \frac{n_m K_1 P_1 (1 + \theta \Sigma K_1 P_1)}{(1 + \Sigma K_1 P_1)} \qquad (2.43)$$

Implicit in its derivation are the assumptions listed before for pure components plus the assumption that the adsorption of a given molecule in a given layer is independent of the identity of the molecule adsorbed beneath it in a previous layer.

González and Holland tested their model against their experimental data on hydrocarbon mixtures on silica gel and activated carbon and the Mason and Cooke[88] experimental data on silica gel. Also, the model has been tested by Sircar and Myers[39] on the experimental data of Szepesy and Illes[89] for hydrocarbon mixtures on activated carbon. Relatively good predictions were obtained in both investigations. No test of this model has been yet made on zeolite molecular sieves.

2.3.1.2 Mixed mobile adsorption

A gaseous mixture is considered to be in equilibrium with a two-dimensional monolayer film on a homogeneous surface. By introducing the concept of surface fugacity, the equation of equilibrium between the two phases is given by[32,45]:

$$f_1^a = \frac{RT}{K_1 \beta_1} P y_1 \qquad (2.44)$$

The surface fugacity f_1^a of component 1 can be calculated from a two-dimensional equation of state by the exact thermodynamic relation[32]:

$$RT \ln f_1^a = \int_A^\infty \left(\left(\frac{\partial \pi}{\partial n_1} \right)_{T,A,n_2} - \frac{RT}{A} \right) dA - RT \ln \frac{A}{n_1 RT} \qquad (2.45)$$

Numerical results for Equation (2.45) can be obtained by the use of an equation of state, e.g. Hill de Boer equation (Equation (2.22)). For a binary mixture the constants α and β are related to those of

the pure components by the following mixing rules:

$$\beta = x_1 \beta_1 + x_2 \beta_2 \qquad (2.46)$$

$$\alpha = \alpha_1 x_1^2 + 2\sqrt{\alpha_1 \alpha_2}\, x_1 x_2 + \alpha_2 x_2^2 \qquad (2.47)$$

Substitution into Equation (2.45) yields the surface fugacity for component 1 and further substitution in Equation (2.44) yields:

$$\ell n\, P\, y_1 = \ell n \left[\frac{x_1 K_1 \beta_1}{a - \beta}\right] + \frac{\beta_1}{a - \beta} - \frac{2}{a\, RT} (\alpha_1 x_1 + \alpha_{12} x_2) \qquad (2.48)$$

where:

$$\alpha_{12} = \sqrt{\alpha_1 \alpha_2}$$

and with a similar equation for component 2. Binary mixture adsorption equilibrium can be predicted by solving Equation (2.48) and its analogous equation for component 2 simultaneously.

This model has been tested for predicting binary equilibrium adsorption of hydrocarbon mixtures on homogeneous carbon black[77] and zeolite, type 13X[78] and O_2-N_2 mixtures on zeolite, type 5A[7]. Although good predictions were obtained, the parameters obtained for the zeolite, type 5A, showed no physical significance[7].

2.3.1.3 Extension of the statistical thermodynamic model

Based on the same assumptions for the pure isotherm model (Equation (2.31)) Ruthven and co-workers[42] extended their earlier work to the binary system producing the following expression for component 1:

$$n_1 = \frac{\bar{K}_1 P_1 + \sum_j \sum_i (\bar{K}_1 P_1)^i (\bar{K}_2 P_2)^j (1 - i\bar{\beta}_1/v - j\bar{\beta}_2/v)^{i+j}/(i-1)!j!}{1 + \bar{K}_1 P_1 + \bar{K}_2 P_2 + \sum_j \sum_i (\bar{K}_1 P_1)^i (\bar{K}_2 P_2)^j (1 - i\bar{\beta}_1/v - j\bar{\beta}_2/v)^{i+j}/i!j!} \qquad (2.49)$$

with a corresponding equation for component 2. The summations in Equation (2.49) are carried out over all values of i (number of molecules of component 1 in zeolite cavity) and j (number of molecules of component 2 in zeolite cavity) satisfying the restrictions $i + j \geq 2$;

$i\,\bar{\beta}_1 + j\,\bar{\beta}_2 \leq v$.

If both $\bar{K}_1 P_1$ and $\bar{K}_2 P_2$ are sufficiently small the higher order terms in Equation (2.49) can be neglected and thus the equation reduces to the extended Langmuir equation for binary gas mixtures.

This model has given relatively good predictions for the adsorption of binary hydrocarbon mixtures[42,78,90], binary mixtures of O_2-N_2, N_2-CO, CO-O_2, CH_4-CO_2 on zeolite molecular sieves[28] and binary mixtures of CH_4-CO_2 on molecular sieves, types 5A and 13X[53].

2.3.2 The potential theory

Lewis and co-workers[30] extended the potential theory to gas mixtures by assuming that the adsorption potential for each gas in the mixture could be obtained from the characteristic curve for the pure gases. They pointed out that the correlation for the pure gases indicated that at constant temperature the amount adsorbed was the important factor in determining the adsorption potential and thus they further assumed that in mixtures the potential value of the individual components was determined by the total amount of adsorbate. Their method of prediction is outlined in the following steps.

(a) An adsorbed phase composition and the total pressure of the mixture are assumed. Then from the pure gas isotherms and the following correlation:

$$\frac{n_1}{n_1^{\circ}(P)} + \frac{n_2}{n_2^{\circ}(P)} = 1 \qquad (2.50)$$

the actual amount adsorbed of both components can be calculated.

In Equation (2.50) $n_1^o(P)$ and $n_2^o(P)$ are the amounts adsorbed for pure component 1 and pure component 2 at the total pressure of the mixture.

(b) The total volume of the adsorbate is then determined by summing the products of the moles of each component adsorbed times its molar volume as a saturated liquid, V_L, at the adsorption pressure.

(c) From the pure gas characteristic curve values of $\left(\frac{1}{V_L} \text{ ℓn } \frac{f_s}{f}\right)$ for each of the gases are read. If both components are on the same correlation curve, the same value of the adsorption potential will be obtained. The value of (f_s/f) is then calculated. The authors have suggested that the value of V_L used may be either the corresponding pure component molar volume or the average molar volume of the mixture.

(d) The fugacities f_s and f are related to composition by the Lewis and Randall type fugacity rule. f_s was taken to be equal to the fugacity of the pure saturated liquid at the adsorption temperature times the mole fraction of that component in the adsorbate. The values of f so calculated were used to determine the gas phase composition by assuming that the fugacity for a component is equal to its mole fraction in the gas phase times its fugacity as pure gas at the same temperature and total pressure of the mixture.

(e) The pressure at which the mole fraction in the gas phase add to unity is compared with the original assumed total pressure. If there is a significant difference the calculations are repeated with a new assumed adsorbed phase composition.

(f) A relative volatility value is then calculated and assumed to be composition independent.

The main disadvantages of this model are its assumption of composition independence of the relative volatility which generally is not the case encountered in most adsorption systems and uncertainties connected with the molar volume, V_L.

In another extension Maslan et al[34] have suggested that both the adsorbate total volume and the mixture potential could be treated as additive functions, i.e.

$$n_T V_{L_T} = n_1 V_{L_1} + n_2 V_{L_2} \qquad (2.51)$$

$$\left(n\ RT\ \ln \frac{f_s}{f}\right)_{12} = \left(n\ RT\ \ln \frac{f_s}{f}\right)_1 + \left(n\ RT\ \ln \frac{f_s}{f}\right)_2 \qquad (2.52)$$

Introducing the concept of mole fraction in the adsorbed phase Equation (2.52) was rearranged as:

$$f_1^{x_1} f_2^{x_2} = f_{s_1}^{x_1} f_{s_2}^{x_2} / (f_{s_{12}} / f_{12}) \qquad (2.53)$$

For a given adsorbate composition the denominator of the right side of Equation (2.53) may be determined from the characteristic curve of the adsorbent. The two fugacities in the numerator are known and thus this will leave the gas composition as represented by the left side of the equation unknown which can be determined by a trial and error procedure.

A third extension of potential theory is reported by Grant and Manes[33]. Their prediction method is based on the assumption that the adsorbate behaves as an ideal liquid mixture with the standard state taken to be the pure adsorbate at the adsorbate volume of the mixture. Using Raoult's law together with the adsorption potential equation:

$$E = \left(n\, RT\, \ell n \left(\frac{f_s}{f} \right) \right)_{\text{pure 1}}$$

they arrived at the following equation:

$$\frac{1}{V_{L_1}} \ell n\, x_1 \left(\frac{f_s}{f} \right)_1 = \frac{1}{V_{L_2}} \ell n\, x_2 \left(\frac{f_s}{f} \right)_2 \qquad (2.54)$$

Equation (2.54) together with the condition $x_1 + x_2 = 1$ determines the compositions of the adsorbed phase from given values of f_i, $(f_s)_i$ and V_{L_i}. Substituting the proper values of x_i into either terms of Equation (2.54) and using the correlation curve the total mixture adsorbate volume can be determined. The individual amount adsorbed of each component can be then determined using the following equations:

$$n_T (x_1 V_{L_1} + x_2 V_{L_2}) = V_{L_T}$$

$$n_1 = x_1 n_T$$

The extensions of the Polanyi theory has been tested by Danner and Wenzel[29] for the adsorption of binary gas mixtures on zeolite molecular sieves, type 5A and 10X and poor results were obtained.

The extension of the Polanyi theory by Grant and Manes is thermodynamically inconsistent for it predicts no separation effect at saturation[39,91].

2.3.3 Empirical methods

In a thermodynamic analysis of gas-mixture adsorption Broughton[92] developed the following equation:

$$\int_o^{n_1^o(P)} \ell n\, P_1^o\, d\, n_1^o - \int_o^{n_1^o(P)} \ell n\, P_1\, d\, n_1 = \int_o^{n_2^o(P)} \ell n\, P_2^o\, d\, n_2^o - \int_o^{n_2^o(P)} \ell n\, P_2\, d\, n_2 \qquad (2.55)$$

Based on the above equation Lewis et al[30] developed their empirical method for prediction of gas mixture adsorption by employing the following relationships:

$$P_1 + P_2 = P$$

$$\frac{n_1}{n_1^{\circ}(P)} + \frac{n_2}{n_2^{\circ}(P)} = 1 \qquad (2.50)$$

$$\frac{y_1}{x_1} \cdot \frac{x_2}{y_2} = \frac{P_1}{P_2}\frac{n_2}{n_1} = \alpha_{1,2} = \text{constant} \qquad (2.39a)$$

Equation (2.50) is an empirical equation based on their experimental observations for the adsorption of hydrocarbon mixtures on both silica gel and carbon. In their analysis of their experimental work they found that the relative volatility $\alpha_{1,2}$ is almost composition independent and thus it was assumed to be constant.

Combining the above four equations yields:

$$\frac{(\alpha_{1,2}-1)}{\alpha_{1,2}\ B-1}\, n_1^{\circ}(P)\ \ell n(\alpha_{1,2}\ B) = (n_2^{\circ}(P) - n_1^{\circ}(P))\ \ell n\ P - \int_o^{n_2^{\circ}(P)} \ell n\ P_2^{\circ}\, d\, n_2^{\circ}$$

$$+ \int_o^{n_1^{\circ}(P)} \ell n\ P_1^{\circ}\ d\ n_1^{\circ} \qquad (2.56)$$

where $B = n_1^{\circ}(P)/n_2^{\circ}(P)$.

The only unknown in the above equation is $\alpha_{1,2}$ for which a unique solution can be obtained by trial and error. Once $\alpha_{1,2}$ is determined the individual amount adsorbed can be evaluated through Equations (2.39a) and (2.50) by assuming a gas phase composition.

Cook and Basmadjian[35] attempted to improve the method of Lewis et al by taking into account the isobaric variation of the relative volatility with composition. The starting point of their approach was

an equation proposed by Basmadjian[93] for predicting the relative volatility when it is small (< 4) and constant:

$$\ell n\ \alpha_{1,2} = \frac{1}{n_1^{o}(P)} \int_{o}^{n_1^{o}(P)} \ell n \left(\frac{P_1^{o}}{P_2^{o}}\right)_{n^{o}} d\ n^{o} \qquad (2.57)$$

Cook and Basmadjian have extended the use of Equation (2.57) to systems with variable relative volatilities. Briefly their method consists of evaluating the relative volatility at both extremes of infinite dilution and interpolating the values at intermediate compositions through an empirical procedure. The detailed steps of the procedure are as follows.

(a) The two limiting relative volatilities are estimated by assuming that they can be described by a relation analogous to Equation (2.57).

$$\ell n(\alpha_{1,2})_{x_1=1} = \frac{1}{n_1^{o}(P)} \int_{o}^{n_1^{o}(P)} \ell n\left(\frac{P_1^{o}}{P_2^{o}}\right) d\ n^{o} \qquad (2.57a)$$

$$\ell n(\alpha_{1,2})_{x_2=1} = \frac{1}{n_2^{o}(P)} \int_{o}^{n_2^{o}(P)} \ell n\left(\frac{P_1^{o}}{P_2^{o}}\right) d\ n^{o} \qquad (2.57b)$$

(b) The limiting relative volatilities are used for evaluating the indeterminate limiting ratios, P/x:

$$\left(\frac{P_1}{x_1}\right)_{x_2=1} = P(\alpha_{1,2})_{x_2=1} \qquad (2.58)$$

$$\left(\frac{P_2}{x_2}\right)_{x_1=1} = P/(\alpha_{1,2})_{x_1=1} \qquad (2.59)$$

These are then entered on a plot of total amount adsorbed, n_T vs P/x. The values are located at the points C and D in

Figure 2.1, which also shows plots of the pure component isotherms 1 and 2.

(c) The binary curves AC and BD are next constructed based on the assumption that they can be represented by the same form of equation as the pure component isotherms over the binary concentration range. In fact the curves AC and BD were found to be linear by an appropriate choice of coordinates (semilog or log-log scale).

(d) The desired binary isotherms $n_1 = f_1(P_1)$ and $n_2 = f_2(P_2)$ can be derived from the curves AC and BD. Values of P_1/x_1 and P_2/x_2 are read off for each total amount adsorbed and one of the unknown mole fractions, say x_2, calculated by combining the equations $x_1 + x_2 = 1$ and $P_1 + P_2 = P$.

$$x_2 = \frac{(P_1/x_1)_{n_T} - P}{(P_1/x_1)_{n_T} - (P_2/x_2)_{n_T}} \qquad (2.60)$$

Cook and Basmadjian tested their method against non-intersecting monolayer adsorption isotherms and intersecting isotherms - multilayer adsorption. They found that their method gave reasonable predictions for monolayer adsorption of binary mixtures but failed to give quantitative results of multilayer adsorption particularly for systems with azeotropes.

Danner and Wenzel[29] tested the above method against their binary mixtures on zeolites, type 5A and 10X and relatively good predictions were obtained especially for the system CO-N_2 on both adsorbents.

Yon and Turnock[40] introduced the concept of loading ratio correlation (LRC) for adsorption on molecular sieves. The LRC is in fact an extension of the Langmuir expression for monolayer adsorption. The concept of monolayer capacity, n_m, is replaced by the maximum

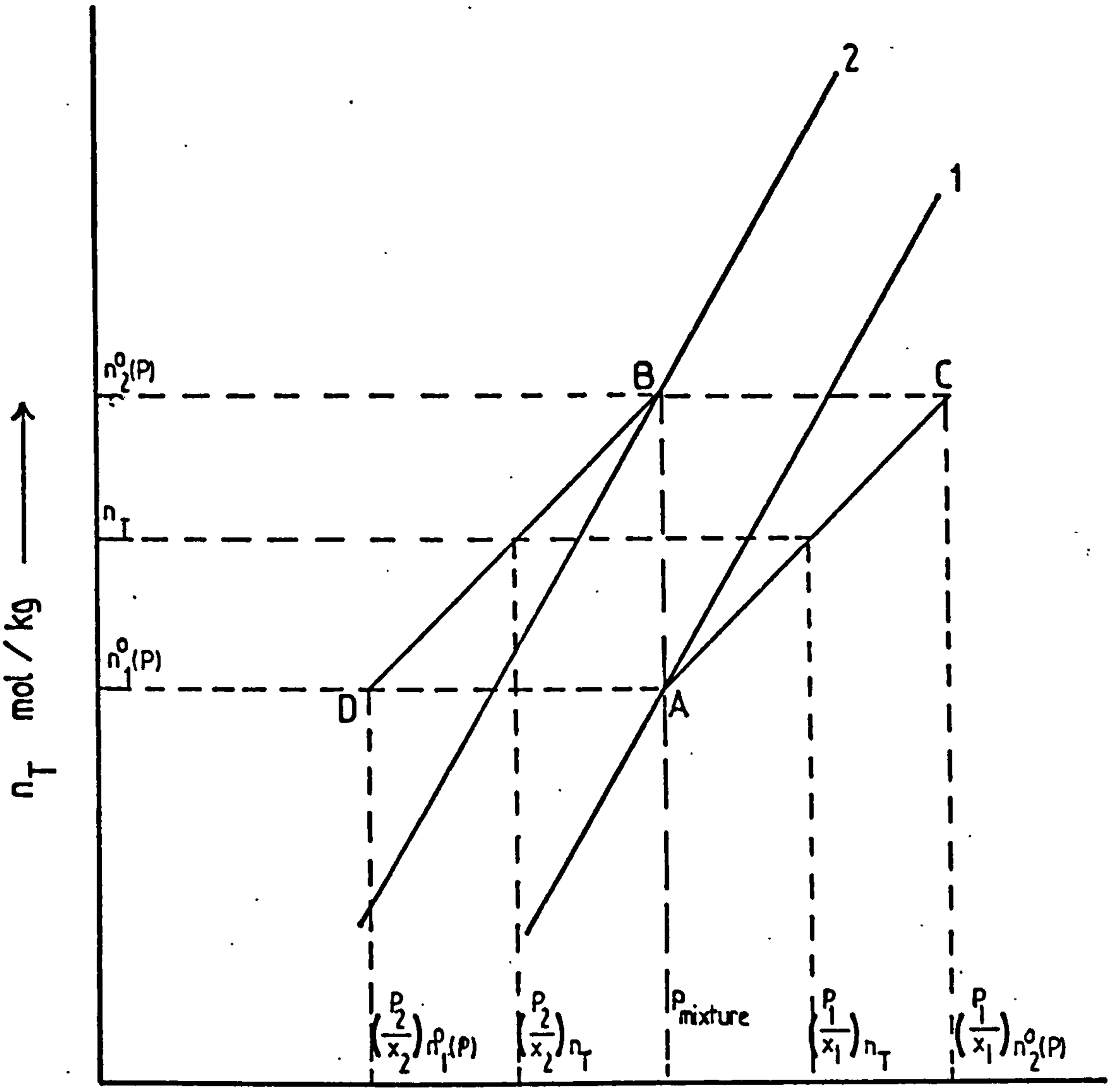

Figure 2.1 Cook and Basmadjian (35) Construction Plot for the Calculation of Binary Isotherms

attainable loading, n_o, for the molecular sieve. The basic LRC equation for the pure component is given by:

$$LRC \equiv \frac{n}{n_o} = (K\,P)^{1/c} / \left[1 + (K\,P)^{1/c}\right] \qquad (2.61)$$

where c is a constant. The correlating equation is produced by taking logarithms and describing K by a temperature dependent function:

$$\ell n\, P = A_1 + A_2/T + c\, \ell n\left[n/(n_o - n)\right] \qquad (2.62)$$

A_1 and A_2 are LRC constants describing the temperature dependence of K.

The value of c can also be described by a temperature dependent function as:

$$c = A_3 + A_4/T$$

Yon and Turnock then extended the LRC to multicomponent systems using the method of Markham and Benton[84]:

$$(LRC)_i = \frac{n_i}{n_{o_i}} = (K_i\,P_i)^{1/c_i} / \left[1 + \sum_{j=1}^{r} (K_j\,P_j)^{1/c_j}\right] \qquad (2.63)$$

or:

$$\ell n\, P_i = A_{1_i} + A_{2_i}/T + c_i\, \ell n\left[(LRC)_i / (1 - \sum_{j=1}^{r} (LRC)_j)\right] \qquad (2.64)$$

Yon and Turnock suggested that if the pure component LRC constants fail to predict adequately the adsorption characteristics of the adsorbates in multicomponent systems, appropriate modified LRC constants can be obtained through correlation of gas mixture experimental results to Equation (2.64). In this way the LRC technique becomes a correlating technique rather than a predictive technique.

Duckett and Dunlop[41] developed a simple empirical method based

on the use of a mean value of the relative volatility and Lewis' equation (Equation (2.50)). The mean relative volatility is given by:

$$\alpha_{m_{1,2}} = \frac{1}{n_1^{o}(P)} \int_{o}^{n_1^{o}(P)} \left[\frac{P_1^{o}}{P_2^{o}}\right]_n d\, n \qquad (2.65)$$

or if the isotherm data are not available at low pressures the following equation is used instead:

$$\alpha_{m_{1,2}} = \frac{1}{n_1^{o}(P) - n_{1,min}} \int_{n_{1,min}}^{n_1^{o}(P)} \left[\frac{P_1^{o}}{P_2^{o}}\right]_n d\, n \qquad (2.66)$$

The individual amounts adsorbed can be calculated by employing Lewis' equation and are given by:

$$n_1 = \frac{1}{\frac{1}{n_1^{o}(P)} + \alpha_{m_{1,2}} \frac{y_2}{y_1} \frac{1}{n_2^{o}(P)}} \qquad (2.67)$$

$$n_2 = \alpha_{m_{1,2}} \frac{y_2}{y_1} n_1 \qquad (2.68)$$

Duckett and Dunlop tested their model against binary data of Lewis et al[30], Ledermann and Williams[71] and Danner and Wenzel[29] but only fair predictions were obtained.

2.3.4 The ideal adsorbed solution theory (IAST)

A significant development in the prediction of gas mixture adsorption behaviour has been accomplished by Myers and Prausnitz[36]. They proposed a method of treating adsorption equilibrium analogous to the description of vapour-liquid equilibrium by solution thermo-

dynamics. An ideal adsorbed solution has been defined whose behaviour is analogous to an equilibrium vapour-liquid system which follows Raoult's law. Deviations from the ideal adsorbed solution can be described in terms of adsorption activity coefficients.

The chemical potential of component i in the adsorbed phase at a constant temperature and spreading pressure is given by[36]:

$$\mu_i(T,\pi,x_i,....) = G_i^{\circ}(T) + RT \ln P_i^{\circ}(\pi) + RT \ln \gamma_i x_i \qquad (2.69)$$

The chemical potential for component i in the gas phase with the same reference state is:

$$\mu_i(T,P,y_i) = G_i^{\circ}(T) + RT \ln P y_i \qquad (2.70)$$

If the equality of chemical potentials of each component in both the gas and adsorbed phase is used as a criterion of equilibrium in an adsorption system, the following equation is obtained:

$$P y_i = P_i^{\circ}(\pi) \gamma_i x_i \quad \text{(constant T)} \qquad (2.71)$$

There is one additional degree of freedom in adsorption equilibrium as compared to vapour-liquid equilibrium. In Myers and Prausnitz treatment the spreading pressure, π, is chosen as the additional intensive property of the adsorbate. In vapour-liquid equilibrium specification of two of the three variables, P, T and x, completely defines the system. In adsorption equilibrium three of the four variables, P, T, x and π must be specified to define the system.

The ideal adsorbed solution is described analytically by Equation (2.71) with γ_i equal to unity. It is also described as an adsorbed mixture for which the area change and enthalpy change of mixing are zero for a hypothetical mixing process at constant temperature and spreading pressure[36]. The criterion of zero area change of mixing

leads to the following expression for a binary mixture:

$$a = a_1^{\circ}(\pi)\, x_1 + a_2^{\circ}\, x_2 \quad \text{(constant T)} \tag{2.72}$$

or:

$$\frac{1}{n_t} = \frac{x_1}{n_1^{\circ}(\pi)} + \frac{x_2}{n_2^{\circ}(\pi)} \tag{2.73}$$

In order to utilize Equations (2.71) and (2.73) for prediction of binary gas mixture adsorption equilibrium, a further relation is needed between the spreading pressure and directly measurable quantities. This relation is given by Gibbs adsorption equation (Equation (2.11)) which can be written in an integral form as:

$$\frac{A\,\pi}{RT} = \int_0^{P^{\circ}} n\, d\, \ell n\, P \tag{2.11a}$$

Another form of Equation (2.11a) is given by Kidnay and Myers[37] as:

$$\frac{A\,\pi}{RT} = \int_0^{n^{\circ}} \frac{d\, \ell n\, P}{d\, \ell n\, n}\, d\, n \tag{2.11b}$$

Calculation of the spreading pressure, π, requires the specific area (A) of the adsorbent which is assumed to be uninfluenced by temperature, pressure or the amount of material adsorbed. In a molecular sieve adsorbent this is not valid and this assumption is overcome by the use of Ω in place of the term $\left(\frac{\pi\, A}{RT}\right)$. Ω is calculated from the right-hand side of Equation (2.11b) and is readily applicable to adsorption in molecular sieves[95].

The prediction calculation for binary gas adsorption by IAST proceeds as follows.

(a) Experimental isotherms are obtained for pure components 1 and 2 (see Figure 2.2a).

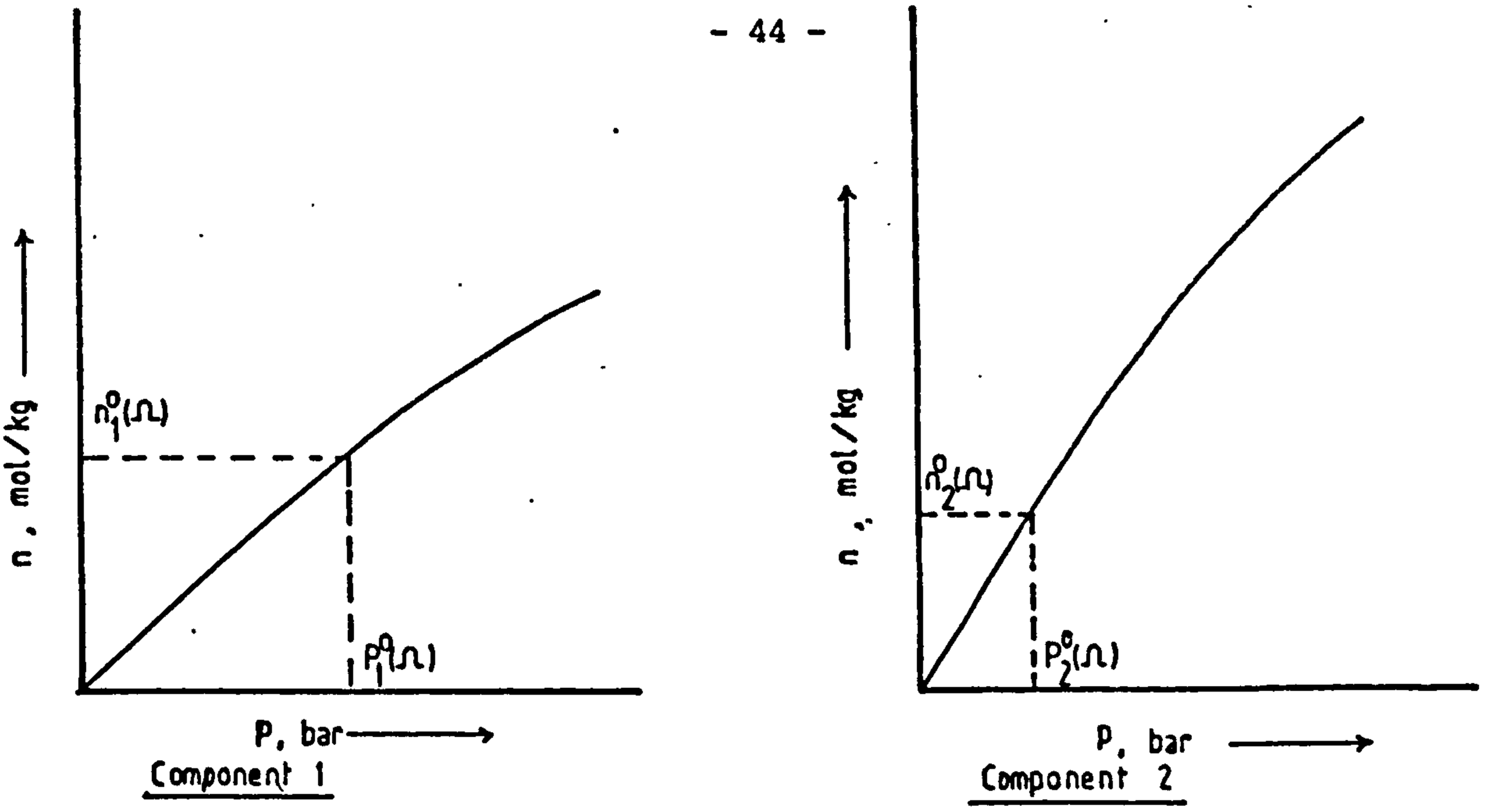

Figure 2·2a Basic Isotherm Data for Components 1 & 2

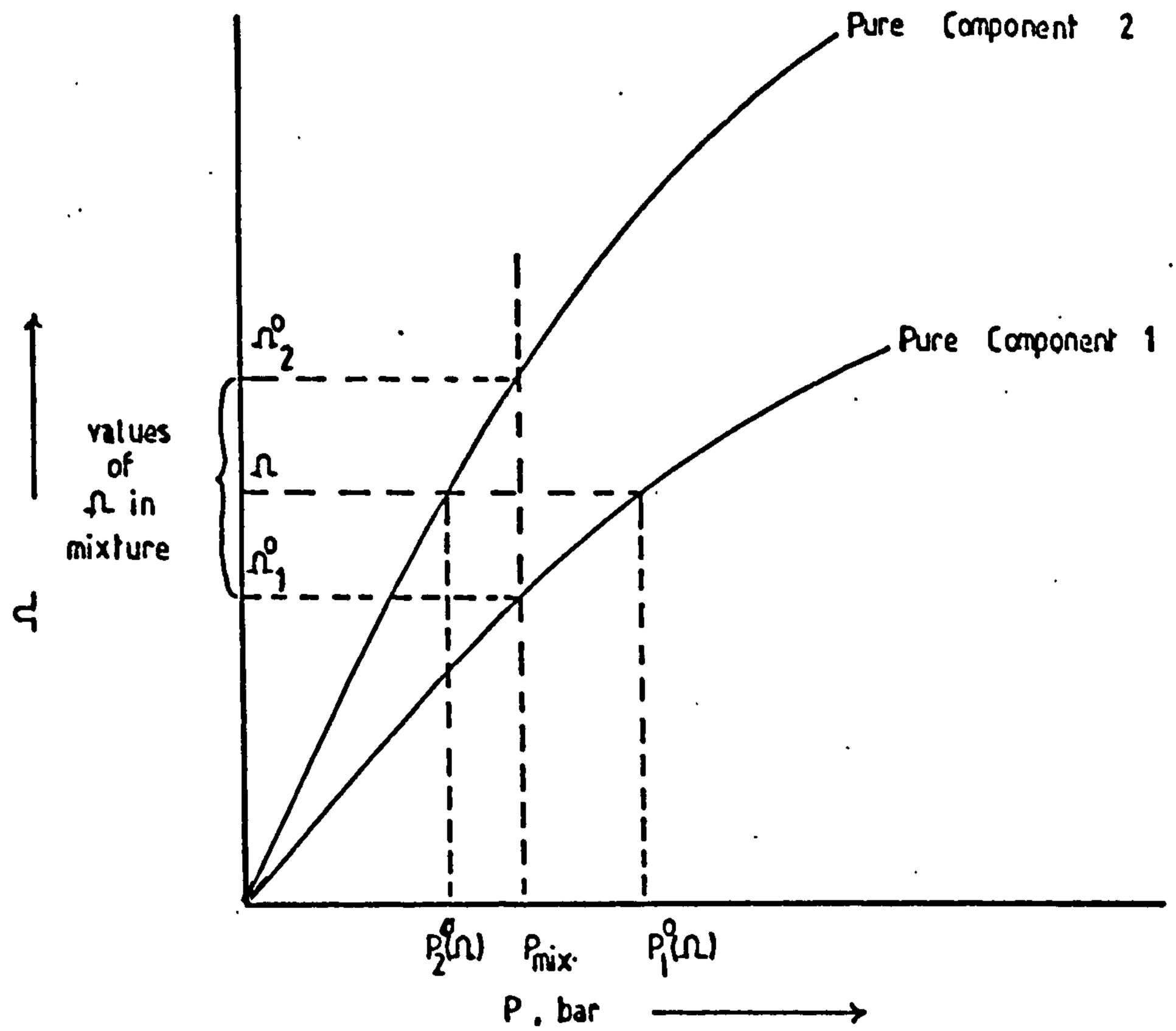

Figure 2·2b Calculation of Mixture Adsorption Equilibria from Pure Components Spreading Pressures

Figure 2·2 Graphical Procedure for Prediction of Binary Adsorption Equilibria by IAST

(b) Equation (2.11a) or (2.11b) is applied to the experimental data for the pure component isotherm yielding two relationships (see Figure 2.2b):

$$\Omega_1^{\circ} = \Omega_1^{\circ}(P_1^{\circ}) \tag{2.74}$$

$$\Omega_2^{\circ} = \Omega_2^{\circ}(P_2^{\circ}) \tag{2.75}$$

(c) Equation (2.71) with γ_i set to unity is written for both components:

$$P\, y_1 = P_1^{\circ}(\pi)\, x_1 \tag{2.71a}$$

$$P\, y_2 = P_2^{\circ}(\pi)\, x_2 \tag{2.71b}$$

(d) The mixing process is carried out at constant values of π or Ω:

$$\pi_1^{\circ} = \pi_2^{\circ}$$

or:

$$\Omega_1^{\circ} = \Omega_2^{\circ} \tag{2.76}$$

(e) In addition there are two mole fractions constraints:

$$x_1 + x_2 = 1$$

$$y_1 + y_2 = 1$$

(f) The above equations in steps (b) to (e) constitute a set of seven independent equations with nine unknowns, x_1, x_2, y_1, y_2, P_1°, P_2°, Ω_1°, Ω_2°, and P. By fixing two thermodynamic degrees of freedom, such as P and Ω, all the remaining

variables can be calculated.

(g) The total amount adsorbed can be calculated by means of Equation (2.73) since the experimental data for pure component adsorption give the values of n_1^o and n_2^o.

IAST has been tested by Myers and Prausnitz on the binary hydrocarbon mixture data of Szepesy and Illes[89] and Bering and Serpenskii[96] and by other investigators[29,37,94,95,97-99]. Good predictions were achieved and deviations from IAST in some cases were accounted for by the activity coefficient[66,95,99].

Although IAST is based on calculating the spreading pressure or Ω from raw pure component equilibrium data, some investigators[78,97,98] have applied IAST using isotherm models quite satisfactorily.

The IAST has the following three major advantages.

(a) The model is thermodynamically consistent, i.e. it satisfies the Gibbs adsorption equation.

(b) It does not depend upon the applicability of a particular isotherm (e.g. Langmuir, BET, ...) to pure component data.

(c) It forms a basis for the calculation of the activity coefficients of adsorbate mixtures. This is achieved by obtaining binary experimental data at constant temperature and pressure for the entire range of gas composition and using Equation (2.10) for calculating the spreading pressure of the mixture. By determining the spreading pressure the corresponding vapour pressure, p^o, of each component can be obtained from the pure component data. The activity coefficients can then be obtained by using Equation (2.71).

The major disadvantage of this method occurs when the spreading pressure curves of the pure components are quite apart from each other. In this case pure gas adsorption data far above the total binary mixture

pressure will be required in order to obtain equal spreading pressures for both components. This difficulty was encountered by Danner[74] on his analysis of his binary data of O_2-CO on molecular sieves, types 10X and 5A.

Different intensive variables that determine the standard state other than the spreading pressure have been used by other investigators[37-39]. Kidnay and Myers[37] used the total amount adsorbed but this method is applicable only if the slopes of the pure isotherms on a logarithmic plot at different values of amount adsorbed are the same. Fernbacher and Wenzel[38] defined the standard state as pure component i adsorbed at the same temperature on the same total adsorbent surface area A and the same adsorbate volume of the mixture. Sircar and Myers[39] applied the reduced potential for condensable vapours which is defined by:

$$\Omega_r = \frac{\Omega_i}{\Omega_s}$$

2.3.5 Real adsorbed solution

A real adsorbed solution is defined by taking into account the possible interaction between the molecules of the different adsorbates competing to occupy the active sites of an adsorbent surface. Using solution thermodynamics such interactions are accounted for by the activity coefficients of all the adsorbates. The activity coefficient for a component i is given by Equation (2.71) which can be rewritten in the form:

$$\gamma_i = \frac{P_i}{x_i \, P_i^{\circ}(\pi)} \qquad (2.71\bar{a})$$

The useful thermodynamic concept for efficiently expressing the non-ideality of an adsorbed mixture is the molar excess Gibbs energy which is given by[36]:

$$G^E = RT \Sigma x_i \ln \gamma_i \qquad (2.77)$$

The molar excess Gibbs energy may be positive or negative or zero. The adsorbed solution is ideal when G^E equals to zero. When the molar excess Gibbs energy of a solution is greater than zero the adsorbed solution is said to exhibit positive deviations from ideality whereas if it is less than zero the deviations from ideality are said to be negative.

In a binary solution system any expression used for correlating the molar excess Gibbs energy in terms of the adsorbed phase compositions must obey the following two boundary conditions.

$$G^E = 0 \qquad \text{when } x_1 = 0$$

$$G^E = 0 \qquad \text{when } x_2 = 0$$

Table 2.2 lists the various models used in gas phase-adsorbed phase equilibria for the molar excess Gibbs energy and the subsequent activity coefficients for a binary system. (These are identical to equations for vapour-liquid equilibria.)

A thermodynamic relation which provides a useful tool for relating activity coefficients is the Gibbs-Duhem equation (Equation (2.6)). Applying the Gibbs-Duhem equation at a constant temperature and spreading pressure gives:

$$\Sigma x_i \, d \ln \gamma_i = 0 \qquad (2.78)$$

which may be written in a differential form for a binary mixture as:

$$x_1 \frac{d \ln \gamma_1}{d x_1} = x_2 \frac{d \ln \gamma_2}{d x_2} \qquad (2.79)$$

The Gibbs-Duhem equation thus says that in a mixture the activity

TABLE 2.2

Some Models for the Excess Gibbs Energy and Subsequent Activity Coefficients for Binary Systems[100]

Name	G^E	Binary Parameters	$\ln \gamma_1$ and $\ln \gamma_2$
Three-suffix Margules	$G^E = x_1 x_2 (A + B(x_1 - x_2))$	A, B	$RT \ln \gamma_1 = (A + 3B) x_2^2 - 4B x_2^3$ $RT \ln \gamma_2 = (A - 3B) x_1^2 + 4B x_1^3$
Van Laar	$G^E = \frac{A x_1 x_2}{x_1 (A/B) + x_2}$	A, B	$RT \ln \gamma_1 = A\left(1 + \frac{A}{B}\frac{x_1}{x_2}\right)^{-2}$ $RT \ln \gamma_2 = B\left(1 + \frac{B}{A}\frac{x_2}{x_1}\right)^{-2}$
Wilson	$\frac{G^E}{RT} = -x_1 \ln(x_1 + \Lambda_{12} x_2) - x_2 \ln(x_2 + \Lambda_{21} x_1)$	Λ_{12}, Λ_{21}	$\ln \gamma_1 = -\ln(x_1 + \Lambda_{12} x_2) + x_2\left(\frac{\Lambda_{12}}{x_1 + \Lambda_{12} x_2} - \frac{\Lambda_{21}}{\Lambda_{21} x_1 + x_2}\right)$ $\ln \gamma_2 = -\ln(x_2 + \Lambda_{21} x_1) - x_1\left(\frac{\Lambda_{12}}{x_1 + \Lambda_{12} x_2} - \frac{\Lambda_{21}}{\Lambda_{21} x_1 + x_2}\right)$
Uniquac	$G^E = G^E(\text{combinatorial}) + G^E(\text{residual})$ $\frac{G^E(\text{combinatorial})}{RT} = x_1 \ln \frac{\phi_1}{x_1} + x_2 \ln \frac{\phi_2}{x_2} + \frac{z}{2}\left(q_1 x_1 \ln \frac{\theta_1}{\phi_1} + q_2 x_2 \ln \frac{\theta_2}{\phi_2}\right)$ $\frac{G^E(\text{residual})}{RT} = - q_1 x_1 \ln(\theta_1 + \theta_2 T_{21}) - q_2 x_2 \ln(\theta_2 + \theta_1 T_{12})$ $\phi_1 = \frac{x_1 r_1}{x_1 r_1 + x_2 r_2}$, $\theta_1 = \frac{x_1 q_1}{x_1 q_1 + x_2 q_2}$ $\ln T_{21} = -\frac{\Delta U_{21}}{RT}$, $\ln T_{12} = -\frac{\Delta U_{12}}{RT}$ r_i, q_i are measures of, respectively, molecular van der Waal's volumes and molecular surface for pure component	ΔU_{12}, ΔU_{21}	$\ln \gamma_i = \ln \frac{\phi_i}{x_i} + \frac{z}{2} q_i \ln \frac{\theta_i}{\phi_i} + \phi_j(\ell_i - \frac{r_i}{r_j}\ell_j) - q_i \ln(\theta_i + \theta_j T_{ji}) + \theta_i q_i\left(\frac{T_{ji}}{\theta_i + \theta_j T_{ji}} - \frac{T_{ij}}{\theta_j + \theta_i T_{ij}}\right)$ where $i = 1, j = 2$ or $i = 2, j = 1$ $\ell_i = \frac{z}{2}(r_i - q_i) - (r_i - 1)$ $\ell_j = \frac{z}{2}(r_j - q_j) - (r_j - 1)$ $z \equiv$ coordination number = 10

coefficients of the individual components are related to each other. The utility of the Gibbs-Duhem equation is best realised through the concept of the total excess Gibbs energy. The total excess Gibbs energy g^E for a binary adsorbed solution containing n_1 moles of component 1 and n_2 moles of component 2 is defined by:

$$g^E = RT(n_1 \ln \gamma_1 + n_2 \ln \gamma_2) \qquad (2.80)$$

Equation (2.80) gives g^E as a function of both γ_1 and γ_2. Upon applying the Gibbs-Duhem equation, the individual activity coefficients γ_1 or γ_2 are related to g^E by differentiation:

$$RT \ln \gamma_1 = \left(\frac{\partial g^E}{\partial n_1}\right)_{T,\pi,n_2} \qquad (2.81)$$

$$RT \ln \gamma_2 = \left(\frac{\partial g^E}{\partial n_2}\right)_{T,\pi,n_1} \qquad (2,82)$$

Equation (2.77) to (2.82) are useful tools for correlating binary experimental data obtained at constant temperature and pressure for the entire range of gas phase compositions. This is achieved by the following steps.

(a) The spreading pressure of the mixture $\left(\frac{\pi A}{RT}\right)$ for the experimental mixture point of interest is calculated using Equation (2.10).

(b) For each spreading pressure value obtained in step (a) the corresponding vapour pressure of each component, $P^o(\pi)$, is obtained using the pure component isotherms. A plot is then made for the vapour pressure of each component vs the mole fraction in the gas phase.

(c) The individual activity coefficients are calculated using Equation (2.71$\bar{a}$) and the corresponding equation for the

other component.

(d) For each of the experimental points the molar excess Gibbs energy is calculated by Equation (2.77).

(e) One of the equations given in Table 2.2 is chosen. The parameters in that equation are adjusted to minimize the deviations between G^E calculated from the equation and G^E found from experiment in step (d).

(f) Selecting an arbitrary value of mole fraction in the gas phase of one of the components, between 0 and 1, and using Equation (2.71$\bar{a}$) together with the expression selected for correlating the experimental activity coefficients and using the plots obtained in step (b), the mole fraction in the adsorbed phase can be determined by an iterative procedure.

The steps outlined above provide a means for correlating the experimental binary equilibria data. No method has been yet published for predicting activity coefficients since all the models used for expressing G^E in terms of composition contain adjustable parameters which are determined by the experimental binary data.

Glessner and Myers[95] used three suffix Margules equation of the form:

$$\ln \gamma_1 = (2B - A)\, x_2^2 + 2(A - B)\, x_2^3 \qquad (2.83)$$

$$\ln \gamma_2 = (2A - B)\, x_1^2 + 2(B - A)\, x_1^3 \qquad (2.84)$$

for correlating their activity coefficients of the binary mixture CO_2-C_2H_6 on molecular sieve, type 5A.

Costa et al[101] used the Wilson and Uniquac equations for correlating the activity coefficients of binary hydrocarbon mixtures on activated carbon. They then used the binary parameters obtained

from Wilson's and Uniquac's to predict their ternary experimental equilibrium results. The predicted ternary data were found to be in good agreement with their experimental data.

2.3.5.1 The vacancy solution model

Suwanayuen and Danner[43] developed a prediction technique for gas mixture adsorption utilizing the vacancy solution model for pure components. According to the vacancy solution model the binary mixture adsorption equilibrium becomes an equilibrium between ternary vacancy solutions, the third component of which is the vacancy defined to be the solvent of the system.

The equilibrium equation governing the distribution of an adsorbate between the adsorbed and gas phase is obtained by equating the chemical potentials in the adsorbed and gas phase.

$$y_i P = \gamma_i x_i \frac{n_T}{n_{m_T}} \exp\left(\frac{\Delta G_i^{\circ}}{RT}\right) \exp\left(\frac{\pi \bar{a}_i}{RT}\right) \qquad (2.85)$$

where:

$$n_{m_T} = n_1 + n_2 + n_3 = x_1 n_{m_1} + x_2 n_{m_2} \qquad (2.86)$$

$$n_T = n_1 + n_2$$

$$x_i^s = x_i n_T / n_{m_T} = x_i \phi$$

The partial molar area $\bar{a}_i$ is given by the following expression:

$$\bar{a}_i = \bar{a}_3 + \left(1 - \frac{n_{m_i}}{n_{m_T}}\right) \frac{A}{n_T} \quad , \quad i = 1 \text{ or } 2 \qquad (2.87)$$

The equation of state expressing the spreading pressure, π, as a function of the vacancy partial molar area, activity coefficient

and the adsorbed phase composition is given by Equation (2.32). Upon applying this equation with Equation (2.87) gives an expression for $(\pi \bar{a}_i/RT)$:

$$-\frac{\pi \bar{a}_i}{RT} = 1 + \left(\frac{n_{m_T} - n_{m_i}}{n_T}\right) \ln \gamma_3 x_3^s \qquad (2.88)$$

The standard free energy of adsorption (ΔG_i^o) is given by:

$$\exp\left(\frac{\Delta G_i^o}{RT}\right) = \frac{n_{m_i}}{b_i} \Lambda_{i3} \exp(\Lambda_{3i} - 1) \qquad (2.89)$$

The final equilibrium equation for the distribution of adsorbate is obtained by substituting Equation (2.89) into Equation (2.85):

$$y_i P = \gamma_i x_i n_T \frac{n_{m_i} \Lambda_{i3}}{n_{m_T} b_i} \exp(\Lambda_{3i} - 1) \exp\left(\frac{\pi \bar{a}_i}{RT}\right) \qquad (2.90)$$

The composition dependence of the activity coefficients is obtained by the use of Wilson's equation[83] for a ternary vacancy solution system:

$$\ln \gamma_i = 1 - \ln(x_i^s + x_j^s \Lambda_{ij} + x_3^s \Lambda_{i3}) - \left(\frac{x_i^s}{x_i^s + x_j^s \Lambda_{ij} + x_3^s \Lambda_{i3}} + \frac{x_j^s \Lambda_{ji}}{x_i^s \Lambda_{ji} + x_j^s + x_3^s \Lambda_{j3}} + \frac{x_3^s \Lambda_{3i}}{x_i^s \Lambda_{3i} + x_j^s \Lambda_{3j} + x_3^s}\right) \quad \text{for } i,j = 1,2 \text{ or } 2,1 \qquad (2.91)$$

$$\ln \gamma_3 = 1 - \ln(x_1^s \Lambda_{31} + x_2^s \Lambda_{32} + x_3^s)$$

Contd/...

$$- \left(\frac{x_1^s \Lambda_{13}}{x_1^s + x_2^s \Lambda_{12} + x_3^s \Lambda_{13}} + \frac{x_2^s \Lambda_{23}}{x_1^s \Lambda_{21} + x_2^s + x_3^s \Lambda_{23}} + \frac{x_3^s}{x_1^s \Lambda_{31} + x_2^s \Lambda_{32} + x_3^s} \right) \qquad (2.92)$$

In these equations for the activity coefficients the parameters Λ_{13}, Λ_{31}, Λ_{23} and Λ_{32} account for adsorbate-vacancy interactions caused by non-ideality in the adsorbed phase and are obtained from regression of the pure component vacancy equation (Equation (2.38)). The parameters Λ_{12} and Λ_{21} represent adsorbate-adsorbate interactions and have to be estimated from theoretical considerations or regressed from experimental binary adsorption data. For systems with similar adsorbates these interactions can be neglected by setting Λ_{12} and Λ_{21} equal to unity.

For systems with similar adsorbates the prediction procedure for the ternary system is outlined below.

(a) Regression of the pure component experimental isotherm data by Equation (2.38) gives the parameters n_{m_i}, b_i, Λ_{i3} and Λ_{3i} for each component.

(b) The mole fraction of component i in the adsorbed phase is selected.

(c) The maximum total number of moles of mixture in the adsorbed phase is obtained using Equation (2.86).

(d) The term $(\pi \bar{a}_i/RT)$ is obtained from Equation (2.88).

(e) Equations (2.91) and (2.92) give the activity coefficients.

(f) Solving the two equilibrium equations, corresponding to adsorbate 1 and 2 as expressed by Equation (2.90) simultaneously gives y_1 and n_T.

Suwanayuen and Danner tested their model with Λ_{12} and Λ_{21} set to unity against two different kinds of systems:

(a) binary mixtures of O_2, N_2 and CO on zeolite, type 10X, and

(b) binary hydrocarbon mixtures on activated carbon.

For the zeolite system the predictions were reasonably accurate but not as accurate as for the carbon system. In the system O_2-N_2 on zeolite 10X the predictions were poor and were improved by taking into consideration the adsorbate-adsorbate interactions.

2.4 Summary of Literature Cited

Previous work on pure component and gas-mixture adsorption on molecular sieves have shown:

(a) The kinetic models such as Langmuir and BET theory have limited applicability for correlation of pure component isotherms. The predictions obtained by the extensions of these models for gas mixture adsorption have been relatively poor.

(b) Two-dimensional isotherm models, such as the Hill-de Boer model, have correlated pure component isotherms with reasonable accuracy. However, the parameters obtained have shown no physical significance. The extension of this model for gas-mixture adsorption has predicted relatively good experimental binary data.

(c) The potential theory depends on the determination of the adsorbed phase volume and this has been interpreted differently by many authors. Generally no accurate correlation of pure component isotherms have been obtained. The extensions of this theory to gas-mixture adsorption has failed to provide reasonable predictions of experimental binary data.

(d) Out of the empirical methods used for prediction of gas-mixture adsorption the Cook and Basmadjian method seems to be the best for the other methods are based on composition

independence of relative volatility, mean relative volatility or a correlating procedure.

(e) The ideal adsorbed solution theory has predicted experimental binary data reasonably good.

(f) The statistical thermodynamic model and the vacancy solution model have correlated pure component data with a good accuracy. The extensions of these models for gas-mixture adsorption have given good predictions of experimental binary data.

CHAPTER 3

EXPERIMENTAL WORK
AND
BASIC RESULTS

CHAPTER 3

EXPERIMENTAL WORK

AND

BASIC RESULTS

This chapter describes the experimental apparatus and procedure used for:

(a) the measurement of pure component isotherms of oxygen and nitrogen on Laportes 4A, 5A and 13X, Eka 5A and Na-mordenite molecular sieve pellets at three temperatures 278.15, 293.15 and 303.15 K with pressure up to 9 bar;

(b) the measurement of binary equilibrium data of oxygen-nitrogen system on the same adsorbents at the same temperatures and two pressures 1.7 and 4.4 bar.

The calculation procedures required to obtain the pure component isotherms and the binary equilibrium data are also described and the basic experimental results are presented.

3.1 Apparatus

The same apparatus was used for measuring both the pure component isotherms and the binary equilibrium data. This apparatus is outlined in Figure 3.1. It comprised an adsorption vessel, a holding vessel, a diaphragm circulating pump and a vacuum system. The gas phase pressure was measured by a high accuracy Bell and Howell pressure transducer, range 0 - 10 bar. The millivolt signal from the transducer was recorded on a pen recorder. The vacuum system comprised a water cooled oil diffusion

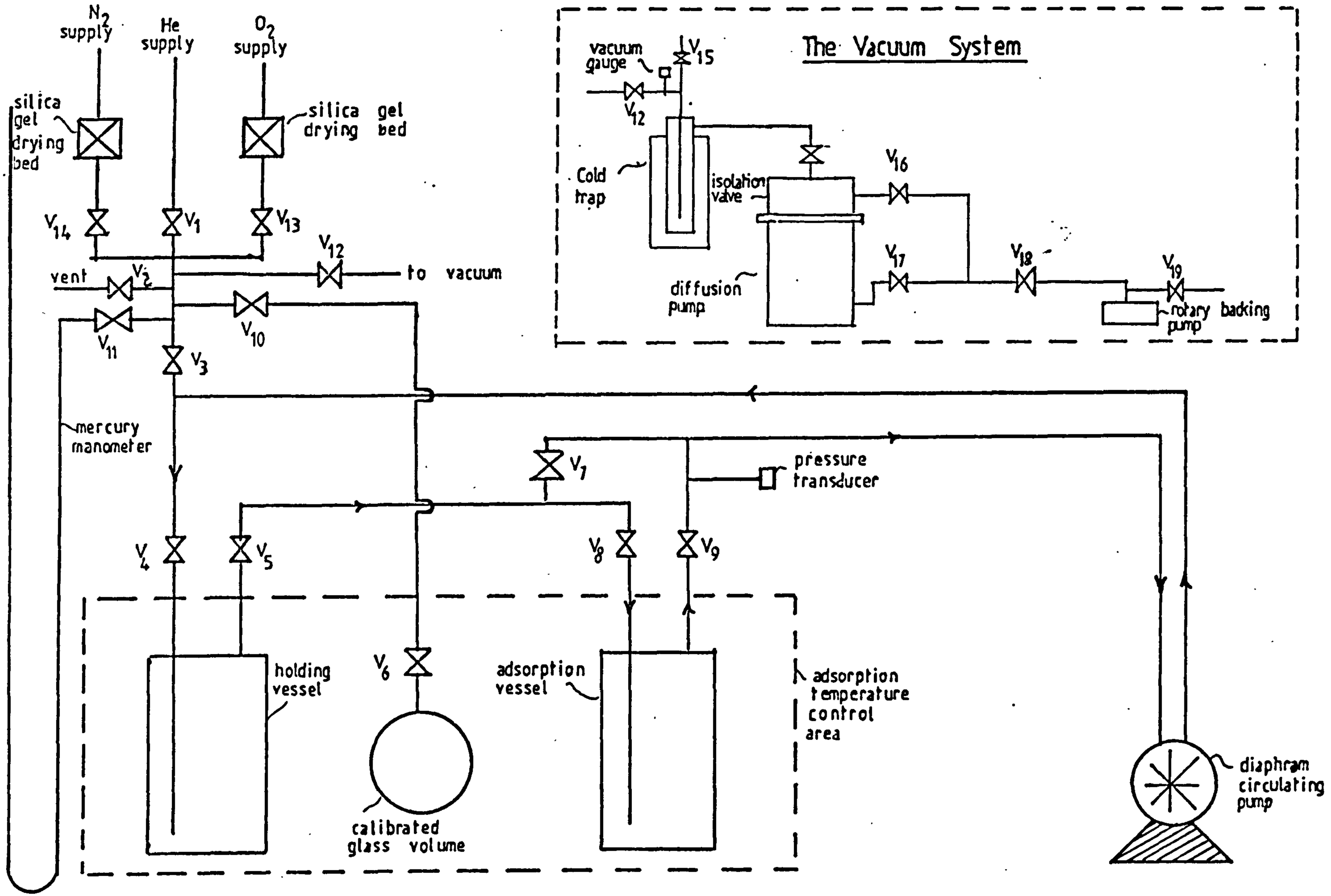

Figure 3-1 Schematic Sketch of the Experimental Apparatus

Legend for FIGURE 3.1

Valves

Number	Type
1, 10, 11, 13, 14	¼" HOKE sealed valves type 4100 series
2, 12, 15	½" Edwards diaphragm vacuum valves
6	¼" Glass stop-cock
3-5, 7-9	¼" HOKE bellow sealed valves type 4600 series
16, 17	1" Edwards diaphragm vacuum valves

Valve Specification

15	cold trap vent
16	roughing valve
17	backing valve
18	throttle valve
19	air admittance valve

Items not illustrated

2 Pen potentiometric recorder, bridge supply, cathetometer, electric furnace and oxygen analyser.

pump, a rotary backing pump, a Penning vacuum gauge and liquid nitrogen cooled cold trap. The vacuum section of the apparatus was constructed mainly from 15 mm copper tube and Edwards diaphragm valves. The testing section of the apparatus was constructed from 6.35 mm stainless steel tubes and HOKE bellow sealed valves. The adsorption and holding vessels were approximately 670 cm^3 constructed from stainless steel and maintained at a constant temperature using a thermostatically controlled 50 litre water bath set at the desired temperature of adsorption. During the calibration of the internal system of the apparatus a calibrated glass volume of 1107.01 cm^3 was submerged in the same bath and connected to the system via a flexible stainless steel tube.

The activation of the adsorbent sample was achieved with the aid of an electric furnace set at 300°C.

When measuring the binary equilibrium data an oxygen analyser was used for determining the oxygen concentration of the gas phase system.

A full specification of the equipment used and operating procedures are given in Appendix II.

3.2 Pure Gas Adsorption

The technique used in measuring pure gas adsorption in this research was a volumetric method. The experimental and calculation procedure for measuring the adsorption isotherms are described below.

3.2.1 Experimental procedure

The internal volumes of the various parts of the system were first accurately determined by expanding helium from the unknown volumes to an accurately calibrated glass-bulb of 1107.01 cm^3. The calibration procedure is outlined in Appendix II.

The cold trap in the vacuum system was filled with 13X molecular sieve pellets. Prior to each activation period of the experimental samples,

the pellets in the cold trap were regenerated to ensure negligible contamination of the experimental samples. The adsorbent samples were activated at 300°C in the adsorption vessel under a vacuum of 10^{-5} torr. The activation period was stopped when the vacuum no longer decreased from 10^{-5} torr on the vacuum gauge. This normally took about 18 - 20 hr. After the activation period was completed, the adsorption vessel was pressurized with helium to a pressure of about 2 bar and left to cool down. It was then evacuated, sealed off and connected to the rest of the system in the water bath.

After the adsorption vessel has reached the desired adsorption temperature, the circulating system which consisted of the holding vessel and the inter-connecting pipe network was evacuated. The pressure transducer was then adjusted to give a zero reading. A quantity of gas was bled into the circulating system from the gas cylinder supply via a silica gel gas drier and the pressure was recorded. The gas was then expanded into the adsorption vessel and left to reach equilibrium with the adsorbent sample. The final pressure was recorded. The adsorption vessel was then sealed off and a new dose of gas again fed to the circulating system and the pressure recorded. The gas was again expanded into the adsorption vessel, left to reach equilibrium and the final pressure recorded. This procedure was repeated for about sixteen consecutive runs until the final equilibrium pressure recorded was up to 9 bar.

The mass of the adsorbent sample used in the experiment could not be accurately determined directly because the mass of the adsorption vessel was out of the limit of the analytical balance. The mass of the samples were hence determined by the following method:

At the end of the experimental run the adsorption vessel was sealed off, disconnected from the experimental system and connected to the vacuum line. It was then heated under vacuum for about 3 hours, sealed off,

connected back to the experimental system in the water bath and left to reach thermal equilibrium. Using helium expansion from the known volumes of the apparatus to the adsorption vessel, the voidage volume in the adsorption vessel was determined. Adsorbent samples from the adsorption vessel were then taken off and a 30 cm^3 HOKE stainless steel cylinder was filled with some of these adsorbents. This cylinder was connected to the vacuum line via a ⅛" HOKE bellow sealed valve. The adsorbent samples in the cylinder were then reactivated by heating the cylinder under vacuum. The cylinder was then sealed off and left to cool down in the water bath. Again using helium expansion the voidage volume in the cylinder was determined. The cylinder was then evacuated, sealed off, disconnected from the system and weighed. The cylinder was next emptied, evacuated, its volume determined by helium expansion, re-evacuated, sealed off and re-weighed. The difference between the two masses yielded the absolute mass of the sample in the cylinder. From the knowledge of the voidage volume and the volume of the cylinder, the absolute density of the adsorbent sample was hence determined. The actual mass of the adsorbent used in the experiment was determined by multiplying the absolute density of the adsorbent by the volume occupied by the adsorbents in the adsorption vessel. The mass used was normally about 500 grams.

3.2.2 Calculation procedure for Gibbs adsorption

In a volumetric apparatus the quantity adsorbed usually determined is the Gibbs adsorption which is defined as the number of moles of gas which must be injected into a fixed evacuated volume containing the adsorbent to bring the equilibrium pressure and temperature to the desired values, less the number of moles which would be injected to produce the same equilibrium conditions if no adsorption occurred[102]. Another definition of adsorption is the absolute adsorption which is the total

number of moles of gas in the range of the operative surface molecular forces between the gas and solid[81]. The difference between the two quantities is due to the volume of the adsorbed phase. The relationship between the Gibbs and the absolute adsorption is given by:

$$n_{abs} = \frac{n_{Gibbs}}{1 - \frac{V}{V^g}} \qquad (3.1)$$

Investigators interpreted differently the determination of the volume of the adsorbed phase. Great variations are found between Dubinin's and Cook and Basmodjian method (see Section 2.2.3). In the earlier stage of this research it had been decided to determine the adsorbed phase volume by comparing isotherms obtained from the volumetric apparatus to those obtained by gravimetric method using the same adsorbent sample. However, due to differences in the degree of adsorbent activation in both processes it was found that the difference between them could not be attributed to the adsorbed phase volume. Hence it was decided to base the calculation procedure of the amount adsorbed on the Gibbs adsorption.

Daly[7] applied the 20 constant equation of state developed by Bender[103] for determining the fugacity coefficients for oxygen and nitrogen within a temperature range of 0 - 50°C and up to a pressure of 100 bar. From his results it was found that both gases could be assumed to behave ideally within the pressure range of this work.

A material balance was performed on the number of moles present in the gas and the adsorbed phase before and after the addition of a new dose of gas to the adsorption vessel, i.e.

$$\text{Number of moles initially present before addition} = \frac{P_D V_D}{R T_B} + \frac{P_{A_1} V_A}{R T_B} + W_1 \qquad (3.2)$$

(In the case of the first addition of gas the last two terms are equated to zero)

$$\text{Number of moles finally present after addition} = \frac{P_{A_2} V_D}{R T_B} + \frac{P_{A_2} V_A}{R T_B} + W_2 \qquad (3.3)$$

The total amount adsorbed per unit mass of adsorbent at a given addition number is given by the expression:

$$n_{Gibbs} = \left(\frac{P_D V_D}{R T_B} + \frac{P_{A_1} V_A}{R T_B} + W_1 - \frac{P_{A_2} V_D}{R T_B} - \frac{P_{A_2} V_A}{R T_B} \right) \Big/ W_A \qquad (3.4)$$

3.3 Binary Gas Adsorption

The measurement of binary gas adsorption equilibria may be achieved using either a dynamic method or a constant volume method[81]. In the dynamic method a gas mixture of known composition is allowed to pass over the outgassed adsorbent until equilibrium is reached, as indicated by constancy of the outlet gas composition. The absorbent container is then isolated from the system and the total amount adsorbed is estimated by pumping off the adsorbed layer and measuring its volume, pressure, composition and temperature. In the constant volume method a gas mixture of known composition is admitted to the outgassed adsorbent within a closed constant volume system. The gas mixture is circulated within the system until equilibrium is reached which is indicated by constancy of the total pressure. A portion of the gas system is then isolated from the adsorbent and its contents withdrawn for analysis. The individual amounts adsorbed can be determined by making a material balance before and after the gas addition to the adsorption chamber.

The constant volume method is the more common method and it is the one used in this research work.

3.3.1 Experimental procedure (constant volume method)

The same adsorbent samples were used in measuring both the pure gas isotherms and the binary equilibrium data.

After reactivation of the adsorbent sample and evacuation of the system, the adsorption vessel was first allowed to reach equilibrium with a known amount of one of the pure gases under a certain pressure. It was then sealed off and the rest of the system evacuated and then pressurized with a certain amount of the other gas such that when expanded to the adsorption vessel, the equilibrium pressure reached the desired value which was approximately 1.7 or 4.4 bar. When gas was then expanded to the adsorption vessel the gas mixture was circulated round the system by the diaphragm pump until equilibrium was reached. The pressure was then recorded with the circulating pump switched off. Both the holding vessel and adsorption vessel were then sealed off. The holding vessel was disconnected from the system and its gas analysed using the oxygen analyser. It was then connected back to the system. The circulating system was evacuated, pressurized with the same second gas and the same procedure again repeated. This procedure was repeated for six consecutive runs, after which the adsorbent sample was reactivated and the whole procedure repeated reversing the roles of the gases. By making a material balance, which is described in the next section, both x, y diagrams (where x and y are mole fractions in the adsorbate and gas phase respectively) and the individual amounts adsorbed were calculated.

3.3.2 Calculation procedure (constant volume method)

The calculation procedure was based on Gibbs adsorption and it was also assumed that both gases, oxygen and nitrogen, behaved ideally within the pressures studied.

Equation (3.4) (with the second and third terms equated to zero) was used to obtain the amount of pure gas adsorbed after the initial addition.

For the next consecutive additions, material balances were performed for each component before and after the addition of a new dose of gas to the adsorption vessel.

For oxygen:

$$\text{Number of moles initially present before addition} = \frac{P_D V_D Y_D}{R T_B} + \frac{P_{A1} V_A Y_{A1}}{R T_B} + W_{O1} \quad (3.5)$$

$$\text{Number of moles finally present after addition} = \frac{P_{A2} V_D Y_{A2}}{R T_B} + \frac{P_{A2} V_A Y_{A2}}{R T_B} + W_{O_2} \quad (3.6)$$

The total amount of oxygen per unit mass of adsorbent at a given addition number is given by the expression:

$$n_{1_{(Gibbs)}} = \left(\frac{P_D V_D Y_D}{R T_B} + \frac{P_{A1} V_A Y_{A1}}{R T_B} + W_{O1} - \frac{P_{A2} V_D Y_{A2}}{R T_B} - \frac{P_{A2} V_A Y_{A2}}{R T_B} \right) \Big/ W_A \quad (3.7)$$

For nitrogen:

$$n_{2_{(Gibbs)}} = \left(\frac{P_D V_D (1-Y_D)}{R T_B} + \frac{P_{A1} V_A (1-Y_{A1})}{R T_B} + W_{N1} - \frac{P_{A2} V_D (1-Y_{A2})}{R T_B} - \frac{P_{A2} V_A (1-Y_{A2})}{R T_B} \right) \Big/ W_A \quad (3.8)$$

3.4 Basic Experimental Results

The basic results presented in this section include pure component adsorption isotherms for O_2 and N_2 and binary gas mixture adsorption data for these gases. These results are presented in graphical form and tabulated results are presented in Appendix I.

3.4.1 Pure gas adsorption results

The adsorption isotherms of oxygen on Laportes 4A, 5A and 13X,

EKA 5A and Na-Mordenite molecular sieve pellets at 278.15, 293.15 and 303.15 K are presented in Figures 3.2 - 3.6. The adsorption isotherms of nitrogen on Laportes 4A, 5A and 13X, EKA 5A and Na-Mordenite molecular sieve pellets at 278.15, 293.15 and 303.15 K are presented in Figures 3.7 - 3.11. The tabulated results are presented in Appendix I.

3.4.2 Binary gas adsorption results

The adsorption data of the binary gas mixtures of nitrogen and oxygen on Laportes 4A, 5A and 13X, EKA 5A and Na-Mordenite molecular sieve pellets were determined at 278.15, 293.15 and 303.15 K and at two pressures of approximately 1.7 and 4.4 bar.

In order to completely specify the adsorption equilibria at a given temperature and total pressure, when a binary gas mixture is adsorbed, the compositions of both the gas and adsorbed phases must be specified together with the total amount adsorbed. The method of presentation of these variables which has been used here is a plot of total amount adsorbed per unit mass of adsorbent as a function of the adsorbed phase composition together with a plot of the adsorbed phase composition versus the gas phase composition. A summary of the results obtained is shown graphically in Figures 3.12 - 3.21 and in tabular form in Appendix I.

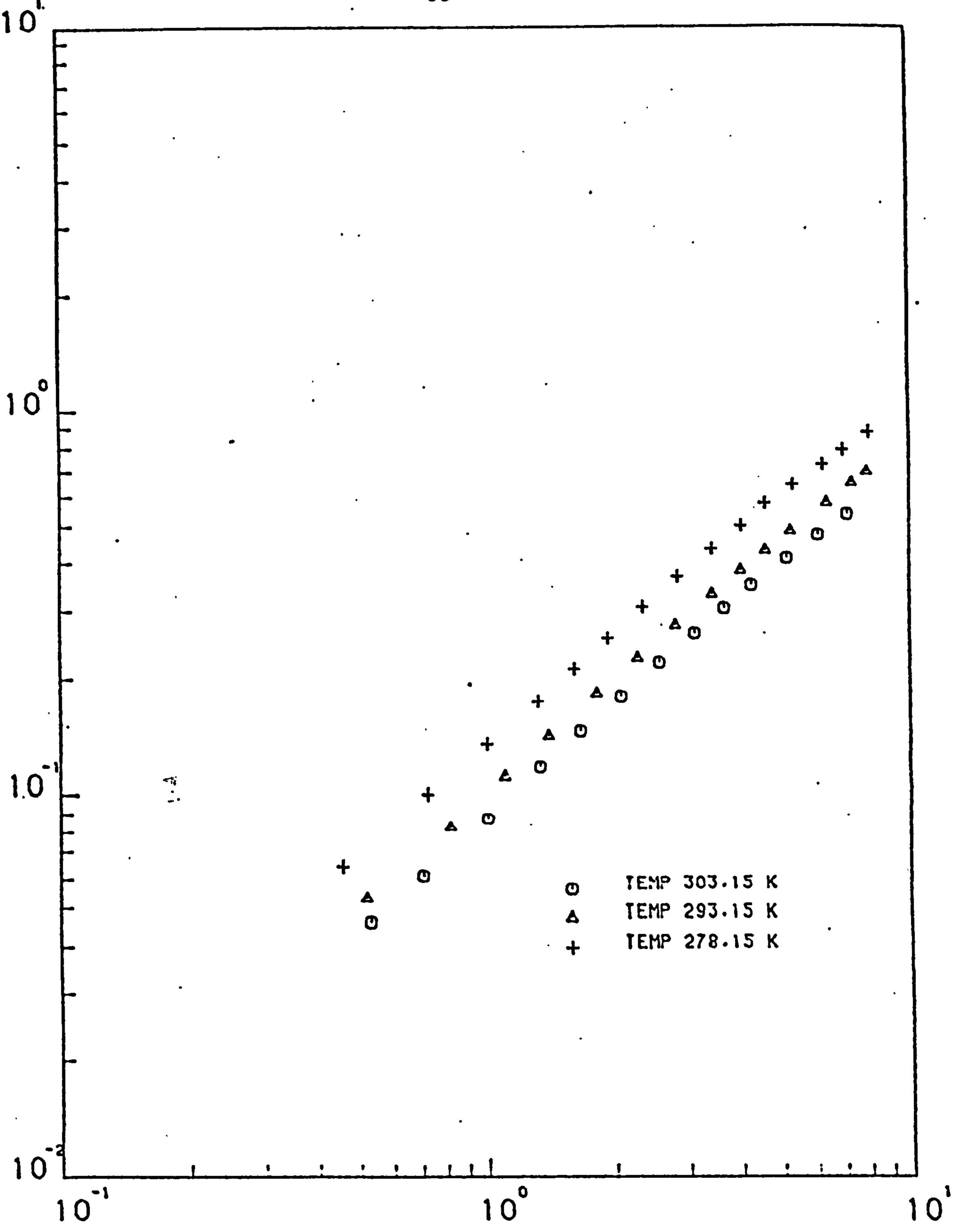

FIGURE (3·2) ADSORPTION ISOTHERMS FOR OXYGEN ON LAPORTE 4A MOLECULAR SIEVE PELLETS AT 278.15.293.15 AND 303.15 K

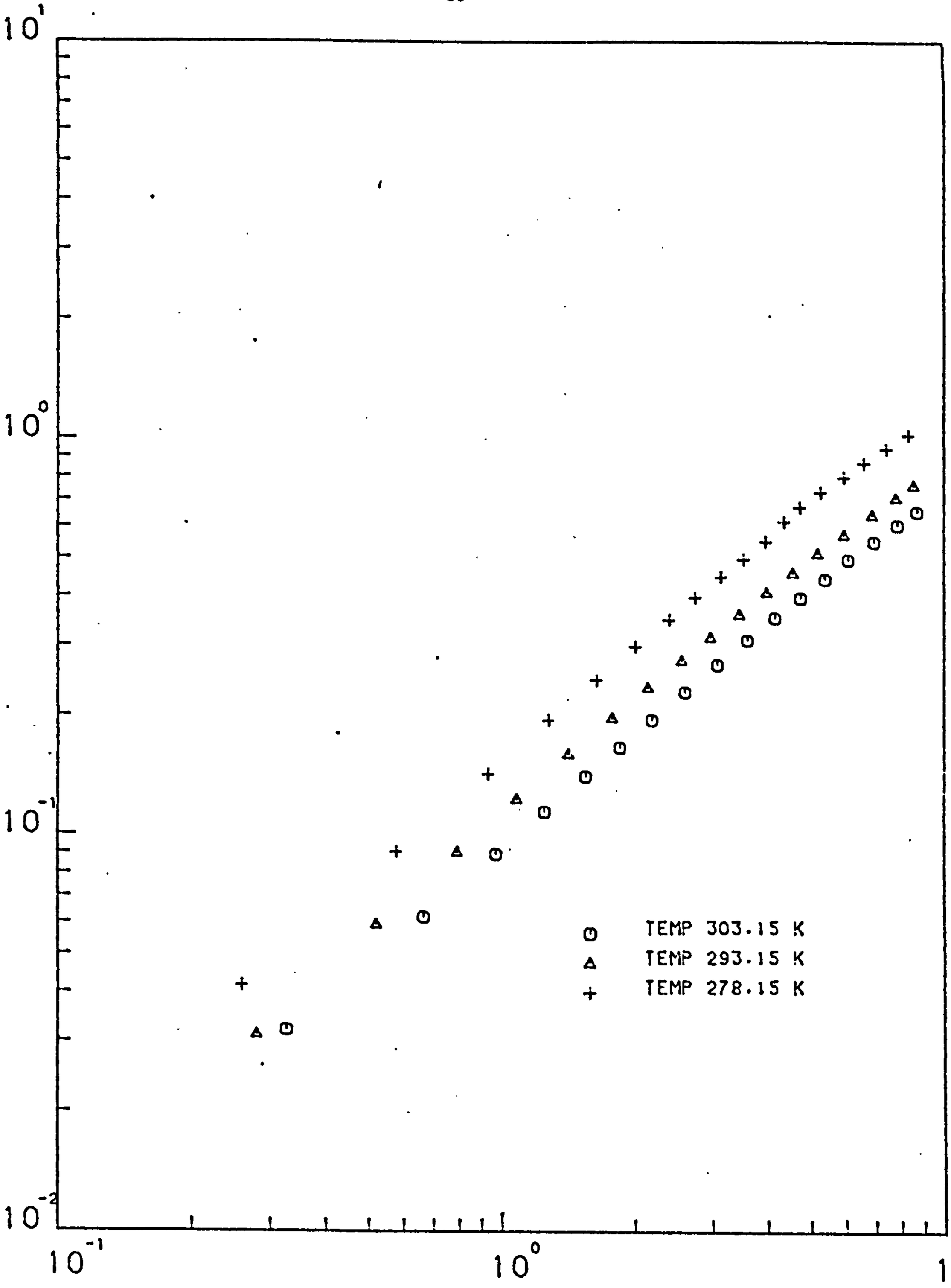

FIGURE (3·3) ADSORPTION ISOTHERMS FOR OXYGEN ON LAPORTE 5A MOLECULAR SIEVE PELLETS AT 303.15 . 293.15 AND 278.15 K

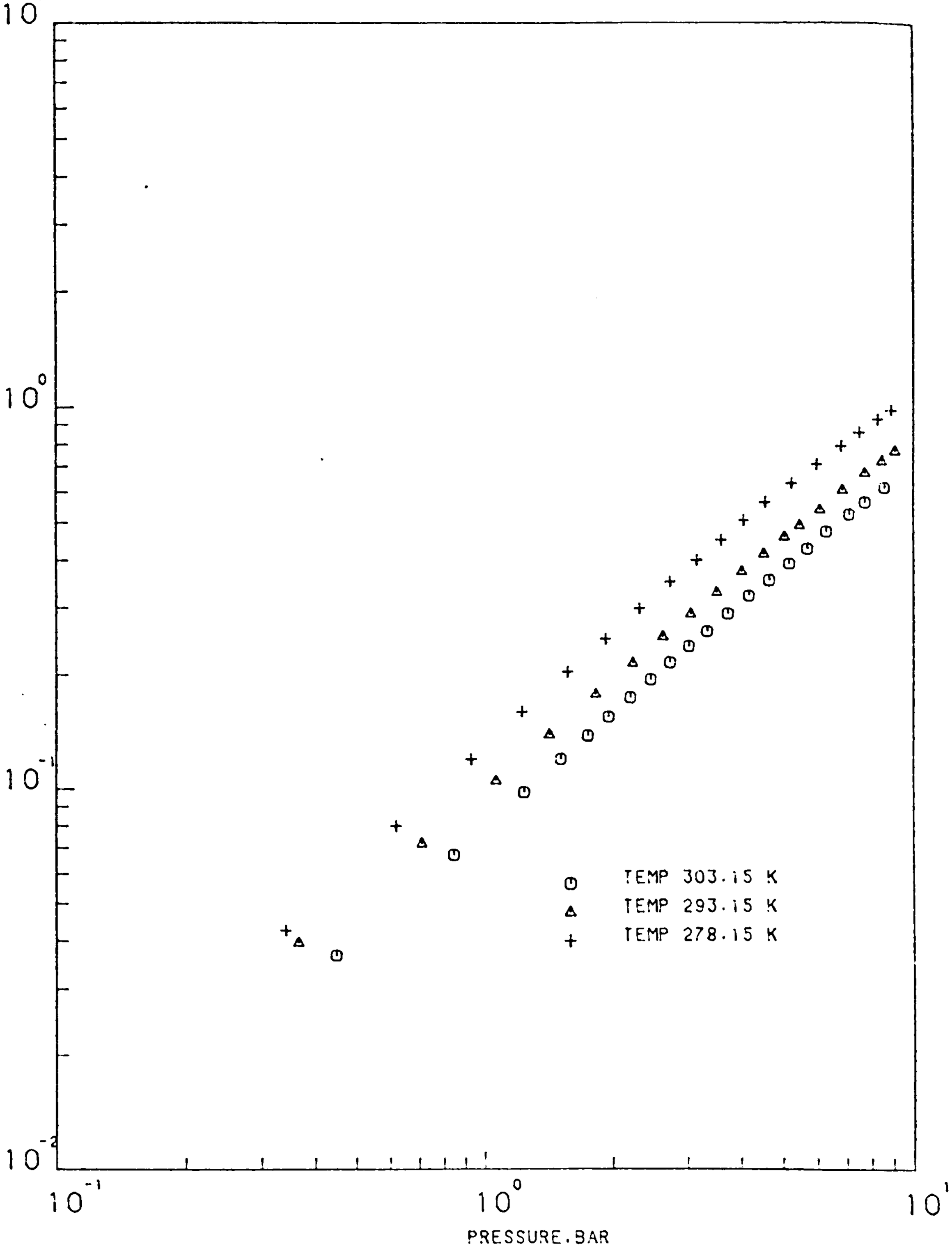

FIGURE (3.4) ADSORPTION ISOTHERMS FOR OXYGEN ON LAPORTE 13X MOLECULAR SIEVE PELLETS AT 278.15, 293.15 AND 303.15 K

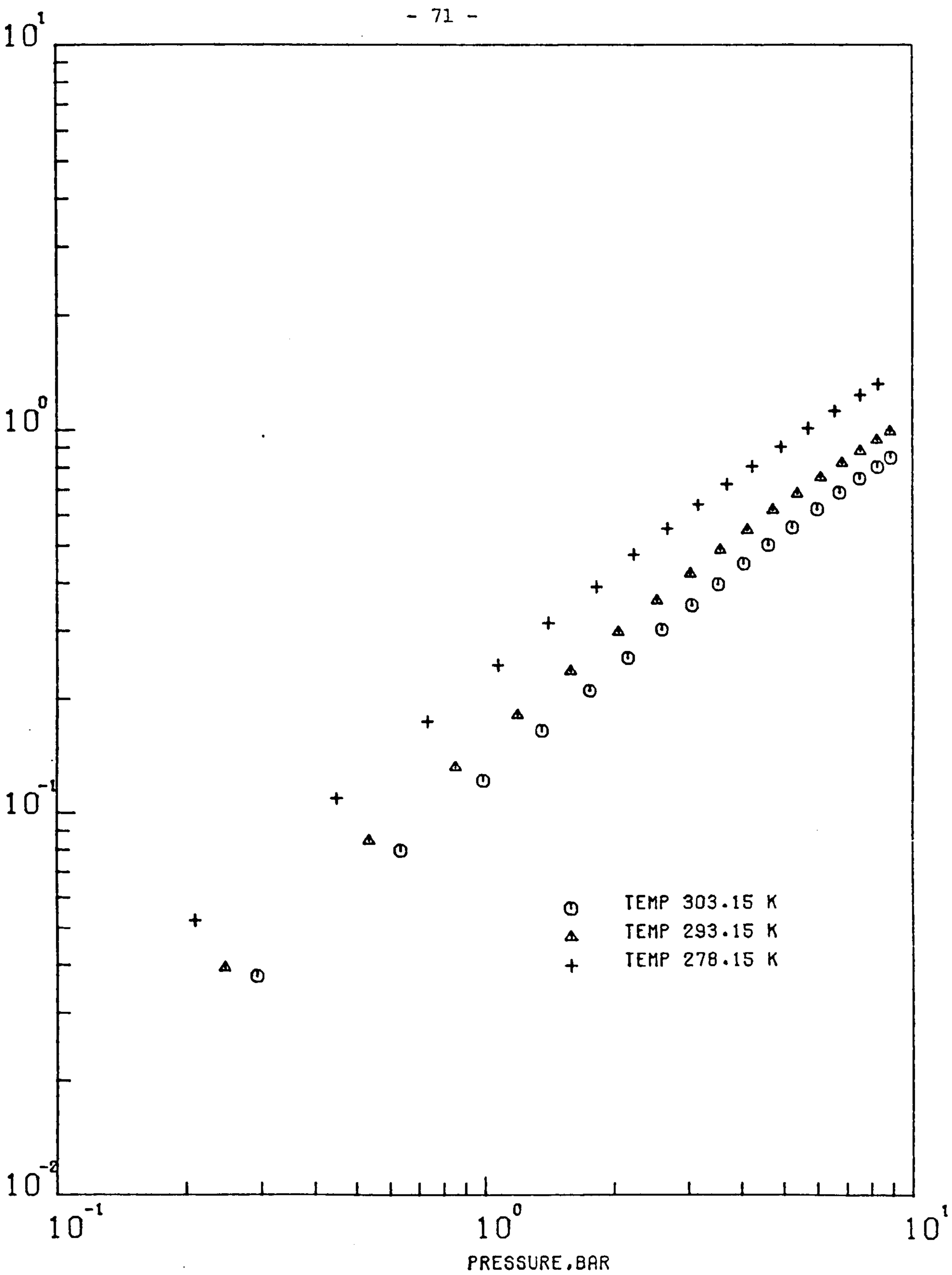

FIGURE (3·5) ADSORPTION ISOTHERMS FOR OXYGEN ON EKA 5A MOLECULAR SIEVE PELLETS AT 303.15 , 293.15 AND 278.15 K

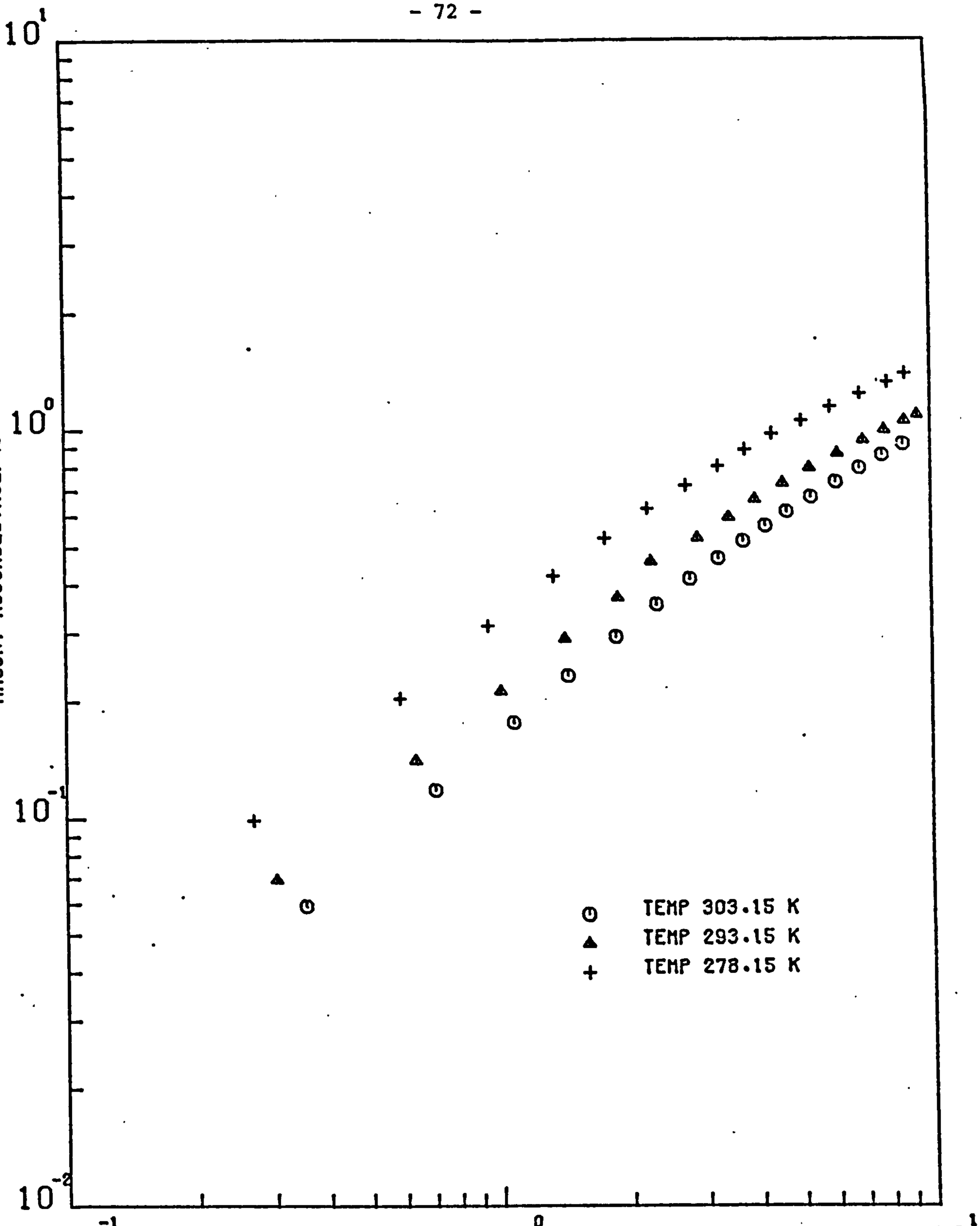

FIGURE (3·6) ADSORPTION ISOTHERMS FOR OXYGEN ON NA-MORDENITE MOLECULAR SIEVE PELLETS AT 303.15 . 293.15 AND 278.15 K

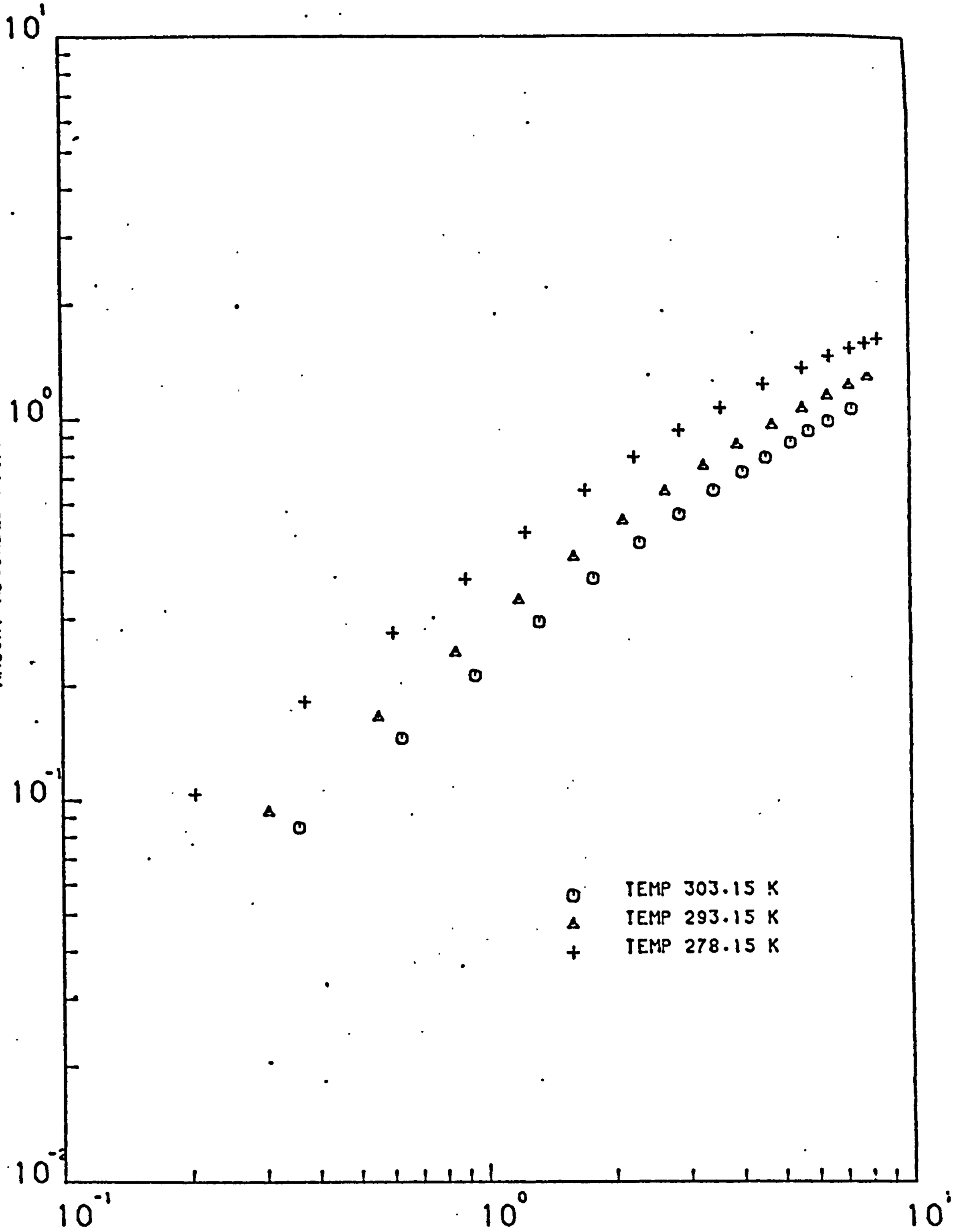

FIGURE (3·7) ADSORPTION ISOTHERMS FOR NITROGEN ON LAPORTE 4A MOLECULAR SIEVE PELLETS AT 278.15.293.15 AND 303.15 K

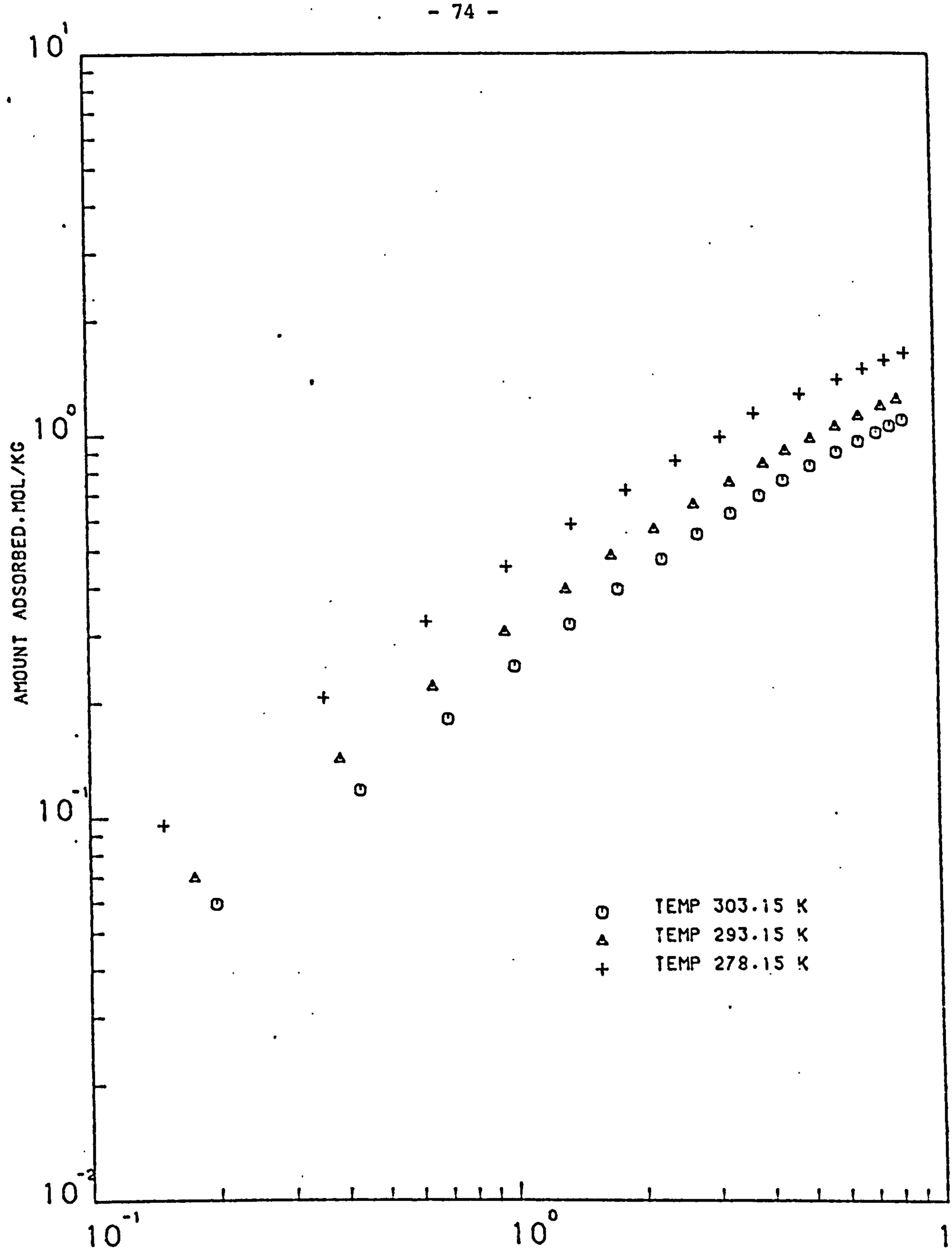

FIGURE (3·8) ADSORPTION ISOTHERMS FOR NITROGEN ON LAPORTE 5A MOLECULAR SIEVE PELLETS AT 303.15 . 293.15 AND 278.15 K

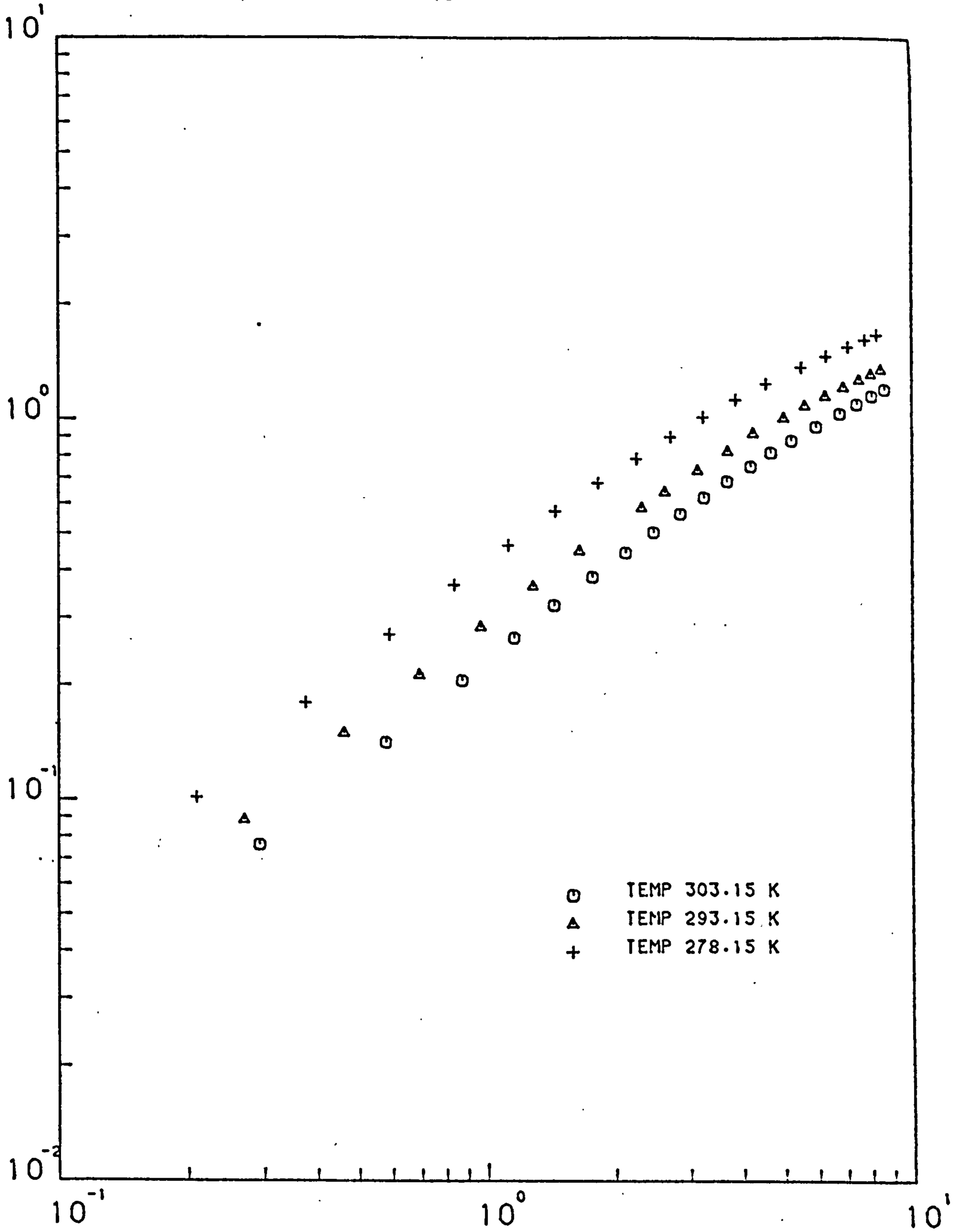

FIGURE (3·9) ADSORPTION ISOTHERMS FOR NITROGEN ON LAPORTE 13X MOLECULAR SIEVE PELLETS AT 278.15, 293.15 AND 303.15 K

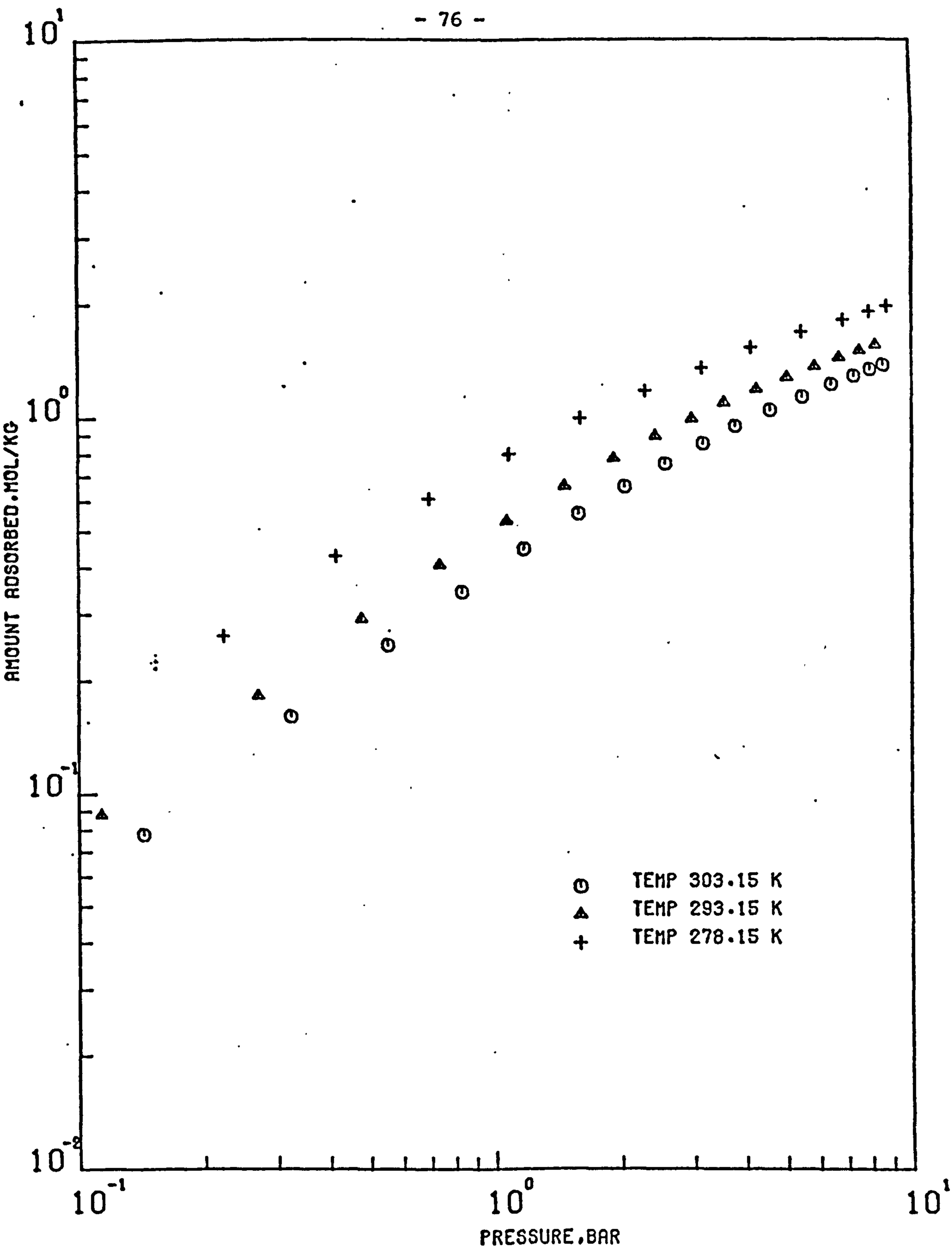

FIGURE (3·10) ADSORPTION ISOTHERMS FOR NITROGEN ON EKA 5A MOLECULAR SIEVE PELLETS AT 303.15 , 293.15 AND 278.15 K

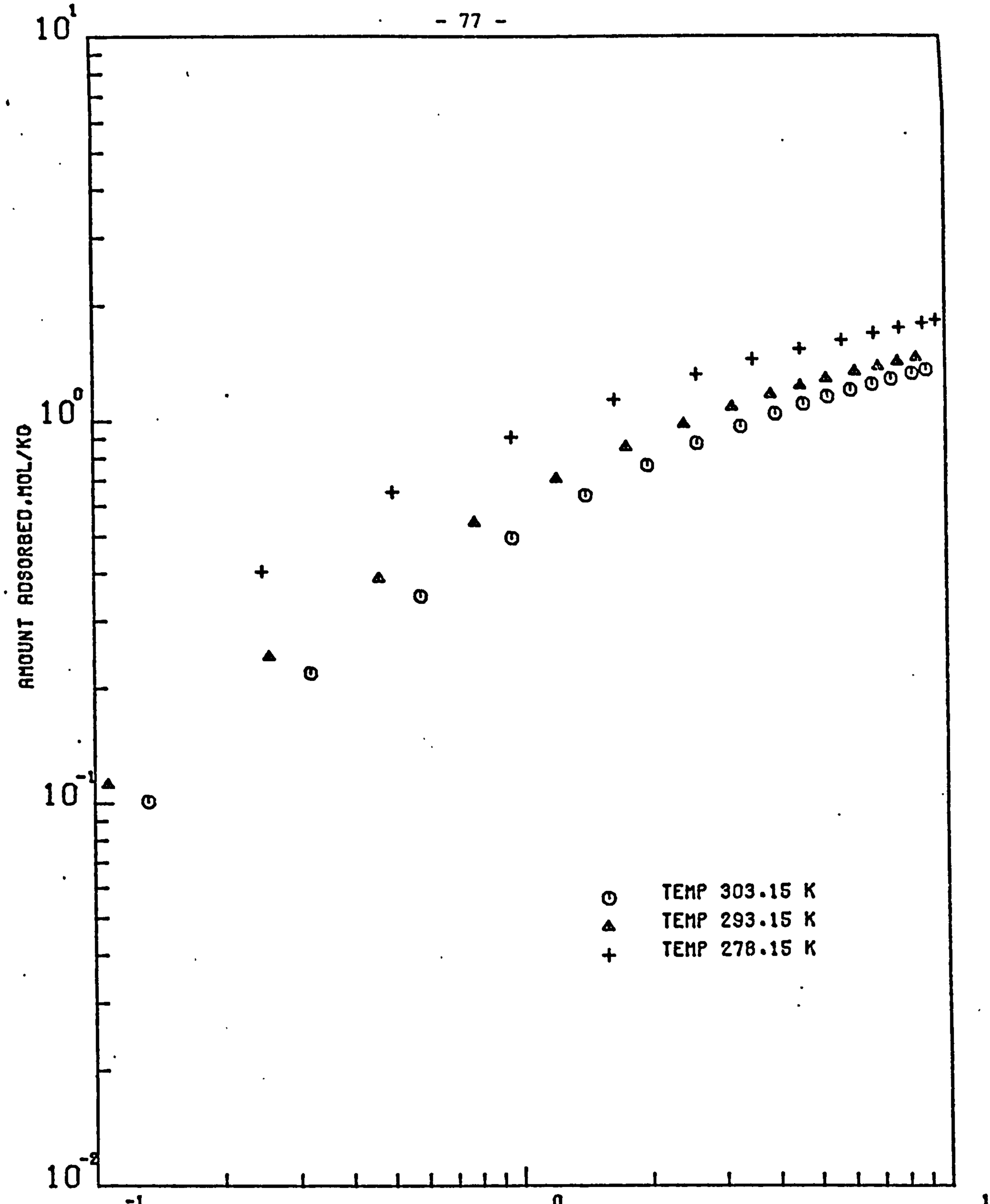

FIGURE (3·11) ADSORPTION ISOTHERMS FOR NITROGEN ON NA-MORDENITE MOLECULAR SIEVE PELLETS AT 303.15 , 293.15 AND 278.15 K

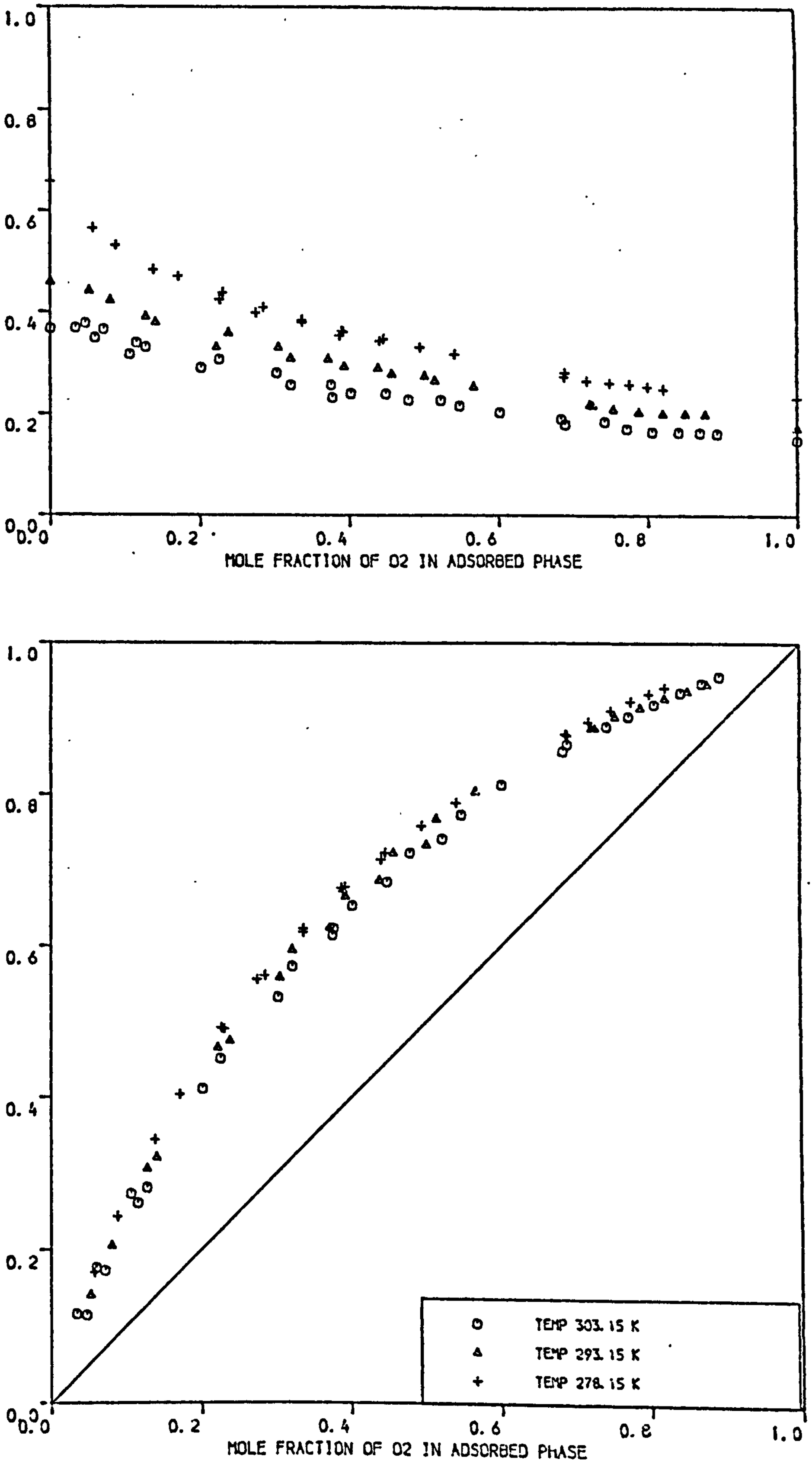

FIGURE 3.12 BINARY ADSORPTION EQUILIBRIA DATA OF O2/N2 ON LAPORTE 4A MOLECULAR SIEVE PELLETS AT 303.15 , 293.15 AND 278.15 K
(PRESSURE ≈ 1.7 BAR)

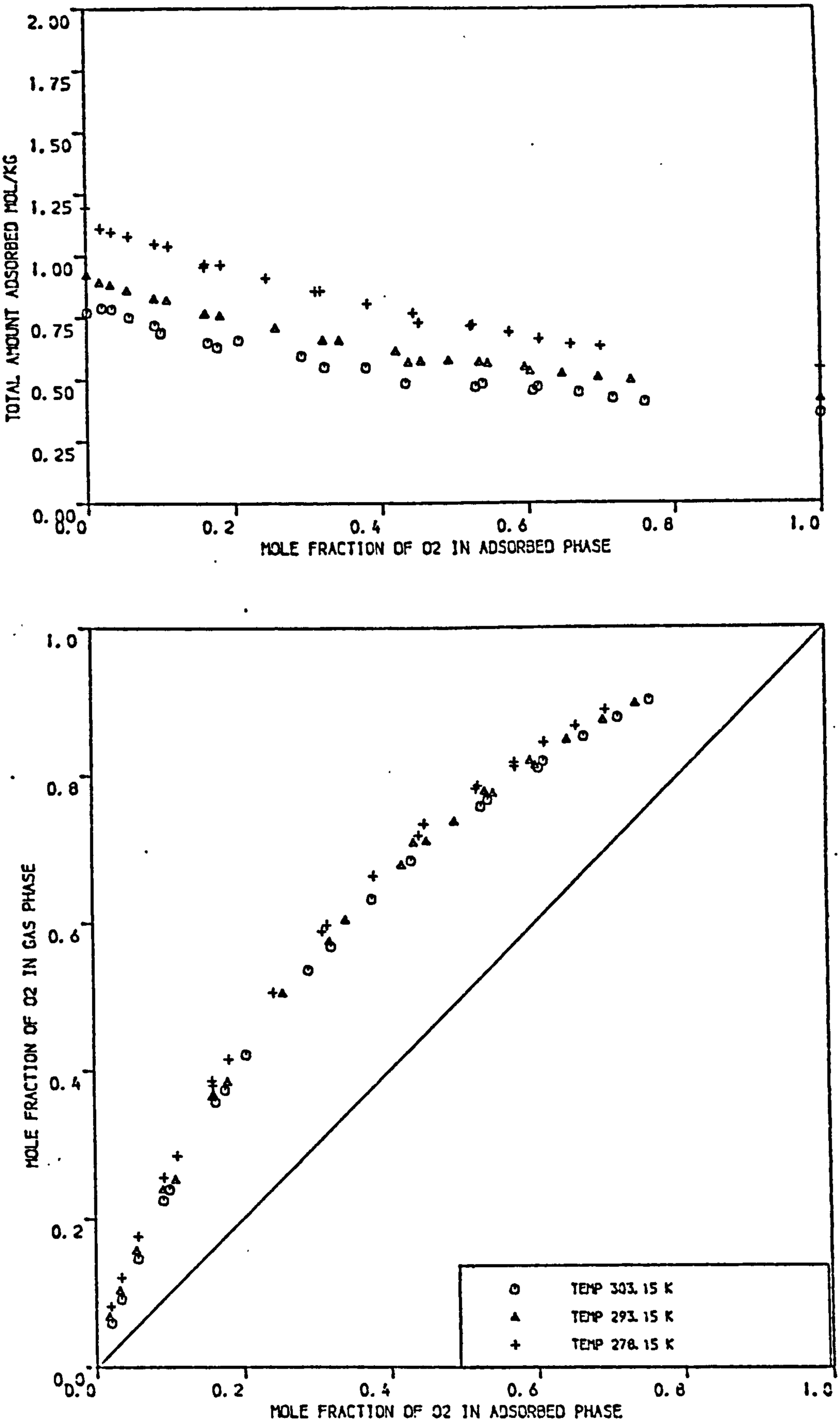

FIGURE 3.13 BINARY ADSORPTION EQUILIBRIA DATA OF O2/N2 ON LAPORTE 4A MOLECULAR SIEVE PELLETS AT 303.15 , 293.15 AND 278.15 K
(PRESSURE ≈ 4.4 BAR)

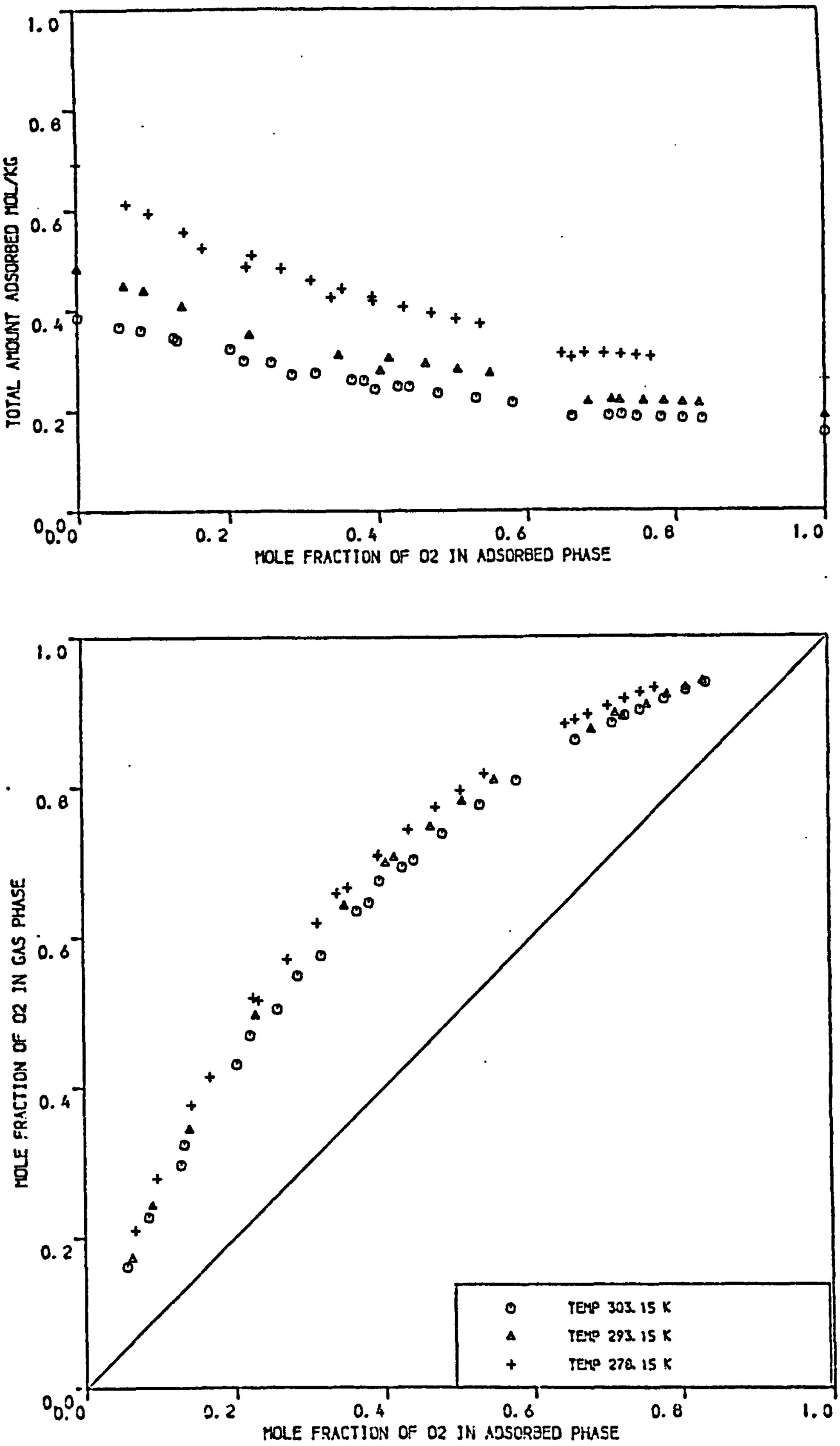

FIGURE 3.14 BINARY ADSORPTION EQUILIBRIA DATA OF O2/N2 ON LAPORTE 5A MOLECULAR SIEVE PELLETS AT 303.15 , 293.15 AND 278.15 K (PRESSURE = 1.7 BAR)

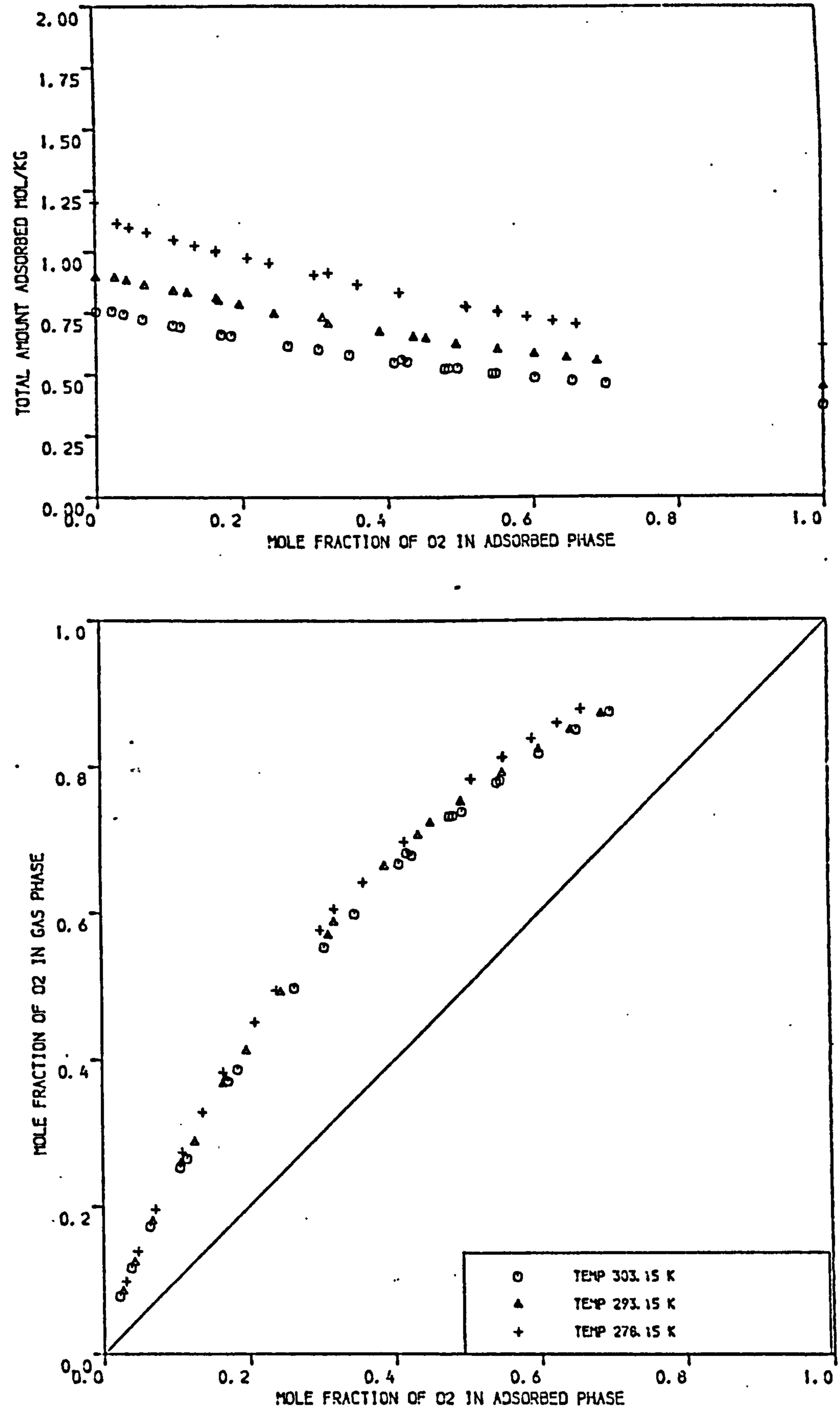

FIGURE 3.15 BINARY ADSORPTION EQUILIBRIA DATA OF O2/N2 ON LAPORTE 5A MOLECULAR SIEVE PELLETS AT 303.15 , 293.15 AND 278.15 K (PRESSURE = 4.4 BAR)

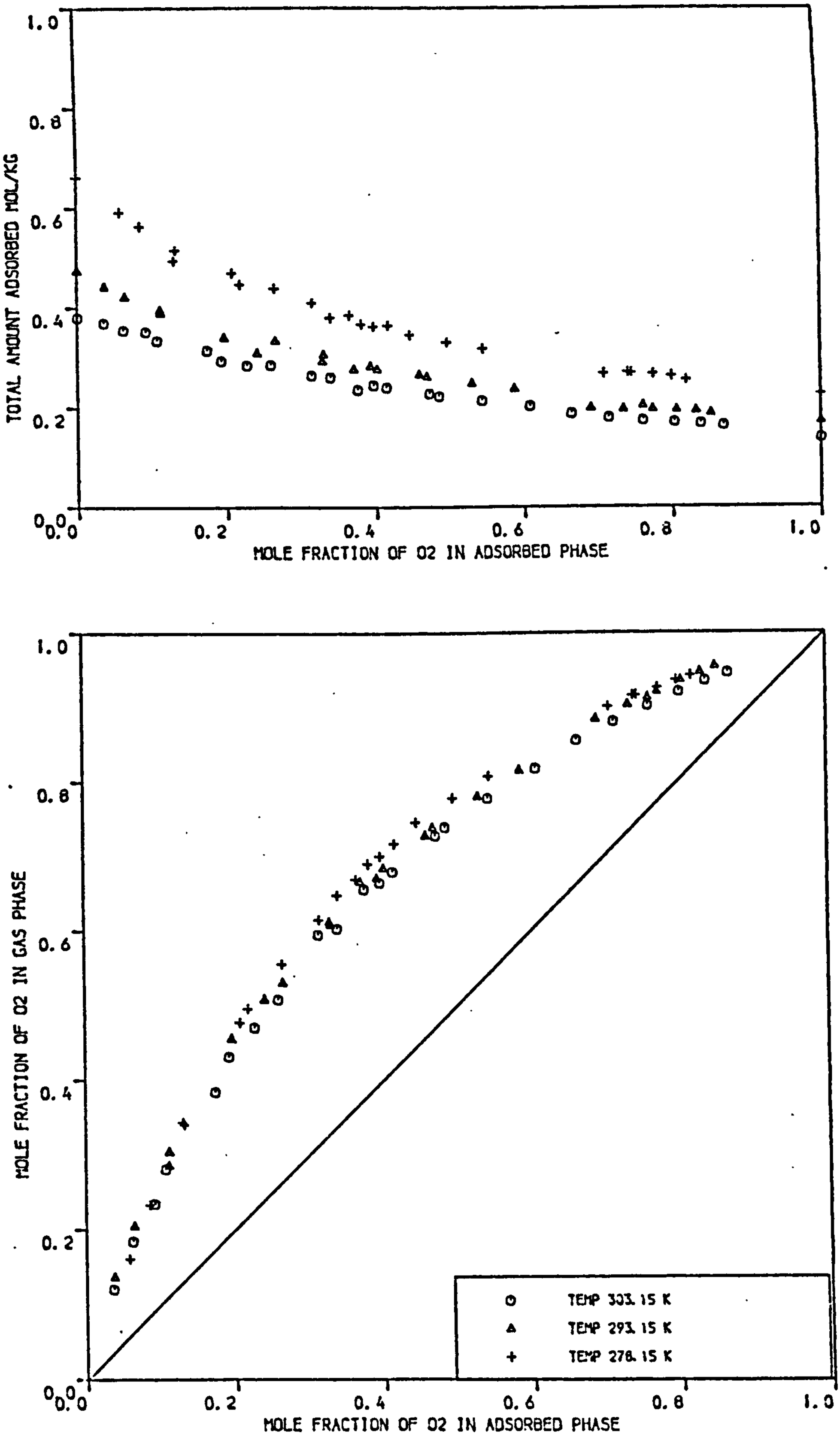

FIGURE 3.16 BINARY ADSORPTION EQUILIBRIA DATA OF O2/N2 ON LAPORTE 13X MOLECULAR SIEVE PELLETS AT 303.15 ,293.15 AND 278.15 K
(PRESSURE = 1.7 BAR)

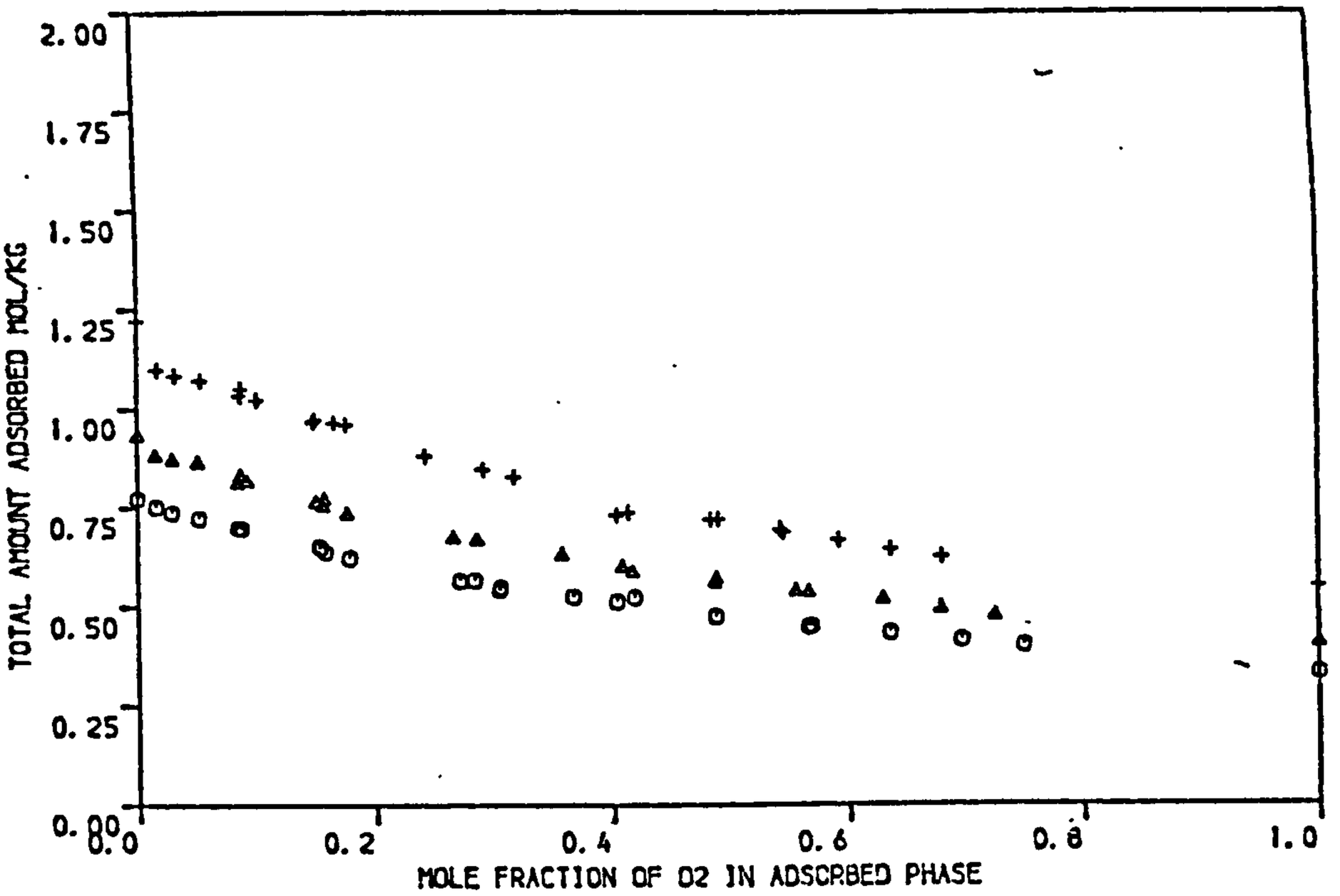

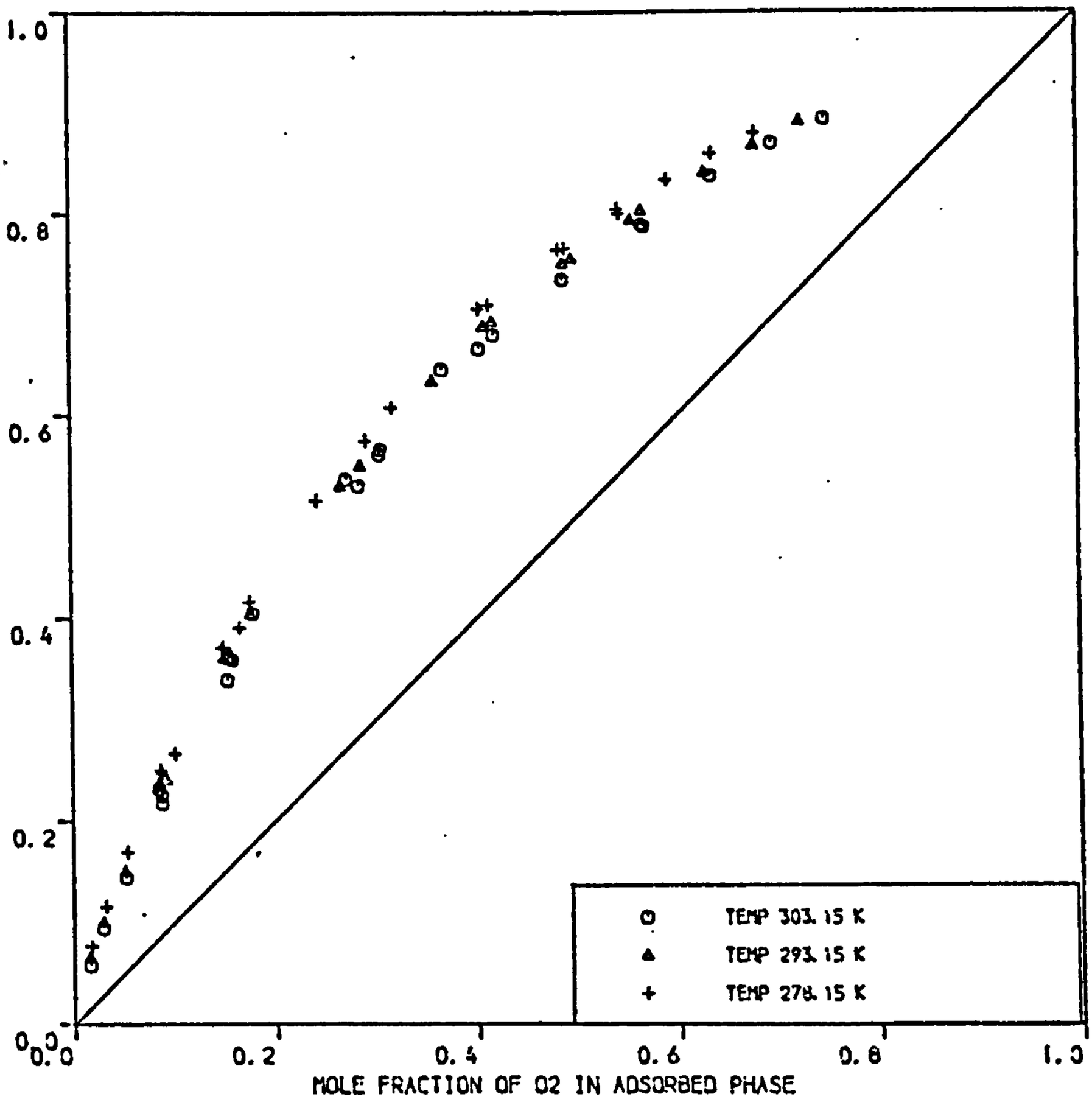

FIGURE 3.17 BINARY ADSORPTION EQUILIBRIA DATA OF O2/N2 ON LAPORTE 13X MOLECULAR SIEVE PELLETS AT 303.15 , 293.15 AND 278.15 K (PRESSURE = 4.4 BAR)

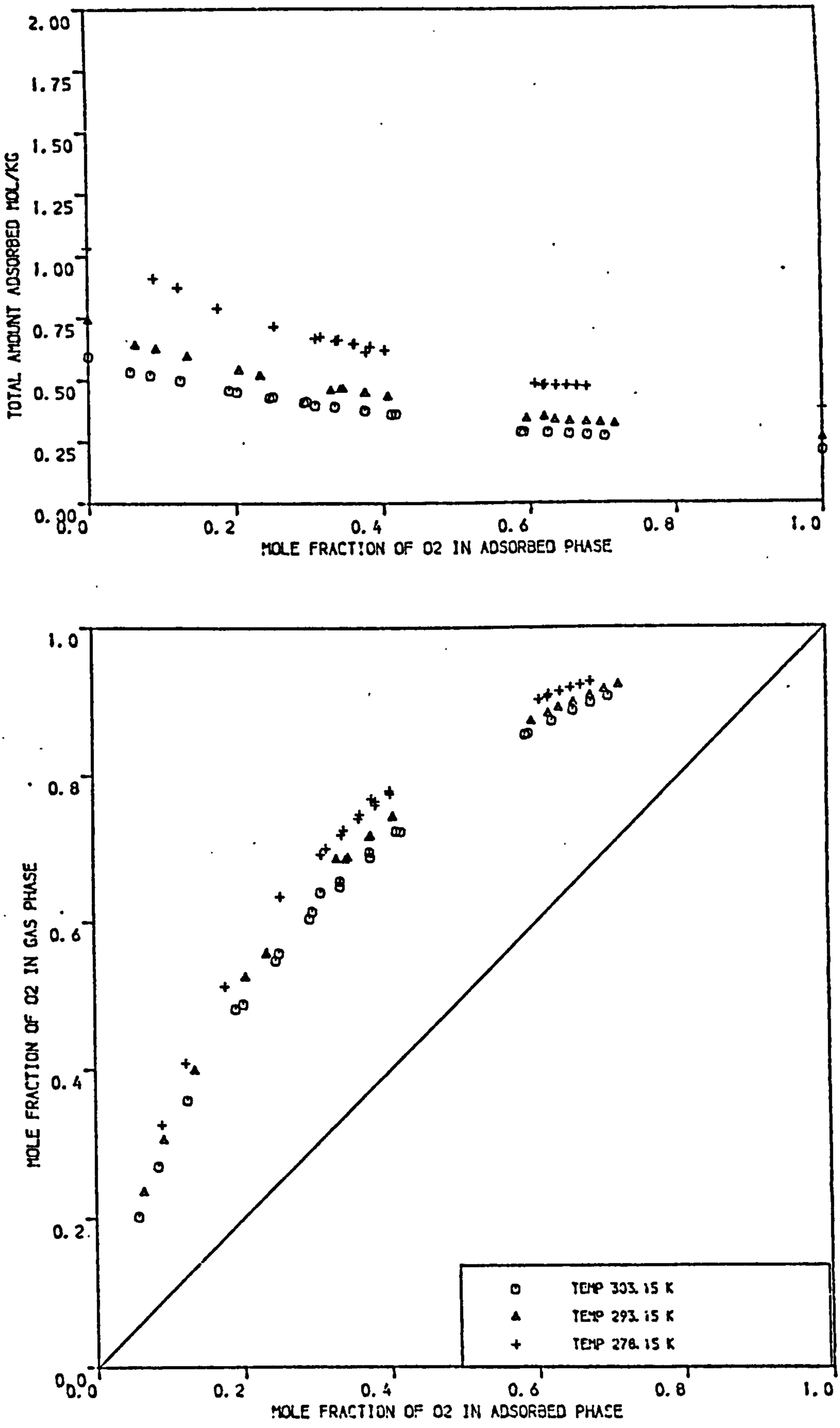

FIGURE 3.19 BINARY ADSORPTION EQUILIBRIA DATA OF O2/N2 ON EKA 5A MOLECULAR SIEVE PELLETS AT 303.15 , 293.15 AND 278.15 K (PRESSURE = 1.7 BAR)

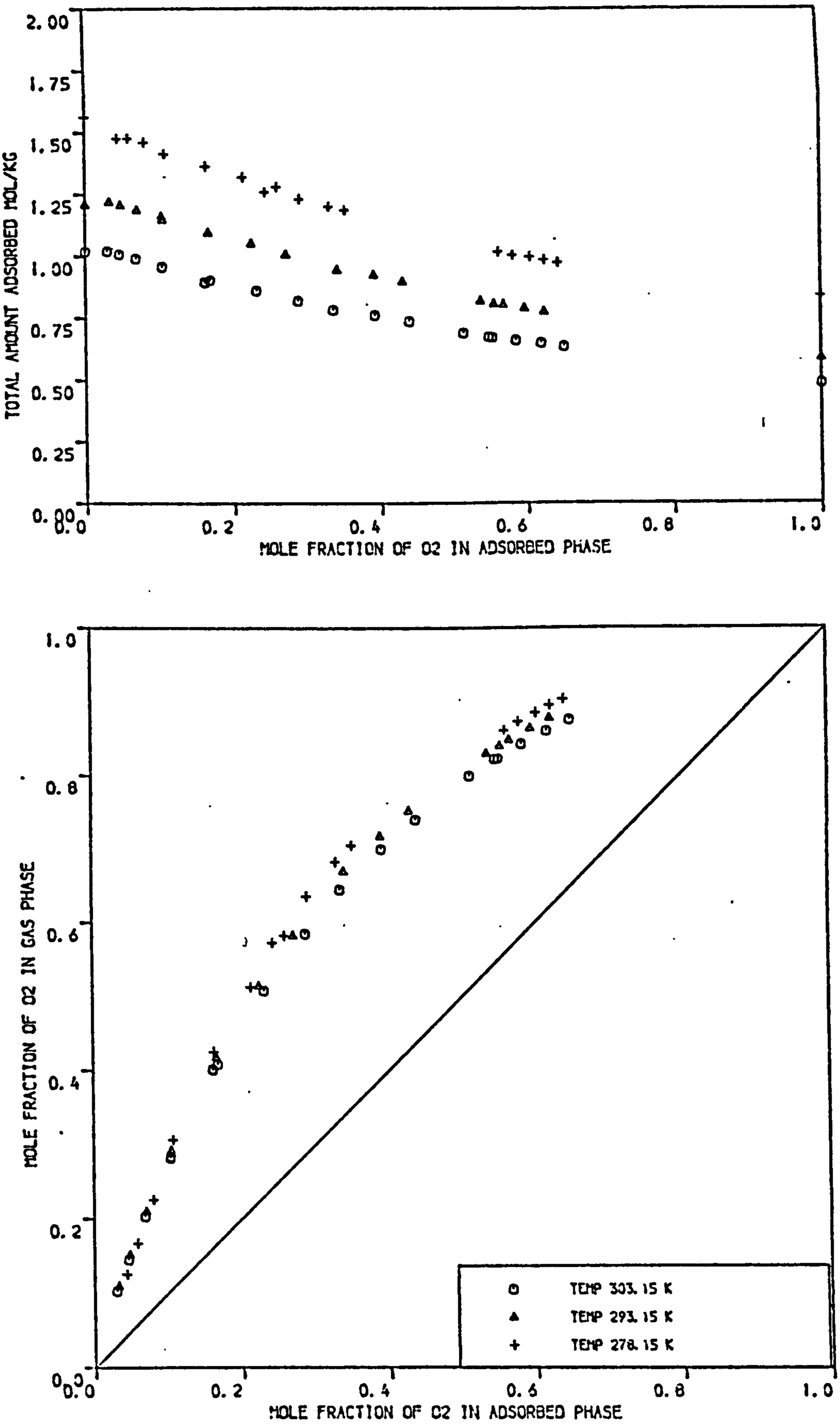

FIGURE 3.19 BINARY ADSORPTION EQUILIBRIA DATA OF O2/N2 ON EKA 5A MOLECULAR SIEVE PELLETS AT 303.15 , 293.15 AND 278.15 K (PRESSURE = 4.4 BAR)

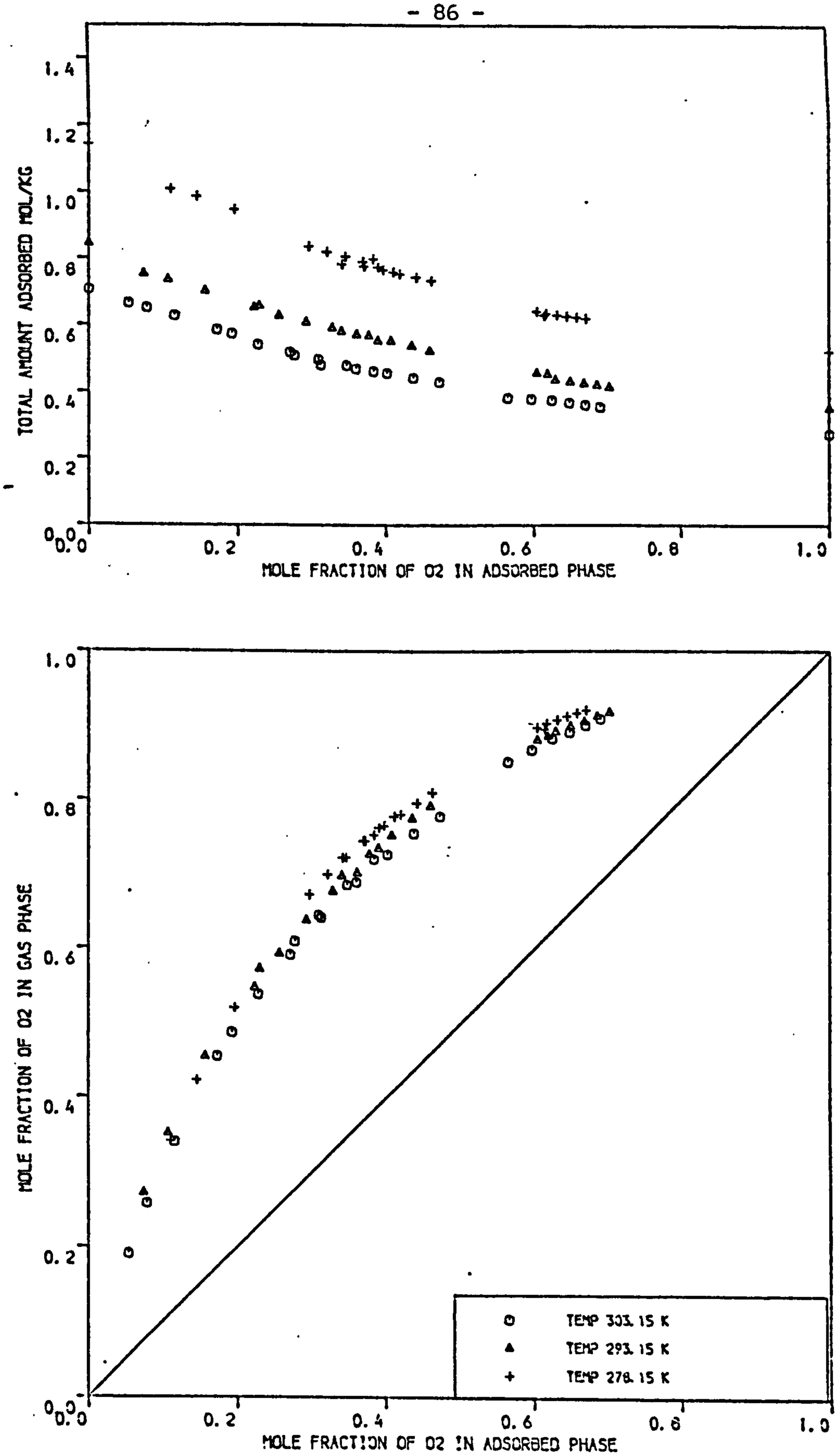

FIGURE 3.20 BINARY ADSORPTION EQUILIBRIA DATA OF O2/N2 ON NA-MORDENITE MOLECULAR SIEVE PELLETS AT 303.15 , 293.15 AND 278.15 K
(PRESSURE = 1.7 BAR)

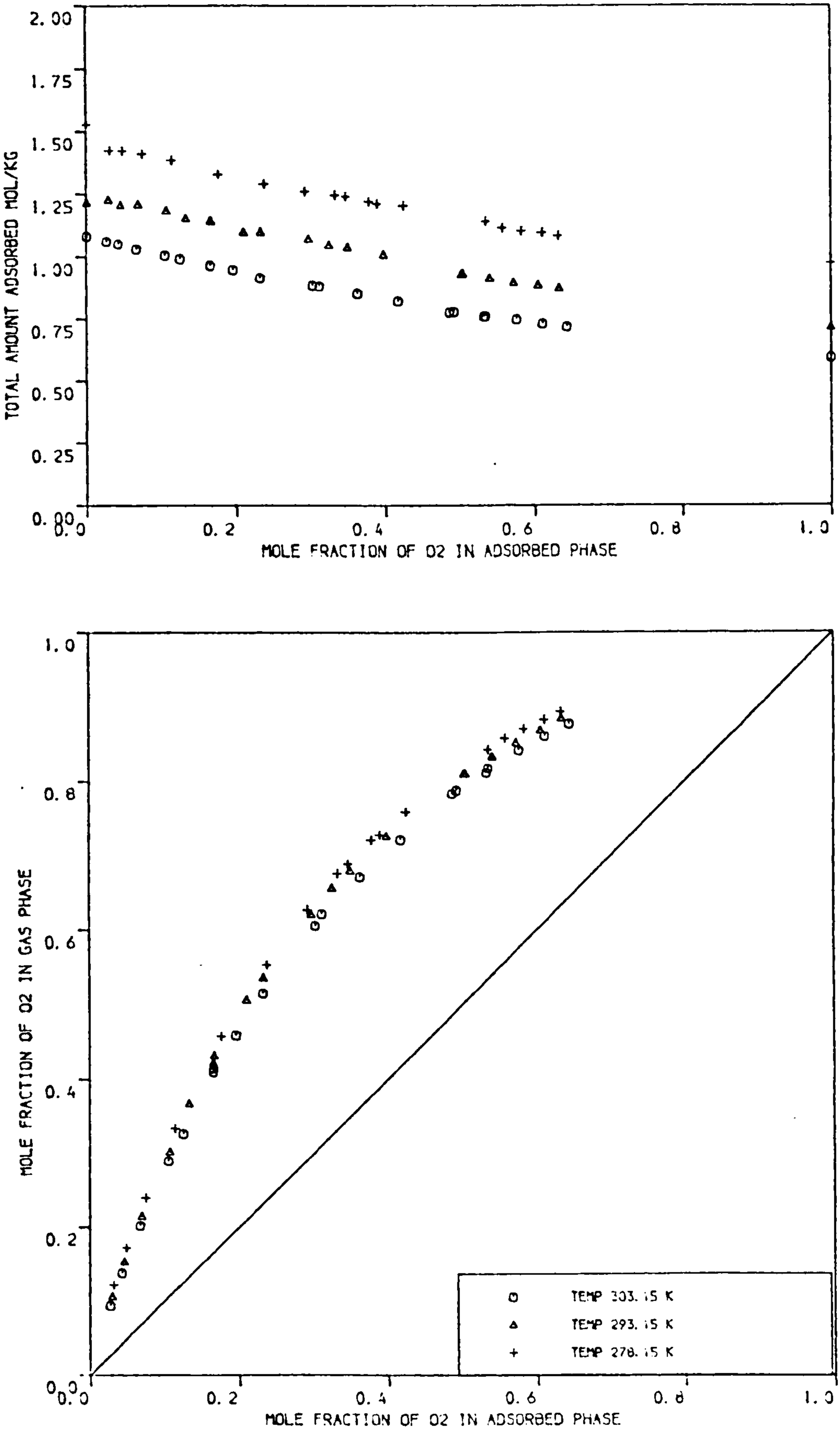

FIGURE 3.21 BINARY ADSORPTION EQUILIBRIA DATA OF O2/N2 ON

CHAPTER 4

ANALYSIS AND INTERPRETATION OF EXPERIMENTAL DATA

CHAPTER 4

ANALYSIS AND INTERPRETATION OF EXPERIMENTAL DATA

In this chapter the experimental data reported in the previous chapter are compared with theoretical models described in Chapter 2. The work conveniently falls into two areas, namely pure component adsorption and binary gas mixture adsorption.

4.1 Pure Gas Adsorption

In this section an analysis and interpretation of the pure component isotherms are made. A comparison of the basic isotherms on the five adsorbents studied is made. The experimental isotherms are correlated with theoretical models. The values of Henry's law constants obtained from the theoretical models are compared. The isosteric heats of adsorption are calculated.

4.1.1 Comparison between adsorbents and adsorbates

The isotherms reported in the previous chapter are all of type I according to BET classification[81].

The oxygen isotherms on Laportes 4A, 5A and 13X, EKA 5A and Na-Mordenite are replotted in Figures 4.1 - 4.3, showing the comparison between adsorbents:

(a) Figure 4.1 shows that at a temperature of 278.15 K

and for pressures up to 1 bar

Adsorption of oxygen on Na-Mordenite > Adsorption of oxygen on EKA 5A > Adsorption of oxygen on Laporte 5A

Adsorption of oxygen on Laporte 5A > Adsorption of oxygen on Laporte 4A > Adsorption of oxygen on Laporte 13X

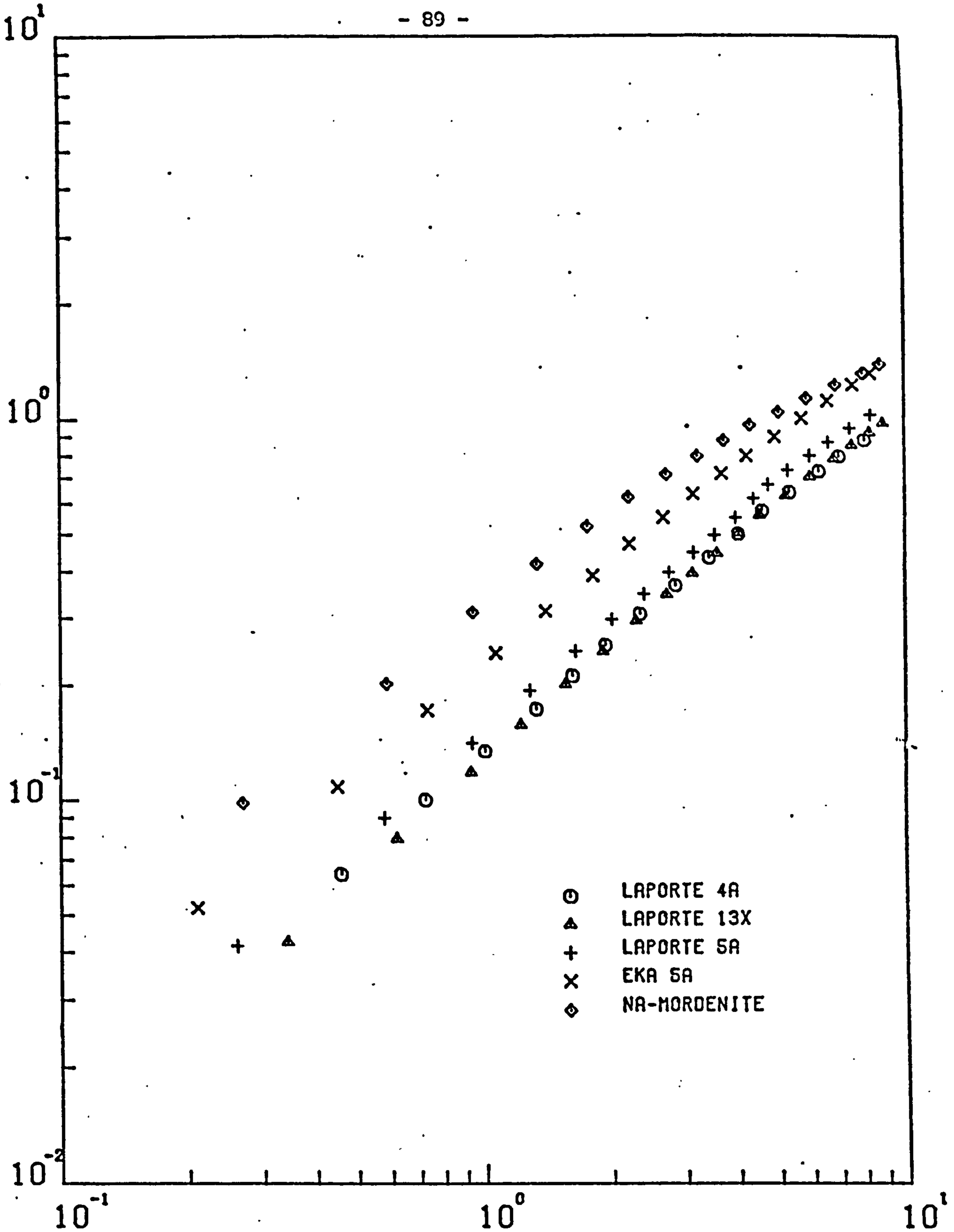

FIGURE (4·1) ADSORPTION ISOTHERMS FOR OXYGEN ON LAPORTE 4A . LAPORTE 13X . LAPORTE 5A . EKA 5A AND NA-MORDENITE MOLECULAR SIEVE PELLETS AT 278.15 K

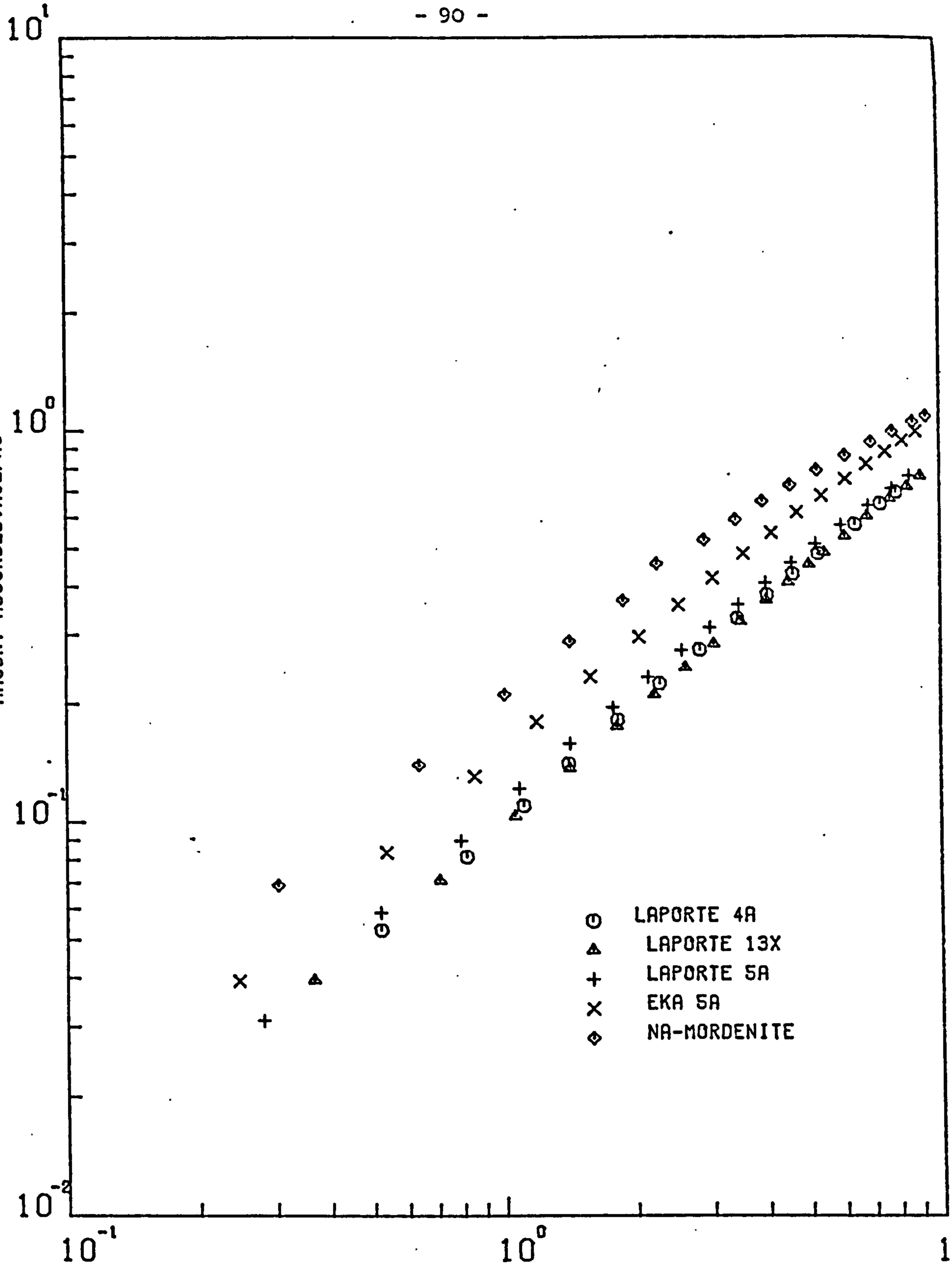

FIGURE (4·2) ADSORPTION ISOTHERMS FOR OXYGEN ON LAPORTE 4A , LAPORTE 13X , LAPORTE 5A , EKA 5A AND NA-MORDENITE MOLECULAR SIEVE PELLETS AT 293.15 K

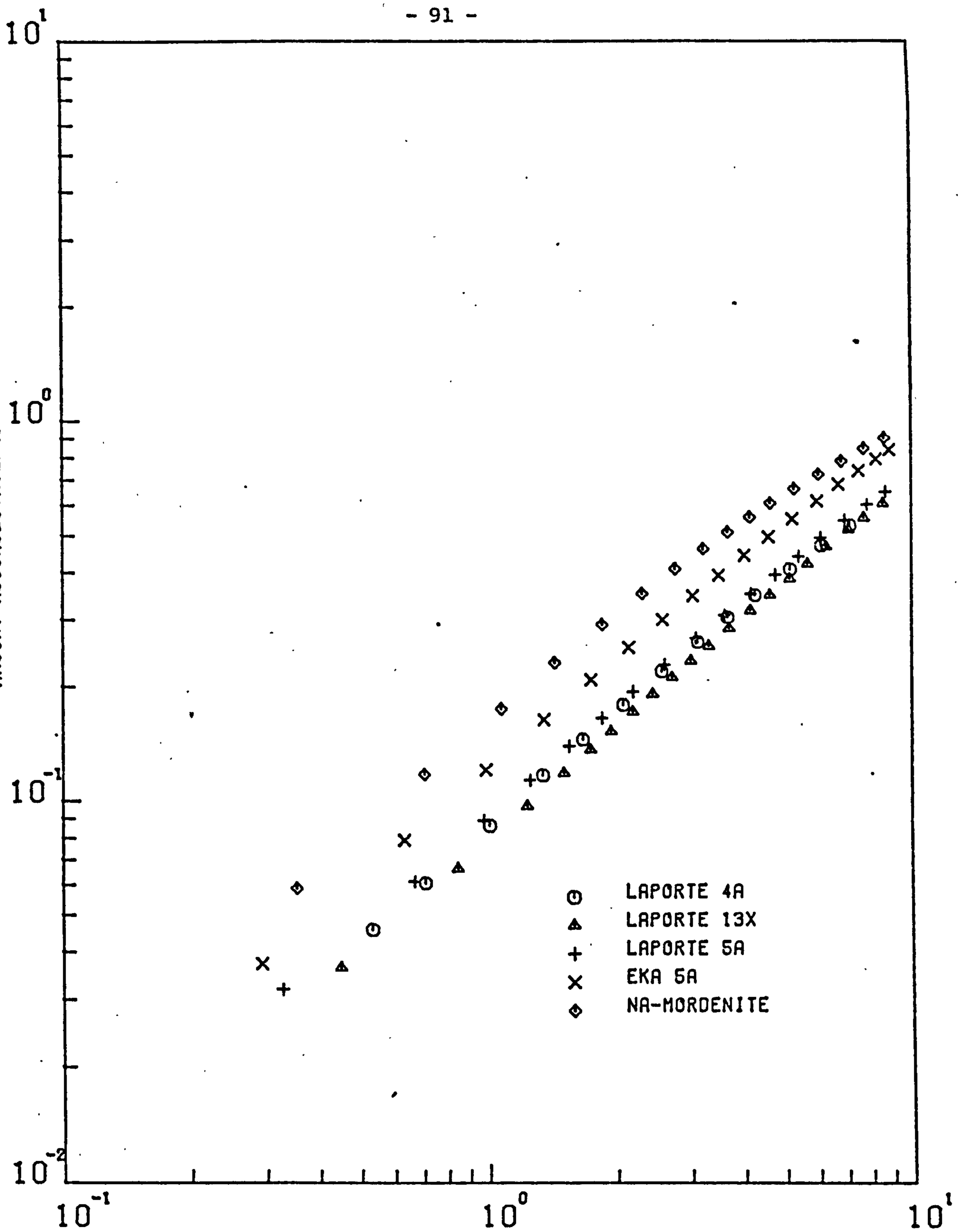

FIGURE (4·3) ADSORPTION ISOTHERMS FOR OXYGEN ON LAPORTE 4A . LAPORTE 13X . LAPORTE 5A . EKA 5A AND NA-MORDENITE MOLECULAR SIEVE PELLETS AT 303.15 K

Between pressures of 1 bar and 10 bar there is less difference between Na-Mordenite and EKA 5A and at pressures approaching 10 bar the adsorption capacity for both adsorbents are approximately the same. The adsorption of oxygen on Laporte 4A is approximately the same as that on Laporte 13X for pressures greater than 1 bar.

(b) Figure 4.2 shows that at a temperature of 293.15 K and for pressures up to 1 bar

Adsorption of oxygen on Na-Mordenite > Adsorption of oxygen on EKA 5A > Adsorption of oxygen on Laporte 5A

Adsorption of oxygen on Laporte 5A > Adsorption of oxygen on Laporte 4A $\underline{\Omega}$ Adsorption of oxygen on Laporte 13X

Between pressures of 1 bar and 10 bar there is again less difference between Na-Mordenite and EKA 5A. The adsorption of oxygen on Laporte 5A approaches the same value for both Laportes 4A and 13X for pressures greater than 1 bar.

(c) Figure 4.3 shows that at a temperature of 303.15 K and for pressures up to 10 bar

Adsorption of oxygen on Na-Mordenite > Adsorption of oxygen on EKA 5A > Adsorption of oxygen on Laporte 5A

Adsorption of oxygen on Laporte 5A $\underline{\Omega}$ Adsorption of oxygen on Laporte 4A > Adsorption of oxygen on Laporte 13X

For pressures greater than 5 bar the adsorption of oxygen on Laportes adsorbents are approximately the same.

From Figures 4.4 - 4.6 for the nitrogen isotherms on the five adsorbents studied the following can be deduced.

At the three temperatures studied and for pressure up to 1 bar

Adsorption of nitrogen on NA-Mordenite > Adsorption of nitrogen on EKA 5A > Adsorption of nitrogen on Laporte 5A

Adsorption of nitrogen on Laporte 5A > Adsorption of nitrogen on Laporte 4A $\underline{\Omega}$ Adsorption of nitrogen on Laporte 13X

Between 1 bar and 10 bar there is less difference between mordenite and EKA 5A and at pressures approaching 10 bar EKA 5A adsorbs more than the mordenite. The adsorption of nitrogen on Laporte 5A approaches that on Laportes 4A and 13X for pressures greater than 1 bar. For adsorption temperatures 293.15 and 303.15 K the adsorption of nitrogen on Laporte 5A tend to be lower than that on Laportes 4A and 13X for pressures greater than 5 bar.

From the above it is clear that the two samples of zeolite type 5A from different manufacturers, Laporte (U.K.) and EKA (Sweden), have significantly different affinities for both gases. Possible explanations that can be offered are different thermal treatment during processing of the zeolite and the type and proportion of binder used. These factors affect both the equilibrium and kinetic properties of zeolite samples[104].

For all the adsorbent samples studied in this work, nitrogen was more strongly adsorbed than oxygen. Table 4.1 shows the ratios of nitrogen to oxygen adsorbed on the five adsorbents at the temperatures and pressures of the gas mixture adsorption studied in this work. For both Na-Mordenite and EKA 5A the ratio decreases with a decrease of temperature and an increase of pressure, whereas for Laportes adsorbents the ratio decreases with an increase of temperature at a pressure of 1.7 bar, and is nearly constant at pressure of 4.4 bar for the three temperatures. These data

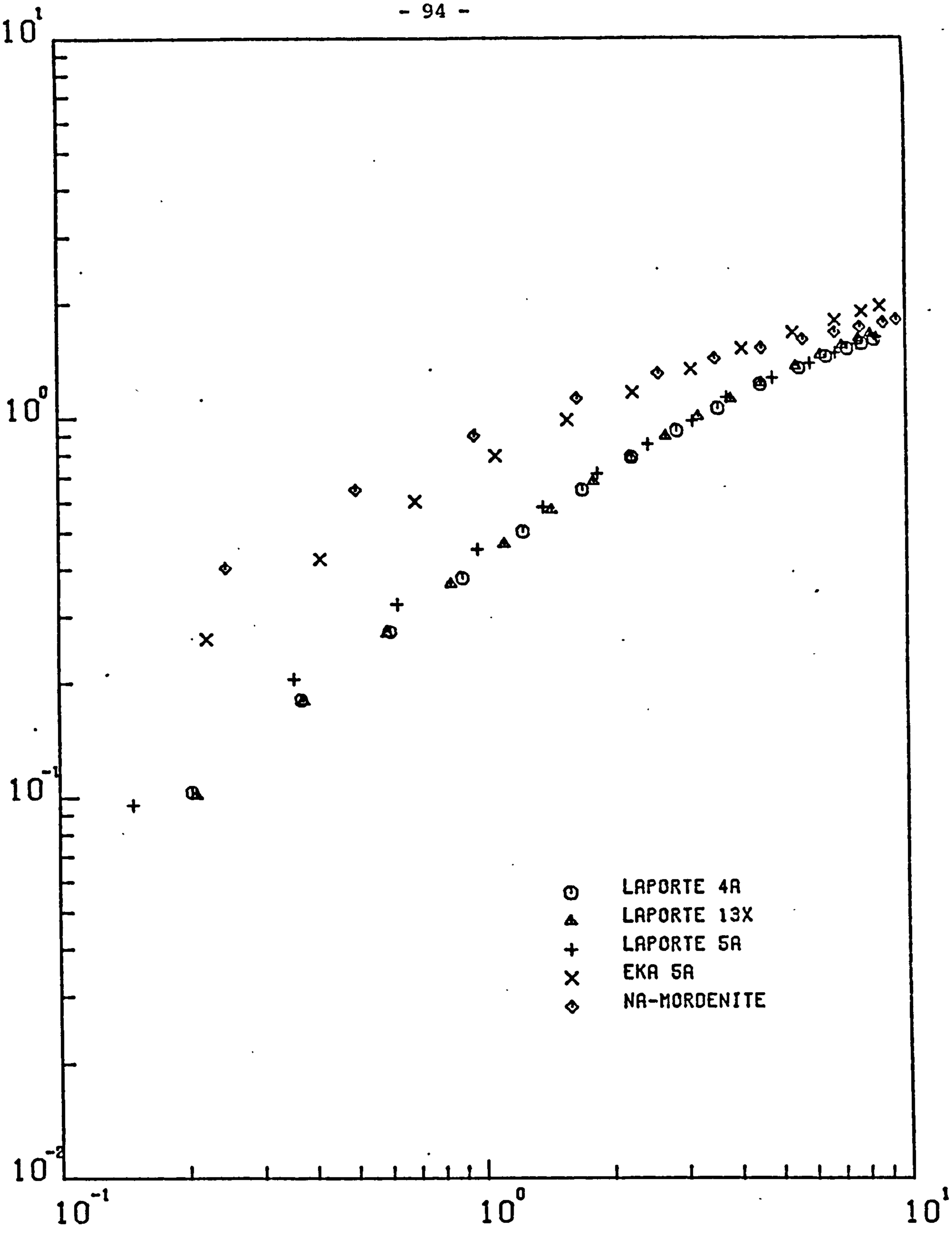

FIGURE (4.4) ADSORPTION ISOTHERMS FOR NITROGEN ON LAPORTE 4A , LAPORTE 13X ,LAPORTE 5A , EKA 5A AND NA-MORDENITE MOLECULAR SIEVE PELLETS AT 278.15 K

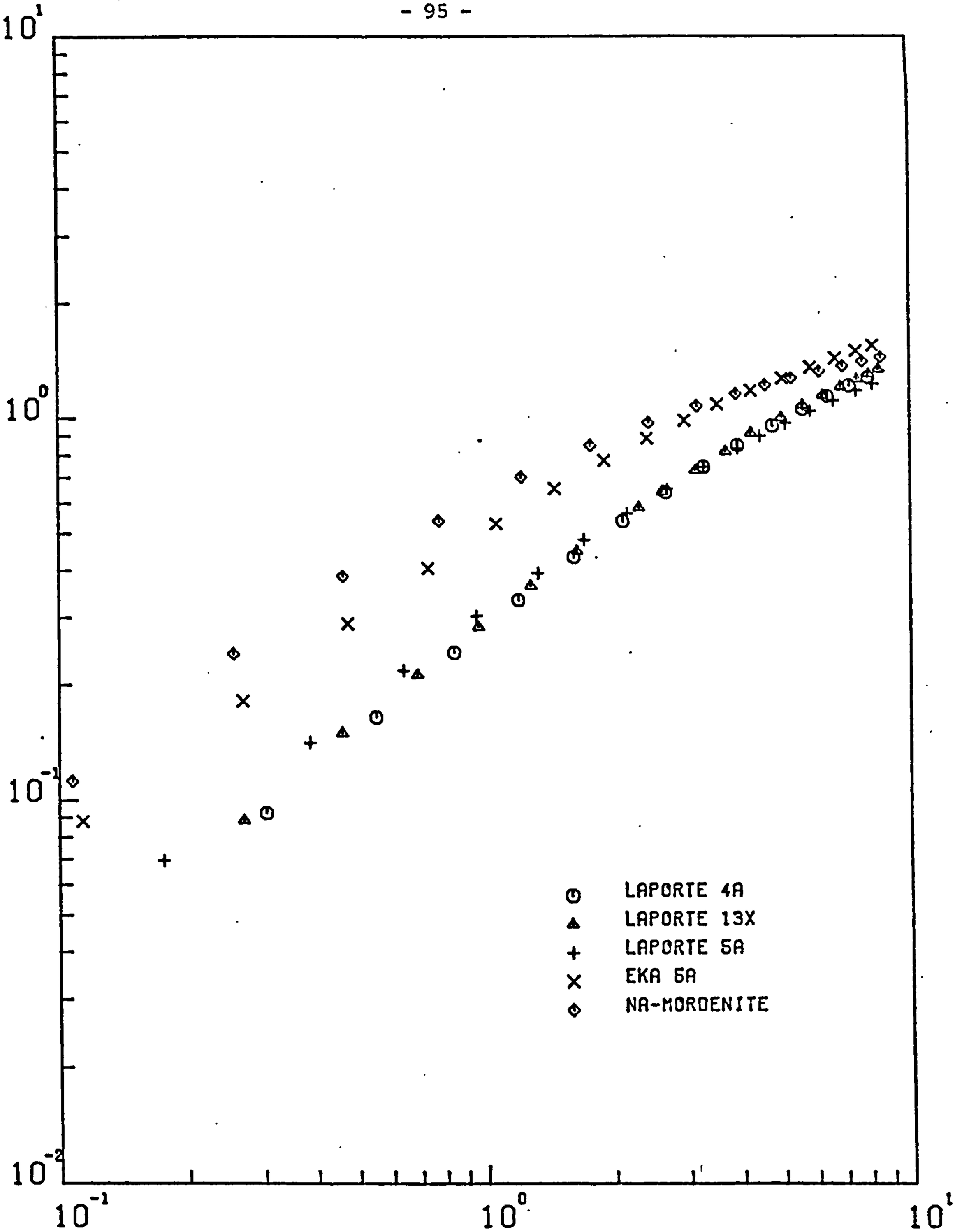

FIGURE (4·5) ADSORPTION ISOTHERMS FOR NITROGEN ON LAPORTE 4A , LAPORTE 13X , LAPORTE 5A , EKA 5A AND NA-MORDENITE MOLECULAR SIEVE PELLETS AT 293.15 K

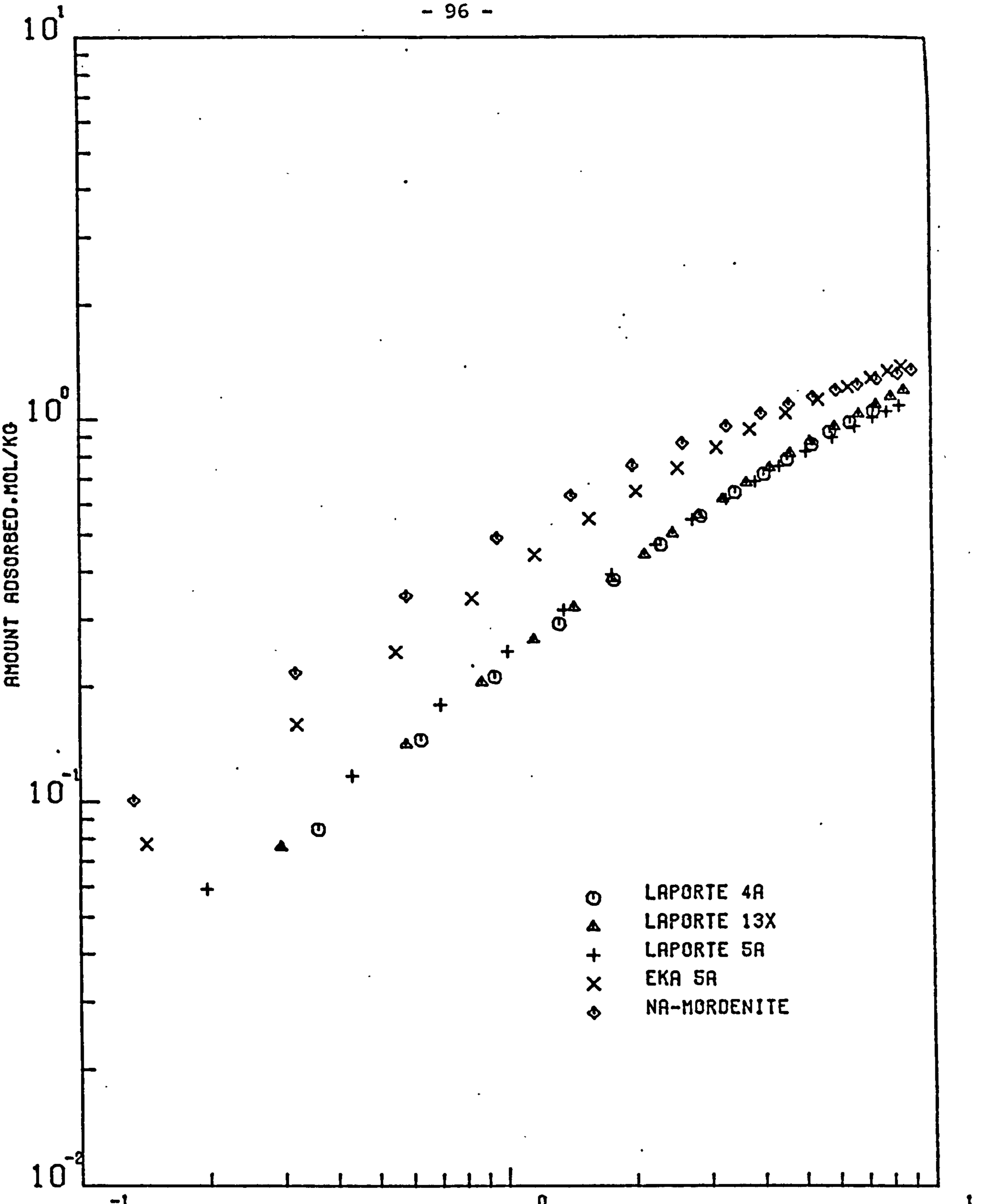

FIGURE (4·6) ADSORPTION ISOTHERMS FOR NITROGEN ON LAPORTE 4A , LAPORTE 13X , LAPORTE 5A , EKA 5A AND NA-MORDENITE MOLECULAR SIEVE PELLETS AT 303.15 K

TABLE 4.1

Affinity Ratio of Nitrogen to Oxygen (pure components)

on Laportes 4A, 5A and 13X, EKA 5A and Na-Mordenite

Molecular Sieve Pellets

Adsorbent	N_2/O_2 mole basis	Temperature K	Pressure bar
Laporte 4A	2.8	278.15	1.76
	2.7	293.15	1.73
	2.5	303.15	1.72
	2.2	278.15	4.41
	2.2	293.15	4.42
	2.1	303.15	4.40
Laporte 5A	2.7	278.15	1.73
	2.6	293.15	1.71
	2.5	303.15	1.71
	2.0	278.15	4.44
	2.0	293.15	4.44
	2.0	303.15	4.44
Laporte 13X	3.0	278.15	1.74
	2.8	293.15	1.74
	2.8	303.15	1.75
	2.2	278.15	4.44
	2.3	293.15	4.41
	2.3	303.15	4.34
EKA 5A	2.7	278.15	1.73
	2.8	293.15	1.76
	2.8	303.15	1.75
	1.9	278.15	4.45
	2.1	293.15	4.45
	2.1	303.15	4.43
Na-Mordenite	2.2	278.15	1.75
	2.4	293.15	1.74
	2.6	303.15	1.73
	1.6	278.15	4.41
	1.7	293.15	4.44
	1.8	303.15	4.45

are for pure components. Separation factors for binary gas mixtures are discussed in Section 4.2.

4.1.2 Analysis and interpretation of results

The purpose of this section is to compare the experimental pure component isotherm data with various theoretical models.

Previous analysis and interpretation of equilibrium data for zeolitic adsorption (see Chapter 2) have indicated the following:

(a) The simple models such as Langmuir and its extensions have limited applicability.

(b) Models based on mobile monolayers such as the Hill de Boer model gave satisfactory correlation of equilibrium data but the basic assumptions from which the model isotherms are derived are generally not fulfilled and it is therefore doubtful whether the parameters have a real significance.

(c) The potential theory depends on the determination of the adsorbed phase volume and this has been interpreted differently by many authors. Generally no accurate correlation of experimental data on molecular sieves has been obtained using this model.

The experimental data of this work has been tested against the following models:

(a) The kinetic model of Holland and Gonzalez[31,75], (hereafter referred to as the kinetic model) as this gives a measure of the applicability of the ideal localised models. This model is represented by Equation (2.15):

$$n = \left(\frac{n_m K_1 P}{1+K_1 P}\right)\left(1 + \theta K_1 P + \theta^3 (K_1 P)^2 + \ldots + \theta^{\frac{(m-1)m}{2}} K_1 P^{m-1}\right) \quad (2.15)$$

(b) A rational function equation of the form:

$$P = \frac{A_1 n}{A_2 - n} \exp\left(\frac{n}{A_3 - n} - A_4 n\right) \quad (4.1)$$

where A_1, A_2, A_3 and A_4 are regression parameters.

This equation has no physical background and it is chosen to be in an identical form to the Hill de Boer equation which proved to correlate the molecular sieve data reasonably well. Equation (4.1) will be used later for prediction of binary gas adsorption using the ideal adsorbed solution theory[36] and the empirical method by Cook and Basmadjian[35].

(c) The statistical thermodynamic model by Ruthven and co-workers[67,68] which is given by:

$$n = \frac{\bar{K} P + (\bar{K}P)^2 (1 - 2\bar{\beta}/v)^2 + \ldots + \frac{(\bar{K} P)^M}{(M-1)!} (1 - M\ \bar{\beta}/v)^M}{1 + \bar{K} P + \frac{1}{2!} (\bar{K} P)^2 (1-2\bar{\beta}/v)^2 + \ldots + \frac{(\bar{K}P)^M}{M!} (1-M\bar{\beta}/v)^M} \quad (2.31)$$

(d) The vacancy solution model by Suwanayuen and Danner[69] which is given by:

$$\dot{p} = \left(\frac{n_m}{b} \frac{\phi}{1-\phi}\right)\left(\Lambda_{13} \cdot \frac{1 - (1 - \Lambda_{31})\ \phi}{\Lambda_{31} + (1-\Lambda_{13})\ \phi}\right)$$

$$\exp\left(-\frac{\Lambda_{31}(1 - \Lambda_{31})\ \phi}{1 - (1-\Lambda_{31})\ \phi} - \frac{(1 - \Lambda_{13})\ \phi}{\Lambda_{13} + (1-\Lambda_{13})\ \phi}\right) \quad (2.38)$$

The above four models were fitted to the experimental data using curvilinear regression analysis. A computer programme was written which

incorporated a NAG[105] subroutine E04FCF. This subroutine used an optimised search technique to obtain the values of the regression parameters corresponding to the minimum sum of squares of the residuals, where the residual was defined as the difference between the experimental and predicted pressures for the vacancy solution model and for Equation (4.1), and as the difference between the experimental and predicted amount adsorbed for the kinetic model and the statistical thermodynamic model.

The kinetic model (Equation (2.15)) was used for two layers because it has been found that the contribution of higher layers offered no better fitness of the experimental data. The parameters K_1 and θ were used in an exponential temperature dependent form. The parameter n_m has been used by Gonzalez and Holland in an exponential temperature dependent form. However, this implies that the surface area of the adsorbent is a function of temperature, which contradicts the third assumption upon which the Gibbs adsorption formula is based (see Section 2.1). In this work n_m has been assumed to be temperature independent. In order to retain the thermodynamic consistency of the model the curve fitting procedure of the experimental data for both gases was done simultaneously for obtaining the same value of n_m and θ for each gas. Table 4.2 contains the regression parameters together with the sum of squares of relative residuals. (The relative residuals are defined as the residuals divided by the experimental values). From Table 4.2 it is seen that the nitrogen data on all the adsorbents were fitted better than the oxygen data. This could be attributed to the fact that the simultaneous fitting affected the oxygen data due to the high affinity of nitrogen on all adsorbents studied. Also Table 4.2 shows that the data on EKA 5A are poorly fitted and for Laporte 4A the value of θ, which is the ratio of K in the second layer to that in the first layer, is negative which gives no physical meaning. In general, it is seen that from the sum of squares of the relative residuals, this model fitted the experimental data poorly and its

TABLE 4.2

Regression Parameters for the Kinetic Model (Equation (2.15)) as Applied to the Adsorption of Oxygen and Nitrogen on Laportes 4A, 5A and 13X, EKA 5A and Na-Mordenite at 278.15, 293.15 and 303.15 K

Gas/Solid	n_m mol/kg	$K_1 = A_1 e^{A_2/T}$ bar^{-1}		$\theta = A_3 e^{A_4/T}$		Sum of Squares of Relative Residuals
		A_1	A_2	A_3	A_4	
O_2/Laporte 4A	2.809	1.594×10^{-5}	2291.42	- 0.0287	- 73.02	0.226
N_2/Laporte 4A		1.108×10^{-4}	2029.49			0.055
O_2/Laporte 5A	1.3446	2.339×10^{-4}	1794.05	0.086	206.71	0.618
N_2/Laporte 5A		2.507×10^{-5}	2720.91			0.161
O_2/Laporte 13X	1.9634	0.0181	256.417	0.215	- 86.97	3.041
N_2/Laporte 13X		6.075×10^{-6}	3033.31			0.868
O_2/EKA 5A	1.5496	1.684×10^{-5}	2775.83	0.139	- 93.03	16.488
N_2/EKA 5A		1.588×10^{-5}	2869.12			3.489
O_2/Na-Mordenite	1.4859	7.465×10^{-7}	3588.31	0.240	- 537.68	0.865
N_2/Na-Mordenite		2.311×10^{-5}	3067.31			0.318

effect will be pronounced when this model is used for prediction of gas mixture adsorption.

Equation (4.1) was curve fitted to each individual isotherm in order to obtain the best fit. The regression parameter together with the sum of squares of relative residuals are presented in Table 4.3 whilst the comparison of the experimental isotherms with the predicted values are presented in graphical form in Appendix I. From Table 4.3 it is seen that for nitrogen on all adsorbents, the parameter A_3 is of a high order which means that the effect of the first term in the exponential expression in Equation (4.1) is negligible. From the graphs in Appendix I it is seen that a reasonably good fitting is obtained.

The curve fitting by the statistical thermodynamic model was obtained by the same least squares technique used for the other models, rather than by the graphical procedure described by Ruthven[28]. The Henry's law constant, $\overline{K}$, and the molecular volume, $\overline{\beta}$, were used in an exponential temperature dependent form. The results are shown in tabular form in Table 4.4 whilst comparisons of the experimental isotherms with the predicted values are presented in graphical form in Figures 4.7 - 4.16. From the graphs it is seen that a good fitting for all the adsorbents is obtained. From Table 4.4 the calculated value of $\overline{\beta}$ for oxygen on Laporte 4A and EKA 5A is approximately temperature independent whilst for nitrogen the calculated value for Laporte 13X is temperature independent. The molecular volume, $\overline{\beta}$, for oxygen on EKA 5A was the closest value to the Van der Waal co-volume for oxygen (53 A^3/molecule). For nitrogen the closest value of $\overline{\beta}$ to the Van der Waal co-volume (65 A^3/molecule) was found to be on Laporte 4A. For the rest of the adsorbents some deviations are encountered between $\overline{\beta}$ and the respective Van der Waal co-volume.

Regression Parameters for Equation (4.1) as Applied to the Adsorption of Oxygen and Nitrogen on Laportes 4A, 5A and 13X EKA 5A and Na-Mordenite at 278.15, 293.15 and 303.15 K

Gas/Solid	Temperature K	A_1	A_2	A_3	A_4	Sum of Squares of Relative Residuals
O_2/Laporte 4A	278.15	19.013	2.6646	102.2551	0.1909	0.0027
	293.15	34.5503	3.5771	5.117	0.2841	0.0004
	303.15	18.2057	1.597	2.204	1.0577	0.00038
N_2/Laporte 4A	278.15	5.27	2.7681	5.5202×10^7	- 0.0815	0.0018
	293.15	7.5285	2.4119	5.2073×10^6	0.0508	0.00027
	303.15	8.8479	2.1805	2.0729×10^5	0.1184	0.00031
O_2/Laporte 5A	278.15	26.7438	4.2318	48.1187	0.06229	0.0044
	293.15	24.414	2.8228	3.9874	0.3686	0.0018
	303.15	388.3417	37.2119	67.8178	- 0.3201	0.0021
N_2/Laporte 5A	278.15	60.31	40.746	9.0484×10^8_7	- 0.7394	0.006
	293.15	11.5215	4.7433	5.5195×10^6	- 0.5643	0.0013
	303.15	20.0963	6.0947	$- 4.884 \times 10^6$	- 0.5944	0.003
O_2/Laporte 13X	278.15	- 7.6706	- 0.9744	265.7976	- 0.8657	0.0009
	293.15	728.839	75.1122	234.7387	- 0.2618	0.006
	303.15	124.3607	10.073	3.9015	0.2048	0.00071
N_2/Laporte 13X	278.15	6.1546	3.2077	5.5206×10^7_7	- 0.1333	0.0009
	293.15	9.2697	3.2013	5.5206×10^7	- 0.1633	0.0014
	303.15	15.92	4.2561	5.207×10^6	- 0.2705	0.00074

TABLE 4.3 continued .....

Gas/Solid	Temperature K	A_1	A_2	A_3	A_4	Sum of Squares of Relative Residuals
O_2/EKA 5A	278.15	301.3749	76.0416	240.2233	- 0.3407	0.00063
	293.15	32.7298	5.2806	- 4.6639	- 0.3426	0.0021
	303.15	- 695.512	- 89.7719	5.5172	- 0.1575	0.0001
N_2/EKA 5A	278.15	2.5607	3.9304	5.0291×10^7	- 0.6229	0.0019
	293.15	4.5213	3.6387	5.0259×10^7	- 0.5673	0.0031
	303.15	- 4.7404	- 2.7079	4.511×10^7	- 1.2077	0.0017
O_2/Na-Mordenite	278.15	9.3038	3.5043	- 1.5937	- 0.6088	0.00074
	293.15	9.824	2.2657	- 1.5179	- 0.4279	0.0052
	303.15	- 4.2839	- 0.7299	89.5064	- 1.4108	0.00019
N_2/Na-Mordenite	278.15	0.8806	2.3225	5.5025×10^8_7	- 0.6306	0.0095
	293.15	1.6018	1.913	5.0259×10^7	- 0.3825	0.0023
	303.15	2.2488	1.8896	5.0259×10^7	- 0.362	0.00047

TABLE 4.4

Regression Parameters for the Statistical Thermodynamics Model[†]

(Equation (2.31)) as Applied to the Adsorption of Oxygen and Nitrogen on Laportes 4A, 5A and 13X, EKA 5A and Na-Mordenite at 278.15, 293.15 and 303.15 K

Gas/Solid	$\bar{K} = A_1 e^{A_2/T}$ molecule/cavity bar		$\bar{\beta} = A_3 e^{A_4/T}$ A^3/molecules		M molecules	Sum of Squares of Relative Residuals
	A_1	A_2	A_3	A_4		
O_2/Laporte 4A	0.00118	1555.857	38.947	- 38.3075	22	0.0093
N_2/Laporte 4A	0.00011	2584.061	13.8418	453.834	11	0.016
O_2/Laporte 5A	0.00069	1741.481	995.31	- 959.063	18	0.015
N_2/Laporte 5A	0.000112	2645.746	156.742	- 175.627	8	0.0066
O_2/Laporte 13X	0.00079	1637.241	213.263	- 568.688	25	0.019
N_2/Laporte 13X	0.00028	2318.083	69.5378	19.9393	12	0.0087
O_2/EKA 5A	0.00018	2244.976	55.6952	- 53.057	16	0.0112
N_2/EKA 5A	0.000031	3223.29	150.914	- 138.131	8	0.0095
O_2/Na-Mordenite	0.00013	2620.545	26.118	66.347	15	0.028
N_2/Na-Mordenite	0.000033	3498.063	114.442	- 241.223	10	0.021

[†]for zeolite type 4A and 5A[24]

v = volume of zeolite cavity = 776 A^3
1 mol/kg = 2.22 molecules/cavity

for zeolite type 13X[24]
v = 822 A^3
1 mol/kg = 2.083 molecules/cavity

for zeolite Na-Mordenite[24]
v = 546 A^3
1 mol/kg = 3.8462 molecules/cavity

for all adsorbents the assumed amount of anhydrous adsorbent in pellet is 80%

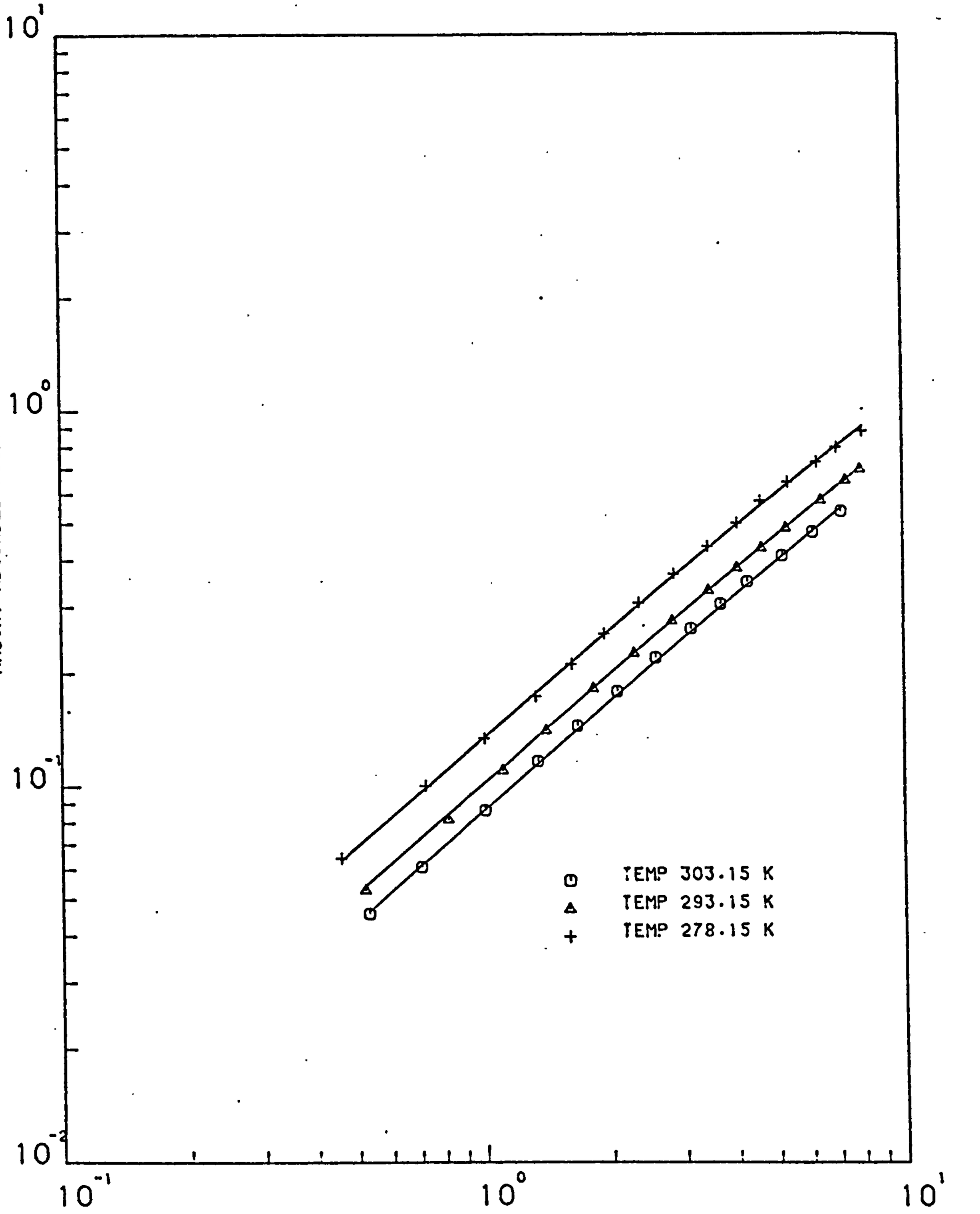

FIGURE (4.7) COMPARISON OF THE STATISTICAL THERMODYNAMICS MODEL (—) WITH THE EXPERIMENTAL DATA OF OXYGEN ON LAPORTE 4A MOLECULAR SIEVE PELLETS AT 278.15, 293.15 AND 303.15 K

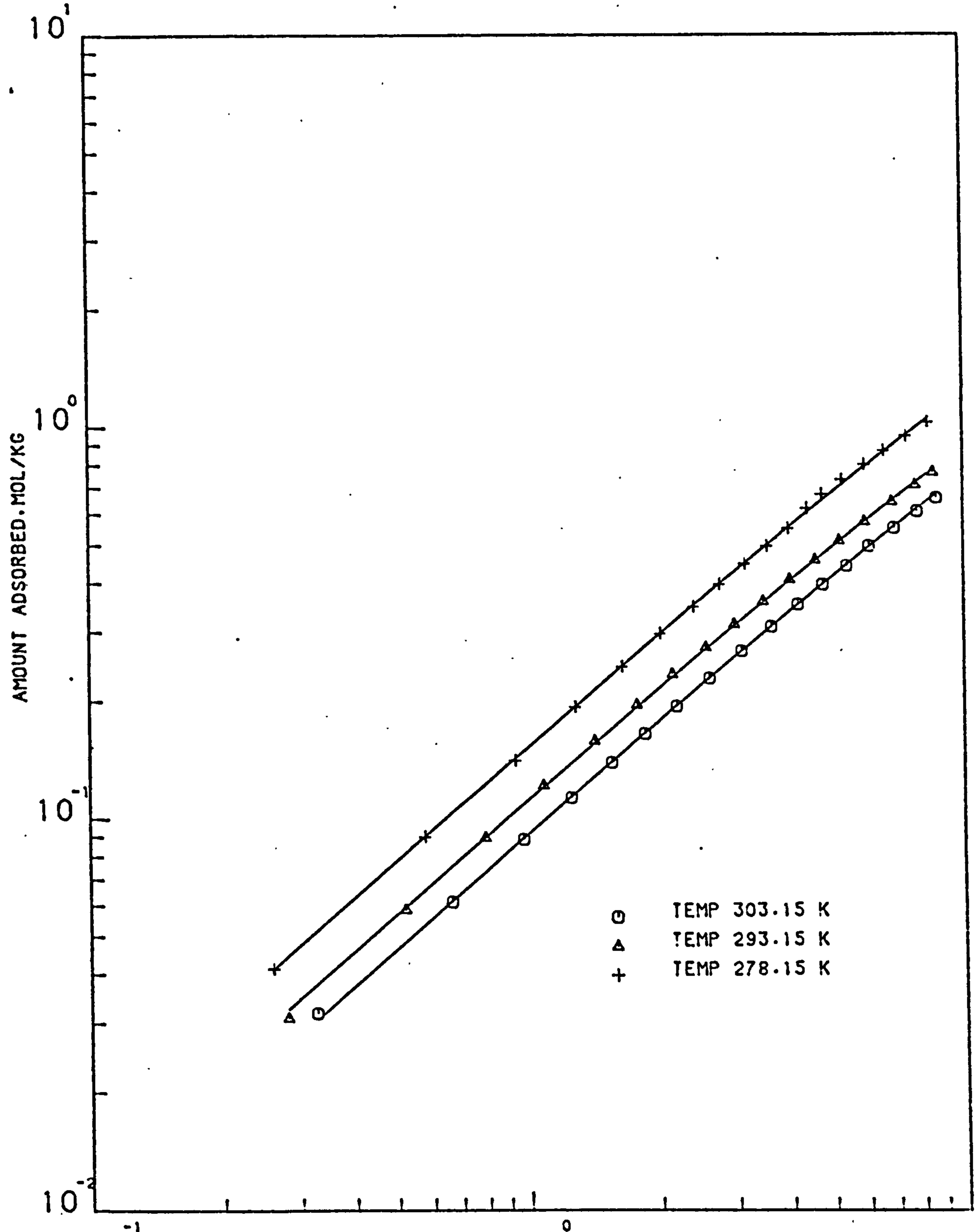

FIGURE (4·8) COMPARISON OF THE STATISTICAL THERMODYNAMICS MODEL WITH EXPERIMENTAL DATA OF OXYGEN ON LAPORTE 5A MOLECULAR SIEVE PELLETS AT 303.15 . 293.15 AND 278.15 K

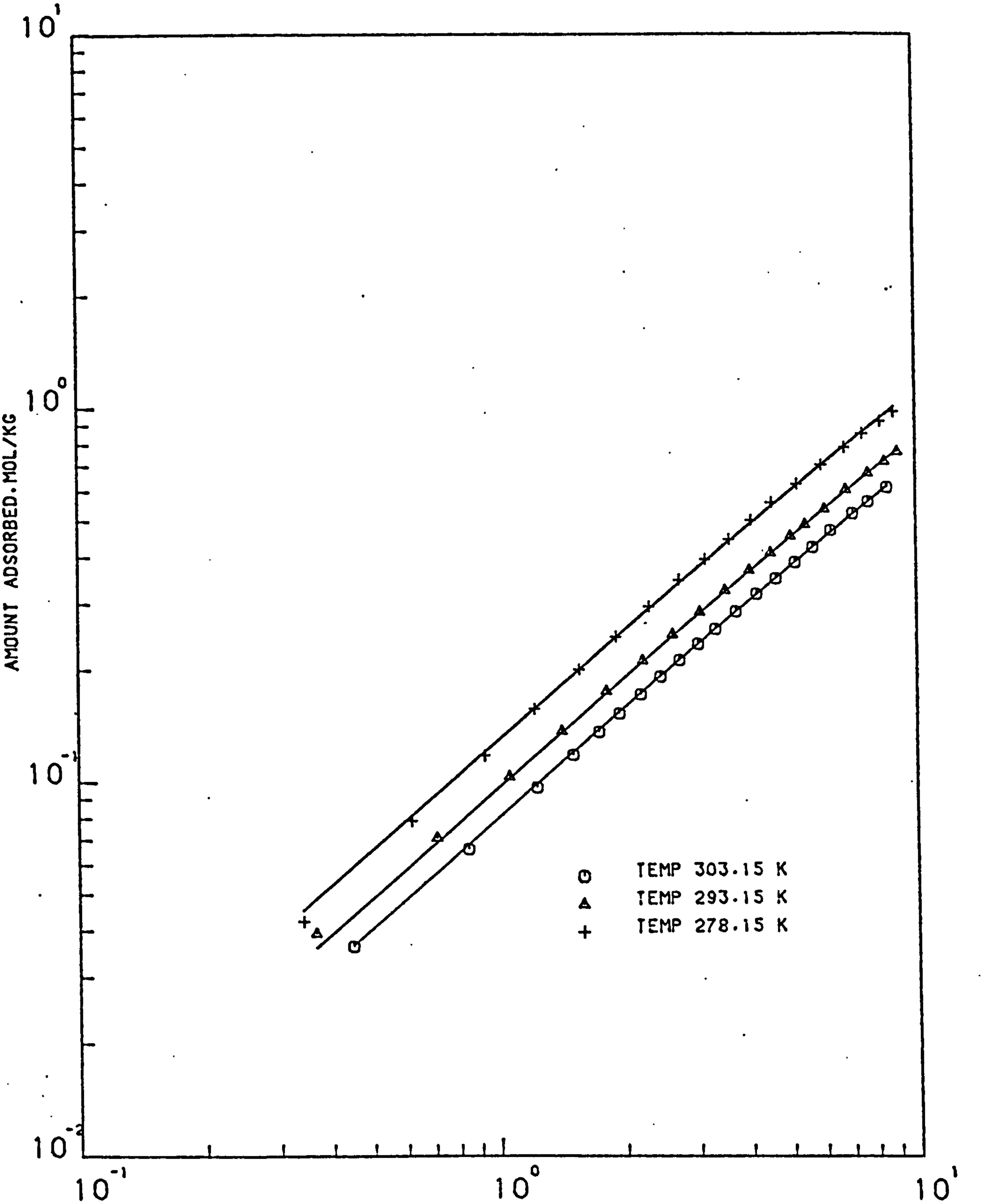

FIGURE (4·9) COMPARISON OF THE STATISTICAL THERMODYNAMICS MODEL (——) WITH THE EXPERIMENTAL DATA OF OXYGEN ON LAPORTE 13X MOLECULAR SIEVE PELLETS AT 278.15.293.15 AND 303.15 K

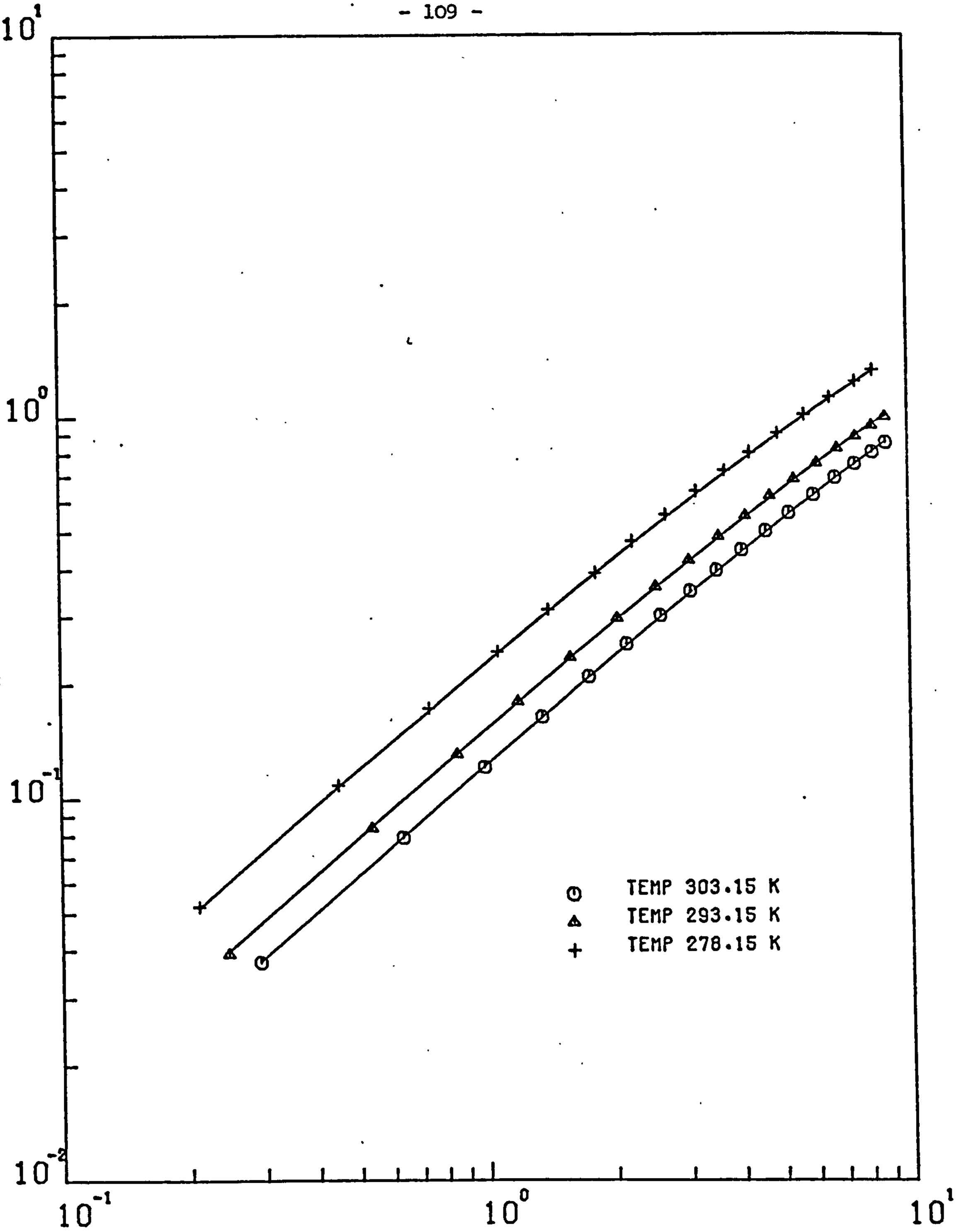

FIGURE (4·10) COMPARISON OF THE STATISTICAL THERMODYNAMICS MODEL (——) WITH EXPERIMENTAL DATA OF OXYGEN ON EKA 5A MOLECULAR SIEVE PELLETS AT 303.15 , 293.15 AND 278.15 K

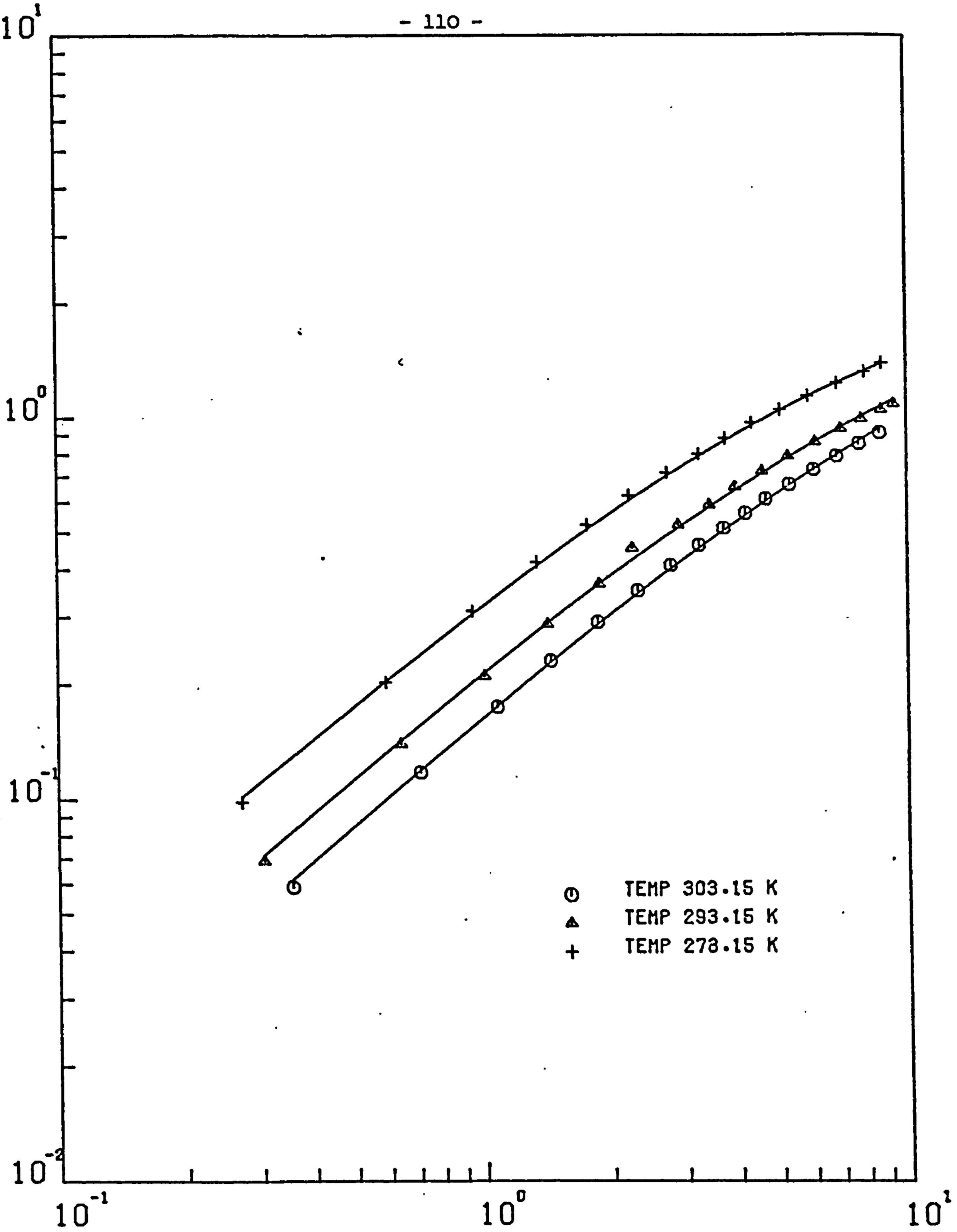

FIGURE (4·11) COMPARISON OF THE STATISTICAL THERMODYNAMICS MODEL (——) WITH EXPERIMENTAL DATA OF OXYGEN ON NA-MORDENITE MOLECULAR SIEVE PELLETS AT 303.15 , 293.15 AND 273.15 K

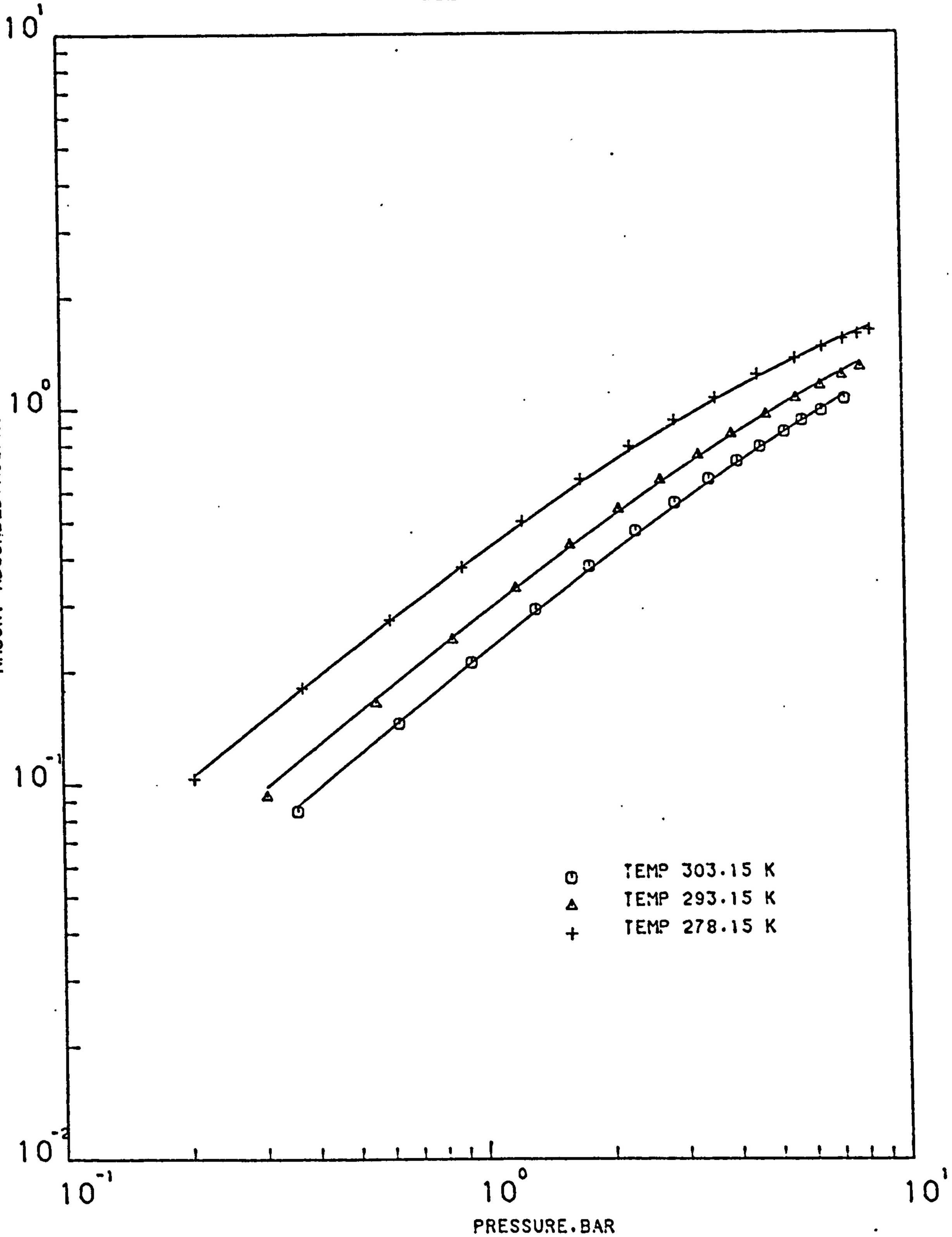

FIGURE (4.12) COMPARISON OF THE STATISTICAL THERMODYNAMICS MODEL (—) WITH THE EXPERIMENTAL DATA OF NITROGEN ON LAPORTE 4A MOLECULAR SIEVE PELLETS AT 278.15, 293.15 AND 303.15 K

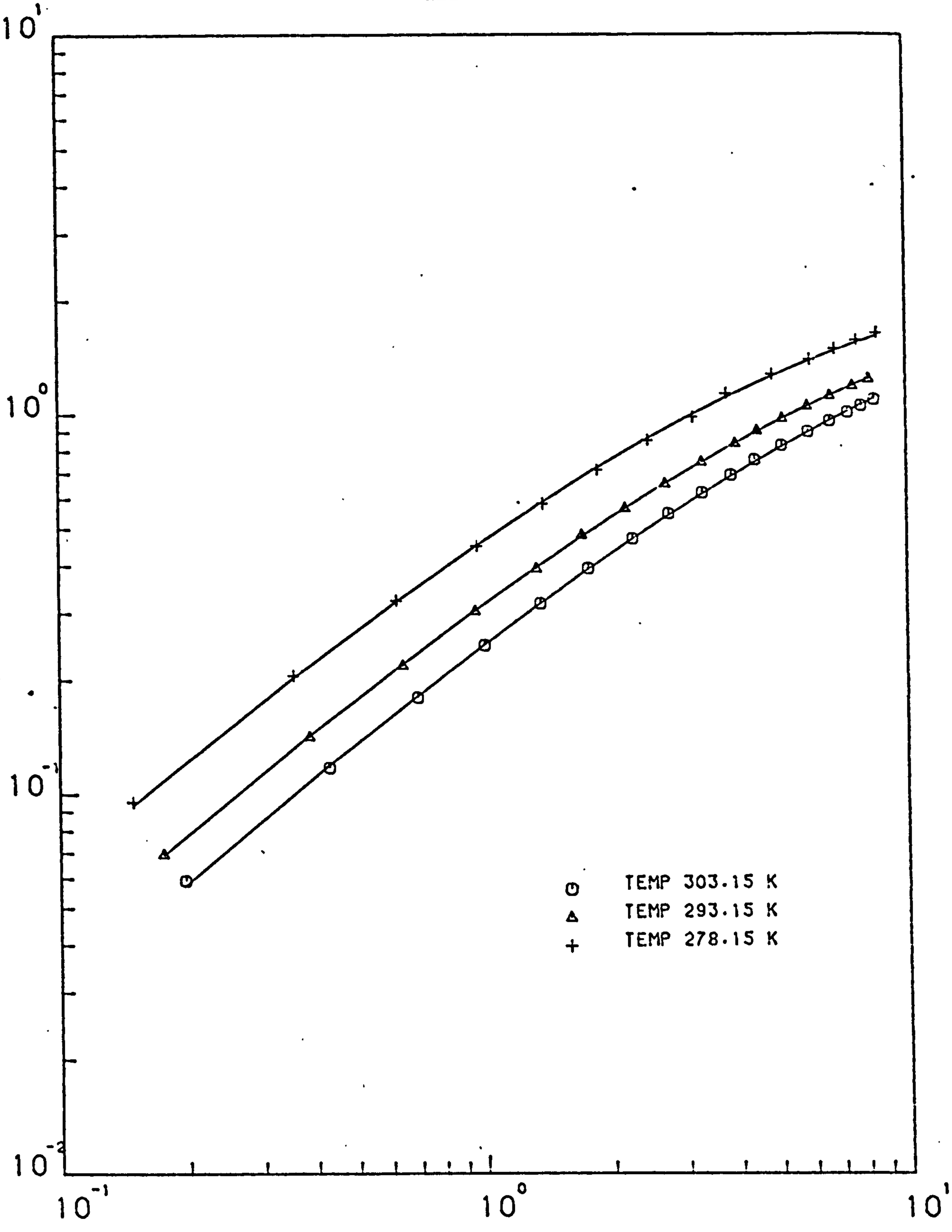

FIGURE (4·13) COMPARISON OF THE STATISTICAL THERMODYNAMICS MODEL (——) WITH EXPERIMENTAL DATA OF NITROGEN ON LAPORTE 5A MOLECULAR SIEVE PELLETS AT 303.15 . 293.15 AND 278.15 K

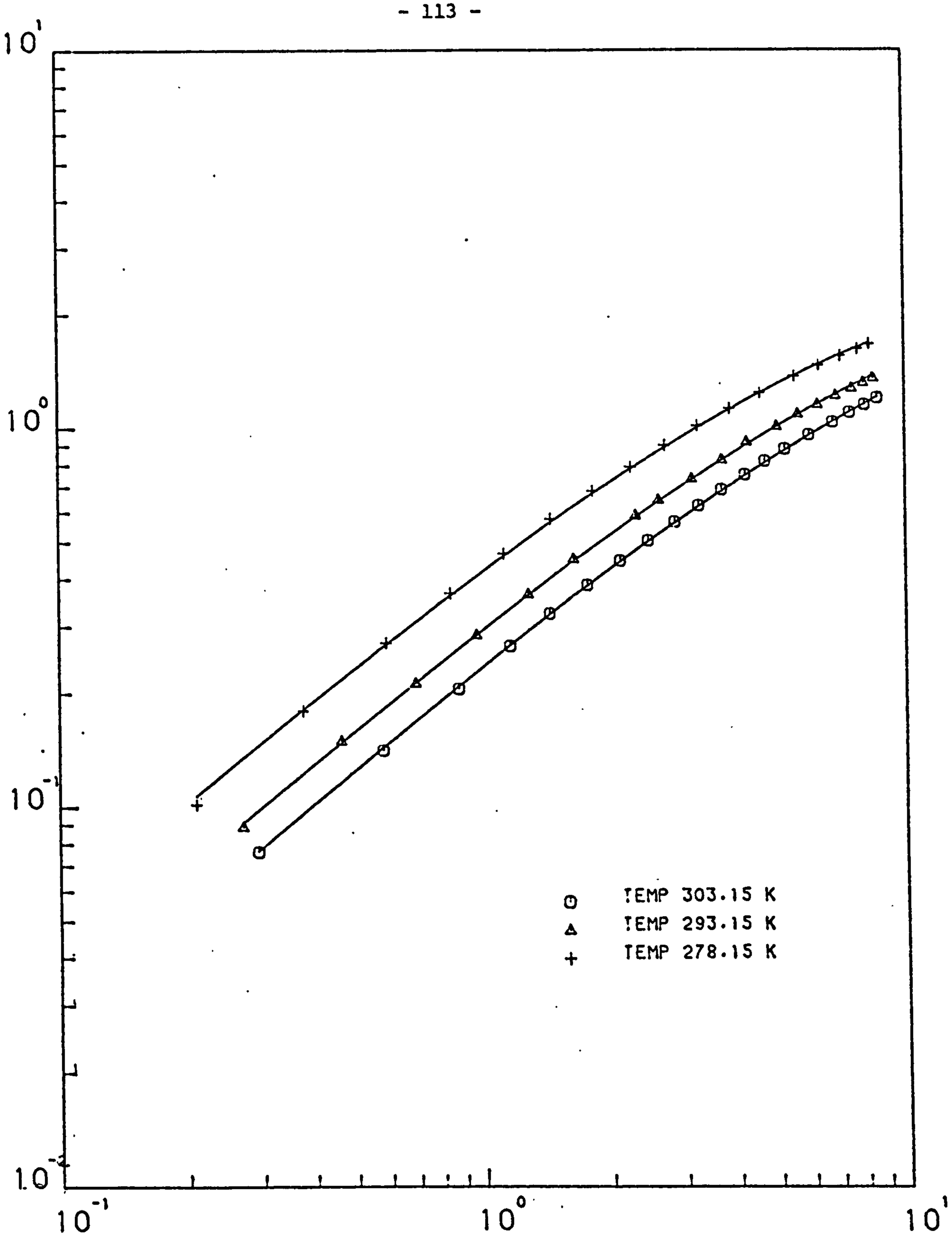

FIGURE (4.14) COMPARISON OF THE STATISTICAL THERMODYNAMICS MODEL (—) WITH THE EXPERIMENTAL DATA OF NITROGEN ON LAPORTE 13X MOLECULAR SIEVE PELLETS AT 278.15.293.15 AND 303.15 K

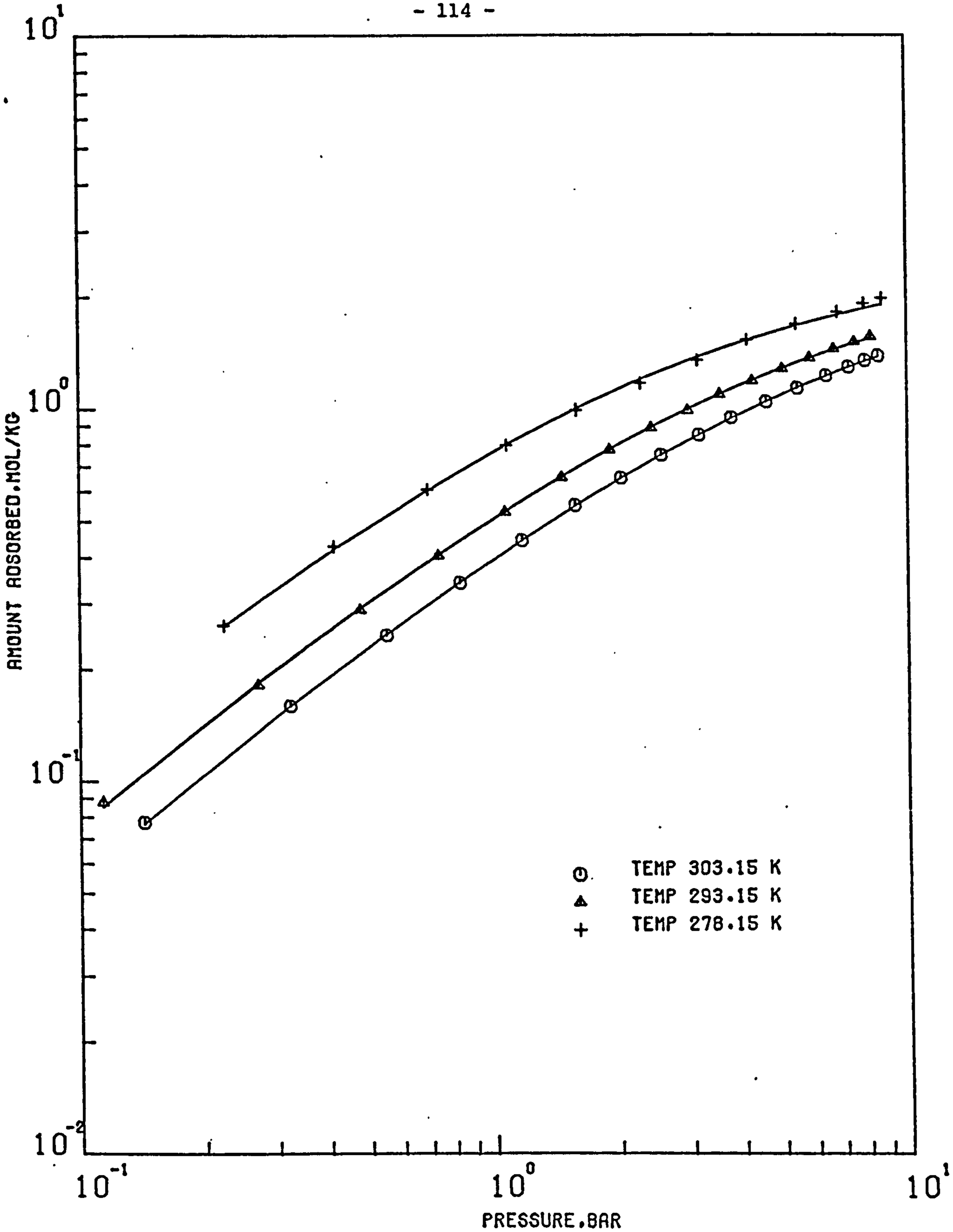

FIGURE (4·15) COMPARISON OF THE STATISTICAL THERMODYNAMICS MODEL (——) WITH EXPERIMENTAL DATA OF NITROGEN ON EKA 5A MOLECULAR SIEVE PELLETS AT 303.15 . 293.15 AND 278.15 K

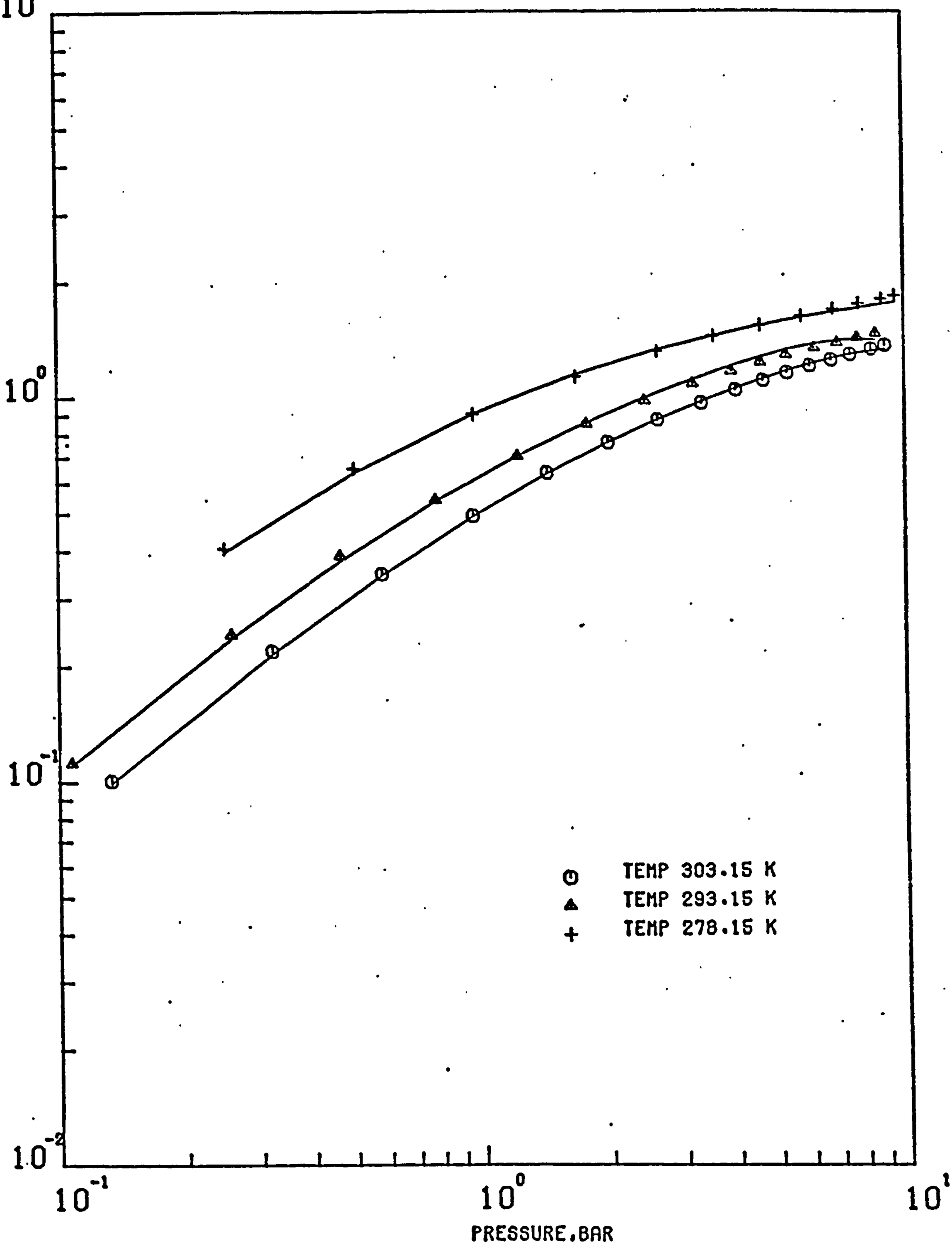

FIGURE (4.16) COMPARISON OF THE STATISTICAL THERMODYNAMICS MODEL (——) WITH EXPERIMENTAL DATA OF NITROGEN ON NA-MORDENITE MOLECULAR SIEVE PELLETS AT 303.15 , 293.15 AND 278.15 K

The vacancy solution model contains four independent parameters: n_m, b, Λ_{13} and Λ_{31}. An initial attempt for curve fitting the experimental data was made using the parameters b, Λ_{13} and Λ_{31} in an exponential temperature dependent form but a poor correlation was obtained. Therefore, it was decided to curve fit each experimental isotherm individually in order to obtain the best fit. The parameter n_m which is the limiting adsorption amount is known to be temperature independent. Consequently, if n_m value is known at one temperature, it should be approximately the same at all temperatures and only three parameters need to be determined. Since the most reliable limiting value from an isotherm is obtained at the lowest temperature, the limiting value, n_m, was determined for 278.15 K isotherms. Only the three remaining parameters were determined for the other adsorption isotherms. One more point to note is that when the vacancy solution model was extended for prediction of gas mixture adsorption, the total limiting adsorption concentration was taken as the average of those of the adsorbates (see Equation (2.86)). This definition has the advantage of being applicable to the description of adsorbed mixtures containing adsorbates which have unequal values of the saturation amount. Thus this allows the individual curve fitting of oxygen and nitrogen isotherms. The results of the regression analysis are shown in tabular form in Table 4.5 whilst comparisons of the experimental isotherms with the predicted values are presented in graphical form in Appendix I. The graphical results show that the model fitted the experimental data reasonably well. From Table 4.5 it is seen that the interaction coefficients Λ_{13} and Λ_{31} show wide variation with temperature especially for O_2 and N_2 on Laporte 4A, O_2 on Laporte 5A, O_2 and N_2 on Laporte 13X and N_2 on Na-Mordenite.

Comparison of Henry's Law Constants

The values of Henry's law constant, K", for oxygen and nitrogen on

TABLE 4.5

Regression Parameters for the Vacancy Solution Model (Equation (2.38)) as Applied to the Adsorption of Oxygen and Nitrogen on Laportes 4A, 5A and 13X, EKA 5A and Na-Mordenite at 278.15, 293.15 and 303.15 K

Gas/Solid	n_m mol/kg	Temperature K	b mol/kg bar	Λ_{13}	Λ_{31}	Sum of Squares of Relative Residuals
O_2/Laporte 4A	7.3848	278.15	0.1415	14.2186	0.0479	0.0029
		293.15	0.103	0.1757	3.2159	0.00034
		303.15	0.0861	0.0843	4.3913	0.00016
N_2/Laporte 4A	4.3712	278.15	0.5269	34.7095	0.025	0.0022
		293.15	0.3006	0.1293	3.484	0.00098
		303.15	0.2365	0.1423	3.3907	0.00052
O_2/Laporte 5A	1.4815	278.15	0.1507	1.0318	0.2406	0.011
		293.15	0.1161	1.1915	0.2840	0.0019
		303.15	0.0957	1.3266	2.663×10^{-5}	0.0026
N_2/Laporte 5A	2.8074	278.15	0.6148	0.529	1.8905	0.0239
		293.15	0.4165	0.6493	1.8648	0.00091
		303.15	0.3065	0.4617	2.1658	0.0024
O_2/Laporte 13X	11.4199	278.15	0.133	18.0603	0.0528	0.0058
		293.15	1.1031	0.3955	2.5287	0.0039
		303.15	0.081	0.1608	3.4769	0.00075
N_2/Laporte 13X	4.7813	278.15	0.5175	132.6518	0.0046	0.00075
		293.15	0.3382	0.1554	3.4495	0.003
		303.15	0.2667	0.2048	3.1449	0.0011

continued .....

TABLE 4.5 continued .....

Gas/Solid	n_m mol/kg	Temperature K	b mol/kg bar	Λ_{13}	Λ_{31}	Sum of Squares of Relative Residuals
O_2/EKA 5A	6.2574	278.15	0.2536	0.4573	2.187	0.00055
		293.15	0.1622	5.0685	0.7275	0.00018
		303.15	0.1291	4.6942	0.6977	0.00012
N_2/EKA 5A	2.9093	278.15	1.5142	0.1770	3.32	0.0028
		293.15	0.8164	0.958	1.661	0.0023
		303.15	0.5757	1.0019	1.6169	0.001
O_2/Na-Mordenite	2.6377	278.15	0.3742	0.266	2.4453	0.00084
		293.15	0.2225	0.1804	2.8727	0.0067
		303.15	0.168	0.2044	2.7098	0.00013
N_2/Na-Mordenite	3.0976	278.15	2.5268	5.8792	1.1021	0.0044
		293.15	1.1852	998.3228	0.7816	0.0017
		303.15	0.8337	1366.435	0.7652	0.00037

the five adsorbents studied were obtained from the kinetic model, statistical thermodynamic model, the vacancy solution model and Equation (4.1). For Equation (4.1), as the pressure approaches zero the value of $A_2 >> n$, hence the value of K" was taken to be equal to A_1/A_2. The values of K" were then used to obtain the values of A_o'' and U_o in the temperature dependent form of the Henry's law constant, i.e.

$$K'' = A_o'' \exp(-U_o/RT)$$

where U_o is + ve. For the kinetic and the statistical thermodynamic models the values of A_o'' and U_o were obtained from Tables 4.2 and 4.4 respectively using the necessary conversion factors. For the vacancy solution model and Equation (4.1) a linear regression analysis was made to obtain the values of A_o'' and U_o. The Henry's law constants for the four models are shown in a tabular form in Table 4.6. From Table 4.6 it is noticed that the values of Henry's law constants obtained from the statistical thermodynamic model, the vacancy solution model and Equation (4.1) are in fairly good agreement with each other whilst the Henry law constants from the kinetic model (with exception of Laporte 5A) are significantly different, especially for oxygen. This deviation could be attributed to the effect caused by the simultaneous fitting (see Table 4.2).

Isosteric Heat of Adsorption

The isosteric heat of adsorption, q_{ST}, (heat of adsorption at constant amount adsorbed) is given by the following expression[56]:

$$q_{ST} = RT^2 \left(\frac{\partial \ln P}{\partial T}\right)_n \qquad (4.2)$$

The isosteric heat of adsorption at any value of the amount adsorbed, n, can be obtained graphically from Equation (4.2), by plotting the adsorption isostere as ln P vs $\frac{1}{T}$ and determining the slope, which equals $- q_{ST}/R$. In

TABLE 4.6

Henry's Law Constants for Oxygen and Nitrogen on Laportes 4A, 5A and 13X, EKA 5A and Na-Mordenite at 278.15, 293.15 and 303.15 K

Gas/Solid	Model	Temperature K	K' bar/mol/kg	A_o" bar/mol/kg	U_o kJ/mol
O_2/Laporte 4A	Kinetic	278.15	5.898	2.23×10^4	19.05
		293.15	8.99		
		303.15	11.63		
	Equation (4.1)	278.15	7.16	2.14×10^3	13.156
		293.15	9.58		
		303.15	11.46		
	Statistical Therm.	278.15	6.99	1.883×10^3	12.94
		293.15	9.31		
		303.15	11.09		
	Vacancy Solution	278.15	7.08	2.99×10^3	13.98
		293.15	9.65		
		303.15	11.66		
N_2/Laporte 4A	Kinetic	278.15	2.18	3.213×10^3	16.87
		293.15	3.168		
		303.15	3.98		
	Equation (4.1)	278.15	1.916	1.94×10^4	21.33
		293.15	3.071		
		303.15	4.1		
	Statistical Therm.	278.15	1.868	2.02×10^4	21.48
		293.15	3.0		
		303.15	4.02		
	Vacancy Solution	278.15	1.91	3.38×10^4	22.62
		293.15	3.16		
		303.15	4.29		

TABLE 4.6 continued .....

Gas/Solid	Model	Temperature K	K" bar/mol/kg	A_o" bar/mol/kg	U_o kJ/mol
O_2/Laporte 5A	Kinetic	278.15 293.15 303.15	5.017 6.98 8.54	3.18×10^3	14.92
	Equation (4.1)	278.15 293.15 303.15	6.32 8.63 10.45	2.78×10^3	14.08
	Statistical Therm.	278.15 293.15 303.15	6.14 8.47 10.3	3.22×10^3	14.48
	Vacancy Solution	278.15 293.15 303.15	6.6 8.74 10.37	1.57×10^3	12.65
N_2/Laporte 5A	Kinetic	278.15 293.15 303.15	1.68 2.77 3.76	2.97×10^4	22.62
	Equation (4.1)	278.15 293.15 303.15	1.48 2.43 3.3	2.44×10^4	22.45
	Statistical Therm.	278.15 293.15 303.15	1.46 2.38 3.21	1.98×10^4	21.997
	Vacancy Solution	278.15 293.15 303.15	1.61 2.47 3.21	6.88×10^3	19.33

TABLE 4.6 continued .....

Gas/Solid	Model	Temperature K	K" bar/mol/kg	A_o" bar/mol/kg	U_o kJ/mol
O_2/Laporte 13X	Kinetic	278.15	11.18	2.81×10^1	2.132
		293.15	11.72		
		303.15	12.06		
	Equation (4.1)	278.15	7.74	1.59×10^3	12.31
		293.15	10.16		
		303.15	12.0		
	Statistical Therm.	278.15	7.34	2.64×10^3	13.61
		293.15	9.92		
		303.15	11.92		
	Vacancy Solution	278.15	7.42	2.73×10^3	13.66
		293.15	10.04		
		303.15	12.08		
N_2/Laporte 13X	Kinetic	278.15	1.54	8.38×10^4	25.22
		293.15	2.69		
		303.15	3.78		
	Equation (4.1)	278.15	1.92	6.25×10^3	18.71
		293.15	2.9		
		303.15	3.74		
	Statistical Therm.	278.15	1.79	7.44×10^3	19.27
		293.15	2.74		
		303.15	3.56		
	Vacancy Solution	278.15	1.94	6.14×10^3	18.64
		293.15	2.93		
		303.15	3.77		

TABLE 4.6 continued .....

Gas/Solid	Model	Temperature K	K" bar/mol/kg	A_o" bar/mol/kg	U_o kJ/mol
O_2/EKA 5A	Kinetic	278.15 293.15 303.15	1.77 2.96 4.04	3.83×10^4	23.08
	Equation (4.1)	278.15 293.15 303.15	3.99 6.07 7.85	1.44×10^4	18.93
	Statistical Therm.	278.15 293.15 303.15	3.85 5.82 7.49	1.23×10^4	18.66
	Vacancy Solution	278.15 293.15 303.15	3.97 6.05 7.83	1.5×10^4	19.05
N_2/EKA 5A	Kinetic	278.15 293.15 303.15	1.347 2.284 3.154	4.06×10^4	23.85
	Equation (4.1)	278.15 293.15 303.15	0.657 1.217 1.774	1.12×10^5	27.86
	Statistical Therm.	278.15 293.15 303.15	0.664 1.2 1.728	7.17×10^4	26.8
	Vacancy Solution	278.15 293.15 303.15	0.663 1.21 1.75	8.5×10^4	27.2

TABLE 4.6 continued .....

Gas/Solid	Model	Temperature K	K" bar/mol/kg	A_o" bar/mol/kg	U_o kJ/mol
O_2/Na-Mordenite	Kinetic	278.15	2.255	9.02×10^5	29.83
		293.15	4.363		
		303.15	6.533		
	Equation (4.1)	278.15	2.654	3.98×10^4	22.24
		293.15	4.341		
		303.15	5.865		
	Statistical Therm.	278.15	2.394	2.96×10^4	21.79
		293.15	3.877		
		303.15	5.207		
	Vacancy Solution	278.15	2.688	4.63×10^4	22.56
		293.15	4.427		
		303.15	6.01		
N_2/Na-Mordenite	Kinetic	278.15	0.473	2.91×10^4	25.5
		293.15	0.832		
		303.15	1.175		
	Equation (4.1)	278.15	0.387	4.79×10^5	32.44
		293.15	0.793		
		303.15	1.231		
	Statistical Therm.	278.15	0.405	1.17×10^5	29.08
		293.15	0.77		
		303.15	1.141		
	Vacancy Solution	278.15	0.403	3.17×10^5	31.4
		293.15	0.807		
		303.15	1.233		

practice, however, it is usual to use an integrated form of Equation (4.2) and apply the equation to isotherms at two temperatures. Thus integrating Equation (4.2) gives:

$$q_{ST} = R \left(\frac{T_2 \, T_1}{T_2 - T_1} \right) \ell n \left(\frac{P_2}{P_1} \right) \qquad (4.3)$$

The temperature to which this value of q_{ST} refers to is given by the expression[56]:

$$\frac{1}{T} = \frac{1}{2} \left(\frac{1}{T_1} + \frac{1}{T_2} \right) \qquad K^{-1} \qquad (4.4)$$

and the pressures are given by the expression[56]:

$$P = (P_1 \, P_2)^{\frac{1}{2}}$$

The experimental isosteric heats of adsorption, q_{ST}, were evaluated from Equation (4.3) using two isotherms of 278.15 and 303.15 K for both oxygen and nitrogen on the five adsorbents studied. The predicted q_{ST} values for the four models were evaluated also from Equation (4.3) by the use of the theoretical isotherms predicted by the models at 278.15 and 303.15 K. For all the adsorbents studied the experimental q_{ST} were in fair agreement with the values predicted by the vacancy solution model, the statistical thermodynamic model and Equation (4.1), whilst the values of q_{ST} predicted from the kinetic model (with exception of Laporte 5A) were significantly different, the highest deviation being encountered for Laporte 13X. The results for Laporte 13X are represented graphically in Figures 4.17 - 4.18. For the four models the values of q_{ST} for the five adsorbents studied were almost constant with loading (i.e. $q_{ST} \; \underline{\Omega} \; U_o$).

General Concluding Remarks on the Pure Component Isotherms

The statistical thermodynamic model, the vacancy solution model and Equation (4.1) fitted the experimental pure component isotherms of oxygen

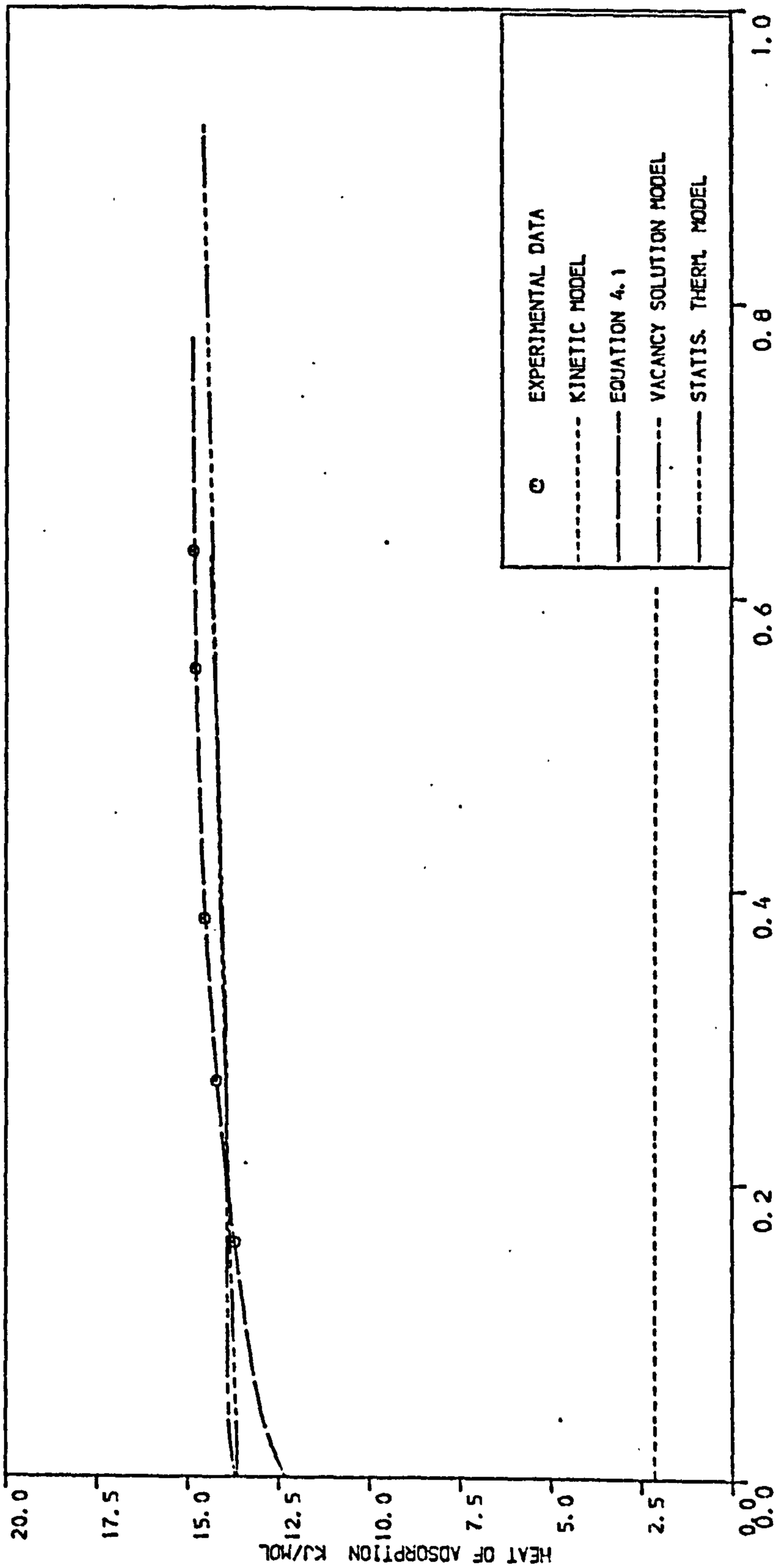

FIGURE 4.17 COMPARISON OF EXPERIMENTAL ISOSTERIC HEAT OF ADSORPTION WITH VALUES PREDICTED BY THE FOUR MODELS FOR OXYGEN ON LAPORTE 13X PELLETS AT 290 K

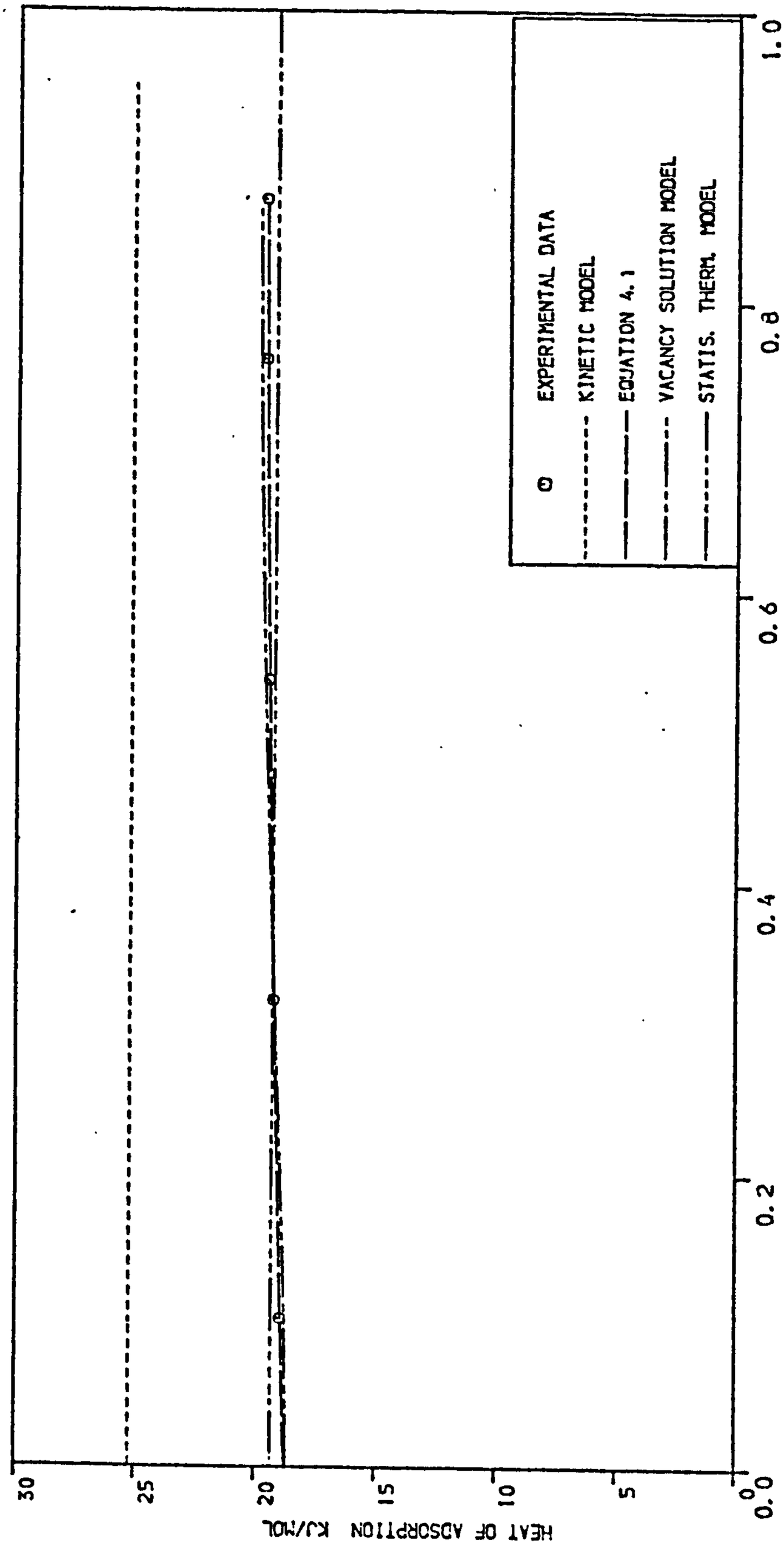

FIGURE 4.18 COMPARISON OF EXPERIMENTAL ISOSTERIC HEAT OF ADSORPTION WITH VALUES PREDICTED BY THE FOUR MODELS FOR NITROGEN ON LAPORTE 13X PELLETS AT 290K

and nitrogen reasonably well. However, the vacancy-adsorbate, Λ_{31}, and the adsorbate-vacancy, Λ_{13}, interactions obtained from the vacancy solution model showed opposite wide variation from unity at a particular temperature on some of the adsorbents studied. This could affect the model when used for gas-mixture adsorption prediction.

The fitted isotherms obtained by the kinetic model were rather poor particularly for EKA 5A isotherms. This could be attributed to the effect caused by the simultaneous fitting and the inheritance of the model on the basic assumptions of the Langmuir model.

4.2 Binary Gas Adsorption

In this section analyses and interpretations of the binary gas equilibria data are made. The effects of both temperature and pressure on separation factors and total amount adsorbed are studied. A comparison of the basic binary equilibria data on the five adsorbents studied is made. The experimental equilibria data are compared with predictions from theoretical models. The activity coefficients for the binary gas-solid systems studied are calculated.

4.2.1 Effect of temperature and pressure on binary gas adsorption

For all the binary gas-solid systems reported in Chapter 3 the following points are deduced from Figures 3.12 - 3.21:

(a) The separation factor ($y_{O_2} x_{N_2}/y_{N_2} x_{O_2}$) decreases slightly with increasing temperature. However, it is less sensitive to temperature change than is the total amount adsorbed.

(b) The effect of temperature on the separation factor is slightly more pronounced at a pressure of 1.7 bar than at a pressure of 4.4 bar.

(c) At a particular pressure the effect of temperature on the separation factor is more pronounced at high oxygen concentration in the adsorbed phase than at low concentration.

(d) The total amount of mixture adsorbed is a strong function of the adsorbed phase composition, decreasing more sharply at high oxygen concentration. This would be expected in view of the stronger affinity of the molecular sieves studied for nitrogen in preference to oxygen.

(e) Within the two pressures studied the effect of increase of pressure tends to decrease the separation factor slightly, whilst of course the total amount adsorbed is affected considerably by increase of pressure.

A comparison of the actual experimental binary loadings for oxygen and nitrogen for a 50 mol% gas mixture with values predicted for pure components at the same partial pressures is presented in Table 4.7. From Table 4.7 it is observed that at all the temperatures and pressures investigated the binary loadings of oxygen and nitrogen are less than the loadings predicted for pure components at the same partial pressures. These data clearly demonstrate the need for models to describe binary adsorption equilibria and a number of models are compared with the experimental data in Section 4.2.3.

4.2.2 Comparison of separation factors between adsorbents

The binary gas mixture adsorption equilibria on Laportes 4A, 5A and 13X, EKA 5A and Na-Mordenite are replotted in Figures 4.19 - 4.24 showing the comparison between adsorbents. The following points are deduced:

PAGE

MISSING

IN

ORIGINAL

TABLE 4.7 continued .....

Adsorbent	Pressure bar	Temperature K	Experimental Loading mol/kg		Loading for independent adsorption mol/kg	
			O_2	N_2	O_2	N_2
EKA 5A	1.7	278.15	0.139	0.647	0.207	0.694
	1.7	293.15	0.11	0.427	0.143	0.451
	1.7	303.15	0.09	0.358	0.107	0.37
	4.4	278.15	0.282	1.034	0.482	1.153
	4.4	293.15	0.236	0.812	0.328	0.839
	4.4	303.15	0.2	0.658	0.266	0.681
Na-Mordenite	1.7	278.15	0.186	0.76	0.304	0.835
	1.7	293.15	0.128	0.549	0.19	0.581
	1.7	303.15	0.111	0.462	0.14	0.47
	4.4	278.15	0.27	1.037	0.62	1.24
	4.4	293.15	0.23	0.866	0.43	0.94
	4.4	303.15	0.212	0.701	0.35	0.8

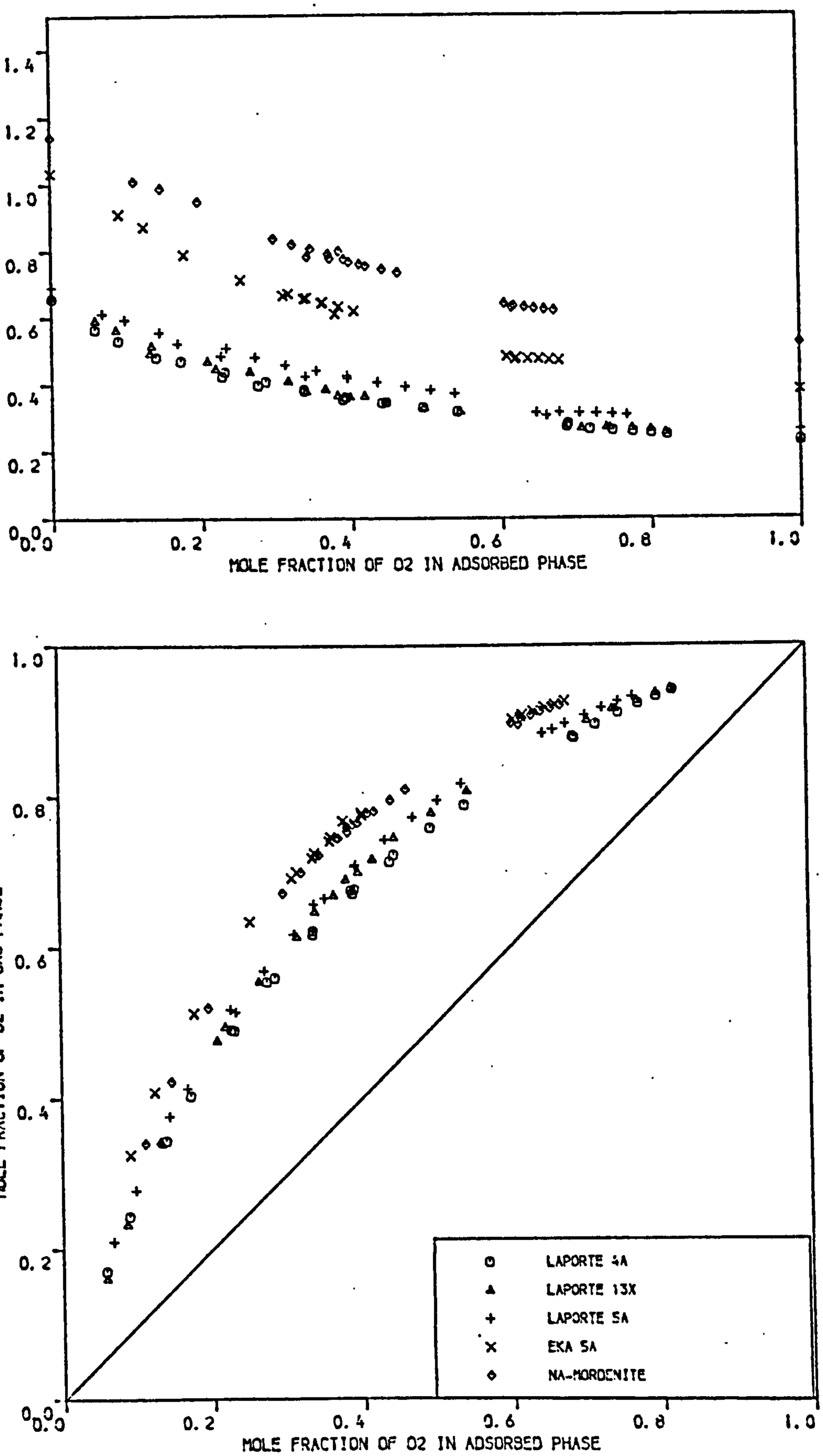

FIGURE 4.19 BINARY ADSORPTION EQUILIBRIA DATA OF O2/N2 ON LAPORTE 4A, LAPORTE 13X, LAPORTE 5A, EKA 5A AND NA-MORDENITE MOLECULAR SIEVE PELLETS AT 278.15 K (PRESSURE = 1.7 BAR)

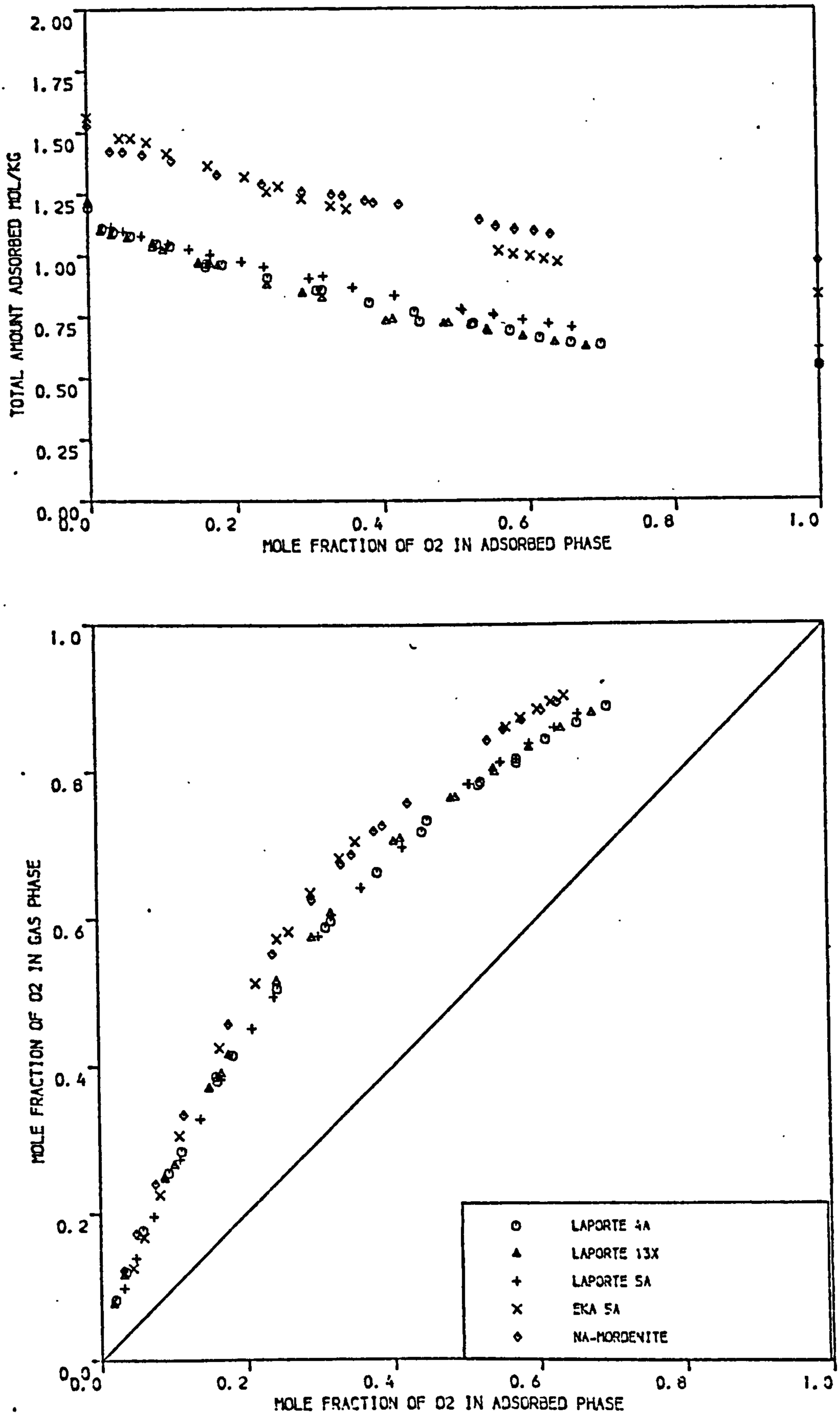

FIGURE 4.20 BINARY ADSORPTION EQUILIBRIA DATA OF O2/N2 ON LAPORTE 4A, LAPORTE 13X, LAPORTE 5A, EKA 5A AND NA-MORDENITE MOLECULAR SIEVE PELLETS AT 278.15 K (PRESSURE = 4.4 BAR)

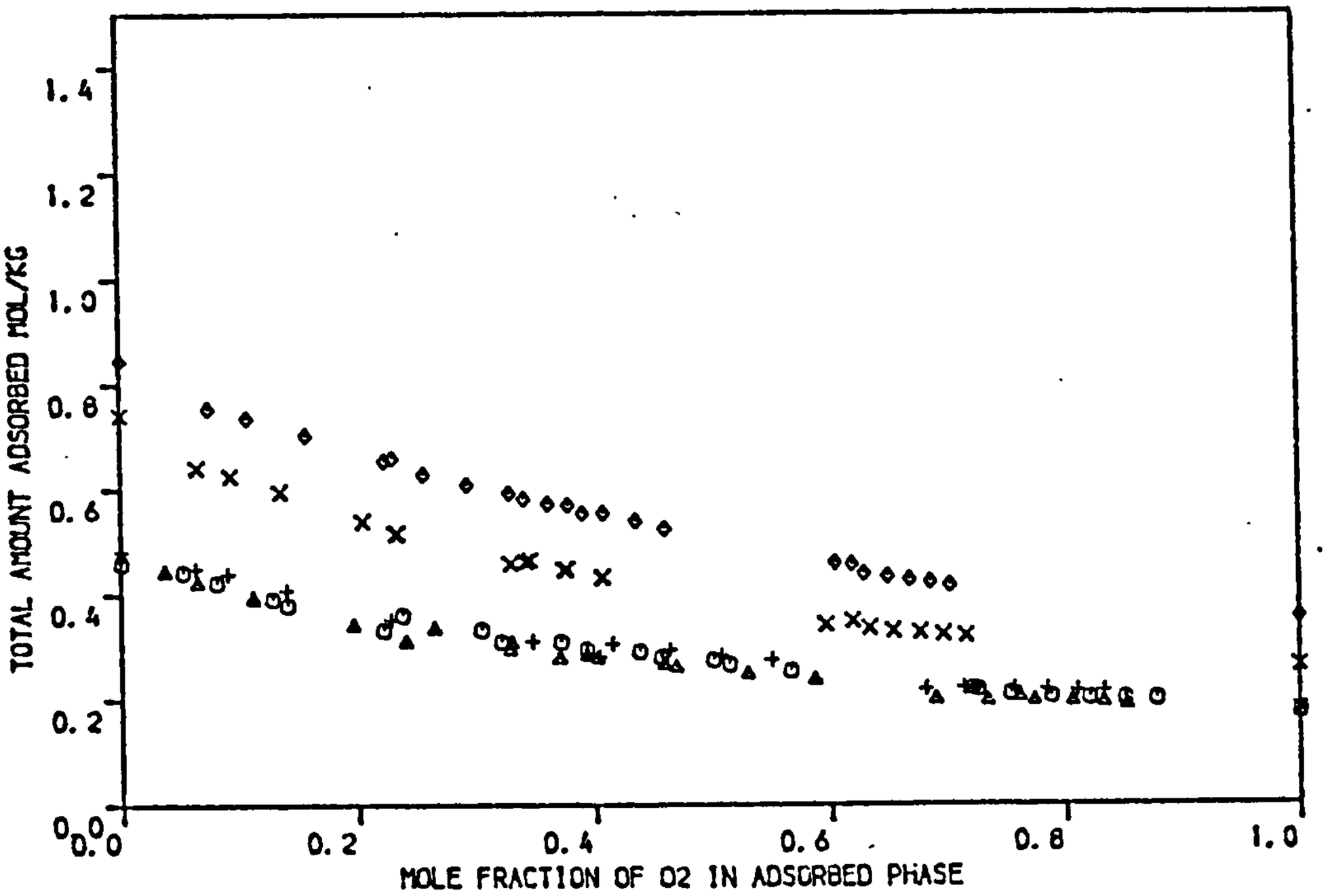

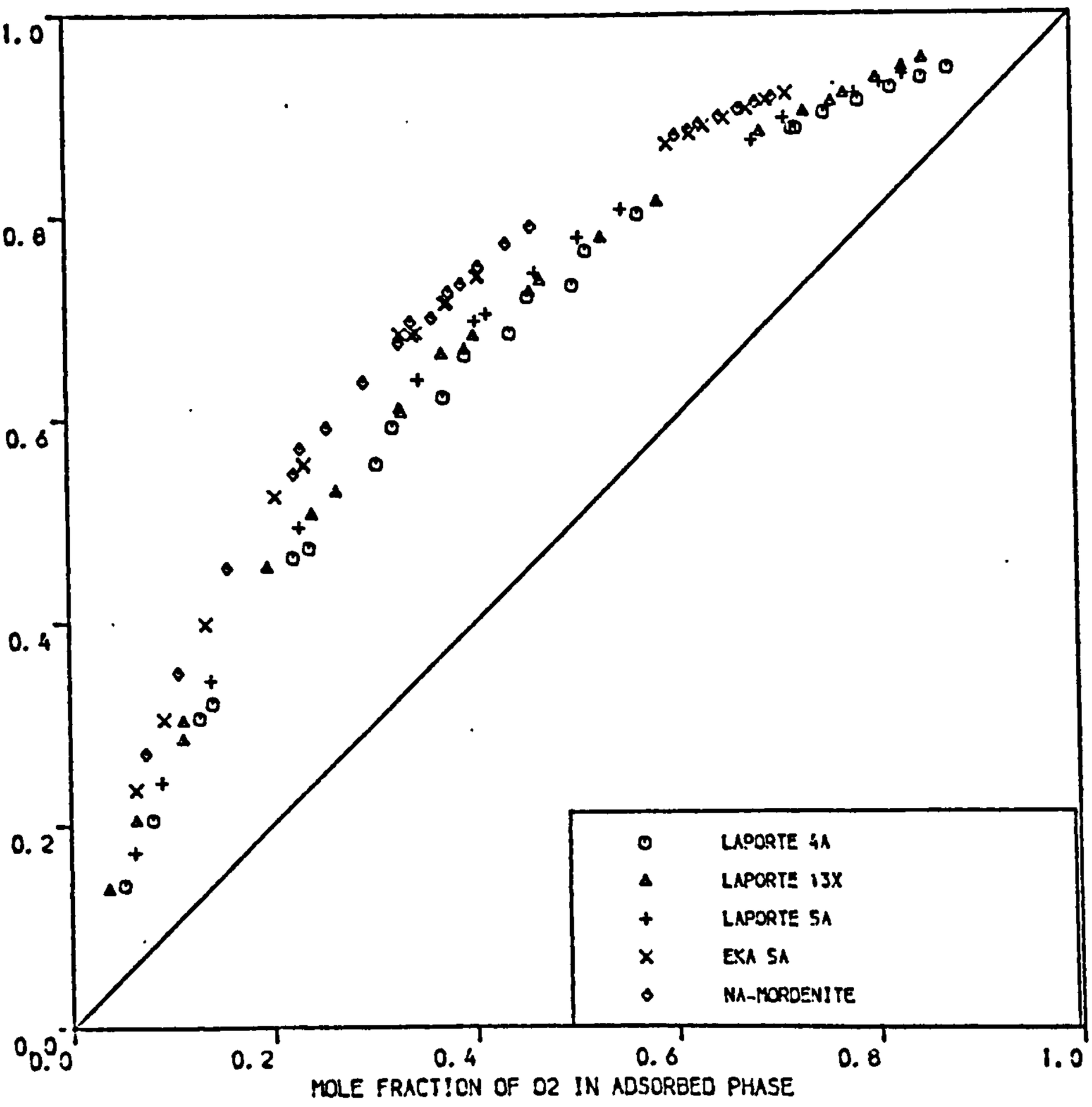

FIGURE 4.21 BINARY ADSORPTION EQUILIBRIA DATA OF O2/N2 ON LAPORTE 4A, LAPORTE 13X, LAPORTE 5A, EKA 5A AND NA-MORDENITE MOLECULAR SIEVE PELLETS AT 293.15 K (PRESSURE = 1.7 BAR)

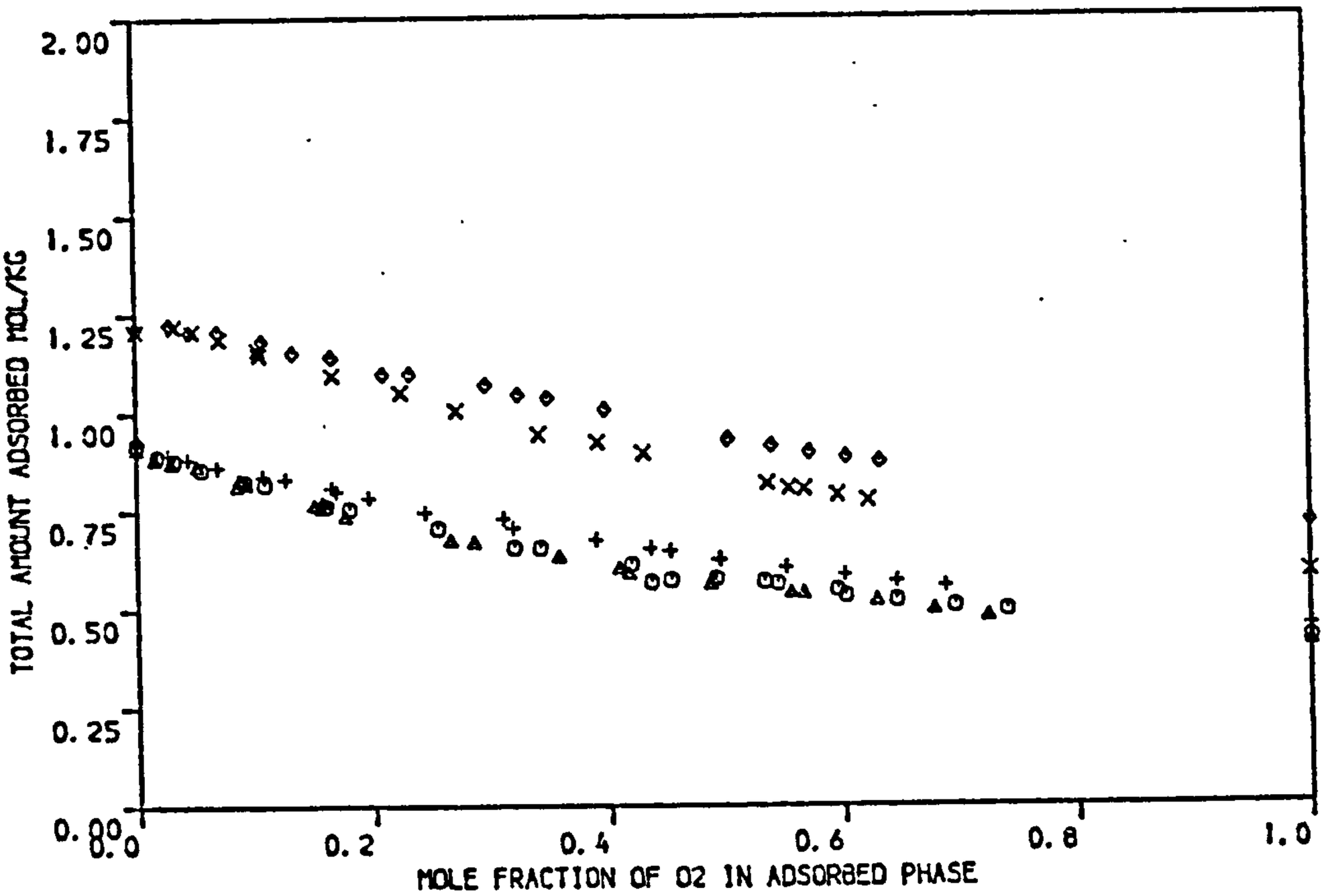

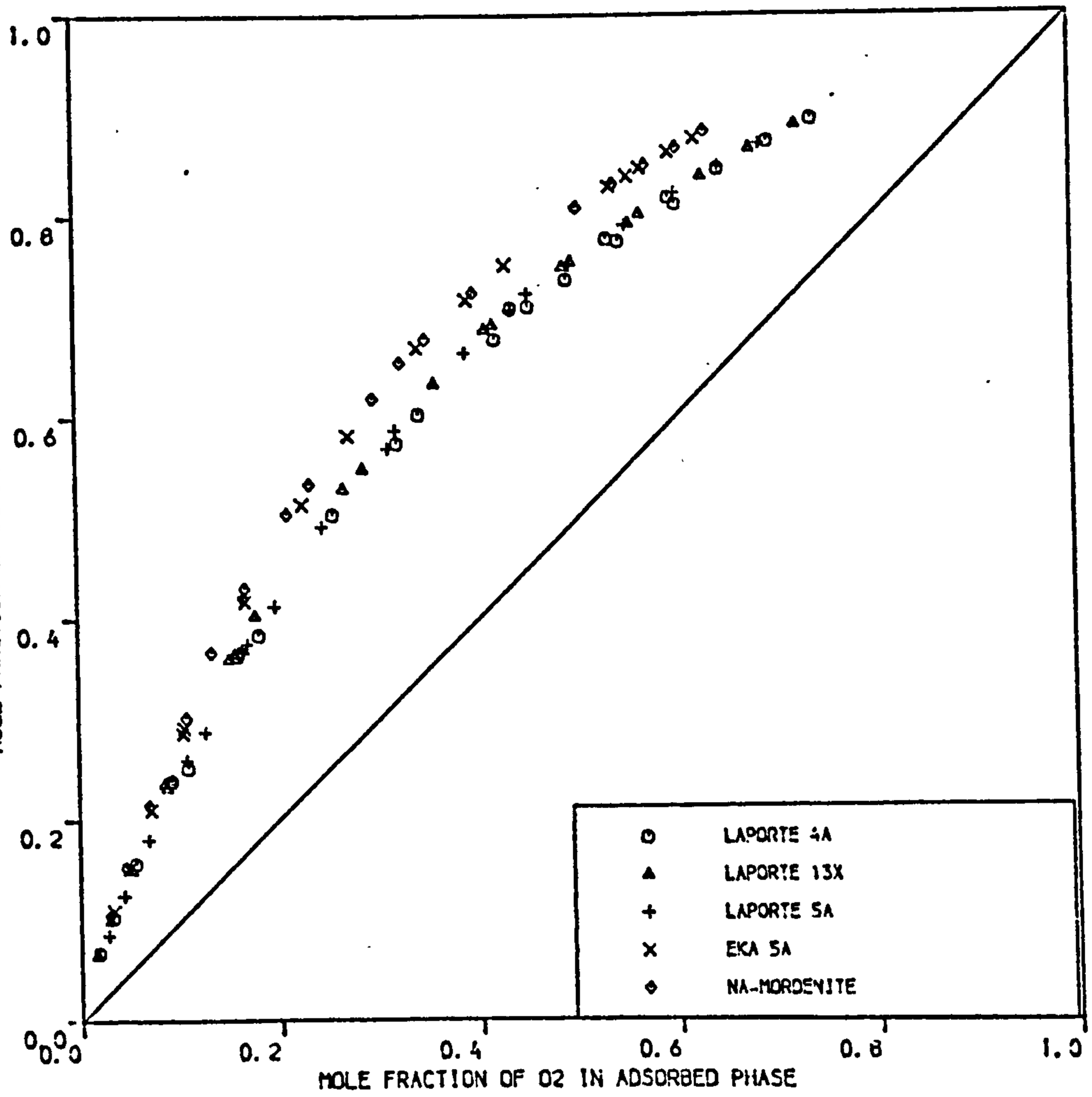

FIGURE 4.22 BINARY ADSORPTION EQUILIBRIA DATA OF O2/N2 ON LAPORTE 4A, LAPORTE 13X, LAPORTE 5A, EKA 5A AND NA-MORDENITE MOLECULAR SIEVE PELLETS AT 293.15 K (PRESSURE ≈ 4.4 BAR)

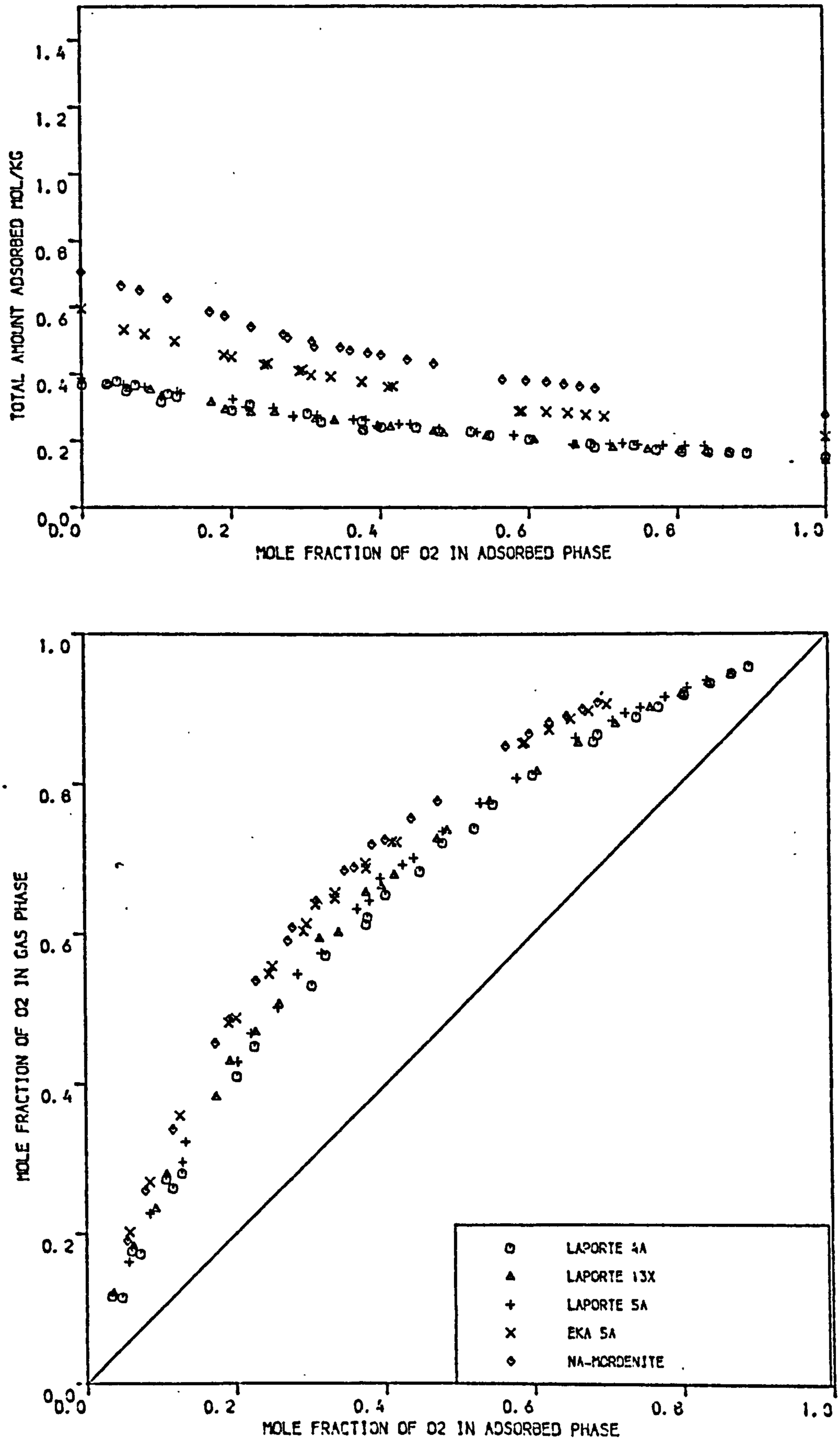

FIGURE 4.23 BINARY ADSORPTION EQUILIBRIA DATA OF O2/N2 ON LAPORTE 4A, LAPORTE 13X, LAPORTE 5A, EKA 5A AND NA-MORDENITE MOLECULAR SIEVE PELLETS AT 303.15 K (PRESSURE ≈ 1.7 BAR)

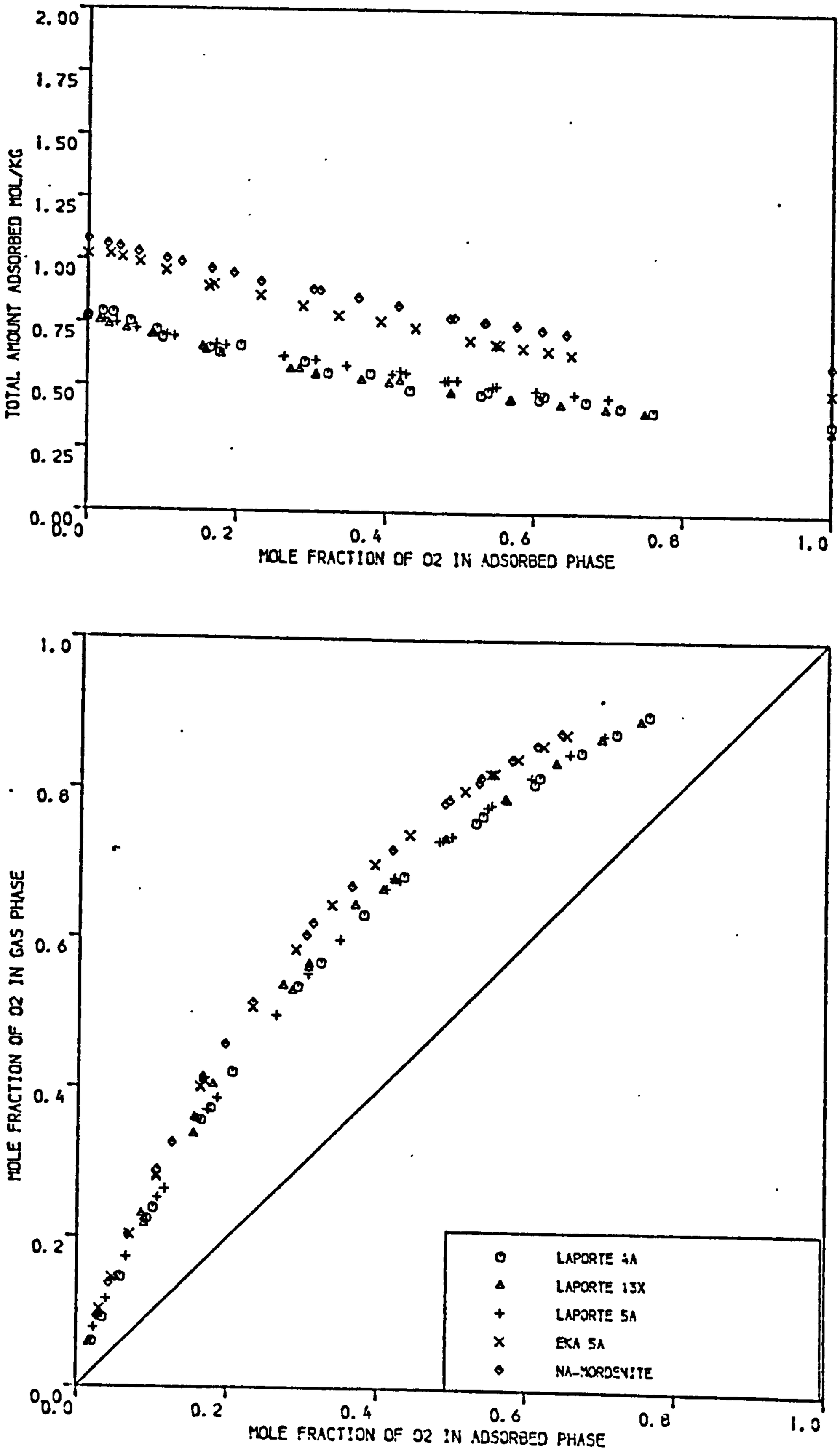

FIGURE 4.24 BINARY ADSORPTION EQUILIBRIA DATA OF O2/N2 ON LAPORTE 4A, LAPORTE 13X, LAPORTE 5A, EKA 5A AND NA-MORDENITE MOLECULAR SIEVE PELLETS AT 303.15 K (PRESSURE = 4.4 BAR)

1. At a temperature 278.15 K and pressure 1.7 bar (Figure 4.19)

(a) For low oxygen concentration in the adsorbed phase up to 30%:

Separation factor on EKA 5A > Separation factor on Na-Mordenite > Separation factor on Laporte 5A Ω Separation factor on Laportes 4A and 13X

(b) For mole fraction of oxygen in the adsorbed phase between 0.3 and 0.8:

Separation factor on Na-Mordenite Ω Separation factor on EKA 5A > Separation factor on Laporte 5A > Separation factor on Laporte 13X > Separation factor on Laporte 4A

For mole fractions of oxygen in the adsorbed phase greater than 0.8 the separation factor on Laporte adsorbents are approximately the same.

(c) For a given adsorbed phase concentration:

Total amount adsorbed on Mordenite > Total amount adsorbed on EKA 5A > Total amount adsorbed on Laporte 5A > Total amount adsorbed on Laporte 13X Ω Total amount adsorbed on Laporte 4A

2. At a temperature 278.15 K and pressure 4.4 bar (Figure 4.20)

(a) For oxygen concentrations in the adsorbed phase up to 20% the separation factor for the five adsorbents is approximately the same and the total amount adsorbed on Laportes adsorbents is approximately the same and less than that of EKA 5A and Na-Mordenite. The total amount adsorbed on EKA 5A is more than that on Na-Mordenite for this concentration range.

(b) For oxygen concentrations in the adsorbed phase greater than 20%:

Separation factor on Mordenite Ω Separation factor on EKA 5A > Separation factor on Laportes adsorbents

The separation on Laportes adsorbents is approximately the same throughout the entire concentration range.

(c) For a given oxygen concentration in the adsorbed phase greater than 20%:

Total amount adsorbed on Mordenite	>	Total amount adsorbed on EKA 5A	>	Total amount adsorbed on Laporte 5A	Ω	Total amount adsorbed on Laporte 13X	>	Total amount adsorbed on Laporte 4A

3. At a temperature 293.15 K and pressure 1.7 bar (Figure 4.21)

For the entire range of oxygen concentration in the adsorbed phase:

Separation factor on Na-Mordenite	Ω	Separation factor on EKA 5A	>	Separation factor on Laporte 5A	Ω	Separation factor on Laporte 13X	>	Separation factor on Laporte 4A

and

Total amount adsorbed on Mordenite	>	Total amount adsorbed on EKA 5A	>	Total amount adsorbed on Laportes adsorbents

4. At a temperature 293.15 K and pressure 4.4 bar (Figure 4.22)

(a) For oxygen concentrations in the adsorbed phase up to 10% the separation factors on the five adsorbents are approxi-mately the same. The total amount adsorbed is also approxi-mately the same for both EKA 5A and Na-Mordenite and is greater than that on Laportes adsorbents.

(b) For oxygen concentrations in the adsorbed phase greater than 10%:

Separation factor on Na-Mordenite	Ω	Separation factor on EKA 5A	>	Separation factor on Laportes adsorbents

and

Total amount adsorbed on Mordenite > Total amount adsorbed on EKA 5A > Total amount adsorbed on Laporte 5A > Total amount adsorbed on Laporte 4A & 13X

5. At a temperature 303.15 K and pressure 1.7 bar (Figure 4.23)

(a) For oxygen concentration in the adsorbed phase up to 10% the separation factor on EKA 5A and Na-Mordenite is approximately the same and is slightly greater than that on Laportes adsorbents.

(b) For oxygen concentrations in the adsorbed phase greater than 10%:

Separation factor on Na-Mordenite > Separation factor on EKA 5A > Separation factor on Laporte 5A $\underline{\Omega}$ Separation factor on Laporte 13X > Separation factor on Laporte 4A

For oxygen concentrations in the adsorbed phase greater than 80% the separation on Laportes adsorbents is approximately the same.

(c) For the entire range of oxygen concentrations in adsorbed phase:

Total amount adsorbed on Na-Mordenite > Total amount adsorbed on EKA 5A > Total amount adsorbed on Laportes adsorbents

6. At a temperature 303.15 K and pressure 4.4 bar (Figure 4.24)

(a) For oxygen concentrations in the adsorbed phase up to 10% the separation factor for the five adsorbents is approximately the same.

(b) For oxygen concentrations in the adsorbed phase greater than 10%:

Separation factor on Na-Mordenite $\underline{\Omega}$ Separation factor on EKA 5A > Separation factor on Laportes adsorbents

(c) For the entire range of oxygen compositions in the adsorbed phase:

Total amount adsorbed on Na-Mordenite > Total amount adsorbed on EKA 5A > Total amount adsorbed on Laportes adsorbents

General Observation

From the above it is clear that the zeolite samples of the Mordenite type and type 5A (EKA) gave better separation factors than the other samples studied. Going back to Table 4.1 it is seen that the highest N_2/O_2 ratio for the pure components is on Laporte 13X and the lowest ratio is on Na-Mordenite. From this one might expect a better separation factor on Laporte 13X than on Na-Mordenite but the opposite is true. The explanation that might be offered to this is that Na-Mordenite has a significantly greater affinity for nitrogen than Laporte 13X which in turn might restrict the active sites of the zeolite for O_2 when the binary mixtures are studied and thus a better separation factor is obtained.

The significant difference in the separation factor between EKA 5A and Laporte 5A could be due to reasons stated before when discussing the pure component isotherm, that is different thermal treatment during processing the zeolite and the type and proportion of binder used.

Comparison with Published Data

The following comparisons are made for the binary equilibria data obtained in this work with other published data:

(a) The binary equilibria data on Laporte 5A and EKA 5A at temperatures 293.15 and 303.15 K and a pressure 1.7 bar are compared with data of Huang[28] on Linde 5A (U.S.A.) at 298 K and a pressure 0.8 in Figure 4.25. From the figure it is seen that the separation factor on Linde 5A is almost identical to Laporte 5A at 293.15 K

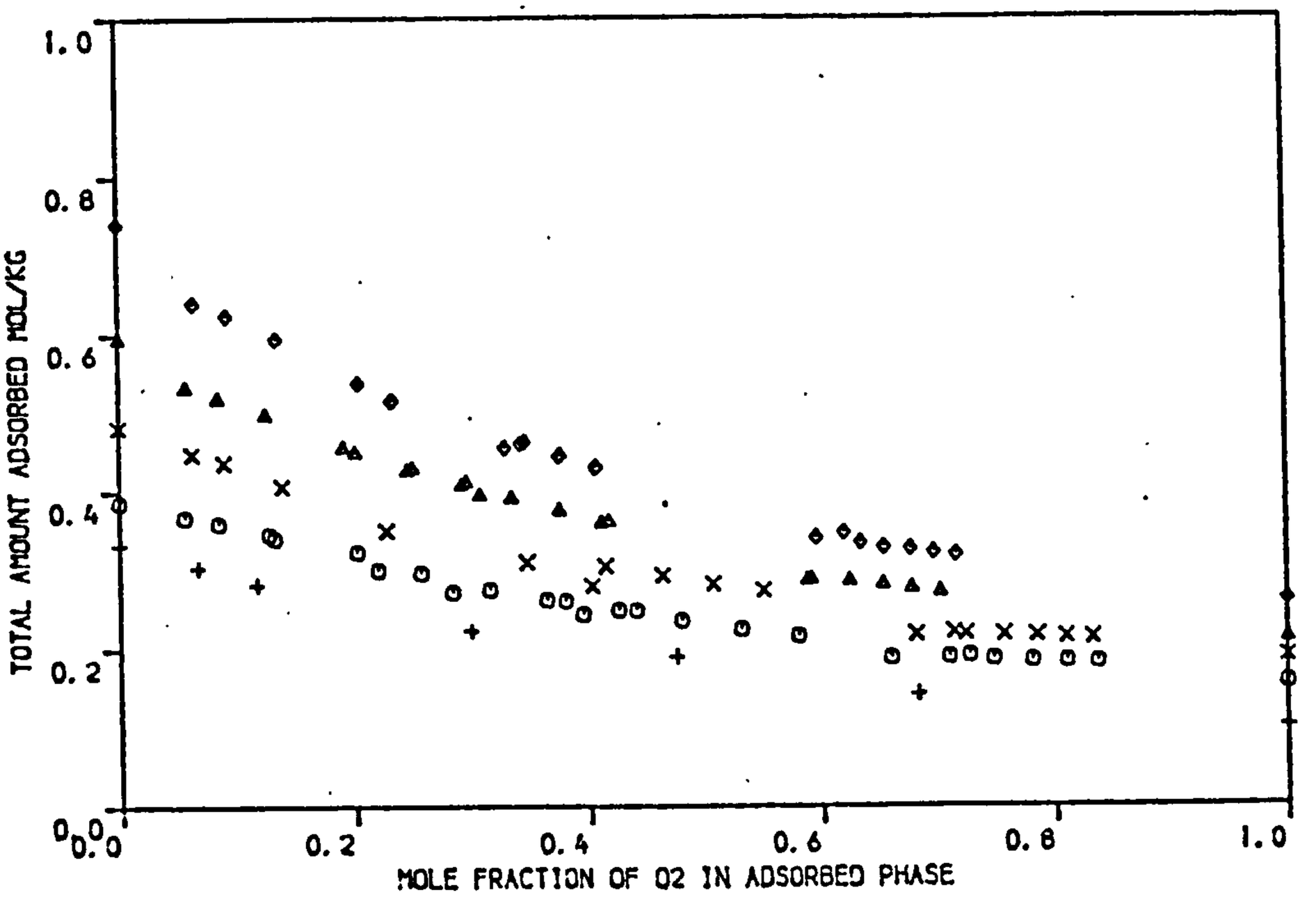

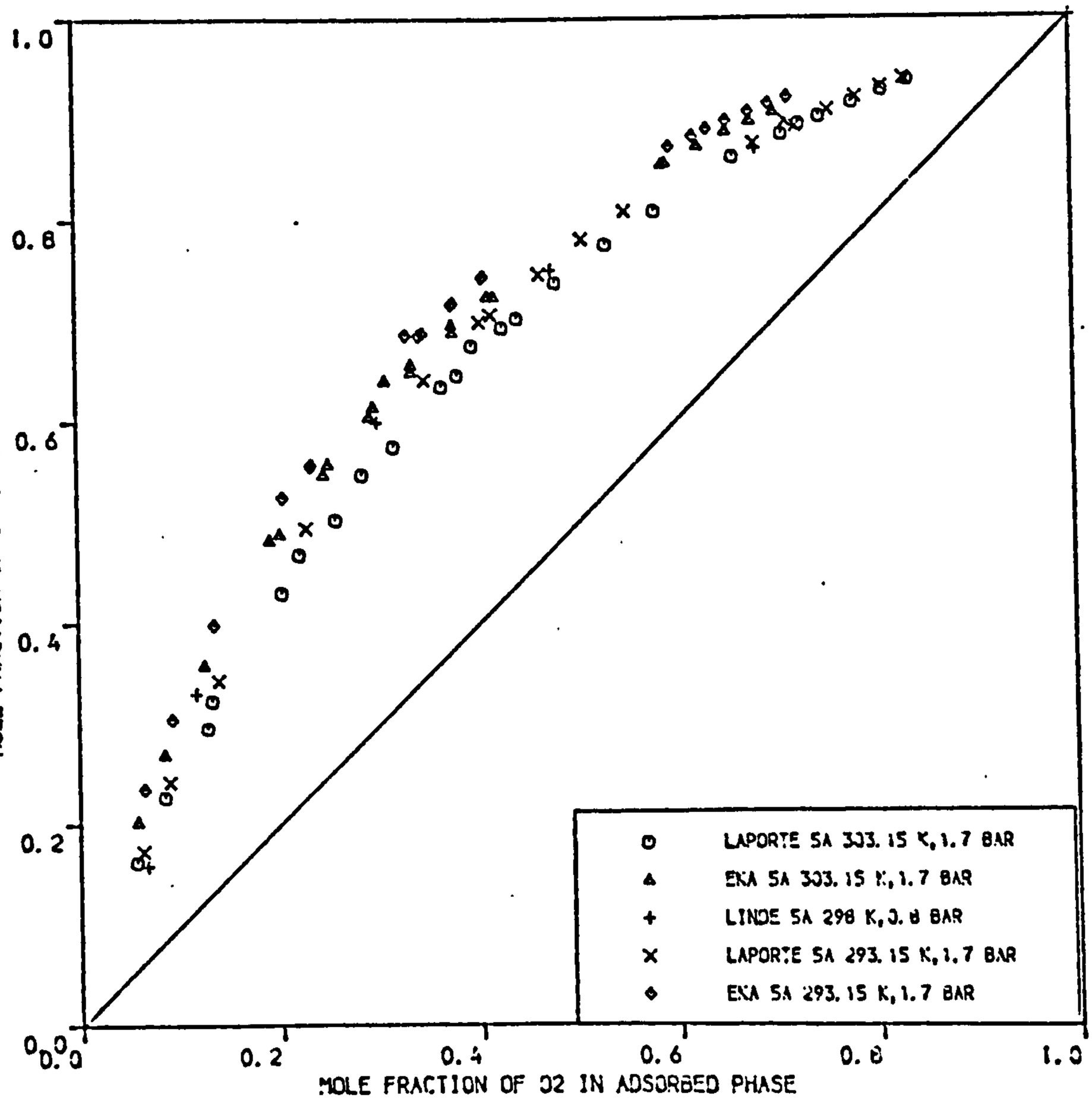

FIGURE 4.25 COMPARISON OF EXPERIMENTAL BINARY EQUILIBRIA DATA OF O2/N2 ON LAPORTE 5A AND EKA 5A WITH REPORTED EXPERIMENTAL DATA OF HUANG (REF. 28) ON LINDE 5A

while the total amount adsorbed could be in line with EKA 5A if the differences in temperature and pressure are considered.

(b) The binary equilibria data on Laporte 5A and EKA 5A at temperatures 293.15 and 303.15 K and pressure 4.4 bar are compared with data of Torii et al[55] on 5A (Japan) at 298.15 K and pressure 4.91 bar in Figure 4.26. From the figure it is noticed that the separation factor on 5A (Japan) at pressure 4.9 bar is almost identical to that on Laporte 5A at 293.15 K while the total amount adsorbed on 5A (Japan) are similar to that on EKA 5A at 293.15 K.

Although there is reported work by Torii et al on 5A at 298.15 K and pressure 0.98 bar, no comparison could be made due to the reported data being below 30 per cent oxygen concentration in the adsorbed phase.

It is worthwhile to note that Torii et al[55] tested their data on 5A at a temperature 298.15 K and pressure 2.94 bar against predicted values from the ideal adsorbed theory (IAST)[36] and the results showed significant deviations. However, in Section 4.2.3 it is shown that the IAST predicted the binary data of this work within good accuracy.

(c) The binary equilibria data on Na-Mordenite at temperature 303.15 and 293.15 K and pressure 1.7 bar are compared with the data of Torii et al[55] on Mordenite (Japan) at 298.15 K and pressure 0.98 bar in Figure 4.27. From the figure it is seen that the separation factor on Mordenite (Japan) is significantly greater than that on Mordenite of this work while the total amount adsorbed could be similar if the differences in temperature and pressure are considered.

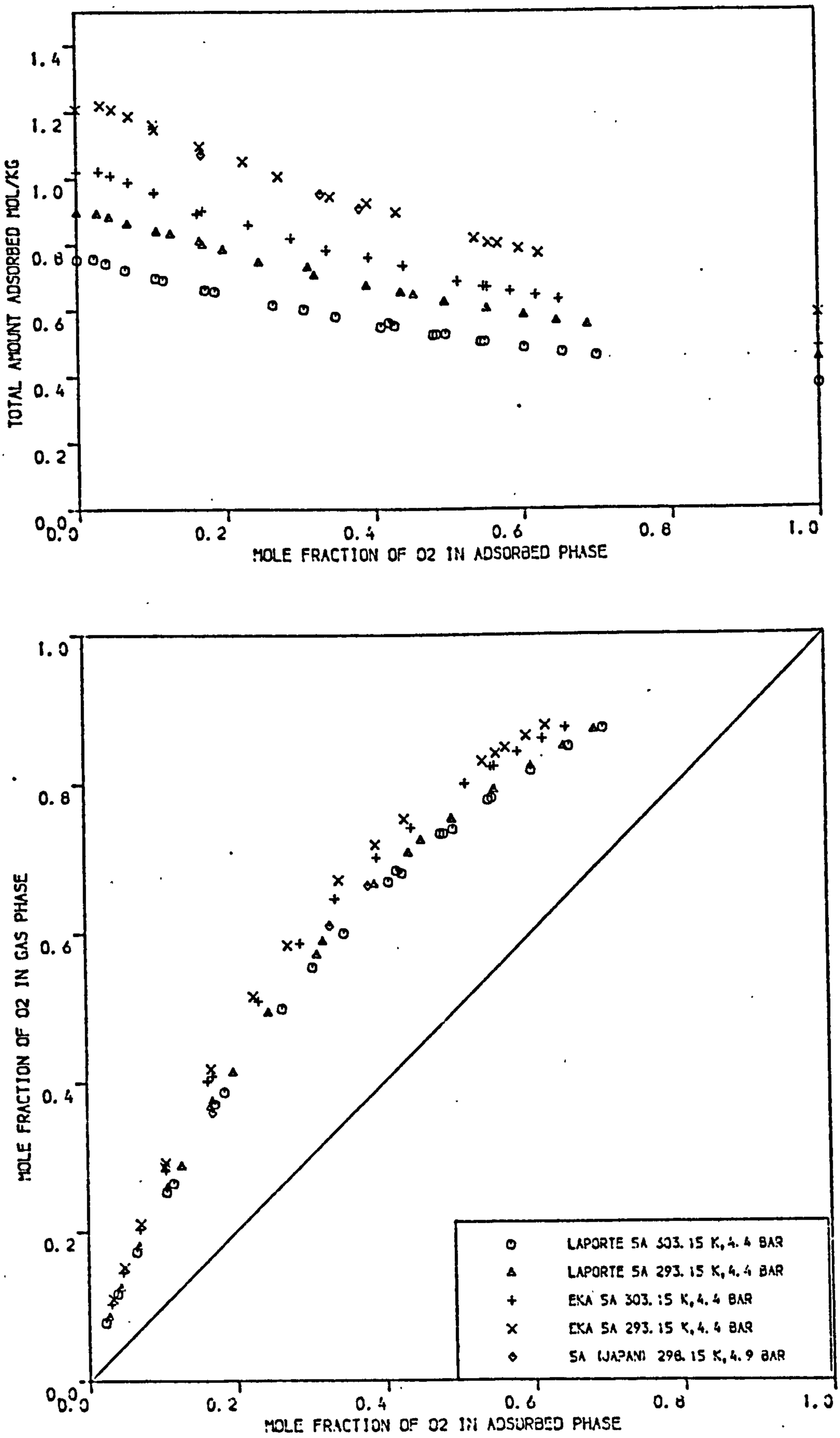

FIGURE 4.26 COMPARISON OF EXPERIMENTAL BINARY EQUILIBRIA DATA OF O2/N2 ON LAPORTE 5A AND EKA 5A WITH REPORTED EXPERIMENTAL DATA OF TORII ET AL (REF. 55) ON 5A (JAPAN)

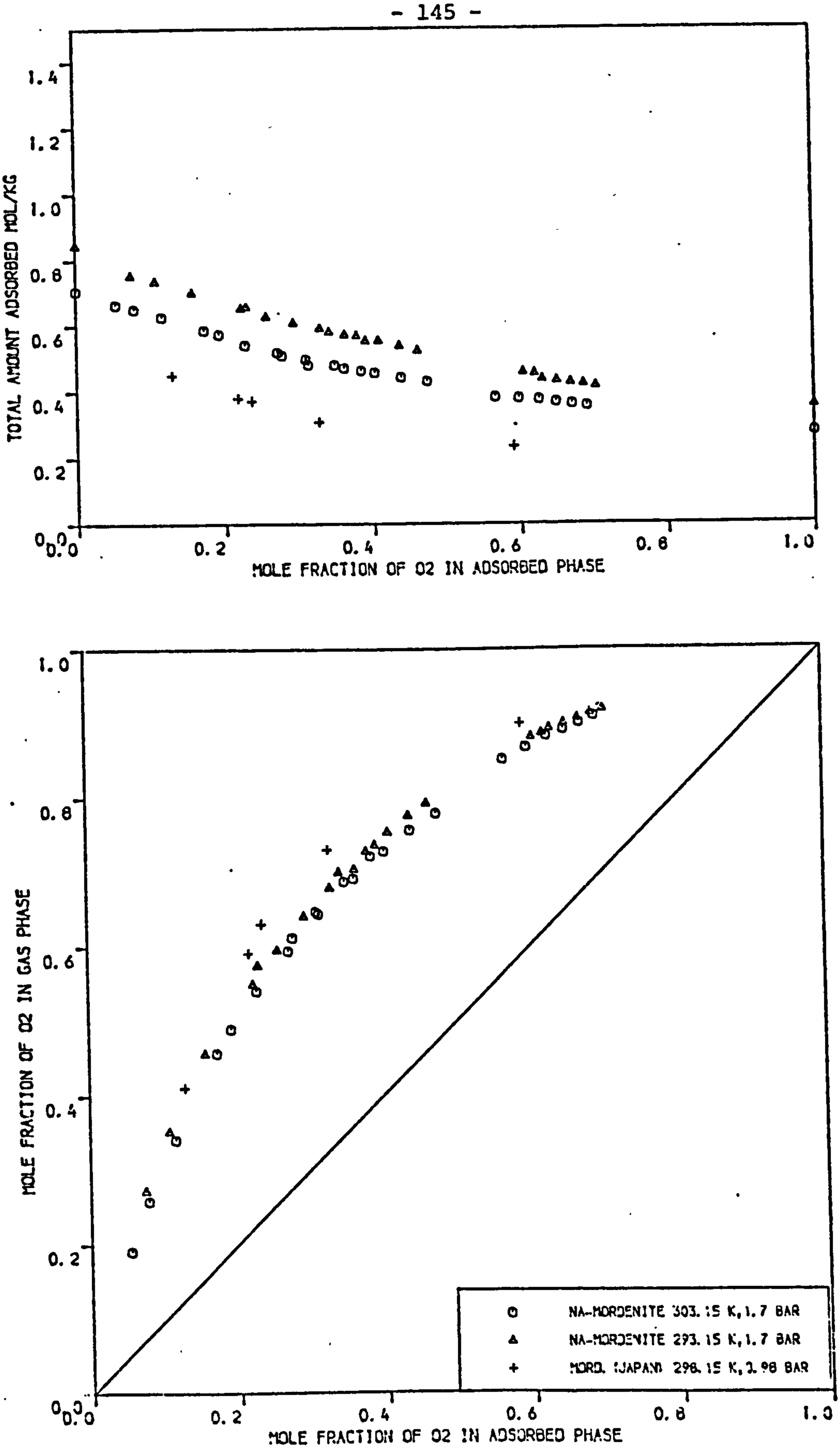

FIGURE 4.27 COMPARISON OF EXPERIMENTAL BINARY EQUILIBRIA DATA OF O2/N2 ON NA-MORDENITE WITH REPORTED EXPERIMENTAL DATA OF TORII ET AL (REF. 55) ON MORDENITE (JAPAN)

(d) The binary equilibria data on Na-Mordenite at temperatures of 303.15 K and 293.15 K and pressure 4.4 bar are compared with the data of Torii et al[55] on Mordenite (Japan) at 298.15 K and pressure 4.91 bar in Figure 4.28. From the figure it is noticed that the separation factors on Mordenite (Japan) is significantly better than that on Mordenite of this work but the total amount adsorbed is significantly less on Mordenite (Japan).

4.2.3 Analysis and interpretation of results

The purpose of this section is to compare the experimental data with predicted values from various theoretical models and to measure the deviation of the experimental binary systems from ideal behaviour in the adsorbed phase by calculating activity coefficients.

4.2.3.1 Models considered

The models considered in this work are:

(a) The kinetic model of Gonzalez and Holland[31,75] given by Equation (2.43):

$$n_1 = \frac{n_m K_1 P_1 (1 + \theta \Sigma K_1 P_1)}{(1 + \Sigma K_1 P_1)} \qquad (2.43)$$

and the corresponding equation for the other component.

(b) The extended statistical thermodynamic model for gas mixtures[28,42] given by Equation (2.49):

$$n_1 = \frac{\bar{K}_1 P_1 + \sum_j \sum_i (\bar{K}_1 P_1)^i (\bar{K}_2 P_2)^j (1 - i\bar{\beta}_1/v - j\bar{\beta}_2/v)^{i+j}/(i-1)!j!}{1 + \bar{K}_1 P_1 + \bar{K}_2 P_2 + \sum_j \sum_i (\bar{K}_1 P_1)^i (\bar{K}_2 P_2)^j (1 - i\bar{\beta}_1/v - j\bar{\beta}_2/v)^{i+j}/i!j!} \qquad (2.49)$$

and the corresponding equation for the other component.

(c) The semi-empirical model of Cook and Basmadjian[35], (see Section 2.3.3).

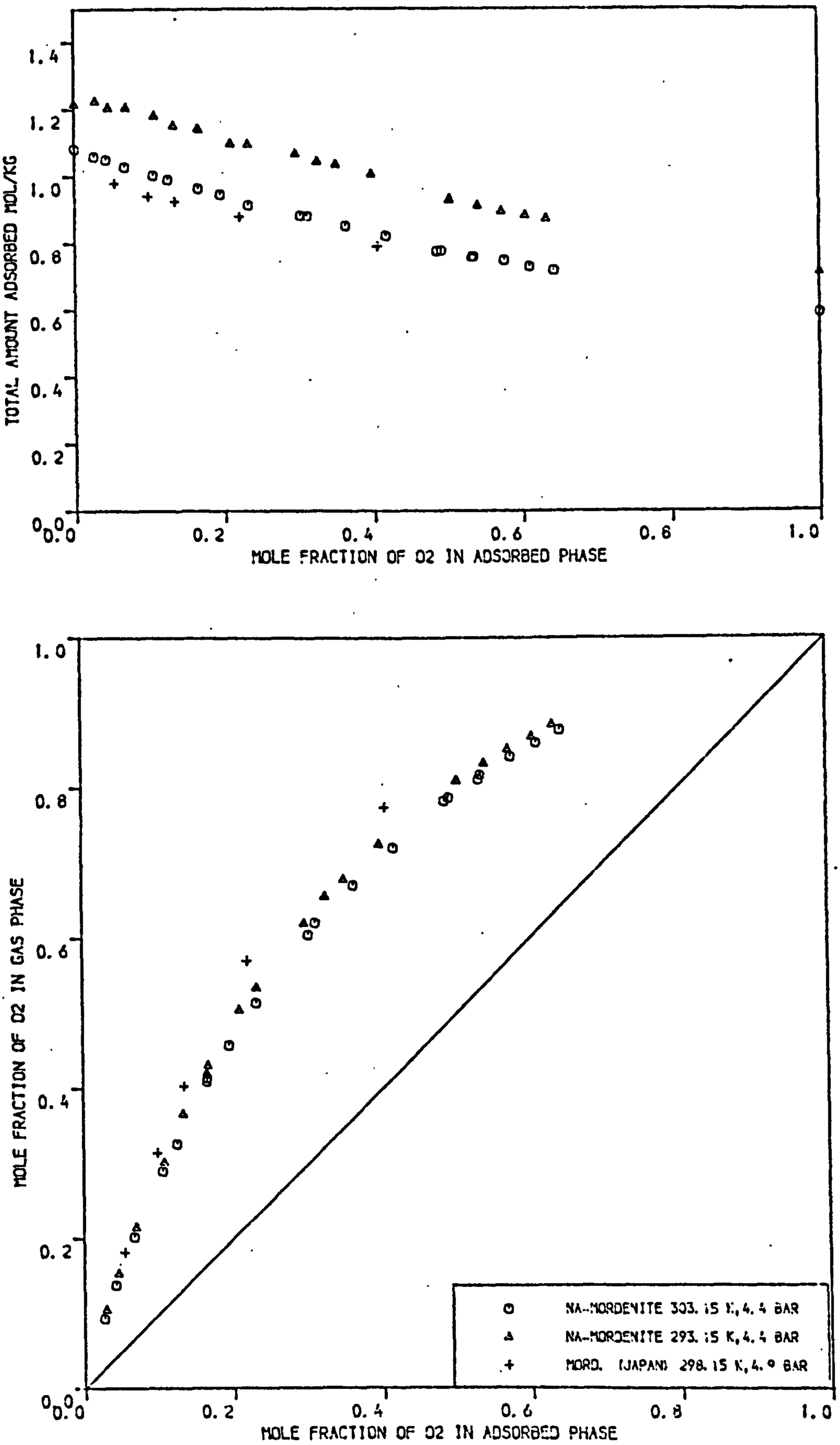

FIGURE 4.28 COMPARISON OF EXPERIMENTAL BINARY EQUILIBRIA DATA OF O2/N2 ON NA-MORDENITE WITH REPORTED EXPERIMENTAL DATA OF TORII ET AL (REF. 55) ON MORDENITE (JAPAN)

(d) The ideal adsorbed solution theory (IAST)[36], (see Section 2.3.4).

(e) The extended vacancy solution model for gas mixtures[43] given by Equations (2.85) to (2.92).

The kinetic model given by Equation (2.43) was used with the regression parameters determined from pure component isotherms (see Table 4.2). For a particular total pressure of gas-mixture and adsorption temperature the mole fraction of one of the components in the gas phase was selected and the partial pressures of both components were calculated. The individual amounts adsorbed were calculated from Equation (2.43) and the corresponding equation for the other component. The mole fraction of each component in the adsorbed phase was then determined. This procedure was again repeated for another selected value of gas phase composition until the system was completely specified.

The statistical thermodynamic model given by Equation (2.49) and the corresponding equation for the other component together with the regression parameters listed on Table 4.4 were used. The prediction procedure is identical to the kinetic model but this model contains two adjustable parameters, i and j, which are the number of molecules of component i and component j in a zeolite cavity respectively. These parameters were first selected arbitrarily and were then adjusted until the total amount adsorbed approached the pure component values at both boundaries. A listing of the computer programme which was written in Fortran 77 version is shown in Appendix III.

For the semi-empirical model of Cook and Basmadjian Equation (4.1) was used as the fitting model for the pure component isotherms. The prediction procedure used is outlined in the following steps:

(a) At a particular total pressure of the gas mixture and adsorption temperature, the amount adsorbed of

each pure component n_1^o, n_2^o was evaluated from Equation (4.1) using regression parameters listed in Table 4.3.

(b) The two limiting relative volatilities were estimated from Equations (2.57a) and (2.57b). Numerical integration was used for evaluating these equations.

(c) Equations (2.58) and (2.59) were used for evaluating the indeterminate limiting ratios P/x.

(d) It was then assumed that the binary curves AC and BD shown in Figure 2.1 could be linearized in a log-log plot. The slope of each of the binary curves were hence determined through the knowledge of the co-ordinates at both ends of the lines by steps (a) and (c).

(e) The total amount adsorbed of the mixture was evaluated by incrementing the distance between the two pure component values evaluated in step (a) into a number of steps.

(f) For each value of the total amount adsorbed evaluated in step (e) the corresponding value of P/x was evaluated through the knowledge of the slopes of the binary lines determined in step (d).

(g) One of the unknown mole fractions in the adsorbed phase was evaluated by Equation (2.60) and using the mole fraction constraint $x_1 + x_2 = 1$, the individual amounts adsorbed were evaluated for each value of total amount adsorbed determined in step (e).

A listing of the computer programme which was written in Fortran 77 version is shown in Appendix III.

For the ideal adsorbed solution theory (IAST) Equation (4.1) was again used as the fitting model for the pure component isotherms. The prediction procedure used is outlined in the following steps:

(a) The amount adsorbed of each pure component at the total pressure of the gas mixture was evaluated from Equation (4.1) using regression parameters listed in Table 4.3.

(b) Knowing the functional relation of the gas pressure to the amount adsorbed (Equation (4.1)), the spreading pressure of each component, or more precisely the term $\frac{\pi A}{RT}$, corresponding to the amount adsorbed for each pure component at the total pressure of the mixture was evaluated by Equation (2.11b) using numerical integration. These spreading pressures represent the mixture spreading pressure at the two ends, i.e. when only pure component 1 is present and in the second case when only pure component 2 is present. The spreading pressure of the mixture will lie between these two values and was evaluated by incrementing the distance between these two values into a number of steps.

(c) For each spreading pressure value evaluated in step (b) the corresponding amount adsorbed of each of the pure components was evaluated from Equation (2.11b) through application of Newton-Raphson search method.

(d) The equilibrium pressure of each pure component (P^o) corresponding to the amount adsorbed evaluated in step (c) was obtained using Equation (4.1).

(e) Combining Equations (2.71a) and (2.71b) the mole fraction of each component was evaluated by:

$$x_1 = (P_2^o - P)/(P_2^o - P_1^o) \qquad (4.5)$$

$$x_2 = 1 - x_1.$$

(f) The mole fraction of each component in the gas phase was evaluated from Equation (2.71a) and applying the mole fraction constraint $y_1 + y_2 = 1$.

(g) The total amount adsorbed was evaluated from Equation (2.73). The individual amounts adsorbed were hence calculated through the knowledge of the mole-fractions in the adsorbed phase determined in step (e).

A listing of the computer programme which was written in Fortran 77 version is shown in Appendix III.

The vacancy solution model given by Equations (2.85) - (2.92) was used with the regression parameters determined from the pure component isotherms (see Table 4.5). It was assumed that the adsorbate-adsorbate interactions parameters Λ_{12} and Λ_{21} are unity. The prediction procedure already outlined in Chapter 2 (Section 2.3.5.1) was used. A listing of the computer programme used is shown in Appendix III.

4.2.3.2 Calculation of activity coefficients

The deviation of an adsorbed solution from ideal behaviour is accounted for by considering the activity coefficients for each component in the adsorbed phase. The activity coefficients can be calculated by Equation (2.71$\bar{a}$) using the binary equilibria data together with the pure component isotherms. The procedure used for calculating the activity coefficients for the binary systems studied is outlined below:

(a) The average mixture pressure was taken to be the adsorption pressure. The amount adsorbed of one of the pure components, say oxygen, at the pressure of the mixture was determined by Equation (4.1) using the regression parameters listed in Table 4.3. Equations (4.1) and (2.11) were then used to determine

the spreading pressure of this pure component, or more precisely the term $\frac{\pi A}{RT}$, corresponding to the amount adsorbed at the pressure of the mixture.

(b) Equation (2.10) which gives the spreading pressure of the mixture can be re-written in an integrated form between the limits $y_1 = 1$, $\Omega = \Omega_1^o$ and $y_1 = y_1$, $\Omega = \Omega$ as

$$\Delta\Omega = \frac{A\ \Delta\pi}{RT} = \int_1^{y_1} n_t \frac{x_1 - y_1}{y_1\ y_2}\ d\ y_1 \quad \text{(constant P and T)} \qquad (4.6)$$

where $\Delta\Omega = \Omega - \Omega_1^o$

$$\therefore \quad \Omega = \Omega_1^o + \Delta\Omega \qquad (4.7)$$

Equations (4.6) and (4.7) can be used to calculate the spreading pressure of any binary mixture, or more precisely Ω, being its value always comprised between the spreading pressure Ω_1^o and Ω_2^o of the less and more adsorbed pure component respectively. The expression $n_t \left(\frac{x_1 - y_1}{y_1\ y_2}\right)$ in Equation (4.6) will be indeterminate at the lower limit $y_1 = 1$. This was overcome by curve fitting this expression to a nth order polynomial using NAG subroutine E02ACF[105]. The order of the polynomial wad adjusted to give the best fit. Generally for all the binary systems studied the best fit was obtained for n = 4. The spreading pressure of a specific binary mixture was hence evaluated using numerical integration of Equation (4.6) and adding the value of the less adsorbed pure component spreading pressure (oxygen) to it.

(c) For each spreading pressure value evaluated in step (b) the corresponding amount adsorbed of each of the pure components was evaluated from Equation (2.11) through

application of Newton-Raphson search method.

(d) The equilibrium pressure of each pure component (P_i^o) corresponding to the amount adsorbed evaluated in step (c) was obtained using Equation (4.1).

(e) The activity coefficients for each experimental point could hence be determined by Equation (2.71$\bar{a}$) and the corresponding equation for the other component.

A listing of the computer programme used for evaluating the activity coefficients is shown in Appendix III.

4.2.3.3 Interpretation of results on Laporte 4A

The binary equilibria experimental results on Laporte 4A molecular sieve pellets are replotted on Figures 4.29 - 4.34 together with the predicted equilibria data by the five models studied. The models were used at the average pressure of the experimental data. For the statistical thermodynamic model the predictions were obtained for the values of i, number of molecules of oxygen in the adsorbed phase, and j, number of molecules of nitrogen in the adsorbed phase, in Equation (2.49), adjusted to 10 and 6 respectively.

For the three temperatures and two pressures studied the statistical thermodynamic model, Cook and Basmadjian model and the ideal adsorbed solution theory (IAST) gave approximately the same predicted separation factors and the predicted values were in good agreement with the experimental values with the exception of a maximum deviation of about 7% with the experimental data at temperature 278.15 K and pressure 1.7 bar. The predicted total amount adsorbed by these three models were almost identical to each other at temperatures 303.15 and 293.15 K and pressure of 1.7 bar while slight deviations between the models were encountered at a temperature 278.15 K and pressure 1.7 bar and at the three temperatures

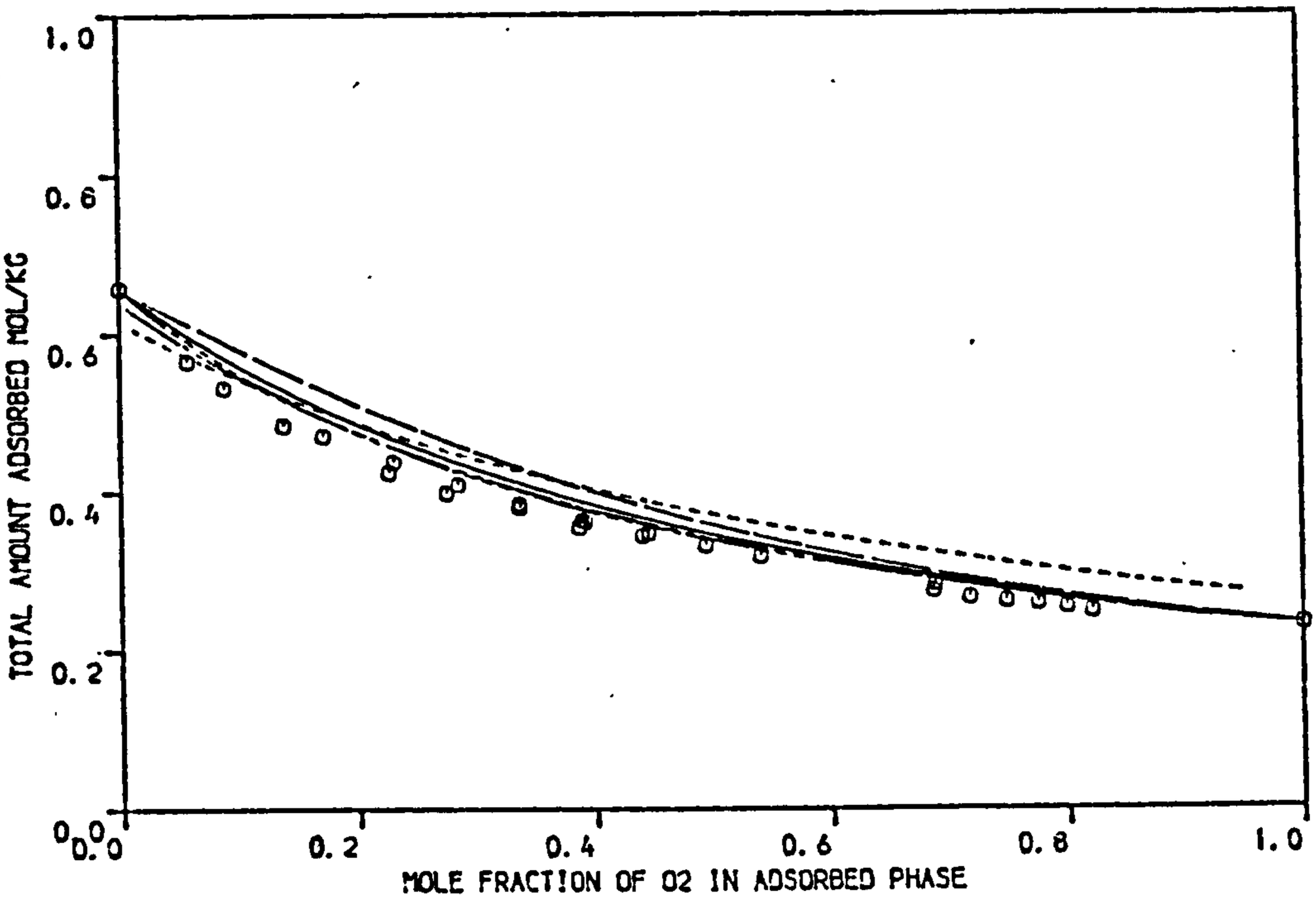

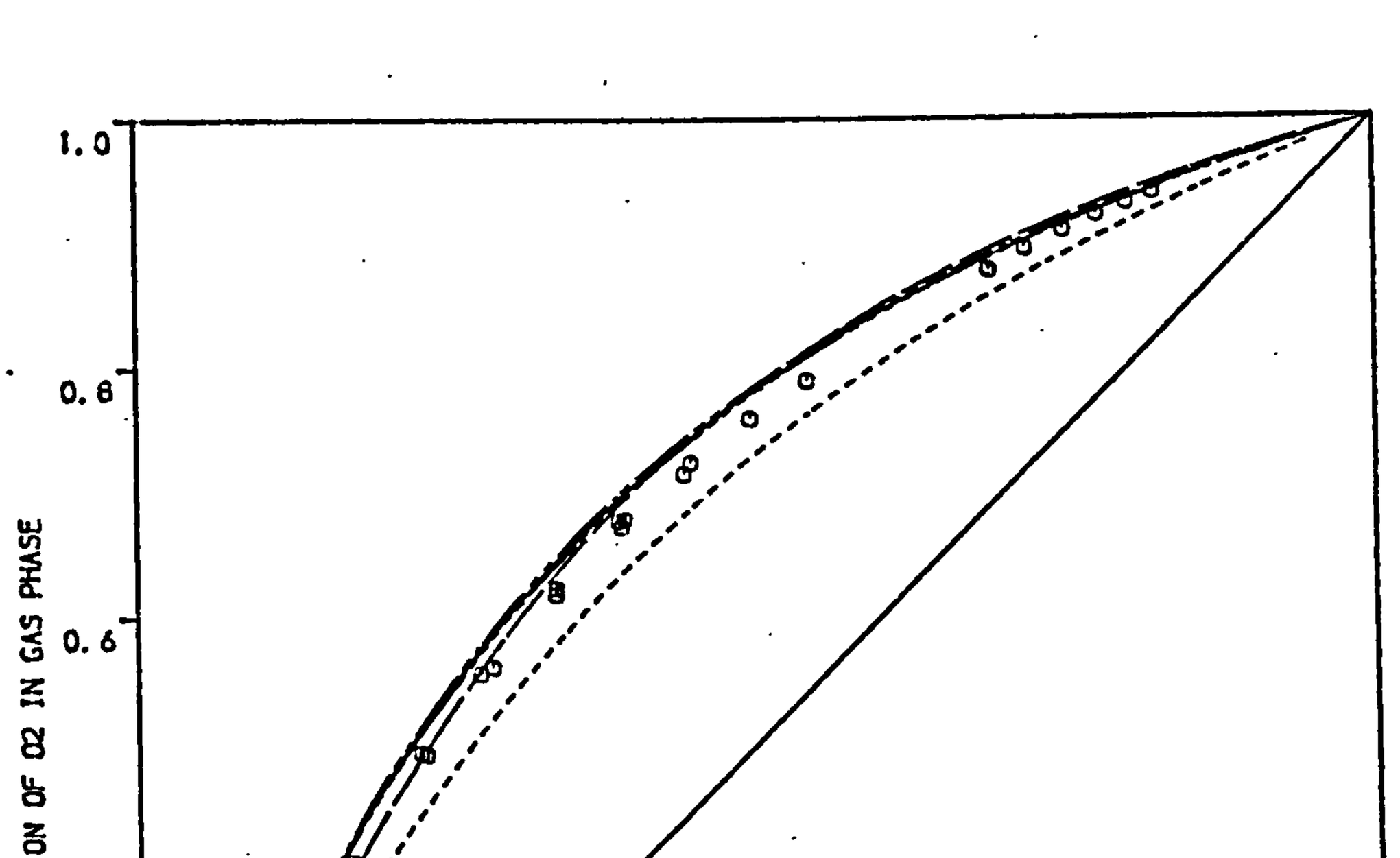

FIGURE 4.29 COMPARISON OF THEORETICAL PREDICTIONS OF VARIOUS MODELS WITH EXPERIMENTAL EQUILIBRIA OF O2/N2 ON LAPORTE 4A MOLECULAR SIEVE PELLETS AT 278.15 K (PRESSURE = 1.7 BAR)

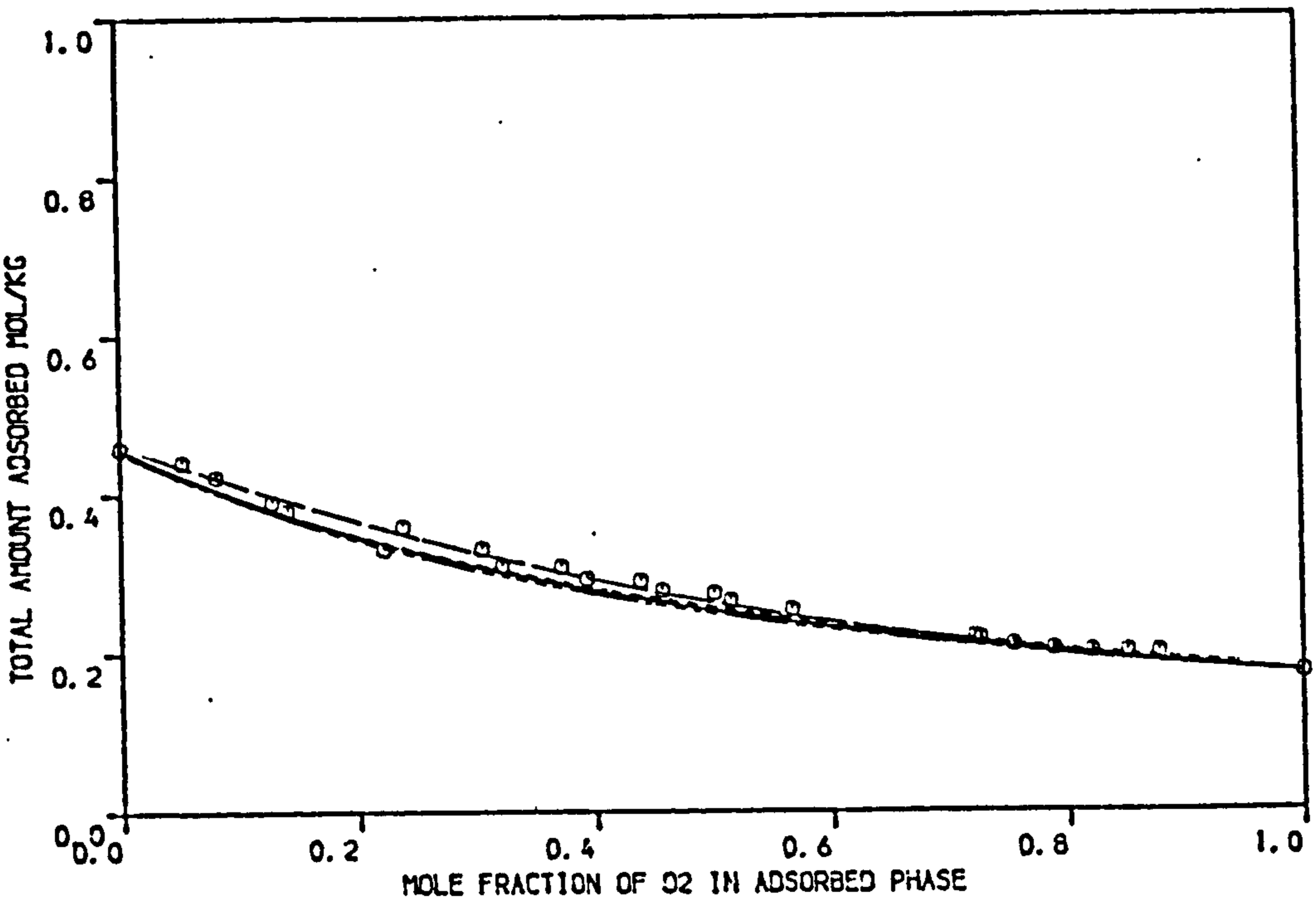

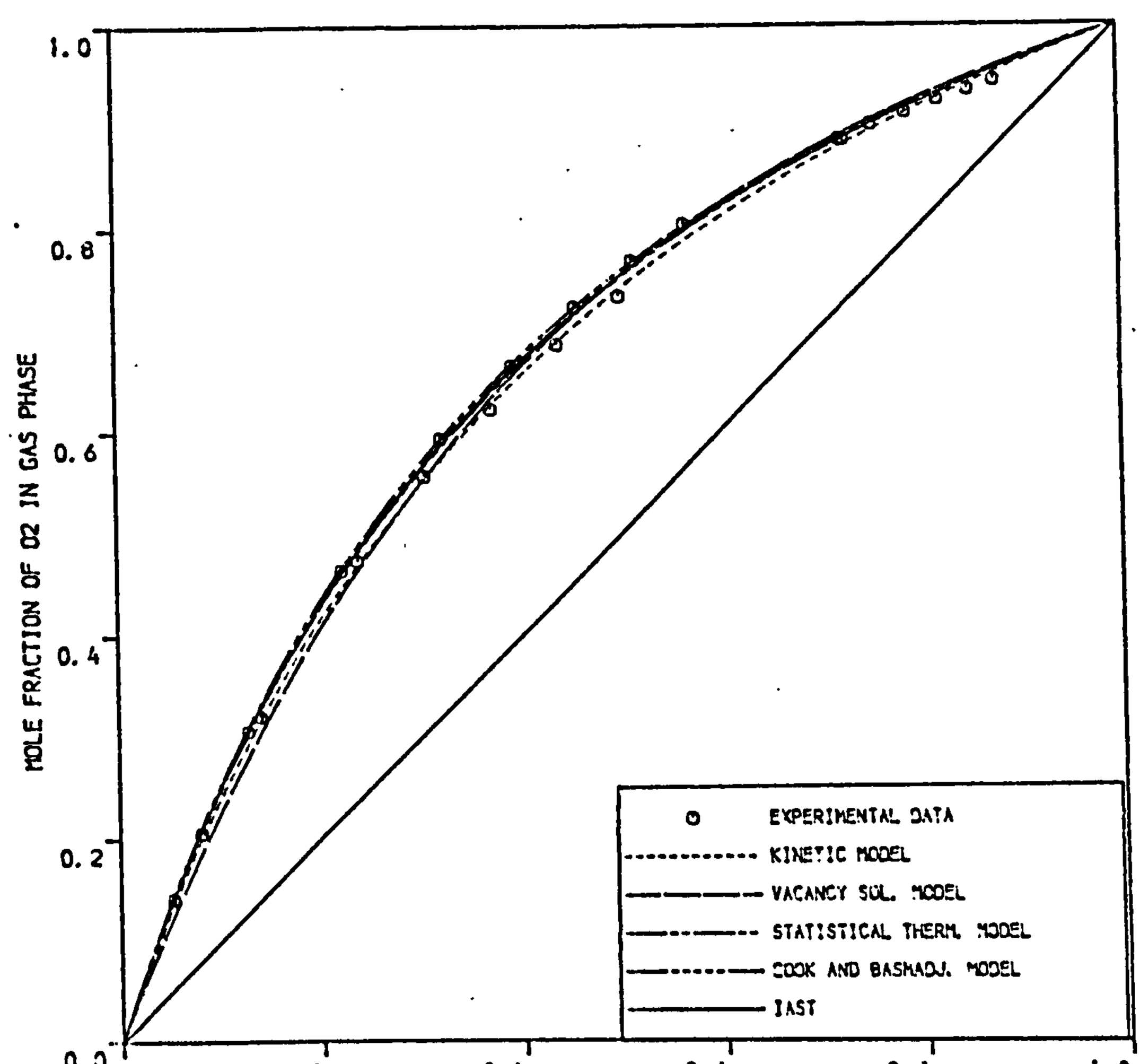

FIGURE 4.30 COMPARISON OF THEORETICAL PREDICTIONS OF VARIOUS MODELS WITH EXPERIMENTAL BINARY EQUILIBRIA OF O2/N2 ON LAPORTE 4A MOLECULAR SIEVE PELLETS AT 293.15 K (PRESSURE = 1.7 BAR)

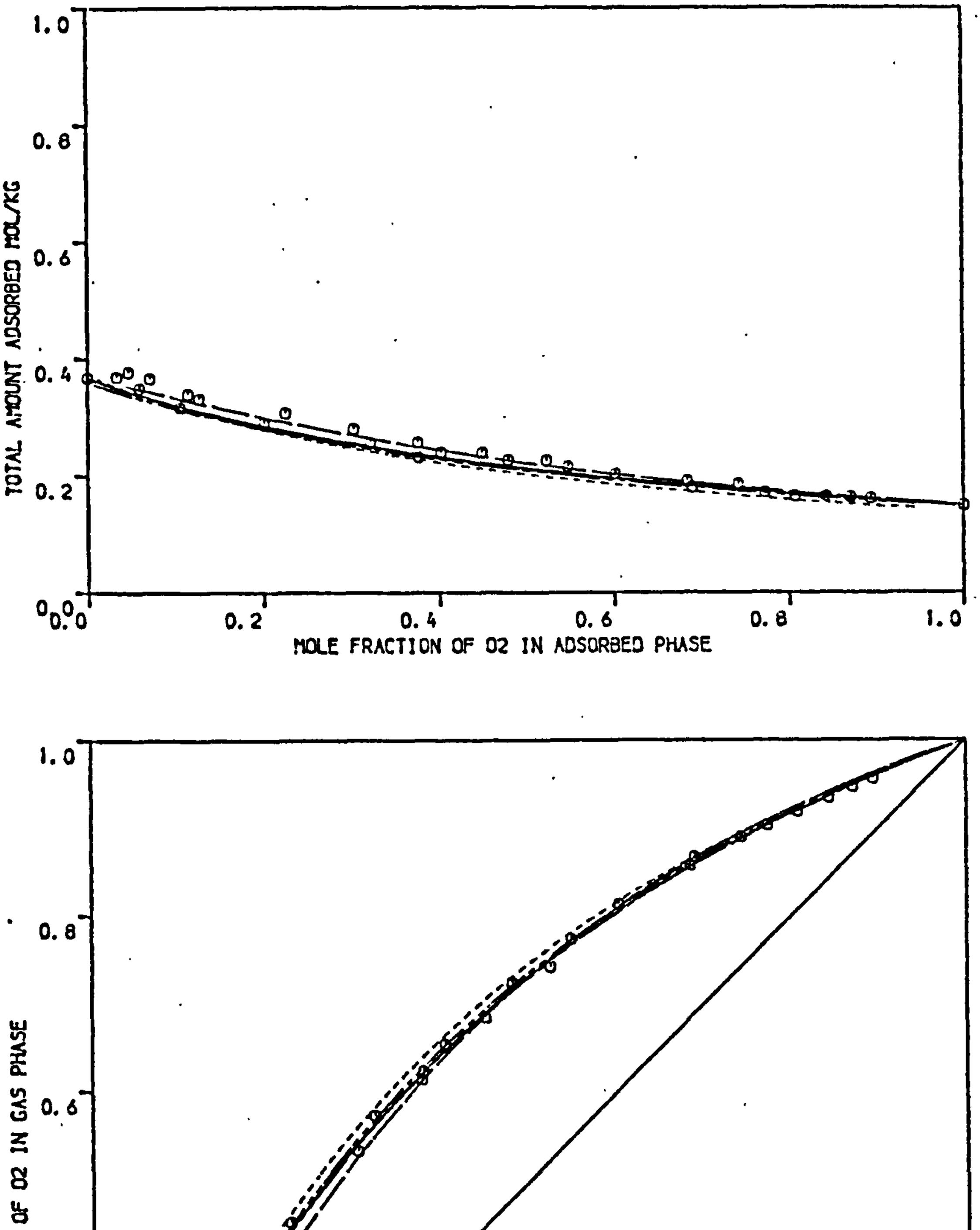

FIGURE 4.31 COMPARISON OF THEORETICAL PREDICTIONS OF VARIOUS MODELS WITH EXPERIMENTAL BINARY EQUILIBRIA OF O2/N2 ON LAPORTE 4A MOLECULAR SIEVE PELLETS AT 303.15 K (PRESSURE = 1.7 BAR)

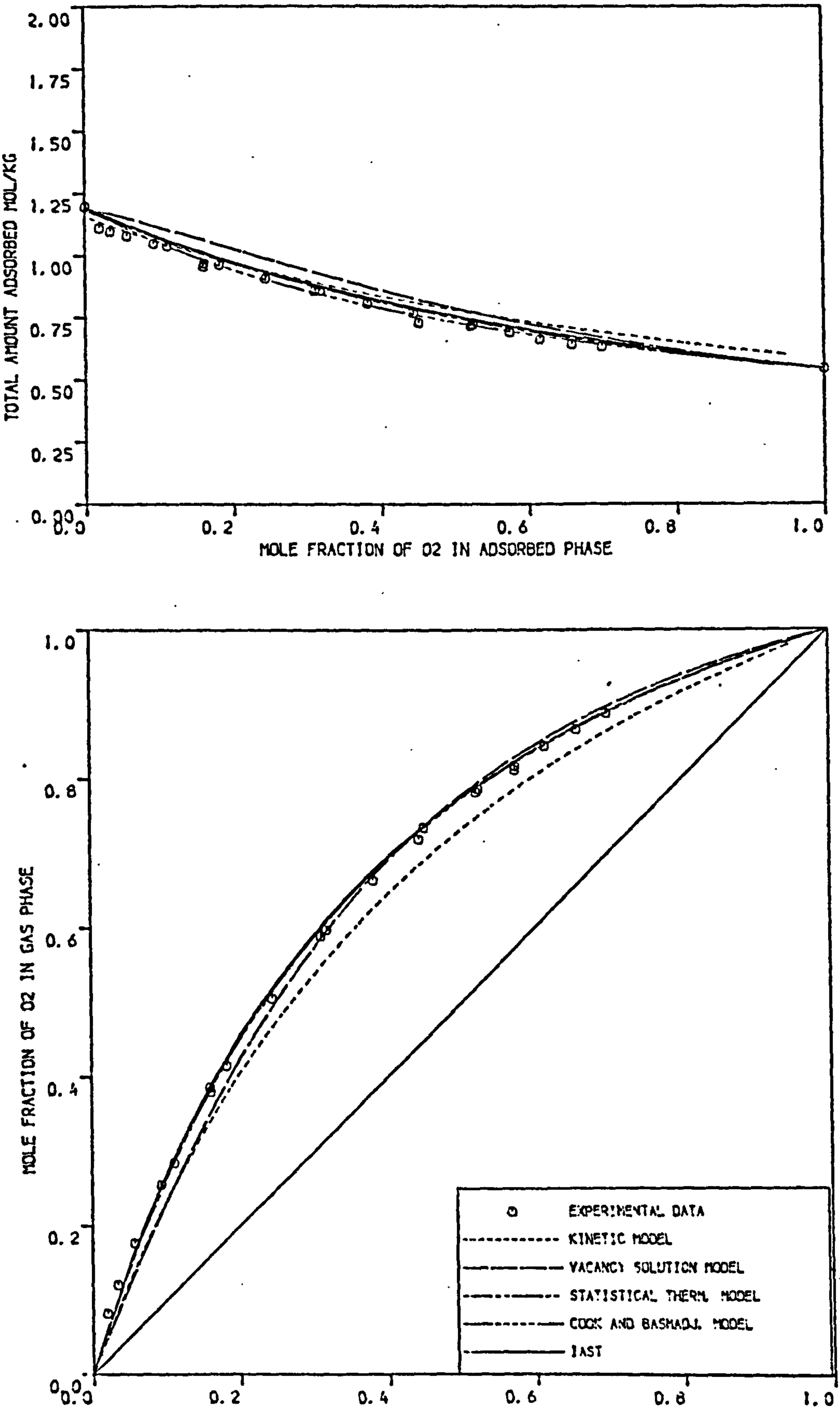

FIGURE 4.32 COMPARISON OF THEORETICAL PREDICTIONS OF VARIOUS MODELS WITH EXPERIMENTAL EQUILIBRIA OF O2/N2 ON LAPORTE 4A MOLECULAR SIEVE PELLETS AT 278.15 K (PRESSURE = 4.4 BAR)

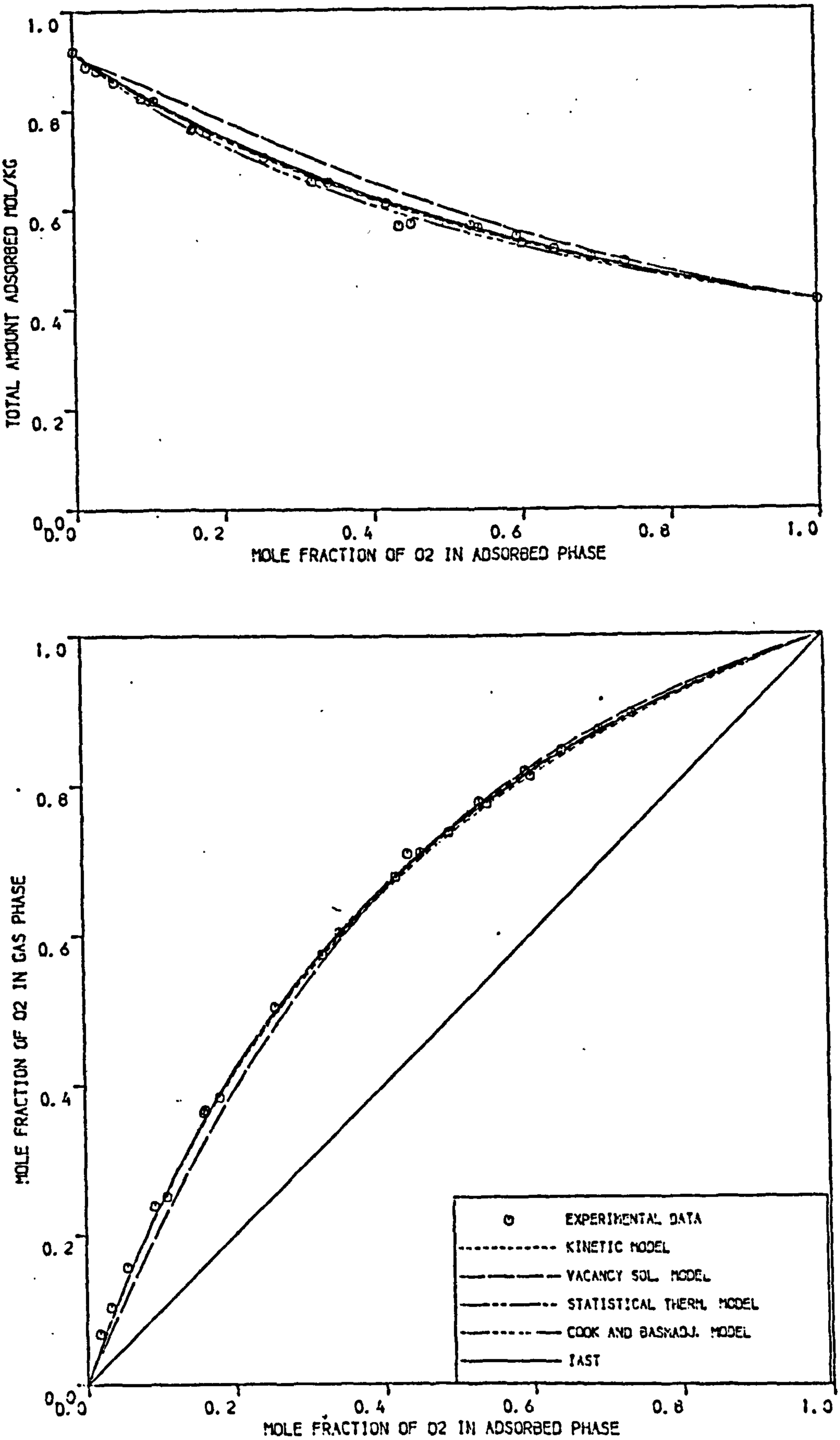

FIGURE 4.33 COMPARISON OF THEORETICAL PREDICTIONS OF VARIOUS MODELS WITH EXPERIMENTAL BINARY EQUILIBRIA OF O2/N2 ON LAPORTE 4A MOLECULAR SIEVE PELLETS AT 293.15 K (PRESSURE = 4.4 BAR)

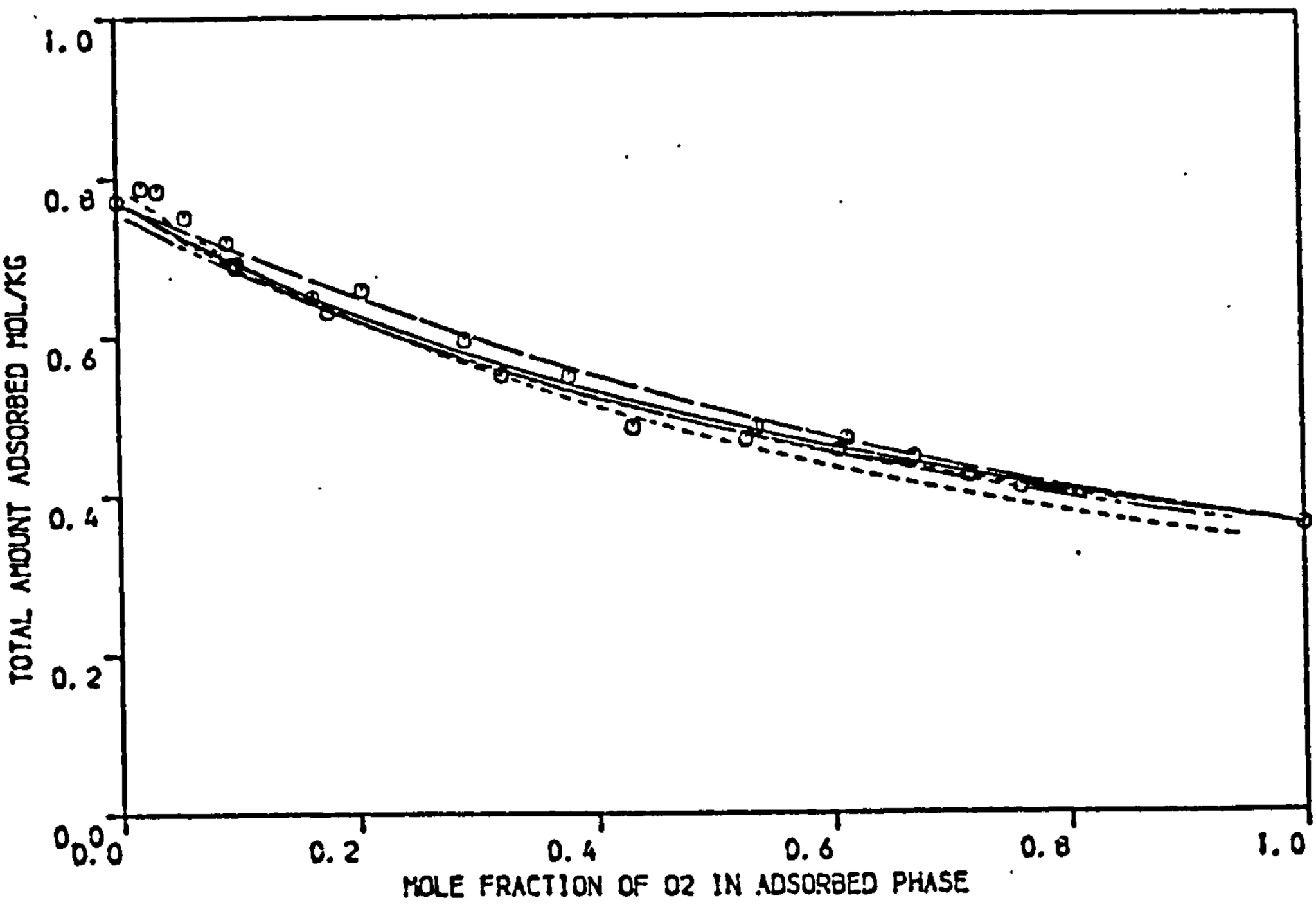

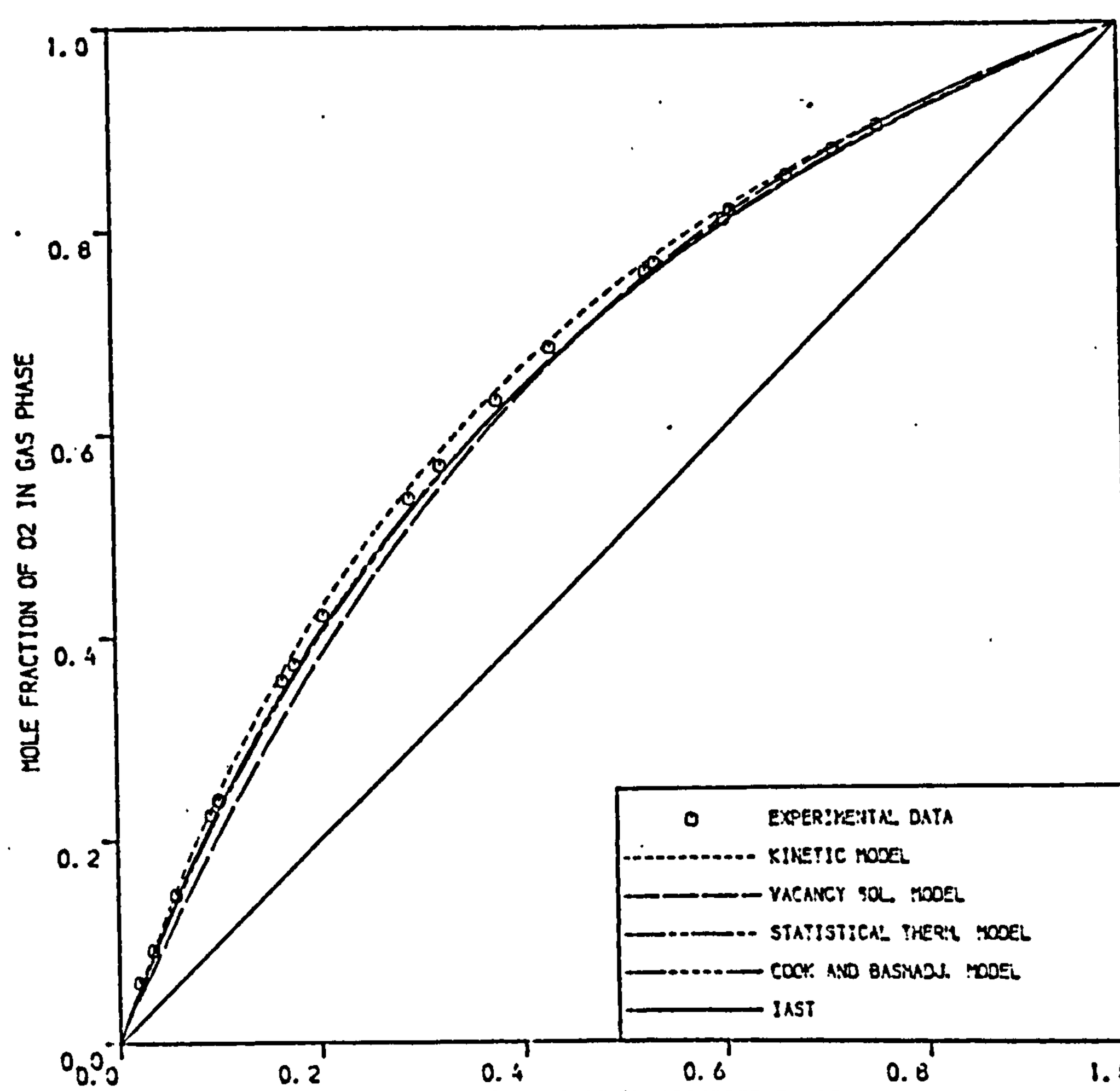

FIGURE 4.34 COMPARISON OF THEORETICAL PREDICTIONS OF VARIOUS MODELS WITH EXPERIMENTAL BINARY EQUILIBRIA OF O2/N2 ON LAPORTE 4A MOLECULAR SIEVE PELLETS AT 303.15 K (PRESSURE =4.4 BAR)

at pressure 4.4 bar. The predicted total amount adsorbed were again in good agreement with the experimental data with the exception of some deviations which could be due to the effect of variation of pressure in the experimental runs.

The vacancy solution model gave reasonably good predicted separation factor for oxygen concentration in the adsorbed phase greater than 50%. For oxygen concentration in the adsorbed phase less than 50%, a slight deviation was encountered with the experimental data and these deviations were more pronounced at mixture pressures of 4.4 bar and were approximately 10%. The predicted total amount adsorbed at temperature 278.15 K and pressure 1.7 bar and at the three temperatures at pressure 4.4 bar showed significant deviations with the experimental data.

Suwanayuen and Danner[43] suggested that some improvement of the vacancy solution model could be achieved by including the interaction parameters Λ_{12} and Λ_{21}. They suggested that the interaction parameters could be estimated from an equation analogous to that introduced by Wilson[83] for a bulk liquid mixture which is given by:

$$\Lambda_{ij} = \frac{n_{m_j}}{n_{m_i}} \exp - \left(\frac{\lambda_{ij} - \lambda_{ii}}{RT} \right) \qquad (4.8)$$

$i = 1, j = 2$

or

$i = 2, j = 1$

where the energies of interactions λ_{ii} and λ_{ij} are given by:

$$\lambda_{ii} = \frac{-2}{z} (- U_{o_i} - RT) \qquad (4.9)$$

$$\lambda_{ij} = \sqrt{\lambda_{ii} \lambda_{jj}} \qquad (4.10)$$

The value of the co-ordination number, Z, is adjusted until a reasonable improvement is achieved. The model hence will be a correlating model rather than a predictive model.

Estimation of the interaction parameters Λ_{12} and Λ_{21}, where component 1 is oxygen and component 2 is nitrogen, through Equations (4.8) - (4.10) showed that Λ_{21} was less than unity and Λ_{12} greater than unity. The effect of these interaction parameters on both separation and total amount adsorbed was hardly significant. This is quite obvious because deviation of an adsorbed solution from ideality is pronounced when either both interaction coefficients are less than unity in which case positive deviation from ideality is encountered or both interaction coefficients are greater than unity in which case negative deviation from ideality is encountered[106].

The predictions obtained by the Kinetic model showed no isobaric variation of the separation factor with concentration and also the separation factor is independent of total pressure. An interesting case obtained on Laporte 4A was that a better separation factor was predicted by the model at the high temperature 303.15 K rather than the low temperature 278.15 K.

The predictions of the Kinetic model were in good agreement with the experimental data at temperature 293.15 K and both pressures. Some deviations between the model and the experimental data were encountered at temperature 303.15 K and both pressures. The predictions obtained by the kinetic model at temperature 278.15 K and both pressures were rather poor. The predictions are far from quantitative agreement with the experimental data. The failure of the Kinetic model at temperature 278.15 K could be due to its inheritance of the three major assumptions of the Langmuir model, i.e. no adsorbate-adsorbate interactions, adsorbent surface is homogeneous and the adsorbed molecules are localized.

These assumptions generally do not conform to the experimental system especially at low temperatures where more is adsorbed. The assumption of the bi-molecular layer formation by the model does not contribute a lot to systems such as molecular sieves since due to their small pore size the number of layers formed are restricted and in fact in these systems the overwhelming contribution to separation is affected in the first molecular layer. From the regression parameters of the pure components shown in Table 4.2 it is seen that the value of θ obtained on Laporte 4A is negative which has no physical meaning but due to its small value its effect was rather insignificant. From Henry's law constants shown in Table 4.6 it is seen that the Henry law constant for oxygen at temperature 278.15 K was significantly low as compared to the other models and its effect may have contributed significantly to the failure of the model at temperature 278.15 K.

The activity coefficients for oxygen and nitrogen on Laporte 4A at the three temperatures and two pressures studied are represented graphically in Figures 4.35 and 4.36. From the figures it is seen that no significant deviations from ideality, i.e. from unity are noticed apart from the data at temperature 293.15 and 278.15 K and pressure 1.7 bar which could be due to the assumption of constant total pressure upon which the calculation of the activity coefficients were based (there were minor variations in pressure) since deviations are noticed only for one component, i.e. nitrogen.

4.2.3.4 Interpretation of results on Laporte 13X

The binary equilibria experimental results on Laporte 13X molecular sieve pellets are replotted on Figures 4.37 - 4.42 together with the predicted equilibria data by the five models studied. For the statistical thermodynamic model the predictions were obtained for values of i and j in Equation (2.49) adjusted to 15 and 6 respectively.

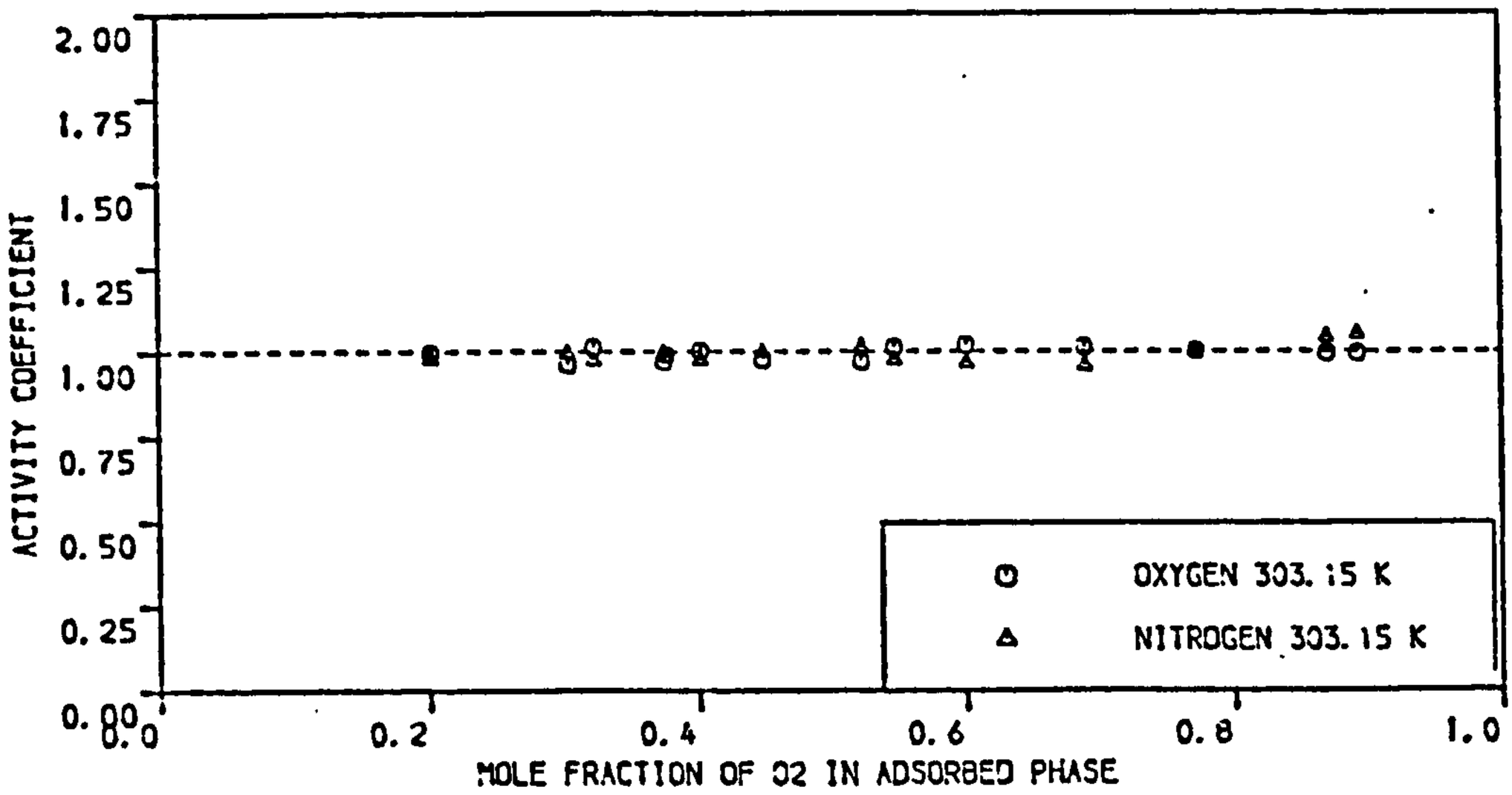

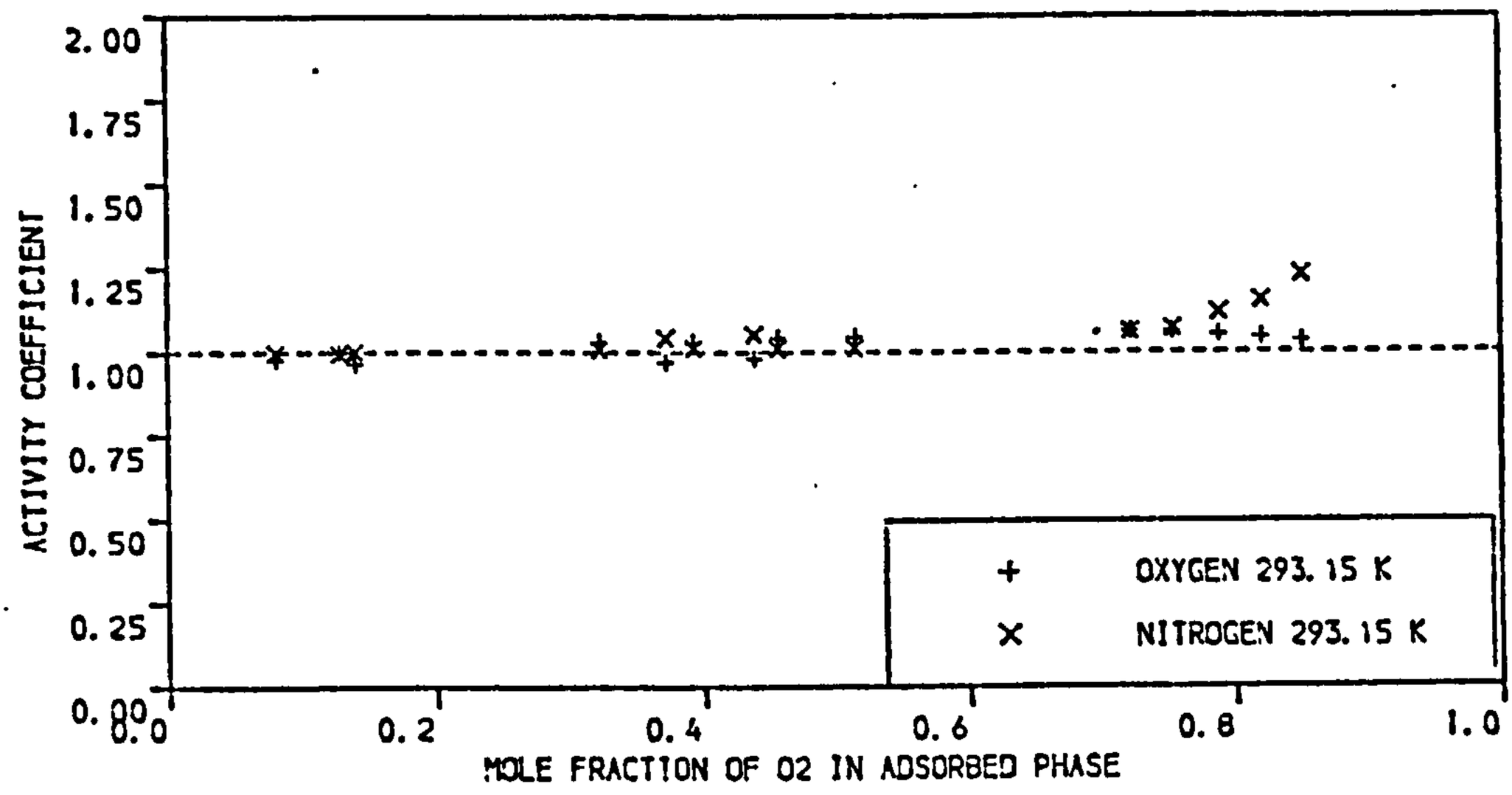

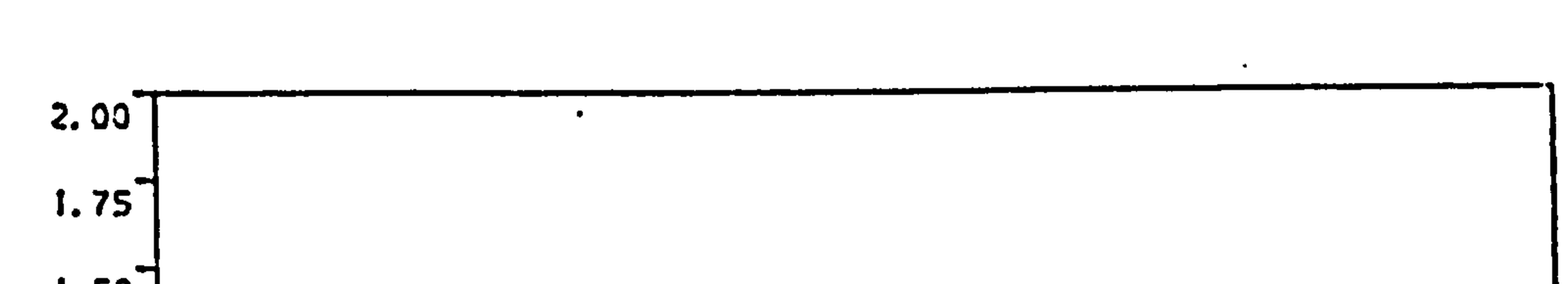

FIGURE 4.35 ACTIVITY COEFFICIENTS FOR O2/N2 ON LAPORTE 4A MOLECULAR SIEVE PELLETS AT 303.15 , 293.15 AND 278.15 K (PRESSURE = 1.7 BAR)

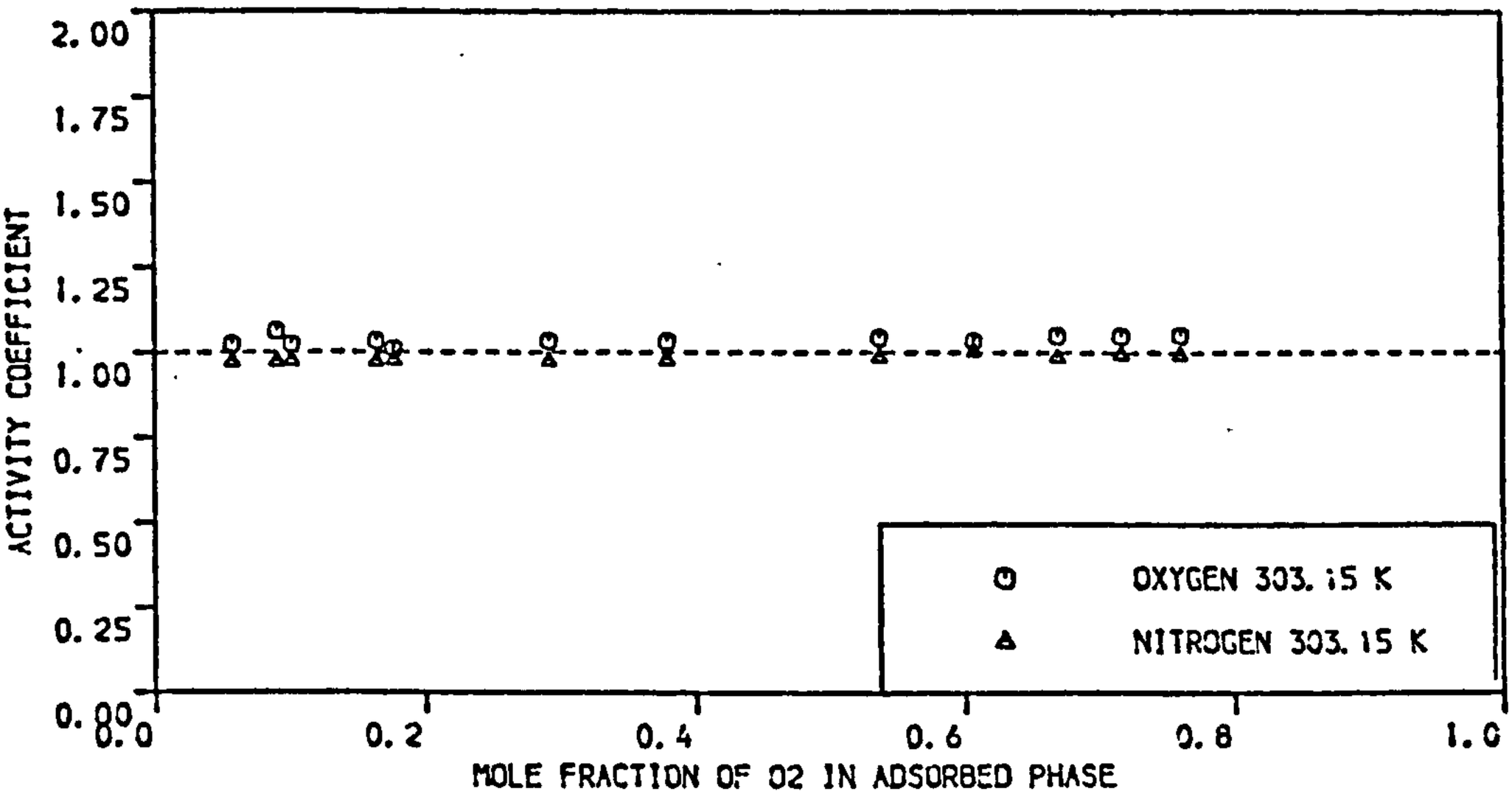

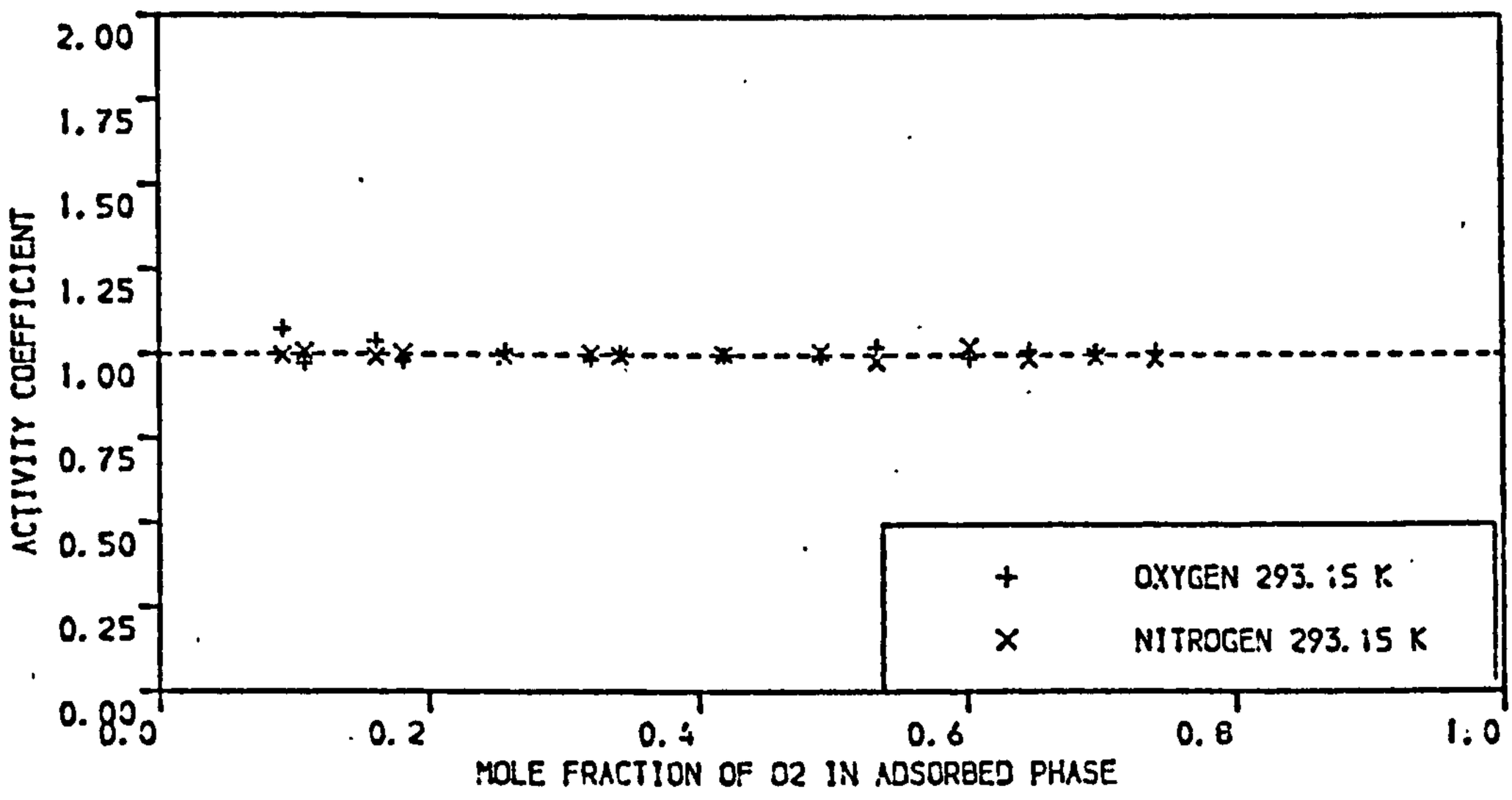

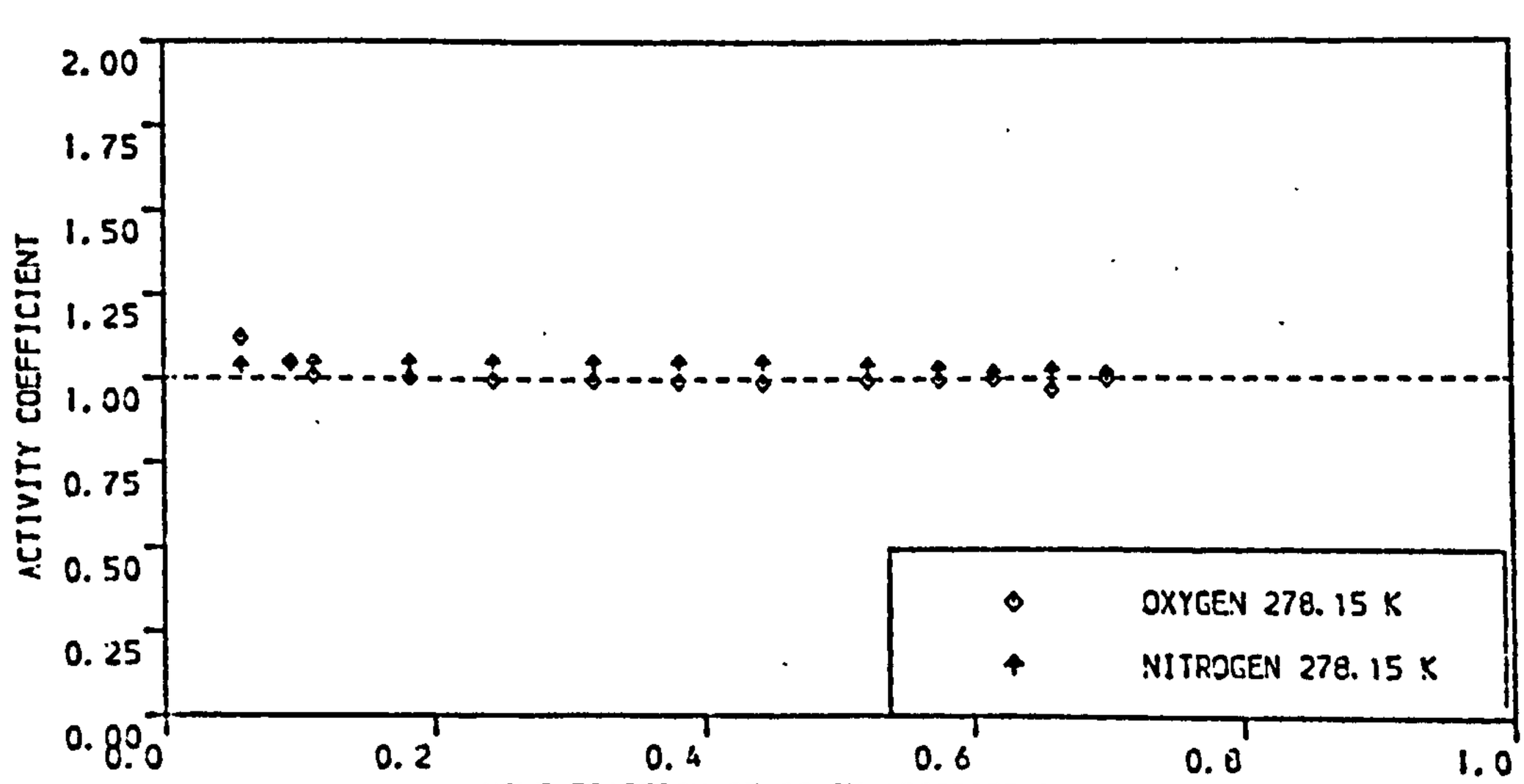

FIGURE 4.56 ACTIVITY COEFFICIENTS FOR O2/N2 ON LAPORTE 4A MOLECULAR SIEVE PELLETS AT 303.15 , 293.15 AND 278.15 K (PRESSURE = 4.4 BAR)

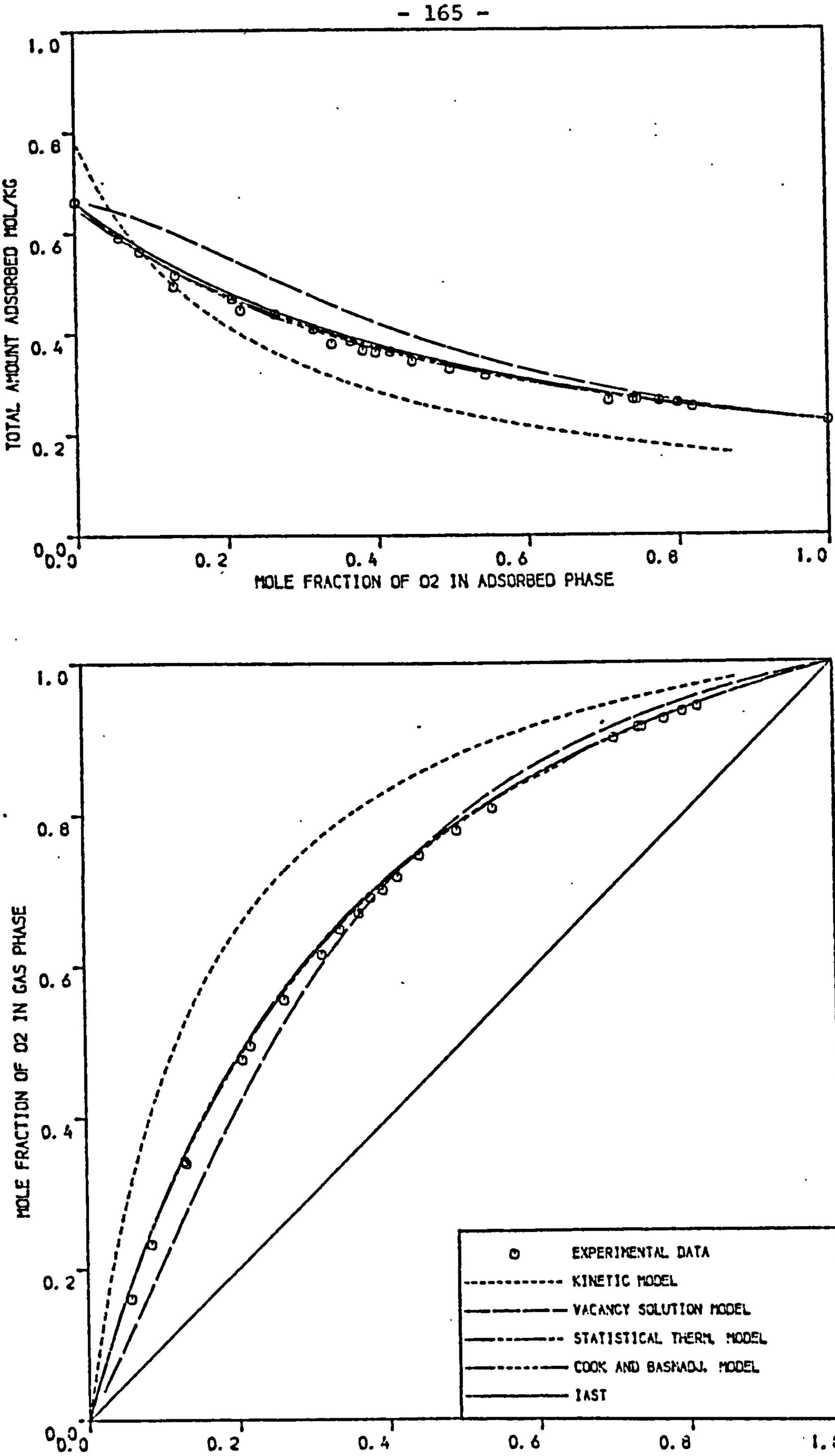

FIGURE 4.37 COMPARISON OF THEORETICAL PREDICTIONS OF VARIOUS MODELS WITH EXPERIMENTAL EQUILIBRIA OF O2/N2 ON LAPORTE 13X MOLECULAR SIEVE PELLETS AT 278.15 K (PRESSURE = 1.7 BAR)

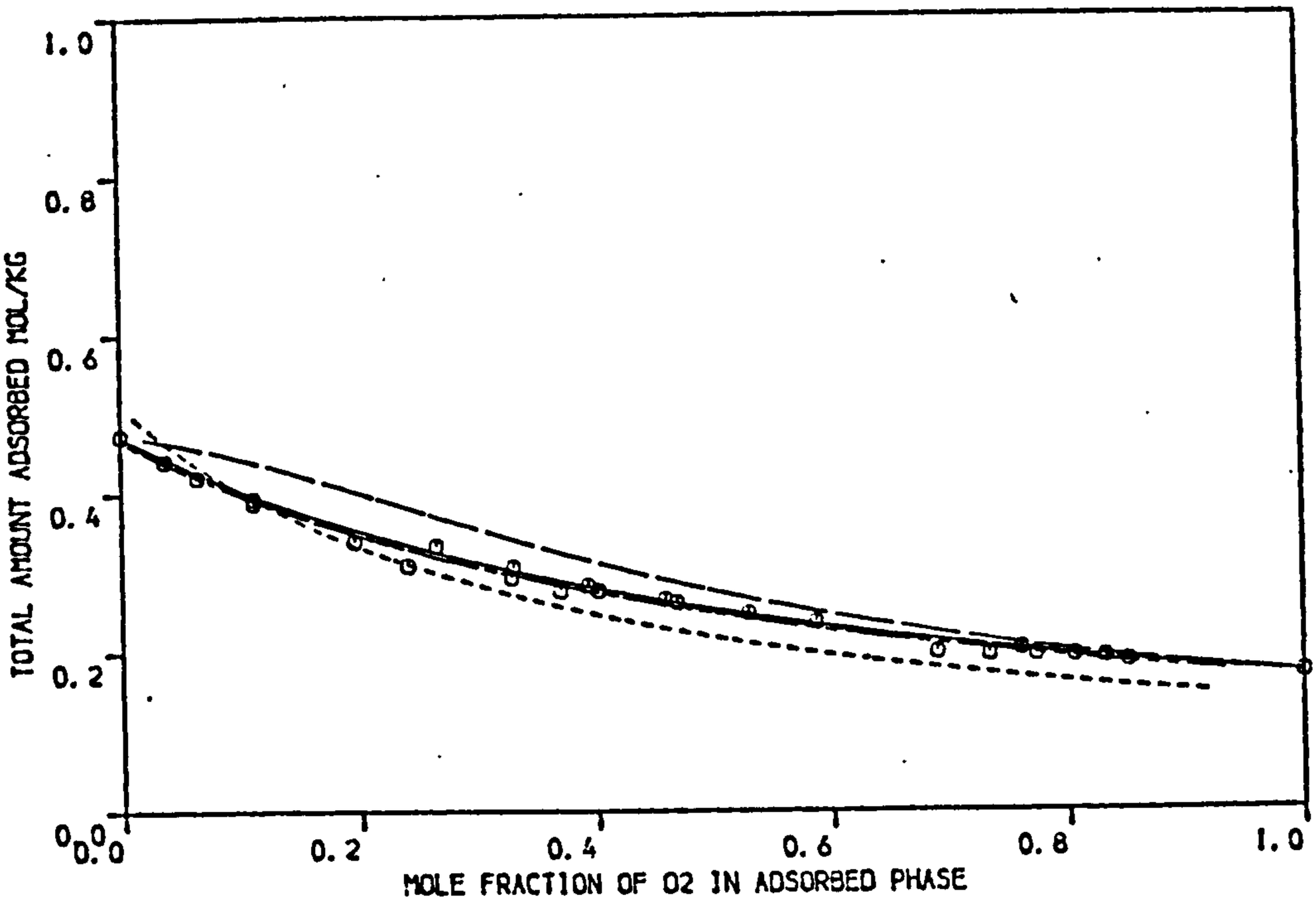

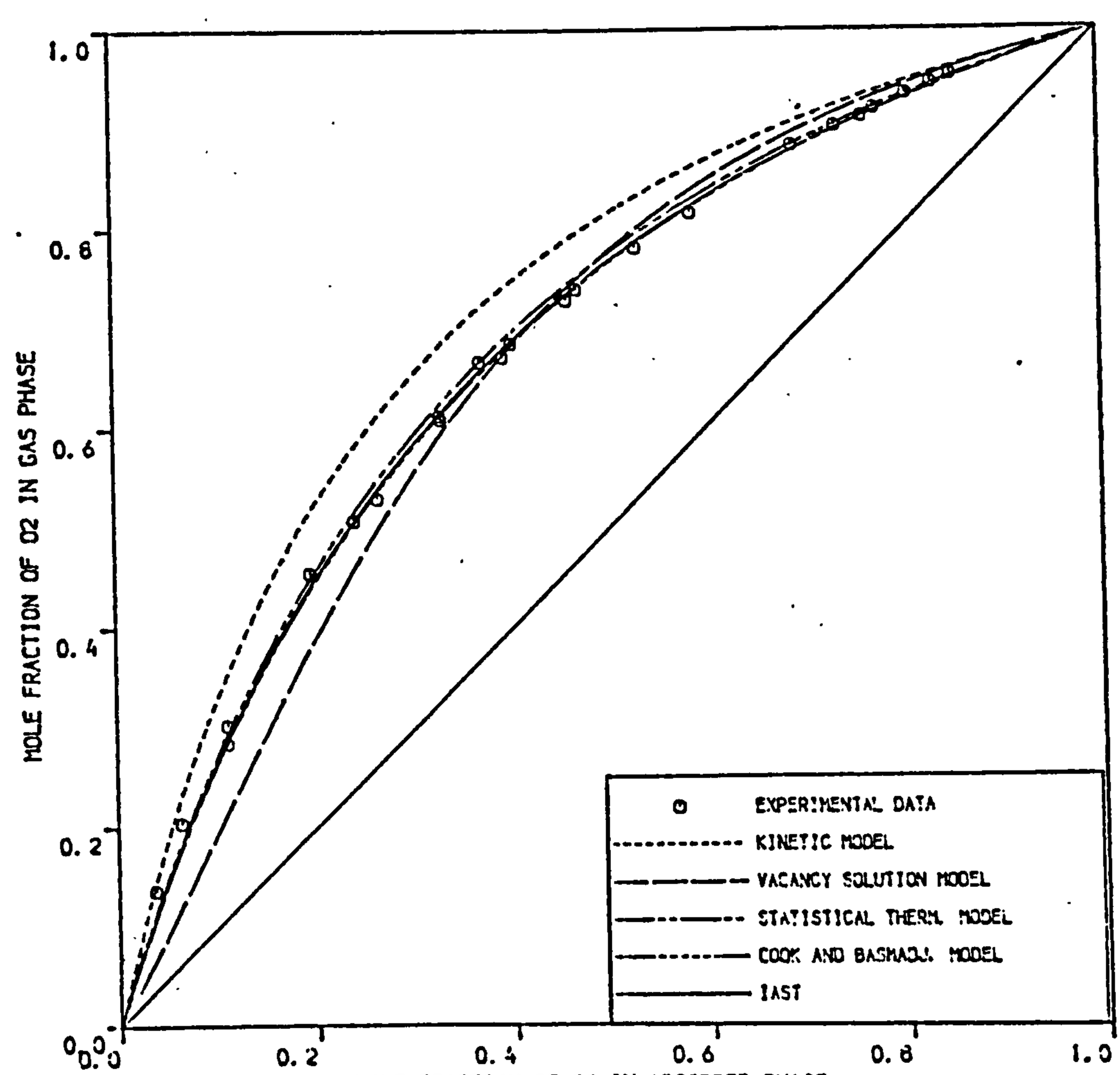

FIGURE 4.38 COMPARISON OF THEORETICAL PREDICTIONS OF VARIOUS MODELS WITH EXPERIMENTAL EQUILIBRIA OF O2/N2 ON LAPORTE 13X MOLECULAR SIEVE PELLETS AT 293.15 K (PRESSURE = 1.7 BAR)

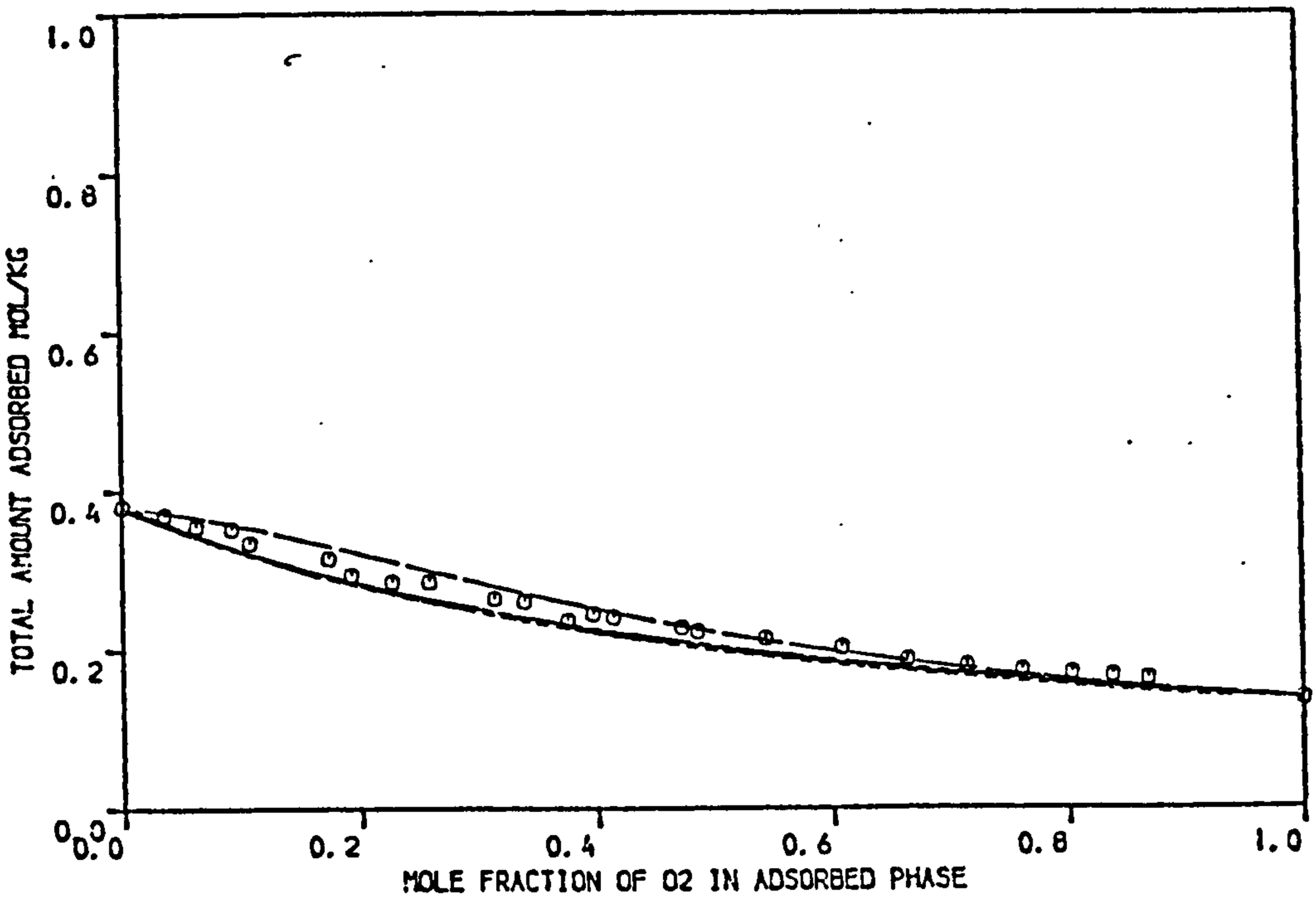

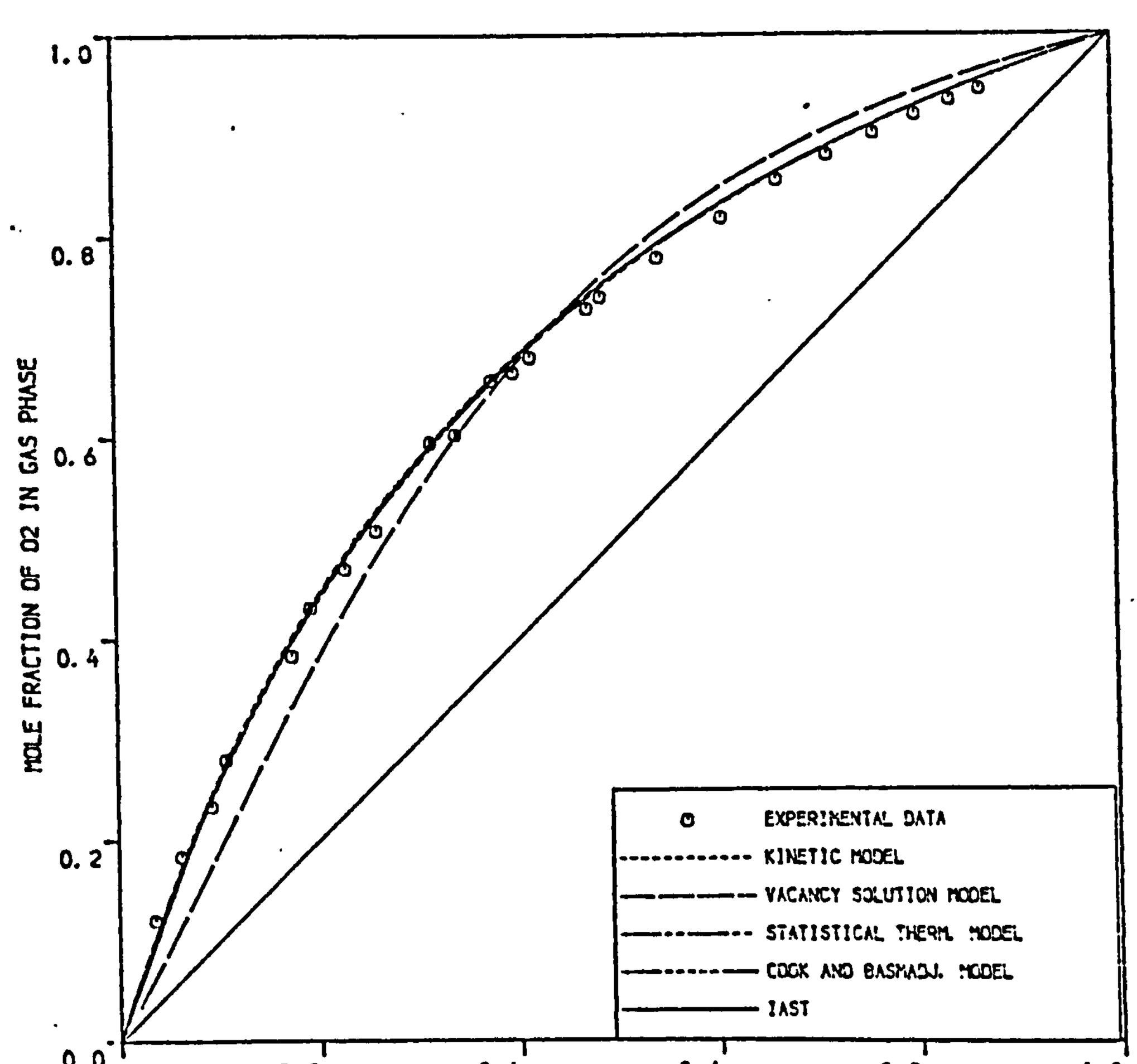

FIGURE 4.39 COMPARISON OF THEORETICAL PREDICTIONS OF VARIOUS MODELS WITH EXPERIMENTAL EQUILIBRIA OF O2/N2 ON LAPORTE 13X MOLECULAR SIEVE PELLETS AT 303.15 K (PRESSURE ≈ 1.7 BAR)

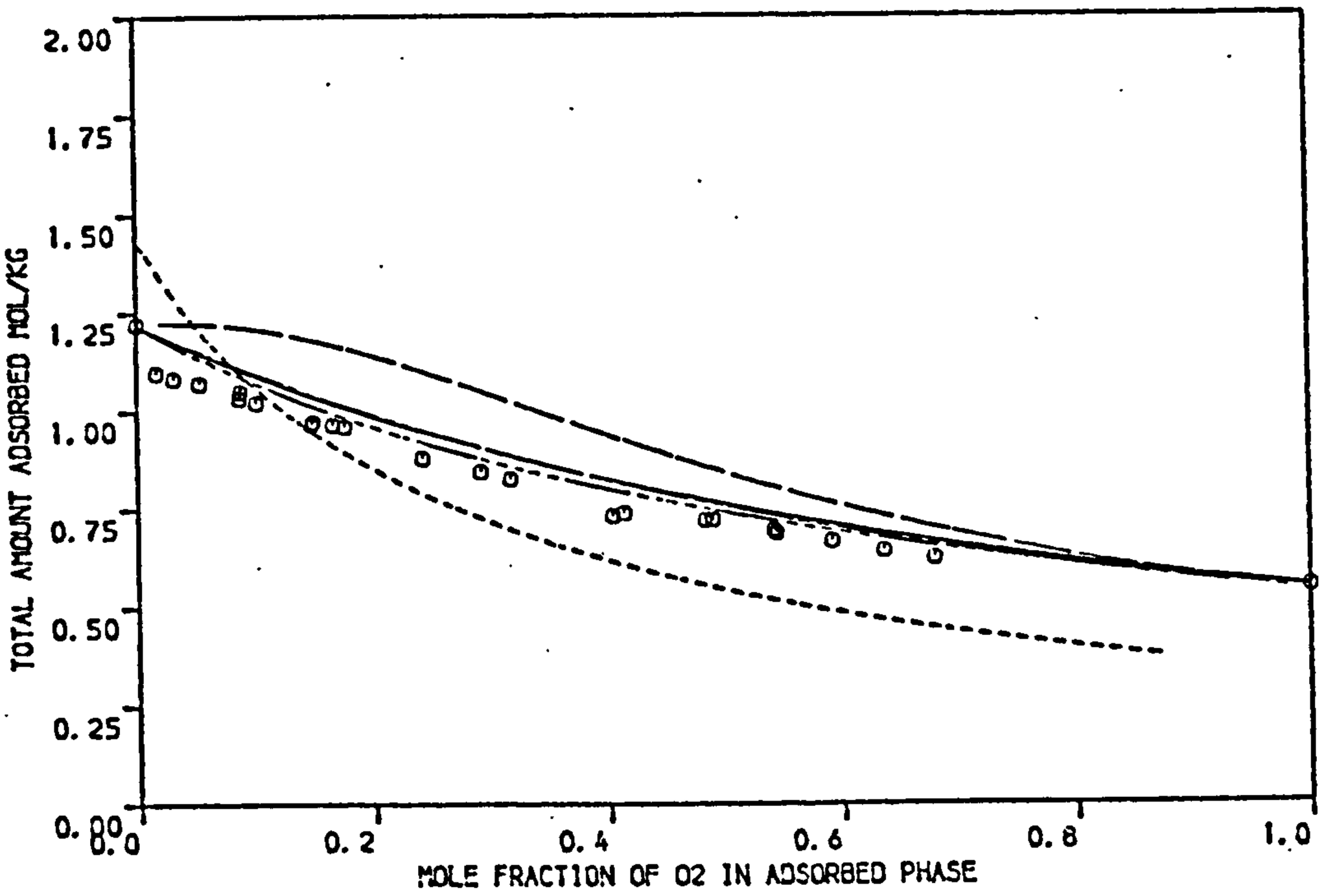

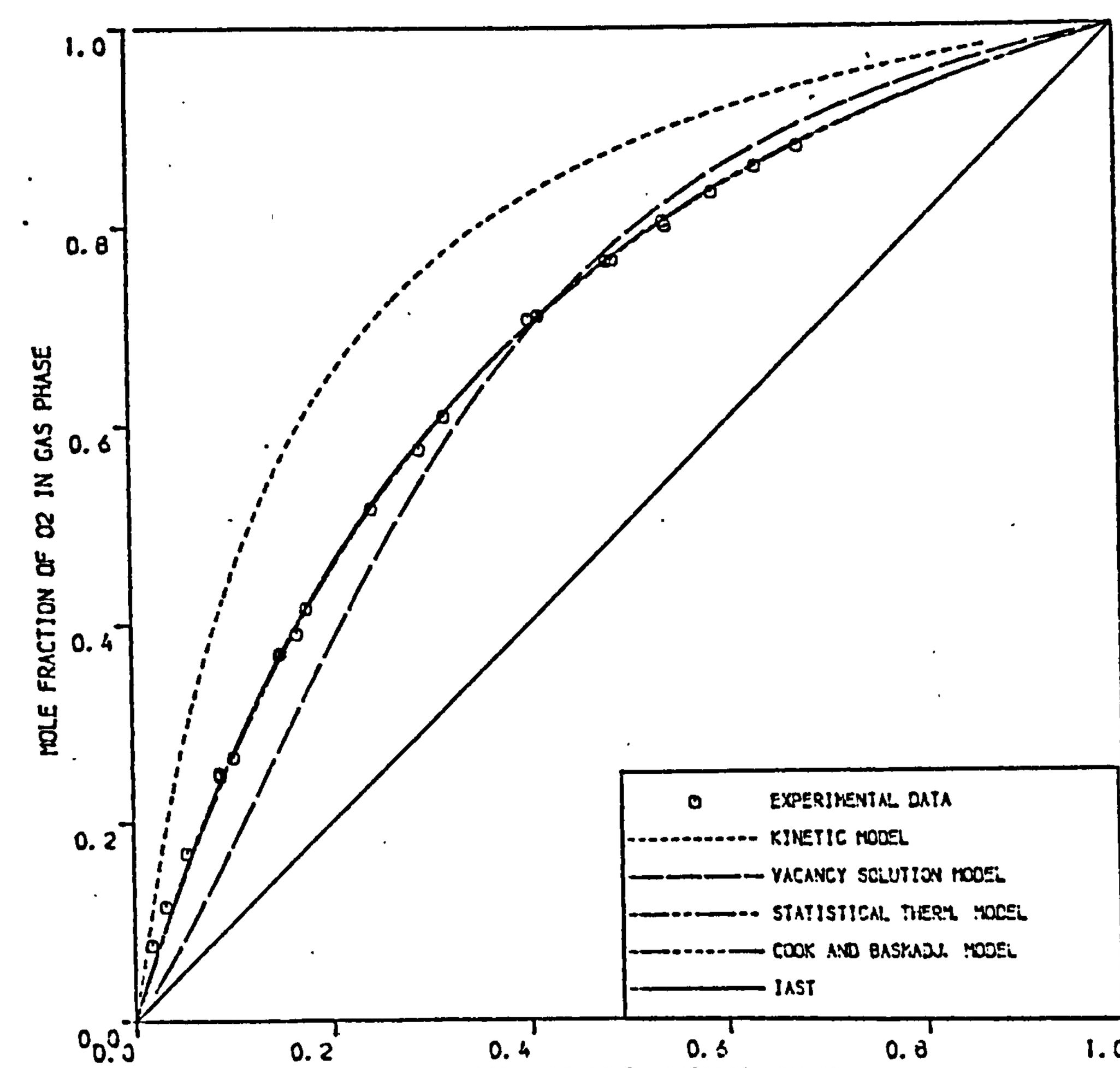

FIGURE 4.40 COMPARISON OF THEORETICAL PREDICTIONS OF VARIOUS MODELS WITH EXPERIMENTAL EQUILIBRIA OF O2/N2 ON LAPORTE 13X MOLECULAR SIEVE PELLETS AT 278.15 K. (PRESSURE ≈ 4.4 BAR)

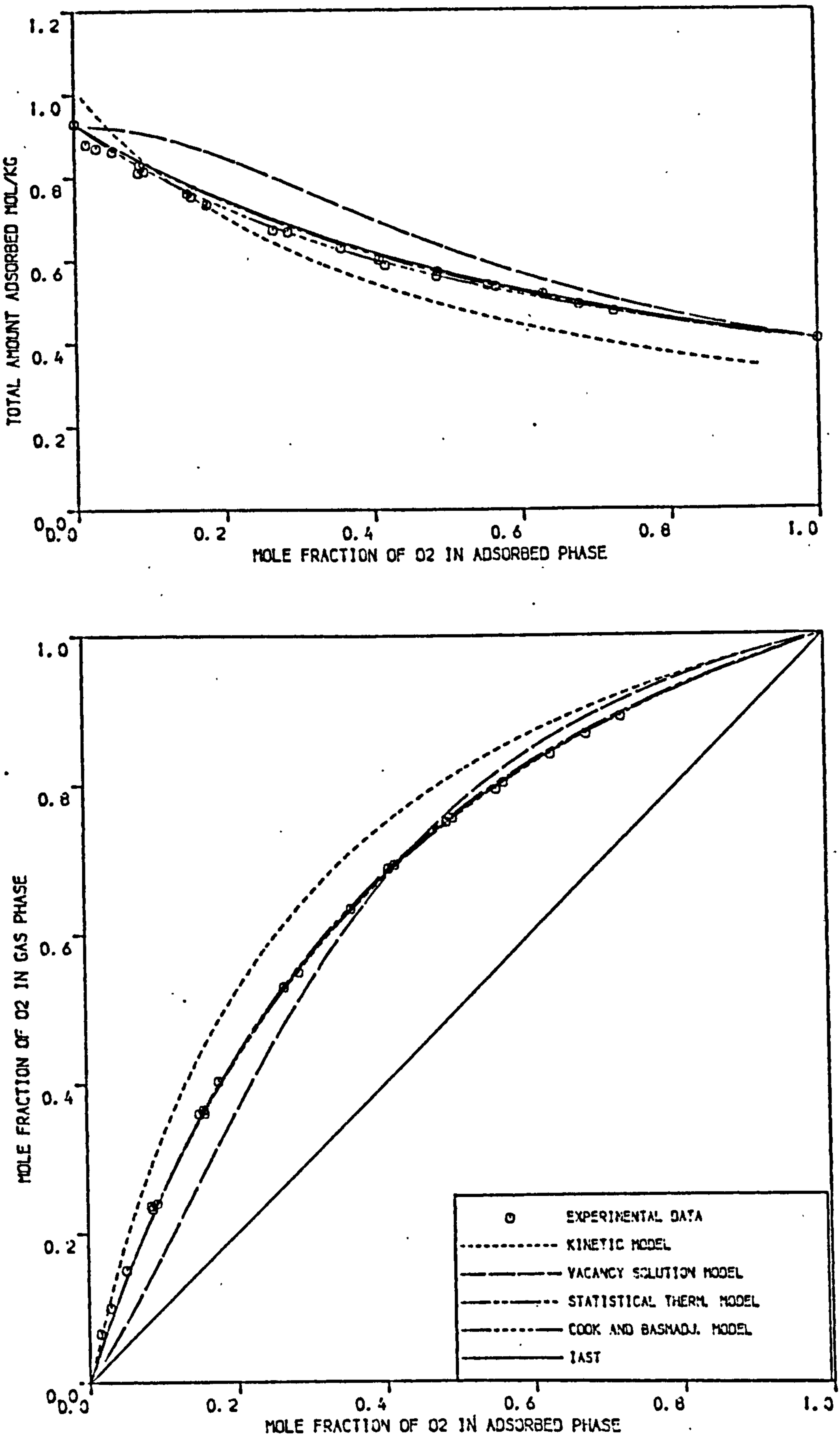

FIGURE 4.41 COMPARISON OF THEORETICAL PREDICTIONS OF VARIOUS MODELS WITH EXPERIMENTAL EQUILIBRIA OF O2/N2 ON LAPORTE 13X MOLECULAR SIEVE PELLETS AT 293.15 K (PRESSURE = 4.4 BAR)

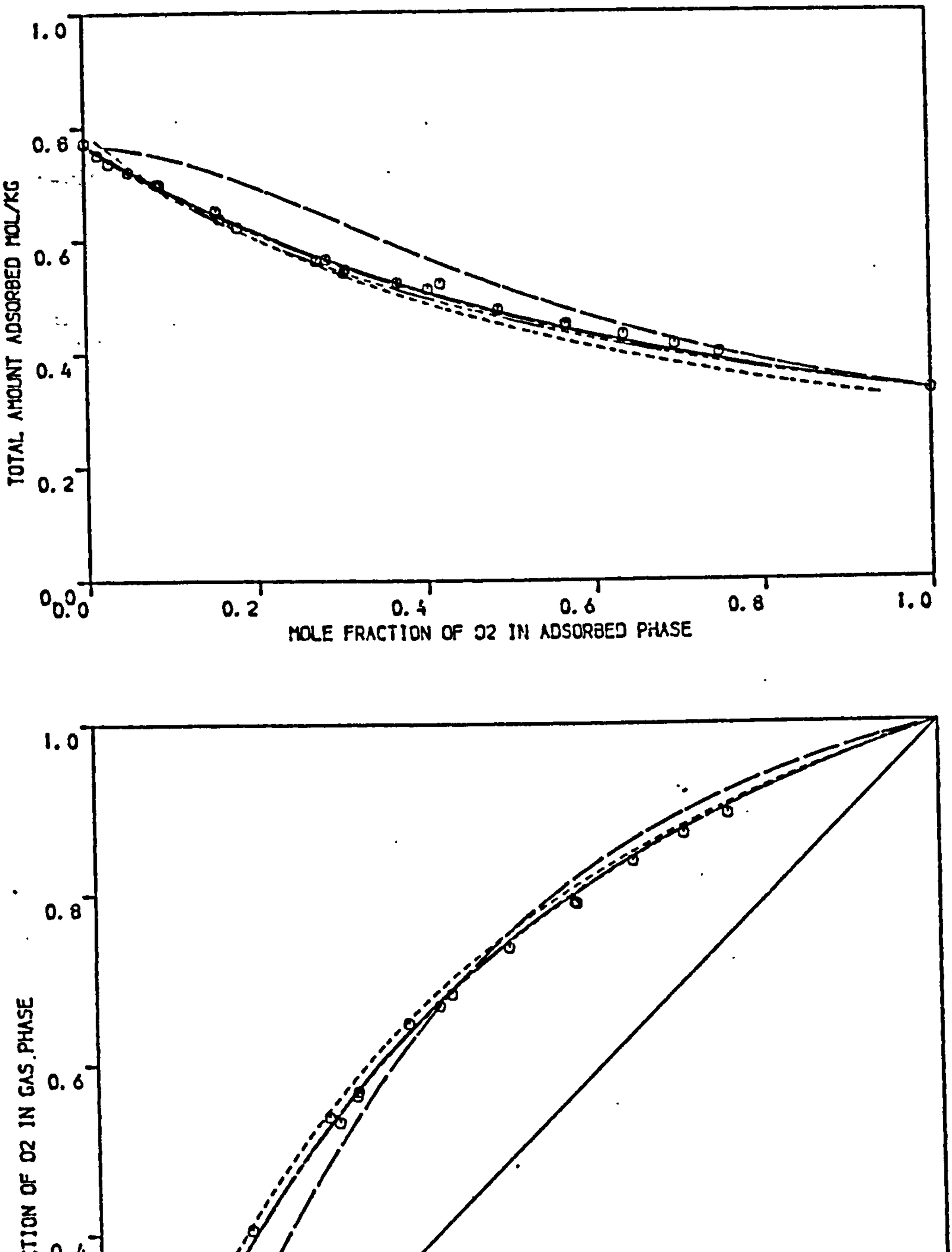

FIGURE 4.42. COMPARISON OF THEORETICAL PREDICTIONS OF VARIOUS MODELS WITH EXPERIMENTAL EQUILIBRIA OF O2/N2 ON LAPORTE 13X MOLECULAR SIEVE PELLETS AT 303.15 K (PRESSURE = 4.4 BAR)

For the three temperatures and two pressures studied the statistical thermodynamic model, Cook and Basmadjian model and the ideal adsorbed solution theory (IAST) gave again approximately the same predicted separation factors and the predicted values were in good agreement with the experimental data. The predicted total amounts adsorbed by the three models are approximately the same and the predicted values were in good agreement with the experimental values with exception of the experimental data at temperature 278.15 K and pressure of 4.4 bar where a deviation of about 5% was noticed.

The predictions obtained by the vacancy solution model were rather poor, significant deviations were encountered between the model and the experimental data and these deviations were increasing with decrease of temperature. The effect of including the interaction parameters Λ_{12} and Λ_{21} served no gain of improvement for again Λ_{12} (O_2 - N_2) was above unity and Λ_{21} (N_2 - O_2) was less than unity. From Figures 4.37 - 4.42 it is seen that for all the experimental data on Laporte 13X the model predicts the total amount adsorbed approaching both experimental values of the pure components adsorbed, hence one could say that the deviation of the model could be due to the effect of the physical meaning of the interactions Λ_{13} and Λ_{31} for both components. From Table 4.5 it is seen that the values of the interactions Λ_{13} and Λ_{31} especially for temperature 278.15 K vary widely, one interaction is high above unity and the other is far below unity.

The prediction obtained by the kinetic model on Laporte 13X at temperature 303.15 K and pressure 1.7 bar was in good agreement with the experimental data. The values predicted by the model coincided with values predicted by the statistical thermodynamic model, Cook and Basmadjian model and IAST. Since the model predicts no effect of pressure on the separation factor, slight deviations were noticed at temperature 303.15 K and pressure 4.4 bar. The predictions obtained at the

other two temperatures were far from quantitative agreement with the experimental values especially for the temperature of 278.15 K. These deviations could be due to similar reasons as that of Laporte 4A.

The activity coefficients for oxygen and nitrogen on Laporte 13X at the three temperatures and the two pressures studied are represented graphically in Figures 4.43 - 4.44. From the figures it is seen that no significant deviations from ideality are encountered, with the exception of data at temperature 303.15 K and 1.7 bar. Since no significant deviations from ideality are encountered at pressure 4.4 bar these deviations could be due to the assumption of constant pressure upon which the calculations of the activity coefficients are based and to errors involved in the evaluation of Equation (4.6).

4.2.3.5 Interpretation of results on Laporte 5A

The binary equilibria results on Laporte 5A molecular sieve pellets are replotted on Figures 4.45 - 4.50 together with the predicted equilibria data by the five models studied. For the statistical thermodynamic model the predictions were obtained for values of i and j in Equation (2.49) adjusted to 10 and 4 respectively.

For the three temperatures and two pressures studied the statistical thermodynamic model, Cook and Basmadjian model, and IAST gave again approximately the same predicted separation factors and the predicted values were in good agreement with the experimental values. The predicted total amounts adsorbed by the three models were also in good agreement with the experimental data at pressure 1.7 bar while at pressure 4.4 bar a maximum deviation of 5% was noticed.

The predicted separation factors obtained by the vacancy solution model were rather poor for oxygen concentration in the adsorbed phase less than 60%. For oxygen concentrations above 60% there was a fairly good agreement between the experimental data and the model. The devia-

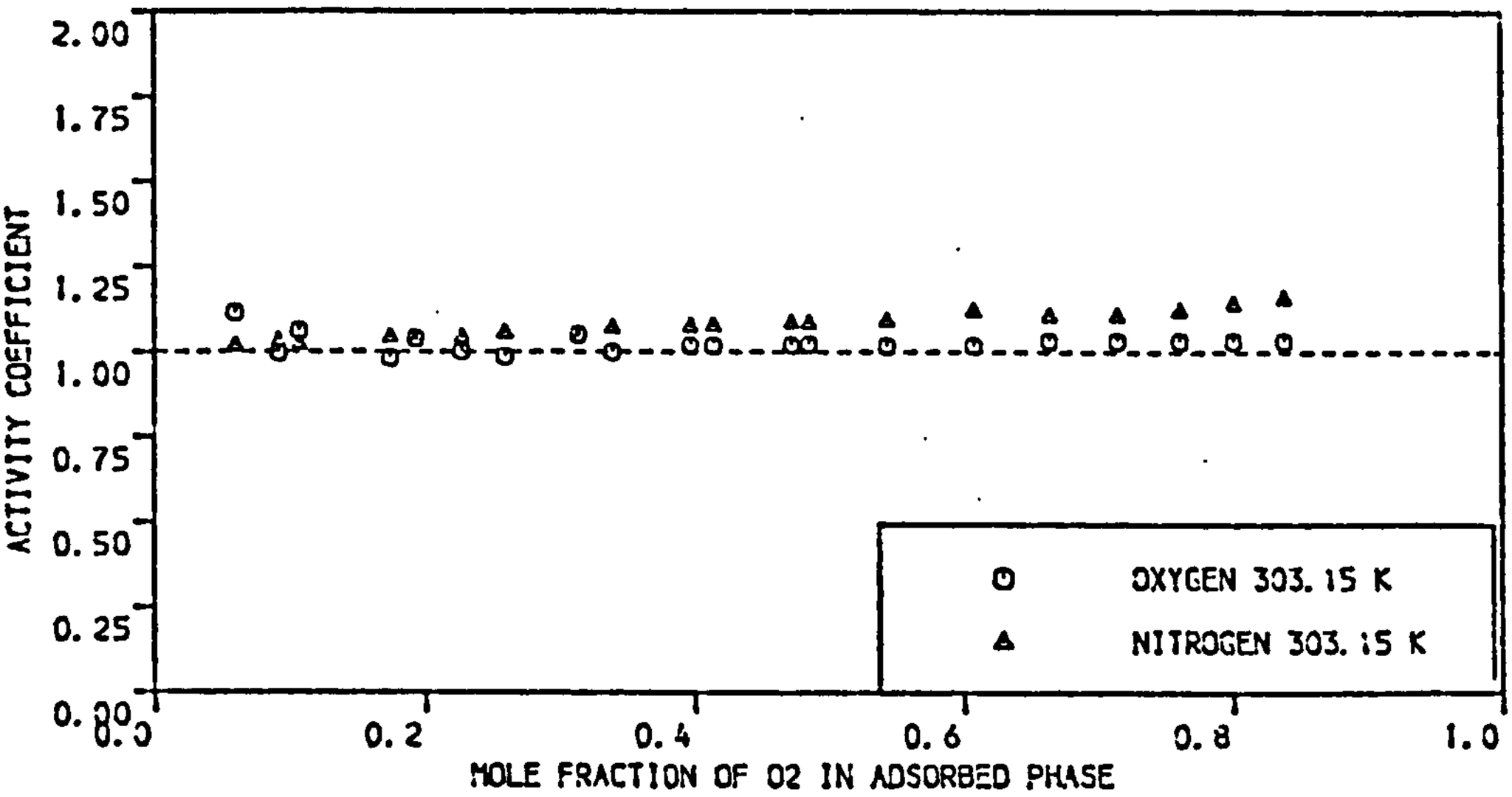

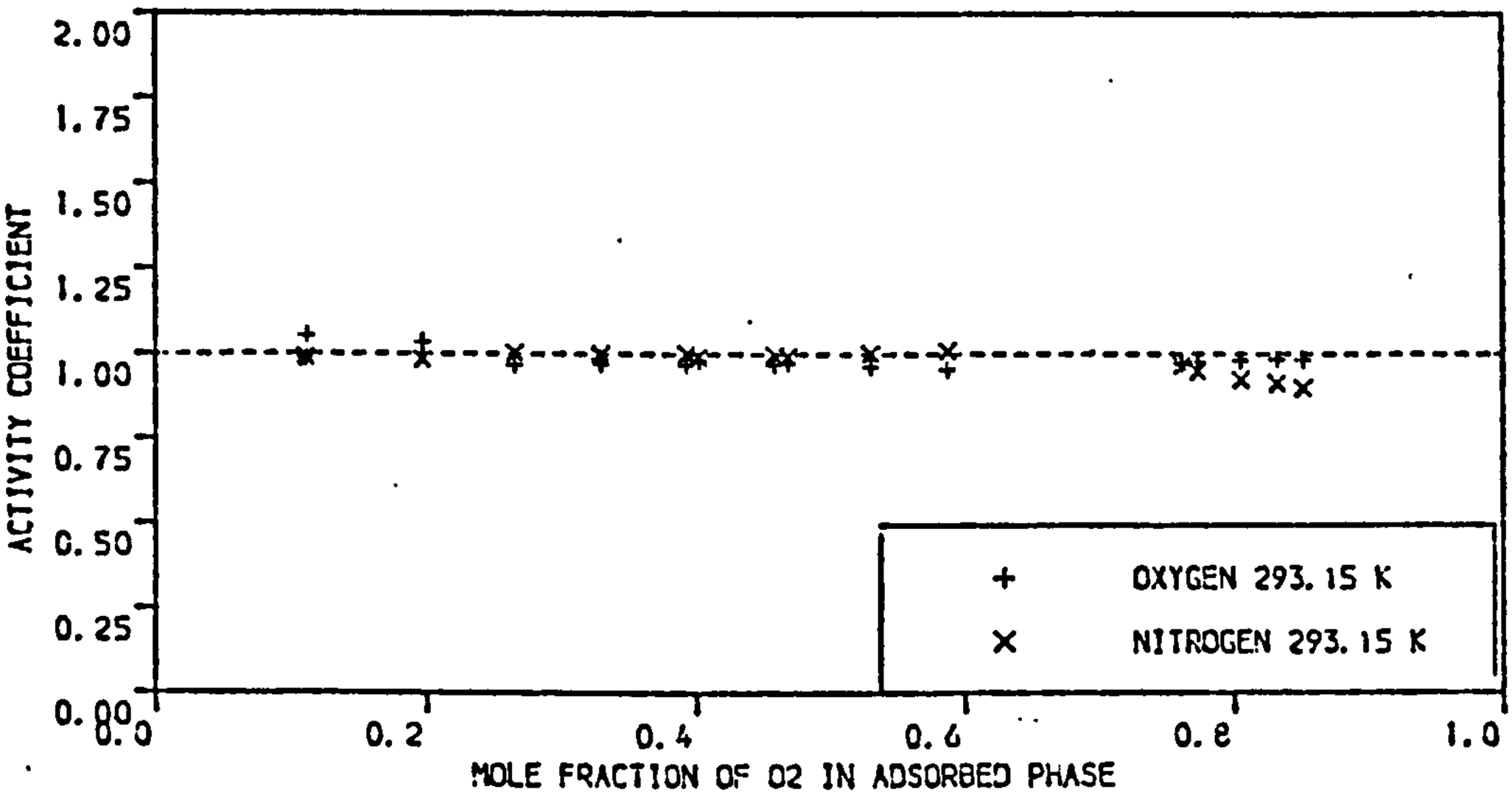

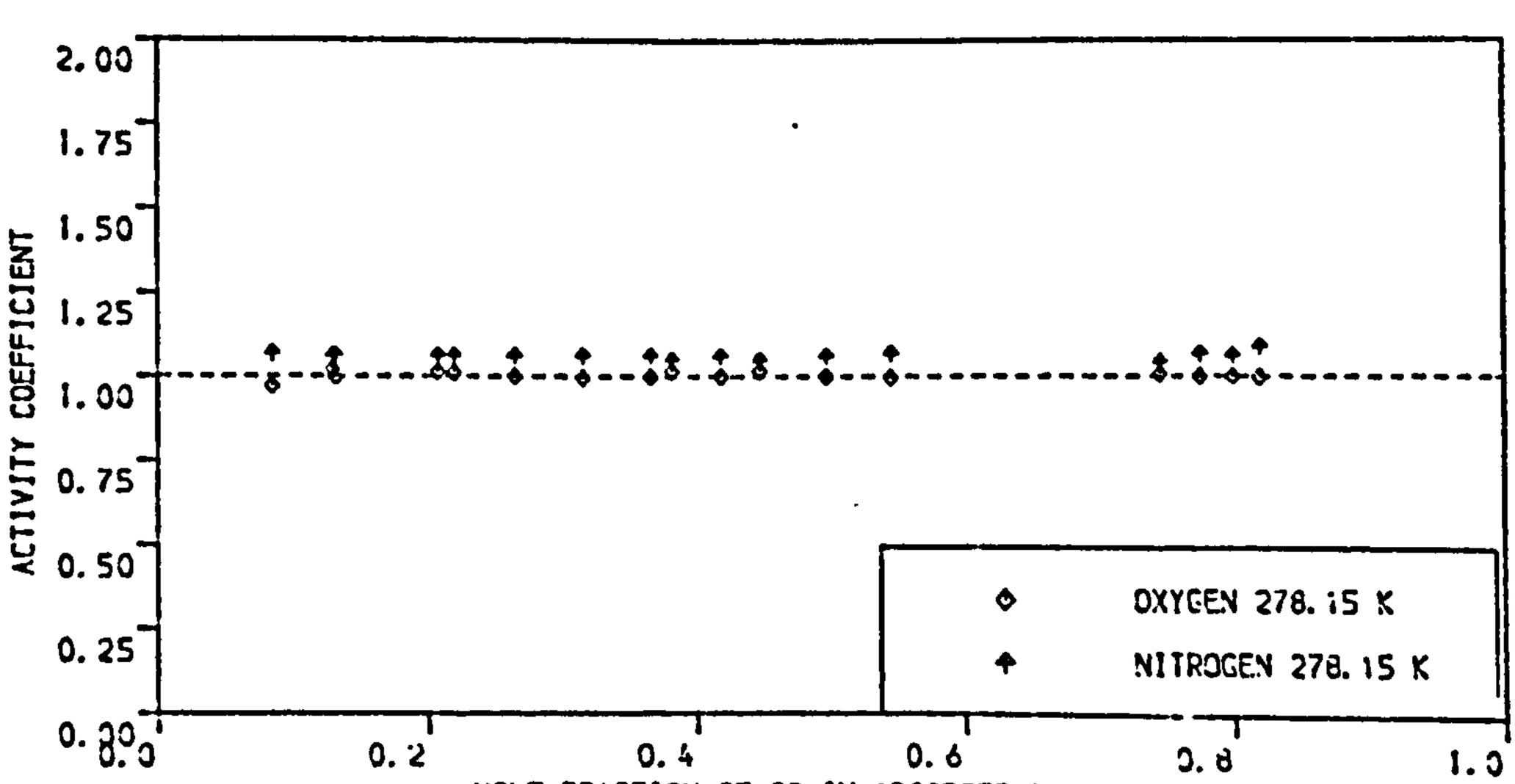

FIGURE 4.43 ACTIVITY COEFFICIENTS FOR O2/N2 ON LAPORTE 13X MOLECULAR SIEVE PELLETS AT 303.15 , 293.15 AND 278.15 K (PRESSURE = 1.7 BAR)

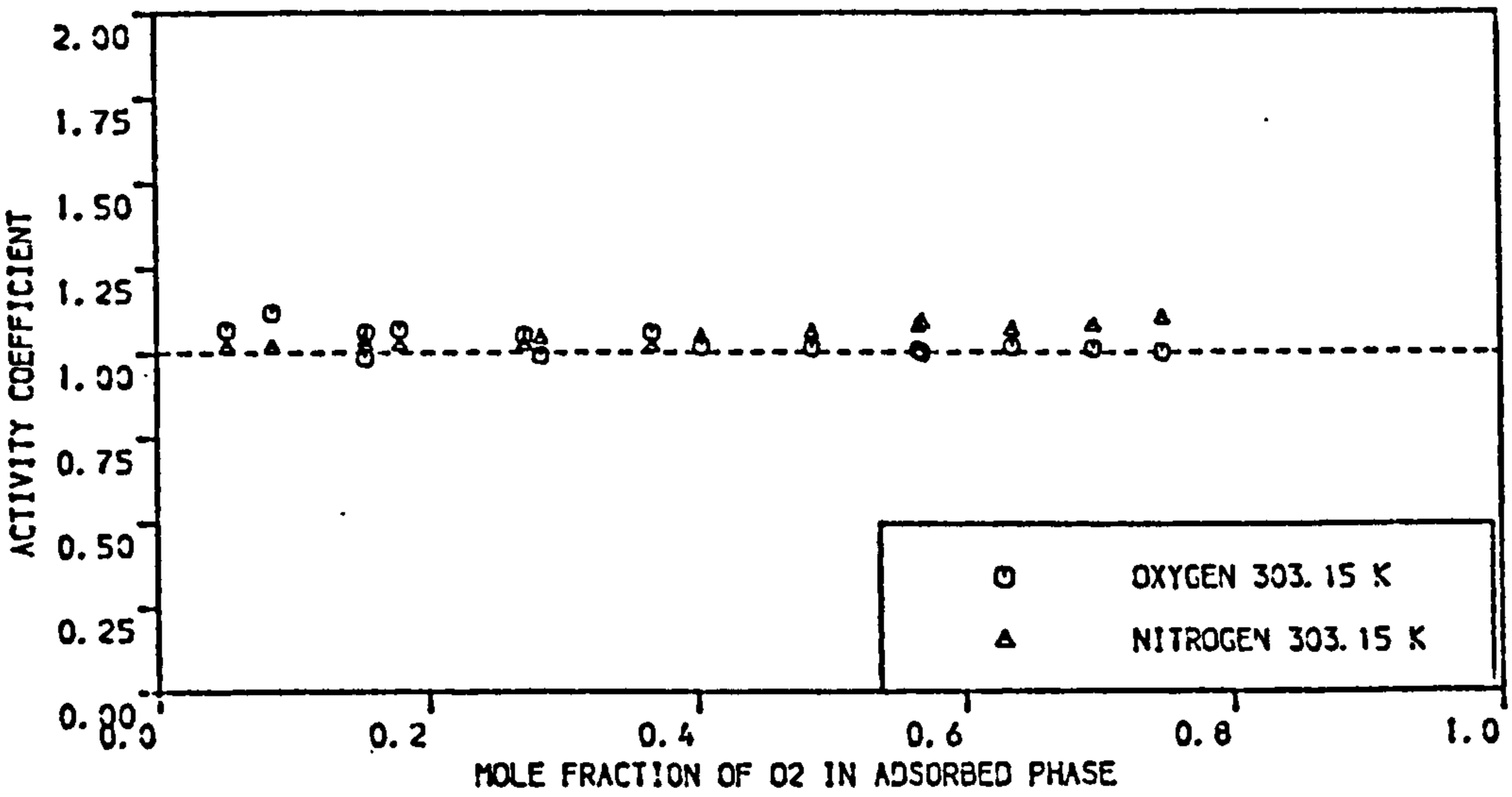

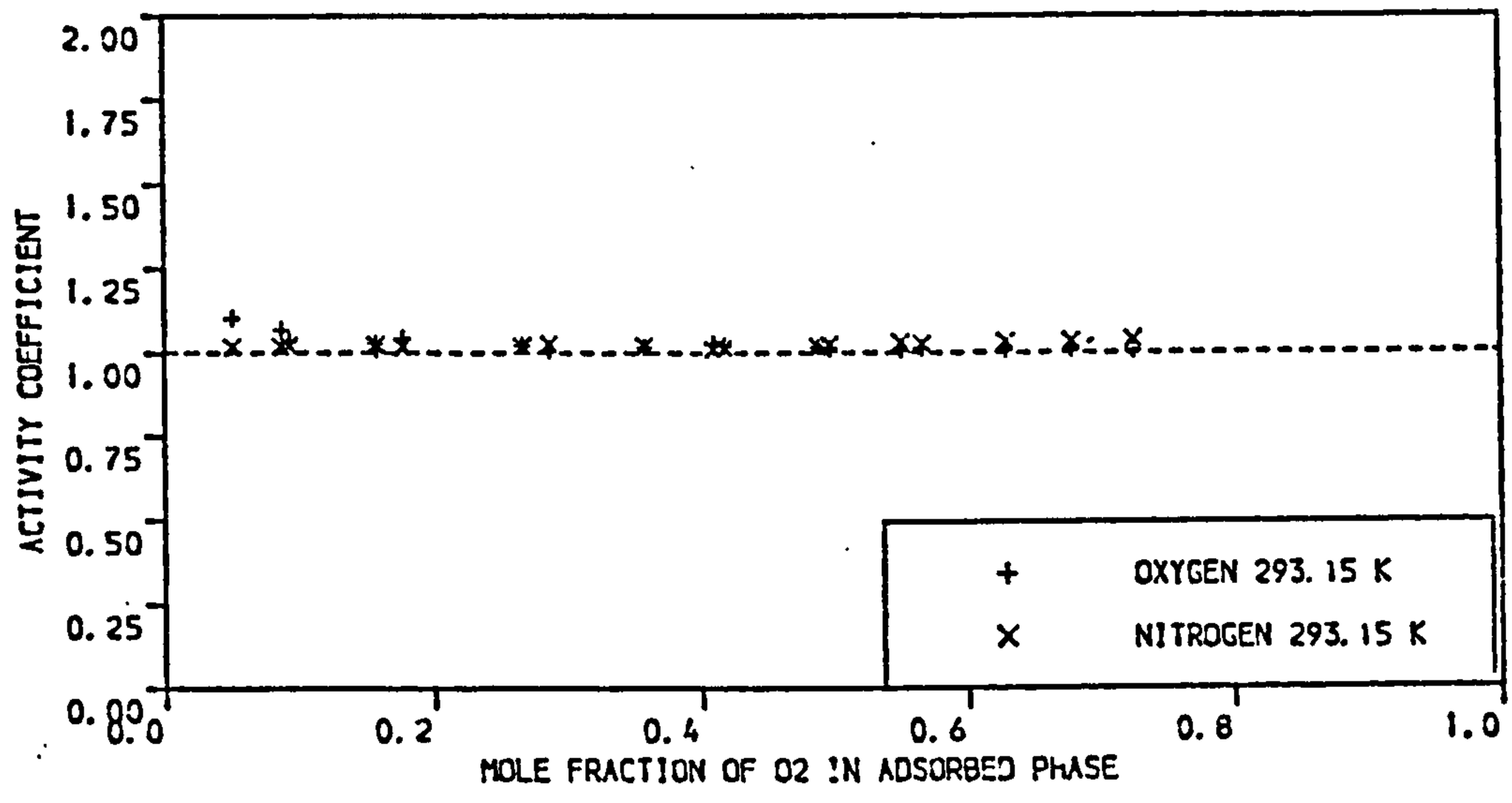

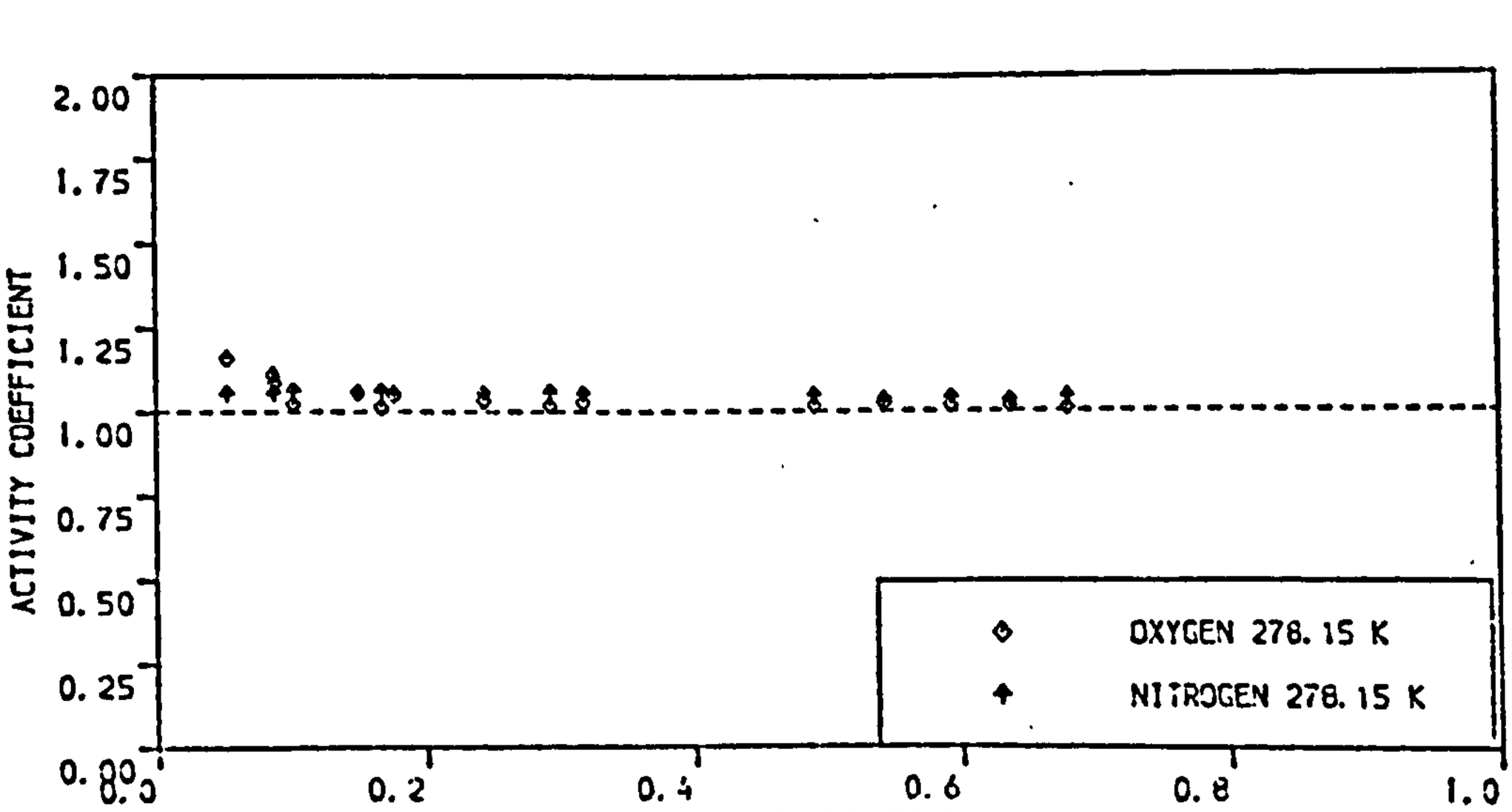

FIGURE 4.44 ACTIVITY COEFFICIENTS FOR O2/N2 ON LAPORTE 13X MOLECULAR SIEVE PELLETS AT 303.15 , 293.15 AND 278.15 K (PRESSURE = 4.4 BAR)

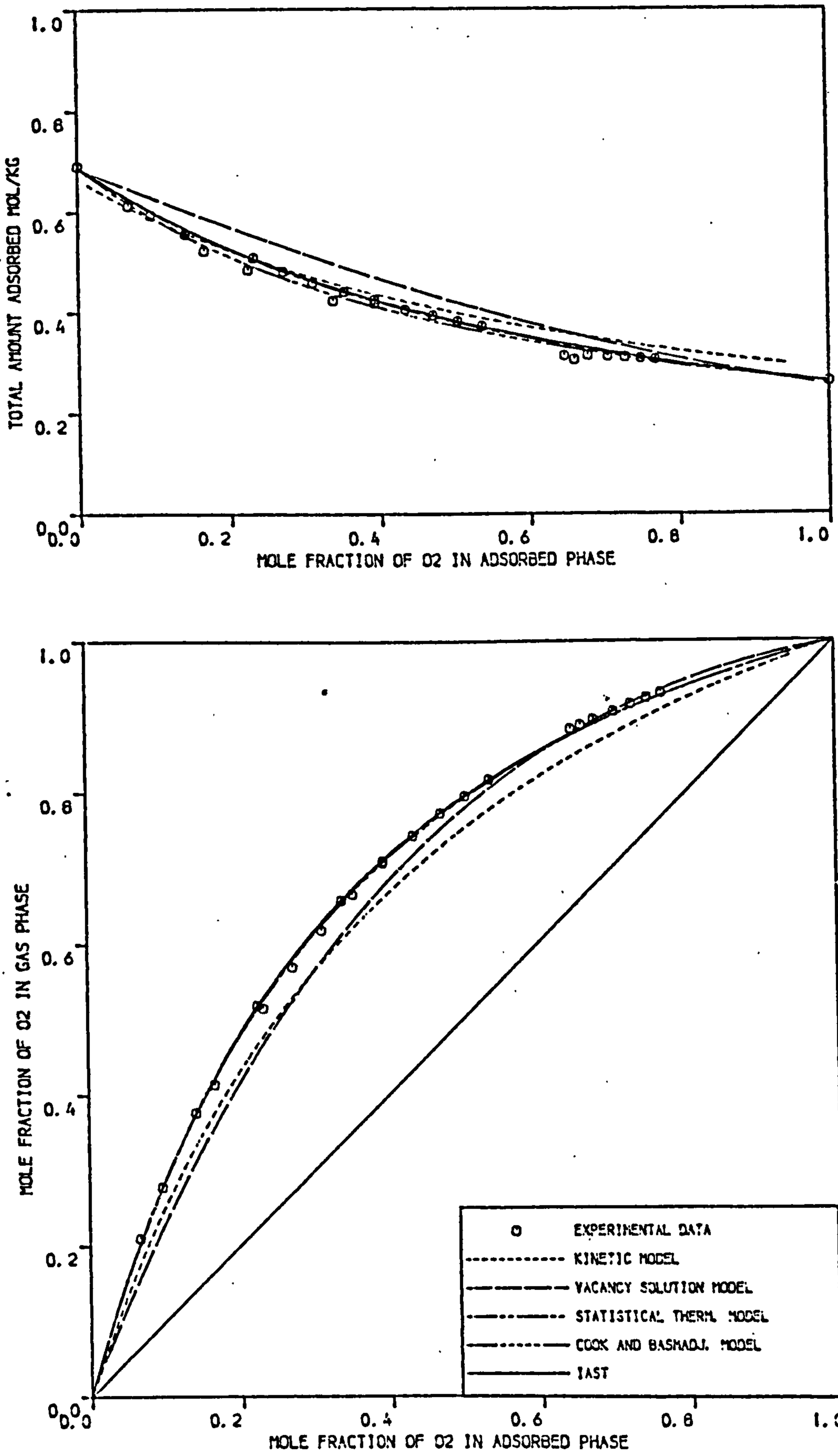

FIGURE 4.45 COMPARISON OF THEORETICAL PREDICTIONS OF VARIOUS MODELS WITH EXPERIMENTAL EQUILIBRIA OF O2/N2 ON LAPORTE 5A MOLECULAR SIEVE PELLETS AT 278.15 K (PRESSURE = 1.7 BAR)

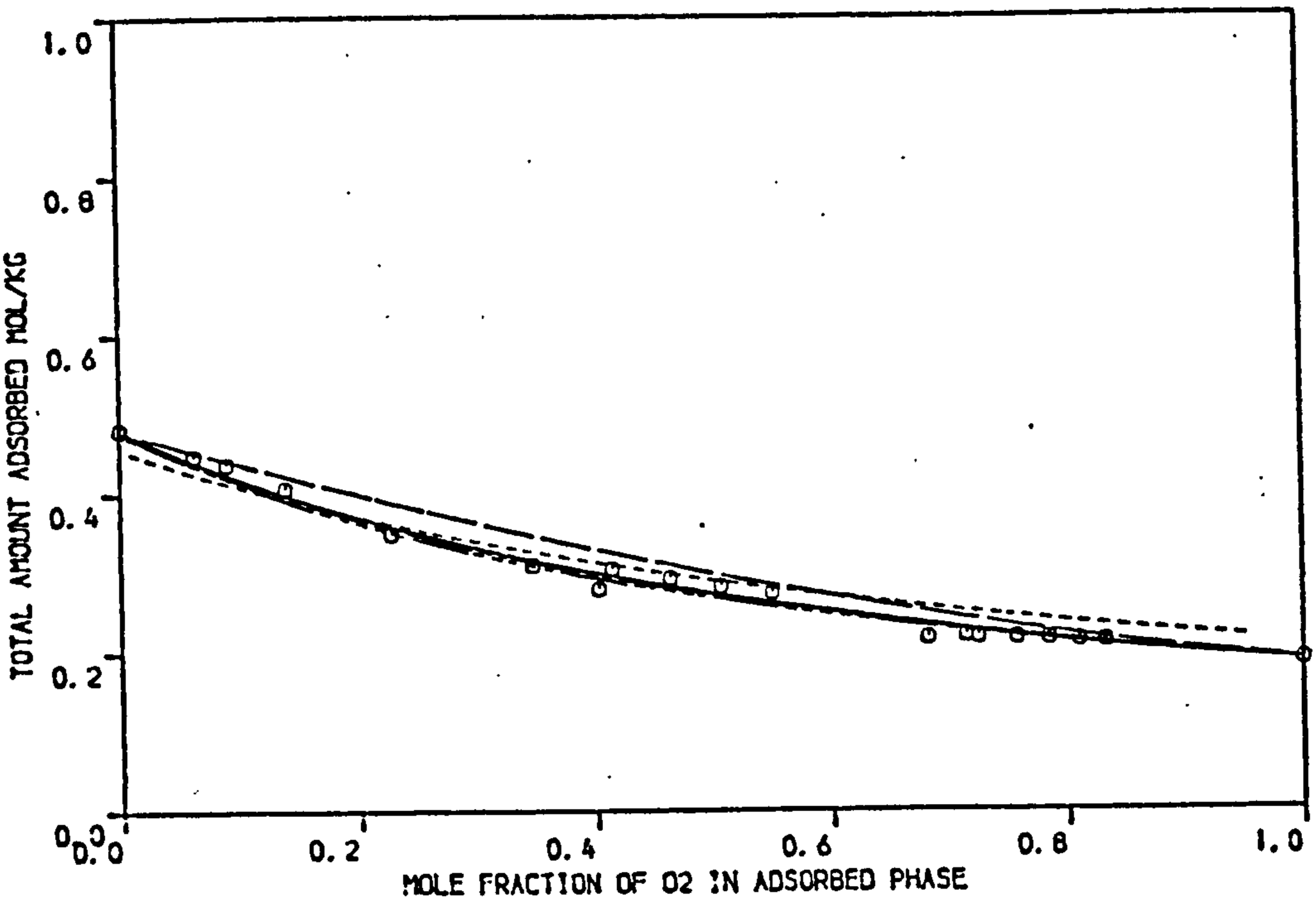

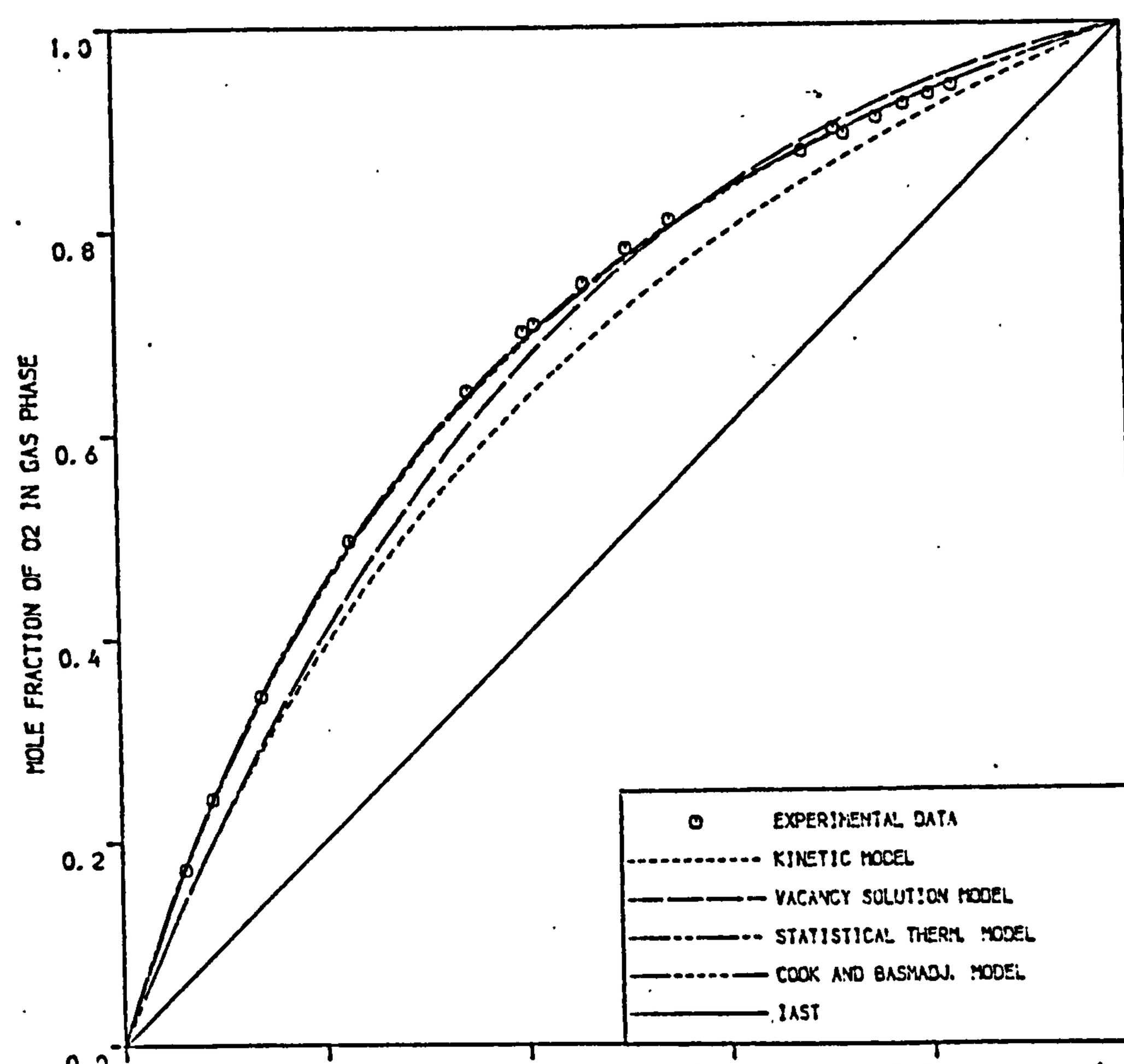

FIGURE 4.46 COMPARISON OF THEORETICAL PREDICTIONS OF VARIOUS MODELS WITH EXPERIMENTAL EQUILIBRIA OF O2/N2 ON LAPORTE 5A MOLECULAR SIEVE PELLETS AT 293.15 K . (PRESSURE ≈ 1.7 BAR)

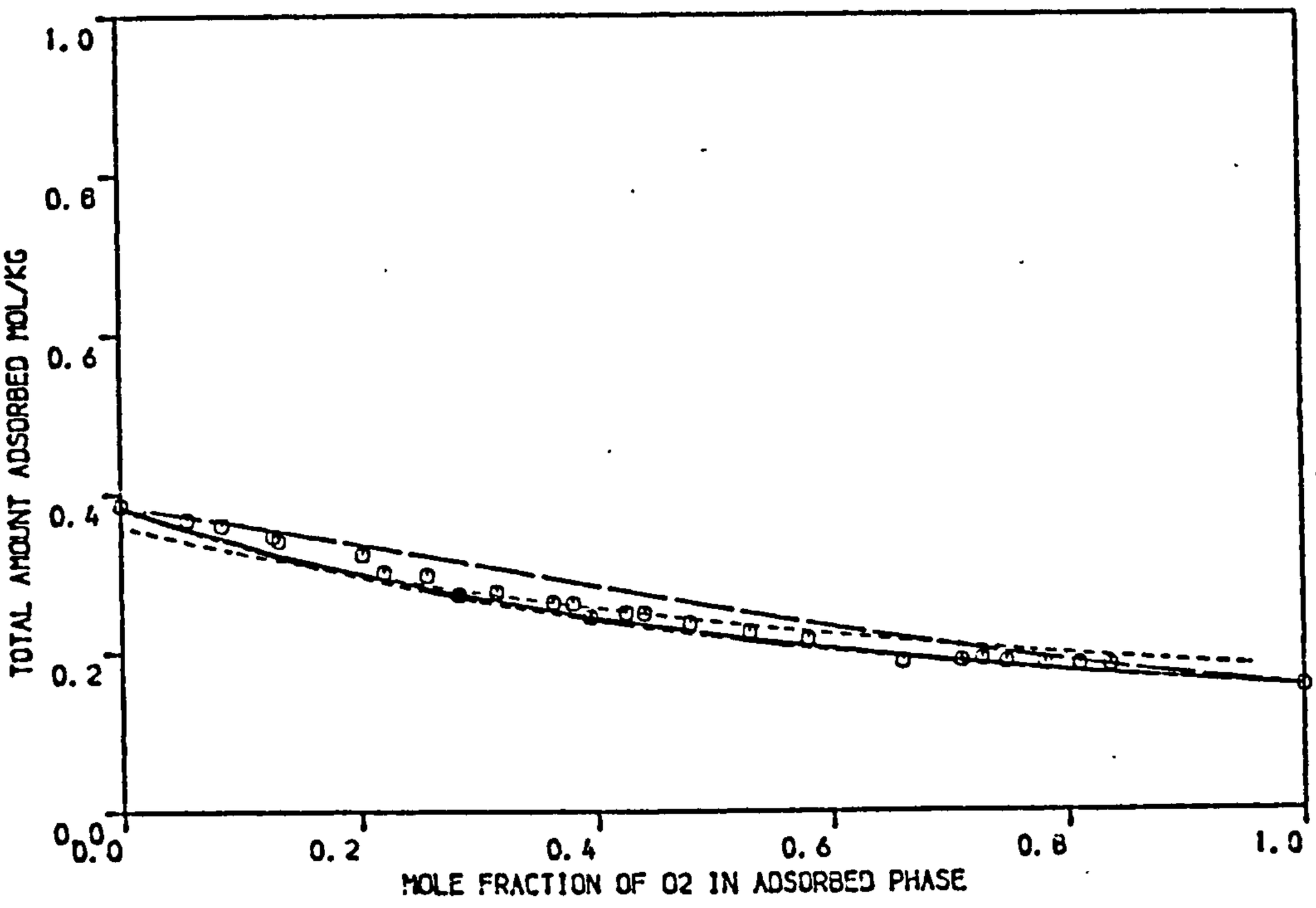

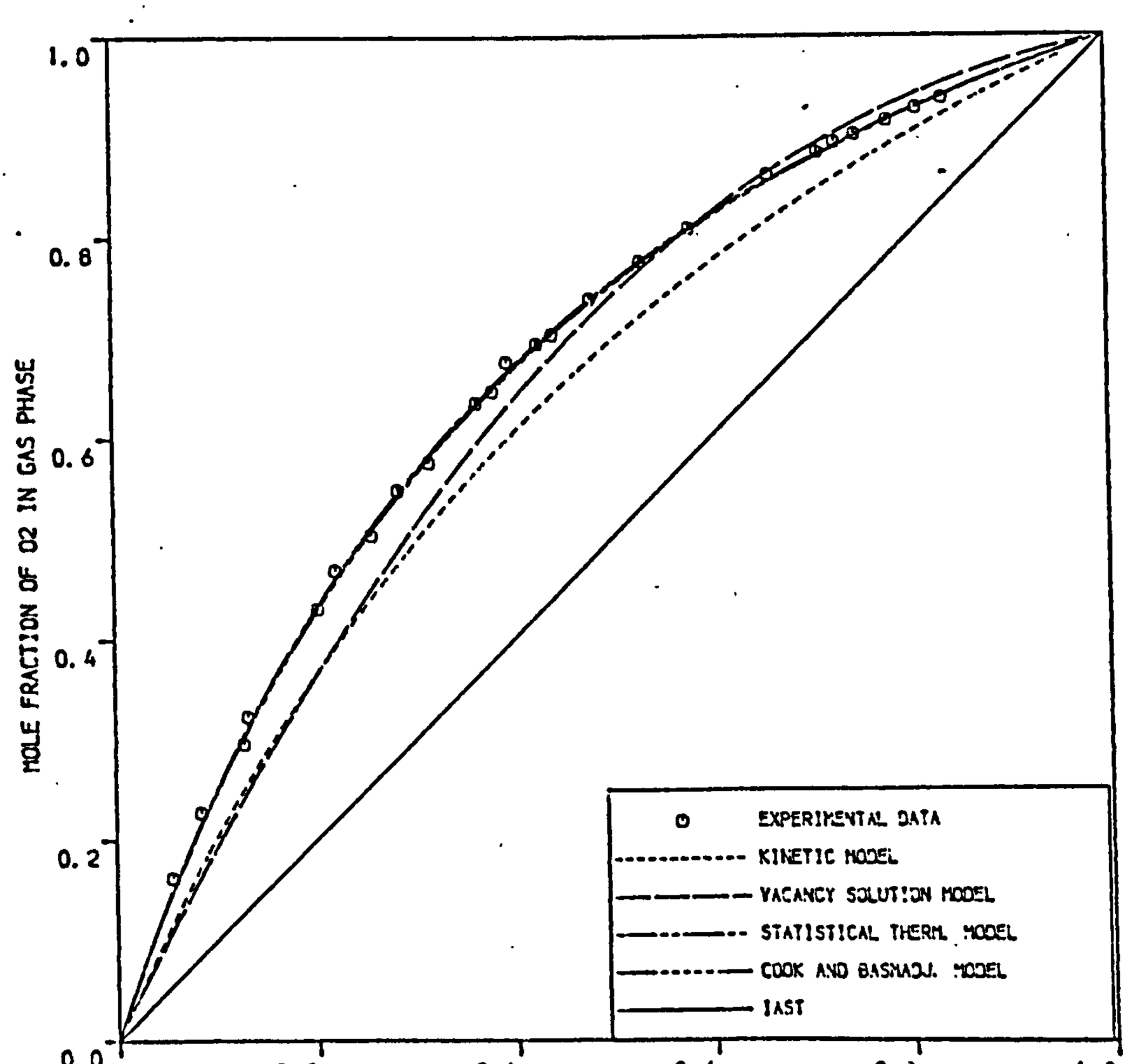

FIGURE 4.47 COMPARISON OF THEORETICAL PREDICTIONS OF VARIOUS MODELS WITH EXPERIMENTAL EQUILIBRIA OF O2/N2 ON LAPORTE 5A MOLECULAR SIEVE PELLETS AT 303.15 K . (PRESSURE ≈ 1.7 BAR)

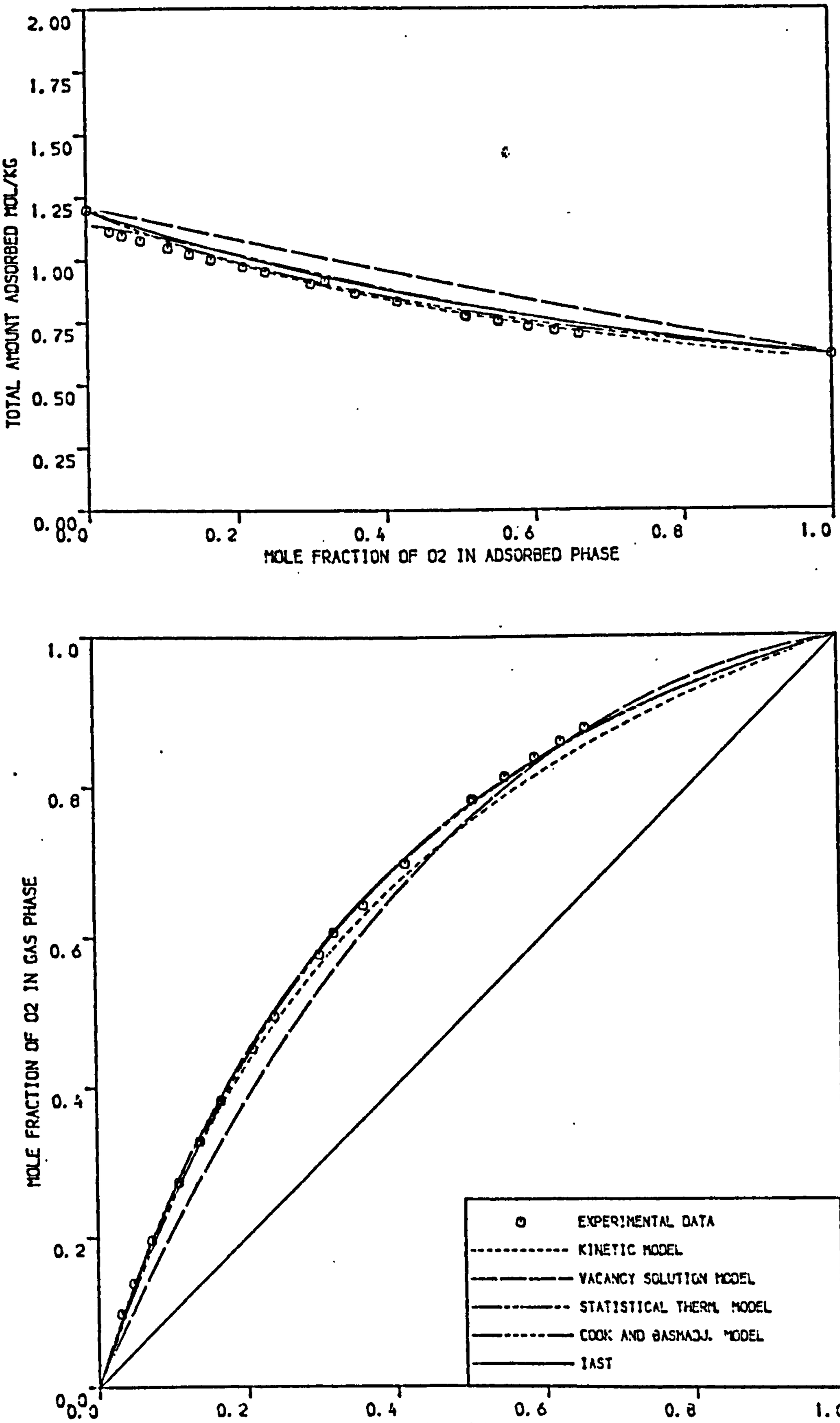

FIGURE 4.48 COMPARISON OF THEORETICAL PREDICTIONS OF VARIOUS MODELS WITH EXPERIMENTAL EQUILIBRIA OF O2/N2 ON LAPORTE 5A MOLECULAR SIEVE PELLETS AT 278.15 K (PRESSURE = 4.4 BAR)

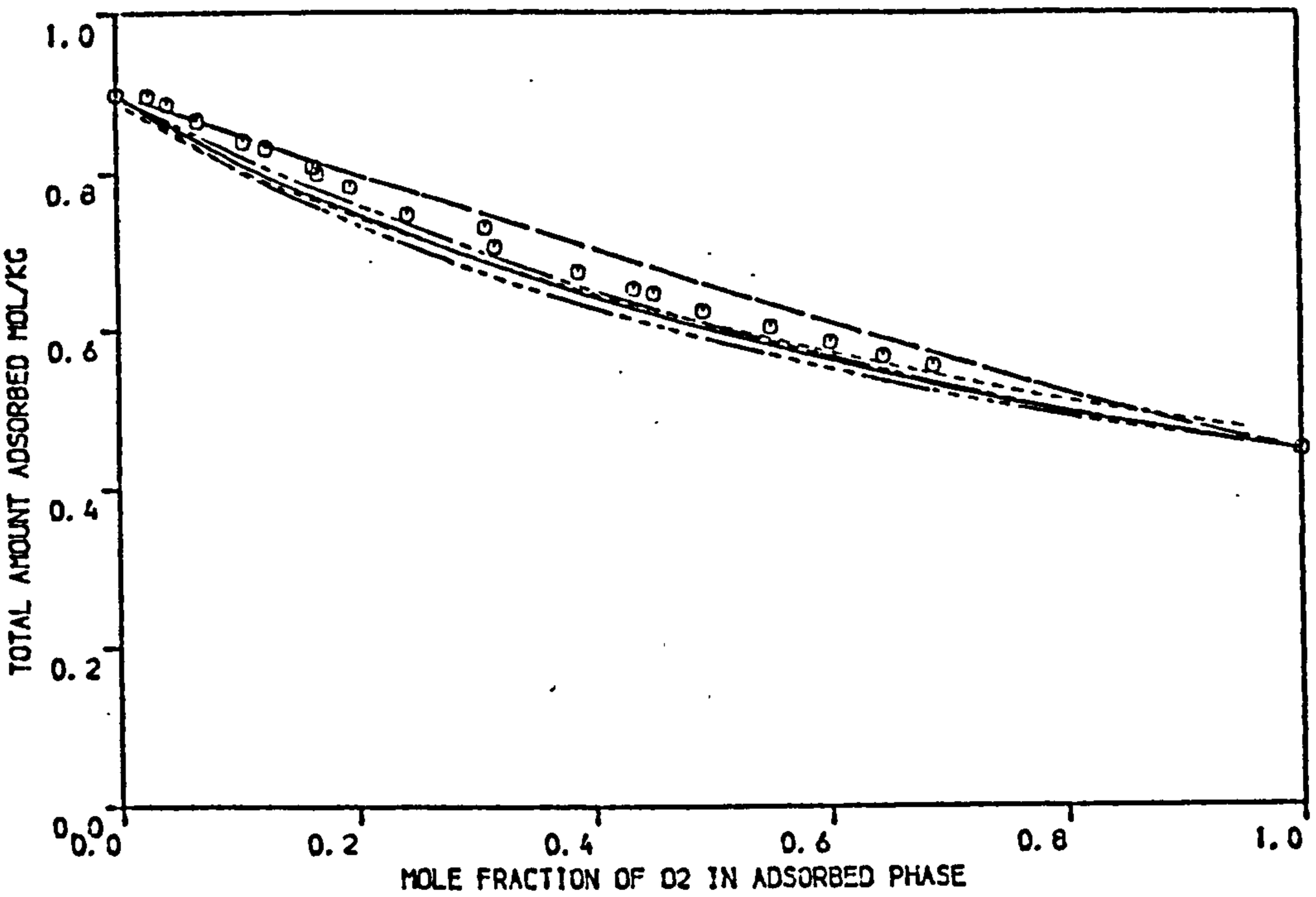

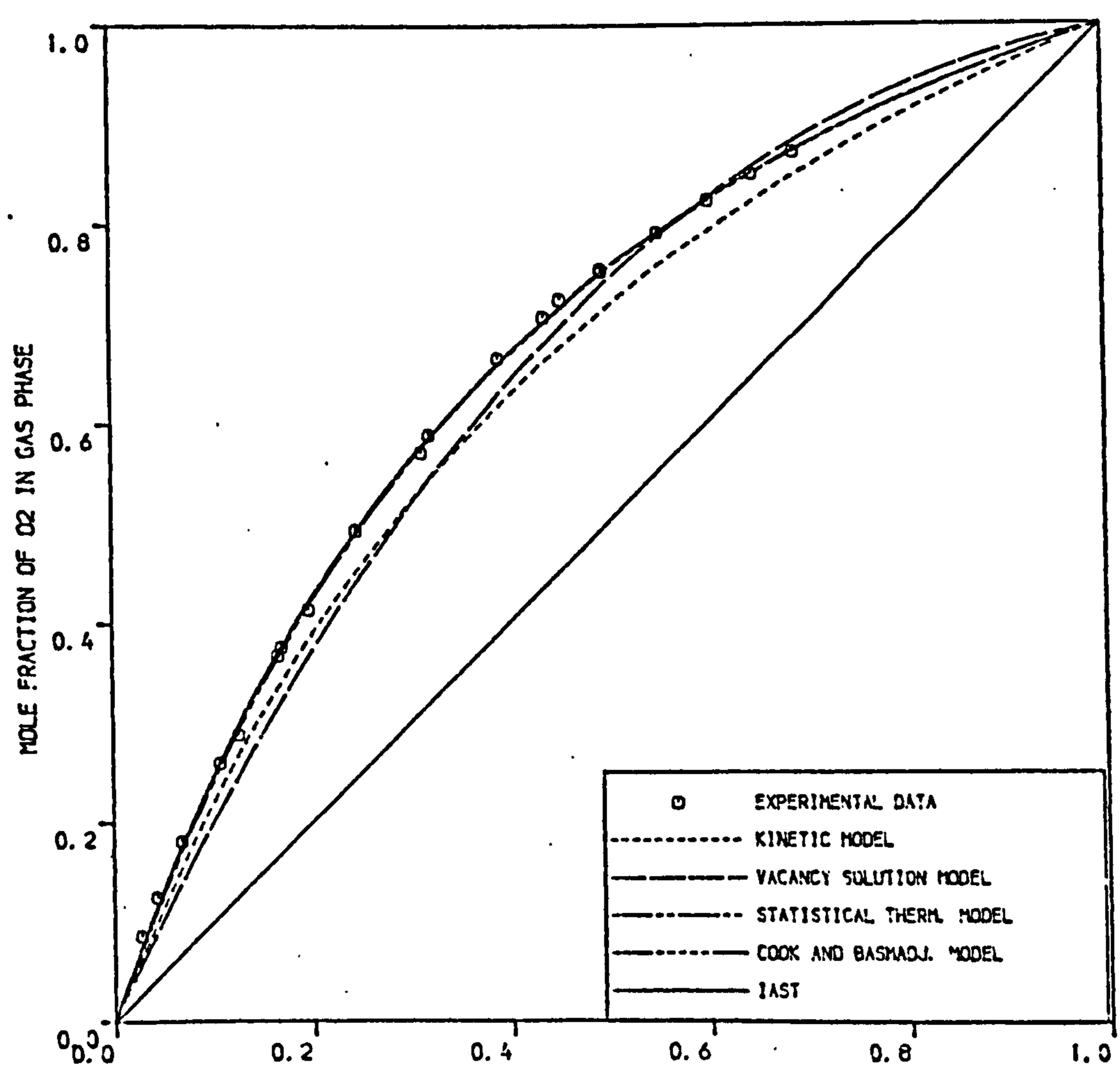

FIGURE 4.49 COMPARISON OF THEORETICAL PREDICTIONS OF VARIOUS MODELS WITH EXPERIMENTAL EQUILIBRIA OF O2/N2 ON LAPORTE 5A MOLECULAR SIEVE PELLETS AT 293.15 K (PRESSURE = 4.4 BAR)

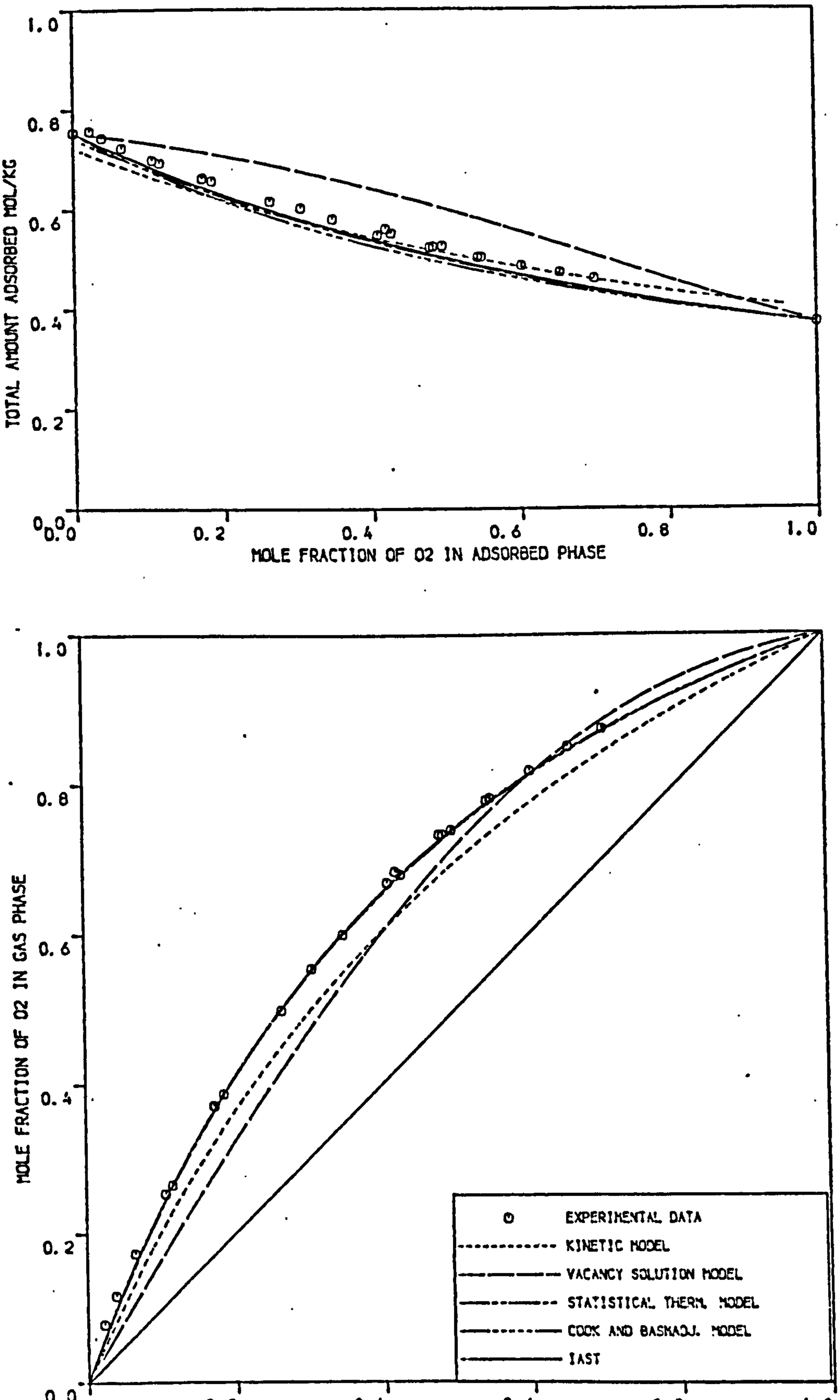

FIGURE 4.50 COMPARISON OF THEORETICAL PREDICTIONS OF VARIOUS MODELS WITH EXPERIMENTAL EQUILIBRIA OF O2/N2 ON LAPORTE 5A MOLECULAR SIEVE PELLETS AT 303.15 K (PRESSURE = 4.4 BAR)

tions between the predicted total amount adsorbed and the experimental values were small at binary mixtures approaching pure components. The predicted total amount adsorbed was significantly different from the experimental values for binary mixtures away from both ends of pure components. The failure of the model could be due to reasons stated before for Laporte 13X and again the effect of including the estimated values of the interaction coefficients Λ_{12} and Λ_{21} as given by Equations (4.8) - (4.10) offered no gain in improvement of the model.

The predicted separation factors obtained by the kinetic model were far from quantitative agreement with the experimental values except for the data at temperature 278.15 K and pressure 4.4 bar, where smaller deviations are noticed. It is surprising to obtain good predictions by this model at the low temperature rather than the high temperature where smaller amounts are adsorbed and hence adsorbate-adsorbate interactions might be less. Inspection of Table 4.6 shows that the Henry law constants obtained by the model for the pure components are close to the values of the other models at temperature 278.15 K and large deviation of about 22% for oxygen is noticed at the higher temperatures.

The activity coefficients for oxygen and nitrogen on Laporte 5A at the three temperatures and two pressures are represented graphically in Figures 4.51 and 4.52. From the plots it is seen that no significant deviations from ideality are encountered.

4.2.3.6 Interpretation of results on EKA 5A

The binary equilibria experimental results on EKA 5A molecular sieve pellets are replotted on Figures 4.53 - 4.58 together with the predicted equilibria data by the five models studied. For the statistical thermodynamic model the predictions were obtained for values of i and j in Equation (2.49) adjusted to 8 and 4 respectively.

For the three temperatures studied at pressure 1.7 bar and for

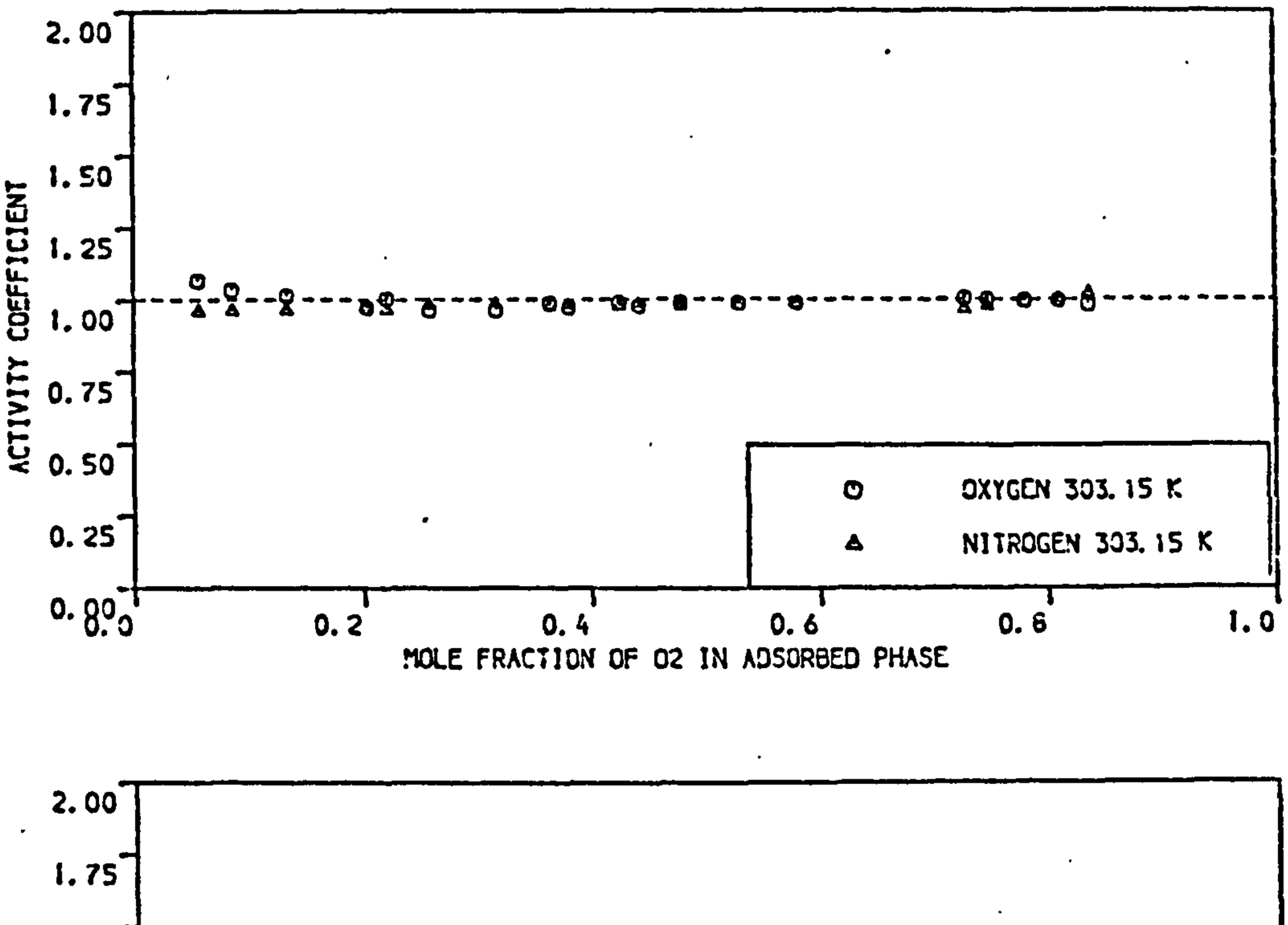

FIGURE 4.51 ACTIVITY COEFFICIENTS FOR O2/N2 ON LAPORTE 5A MOLECULAR SIEVE PELLETS AT 303.15 , 293.15 AND 278.15 K (PRESSURE = 1.7 BAR)

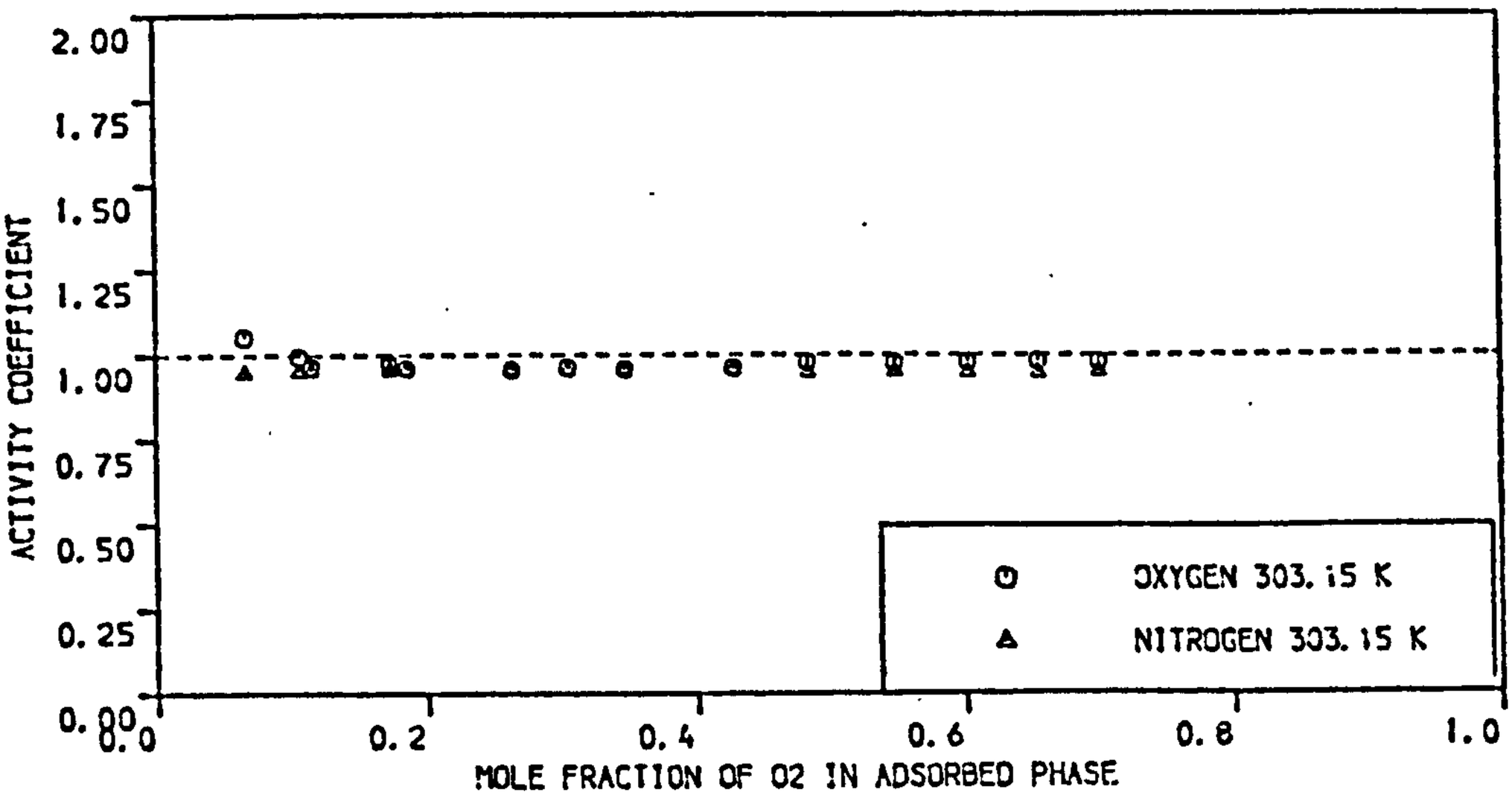

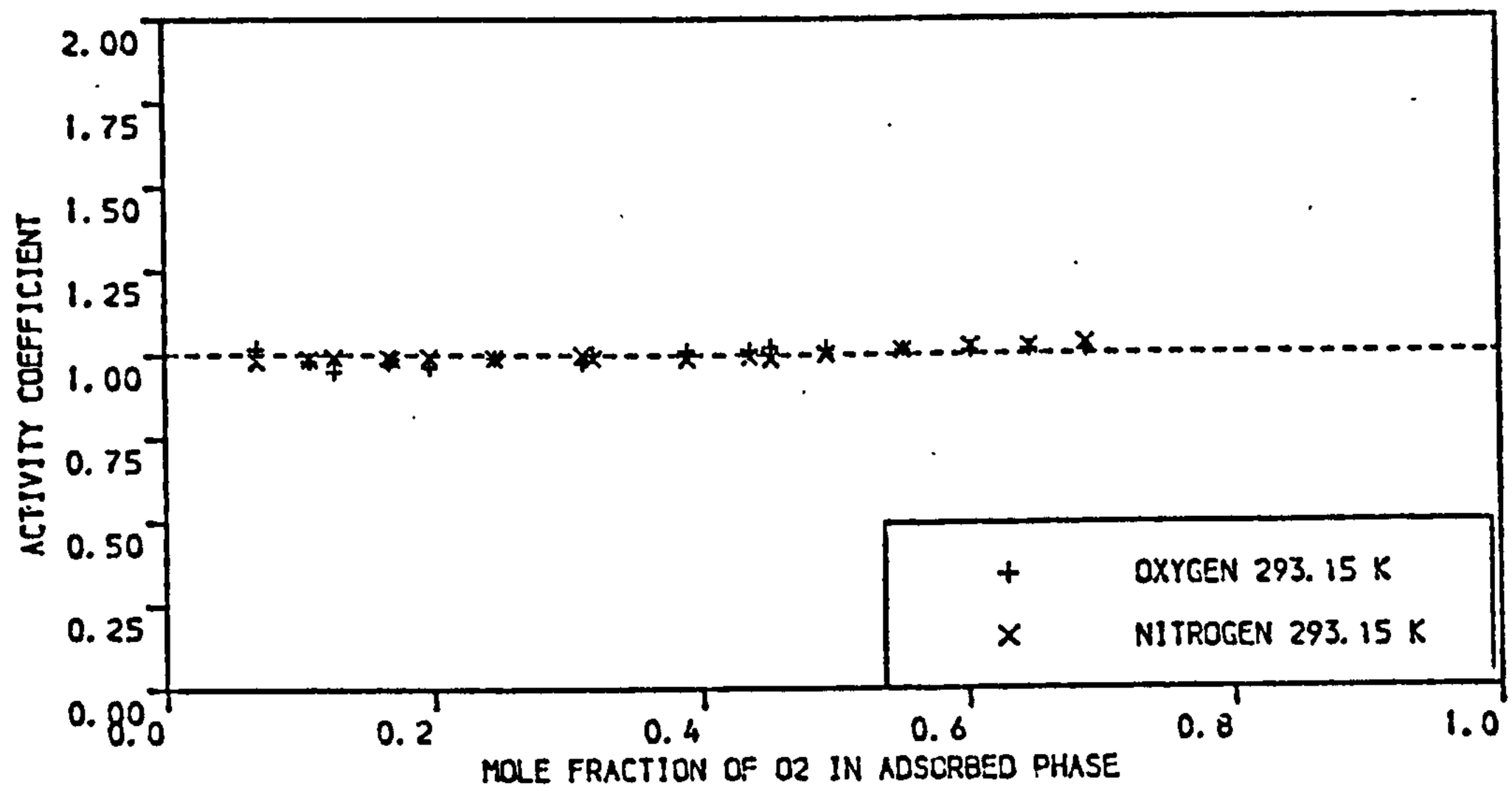

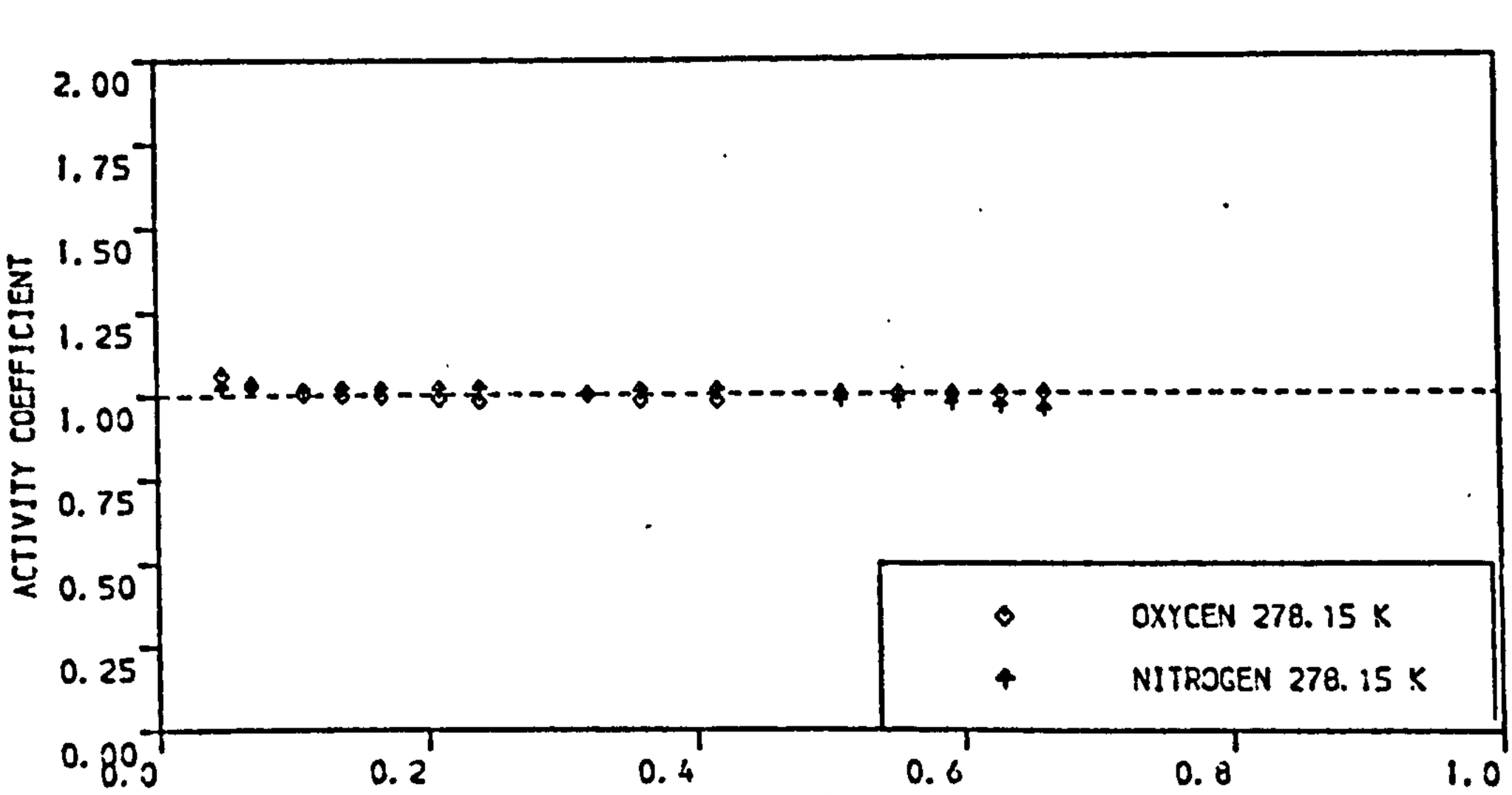

FIGURE 4.52 ACTIVITY COEFFICIENTS FOR O2/N2 ON LAPORTE 5A MOLECULAR SIEVE PELLETS AT 303.15 , 293.15 AND 278.15 K (PRESSURE = 4.4 BAR)

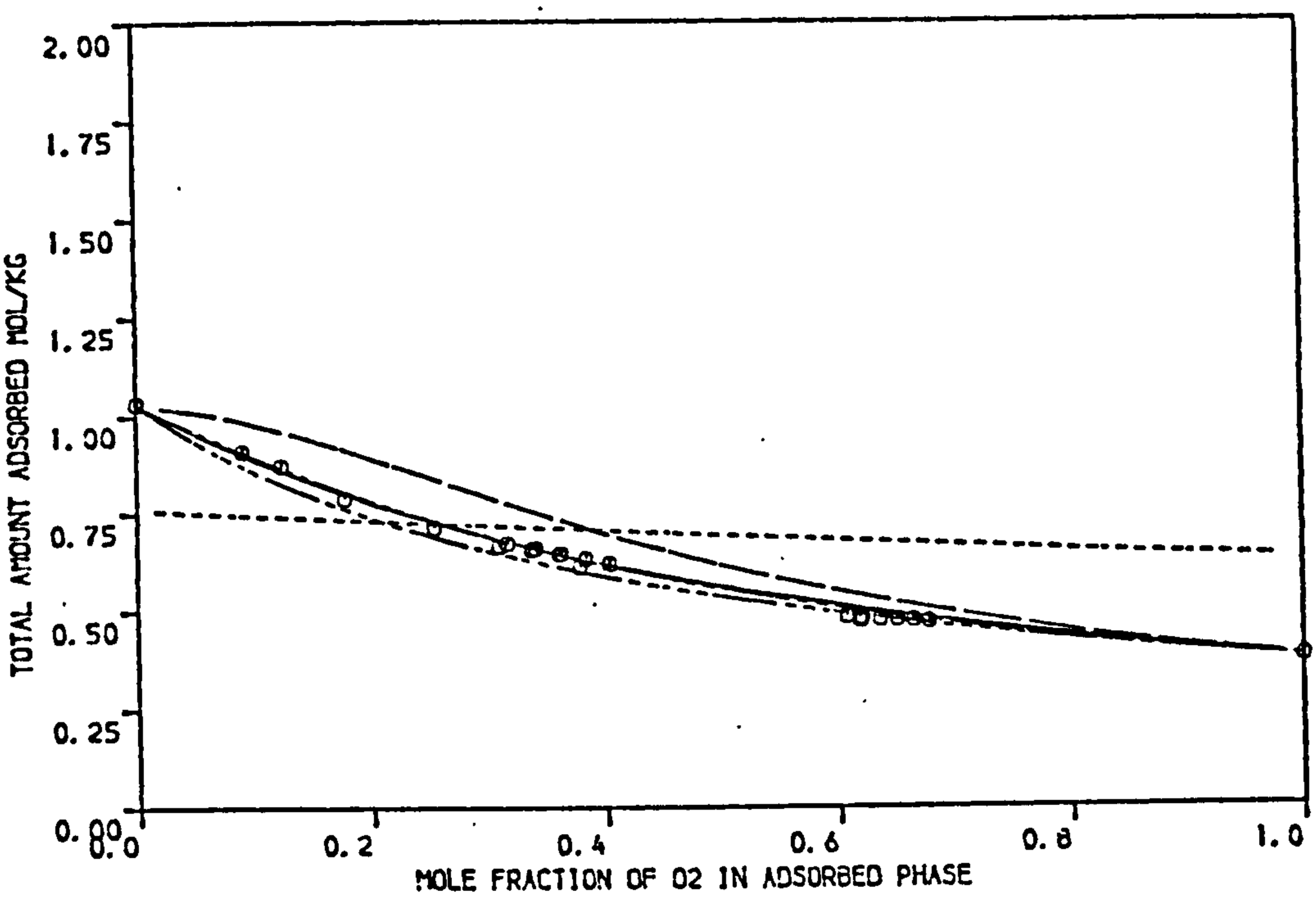

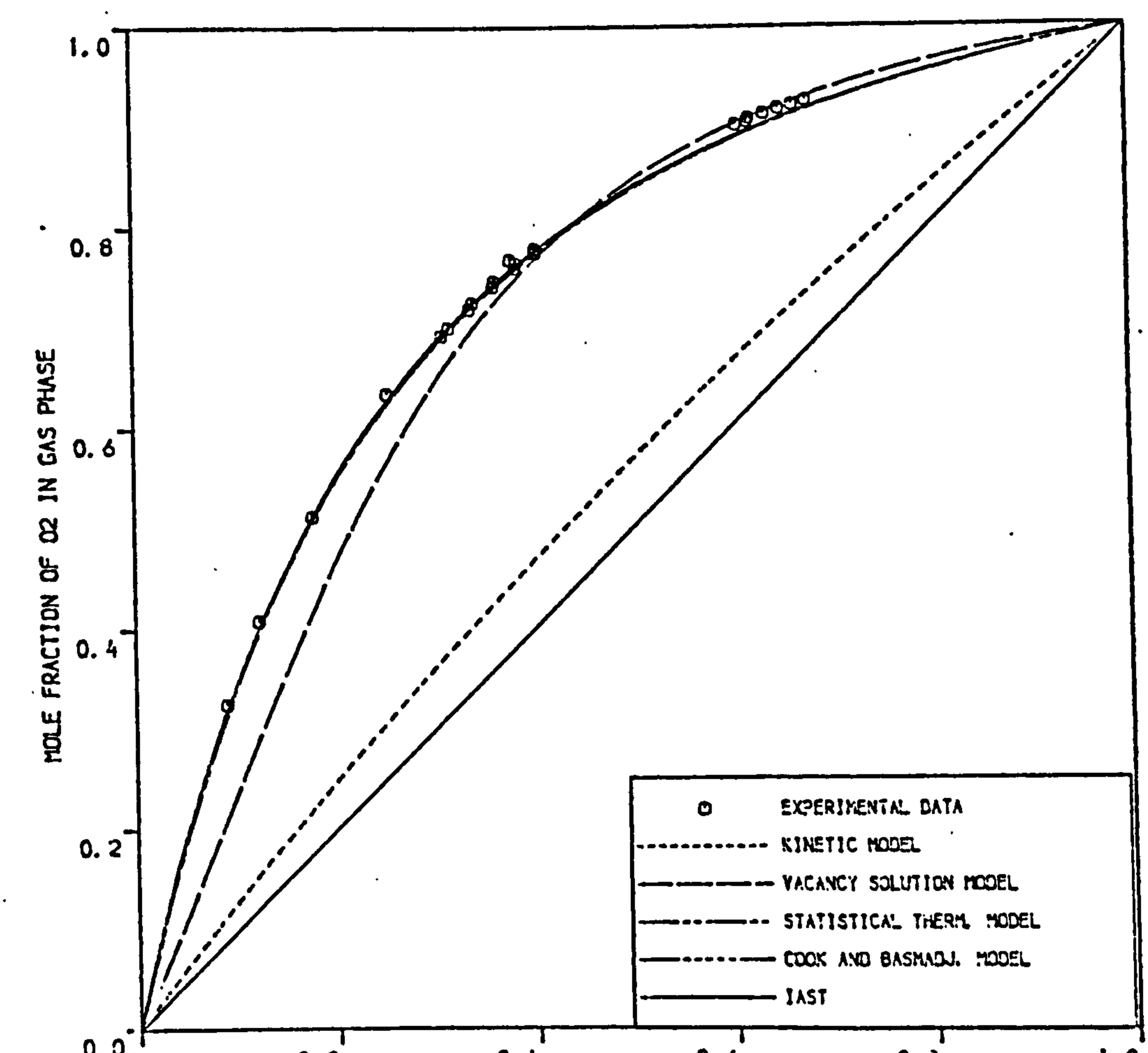

FIGURE 4.53 COMPARISON OF THEORETICAL PREDICTIONS OF VARIOUS MODELS WITH EXPERIMENTAL EQUILIBRIA OF O2/N2 ON EKA 5A MOLECULAR SIEVE PELLETS AT 278.15 K (PRESSURE = 1.7 BAR)

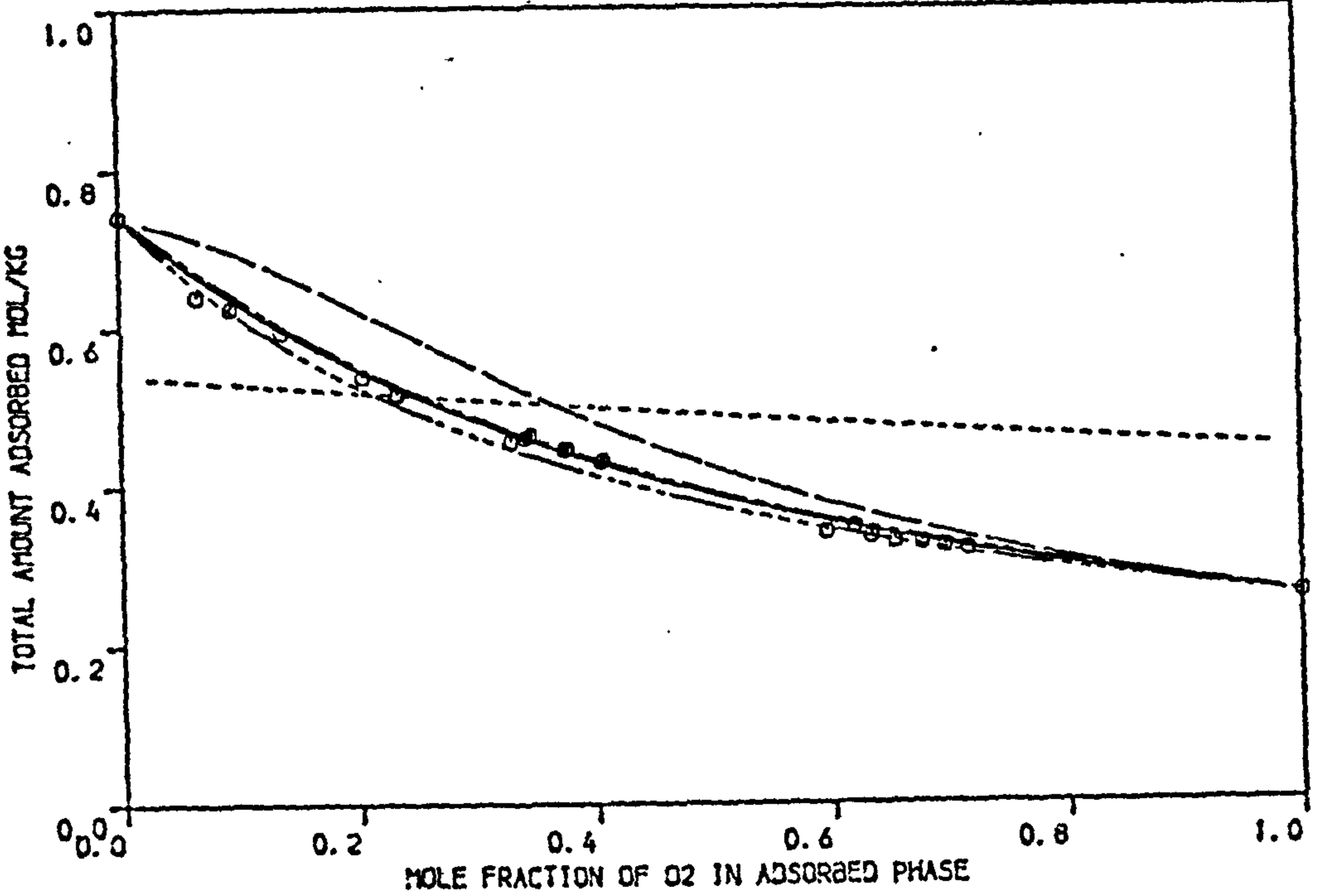

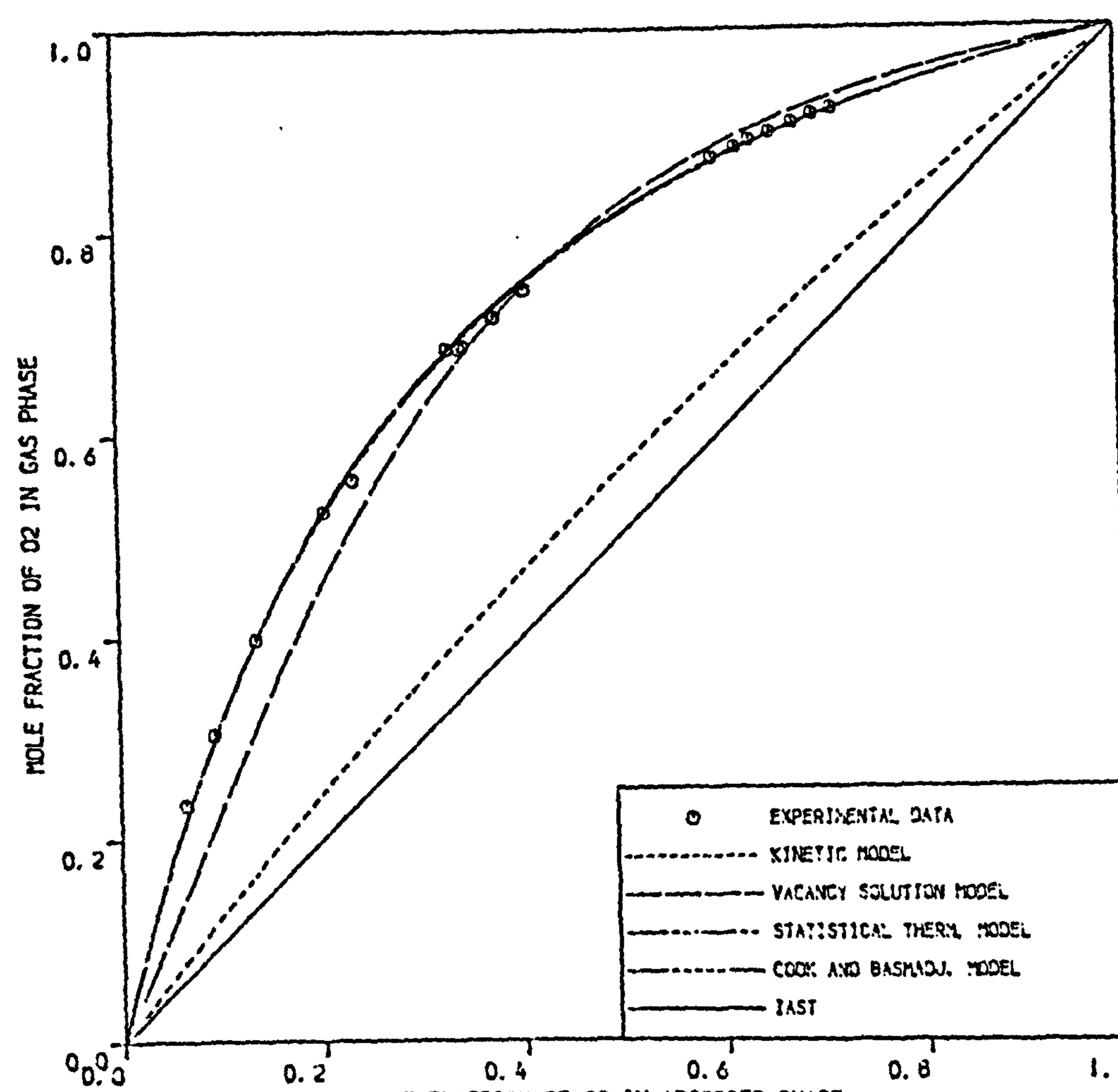

FIGURE 4.54 COMPARISON OF THEORETICAL PREDICTIONS OF VARIOUS MODELS WITH EXPERIMENTAL EQUILIBRIA OF O2/N2 ON EKA 5A MOLECULAR SIEVE PELLETS AT 293.15 K (PRESSURE ≈ 1.7 BAR)

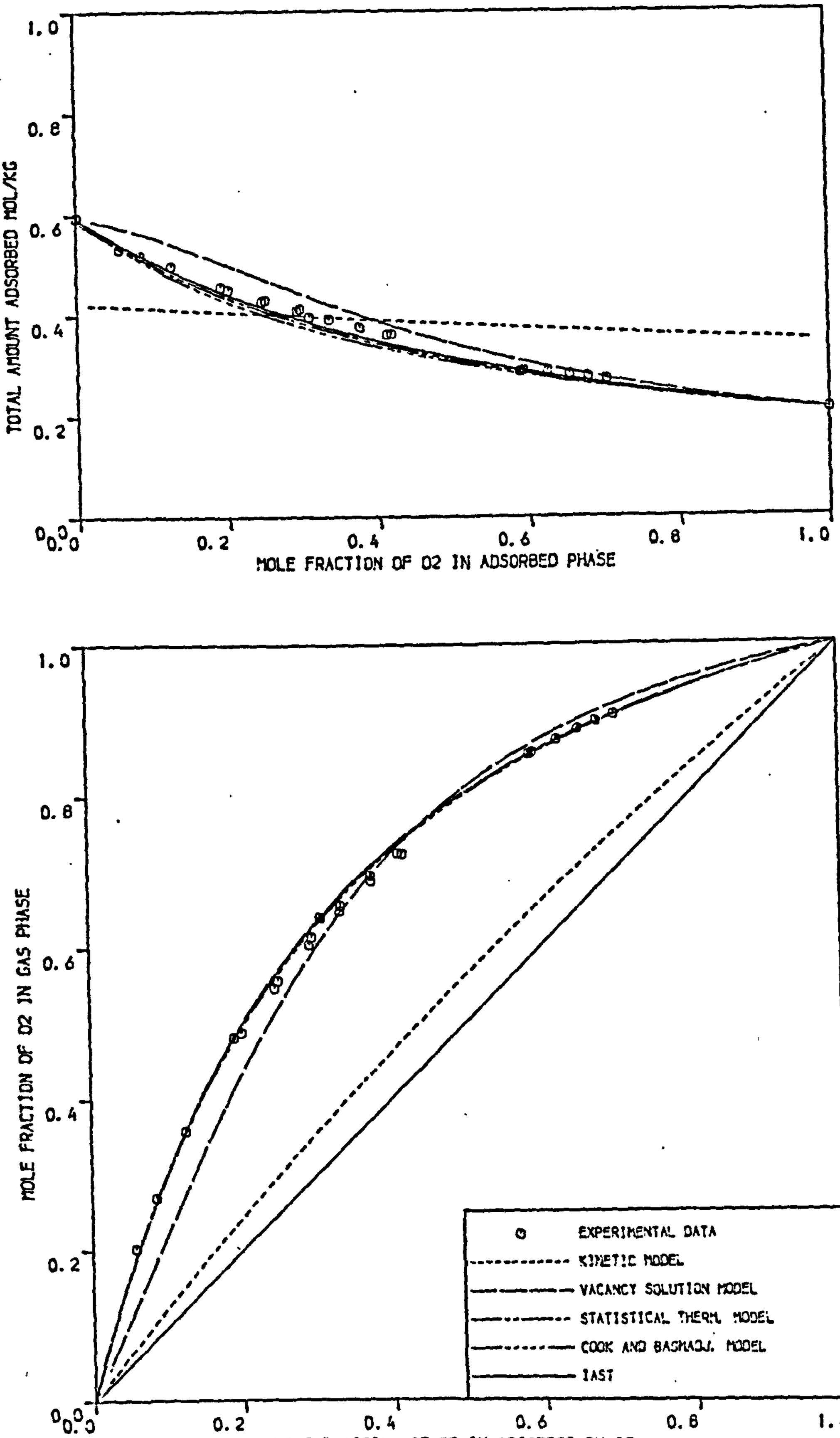

FIGURE 4.55 COMPARISON OF THEORETICAL PREDICTIONS OF VARIOUS MODELS WITH EXPERIMENTAL EQUILIBRIA OF O2/N2 ON EKA 5A MOLECULAR SIEVE PELLETS AT 303.15 K (PRESSURE ≈ 1.7 BAR)

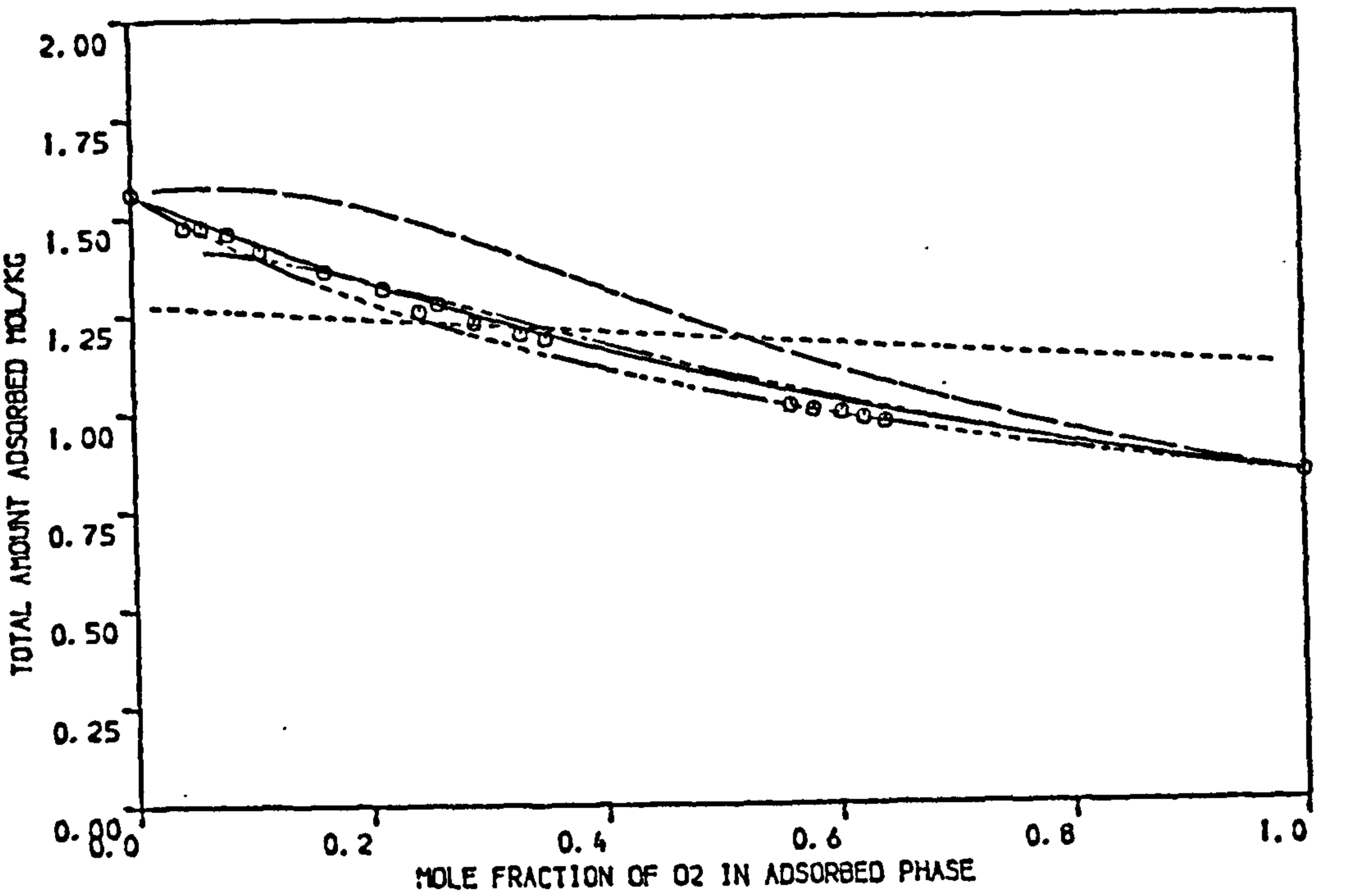

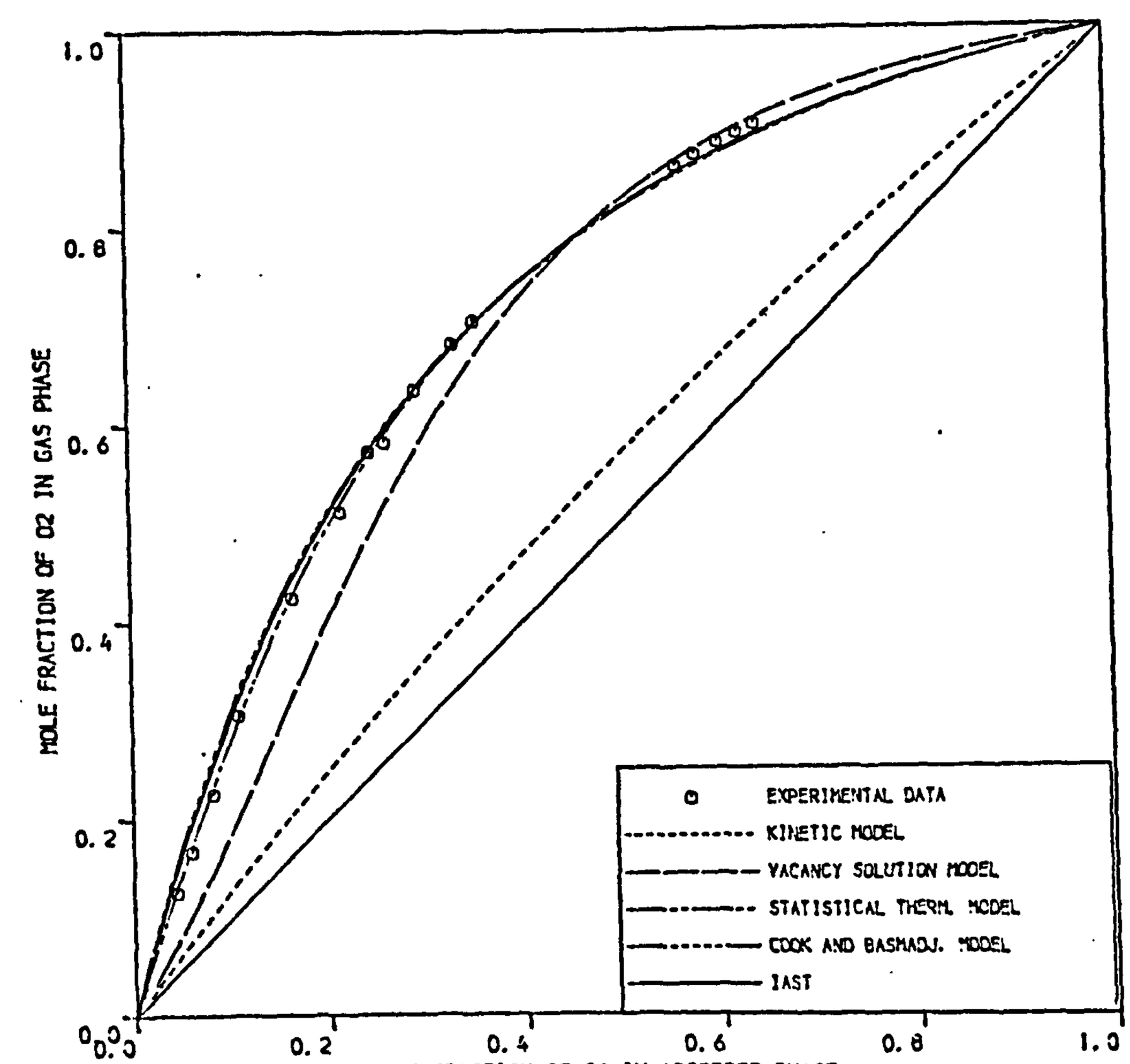

FIGURE 4.56 COMPARISON OF THEORETICAL PREDICTIONS OF VARIOUS MODELS WITH EXPERIMENTAL EQUILIBRIA OF O2/N2 ON EKA 5A MOLECULAR SIEVE PELLETS AT 278.15 K (PRESSURE ≈ 4.4 BAR)

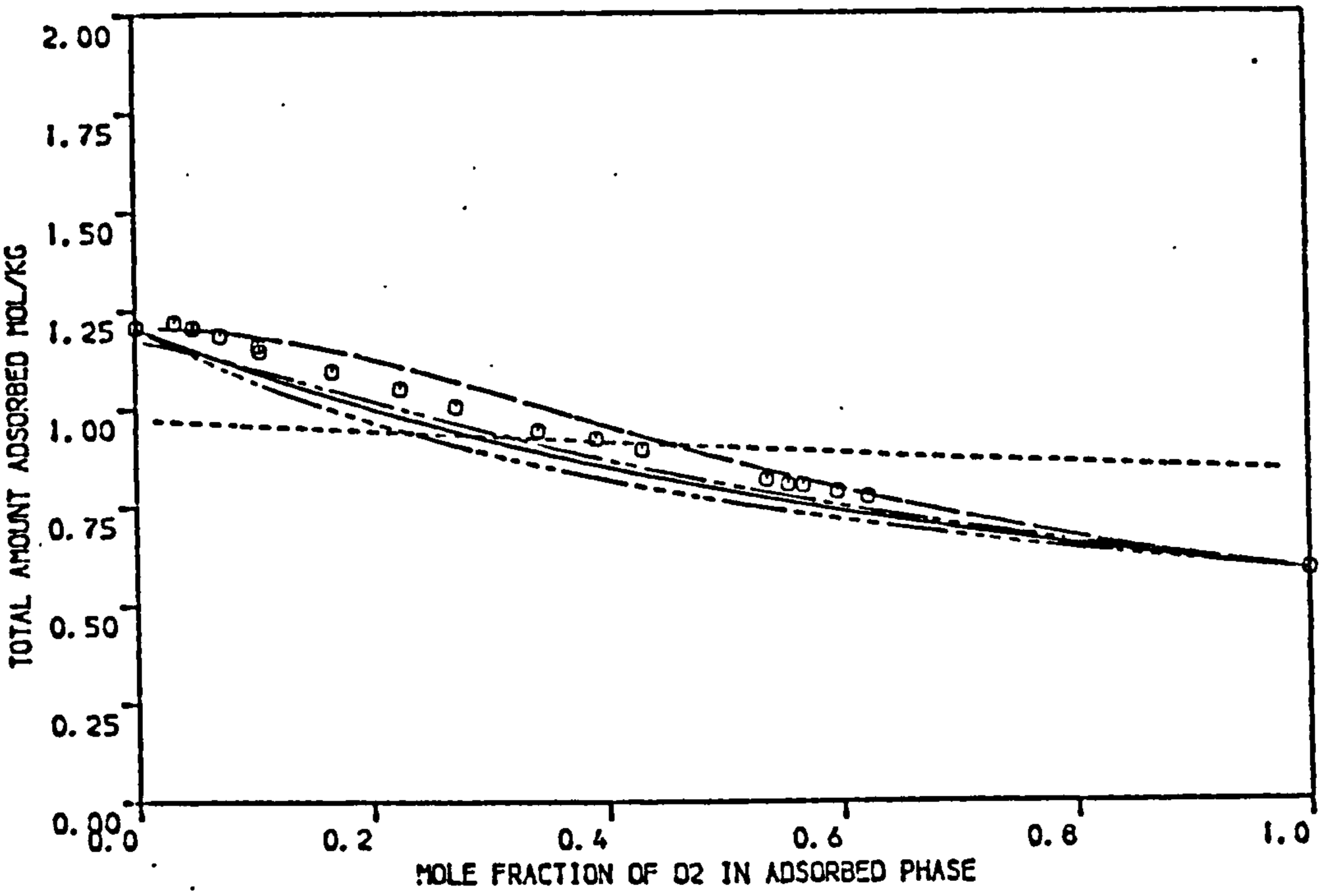

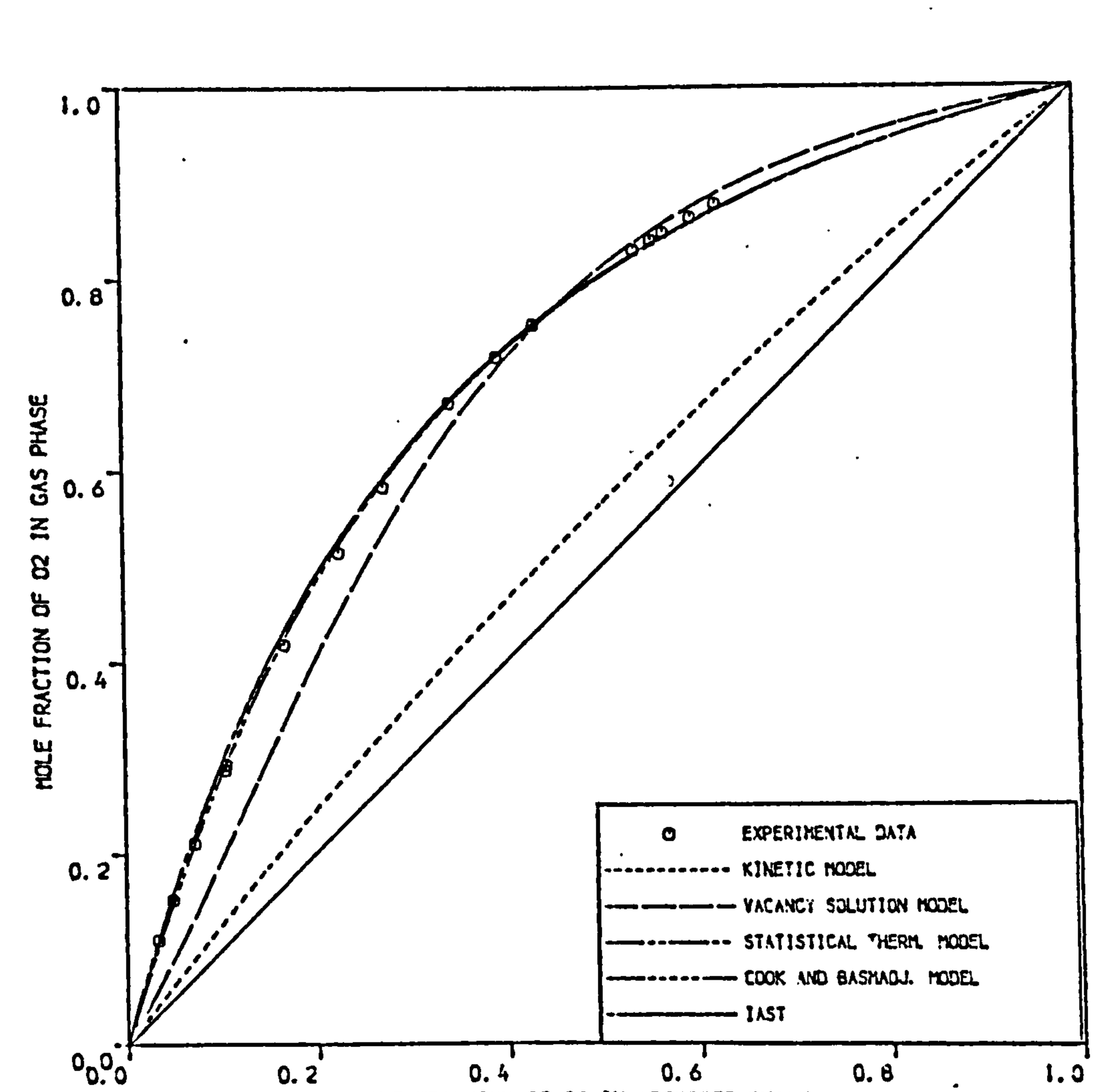

FIGURE 4.57 COMPARISON OF THEORETICAL PREDICTIONS OF VARIOUS MODELS WITH EXPERIMENTAL EQUILIBRIA OF O2/N2 ON EKA 5A MOLECULAR SIEVE PELLETS AT 293.15 K (PRESSURE = 4.4 BAR)

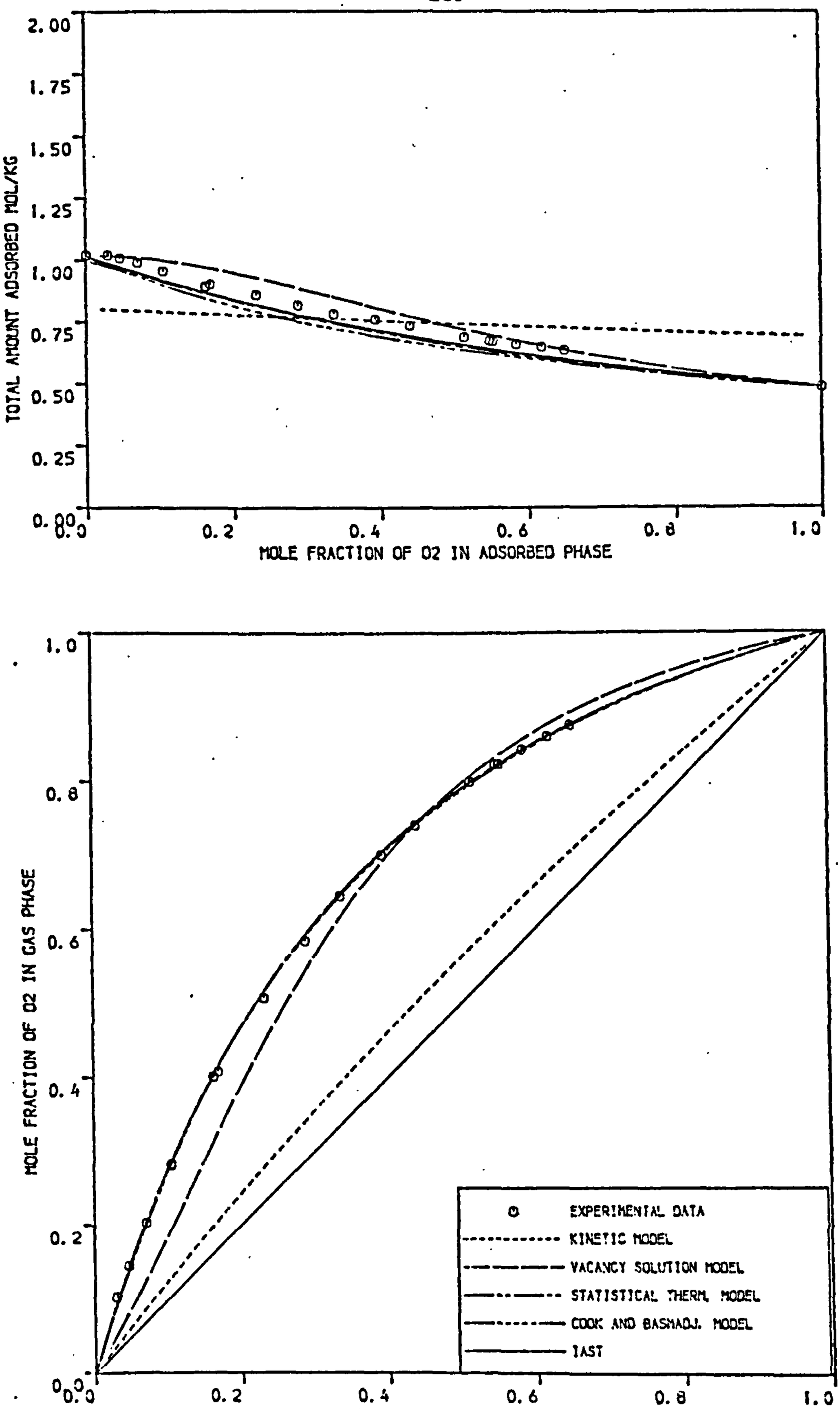

FIGURE 4.58 COMPARISON OF THEORETICAL PREDICTIONS OF VARIOUS MODELS WITH EXPERIMENTAL EQUILIBRIA OF O2/N2 ON EKA 5A MOLECULAR SIEVE PELLETS AT 303.15 K (PRESSURE = 4.4 BAR)

temperature at 303.15 K and pressure 4.4 bar, the separation factors predicted by the statistical thermodynamic model, Cook and Basmadjian model and IAST were approximately the same and were in good agreement with the experimental data. For temperatures 293.15 and 278.15 K at pressure 4.4 bar there was slight deviation between the statistical thermodynamic model and the other two models, i.e. Cook and Basmadjian model and IAST, and the separation factors predicted by the statistical thermodynamic model coincided with the experimental data. The predicted total amounts adsorbed by the statistical thermodynamic model and IAST were approximately the same for the three temperatures at the two pressures studied, whilst the total amount adsorbed predicted by Cook and Basmadjian was slightly different. The experimental total amounts adsorbed were in good agreement with the predicted values at 1.7 bar pressure while a maximum deviation of 5% was noticed for data at pressure 4.4 bar.

The predictions obtained by the vacancy solution model followed the same trend as that on Laporte 5A and the reasons for failure could be due to reasons stated before.

The Kinetic model hardly predicted any separation and its failure is due to the poor fitting of the pure component isotherms by the model.

The activity coefficients for oxygen and nitrogen on EKA 5A at the three temperatures and two pressures studied are represented graphically in Figures 4.59 and 4.60. At pressure 1.7 bar no appreciable deviation from ideality is noticed except at temperature of 278.15 K which could be due to the effect of assuming constant adsorption pressure since deviations are noticed for one component only (nitrogen). At pressure 4.4 bar and temperature 303.15 K no appreciable deviations from ideality are noticed but for the other two temperatures negative deviations from ideality are noticeable especially for temperature 278.15 K and explains why the

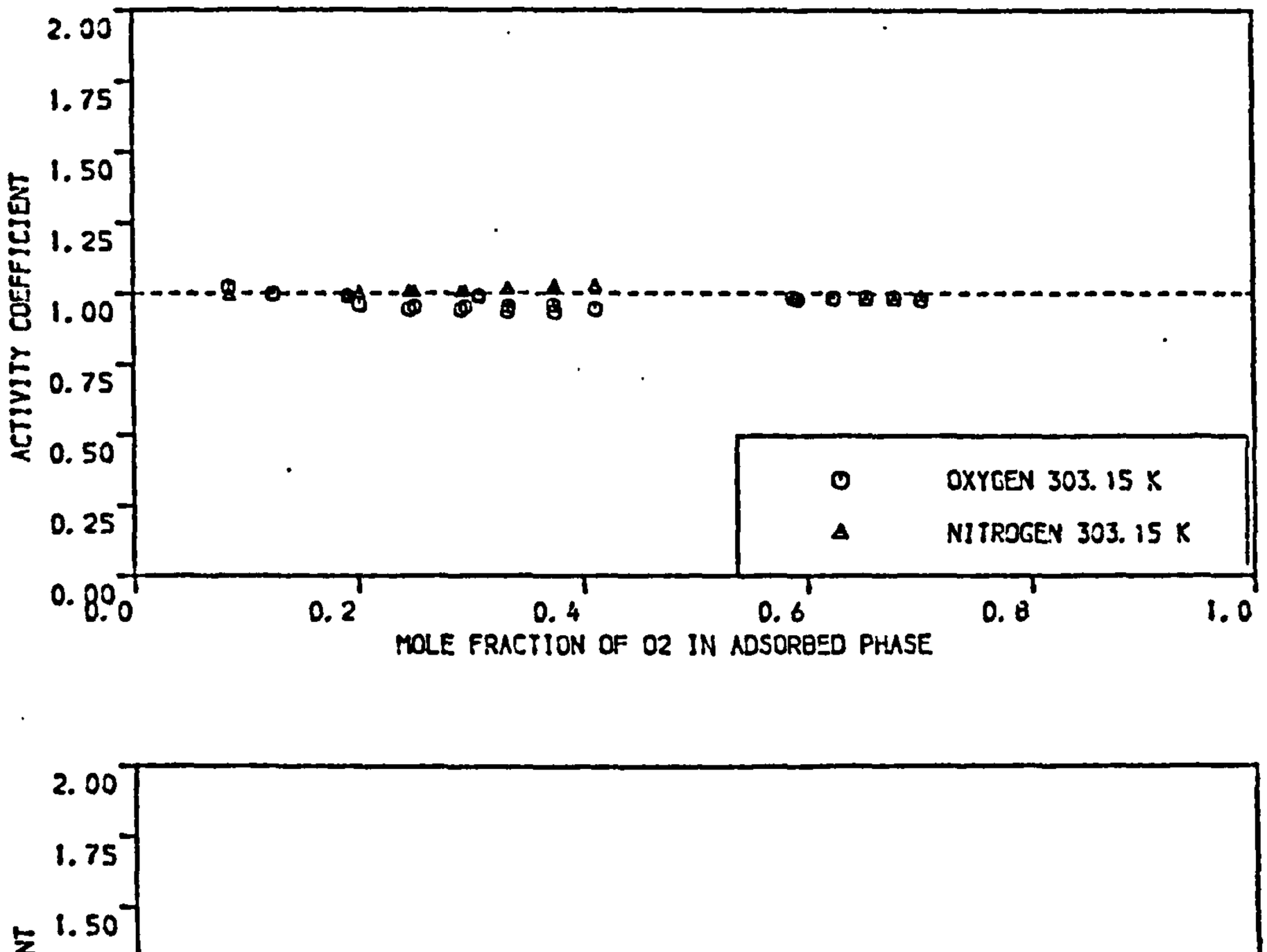

FIGURE 4.59 ACTIVITY COEFFICIENTS FOR O2/N2 ON EKA 5A MOLECULAR SIEVE PELLETS AT 303.15 , 293.15 AND 278.15 K (PRESSURE = 1.7 BAR)

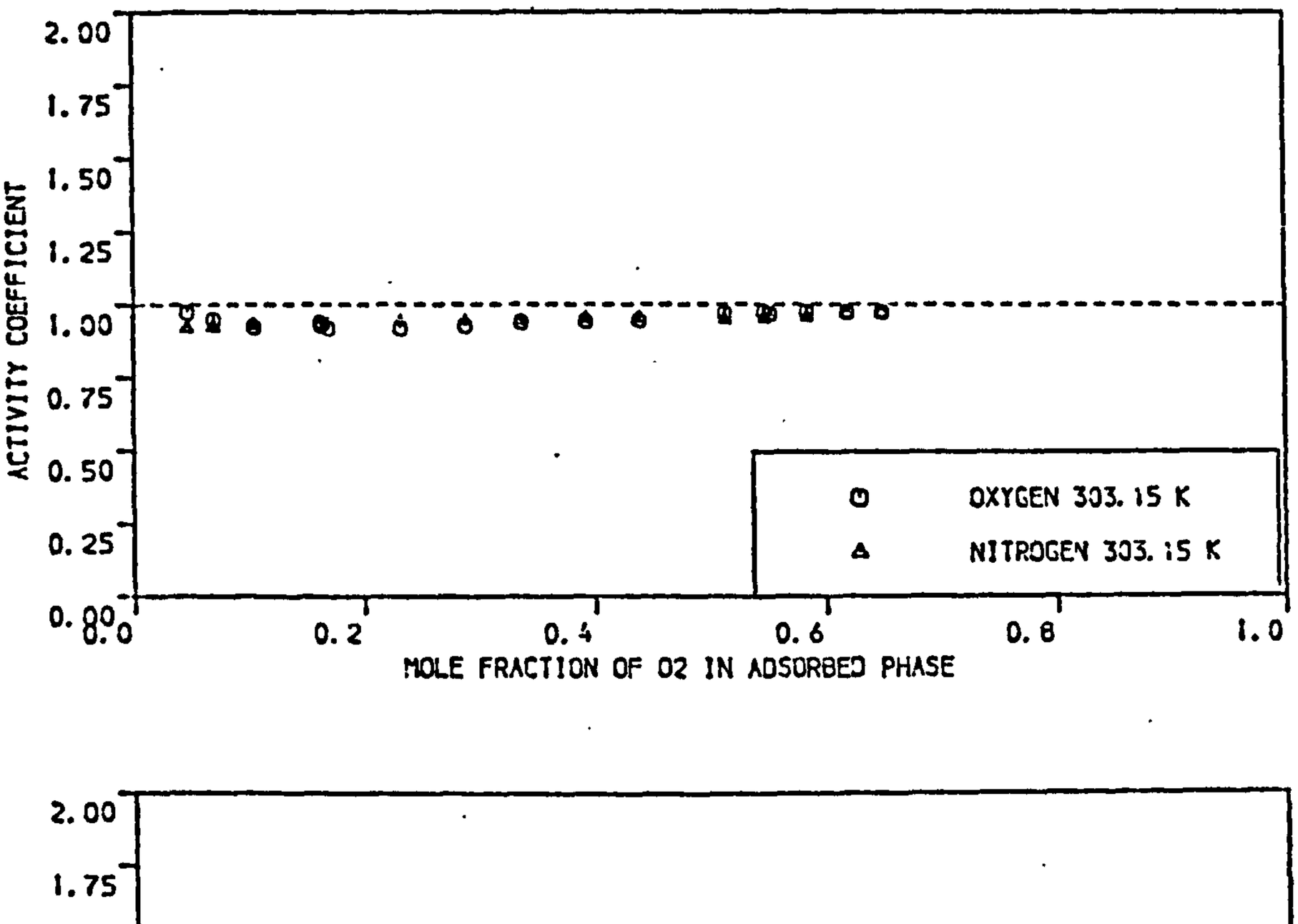

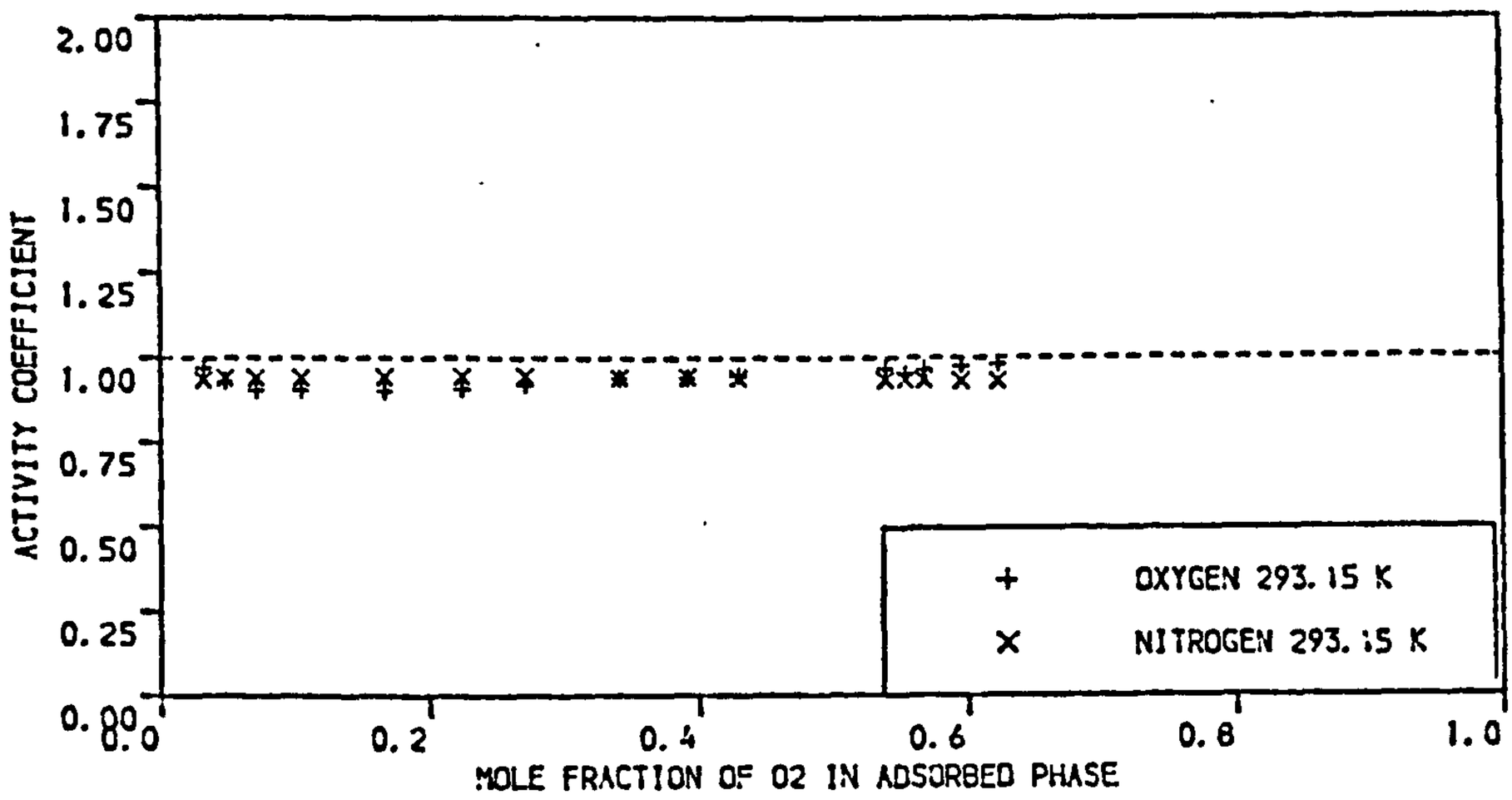

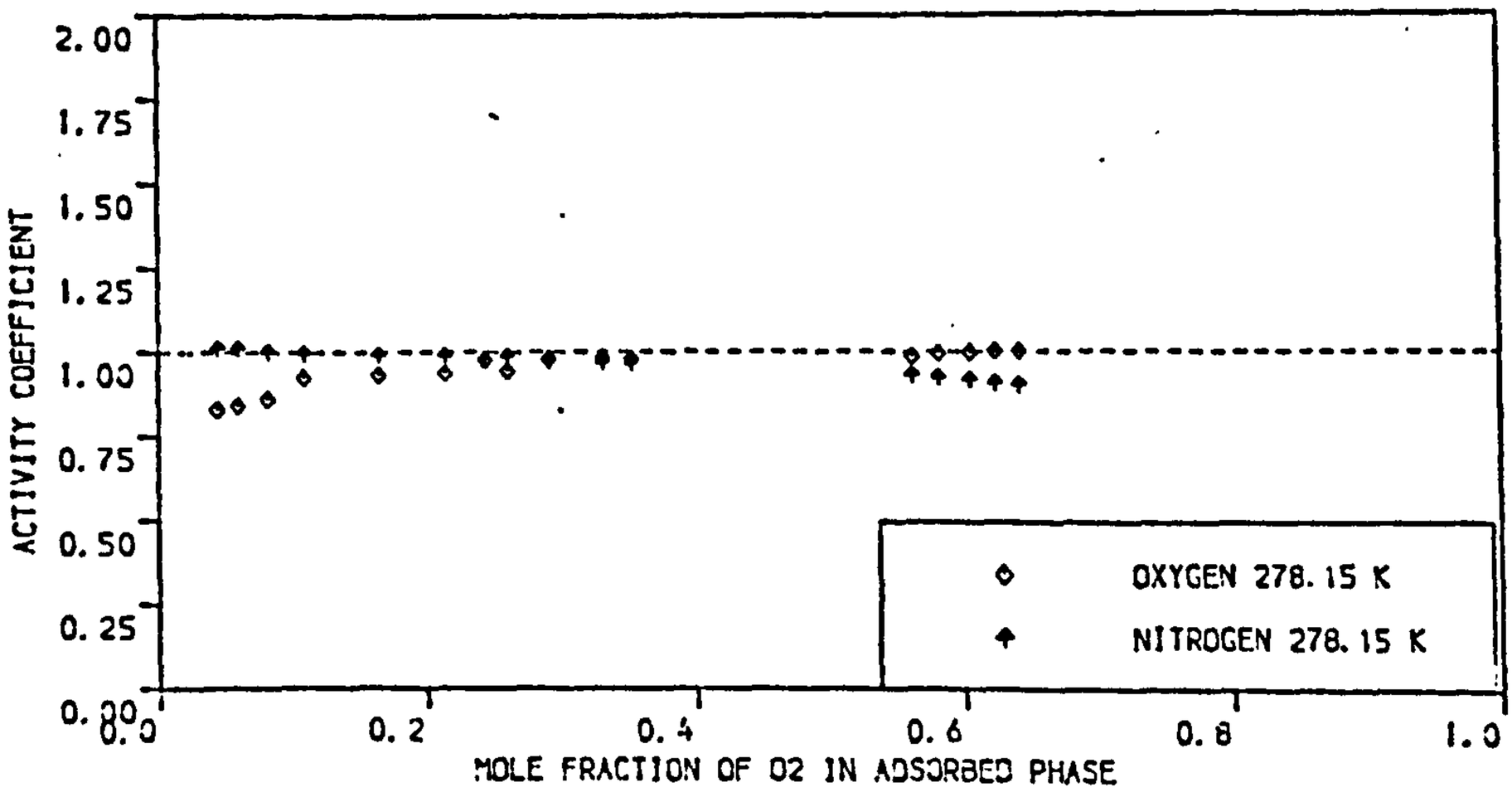

FIGURE 4.60 ACTIVITY COEFFICIENTS FOR O2/N2 ON EKA 5A MOLECULAR SIEVE PELLETS AT 303.15 , 293.15 AND 278.15 K (PRESSURE = 4.4 BAR)

ideal adsorbed solution showed slight deviations from the experimental equilibrium data.

4.2.3.7 Interpretation of results on Na-Mordenite

The binary equilibria experimental results on Na-Mordenite molecular sieve pellets are replotted on Figures 4.61 - 4.66 together with the predicted equilibria data by the five models studied. For the statistical thermodynamic model the predictions were obtained for values of i and j in Equation (2.49) adjusted to 7 and 6 respectively.

For the three temperatures and two pressures studied the separation factors predicted by the statistical thermodynamic model, Cook and Basmadjian model and IAST were approximately the same but deviations of about 10% between the statistical thermodynamic model and the other two models were noticed for temperature 278.15 K at pressure of 1.7 bar for oxygen concentration in the adsorbed phase below 40%. The predicted separation factors by these three models were in good agreement with the experimental data and the predictions by the statistical thermodynamic model for temperature 278.15 K and pressure 1.7 bar gave better representation of the experimental data than the other two models. The predicted total amount adsorbed by the three models varied and the lowest predictions were obtained by the Cook and Basmadjian model. The experimental total amount adsorbed at pressure 1.7 bar and the three temperatures studied were in good agreement with the statistical thermodynamic model and IAST, the maximum deviation noticed was 5% which was at temperature 303.15 K. The total amount adsorbed predicted by Cook and Basmadjian model showed a maximum deviation of about 15% below the experimental data. The experimental total amount adsorbed at pressure 4.4 bar and temperatures 303.15 and 278.15 K were in good agreement with the predicted values by the statistical thermodynamic model and IAST but a maximum deviation of about 8% was noticed between these two models and the experimental data at

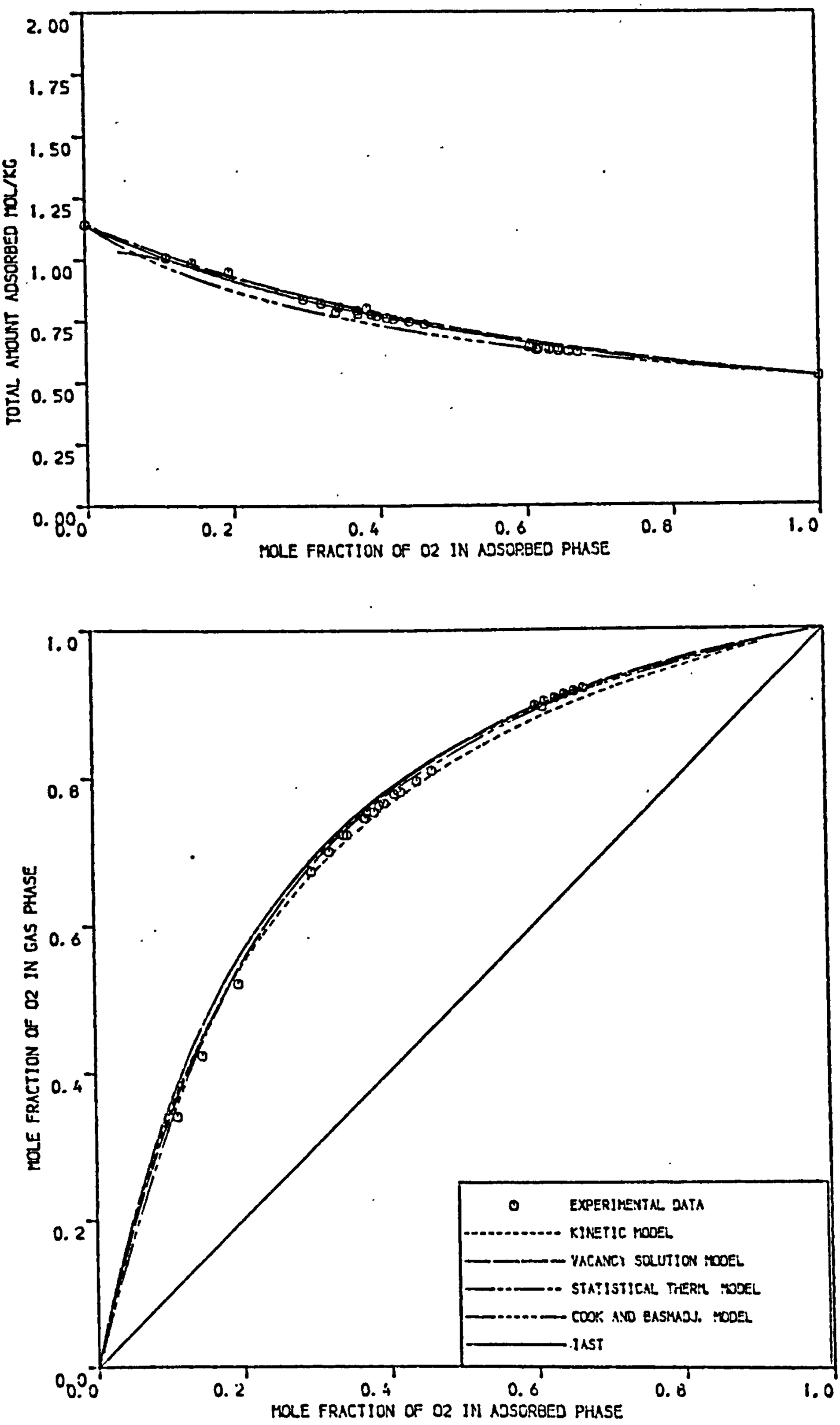

FIGURE 4.61 COMPARISON OF THEORETICAL PREDICTIONS OF VARIOUS MODELS WITH EXPERIMENTAL EQUILIBRIA OF O2/N2 ON NA-MORDENITE MOLECULAR SIEVE PELLETS AT 278.15 K (PRESSURE ≈ 1.7 BAR)

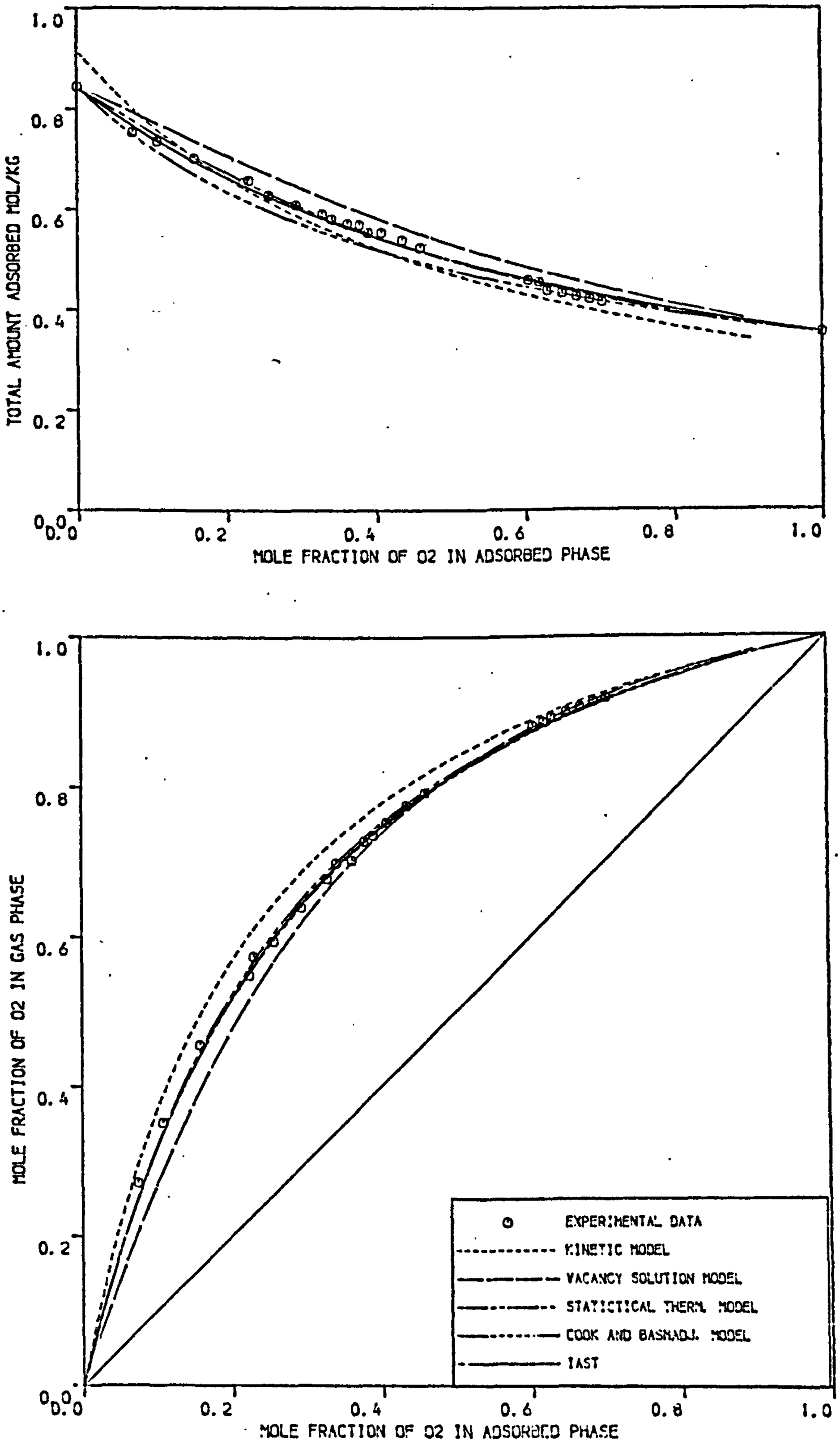

FIGURE 4.62 COMPARISON OF THEORETICAL PREDICTIONS OF VARIOUS MODELS WITH EXPERIMENTAL EQUILIBRIA OF O2/N2 ON NA-MORDENITE MOLECULAR SIEVE PELLETS AT 293.15 K (PRESSURE ≈ 1.7 BAR)

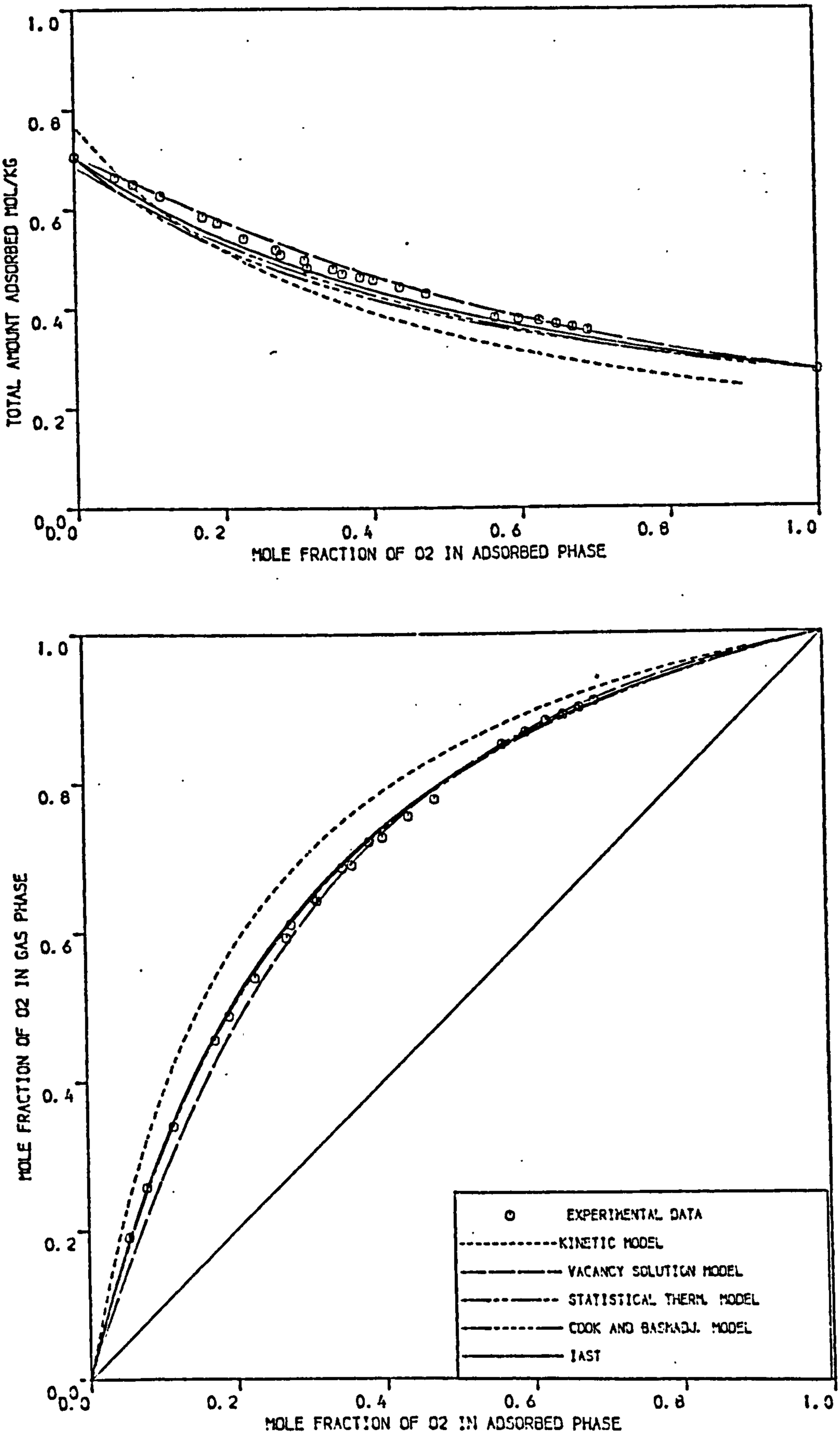

FIGURE 4.63 COMPARISON OF THEORETICAL PREDICTIONS OF VARIOUS MODELS WITH EXPERIMENTAL EQUILIBRIA OF O2/N2 ON NA-MORDENITE MOLECULAR SIEVE PELLETS AT 303.15 K (PRESSURE = 1.7 BAR)

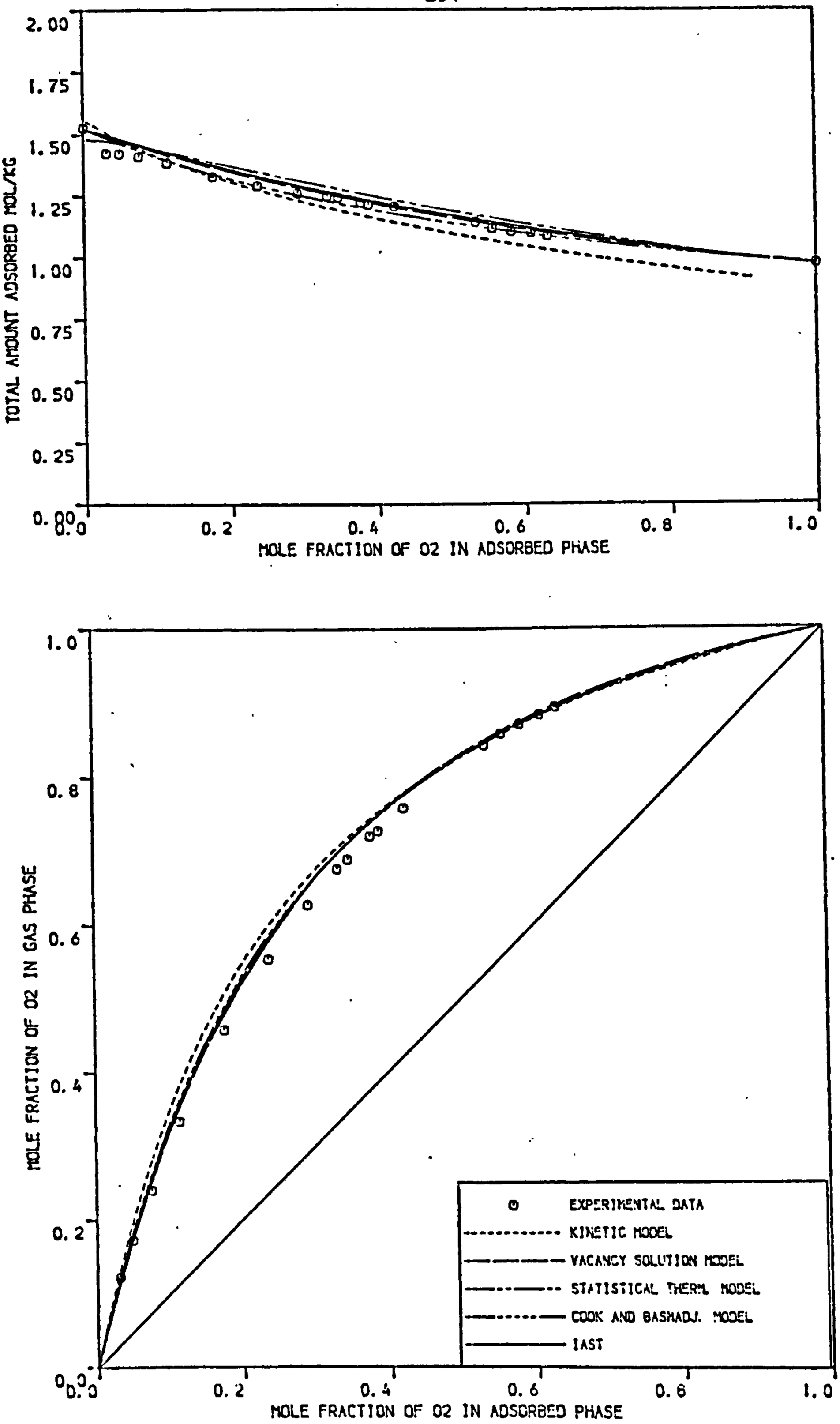

FIGURE 4.64 COMPARISON OF THEORETICAL PREDICTIONS OF VARIOUS MODELS WITH EXPERIMENTAL EQUILIBRIA OF O2/N2 ON NA-MORDENITE MOLECULAR SIEVE PELLETS AT 278.15 K (PRESSURE = 4.4 BAR)

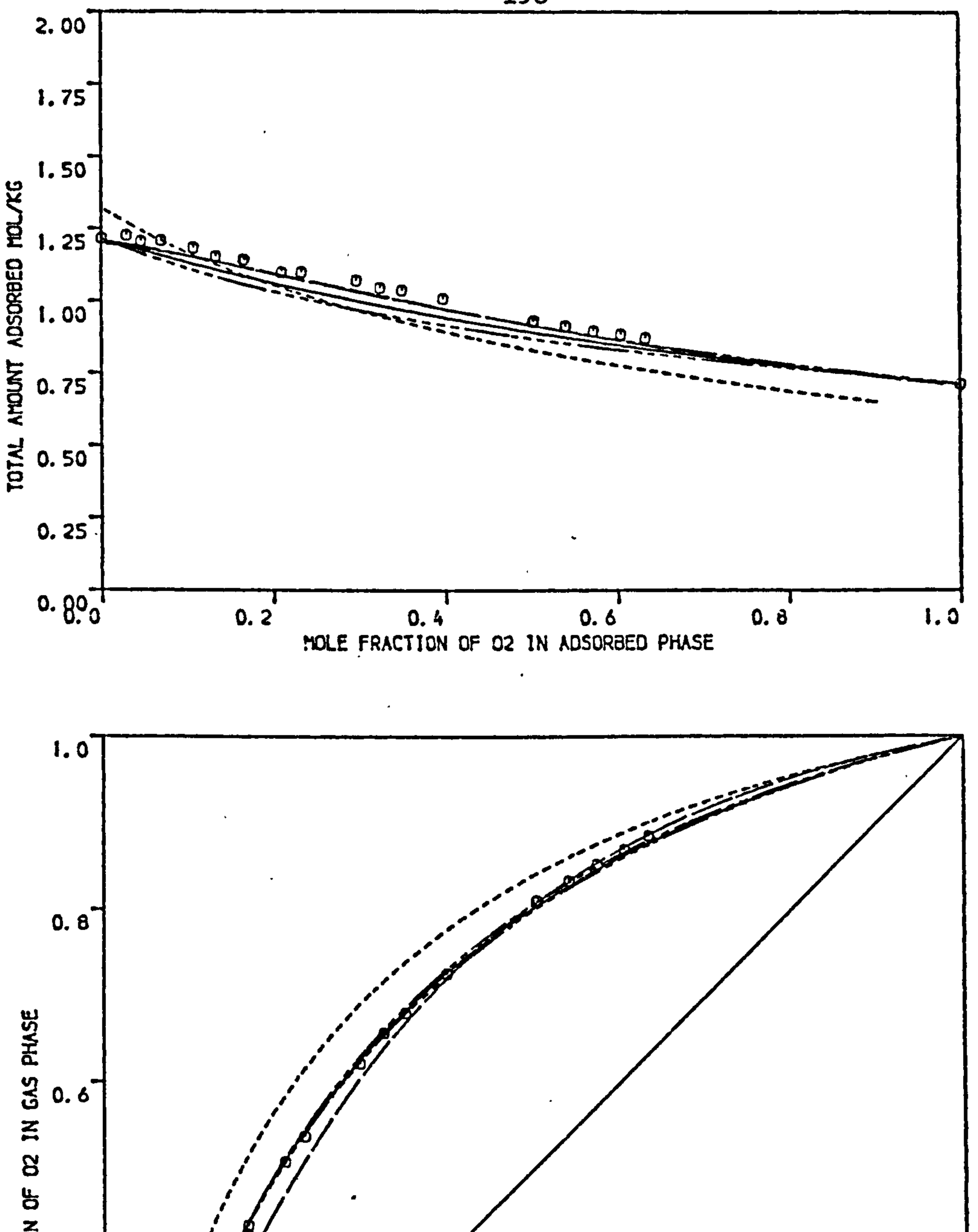

FIGURE 4.65 COMPARISON OF THEORETICAL PREDICTIONS OF VARIOUS MODELS WITH EXPERIMENTAL EQUILIBRIA OF O2/N2 ON NA-MORDENITE MOLECULAR SIEVE PELLETS AT 293.15 K (PRESSURE = 4.4 BAR)

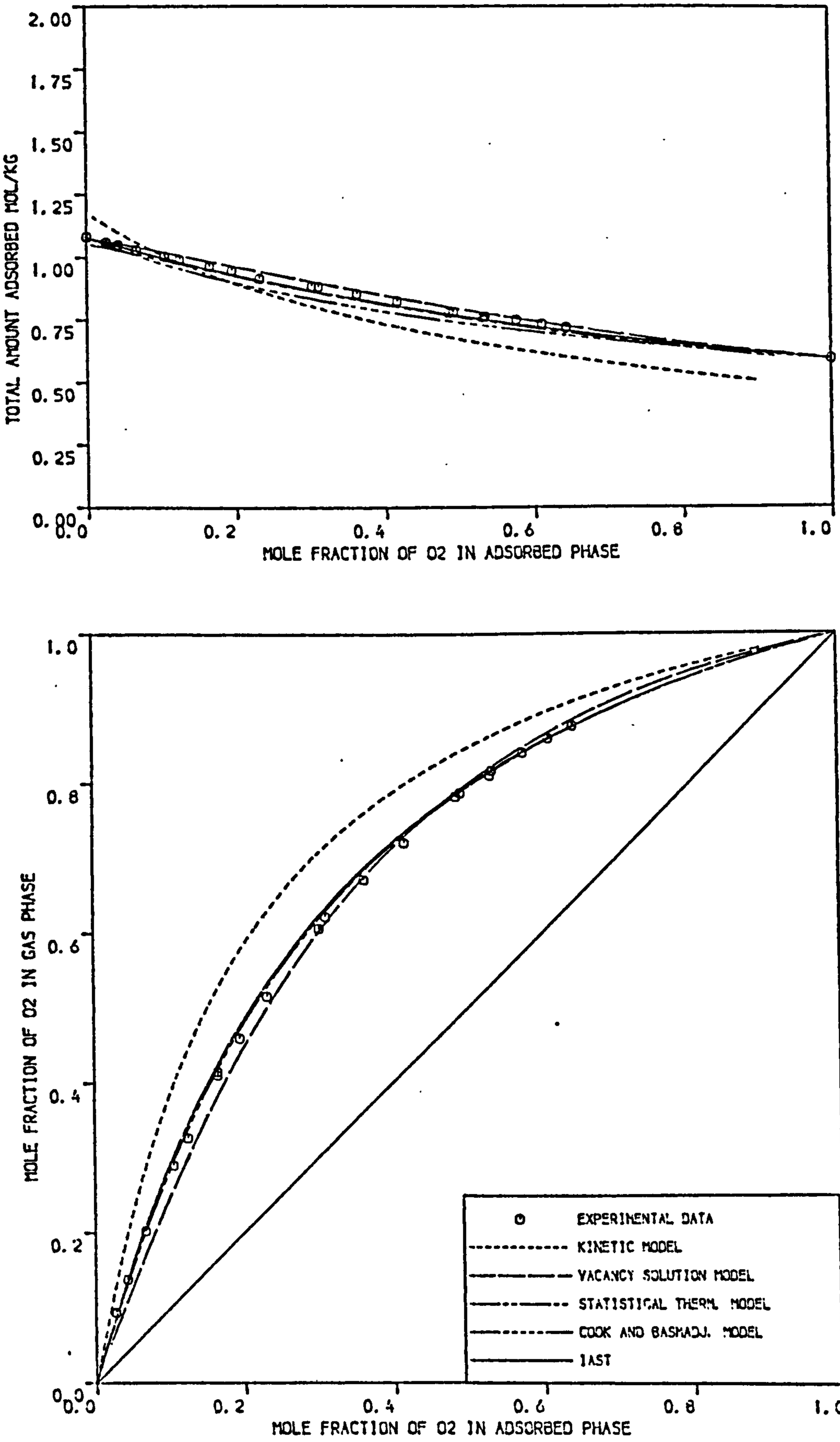

FIGURE 4.66 COMPARISON OF THEORETICAL PREDICTIONS OF VARIOUS MODELS WITH EXPERIMENTAL EQUILIBRIA OF O2/N2 ON NA-MORDENITE MOLECULAR SIEVE PELLETS AT 303.15 K (PPESSURE = 4.4 BAR)

293.15 K. The predicted total amount adsorbed by Cook and Basmadjian model showed a maximum deviation of about 15% for temperature 293.15 K.

The predicted separation factors obtained by the vacancy solution model showed significant deviations from the experimental data for oxygen concentration in the adsorbed phase below 40% at temperatures 303.15 and 293.15 K for both pressures studied. Inspection of Table 4.5 showed that the regression interaction parameters Λ_{13} and Λ_{31} for pure nitrogen vary widely at these two temperatures, one interaction is far above unity and the other is below unity and this could be the possible explanation for the failure of the model at low oxygen concentration. For temperature 278.15 K at both pressures studied the model showed good agreement with the experimental total amount adsorbed and separation factors.

The predictions obtained by the Kinetic model showed that better separation factors are obtained at the high temperatures rather than the low temperatures. The predictions were rather poor for temperatures 293.15 and 303.15 K. The best predictions obtained that were in a reasonable agreement with the experimental data were at temperature 278.15 K and pressure 1.7 bar.

The activity coefficients for oxygen and nitrogen on Na-Mordenite at the three temperatures and two pressures studied are represented graphically in Figures 4.67 - 4.68. From the plots it is seen that no significant deviations from ideality are encountered.

General Concluding Remarks on Binary Gas Adsorption

The statistical thermodynamic model and IAST gave reasonably good predictions of the binary equilibria data obtained in this work. The Cook and Badmadjian model also predicted the data within a good accuracy but significant deviations between the model and the experimental total amount adsorbed on Na-Mordenite were noticed. The vacancy solution model showed fairly good predictions on Laporte 4A and Na-Mordenite. The

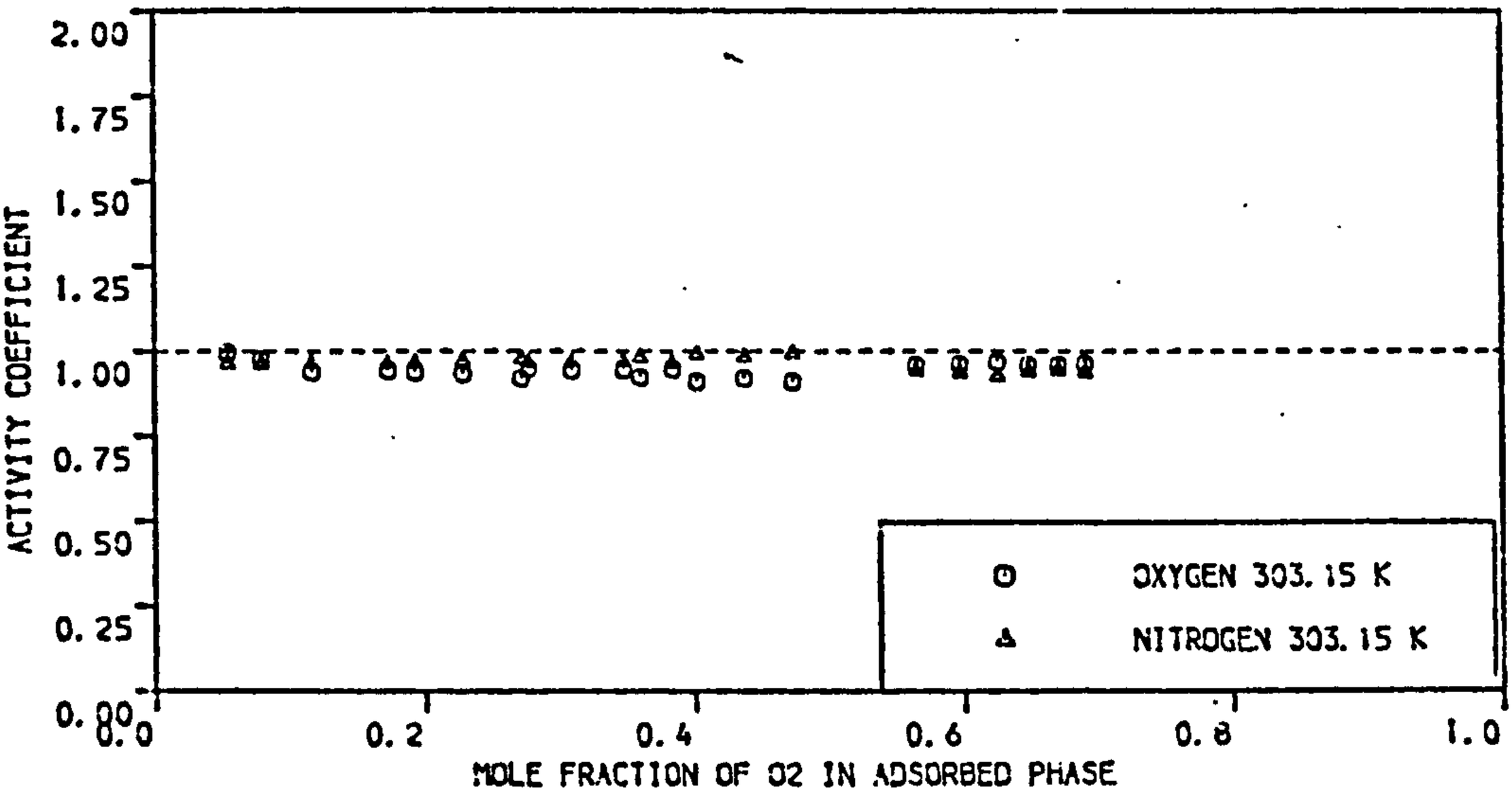

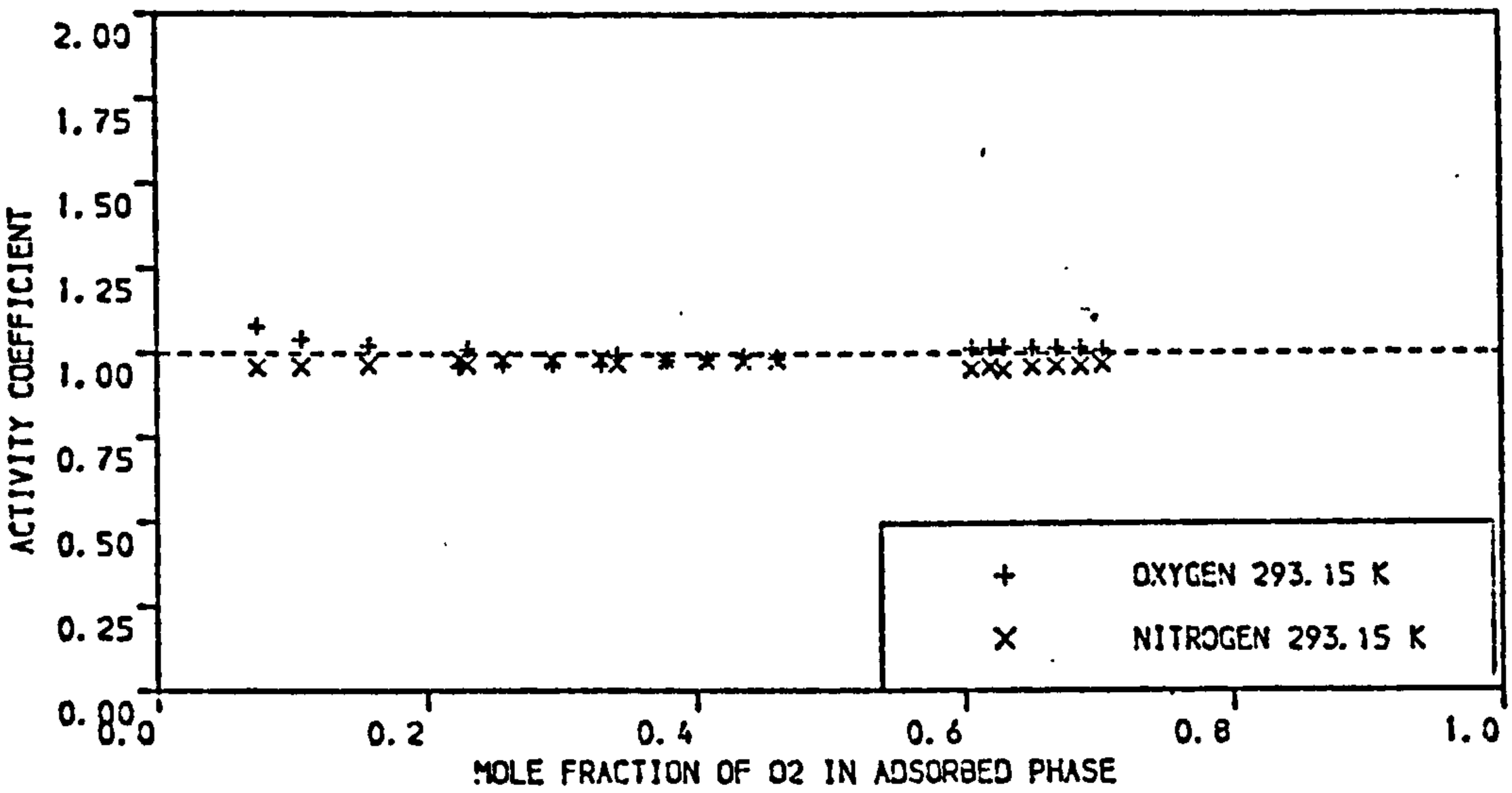

FIGURE 4.67 ACTIVITY COEFFICIENTS FOR O2/N2 ON NA-MORDENITE MOLECULAR SIEVE PELLETS AT 303.15 , 293.15 AND 278.15 K (PRESSURE ≈ 1.7 BAR)

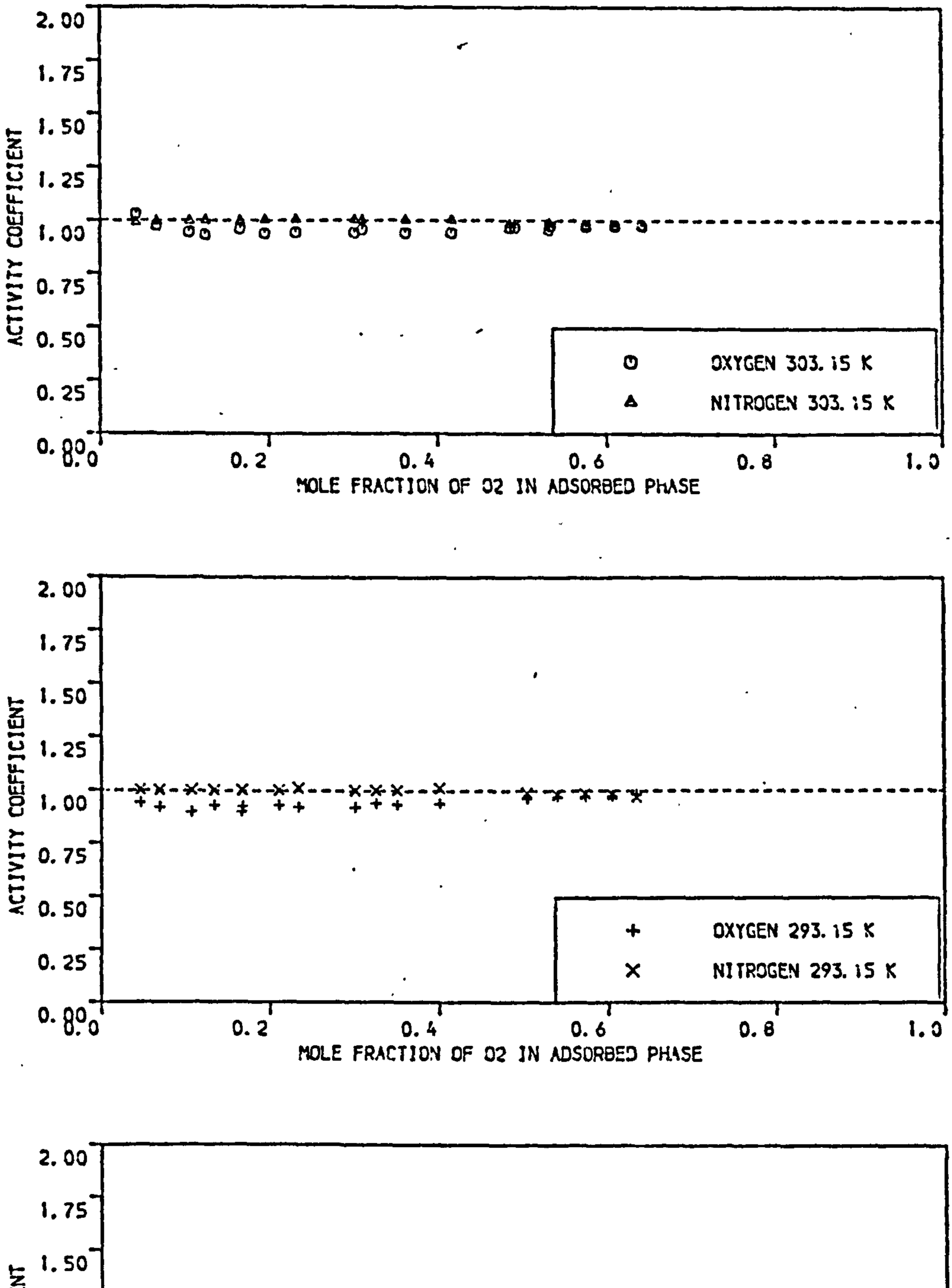

FIGURE 4.68 ACTIVITY COEFFICIENTS FOR O2/N2 ON NA-MORDENITE MOLECULAR SIEVE PELLETS AT 303.15 , 293.15 AND 278.15 K (PRESSURE = 4.4 BAR)

failure of the model on the other systems studied was attributed to the physical significance of the interaction coefficients Λ_{13} and Λ_{31}. Improvement of the vacancy solution model by including the interactions Λ_{12} and Λ_{21} as estimated by Equations (4.8) - (4.10) was insignificant since the interactions were above and below unity. The predictions obtained by the Kinetic model were rather poor in most cases and a complete failure of the model was noticed on EKA 5A. Although the kinetic model showed good predictions in some cases, it is not recommended for use since it fails to offer reasonable predictions at certain temperatures with the same adsorbent where relatively good predictions have been obtained on other temperatures.

Generally speaking, for all the systems studied in this work no significant deviations from ideality were noticed and thus no attempt has been made to correlate the activity coefficients by expressions from Table 2.2.

CHAPTER 5

CONCLUSIONS AND RECOMMENDATIONS

CHAPTER 5

CONCLUSIONS AND RECOMMENDATIONS

This thesis comprises experimental work and a comparison with theoretical models associated with pure gas and binary gas adsorption of oxygen and nitrogen on molecular sieve pellets, types 4A, 5A and 13X, supplied by Laporte Chemicals Ltd. (U.K.) and 5A and Na-Mordenite, supplied by EKA (Sweden). The following conclusions have been drawn.

5.1 Experimental Isotherm Data (Figures 4.1 to 4.6)

(i) The isotherms measured on Na-Mordenite molecular sieve pellets for both gases, oxygen and nitrogen, gave the highest affinity as compared to the other adsorbents studied, for pressures up to 1 bar.

(ii) For pressures more than one bar the affinity on EKA 5A for both gases approached that on Na-Mordenite and for pressures approaching 10 bar EKA 5A adsorbed more nitrogen than Na-Mordenite.

(iii) The affinity on Laporte's 4A and 13X for oxygen and nitrogen were approximately the same with the pressure range 1-9 bar but for temperature 303.15 K Laporte 4A adsorbed more oxygen than Laporte 13X.

(iv) For pressures up to 1 bar Laporte 5A adsorbed more oxygen and nitrogen than Laporte's 4A and 13X.

(v) For pressures greater than 1 bar the affinity on Laporte 5A for oxygen and nitrogen approached that on Laporte 4A and 13X. For adsorption temperatures 293.15 and 303.15 K the adsorption of nitrogen on Laporte 5A tends to be lower than that on Laporte's 4A and 13X for pressures greater

than 5 bar.

5.2 Theoretical Isotherm Models (Figures 4.7 to 4.16, I.1 to I.20)

Models have been used for curve fitting the experimental pure component isotherm data, determining Henry's law constants and predicting the isosteric heats of adsorption of oxygen and nitrogen on Laporte's 4A, 5A and 13X, EKA 5A and Na-Mordenite molecular sieve pellets.

(i) Curve fitting of the experimental pure component isotherm data was attempted using the kinetic model of Gonzalez and Holland, the vacancy solution model, the statistical thermodynamic model and a mathematical equation given by Equation (4.1). The vacancy solution model, the statistical thermodynamic model and Equation (4.1) fitted the experimental data within a good accuracy. The curve fitted isotherms obtained by the kinetic model were rather poor, particularly for EKA 5A (see Table 4.2).

(ii) In the case of the vacancy solution model, the vacancy-adsorbate, Λ_{31}, and the adsorbate-vacancy, Λ_{13}, interactions showed opposite and wide variation from unity indicating no physical significance (see Table 4.5).

(iii) The Henry's law constants determined from the statistical thermodynamic model, the vacancy solution model and Equation (4.1) were in a fairly good agreement with each other whilst the Henry's law constants determined from the kinetic model were significantly different (see Table 4.6).

(iv) The predicted isosteric heats of adsorption for oxygen and nitrogen by the statistical thermodynamic model, the vacancy solution model and Equation (4.1) were in fair agreement with each other and almost constant with loading. The values were approximately equal to the values of U_o

in Table 4.6.

5.3 Experimental Binary Data (Figures 3.12 to 3.21, 4.19 to 4.28)

(i) The experimental binary loadings for oxygen and nitrogen were less than the loadings predicted for the pure components at the same partial pressures (see Table 4.7 for 50 mol % gas mixtures).

(ii) The separation factor ($y_{O_2} x_{N_2} / y_{N_2} x_{O_2}$) is much less sensitive to temperature or pressure change than is the total amount adsorbed.

(iii) The separation factor decreased with increasing temperatures and this effect was more pronounced at 1.7 bar than at 4.4 bar.

(iv) The separation factors obtained on EKA 5A and Na-Mordenite were almost identical and greater than those obtained on Laporte's adsorbents. However, for adsorption at 303.15 K and 1.7 bar, the separation factors on Na-Mordenite were greater than that on EKA 5A.

(v) The separation factors on Laporte 5A were greater than those on Laporte 4A and 13X at 278.15 K and 1.7 bar. For temperatures 293.15 and 303.15 K at 1.7 bar the separation factors on Laporte 5A were approximately the same as those on Laporte 13X and greater than those on Laporte 4A. For the three temperatures studied at 4.4 bar the separation factors on Laporte adsorbents were approximately the same.

(vi) The total amount adsorbed on Na-Mordenite was the highest as compared to the other adsorbents studied, EKA 5A gave greater total amount adsorbed than Laporte adsorbents and generally Laporte 5A showed the highest total amount adsorbed as compared to Laporte adsorbents 4A and 13X.

(vii) The separation factors on Laporte 5A were similar to published data on zeolite type 5A from two different origins. However, the total amount adsorbed on Laporte 5A was significantly less.

(viii) Comparison of binary data on Na-Mordenite obtained in this work with published data showed that the separation factors on Na-Mordenite of this work were less but the total amounts adsorbed were significantly higher.

5.4 Theoretical Gas-Mixtures Models (Figures 4.29 to 4.68)

Predictions of the experimental binary equilibria data obtained on Laporte's 4A, 5A and 13X, EKA 5A and Na-Mordenite molecular sieve pellets were attempted using the kinetic model of Gonzalez and Holland, the vacancy solution model, the statistical thermodynamic model, Cook and Basmadjian model and the ideal adsorbed solution theory (IAST). Activity coefficients were calculated.

(i) The calculated activity coefficients for all the binary gas-solid systems studied in this work showed no appreciable deviation from ideality.

(ii) The statistical thermodynamic model and IAST predicted the binary experimental equilibrium data to a reasonable accuracy.

(iii) The Cook and Basmadjian model also predicted the binary experimental data with a good accuracy except that significant deviations between the model and the experimental total amount adsorbed on Na-Mordenite were noticed.

(iv) The vacancy solution model showed fairly good predictions on Laporte 4A and Na-Mordenite. The failure of the model on the other systems studied was attributed to the physical significance of the interaction coefficients Λ_{13} and Λ_{31}

for both pure gases, oxygen and nitrogen. Improvement of the model by taking into account the interaction coefficients Λ_{12} and Λ_{21} as estimated by Equations (4.8) to (4.10) was insignificant since the interaction coefficients were above and below unity.

(v) The predictions obtained by the kinetic model were rather poor in most cases and a complete failure of the model was noticed on EKA 5A.

5.5 Recommendations for Further Work

(a) Industrial separation of air by adsorption involves mainly a ternary mixture of nitrogen, oxygen and argon. Hence it is recommended to obtain binary equilibrium data of O_2-Ar and N_2-Ar and ternary equilibrium data of N_2-O_2-Ar. A further test of the validity of the gas mixture models will also be required.

(b) No reported work appear in literature for determining the rates of diffusion in the binary gas mixture O_2-N_2 on zeolites. Hence it is recommended that experimental rate data be obtained and a realistic model proposed for this system.

REFERENCES

1. KELLER, G.E. and JONES, R.L., in 'Adsorption and Ion Exchange with Synthetic Zeolites', ACS Symposium Series 135, pp 275-286, 1980.

2. ARMOND, J.W., in 'The Properties and Application of Zeolites', Special Publication No. 33, pp 92-102, 1979.

3. LEE, H. and STAHL, D.E., A.I.Ch.E. Sym. Series 69, No. 134, pp 1-8, 1973.

4. SKARSTROM, C.W., U.S. Patent 2, 944, 627 (1960).

5. BERLIN, N.H., U.S. Patent 3, 280, 536 (1966).

6. MARSH, W.D., HOKE, R.C., PRAMUK, F.S. and SKARSTROM, C.W., U.S. Patent 3, 142, 547 (1964).

7. DALY, W.O., Ph.D. Thesis, University of Bradford, 1977.

8. DALY, W.O. and GRANVILLE, W.H., in 'The Properties and Application of Zeolites', Special Publication No. 33, pp 184-197, 1979.

9. RUTHVEN, D.M. and LOUGHLIN, R.K., A.I.Ch.E. Sym. Series, 67, No. 117, pp 35-41, 1971.

10. RUTHVEN, D.M. and GARG, D.R., Chem. Eng. Sci., 28, pp 791-798, 1973.

11. HABGOOD, H.W., Can. J. Chem., 36, pp 1384-1397, 1958.

12. RUTHVEN, D.M., in 'Molecular Sieve II', ACS Sym. Series 40, pp 320-334, 1977.

13. RUTHVEN, D.M., in 'The Properties and Application of Zeolites', Special Publication No. 33, pp 43-57, 1979.

14. RUTHVEN, D.M., LOUGHLIN, K.F. and DERRAH, R.I., in 'Molecular Sieves', Adv. Chem. Ser. 121, pp 330-344, 1973.

15. RUTHVEN, D.M., LOUGHLIN, K.F. and DERRAH, R.I., Cand. J. Chem. Eng., 49, pp 66-70 (1971).

16. RUTHVEN, D.M. and DERRAH, K.F., J. Chem. Soc. Faraday Trans. I., 71, pp 2031-2044, 1975.

17. RUTHVEN, D.M. and LOUGHLIN, K.F., Chem. Eng. Sci., 27, pp 1401-1408, 1972.

18. RUTHVEN, D.M. and LOUGHLIN, K.F., ibid, 26, pp 1145-1154, 1971.

19. TAKEUCHI, Y. and KAWAZOE, K., J. Chem. Eng., Japan, 9, No. 1, pp 46-52, 1976.

20. RUTHVEN, D.M. and DERRAH, R.I., J. Coll. and Inter. Sci., 52, No. 2, pp 397-403, 1975.

21. RUTHVEN, D.M. and KUMAR, R., Cand. J. Chem. Eng., 57, pp 342-348, 1979.

22. RUTHVEN, D.M. and LOUGHLIN, K.F., Trans. Farad. Soc., 67, pp 1661-1671, 1971.

23. COLLINS, J.J., Chem. Eng. Progr., 64, 66-71, 1968.

24. BRECK, D.W., 'Zeolite Molecular Sieves', Wiley and Sons, New York, 1973.

25. BARRER, R.M. and MEIRER, W.M., Trans. Faraday Soc., 54, 1074-1085 (1958).

26. BARRER, R.M. and PETERSON, D.L., Proc. Roy. Soc., 280A, pp 446-485, 1964.

27. BRECK, D.W., Chem. Eng. Progr., 73, No. 10, pp 44-48, 1977.

28. RUTHVEN, D.M., A.I.Ch.E. Journal, 22, No. 4, pp 753-759, 1976.

29. DANNER, R.P. and WENZEL, L.A., ibid, 15, No. 4, pp 515-520, 1969.

30. LEWIS, W.K., GILLILAND, E.R., CHERTOW, B. and CADOGAN, W.P., I. & E.C. 42, No. 7, pp 1319-1325, 1950.

31. GONZALEZ, A.J. and HOLLAND, C.D., A.I.Ch.E. Journal, 16, No. 5, pp 718-724, 1970.

32. HOORY, S.E. and PRAUSNITZ, J.M., Chem. Eng. Sci., 22, pp 1025-1033, 1967.

33. GRANT, R.J. and MANES, M., I. & E.C. Fundam. 5, No. 4, pp 490-498, 1966.

34. MASLAN, F.D., ALTMAN, M. and ABERTH, E.R., J. Phys. Chem. 57, pp 106-109, 1953.

35. COOK, W.H. and BASMADJIAN, D., Can. J. Chem. Eng., 43, pp 78-83, 1965.

36. MYERS, A.L. and PRAUSNITZ, J.M., A.I.Ch.E. Journal, 11, No. 1, pp 121-127, 1965.

37. KIDNAY, A.J. and MYERS, A.L., ibid, 12, No. 5, pp 981-986, 1966.

38. FERNBACHER, J.M. and WENZEL, L.A., I. & E.C. Fundam. 11, No. 4, pp 457-465, 1972.

39. MYERS, A.L. and SIRCAR, S., Chem. Eng. Sci., 28, pp. 489-499, 1973.

40. YON, C.M. and TURNACK, P.H., A.I.Ch.E. Sym. Series, 67, No. 117, pp 75-83, 1971.

41. DUCKETT, M. and DUNLOP, A., I.Chem.E. Sym. Series 54, pp 173-183, 1978.

42. RUTHVEN, D.M., LOUGHLIN, K.F. and HOLBOROW, K.A., Chem. Eng. Sci., 28, pp 701-709, 1973.

43. SUWANAYUEN, S. and DANNER, R.P., A.I.Ch.E. Journal, 26, No. 1, pp 76-83, 1980.

44. HILL, T.L., J. Chem. Phys., 17, pp 520-524, 1949.

45. VAN NESS, H.C., I. & E.C. Fundam. 8, No. 3, pp 464-473, 1969.

46. LANGMUIR, I., Phs. Rev. 8, p 149, 1916.

47. LANGMUIR, I., J. Am. Chem. Soc. 40, p 1361, 1918.

48. FOWLER, R.H. and GUGGENHEIM, E.A., 'Statistical Thermodynamics', Macmillan, New York, 1939.

49. PEIERLS, R., Proc. Cambridge Phil. Soc., 32, pp 471-476, 1936.

50. WANG, J., Proc. Roy. Soc., A161, pp 127-140, 1937.

51. BRUNAUER, S., EMMETT, P.H. and TELLER, E., J. Am. Chem. Soc., 60, pp 309-319, 1938.

52. HILL, T.L., J. Chem. Phys., 14, pp 268-275, 1946.

53. ROLNIAK, P.D. and KOBAYASHI, R., A.I.Ch.E. Journal, 26, No. 4, pp 616-625 (1980).

54. DE BOER, J.H., 'The Dynamical Nature of Adsorption', 2nd Edition, Claredon Press, Oxford, 1968.

55. TORII, K., HOTTA, M., ONODERA, Y. and ASAKA, M., Trans. Chem. Soc., Japan, No. 2, pp 225-232, 1973.

56. ROSS, S. and OLIVIER, J.P., 'On Physical Adsorption', Interscience Publishers, 1964.

57. ROSS, S., A.I.Ch.E. Sym. Series, 67, No. 117, pp 1-10, 1971.

58. HOORY, S.E. and PRAUSNITZ, J.M., Chem. Eng. Progr. Sym. Series 63, No. 74, pp 3-9, 1967.

59. HOORY, S.E. and PRAUSNITZ, J.M., Trans. Faraday Soc., 63, pp 455-460, 1967.

60. EAGAN, J.D. and ANDERSON, R.B., J. Coll. and Int. Sci., 50, pp 419-433, 1975.

61. EAGAN, J.D., ANDERSON, R.B. and KINDL, B., A.I.Ch.E. Sym. Series 69, No. 134, pp 39-44, 1973.

62. BARRER, R.M. and DAVIES, J.A., Proc. Roy. Soc., Lond., A320, pp 289-308, 1970.

63. BARRER, R.M. and LEE, J.A., Surface Sci., 12, p 341, 1968.

64. DUBININ, M.M., Chem. Rev., 60, pp 235-241, 1960.

65. LEWIS, W.K., GILLILAND, E.R., CHERTOW, B. and CADOGAN, W.P., I. & E.C., 42, No. 7, pp 1326-1332, 1950.

66. HENSON, T.L. and KABEL, R.L., Chem. Eng. Progr. Sym. Series 63, No. 74, pp 36-41, 1967.

67. RUTHVEN, D.M., Nature, Phys. Sci., 232, No. 29, pp 70-71, 1971.

68. RUTHVEN, D.M. and LOUGHLIN, K.F., J. Chem. Soc. Faraday Trans., 68, pp 696-708, 1972.

69. SUWANAYUEN, S. and DANNER, R.P., A.I.Ch.E. Journal, 26, No. 1, pp 68-76, 1980.

70. ROUND, G.F., HABGOOD, H.W. and NEWTON, R., Sep. Sci., 1, pp 219-244, 1966.

71. LEDERMANN, P.B. and WILLIAMS, B., A.I.Ch.E. Journal, 10, No. 1, pp 30-34, 1964.

72. CARTER, J.W. and HUSAIN, H., Trans. Instn. Chem. Engrs., 50, pp 69-75, 1972.

73. CARTER, J.W. and HUSAIN, H., Chem. Eng. Sci., 29, pp 267-273, 1974.

74. DANNER, R.P., Ph.D. Dissertation, Lehigh University, Pennsylvania, U.S.A., 1966.

75. GONZALEZ, A.J. and HOLLAND, C.D., A.I.Ch.E. Journal, 17, No. 2, pp 470-474, 1971.

76. ALLEN, T., 'Particle Size Measurement', Powder Technology Series, Chapman and Hall, 3rd Edition, 1981.

77. FRIEDERICH, R.O. and MULLINS, J.C., I. & E.C. Fundam., 11, No. 4, pp 439-445, 1972.

78. DANNER, R.P. and CHOI, E.C.F., ibid, 17, No. 4, pp 248-253, 1978.

79. KISELEV, A.V., in 'Molecular Seive Zeolite II', Adv. Chem. Series 102, pp 37-68, 1971.

80. BARRER, R.M., ibid, pp 1-36.

81. YOUNG, D.M. and CROWELL, A.D., 'Physical Adsorption of Gases', Butterworth, London, 1962.

82. COOK, W.H. and BASMADJIAN, D., Can. J. Chem. Eng., 42, p 146, 1964.

83. PRAUSNITZ, J.M., 'Molecular Thermodynamics of Fluid-Phase Equilibria', Prentice Hall, Englewood Cliffs, N.J., 1969.

84. MARKHAM, E.C. and BENTON, A.F., J. Am. Chem. Soc., 53, 497-507, 1931.

85. KEMBALL, C., RIDEAL, E.K. and GUGGENHEIM, E.A., Trans. Faraday Soc., 44, pp 948-954, 1948.

86. ARNOLD, J.R., J. Am. Chem. Soc., 71, pp 104-110, 1949.

87. WHITE, Jr., L. and SCHNEIDER, C.H., ibid, 71, pp 2593-2600, 1949.

88. MASON, J.P. and COOKE, C.E., A.I.Ch.E. Journal, 12, No. 6, pp 1097-1103, 1966.

89. SZEPESY, L. and ILLES, V., Acta Chim. Hung., 35, 37, 1963.

90. LOUGHLIN, K.F., HOLBOROW, K.A. and RUTHVEN, D.M., A.I.Ch.E. Sym. Series 71, No. 152, pp 24-29, 1975.

91. SIRCAR, S. and MYERS, A.L., J. Phys. Chem., 74, pp 2828-2835, 1970.

92. BROUGHTON, D.B., I. & E.C., 40, No. 8, pp 1506-1507, 1948.

93. BASMADJIAN, D., Can. J. Chem., 38, pp 149-156, 1960.

94. MYERS, A.L., I. & E.C., 60, No. 5, pp 45-49, 1968.

95. GLESSNER, A.J. and MYERS, A.L., Chem. Eng. Progr. Sym., Series 65, No. 96, pp 73-79, 1969.

96. BERING, B.P. and SERPENSKII, V.V., Zhur, Fiz. Khim. (USSR), 26, 253, 1952.

97. DREHER, H. and KAST, W., Ger. Chem. Eng., 3, pp 222-228, 1980.

98. SINGHAL, A.K., A.I.Ch.E., Symp. Series 74, No. 179, pp 36-41, 1978.

99. HENSON, T.L. and KABEL, R.L., A.I.Ch.E. Journal, 12, No. 3, pp 606-608, 1966.

100. REID, R.C., PRAUSNITZ, J.M. and SHERWOOD, T.K., 'The Properties of Gases and Liquids', (3rd Edition), McGraw Hill, New York, 1977.

101. COSTA, E., SOTELO, J.L., COLLEJA, G. and MARRON, C., A.I.Ch.E. Journal 27, No. 1, pp 5-12, 1981.

102. PAYNE, H.K., STURDEVANT, G.A. and LELAND, T.W., I. & E.C., Fundam. 7, No. 3, p 366, 1968.

103. BENDER, E., Cryogenics, 13, p 11, 1973.

104. ROBERTS, C.W., in 'The Properties and Application of Zeolites', Special Publication No. 33, pp 103-119 (1979).

105. 'NAG Mini Manual Mark 7', Numerical Algorithms Group, Oxford (1978).

106. PRAUSNITZ, J.M., ECKERT, C.A., ORYE, R.V. and O'CONNELL, J.P., 'Computer Calculations for Multicomponent Vapor-Liquid Equilibria', Prentice-Hall, Englewood Cliffs, N.J., 1967.

APPENDICES

APPENDIX I

EXPERIMENTAL RESULTS

Tables I.1 - I.10	Adsorption isotherms for O_2 and N_2 on Laportes 4A, 5A and 13X, EKA 5A and Na-Mordenite molecular sieve pellets at temperatures 278.15, 293.15 and 303.15 K.
Tables I.11 - I.15	Binary adsorption equilibrium data for O_2/N_2 on Laportes 4A, 5A and 13X, EKA 5A and Na-Mordenite molecular sieve pellets at temperatures 278.15, 293.15 and 303.15 K and pressures 1.7 and 4.4 bar.
Figures I.1 - I.10	Comparison of Equation (4.1) with experimental isotherms data of oxygen and nitrogen on Laportes 4A, 5A and 13X, EKA 5A and Na-Mordenite molecular sieve pellets at temperatures 278.15, 293.15 and 303.15 K.
Figures I.11 - I.20	Comparison of the vacancy solution model with experimental isotherms data of O_2 and N_2 on Laportes 4A, 5A and 13X, EKA 5A and Na-Mordenite molecular sieve pellets at temperatures 278.15, 293.15 and 303.15 K.

TABLE I.1

Adsorption Isotherms for Oxygen on Laporte 4A Molecular Sieve Pellets at 278.15, 293.15 and 303.15 K

T = 278.15 K

Pressure bar	Amount adsorbed mol/kg of adsorbent
0.457	0.065
0.724	0.101
1.0	0.135
1.324	0.175
1.614	0.212
1.937	0.255
2.349	0.308
2.851	0.368
3.435	0.435
4.032	0.5009
4.588	0.573
5.331	0.642
6.261	0.727
6.987	0.795
8.04	0.877

T = 293.15 K

Pressure bar	Amount adsorbed mol/kg of adsorbent
0.520	0.053
0.816	0.082
1.102	0.111
1.401	0.142
1.819	0.183
2.278	0.226
2.814	0.276
3.441	0.332
4.02	0.381
4.599	0.430
5.262	0.485
6.403	0.574
7.331	0.648
7.955	0.694

T = 303.15 K

Pressure bar	Amount adsorbed mol/kg of adsorbent
0.531	0.046
0.707	0.062
1.003	0.087
1.34	0.118
1.666	0.146
2.079	0.18
2.572	0.221
3.125	0.263
3.679	0.306
4.261	0.350
5.163	0.41
6.115	0.474
7.158	0.536

TABLE I.2

Adsorption Isotherms for Oxygen on Laporte 5A Molecular Sieve Pellets at 278.15, 293.15 and 303.15 K

T = 278.15 K

Pressure bar	Amount adsorbed mol/kg of adsorbent
0.26	0.042
0.579	0.091
0.932	0.143
1.279	0.195
1.642	0.246
2.01	0.298
2.402	0.348
2.757	0.397
3.155	0.448
3.547	0.497
3.975	0.551
4.257	0.618
4.750	0.672
5.287	0.732
5.962	0.799
6.610	0.866
7.433	0.943
8.332	1.022

T = 293.15 K

Pressure bar	Amount adsorbed mol/kg of adsorbent
0.280	0.0312
0.520	0.059
0.792	0.09
1.078	0.123
1.413	0.159
1.774	0.196
2.140	0.235
2.558	0.274
2.975	0.314
3.462	0.359
3.989	0.408
4.571	0.457
5.197	0.512
5.949	0.571
6.878	0.641
7.796	0.707
8.547	0.761

T = 303.15 K

Pressure bar	Amount adsorbed mol/kg of adsorbent
0.327	0.032
0.666	0.062
0.972	0.089
1.251	0.114
1.55	0.140
1.852	0.166
2.193	0.195
2.609	0.229
3.092	0.269
3.620	0.310
4.170	0.352
4.763	0.396
5.411	0.442
6.096	0.495
6.963	0.55
7.869	0.606
8.710	0.654

TABLE I.3

Adsorption Isotherms for Oxygen on Laporte 13X Molecular Sieve Pellets at 278.15, 293.15 and 303.15 K

T = 278.15 K

Pressure bar	Amount adsorbed mol/kg of adsorbent
0.341	0.043
0.619	0.0799
0.926	0.119
1.218	0.159
1.559	0.202
1.915	0.246
2.302	0.296
2.719	0.348
3.139	0.396
3.584	0.447
4.044	0.502
4.532	0.560
5.214	0.627
5.964	0.704
6.792	0.784
7.498	0.852
8.259	0.920
8.880	0.973

T = 293.15 K

Pressure bar	Amount adsorbed mol/kg of adsorbent
0.365	0.0397
0.709	0.072
1.057	0.105
1.413	0.138
1.813	0.176
2.218	0.212
2.615	0.249
3.039	0.286
3.496	0.326
3.998	0.369
4.497	0.411
5.021	0.455
5.448	0.488
6.071	0.536
6.836	0.603
7.718	0.667
8.449	0.717
9.068	0.761

T = 303.15 K

Pressure bar	Amount adsorbed mol/kg of adsorbent
0.448	0.037
0.845	0.067
1.234	0.098
1.506	0.119
1.740	0.137
1.947	0.153
2.193	0.173
2.446	0.192
2.719	0.213
3.011	0.235
3.320	0.257
3.713	0.287
4.159	0.319
4.625	0.351
5.148	0.387
5.677	0.424
6.281	0.470
7.095	0.521
7.728	0.560
8.571	0.611

TABLE I.4

Adsorption Isotherms for Oxygen on EKA 5A Molecular Sieve Pellets at 278.15, 293.15 and 303.15 K

T = 278.15 K

Pressure bar	Amount adsorbed mol/kg of adsorbent
0.2095	0.052
0.449	0.109
0.730	0.174
1.063	0.245
1.40	0.314
1.813	0.390
2.220	0.472
2.670	0.553
3.153	0.636
3.680	0.719
4.217	0.801
4.924	0.899
5.706	1.006
6.576	1.115
7.553	1.226
8.305	1.313

T = 293.15 K

Pressure bar	Amount adsorbed mol/kg of adsorbent
0.246	0.039
0.536	0.084
0.853	0.132
1.185	0.181
1.579	0.236
2.044	0.298
2.523	0.359
3.025	0.421
3.561	0.485
4.123	0.547
4.717	0.617
5.384	0.680
6.113	0.750
6.834	0.818
7.553	0.879
8.247	0.938
8.873	0.988

T = 303.15 K

Pressure bar	Amount adsorbed mol/kg of adsorbent
0.292	0.037
0.633	0.0796
0.987	0.122
1.351	0.165
1.747	0.2096
2.146	0.255
2.586	0.302
3.042	0.349
3.508	0.396
4.032	0.447
4.60	0.4998
5.233	0.556
5.986	0.619
6.734	0.685
7.511	0.745
8.259	0.799
8.885	0.845

TABLE I.5

Adsorption Isotherms for Oxygen on Na-Mordenite Molecular Sieve Pellets at 278.15, 293.15 and 303.15 K

T = 278.15 K

Pressure bar	Amount adsorbed mol/kg of adsorbent
0.269	0.099
0.586	0.204
0.937	0.313
1.333	0.4197
1.755	0.525
2.209	0.624
2.718	0.715
3.228	0.80
3.732	0.88
4.312	0.967
5.038	1.044
5.867	1.134
6.870	1.227
7.967	1.311
8.744	1.383

T = 293.15 K

Pressure bar	Amount adsorbed mol/kg of adsorbent
0.303	0.069
0.636	0.141
1.0	0.213
1.412	0.29
1.876	0.369
2.249	0.457
2.887	0.526
3.419	0.592
3.935	0.659
4.553	0.723
5.253	0.791
6.098	0.861
6.997	0.930
7.833	0.989
8.722	1.045
9.329	1.079

T = 303.15 K

Pressure bar	Amount adsorbed mol/kg of adsorbent
0.353	0.059
0.704	0.119
1.071	0.176
1.435	0.232
1.855	0.292
2.311	0.353
2.765	0.411
3.223	0.464
3.686	0.514
4.152	0.561
4.644	0.611
5.287	0.667
6.032	0.728
6.841	0.790
7.730	0.853
8.644	0.908

TABLE I.6

Adsorption Isotherms for Nitrogen on Laporte 4A Molecular Sieve Pellets at 278.15, 293.15 and 303.15 K

T = 278.15 K

Pressure bar	Amount adsorbed mol/kg of adsorbent
0.205	0.104
0.370	0.182
0.599	0.277
0.892	0.382
1.240	0.505
1.715	0.649
2.248	0.792
2.877	0.93
3.603	1.063
4.544	1.226
5.604	1.354
6.495	1.452
7.285	1.523
7.894	1.572
8.43	1.609

T = 293.15 K

Pressure bar	Amount adsorbed mol/kg of adsorbent
0.305	0.093
0.552	0.166
0.842	0.246
1.193	0.336
1.610	0.435
2.110	0.541
2.657	0.644
3.277	0.749
3.935	0.852
4.756	0.958
5.603	1.059
6.420	1.145
7.224	1.219
7.991	1.283

T = 303.15 K

Pressure bar	Amount adsorbed mol/kg of adsorbent
0.359	0.085
0.627	0.147
0.936	0.214
1.330	0.295
1.791	0.382
2.314	0.474
2.877	0.562
3.466	0.648
4.054	0.723
4.599	0.789
5.262	0.864
5.798	0.926
6.461	0.984
7.333	1.055

TABLE I.7

Adsorption Isotherms for Nitrogen on Laporte 5A Molecular Sieve Pellets at 278.15, 293.15 and 303.15 K

T = 278.15 K

Pressure bar	Amount adsorbed mol/kg of adsorbent
0.149	0.096
0.356	0.207
0.624	0.327
0.966	0.454
1.381	0.585
1.864	0.716
2.457	0.855
3.139	0.984
3.776	1.131
4.843	1.271
5.945	1.3917
6.819	1.483
7.679	1.562
8.547	1.629

T = 293.15 K

Pressure bar	Amount adsorbed mol/kg of adsorbent
0.175	0.07
0.386	0.142
0.641	0.220
0.95	0.306
1.328	0.394
1.705	0.482
2.160	0.566
2.689	0.655
3.279	0.748
3.941	0.836
4.444	0.903
5.102	0.972
5.847	1.047
6.627	1.115
7.499	1.183
8.186	1.231

T = 303.15 K

Pressure bar	Amount adsorbed mol/kg of adsorbent
0.197	0.059
0.432	0.118
0.697	0.182
1.004	0.249
1.361	0.320
1.77	0.395
2.257	0.472
2.747	0.548
3.3	0.622
3.859	0.691
4.395	0.757
5.087	0.826
5.876	0.898
6.622	0.958
7.303	1.010
7.864	1.051
8.422	1.088

TABLE I.8

Adsorption Isotherms for Nitrogen on Laporte 13X Molecular Sieve Pellets at 278.15, 293.15 and 303.15 K

T = 278.15 K

Pressure bar	Amount adsorbed mol/kg of adsorbent
0.21	0.102
0.375	0.182
0.59	0.274
0.837	0.370
1.121	0.470
1.45	0.576
1.827	0.683
2.25	0.789
2.713	0.9
3.243	1.013
3.868	1.125
4.568	1.238
5.511	1.37
6.298	1.465
7.085	1.55
7.767	1.618
8.279	1.666

T = 293.15 K

Pressure bar	Amount adsorbed mol/kg of adsorbent
0.270	0.089
0.461	0.151
0.691	0.215
0.962	0.287
1.279	0.366
1.645	0.452
2.307	0.587
2.619	0.646
3.136	0.734
3.693	0.823
4.239	0.917
4.999	1.007
5.611	1.086
6.256	1.151
6.90	1.214
7.523	1.269
8.011	1.312
8.454	1.349

T = 303.15 K

Pressure bar	Amount adsorbed mol/kg of adsorbent
0.294	0.077
0.579	0.143
0.873	0.208
1.157	0.268
1.439	0.326
1.771	0.387
2.12	0.448
2.473	0.506
2.859	0.566
3.255	0.625
3.691	0.688
4.197	0.753
4.680	0.818
5.226	0.88
5.964	0.958
6.785	1.036
7.441	1.097
8.064	1.15
8.644	1.196

TABLE I.9

Adsorption Isotherms for Nitrcgen on EKA 5A Molecular Sieve Pellets at 278.15, 293.15 and 303.15 K

T = 278.15 K

Pressure bar	Amount adsorbed mol/kg of adsorbent
0.088	0.123
0.222	0.263
0.412	0.431
0.691	0.61
1.072	0.801
1.586	0.991
2.274	1.171
3.121	1.346
4.117	1.525
5.423	1.68
6.829	1.808
7.91	1.906
8.717	1.968

T = 293.15 K

Pressure bar	Amount adsorbed mol/kg of adsorbent
0.113	0.088
0.269	0.183
0.475	0.292
0.732	0.409
1.061	0.533
1.459	0.658
1.911	0.777
2.412	0.889
2.961	0.991
3.539	1.092
4.242	1.185
5.019	1.277
5.854	1.362
6.70	1.439
7.504	1.503
8.206	1.554

T = 303.15 K

Pressure bar	Amount adsorbed mol/kg of adsorbent
0.143	0.078
0.322	0.161
0.548	0.25
0.826	0.345
1.166	0.447
1.573	0.553
2.031	0.653
2.546	0.751
3.140	0.849
3.768	0.945
4.580	1.041
5.452	1.132
6.408	1.22
7.25	1.288
7.947	1.339
8.537	1.376

TABLE I.10

Adsorption Isotherms for Nitrogen on Na-Mordenite Molecular Sieve Pellets at 278.15, 293.15 and 303.15 K

T = 278.15 K

Pressure bar	Amount adsorbed mol/kg of adsorbent
0.088	0.184
0.246	0.406
0.499	0.654
0.954	0.905
1.671	1.129
2.609	1.313
3.547	1.434
4.573	1.528
5.728	1.612
6.817	1.683
7.816	1.736
8.863	1.782
9.519	1.815

T = 293.15 K

Pressure bar	Amount adsorbed mol/kg of adsorbent
0.107	0.112
0.256	0.243
0.463	0.390
0.777	0.545
1.216	0.705
1.772	0.852
2.434	0.977
3.165	1.080
3.910	1.163
4.580	1.225
5.275	1.277
6.144	1.332
6.968	1.376
7.762	1.414
8.581	1.449

T = 303.15 K

Pressure bar	Amount adsorbed mol/kg of adsorbent
0.133	0.101
0.319	0.219
0.58	0.35
0.951	0.494
1.425	0.637
1.992	0.761
2.614	0.8696
3.316	0.961
3.997	1.037
4.647	1.098
5.299	1.149
5.993	1.195
6.736	1.237
7.465	1.277
8.371	1.320
9.014	1.347

TABLE I.11

Binary Adsorption Equilibrium Data for O_2/N_2 on Laporte 4A

Adsorption Temperature = 278.15 K

Average Equilibrium Pressure = 1.76 bar

Mole Fraction Gas Phase (oxygen)	Mole Fraction Adsorbed Phase (oxygen)	Amount Adsorbed mol/kg			Equilibrium Pressure bar	Selectivity Coefficient $S_{1,2}$
		Component 1 (oxygen)	Component 2 (nitrogen)	Total		
0.94	0.82	0.203	0.045	0.248	1.792	0.292
0.932	0.799	0.202	0.051	0.253	1.774	0.292
0.922	0.775	0.199	0.058	0.257	1.764	0.292
0.91	0.748	0.195	0.066	0.26	1.754	0.293
0.895	0.717	0.189	0.075	0.264	1.757	0.298
0.879	0.687	0.187	0.085	0.272	1.774	0.301
0.878	0.689	0.193	0.087	0.280	1.816	0.309
0.676	0.388	0.137	0.216	0.353	1.718	0.303
0.491	0.227	0.096	0.327	0.423	1.719	0.304
0.344	0.138	0.067	0.415	0.482	1.779	0.307
0.243	0.088	0.047	0.483	0.530	1.768	0.301
0.170	0.057	0.032	0.532	0.564	1.803	0.297
0.789	0.540	0.171	0.145	0.316	1.763	0.315
0.758	0.494	0.163	0.167	0.33	1.766	0.312
0.723	0.445	0.154	0.192	0.345	1.732	0.308
0.714	0.440	0.151	0.192	0.342	1.766	0.315

TABLE I.11 continued .....

Mole Fraction Gas Phase (oxygen)	Mole Fraction Adsorbed Phase (oxygen)	Amount Adsorbed mol/kg			Equilibrium Pressure bar	Selectivity Coefficient $S_{1,2}$
		Component 1 (oxygen)	Component 2 (nitrogen)	Total		
0.678	0.393	0.141	0.219	0.360	1.757	0.308
0.672	0.390	0.141	0.221	0.362	1.766	0.313
0.623	0.337	0.127	0.251	0.378	1.740	0.308
0.618	0.336	0.129	0.254	0.383	1.744	0.313
0.56	0.285	0.116	0.291	0.407	1.783	0.313
0.555	0.275	0.109	0.288	0.397	1.735	0.303
0.49	0.23	0.101	0.336	0.437	1.796	0.312
0.403	0.172	0.081	0.389	0.469	1.759	0.307

TABLE I.11 continued .....

Adsorption Temperature = 293.15 K

Average Equilibrium Pressure = 1.73 bar

Mole Fraction Gas Phase (oxygen)	Mole Fraction Adsorbed Phase (oxygen)	Amount Adsorbed mol/kg			Equilibrium Pressure bar	Selectivity Coefficient $S_{1,2}$
		Component 1 (oxygen)	Component 2 (nitrogen)	Total		
0.945	0.877	0.174	0.024	0.199	1.742	0.415
0.936	0.851	0.170	0.0298	0.2	1.718	0.39
0.926	0.820	0.164	0.036	0.2	1.719	0.363
0.914	0.788	0.16	0.043	0.203	1.702	0.350
0.902	0.753	0.157	0.051	0.209	1.731	0.332
0.887	0.721	0.157	0.061	0.218	1.779	0.329
0.887	0.726	0.157	0.059	0.217	1.763	0.337
0.804	0.566	0.143	0.110	0.253	1.733	0.319
0.768	0.514	0.136	0.128	0.264	1.746	0.320
0.733	0.501	0.137	0.137	0.274	1.752	0.364
0.723	0.456	0.127	0.151	0.277	1.74	0.322
0.687	0.438	0.127	0.162	0.289	1.776	0.355
0.665	0.393	0.115	0.177	0.292	1.724	0.326
0.624	0.372	0.114	0.193	0.307	1.766	0.357
0.594	0.322	0.099	0.209	0.308	1.697	0.323
0.465	0.222	0.073	0.257	0.33	1.637	0.328
0.32	0.140	0.053	0.325	0.379	1.682	0.347
0.306	0.128	0.05	0.34	0.39	1.718	0.332
0.205	0.081	0.34	0.388	0.422	1.744	0.340
0.141	0.052	0.023	0.418	0.441	1.758	0.337

TABLE I.11 continued .....

Adsorption Temperature = 303.15 K

Average Equilibrium Pressure = 1.72 bar

Mole Fraction Gas Phase (oxygen)	Mole Fraction Adsorbed Phase (oxygen)	Amount Adsorbed mol/kg			Equilibrium Pressure bar	Selectivity Coefficient $S_{1,2}$
		Component 1 (oxygen)	Component 2 (nitrogen)	Total		
0.956	0.893	0.144	0.017	0.161	1.715	0.39
0.946	0.87	0.142	0.021	0.163	1.721	0.381
0.934	0.842	0.138	0.026	0.164	1.699	0.375
0.919	0.807	0.133	0.032	0.165	1.666	0.37
0.903	0.772	0.132	0.039	0.171	1.696	0.366
0.889	0.742	0.137	0.048	0.185	1.805	0.359
0.866	0.689	0.123	0.056	0.179	1.705	0.343
0.857	0.683	0.13	0.06	0.19	1.76	0.362
0.813	0.601	0.122	0.081	0.20	1.714	0.348
0.773	0.547	0.118	0.097	0.215	1.74	0.354
0.741	0.522	0.118	0.108	0.226	1.733	0.381
0.723	0.479	0.109	0.118	0.227	1.72	0.353
0.684	0.448	0.107	0.131	0.238	1.733	0.376
0.653	0.402	0.096	0.143	0.239	1.691	0.357
0.623	0.377	0.087	0.144	0.232	1.623	0.366
0.614	0.375	0.096	0.16	0.256	1.735	0.377
0.573	0.322	0.082	0.173	0.255	1.691	0.354

TABLE I.11 continued .....

Adsorption Temperature = 303.15 K

Average Equilibrium Pressure = 1.72 bar

Mole Fraction Gas Phase (oxygen)	Mole Fraction Adsorbed Phase (oxygen)	Amount adsorbed mol/kg			Equilibrium Pressure bar	Selectivity Coefficient $S_{1,2}$
		Component 1 (oxygen)	Component 2 (nitrogen)	Total		
0.532	0.303	0.084	0.195	0.279	1.754	0.382
0.447	0.219	0.059	0.211	0.27	1.593	0.348
0.426	0.197	0.053	0.216	0.269	1.581	0.329
0.411	0.202	0.058	0.231	0.289	1.673	0.363
0.273	0.106	0.034	0.282	0.316	1.675	0.317
0.261	0.115	0.039	0.3	0.339	1.766	0.369
0.281	0.127	0.042	0.289	0.331	1.751	0.373
0.176	0.06	0.021	0.328	0.349	1.742	0.296
0.173	0.071	0.026	0.339	0.365	1.80	0.368
0.116	0.033	0.012	0.356	0.368	1.772	0.262
0.114	0.047	0.018	0.359	0.377	1.796	0.381

TABLE I.11 continued .....

Adsorption Temperature = 278.15 K

Average Equilibrium Pressure = 4.41 bar

Mole Fraction Gas Phase (oxygen)	Mole Fraction Adsorbed Phase (oxygen)	Amount Adsorbed mol/kg			Equilibrium Pressure bar	Selectivity Coefficient $S_{1,2}$
		Component 1 (oxygen)	Component 2 (nitrogen)	Total		
0.888	0.699	0.442	0.19	0.632	4.419	0.295
0.866	0.658	0.421	0.219	0.640	4.429	0.298
0.844	0.615	0.406	0.254	0.660	4.381	0.297
0.817	0.574	0.396	0.294	0.69	4.478	0.303
0.812	0.574	0.395	0.293	0.688	4.393	0.313
0.785	0.524	0.377	0.342	0.719	4.488	0.302
0.781	0.521	0.372	0.342	0.714	4.429	0.305
0.719	0.443	0.339	0.426	0.764	4.429	0.312
0.664	0.381	0.307	0.498	0.804	4.441	0.312
0.598	0.317	0.271	0.584	0.855	4.463	0.313
0.589	0.31	0.265	0.589	0.854	4.393	0.314
0.505	0.243	0.221	0.686	0.907	4.429	0.315
0.415	0.182	0.175	0.787	0.962	4.424	0.314
0.38	0.161	0.155	0.811	0.966	4.307	0.313
0.386	0.16	0.153	0.801	0.953	4.259	0.304
0.284	0.111	0.115	0.922	1.037	4.471	0.315
0.255	0.094	0.098	0.949	1.047	4.478	0.302
0.176	0.057	0.062	1.017	1.079	4.439	0.284
0.12	0.034	0.038	1.058	1.095	4.39	0.260
0.08	0.019	0.021	1.088	1.109	4.342	0.222

TABLE I.11 continued .....

Adsorption Temperature = 293.15 K

Average Equilibrium Pressure = 4.42 bar

Mole Fraction Gas Phase (oxygen)	Mole Fraction Adsorbed Phase (oxygen)	Amount Adsorbed mol/kg			Equilibrium Pressure bar	Selectivity Coefficient $S_{1,2}$
		Component 1 (oxygen)	Component 2 (nitrogen)	Total		
0.896	0.74	0.365	0.128	0.494	4.437	0.332
0.873	0.696	0.351	0.154	0.505	4.405	0.332
0.847	0.646	0.336	0.184	0.520	4.395	0.331
0.819	0.596	0.325	0.221	0.546	4.488	0.327
0.812	0.602	0.32	0.211	0.531	4.429	0.350
0.778	0.533	0.302	0.265	0.567	4.441	0.326
0.775	0.544	0.306	0.256	0.562	4.502	0.347
0.737	0.491	0.283	0.292	0.575	4.402	0.345
0.678	0.419	0.256	0.355	0.611	4.419	0.343
0.604	0.342	0.224	0.43	0.653	4.473	0.341
0.575	0.320	0.21	0.445	0.655	4.30	0.348
0.504	0.256	0.18	0.523	0.703	4.456	0.338
0.384	0.181	0.136	0.617	0.753	4.376	0.354
0.367	0.161	0.123	0.64	0.763	4.361	0.332
0.363	0.16	0.121	0.639	0.76	4.344	0.333

TABLE I.11 continued .....

Adsorption Temperature = 293.15 K

Average Equilibrium Pressure = 4.42 bar

Mole Fraction Gas Phase (oxygen)	Mole Fraction Adsorbed Phase (oxygen)	Amount Adsorbed mol/kg			Equilibrium Pressure bar	Selectivity Coefficient $S_{1,2}$
		Component 1 (oxygen)	Component 2 (nitrogen)	Total		
0.252	0.108	0.089	0.729	0.818	4.434	0.362
0.239	0.092	0.076	0.748	0.823	4.437	0.323
0.157	0.055	0.047	0.809	0.856	4.429	0.312
0.103	0.032	0.028	0.851	0.879	4.432	0.287
0.068	0.017	0.015	0.873	0.888	4.446	0.240

TABLE I.11 continued .....

Adsorption Temperature = 303.15 K

Average Equilibrium Pressure = 4.4 bar

Mole Fraction Gas Phase (oxygen)	Mole Fraction Adsorbed Phase (oxygen)	Amount Adsorbed mol/kg			Equilibrium Pressure bar	Selectivity Coefficient $S_{1,2}$
		Component 1 (oxygen)	Component 2 (nitrogen)	Total		
0.9	0.76	0.31	0.098	0.408	4.307	0.35
0.877	0.716	0.302	0.12	0.422	4.344	0.352
0.852	0.669	0.298	0.147	0.445	4.468	0.353
0.818	0.613	0.287	0.181	0.469	4.551	0.353
0.81	0.607	0.276	0.179	0.454	4.378	0.363
0.767	0.537	0.259	0.224	0.482	4.424	0.353
0.758	0.528	0.248	0.222	0.469	4.271	0.358
0.633	0.379	0.208	0.34	0.548	4.385	0.354
0.537	0.291	0.173	0.421	0.594	4.419	0.355
0.421	0.206	0.135	0.522	0.657	4.575	0.356
0.373	0.177	0.112	0.518	0.63	4.244	0.362
0.357	0.164	0.106	0.542	0.648	4.298	0.354
0.24	0.101	0.07	0.622	0.692	4.32	0.356
0.239	0.1	0.069	0.618	0.686	4.215	0.355
0.225	0.09	0.066	0.651	0.718	4.463	0.352
0.146	0.057	0.043	0.707	0.75	4.468	0.355
0.092	0.034	0.026	0.757	0.783	4.585	0.344
0.06	0.02	0.016	0.771	0.787	4.527	0.324

TABLE I.12

Binary Adsorption Equilibrium Data for O_2/N_2 on Laporte 5A

Adsorption Temperature = 278.15 K

Average Equilibrium Pressure = 1.73 bar

Mole Fraction Gas Phase (oxygen)	Mole Fraction Adsorbed Phase (oxygen)	Amount Adsorbed mol/kg			Equilibrium Pressure bar	Selectivity Coefficient $S_{1,2}$
		Component 1 (oxygen)	Component 2 (nitrogen)	Total		
0.931	0.767	0.234	0.071	0.305	1.768	0.245
0.925	0.748	0.23	0.078	0.308	1.759	0.242
0.916	0.726	0.225	0.085	0.31	1.737	0.243
0.907	0.703	0.219	0.093	0.312	1.715	0.244
0.896	0.677	0.212	0.101	0.313	1.684	0.244
0.889	0.66	0.201	0.103	0.304	1.626	0.244
0.883	0.647	0.202	0.11	0.313	1.657	0.242
0.817	0.536	0.199	0.172	0.371	1.747	0.259
0.795	0.504	0.192	0.189	0.381	1.752	0.263
0.772	0.471	0.185	0.208	0.393	1.771	0.263
0.743	0.434	0.175	0.229	0.405	1.741	0.266
0.709	0.394	0.164	0.253	0.417	1.74	0.266
0.707	0.393	0.167	0.258	0.425	1.769	0.269
0.666	0.353	0.155	0.285	0.44	1.759	0.274
0.657	0.338	0.143	0.279	0.422	1.642	0.267

TABLE I.12 continued .....

Adsorption Temperature = 278.15 K

Average Equilibrium Pressure = 1.73 bar

Mole Fraction Gas Phase (oxygen)	Mole Fraction Adsorbed Phase (oxygen)	Amount Adsorbed mol/kg			Equilibrium Pressure bar	Selectivity Coefficient $S_{1,2}$
		Component 1 (oxygen)	Component 2 (nitrogen)	Total		
0.618	0.311	0.142	0.315	0.458	1.753	0.279
0.569	0.271	0.130	0.35	0.481	1.769	0.282
0.518	0.225	0.109	0.376	0.485	1.666	0.271
0.413	0.167	0.087	0.435	0.522	1.715	0.286
0.376	0.143	0.079	0.476	0.555	1.754	0.276
0.278	0.097	0.057	0.536	0.593	1.77	0.278
0.21	0.067	0.041	0.571	0.612	1.757	0.271
0.515	0.233	0.118	0.39	0.508	1.8	0.286

TABLE I.12 continued .....

Adsorption Temperature = 293.15 K

Average Equilibrium Pressure = 1.7 bar

Mole Fraction Gas Phase (oxygen)	Mole Fraction Adsorbed Phase (oxygen)	Amount Adsorbed mol/kg			Equilibrium Pressure bar	Selectivity Coefficient $S_{1,2}$
		Component 1 (oxygen)	Component 2 (nitrogen)	Total		
0.939	0.832	0.177	0.036	0.213	1.741	0.32
0.93	0.81	0.174	0.041	0.214	1.727	0.317
0.921	0.784	0.169	0.047	0.216	1.708	0.312
0.908	0.757	0.164	0.053	0.217	1.69	0.315
0.897	0.714	0.157	0.063	0.22	1.653	0.286
0.892	0.724	0.158	0.06	0.218	1.659	0.317
0.876	0.681	0.147	0.069	0.216	1.596	0.304
0.808	0.55	0.15	0.123	0.273	1.738	0.29
0.781	0.507	0.143	0.139	0.281	1.737	0.289
0.746	0.463	0.135	0.156	0.292	1.738	0.294
0.706	0.415	0.126	0.177	0.303	1.727	0.296
0.641	0.348	0.107	0.201	0.309	1.637	0.298
0.699	0.404	0.112	0.166	0.278	1.57	0.292
0.495	0.229	0.08	0.269	0.349	1.637	0.303
0.343	0.139	0.057	0.35	0.406	1.713	0.31
0.242	0.09	0.039	0.398	0.437	1.781	0.309
0.173	0.063	0.028	0.42	0.448	1.737	0.321

TABLE I.12 continued .....

Adsorption Temperature = 303.15 K

Average Equilibrium Pressure = 1.71 bar

Mole Fraction Gas Phase (oxygen)	Mole Fraction Adsorbed Phase (oxygen)	Amount Adsorbed mol/kg			Equilibrium Pressure bar	Selectivity Coefficient $S_{1,2}$
		Component 1 (oxygen)	Component 2 (nitrogen)	Total		
0.938	0.836	0.152	0.03	0.182	1.742	0.341
0.928	0.81	0.148	0.035	0.183	1.727	0.331
0.916	0.78	0.144	0.04	0.184	1.721	0.328
0.902	0.747	0.139	0.047	0.186	1.705	0.322
0.894	0.727	0.138	0.052	0.19	1.723	0.316
0.884	0.709	0.133	0.055	0.188	1.671	0.32
0.862	0.66	0.123	0.064	0.187	1.596	0.311
0.808	0.58	0.125	0.09	0.215	1.702	0.328
0.775	0.53	0.119	0.105	0.224	1.701	0.328
0.738	0.479	0.112	0.122	0.235	1.718	0.328
0.702	0.441	0.109	0.138	0.247	1.703	0.334
0.693	0.425	0.105	0.142	0.248	1.723	0.328
0.675	0.396	0.096	0.147	0.243	1.648	0.315
0.646	0.38	0.099	0.161	0.26	1.692	0.337
0.635	0.364	0.096	0.166	0.261	1.718	0.33
0.575	0.316	0.087	0.188	0.274	1.679	0.341

TABLE I.12 continued .....

Adsorption Temperature = 303.15 K

Average Equilibrium Pressure = 1.71 bar

Mole Fraction Gas Phase (oxygen)	Mole Fraction Adsorbed Phase (oxygen)	Amount Adsorbed mol/kg			Equilibrium Pressure bar	Selectivity Coefficient $S_{1,2}$
		Component 1 (oxygen)	Component 2 (nitrogen)	Total		
0.548	0.284	0.077	0.194	0.271	1.638	0.328
0.503	0.257	0.076	0.219	0.295	1.708	0.342
0.468	0.221	0.066	0.233	0.299	1.698	0.322
0.43	0.203	0.065	0.257	0.322	1.779	0.338
0.323	0.133	0.045	0.295	0.34	1.751	0.321
0.296	0.128	0.044	0.301	0.345	1.743	0.35
0.227	0.085	0.031	0.329	0.36	1.748	0.316
0.162	0.056	0.02	0.346	0.367	1.709	0.306

TABLE I.12 continued .....

Adsorption Temperature = 278.15 K

Average Equilibrium Pressure = 4.44 bar

Mole Fraction Gas Phase (oxygen)	Mole Fraction Adsorbed Phase (oxygen)	Amount Adsorbed mol/kg			Equilibrium Pressure bar	Selectivity Coefficient $S_{1,2}$
		Component 1 (oxygen)	Component 2 (nitrogen)	Total		
0.878	0.66	0.462	0.238	0.701	4.468	0.271
0.859	0.628	0.45	0.267	0.717	4.419	0.276
0.838	0.592	0.434	0.299	0.733	4.446	0.281
0.813	0.552	0.415	0.336	0.751	4.434	0.284
0.812	0.551	0.417	0.339	0.756	4.434	0.286
0.783	0.509	0.392	0.378	0.771	4.429	0.288
0.783	0.507	0.393	0.382	0.776	4.429	0.286
0.698	0.416	0.346	0.485	0.831	4.422	0.309
0.643	0.359	0.31	0.553	0.864	4.395	0.312
0.606	0.32	0.292	0.62	0.912	4.544	0.307
0.577	0.3	0.271	0.632	0.903	4.434	0.315
0.494	0.239	0.227	0.724	0.951	4.502	0.321
0.451	0.209	0.203	0.769	0.972	4.483	0.322
0.382	0.166	0.166	0.832	0.998	4.405	0.322
0.381	0.166	0.167	0.837	1.004	4.441	0.324
0.328	0.137	0.141	0.883	1.024	4.468	0.327
0.273	0.109	0.113	0.933	1.047	4.444	0.325
0.195	0.072	0.078	0.999	1.076	4.429	0.321
0.138	0.048	0.052	1.045	1.097	4.419	0.312
0.098	0.031	0.034	1.08	1.114	4.439	0.293

TABLE I.12 continued .....

Adsorption Temperature = 293.15 K

Average Equilibrium Pressure = 4.44 bar

Mole Fraction Gas Phase (oxygen)	Mole Fraction Adsorbed Phase (oxygen)	Amount Adsorbed mol/kg			Equilibrium Pressure bar	Selectivity Coefficient $S_{1,2}$
		Component 1 (oxygen)	Component 2 (nitrogen)	Total		
0.871	0.688	0.381	0.173	0.554	4.402	0.325
0.85	0.646	0.365	0.20	0.566	4.432	0.323
0.823	0.602	0.351	0.232	0.583	4.463	0.324
0.791	0.551	0.332	0.27	0.601	4.468	0.325
0.791	0.551	0.331	0.27	0.602	4.468	0.324
0.753	0.494	0.307	0.315	0.622	4.454	0.321
0.751	0.495	0.307	0.314	0.622	4.485	0.325
0.724	0.452	0.291	0.353	0.644	4.419	0.315
0.707	0.436	0.283	0.367	0.651	4.466	0.32
0.694	0.422	0.269	0.368	0.637	4.303	0.323
0.665	0.389	0.261	0.41	0.672	4.405	0.322
0.588	0.319	0.224	0.479	0.703	4.371	0.328
0.57	0.311	0.226	0.501	0.728	4.507	0.34
0.492	0.245	0.182	0.562	0.744	4.383	0.333
0.413	0.197	0.154	0.627	0.781	4.417	0.349
0.375	0.169	0.135	0.663	0.798	4.439	0.339

TABLE I.12 continued .....

Adsorption Temperature = 293.15 K

Average Equilibrium Pressure = 4.44 bar

Mole Fraction Gas Phase (oxygen)	Mole Fraction Adsorbed Phase (oxygen)	Amount Adsorbed mol/kg			Equilibrium Pressure bar	Selectivity Coefficient $S_{1,2}$
		Component 1 (oxygen)	Component 2 (nitrogen)	Total		
0.367	0.166	0.134	0.674	0.808	4.529	0.343
0.288	0.126	0.104	0.725	0.83	4.417	0.357
0.26	0.108	0.09	0.747	0.837	4.415	0.344
0.18	0.068	0.058	0.803	0.861	4.463	0.331
0.124	0.043	0.038	0.843	0.881	4.39	0.318
0.085	0.027	0.024	0.869	0.892	4.415	0.294

TABLE I.12 continued .....

Adsorption Temperature = 303.15 K

Average Equilibrium Pressure = 4.44 bar

Mole Fraction Gas Phase (oxygen)	Mole Fraction Adsorbed Phase (oxygen)	Amount Adsorbed mol/kg			Equilibrium Pressure bar	Selectivity Coefficient $S_{1,2}$
		Component 1 (oxygen)	Component 2 (nitrogen)	Total		
0.874	0.699	0.323	0.139	0.462	4.434	0.336
0.85	0.654	0.309	0.164	0.473	4.434	0.334
0.818	0.602	0.293	0.193	0.486	4.429	0.338
0.781	0.548	0.276	0.227	0.503	4.483	0.341
0.778	0.543	0.273	0.229	0.502	4.390	0.341
0.733	0.483	0.253	0.271	0.524	4.473	0.341
0.739	0.496	0.26	0.265	0.525	4.451	0.348
0.679	0.427	0.235	0.316	0.55	4.451	0.351
0.668	0.409	0.223	0.323	0.547	4.395	0.343
0.599	0.347	0.201	0.377	0.578	4.415	0.356
0.553	0.305	0.183	0.418	0.601	4.458	0.355
0.498	0.263	0.162	0.453	0.615	4.415	0.36
0.386	0.185	0.122	0.535	0.656	4.41	0.362
0.371	0.172	0.114	0.547	0.661	4.444	0.353
0.37	0.173	0.114	0.548	0.662	4.444	0.355
0.264	0.115	0.08	0.613	0.693	4.398	0.364
0.253	0.106	0.074	0.624	0.698	4.429	0.35
0.173	0.065	0.047	0.676	0.722	4.415	0.332
0.116	0.038	0.029	0.715	0.743	4.434	0.304
0.078	0.022	0.017	0.74	0.756	4.412	0.268

TABLE I.13

Binary Adsorption Equilibrium Data for O_2/N_2 on Laporte 13X

Adsorption Temperature = 278.15 K

Average Equilibrium Pressure = 1.74 bar

Mole Fraction Gas Phase (oxygen)	Mole Fraction Adsorbed Phase (oxygen)	Amount Adsorbed mol/kg			Equilibrium Pressure bar	Selectivity Coefficient $S_{1,2}$
		Component 1 (oxygen)	Component 2 (nitrogen)	Total		
0.941	0.819	0.208	0.046	0.254	1.761	0.282
0.935	0.799	0.209	0.053	0.261	1.782	0.276
0.925	0.774	0.205	0.06	0.265	1.782	0.278
0.915	0.744	0.199	0.068	0.268	1.76	0.271
0.915	0.74	0.199	0.07	0.269	1.752	0.266
0.90	0.707	0.188	0.078	0.266	1.692	0.268
0.808	0.544	0.172	0.144	0.316	1.764	0.284
0.778	0.496	0.163	0.166	0.329	1.752	0.281
0.746	0.446	0.153	0.19	0.343	1.7383	0.275
0.717	0.417	0.151	0.212	0.363	1.796	0.283
0.69	0.381	0.139	0.226	0.365	1.671	0.277
0.669	0.365	0.14	0.244	0.384	1.77	0.284
0.648	0.339	0.128	0.25	0.378	1.699	0.279
0.615	0.315	0.129	0.28	0.409	1.78	0.288

TABLE I.13 continued .....

Adsorption Temperature = 278.15 K

Average Equilibrium Pressure = 1.74 bar

Mole Fraction Gas Phase (oxygen)	Mole Fraction Adsorbed Phase (oxygen)	Amount Adsorbed mol/kg			Equilibrium Pressure bar	Selectivity Coefficient $S_{1,2}$
		Component 1 (oxygen)	Component 2 (nitrogen)	Total		
0.555	0.264	0.116	0.322	0.438	1.799	0.288
0.495	0.219	0.097	0.348	0.446	1.663	0.285
0.477	0.207	0.097	0.371	0.469	1.797	0.288
0.343	0.13	0.064	0.429	0.493	1.681	0.287
0.34	0.132	0.068	0.447	0.515	1.714	0.297
0.233	0.085	0.048	0.514	0.562	1.757	0.307
0.16	0.058	0.034	0.557	0.591	1.77	0.321

TABLE I.13 continued .....

Adsorption Temperature = 293.15 K

Average Equilibrium Pressure = 1.74 bar

Mole Fraction Gas Phase (oxygen)	Mole Fraction Adsorbed Phase (oxygen)	Amount Adsorbed mol/kg			Equilibrium Pressure bar	Selectivity Coefficient $S_{1,2}$
		Component 1 (oxygen)	Component 2 (nitrogen)	Total		
0.954	0.852	0.159	0.028	0.187	1.735	0.277
0.946	0.832	0.16	0.032	0.192	1.764	0.283
0.935	0.805	0.156	0.038	0.194	1.744	0.287
0.92	0.773	0.151	0.044	0.195	1.699	0.296
0.913	0.761	0.154	0.049	0.203	1.794	0.305
0.903	0.733	0.143	0.052	0.195	1.654	0.297
0.883	0.689	0.136	0.061	0.198	1.642	0.293
0.815	0.587	0.138	0.097	0.236	1.754	0.322
0.78	0.53	0.131	0.116	0.245	1.752	0.317
0.738	0.468	0.122	0.138	0.26	1.749	0.312
0.728	0.458	0.121	0.143	0.265	1.77	0.317
0.684	0.402	0.111	0.165	0.276	1.731	0.31
0.671	0.393	0.111	0.171	0.282	1.769	0.318
0.666	0.371	0.102	0.173	0.276	1.697	0.296
0.612	0.329	0.096	0.196	0.292	1.699	0.311

TABLE I.13 continued .....

Adsorption Temperature = 293.15 K

Average Equilibrium Pressure = 1.74 bar

Mole Fraction Gas Phase (oxygen)	Mole Fraction Adsorbed Phase (oxygen)	Amount Adsorbed mol/kg			Equilibrium Pressure bar	Selectivity Coefficient $S_{1,2}$
		Component 1 (oxygen)	Component 2 (nitrogen)	Total		
0.608	0.33	0.101	0.204	0.305	1.788	0.317
0.53	0.265	0.088	0.244	0.332	1.799	0.32
0.455	0.197	0.067	0.272	0.339	1.705	0.293
0.303	0.112	0.043	0.345	0.388	1.726	0.289
0.285	0.111	0.044	0.35	0.393	1.747	0.314
0.204	0.064	0.027	0.394	0.421	1.757	0.269
0.136	0.037	0.016	0.425	0.441	1.781	0.242

TABLE I.13 continued .....

Adsorption Temperature = 303.15 K

Average Equilibrium Pressure = 1.75 bar

Mole Fraction Gas Phase (oxygen)	Mole Fraction Adsorbed Phase (oxygen)	Amount Adsorbed mol/kg			Equilibrium Pressure bar	Selectivity Coefficient $S_{1,2}$
		Component 1 (oxygen)	Component 2 (nitrogen)	Total		
0.945	0.869	0.141	0.021	0.162	1.764	0.385
0.935	0.838	0.14	0.027	0.166	1.764	0.362
0.92	0.80	0.136	0.034	0.17	1.743	0.353
0.902	0.76	0.131	0.041	0.173	1.731	0.346
0.88	0.713	0.127	0.051	0.178	1.72	0.339
0.855	0.663	0.124	0.063	0.186	1.72	0.333
0.818	0.607	0.122	0.079	0.202	1.77	0.346
0.778	0.543	0.116	0.097	0.213	1.779	0.34
0.739	0.485	0.108	0.114	0.222	1.766	0.333
0.728	0.472	0.107	0.12	0.227	1.766	0.334
0.68	0.414	0.099	0.14	0.239	1.768	0.334
0.665	0.397	0.097	0.15	0.243	1.766	0.332
0.656	0.376	0.088	0.146	0.234	1.693	0.315
0.603	0.339	0.088	0.171	0.259	1.776	0.338
0.595	0.314	0.082	0.18	0.263	1.759	0.311

TABLE I.13 continued .....

Adsorption Temperature = 303.15 K

Average Equilibrium Pressure = 1.75 bar

Mole Fraction Gas Phase (oxygen)	Mole Fraction Adsorbed Phase (oxygen)	Amount Adsorbed mol/kg			Equilibrium Pressure bar	Selectivity Coefficient $S_{1,2}$
		Component 1 (oxygen)	Component 2 (nitrogen)	Total		
0.508	0.259	0.074	0.21	0.284	1.779	0.339
0.47	0.227	0.064	0.219	0.283	1.704	0.331
0.431	0.193	0.056	0.236	0.292	1.705	0.316
0.384	0.174	0.055	0.259	0.313	1.768	0.339
0.28	0.107	0.036	0.297	0.333	1.719	0.309
0.234	0.092	0.032	0.319	0.351	1.781	0.333
0.184	0.062	0.022	0.333	0.355	1.735	0.294
0.12	0.035	0.013	0.356	0.369	1.74	0.269

TABLE I.13 continued .....

Adsorption Temperature = 278.15 K

Average Equilibrium Pressure = 4.44 bar

Mole Fraction Gas Phase (oxygen)	Mole Fraction Adsorbed Phase (oxygen)	Amount Adsorbed mol/kg			Equilibrium Pressure bar	Selectivity Coefficient $S_{1,2}$
		Component 1 (oxygen)	Component 2 (nitrogen)	Total		
0.879	0.679	0.423	0.2	0.623	4.439	0.292
0.859	0.636	0.407	0.233	0.64	4.434	0.288
0.833	0.592	0.393	0.272	0.665	4.451	0.29
0.804	0.542	0.376	0.317	0.693	4.468	0.289
0.799	0.544	0.372	0.312	0.684	4.439	0.3
0.765	0.49	0.352	0.367	0.718	4.473	0.295
0.764	0.483	0.347	0.371	0.717	4.385	0.289
0.608	0.317	0.261	0.562	0.824	4.439	0.3
0.575	0.292	0.246	0.597	0.843	4.373	0.304
0.516	0.243	0.213	0.665	0.878	4.402	0.3
0.416	0.176	0.169	0.789	0.958	4.539	0.301
0.39	0.167	0.161	0.803	0.963	4.466	0.313
0.371	0.15	0.146	0.825	0.971	4.402	0.301
0.37	0.149	0.143	0.821	0.964	4.415	0.298
0.266	0.102	0.104	0.917	1.021	4.473	0.312
0.25	0.087	0.09	0.942	1.032	4.456	0.288
0.247	0.088	0.092	0.956	1.047	4.536	0.294
0.169	0.053	0.057	1.012	1.069	4.454	0.277
0.115	0.031	0.034	1.048	1.082	4.371	0.247
0.076	0.017	0.018	1.079	1.097	4.405	0.205

TABLE I.13 continued .....

Adsorption Temperature = 293.15 K

Average Equilibrium Pressure = 4.41 bar

Mole Fraction Gas Phase (oxygen)	Mole Fraction Adsorbed Phase (oxygen)	Amount Adsorbed mol/kg			Equilibrium Pressure bar	Selectivity Coefficient $S_{1,2}$
		Component 1 (oxygen)	Component 2 (nitrogen)	Total		
0.89	0.724	0.344	0.131	0.475	4.402	0.325
0.867	0.678	0.333	0.158	0.491	4.415	0.324
0.84	0.629	0.325	0.191	0.516	4.5	0.323
0.803	0.566	0.302	0.232	0.534	4.454	0.321
0.793	0.555	0.299	0.239	0.538	4.463	0.326
0.755	0.497	0.277	0.281	0.559	4.395	0.32
0.75	0.488	0.278	0.292	0.57	4.434	0.317
0.693	0.417	0.244	0.342	0.586	4.298	0.318
0.688	0.409	0.245	0.354	0.599	4.361	0.314
0.635	0.358	0.225	0.403	0.628	4.454	0.321
0.55	0.286	0.191	0.476	0.666	4.366	0.328
0.53	0.266	0.178	0.492	0.671	4.361	0.321
0.404	0.177	0.13	0.603	0.733	4.381	0.318
0.365	0.157	0.118	0.634	0.752	4.293	0.323
0.361	0.158	0.121	0.648	0.769	4.41	0.332

TABLE I.13 continued .....

Adsorption Temperature = 293.15 K

Average Equilibrium Pressure = 4.41 bar

Mole Fraction Gas Phase (oxygen)	Mole Fraction Adsorbed Phase (oxygen)	Amount Adsorbed mol/kg			Equilibrium Pressure bar	Selectivity Coefficient $S_{1,2}$
		Component 1 (oxygen)	Component 2 (nitrogen)	Total		
0.36	0.151	0.115	0.646	0.761	4.385	0.316
0.24	0.093	0.076	0.738	0.814	4.393	0.326
0.237	0.085	0.069	0.741	0.81	4.441	0.3
0.233	0.087	0.072	0.756	0.828	4.488	0.315
0.15	0.051	0.044	0.818	0.861	4.502	0.303
0.1	0.029	0.026	0.844	0.87	4.427	0.268
0.065	0.015	0.013	0.866	0.88	4.395	0.218

TABLE I.13 continued .....

Adsorption Temperature = 303.15 K

Average Equilibrium Pressure = 4.34 bar

Mole Fraction Gas Phase (oxygen)	Mole Fraction Adsorbed Phase (oxygen)	Amount Adsorbed mol/kg			Equilibrium Pressure bar	Selectivity Coefficient $S_{1,2}$
		Component 1 (oxygen)	Component 2 (nitrogen)	Total		
0.893	0.748	0.299	0.101	0.4	4.39	0.357
0.869	0.696	0.288	0.126	0.415	4.41	0.345
0.837	0.636	0.274	0.157	0.431	4.39	0.34
0.789	0.566	0.254	0.194	0.448	4.329	0.349
0.788	0.569	0.256	0.194	0.45	4.366	0.356
0.735	0.487	0.231	0.243	0.474	4.317	0.343
0.735	0.488	0.232	0.244	0.476	4.342	0.344
0.667	0.404	0.207	0.305	0.512	4.349	0.339
0.646	0.367	0.192	0.331	0.523	4.305	0.318
0.537	0.272	0.153	0.41	0.563	4.244	0.322
0.531	0.284	0.16	0.4	0.565	4.283	0.351
0.404	0.179	0.111	0.511	0.622	4.283	0.321
0.36	0.155	0.101	0.548	0.649	4.366	0.326
0.359	0.159	0.101	0.536	0.637	4.3	0.338
0.339	0.154	0.1	0.551	0.651	4.356	0.355
0.231	0.085	0.0595	0.638	0.698	4.393	0.31
0.225	0.088	0.062	0.635	0.697	4.4	0.334
0.218	0.089	0.062	0.637	0.698	4.366	0.35
0.144	0.052	0.037	0.683	0.721	4.332	0.323
0.094	0.028	0.021	0.715	0.736	4.295	0.279
0.058	0.015	0.012	0.739	0.751	4.329	0.255

TABLE I.14

Binary Adsorption Equilibrium Data for O_2/N_2 on EKA 5A

Adsorption Temperature = 278.15 K

Average Equilibrium Pressure = 1.73 bar

Mole Fraction Gas Phase (oxygen)	Mole Fraction Adsorbed Phase (oxygen)	Amount Adsorbed mol/kg			Equilibrium Pressure bar	Selectivity Coefficient $S_{1,2}$
		Component 1 (oxygen)	Component 2 (nitrogen)	Total		
0.926	0.677	0.318	0.152	0.47	1.753	0.169
0.921	0.664	0.313	0.158	0.472	1.74	0.169
0.918	0.65	0.308	0.166	0.477	1.724	0.167
0.913	0.636	0.302	0.173	0.475	1.727	0.167
0.908	0.62	0.296	0.181	0.477	1.685	0.165
0.905	0.618	0.292	0.18	0.473	1.684	0.171
0.902	0.607	0.292	0.189	0.481	1.691	0.168
0.779	0.404	0.249	0.369	0.617	1.77	0.192
0.775	0.404	0.249	0.368	0.618	1.758	0.197
0.768	0.378	0.231	0.379	0.61	1.687	0.184
0.765	0.384	0.242	0.389	0.631	1.769	0.192
0.76	0.383	0.241	0.389	0.63	1.752	0.197
0.746	0.362	0.233	0.41	0.643	1.764	0.193
0.741	0.361	0.232	0.41	0.642	1.752	0.197
0.725	0.34	0.224	0.433	0.657	1.753	0.196

TABLE I.14 continued .....

Adsorption Temperature = 278.15 K

Average Equilibrium Pressure = 1.73 bar

Mole Fraction Gas Phase (oxygen)	Mole Fraction Adsorbed Phase (oxygen)	Amount Adsorbed mol/kg			Equilibrium Pressure bar	Selectivity Coefficient $S_{1,2}$
		Component 1 (oxygen)	Component 2 (nitrogen)	Total		
0.719	0.337	0.22	0.434	0.654	1.716	0.199
0.70	0.316	0.212	0.458	0.67	1.74	0.198
0.692	0.309	0.205	0.459	0.664	1.668	0.199
0.634	0.253	0.18	0.531	0.711	1.704	0.195
0.513	0.177	0.139	0.647	0.786	1.725	0.205
0.408	0.123	0.107	0.763	0.87	1.742	0.203
0.325	0.09	0.082	0.826	0.908	1.73	0.206

TABLE I.14 continued .....

Adsorption Temperature = 293.15 K

Average Equilibrium Pressure = 1.76 bar

Mole Fraction Gas Phase (oxygen)	Mole Fraction Adsorbed Phase (oxygen)	Amount Adsorbed mol/kg			Equilibrium Pressure bar	Selectivity Coefficient $S_{1,2}$
		Component 1 (oxygen)	Component 2 (nitrogen)	Total		
0.921	0.716	0.228	0.09	0.318	1.769	0.216
0.915	0.696	0.224	0.097	0.321	1.764	0.215
0.907	0.677	0.22	0.105	0.325	1.754	0.216
0.898	0.654	0.214	0.113	0.327	1.726	0.216
0.89	0.634	0.211	0.122	0.334	1.743	0.214
0.882	0.62	0.215	0.132	0.346	1.794	0.218
0.873	0.596	0.203	0.137	0.34	1.7	0.216
0.744	0.408	0.175	0.255	0.43	1.77	0.237
0.743	0.406	0.174	0.255	0.429	1.769	0.237
0.718	0.377	0.168	0.277	0.445	1.772	0.238
0.716	0.375	0.166	0.277	0.444	1.764	0.238
0.686	0.33	0.15	0.305	0.455	1.727	0.226
0.685	0.342	0.157	0.302	0.459	1.766	0.239
0.688	0.346	0.16	0.302	0.462	1.78	0.24
0.659	0.317	0.153	0.33	0.483	1.811	0.241

TABLE I.14 continued .....

Adsorption Temperature = 293.15 K

Average Equilibrium Pressure = 1.76 bar

Mole Fraction Gas Phase (oxygen)	Mole Fraction Adsorbed Phase (oxygen)	Amount Adsorbed mol/kg			Equilibrium Pressure bar	Selectivity Coefficient $S_{1,2}$
		Component 1 (oxygen)	Component 2 (nitrogen)	Total		
0.618	0.282	0.142	0.36	0.502	1.805	0.244
0.558	0.234	0.121	0.394	0.515	1.73	0.243
0.556	0.233	0.12	0.394	0.514	1.727	0.243
0.525	0.205	0.11	0.427	0.537	1.76	0.233
0.399	0.135	0.080	0.514	0.594	1.776	0.235
0.305	0.093	0.058	0.566	0.624	1.749	0.234
0.235	0.064	0.041	0.598	0.639	1.708	0.224

TABLE I.14 continued .....

Adsorption Temperature = 303.15 K

Average Equilibrium Pressure = 1.75 bar

Mole Fraction Gas Phase (oxygen)	Mole Fraction Adsorbed Phase (oxygen)	Amount Adsorbed mol/kg			Equilibrium Pressure bar	Selectivity Coefficient $S_{1,2}$
		Component 1 (oxygen)	Component 2 (nitrogen)	Total		
0.906	0.702	0.19	0.081	0.271	1.754	0.243
0.898	0.678	0.186	0.089	0.275	1.764	0.240
0.887	0.653	0.183	0.097	0.28	1.763	0.240
0.873	0.624	0.178	0.107	0.285	1.742	0.242
0.856	0.592	0.17	0.117	0.288	1.705	0.243
0.855	0.588	0.168	0.118	0.286	1.69	0.243
0.724	0.412	0.148	0.211	0.359	1.754	0.267
0.724	0.417	0.15	0.21	0.36	1.77	0.274
0.696	0.375	0.141	0.234	0.375	1.788	0.263
0.689	0.376	0.141	0.233	0.374	1.761	0.273
0.656	0.335	0.131	0.26	0.391	1.781	0.264
0.649	0.334	0.13	0.259	0.389	1.757	0.272
0.64	0.308	0.121	0.273	0.394	1.752	0.25
0.614	0.296	0.122	0.289	0.411	1.796	0.265
0.605	0.292	0.119	0.288	0.407	1.768	0.269
0.558	0.251	0.108	0.321	0.429	1.768	0.266

TABLE I.14 continued .....

Adsorption Temperature = 303.15 K

Average Equilibrium Pressure = 1.75 bar

Mole Fraction Gas Phase (oxygen)	Mole Fraction Adsorbed Phase (oxygen)	Amount Adsorbed mol/kg			Equilibrium Pressure bar	Selectivity Coefficient $S_{1,2}$
		Component 1 (oxygen)	Component 2 (nitrogen)	Total		
0.548	0.246	0.105	0.321	0.426	1.747	0.269
0.489	0.202	0.09	0.358	0.448	1.744	0.264
0.482	0.192	0.087	0.368	0.455	1.755	0.255
0.358	0.125	0.062	0.435	0.497	1.755	0.257
0.269	0.085	0.044	0.474	0.518	1.727	0.251
0.202	0.057	0.03	0.501	0.531	1.688	0.24

TABLE I.14 continued .....

Adsorption Temperature = 278.15 K

Average Equilibrium Pressure = 4.45 bar

Mole Fraction Gas Phase (oxygen)	Mole Fraction Adsorbed Phase (oxygen)	Amount Adsorbed mol/kg			Equilibrium Pressure bar	Selectivity Coefficient $S_{1,2}$
		Component 1 (oxygen)	Component 2 (nitrogen)	Total		
0.903	0.641	0.621	0.348	0.969	4.451	0.193
0.895	0.623	0.611	0.37	0.981	4.439	0.195
0.885	0.604	0.6	0.393	0.993	4.449	0.199
0.873	0.581	0.581	0.42	1.001	4.398	0.201
0.861	0.561	0.568	0.445	1.013	4.383	0.207
0.705	0.353	0.417	0.766	1.183	4.51	0.228
0.683	0.331	0.396	0.801	1.198	4.463	0.23
0.583	0.26	0.332	0.944	1.276	4.483	0.252
0.636	0.291	0.357	0.871	1.228	4.439	0.235
0.573	0.244	0.307	0.949	1.256	4.354	0.241
0.513	0.214	0.282	1.034	1.316	4.463	0.26
0.425	0.164	0.224	1.138	1.362	4.483	0.266
0.305	0.108	0.153	1.258	1.411	4.458	0.276
0.225	0.081	0.118	1.339	1.457	4.527	0.304
0.166	0.059	0.087	1.387	1.474	4.558	0.313
0.125	0.044	0.064	1.409	1.474	4.39	0.32

TABLE I.14 continued .....

Adsorption Temperature = 293.15 K

Average Equilibrium Pressure = 4.45 bar

Mole Fraction Gas Phase (oxygen)	Mole Fraction Adsorbed Phase (oxygen)	Amount Adsorbed mol/kg			Equilibrium Pressure bar	Selectivity Coefficient $S_{1,2}$
		Component 1 (oxygen)	Component 2 (nitrogen)	Total		
0.878	0.623	0.48	0.291	0.771	4.441	0.23
0.864	0.596	0.468	0.317	0.785	4.463	0.233
0.848	0.568	0.454	0.346	0.8	4.456	0.235
0.84	0.554	0.445	0.357	0.802	4.373	0.237
0.83	0.536	0.437	0.378	0.815	4.437	0.237
0.752	0.43	0.384	0.509	0.893	4.466	0.249
0.718	0.392	0.361	0.56	0.921	4.461	0.254
0.67	0.342	0.32	0.619	0.94	4.342	0.256
0.583	0.272	0.273	0.73	1.003	4.415	0.268
0.514	0.225	0.236	0.812	1.048	4.502	0.275
0.417	0.167	0.183	0.91	1.094	4.451	0.28
0.292	0.105	0.123	1.025	1.146	4.441	0.285
0.287	0.104	0.12	1.04	1.16	4.515	0.288
0.21	0.071	0.084	1.101	1.185	4.48	0.287
0.152	0.048	0.058	1.148	1.206	4.476	0.283
0.109	0.032	0.04	1.179	1.218	4.466	0.274

TABLE I.14 continued .....

Adsorption Temperature = 303.15 K

Average Equilibrium Pressure = 4.43 bar

Mole Fraction Gas Phase (oxygen)	Mole Fraction Adsorbed Phase (oxygen)	Amount Adsorbed mol/kg			Equilibrium Pressure bar	Selectivity Coefficient $S_{1,2}$
		Component 1 (oxygen)	Component 2 (nitrogen)	Total		
0.875	0.649	0.41	0.221	0.631	4.468	0.264
0.86	0.619	0.399	0.246	0.644	4.456	0.264
0.843	0.584	0.384	0.273	0.657	4.437	0.263
0.823	0.552	0.369	0.299	0.668	4.471	0.265
0.822	0.547	0.366	0.303	0.67	4.419	0.261
0.8	0.513	0.351	0.333	0.685	4.456	0.264
0.74	0.439	0.322	0.410	0.732	4.471	0.275
0.7	0.393	0.298	0.460	0.758	4.48	0.277
0.645	0.337	0.262	0.517	0.779	4.363	0.279
0.585	0.288	0.235	0.580	0.815	4.483	0.287
0.508	0.232	0.199	0.658	0.857	4.441	0.292
0.408	0.169	0.152	0.748	0.9	4.434	0.296
0.402	0.162	0.145	0.748	0.893	4.261	0.289
0.4	0.163	0.145	0.745	0.89	4.276	0.292
0.283	0.105	0.1	0.856	0.956	4.412	0.296
0.281	0.104	0.099	0.854	0.953	4.483	0.298
0.203	0.069	0.069	0.919	0.988	4.429	0.294
0.145	0.046	0.046	0.961	1.007	4.434	0.283
0.103	0.03	0.03	0.989	1.019	4.434	0.269

TABLE I.15

Binary Adsorption Equilibrium for O_2/N_2 on Na-Mordenite

Adsorption Temperature = 278.15 K

Average Equilibrium Pressure = 1.75 bar

Mole Fraction Gas Phase (oxygen)	Mole Fraction Adsorbed Phase (oxygen)	Amount Adsorbed mol/kg			Equilibrium Pressure bar	Selectivity Coefficient $S_{1,2}$
		Component 1 (oxygen)	Component 2 (nitrogen)	Total		
0.92	0.671	0.415	0.204	0.619	1.769	0.177
0.916	0.658	0.41	0.213	0.623	1.755	0.176
0.912	0.645	0.403	0.222	0.625	1.748	0.175
0.907	0.632	0.398	0.232	0.629	1.748	0.175
0.903	0.618	0.391	0.242	0.633	1.723	0.175
0.897	0.605	0.387	0.253	0.639	1.718	0.176
0.895	0.615	0.386	0.242	0.628	1.66	0.187
0.81	0.462	0.338	0.394	0.732	1.758	0.202
0.796	0.442	0.328	0.415	0.743	1.744	0.203
0.781	0.42	0.316	0.437	0.753	1.757	0.203
0.778	0.411	0.312	0.446	0.758	1.764	0.20
0.765	0.397	0.304	0.461	0.765	1.742	0.203
0.763	0.391	0.302	0.471	0.773	1.76	0.2
0.753	0.384	0.306	0.49	0.796	1.77	0.205

TABLE I.15 continued .....

Adsorption Temperature = 278.15 K

Average Equilibrium Pressure = 1.75 bar

Mole Fraction Gas Phase (oxygen)	Mole Fraction Adsorbed Phase (oxygen)	Amount Adsorbed mol/kg			Equilibrium Pressure bar	Selectivity Coefficient $S_{1,2}$
		Component 1 (oxygen)	Component 2 (nitrogen)	Total		
0.745	0.372	0.288	0.486	0.774	1.719	0.203
0.745	0.37	0.292	0.497	0.788	1.769	0.201
0.723	0.347	0.278	0.525	0.803	1.736	0.204
0.722	0.342	0.267	0.514	0.781	1.648	0.2
0.70	0.322	0.263	0.554	0.817	1.73	0.204
0.673	0.297	0.248	0.586	0.834	1.732	0.206
0.52	0.196	0.186	0.76	0.946	1.818	0.225
0.423	0.146	0.144	0.841	0.984	1.805	0.233
0.34	0.111	0.111	0.894	1.006	1.766	0.242

TABLE I.15 continued .....

Adsorption Temperature = 293.15 K

Average Equilibrium Pressure = 1.74 bar

Mole Fraction Gas Phase (oxygen)	Mole Fraction Adsorbed Phase (oxygen)	Amount Adsorbed mol/kg			Equilibrium Pressure bar	Selectivity Coefficient $S_{1,2}$
		Component 1 (oxygen)	Component 2 (nitrogen)	Total		
0.918	0.702	0.291	0.123	0.414	1.732	0.212
0.913	0.686	0.288	0.132	0.42	1.732	0.209
0.906	0.668	0.284	0.141	0.425	1.732	0.209
0.899	0.65	0.28	0.151	0.431	1.732	0.208
0.892	0.629	0.275	0.162	0.436	1.725	0.206
0.886	0.619	0.281	0.173	0.453	1.791	0.209
0.881	0.605	0.276	0.181	0.457	1.769	0.207
0.792	0.46	0.24	0.282	0.522	1.746	0.224
0.775	0.435	0.234	0.304	0.537	1.764	0.223
0.753	0.408	0.225	0.327	0.552	1.759	0.226
0.735	0.39	0.215	0.337	0.552	1.751	0.230
0.727	0.378	0.214	0.353	0.567	1.754	0.228
0.698	0.341	0.197	0.382	0.579	1.703	0.224
0.702	0.361	0.206	0.364	0.57	1.775	0.24
0.677	0.329	0.194	0.396	0.589	1.758	0.234

TABLE I.15 continued .....

Adsorption Temperature = 293.15 K

Average Equilibrium Pressure = 1.74 bar

Mole Fraction Gas Phase (oxygen)	Mole Fraction Adsorbed Phase (oxygen)	Amount Adsorbed mol/kg			Equilibrium Pressure bar	Selectivity Coefficient $S_{1,2}$
		Component 1 (oxygen)	Component 2 (nitrogen)	Total		
0.639	0.293	0.178	0.429	0.607	1.74	0.234
0.593	0.256	0.16	0.466	0.626	1.727	0.237
0.573	0.23	0.151	0.505	0.656	1.799	0.223
0.548	0.224	0.146	0.506	0.652	1.754	0.238
0.455	0.157	0.11	0.591	0.701	1.763	0.223
0.351	0.107	0.079	0.656	0.735	1.748	0.222
0.271	0.074	0.056	0.697	0.753	1.703	0.216

TABLE I.15 continued .....

Adsorption Temperature = 303.15 K

Average Equilibrium Pressure = 1.73 bar

Mole Fraction Gas Phase (oxygen)	Mole Fraction Adsorbed Phase (oxygen)	Amount Adsorbed mol/kg			Equilibrium Pressure bar	Selectivity Coefficient $S_{1,2}$
		Component 1 (oxygen)	Component 2 (nitrogen)	Total		
0.909	0.69	0.245	0.11	0.355	1.749	0.223
0.90	0.67	0.242	0.119	0.361	1.757	0.225
0.891	0.648	0.238	0.129	0.367	1.766	0.226
0.883	0.625	0.234	0.141	0.374	1.77	0.222
0.868	0.597	0.226	0.152	0.378	1.733	0.226
0.851	0.565	0.215	0.166	0.381	1.679	0.227
0.778	0.473	0.203	0.226	0.429	1.748	0.256
0.755	0.437	0.193	0.248	0.441	1.749	0.252
0.723	0.402	0.183	0.273	0.456	1.752	0.253
0.721	0.384	0.177	0.284	0.461	1.754	0.242
0.69	0.36	0.169	0.3	0.469	1.73	0.254
0.686	0.348	0.166	0.312	0.478	1.757	0.244
0.645	0.309	0.153	0.343	0.496	1.752	0.246
0.642	0.313	0.15	0.33	0.48	1.679	0.254
0.61	0.277	0.141	0.367	0.508	1.702	0.245

TABLE I.15 continued .....

Adsorption Temperature = 303.15 K

Average Equilibrium Pressure = 1.73 bar

Mole Fraction Gas Phase (oxygen)	Mole Fraction Adsorbed Phase (oxygen)	Amount Adsorbed mol/kg			Equilibrium Pressure bar	Selectivity Coefficient $S_{1,2}$
		Component 1 (oxygen)	Component 2 (nitrogen)	Total		
0.592	0.271	0.14	0.377	0.517	1.752	0.256
0.539	0.228	0.123	0.417	0.541	1.746	0.253
0.487	0.193	0.111	0.462	0.572	1.791	0.252
0.455	0.173	0.101	0.483	0.585	1.759	0.251
0.34	0.116	0.073	0.554	0.627	1.764	0.255
0.258	0.079	0.051	0.598	0.649	1.743	0.246
0.19	0.054	0.036	0.628	0.664	1.721	0.243

TABLE I.15 continued .....

Adsorption Temperature = 278.15 K

Average Equilibrium Pressure = 4.41 bar

Mole Fraction Gas Phase (oxygen)	Mole Fraction Adsorbed Phase (oxygen)	Amount Adsorbed mol/kg			Equilibrium Pressure bar	Selectivity Coefficient $S_{1,2}$
		Component 1 (oxygen)	Component 2 (nitrogen)	Total		
0.893	0.632	0.684	0.399	1.082	4.41	0.205
0.883	0.61	0.667	0.427	1.094	4.458	0.207
0.87	0.583	0.641	0.459	1.101	4.373	0.208
0.857	0.557	0.62	0.494	1.113	4.41	0.209
0.843	0.534	0.608	0.531	1.139	4.532	0.214
0.758	0.424	0.51	0.693	1.203	4.483	0.235
0.72	0.378	0.46	0.758	1.218	4.385	0.237
0.727	0.389	0.47	0.739	1.209	4.39	0.239
0.688	0.347	0.43	0.809	1.239	4.463	0.241
0.675	0.333	0.414	0.83	1.244	4.361	0.24
0.626	0.292	0.367	0.891	1.258	4.322	0.246
0.553	0.237	0.306	0.982	1.288	4.346	0.252
0.457	0.177	0.234	1.092	1.326	4.307	0.255
0.333	0.115	0.158	1.224	1.382	4.454	0.259
0.24	0.075	0.106	1.302	1.408	4.471	0.258
0.172	0.049	0.069	1.352	1.421	4.461	0.246
0.122	0.031	0.044	1.377	1.421	4.41	0.231

TABLE I.15 continued .....

Adsorption Temperature = 293.15 K

Average Equilibrium Pressure = 4.44 bar

Mole Fraction Gas Phase (oxygen)	Mole Fraction Adsorbed Phase (oxygen)	Amount Adsorbed mol/kg			Equilibrium Pressure bar	Selectivity Coefficient $S_{1,2}$
		Component 1 (oxygen)	Component 2 (nitrogen)	Total		
0.884	0.633	0.551	0.32	0.871	4.458	0.226
0.868	0.604	0.533	0.349	0.882	4.441	0.232
0.851	0.572	0.511	0.382	0.893	4.434	0.234
0.833	0.539	0.491	0.419	0.91	4.454	0.235
0.833	0.54	0.492	0.418	0.91	4.461	0.237
0.809	0.503	0.467	0.462	0.929	4.446	0.239
0.809	0.502	0.464	0.461	0.925	4.41	0.238
0.725	0.40	0.4	0.605	1.005	4.434	0.251
0.678	0.35	0.362	0.672	1.034	4.458	0.255
0.656	0.325	0.338	0.703	1.041	4.534	0.253
0.62	0.30	0.317	0.75	1.067	4.468	0.259
0.535	0.233	0.255	0.841	1.096	4.398	0.264
0.505	0.21	0.23	0.866	1.096	4.41	0.261
0.431	0.167	0.19	0.948	1.138	4.419	0.265
0.421	0.166	0.189	0.952	1.141	4.483	0.273
0.367	0.133	0.153	0.997	1.151	4.449	0.265
0.302	0.107	0.127	1.054	1.181	4.478	0.278
0.214	0.069	0.084	1.122	1.206	4.458	0.274
0.153	0.046	0.055	1.149	1.204	4.328	0.265
0.105	0.029	0.035	1.19	1.225	4.307	0.252

TABLE I.15 continued .....

Adsorption Temperature = 303.15 K

Average Equilibrium Pressure = 4.45 bar

Mole Fraction Gas Phase (oxygen)	Mole Fraction Adsorbed Phase (oxygen)	Amount Adsorbed mol/kg			Equilibrium Pressure bar	Selectivity Coefficient $S_{1,2}$
		Component 1 (oxygen)	Component 2 (nitrogen)	Total		
0.877	0.642	0.46	0.256	0.716	4.429	0.252
0.861	0.61	0.445	0.284	0.729	4.454	0.254
0.842	0.576	0.43	0.317	0.746	4.473	0.255
0.818	0.534	0.405	0.353	0.758	4.434	0.256
0.811	0.532	0.403	0.355	0.757	4.444	0.264
0.788	0.492	0.382	0.395	0.776	4.434	0.261
0.783	0.486	0.376	0.398	0.774	4.429	0.263
0.72	0.417	0.342	0.478	0.82	4.451	0.278
0.671	0.363	0.308	0.541	0.849	4.466	0.280
0.621	0.311	0.274	0.606	0.88	4.483	0.276
0.605	0.302	0.266	0.615	0.881	4.444	0.283
0.514	0.232	0.212	0.701	0.913	4.398	0.285
0.458	0.196	0.185	0.76	0.945	4.434	0.288
0.414	0.166	0.16	0.802	0.962	4.424	0.282
0.41	0.166	0.16	0.804	0.964	4.488	0.287
0.327	0.125	0.124	0.866	0.99	4.434	0.295
0.29	0.106	0.106	0.897	1.003	4.454	0.289
0.202	0.067	0.069	0.96	1.029	4.434	0.284
0.14	0.042	0.044	1.005	1.049	4.456	0.277
0.094	0.026	0.028	1.032	1.059	4.461	0.26

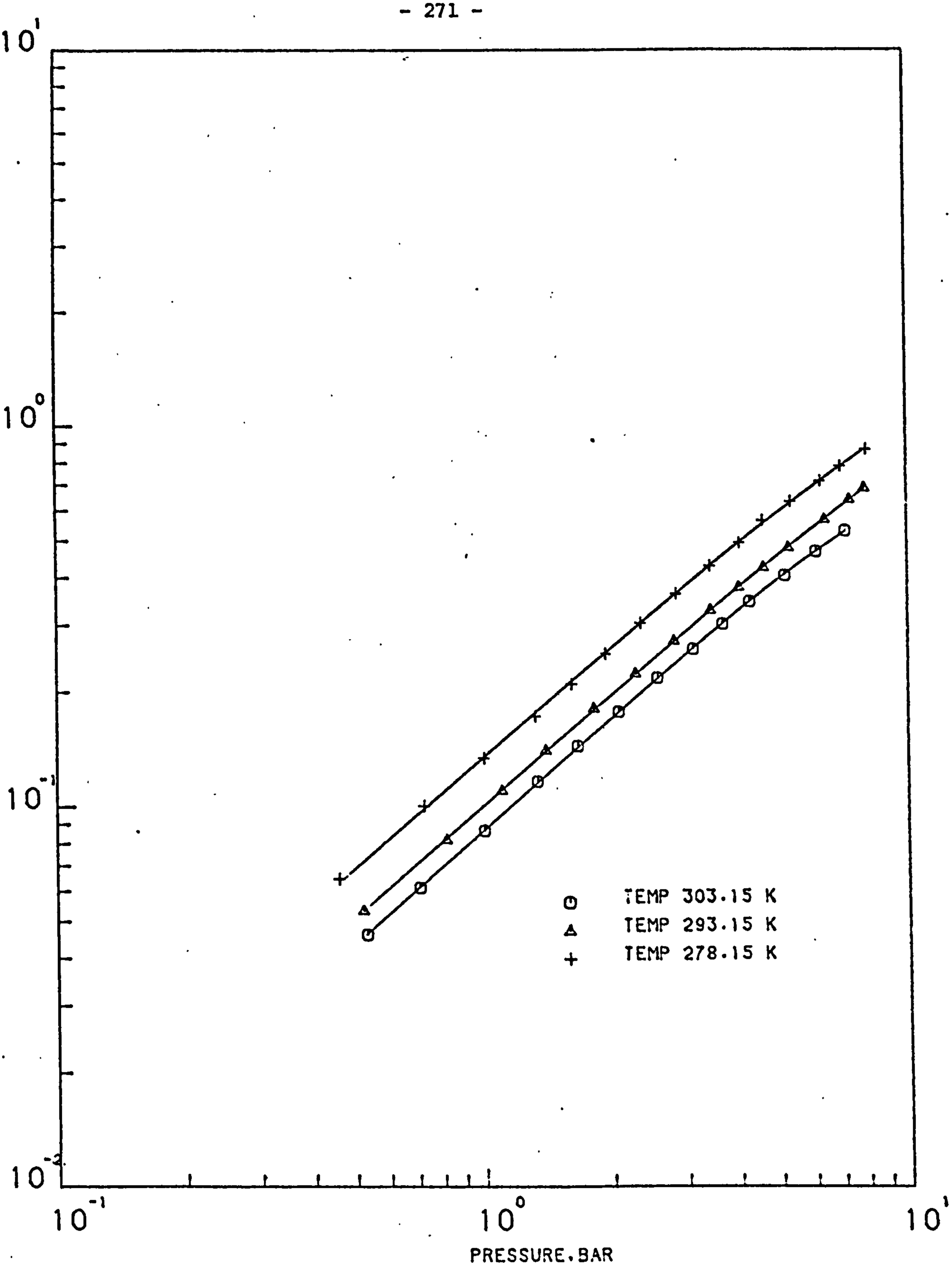

FIGURE (I·1) COMPARISON OF EQUATION (4·1) WITH EXPERIMENTAL DATA OF OXYGEN ON LAPORTE 4A MOLECULAR SIEVE PELLETS AT 278.15. 293.15 AND 303.15 K

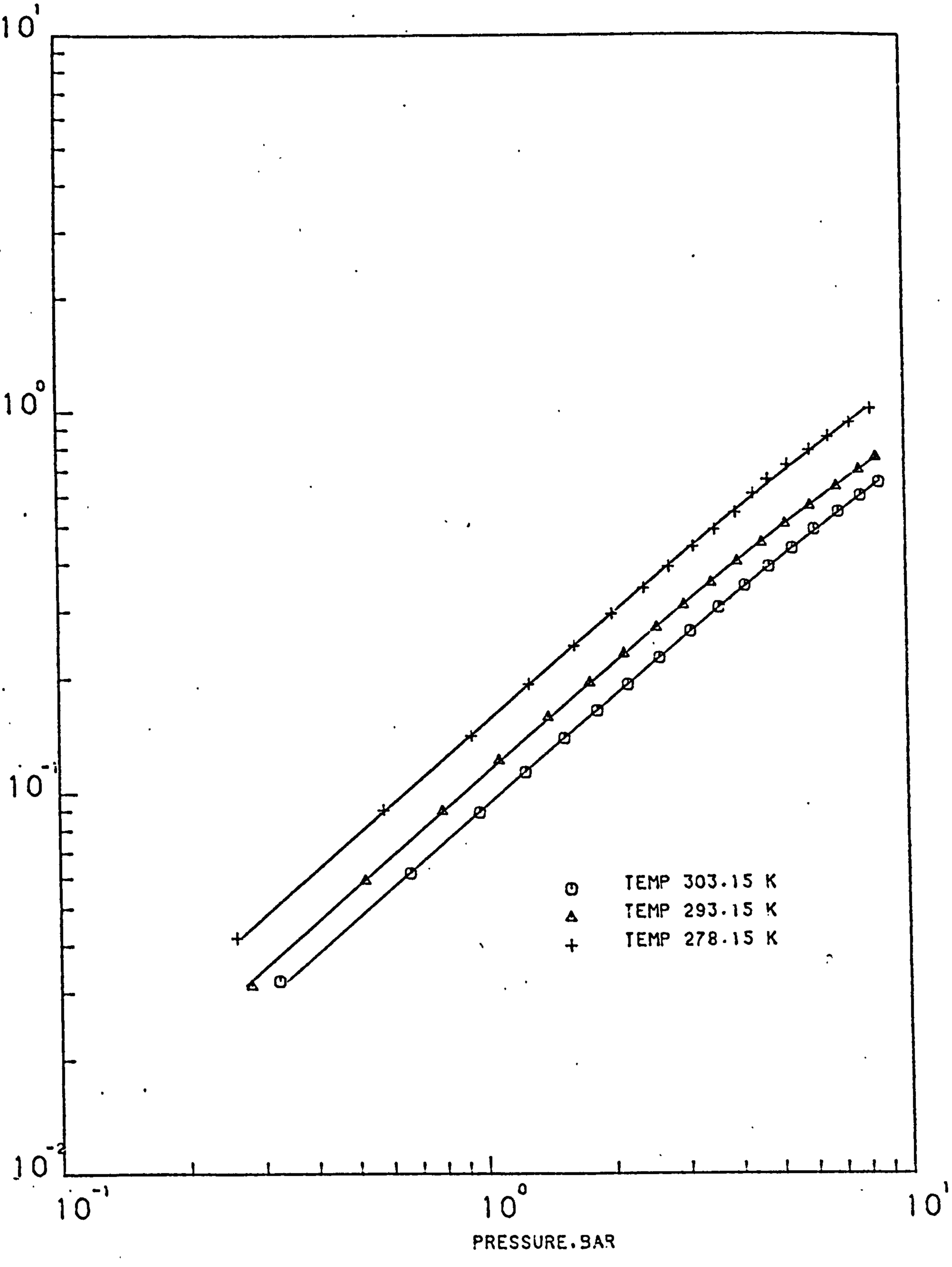

FIGURE (I.2) COMPARISON OF EQUATION (4.1) WITH THE EXPERIMENTAL DATA OF OXYGEN ON LAPORTE 5A MOLECULAR SIEVE PELLETS AT 303.15 . 293.15 AND 278.15 K

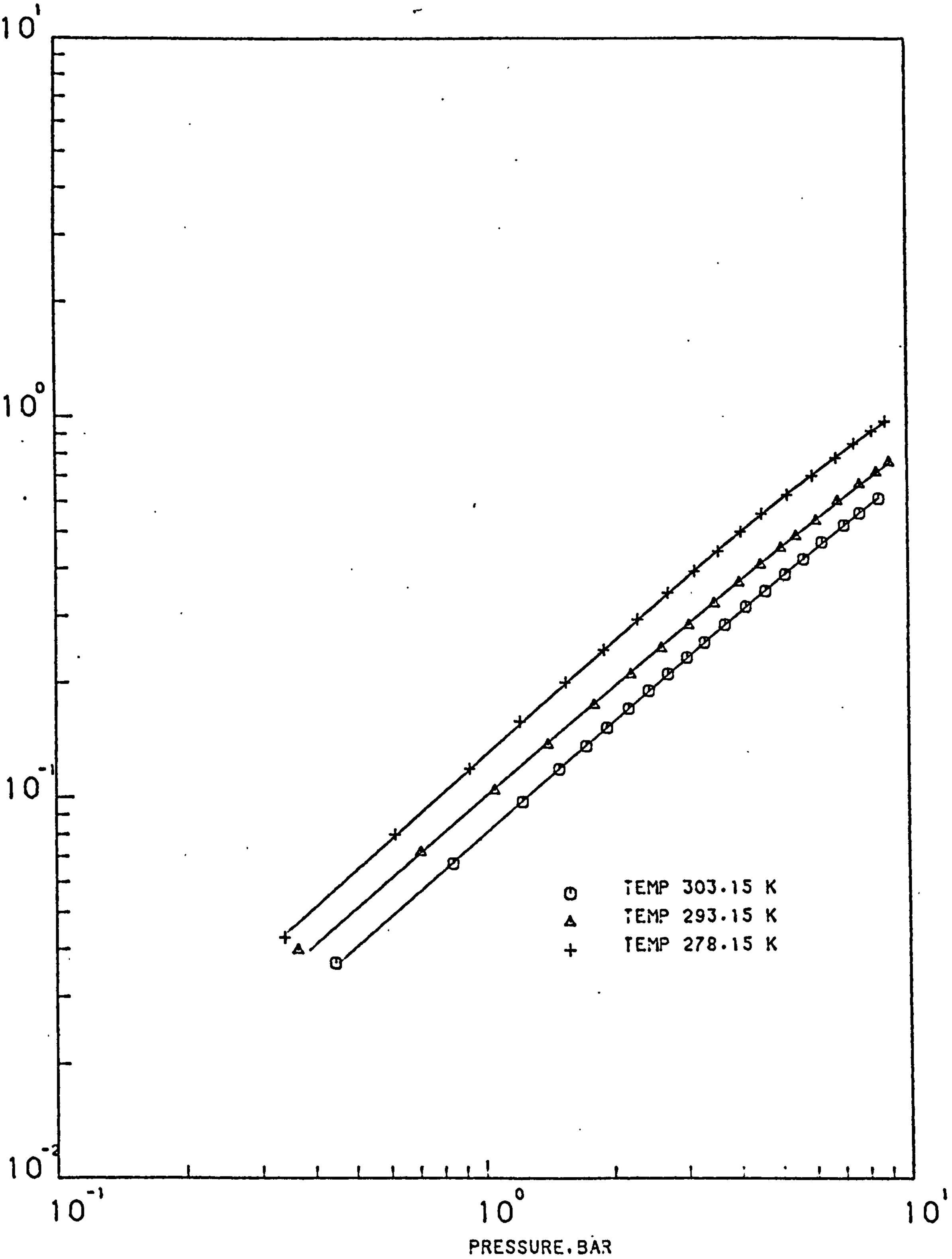

FIGURE (I·3) COMPARISON OF EQUATION (4·1) WITH EXPERIMENTAL DATA OF OXYGEN ON LAPORTE 13X MOLECULAR SIEVE PELLETS AT 278.15, 293.15 AND 303.15 K

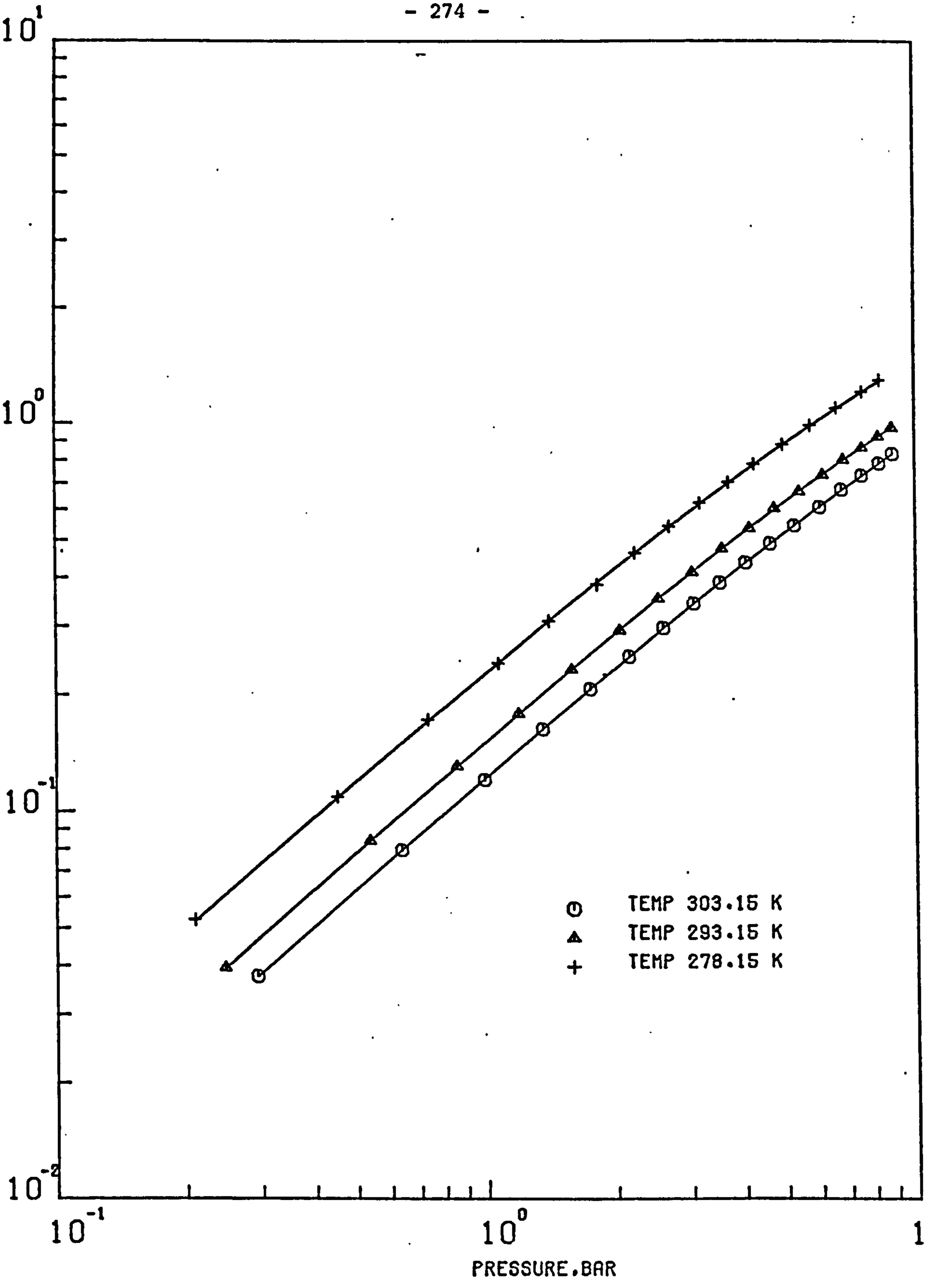

FIGURE (I·4) COMPARISON OF EQUATION (4·1) WITH EXPERIMENTAL DATA OF OXYGEN ON EKA 5A MOLECULAR SIEVE PELLETS AT 303.15 , 293.15 AND 278.15 K

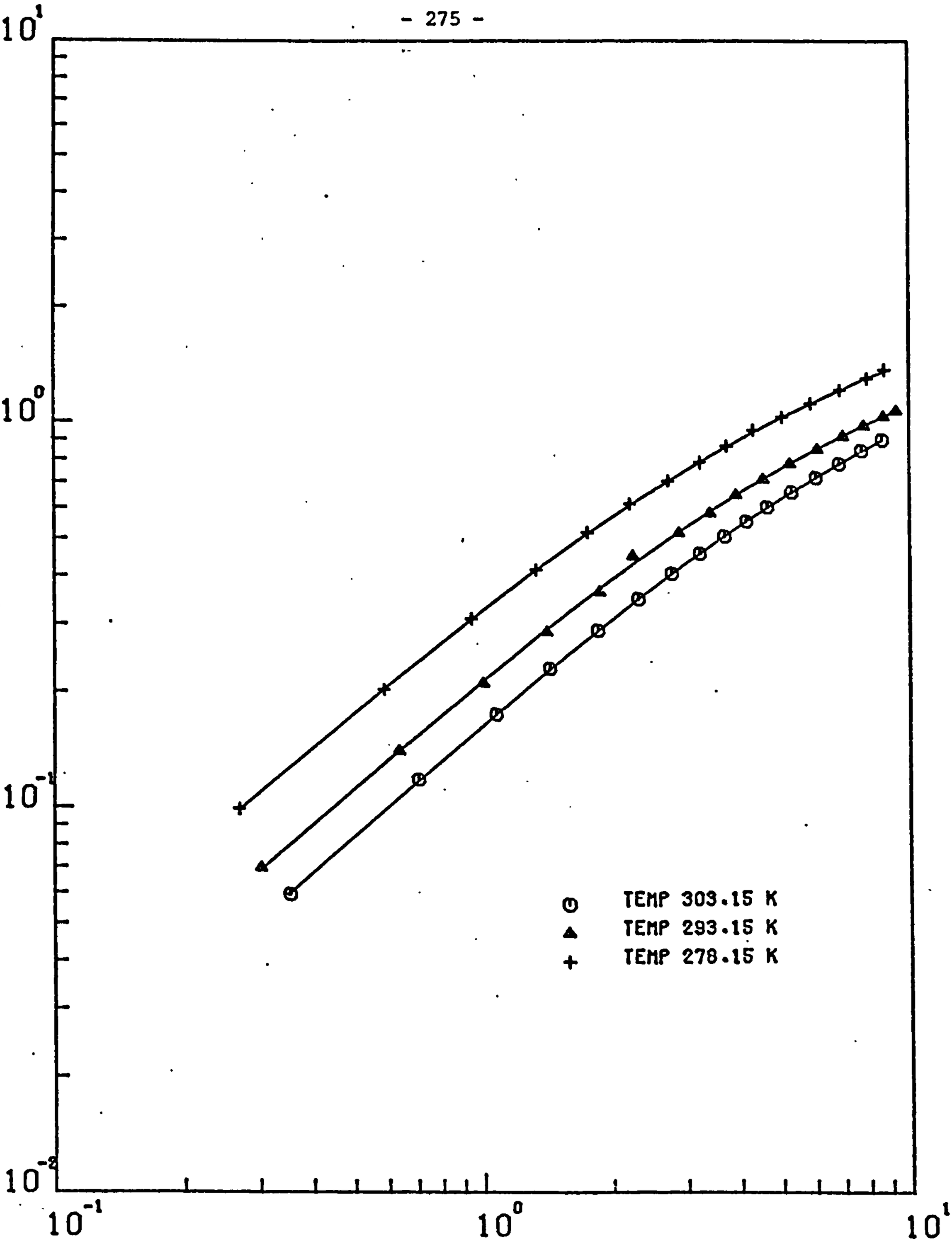

FIGURE (I·5) COMPARISON OF EQUATION (4·1) WITH EXPERIMENTAL DATA OF OXYGEN ON NA-MORDENITE MOLECULAR SIEVE PELLETS AT 303.15 , 293.15 AND 278.15 K

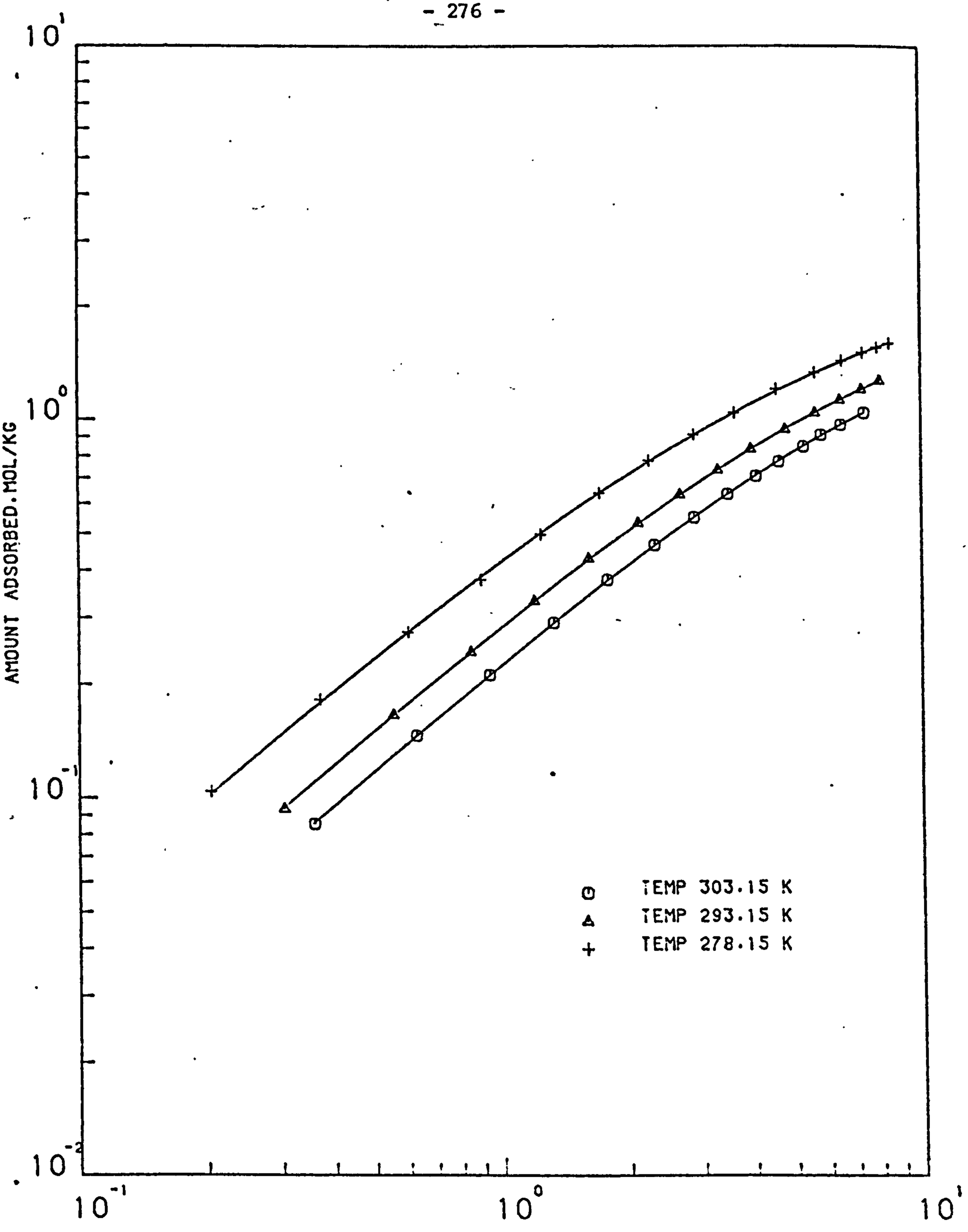

FIGURE (I·6) COMPARISON OF EQUATION (4·1) WITH EXPERIMENTAL DATA OF NITROGEN ON LAPORTE 4A MOLECULAR SIEVE PELLETS AT 278.15, 293.15 AND 303.15 K

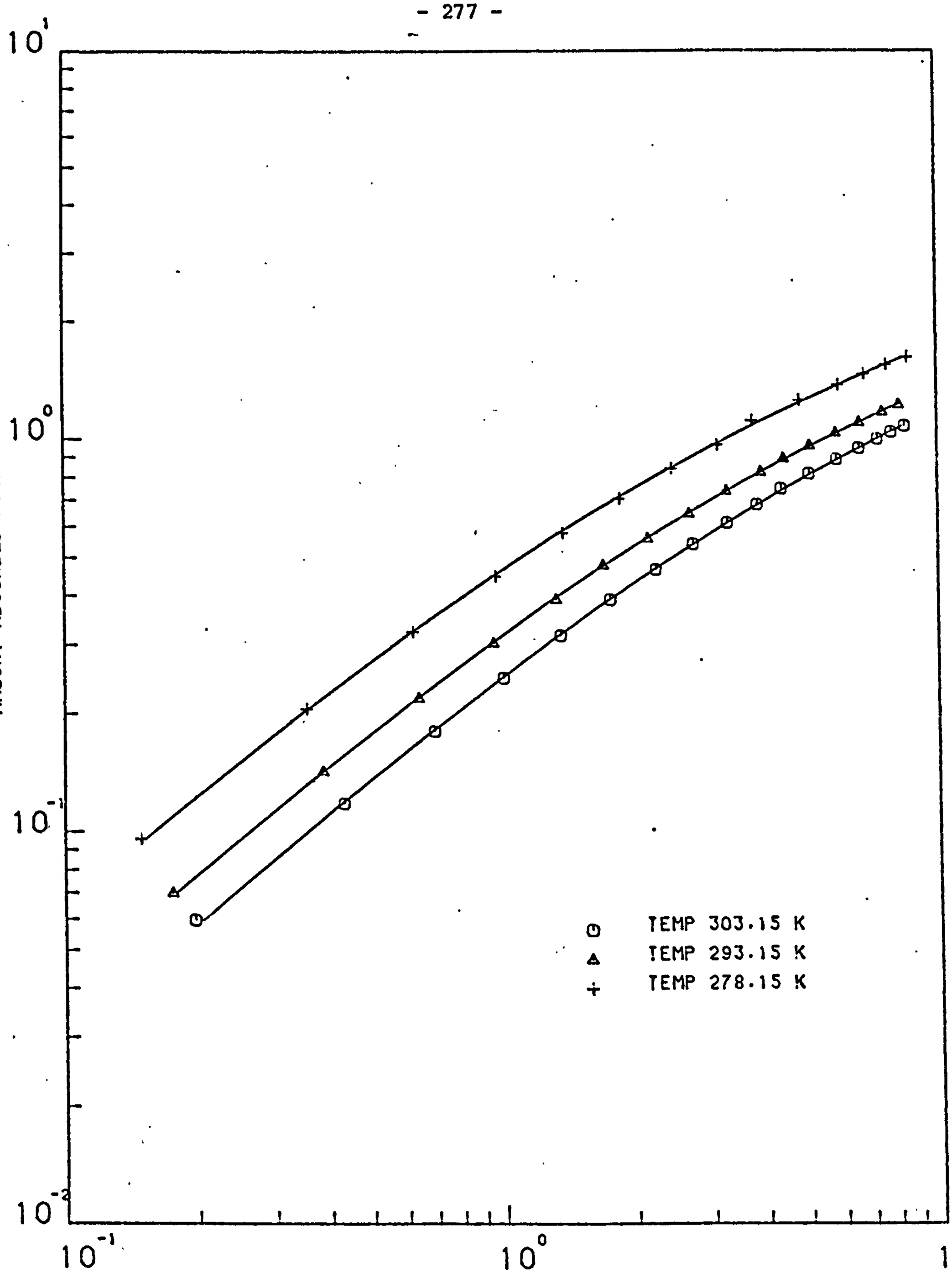

FIGURE (I·7) COMPARISON OF EQUATION (4·1) WITH THE EXPERIMENTAL DATA OF NITROGEN ON LAPORTE 5A MOLECULAR SIEVE PELLETS AT 303.15 . 293.15 AND 278.15 K

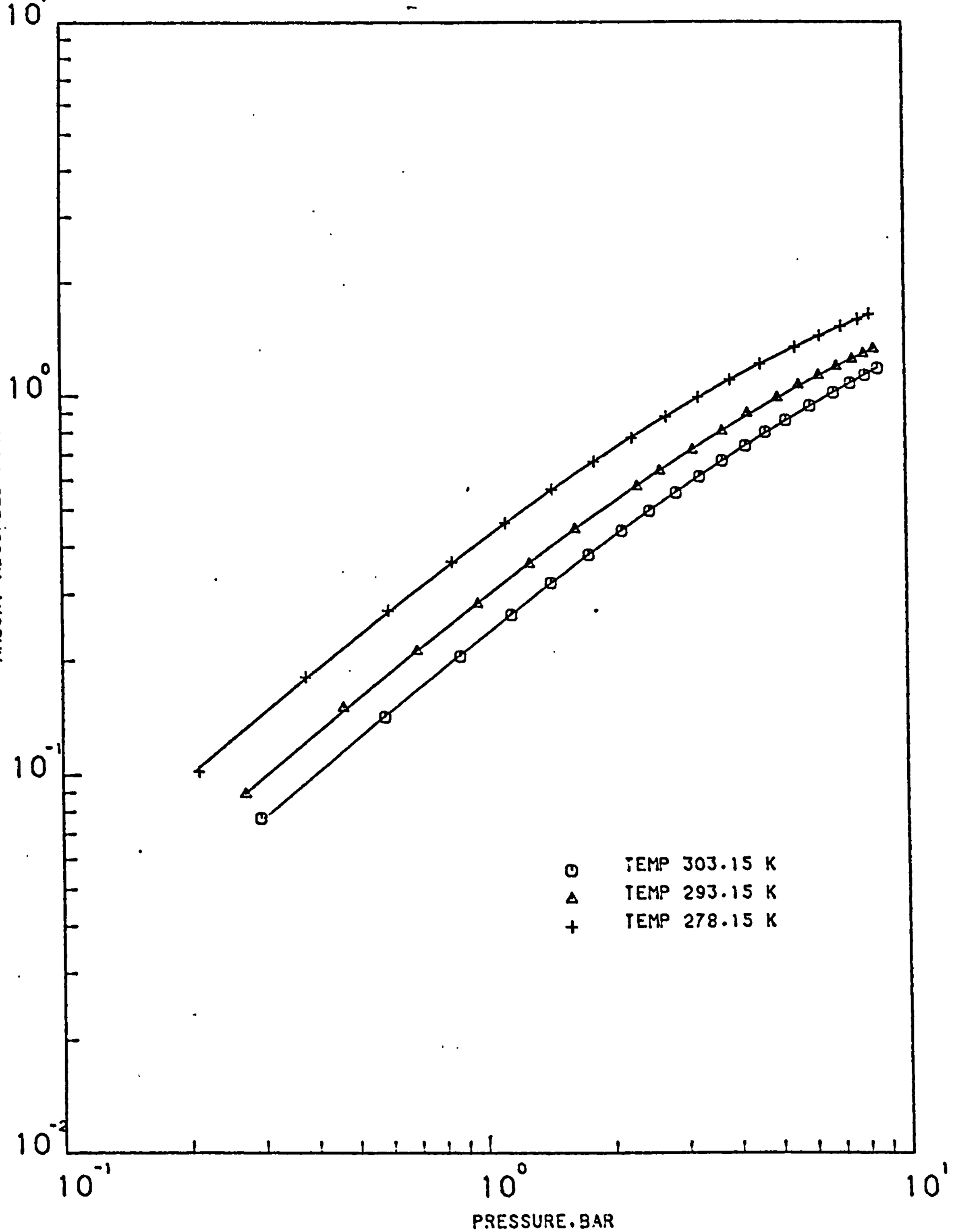

FIGURE (I-8) COMPARISON OF EQUATION (4-1) WITH EXPERIMENTAL DATA OF NITROGEN ON LAPORTE 13X MOLECULAR SIEVE PELLETS AT 278.15, 293.15 AND 303.15 K

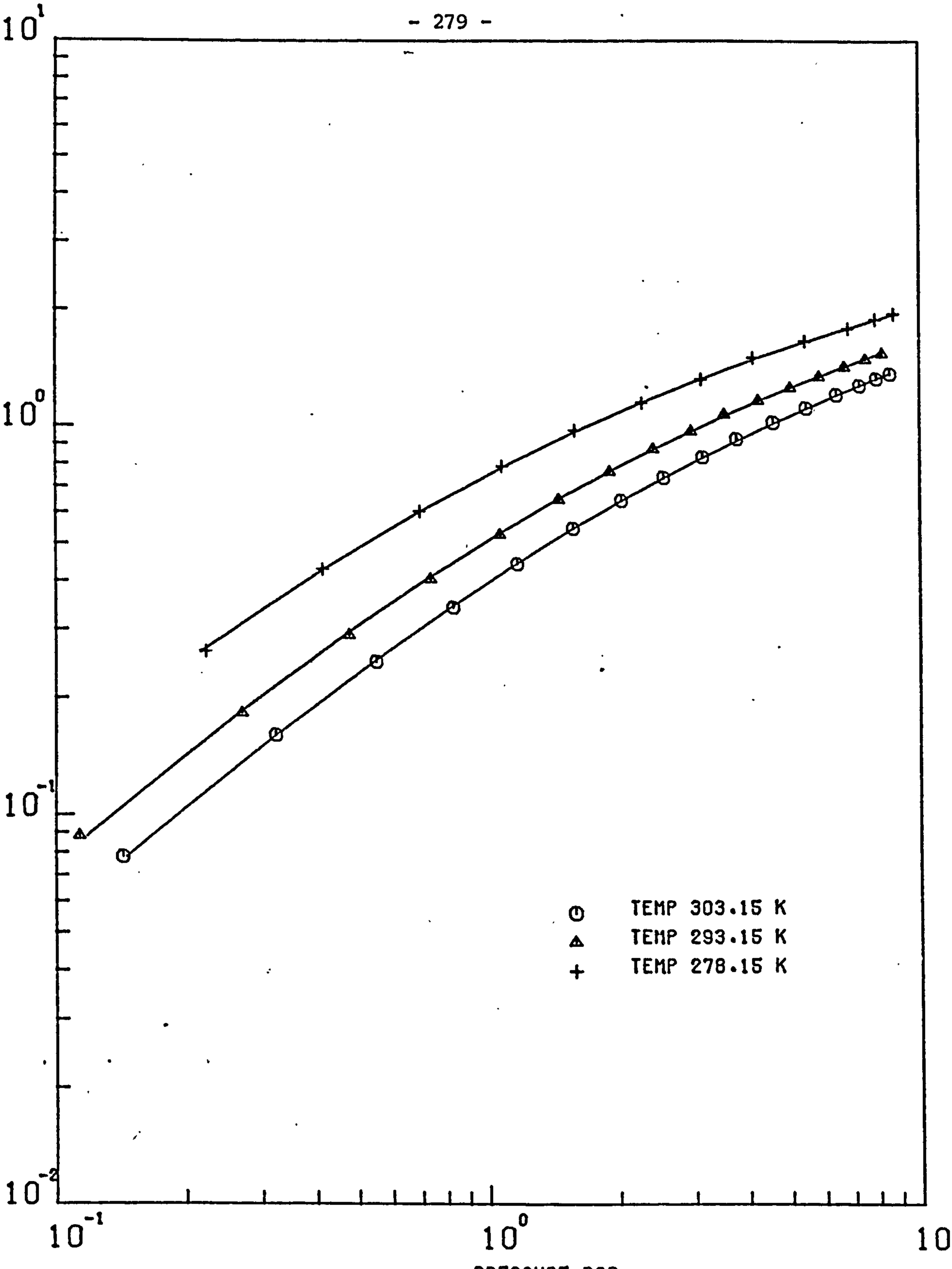

FIGURE (I·9) COMPARISON OF EQUATION (4·1) WITH EXPERIMENTAL DATA OF NITROGEN ON EKA 5A MOLECULAR SIEVE PELLETS AT 303.15 , 293.15 AND 278.15 K

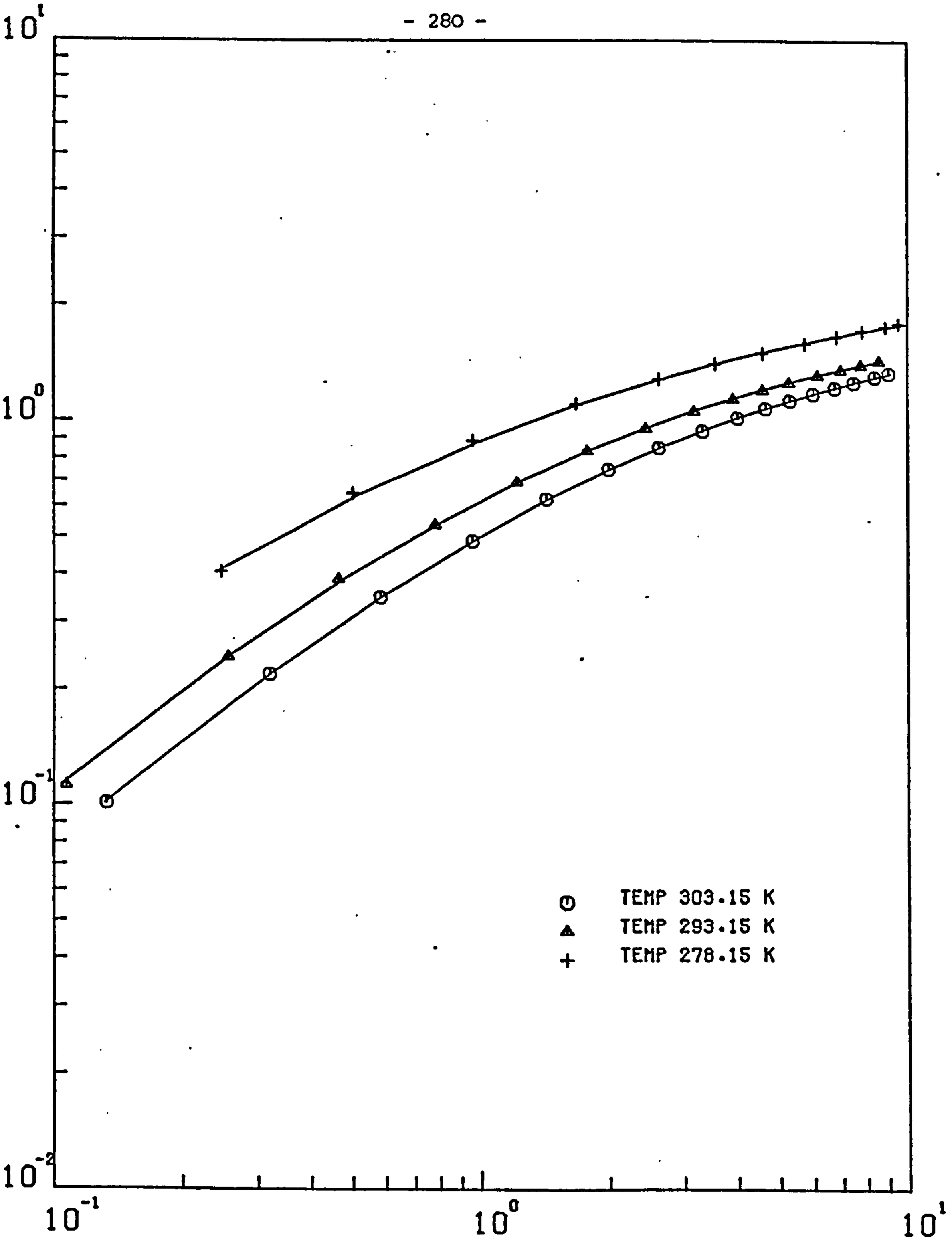

FIGURE (I·10) COMPARISON OF EQUATION (4·1) WITH EXPERIMENTAL DATA OF NITROGEN ON NA-MORDENITE MOLECULAR SIEVE PELLETS AT 303.15 , 293.15 AND 278.15 K

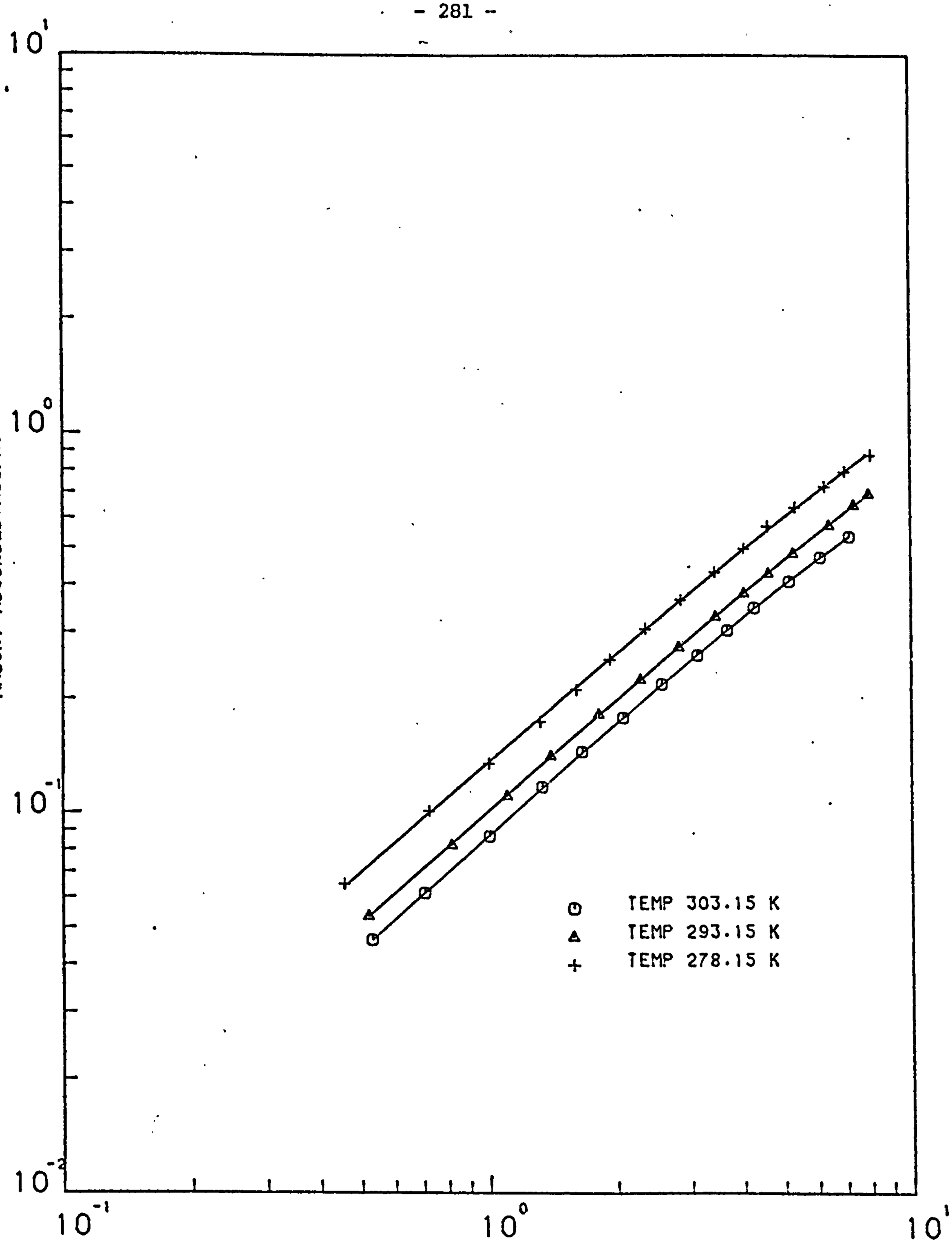

FIGURE (I·11) COMPARISON OF THE VACANCY SOLUTION MODEL (——) WITH THE EXPERIMENTAL DATA OF OXYGEN ON LAPORTE 4A MOLECULAR SIEVE PELLETS AT 278.15, 293.15 AND 303.15 K

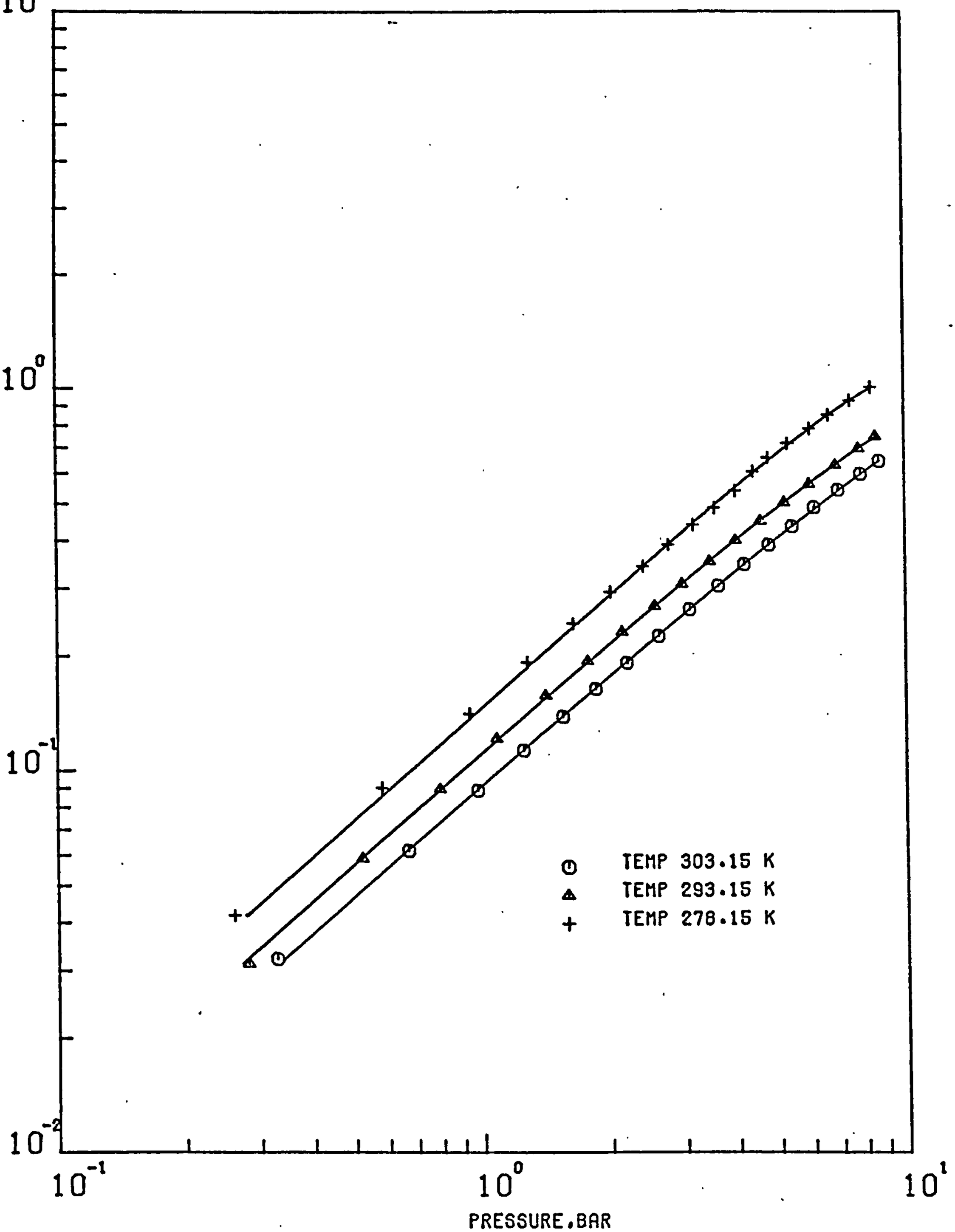

FIGURE (I·12) COMPARISON OF THE VACANCY SOLUTION MODEL (——) WITH EXPERIMENTAL DATA OF OXYGEN ON LAPORTE 5A MOLECULAR SIEVE PELLETS AT 303.15 , 293.15 AND 278.15 K

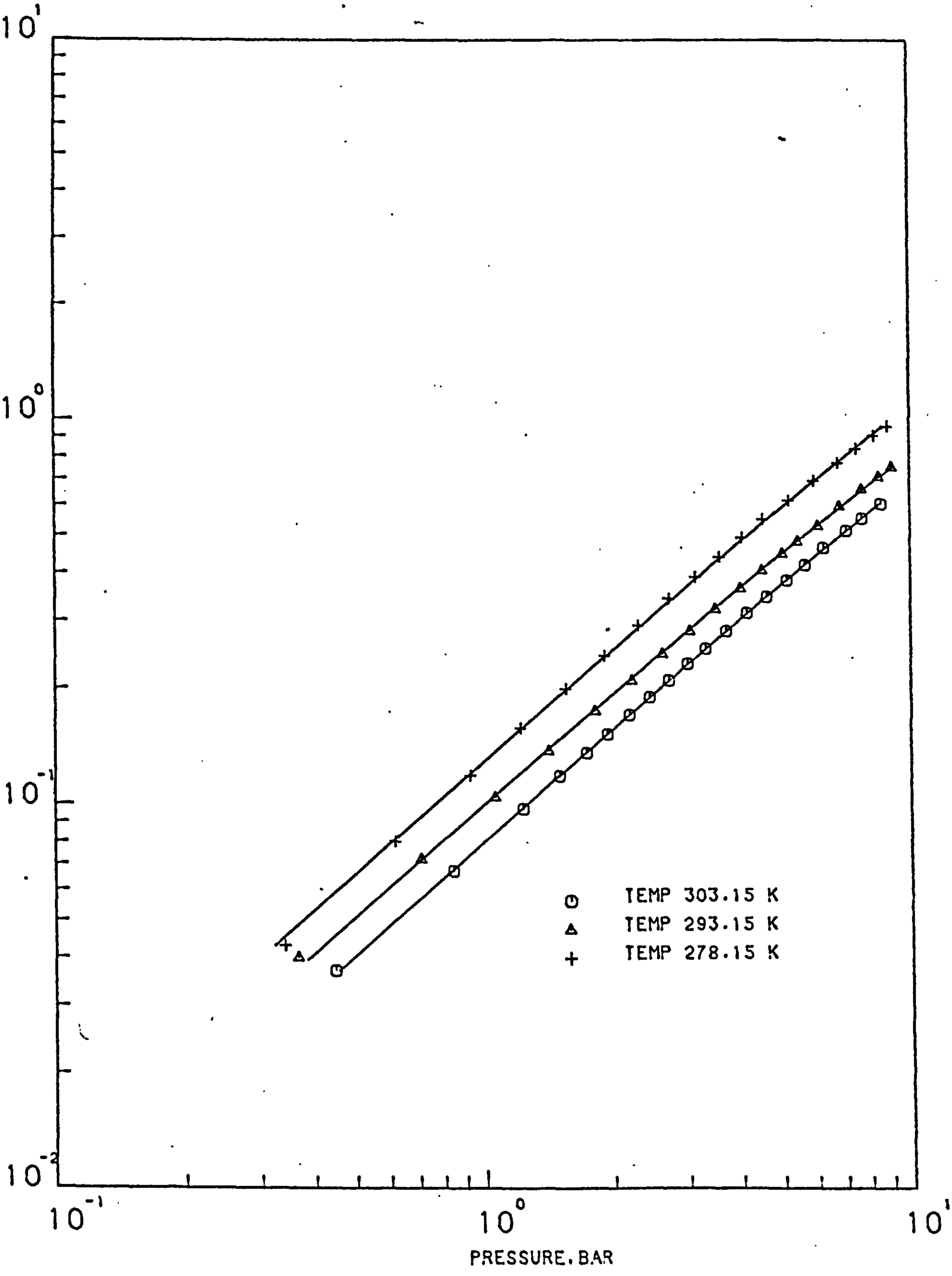

FIGURE (I·13) COMPARISON OF THE VACANCY SOLUTION MODEL (——)
WITH THE EXPERIMENTAL DATA OF OXYGEN ON LAPORTE 13X
MOLECULAR SIEVE PELLETS AT 278.15 .293.15
AND 303.15 K

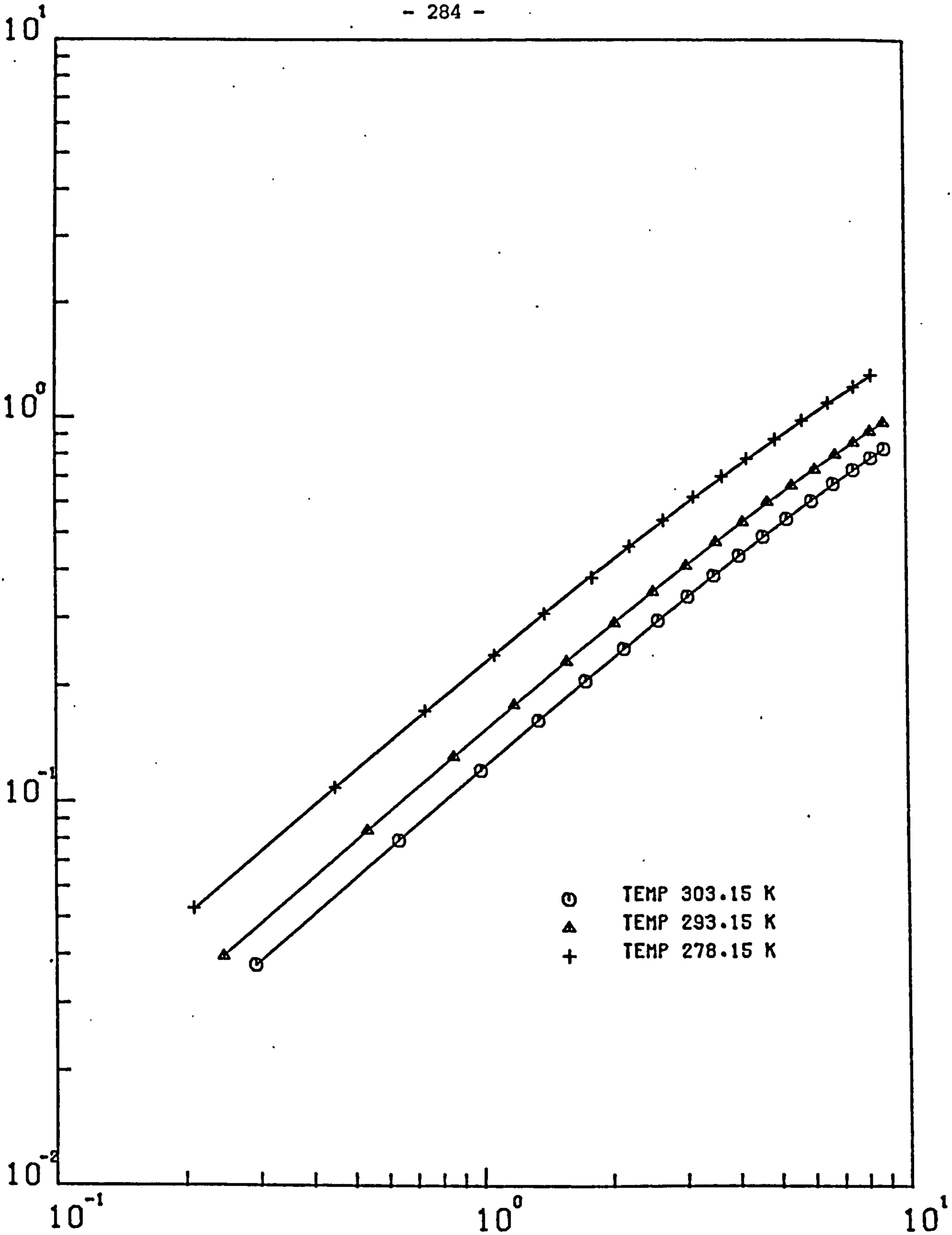

FIGURE (I·14) COMPARISON OF THE VACANCY SOLUTION MODEL (——)
WITH EXPERIMENTAL DATA OF OXYGEN ON
EKA 5A MOLECULAR SIEVE PELLETS AT
303.15 , 293.15 AND 278.15 K

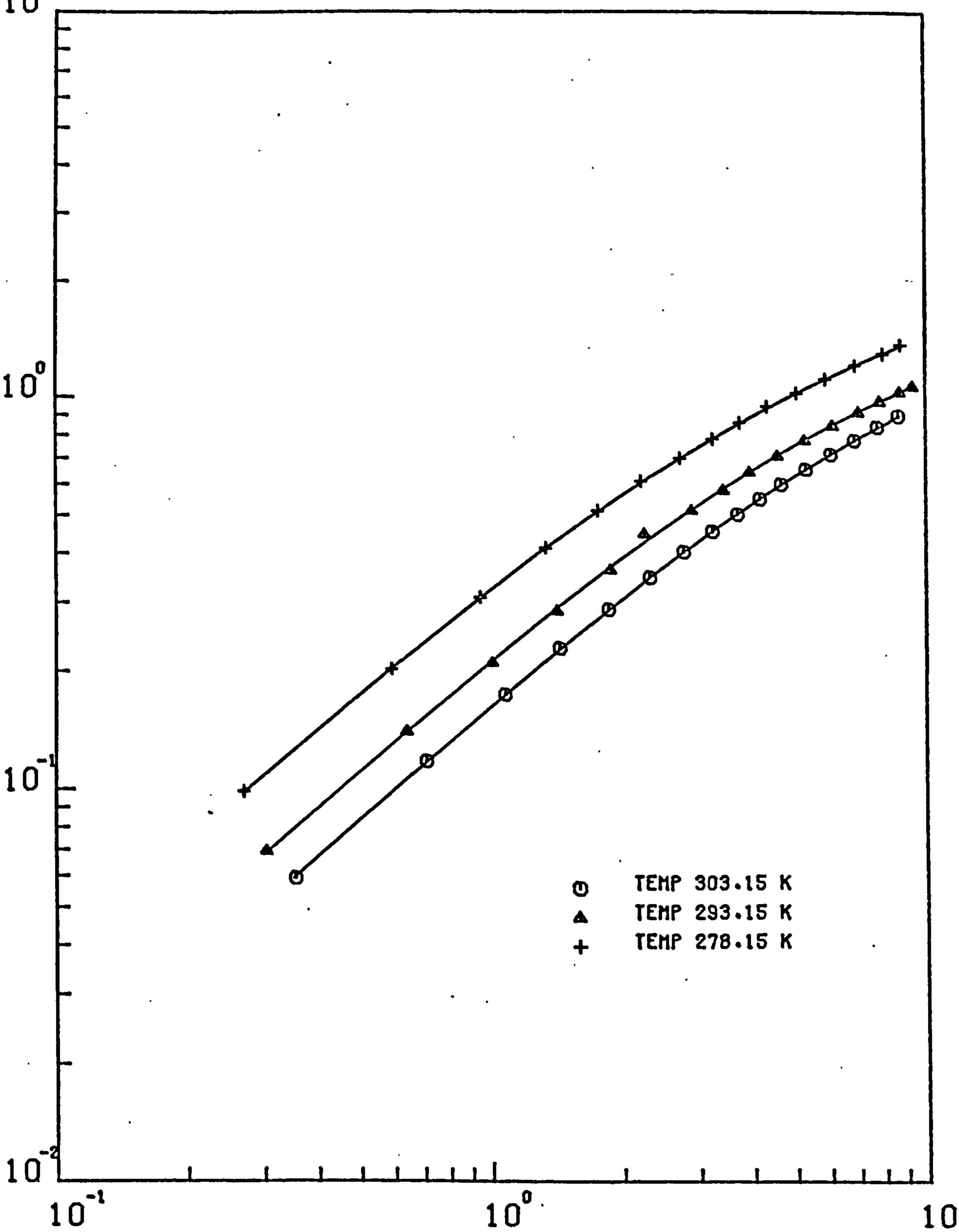

FIGURE (I·15) COMPARISON OF THE VACANCY SOLUTION MODEL (——) WITH EXPERIMENTAL DATA OF OXYGEN ON NA-MORDENITE MOLECULAR SIEVE PELLETS AT 303.15 , 293.15 AND 278.15 K

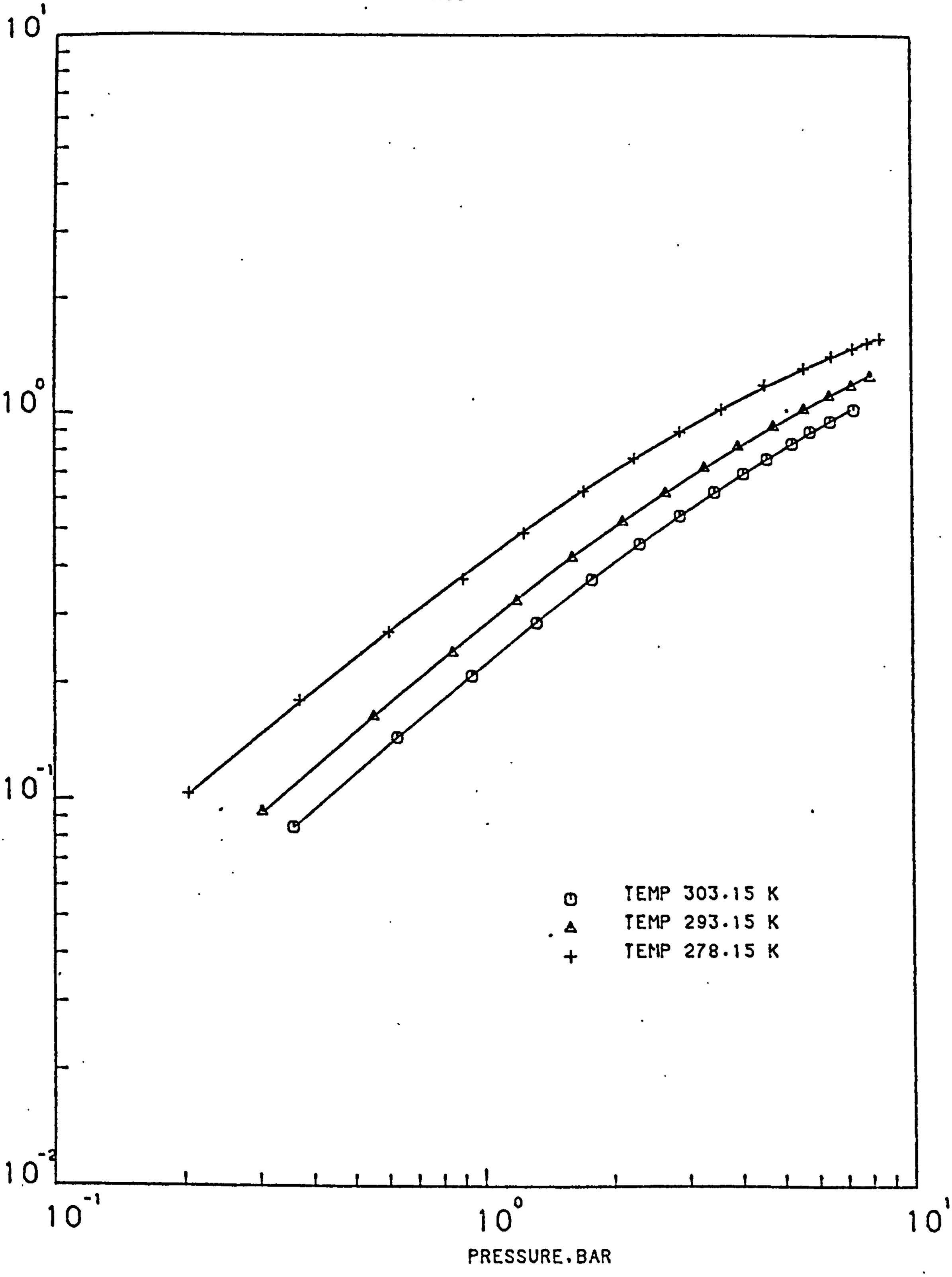

FIGURE (I·16) COMPARISON OF THE VACANCY SOLUTION MODEL (——)
WITH THE EXPERIMENTAL DATA OF NITROGEN ON LAPORTE 4A
MOLECULAR SIEVE PELLETS AT 278.15 .
293.15 AND 303.15 K

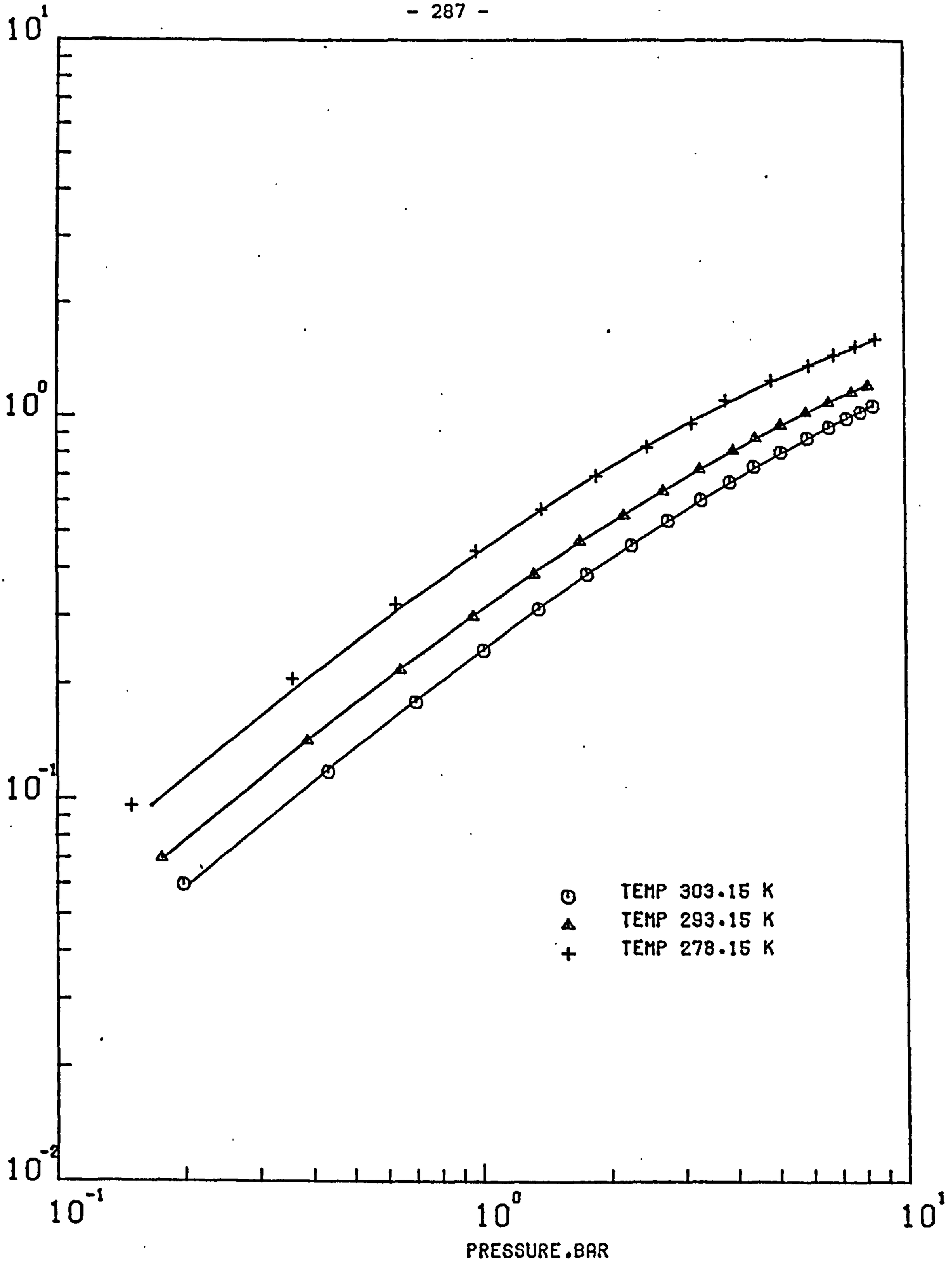

FIGURE (I·17) COMPARISON OF THE VACANCY SOLUTION MODEL (——)
WITH EXPERIMENTAL DATA OF NITROGEN ON
LAPORTE 5A MOLECULAR SIEVE PELLETS AT
303.15 , 293.15 AND 278.15 K

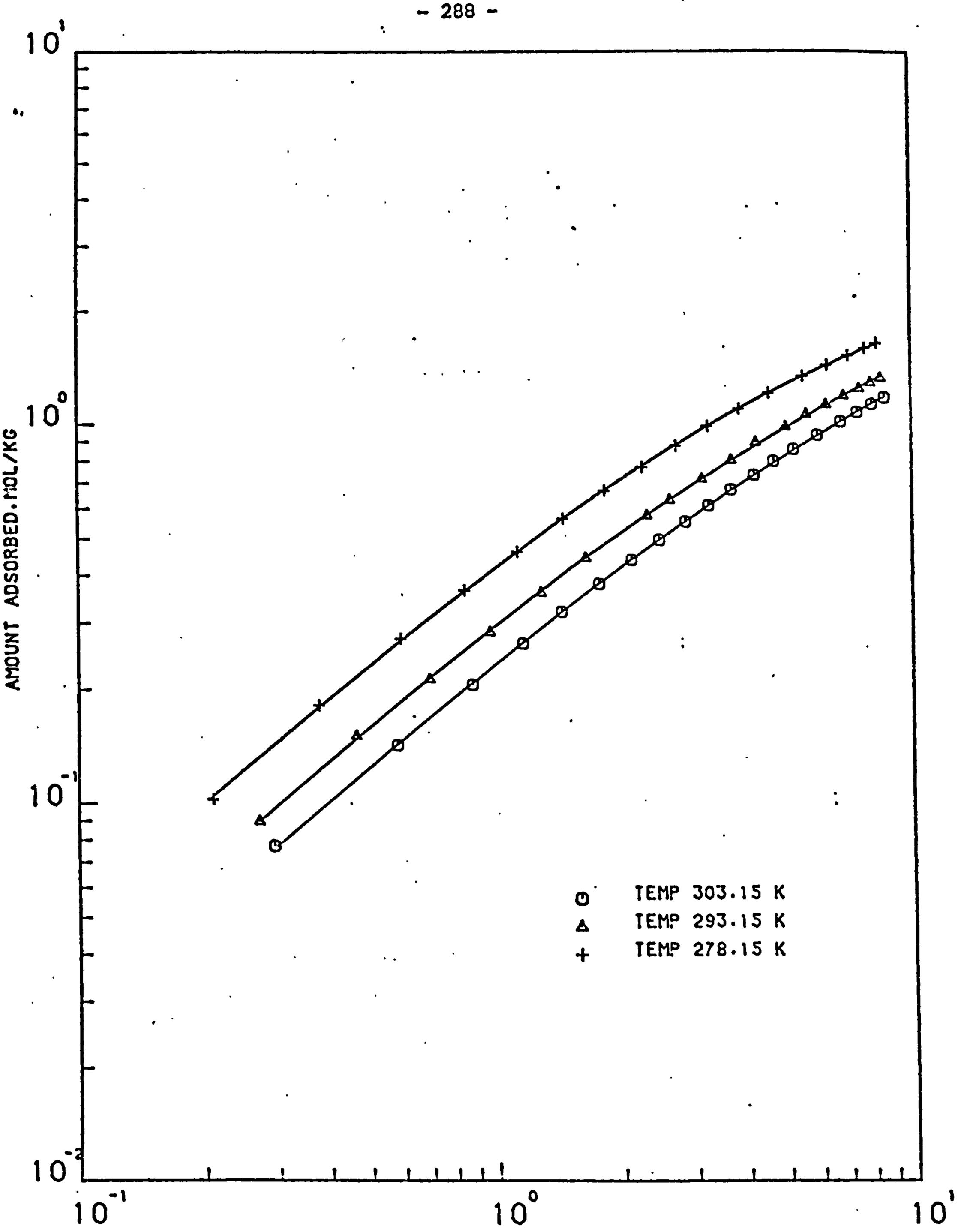

FIGURE (1-18) COMPARISON OF THE VACANCY SOLUTION MODEL (——) WITH THE EXPERIMENTAL DATA OF NITROGEN ON LAPORTE 13X MOLECULAR SIEVE PELLETS AT 278.15.293.15 AND 303.15 K

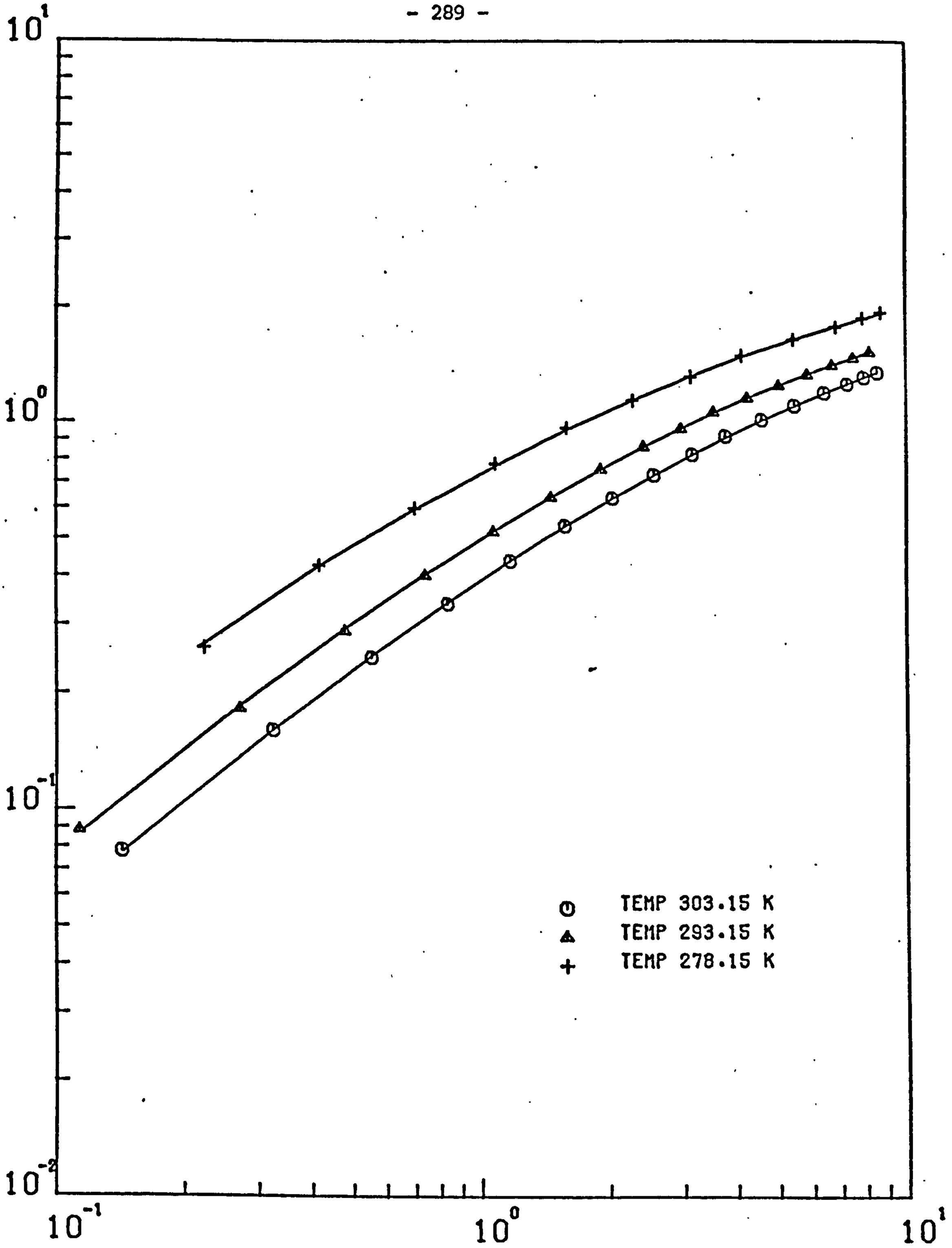

FIGURE (I·19) COMPARISON OF THE VACANCY SOLUTION MODEL (——) WITH EXPERIMENTAL DATA OF NITROGEN ON EKA 5A MOLECULAR SIEVE PELLETS AT 303.15 , 293.15 AND 278.15 K

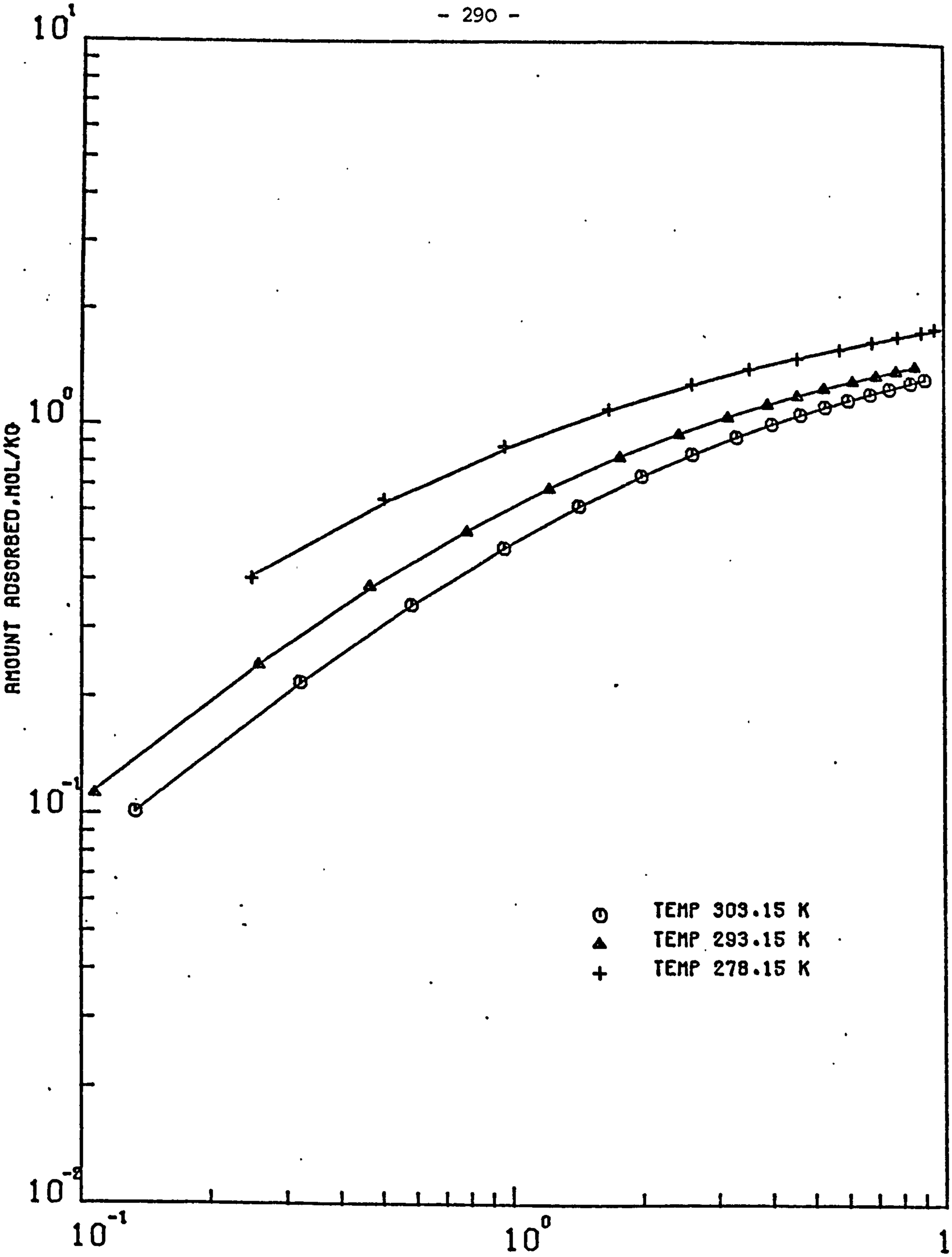

FIGURE (1·20) COMPARISON OF THE VACANCY SOLUTION MODEL (——)
WITH EXPERIMENTAL DATA OF NITROGEN ON
NA-MORDENITE MOLECULAR SIEVE PELLETS AT
303.15 , 293.15 AND 278.15 K

APPENDIX II

DETAILED CALIBRATION PROCEDURES AND EQUIPMENT SPECIFICATIONS

A Calibration Procedures

(a) Calibration of the system

(b) Operating procedure for the oxygen analyser

B Equipment Specifications

Table II.1 Uncertainties in Volume Determination

Table II.2 Determined Absolutes Densities for Laporte's 4A, 5A and 13X, EKA 5A and Na-Mordenite at Temperature 293.15 K

Figure II.1 Schematic Sketch of the Adsorption Vessel

A. Calibration Procedures

(a) Calibration of the system

(i) Measure the internal volume of the glass sphere V_c (see Figure 3.1). This is done in the following way.

(a) Clean the glass sphere thoroughly by hot water and soap and then by acetone.

(b) Weigh the glass sphere several times when empty and when full of water at a known temperature. Obtain an average value.

(c) Determine the density of water used.

(d) The volume hence can be evaluated by dividing the mass of water in the glass sphere by the water's density.

(ii) Measure the internal volume of the system by using the calibrated glass bulb, a mercury manometer and a cathetometer. The volumes to be measured are defined below.

Volume No.	Defined by Valves (see Figure 3.1)
V_d	Pipe network between valves 1, 2, 3, 12, 13, 14 and 6 with valves 10 and 11 open and mercury at datum level.
V_{CR}	Circulation volume defined by valves 4, 5, 7 open and valves 3, 8 and 9 closed.
V_A	Adsorption vessel volume with valves 8 and 9 closed.
V_{AD}	Voidage volume in adsorption vessel when full of adsorbents.

The technique for measuring these volumes are presented below.

V_d

(a) Measure the datum level of the mercury column, h_o, in the manometer using the cathetometer, the atmospheric pressure, P_A, using the barometer, and the room temperature, T_R.

(b) Close valves 1 and 3.

(c) Evacuate the system and then close valve 6.

(d) Close valve 2 and bleed helium into the system using valve 1.

(e) Measure the new mercury level, h_1, corresponding to an internal pressure, P_1.

(f) Open valve 6 and record the new mercury level, h_2, corresponding to the final pressure, P_2.

(g) Compute the value of V_d from the following equation:

$$V_d = \frac{P_2 V_c T_R}{(P_1 - P_2) T_B} + \frac{(P_2 \Delta h_2 - P_1 \Delta h_1) A_2}{(P_1 - P_2)}$$

where $\Delta h_1 = h_o - h_1$ $\qquad P_1 = P_A + \Delta h_1 \rho \left\{1 + \frac{A_2}{A_1}\right\}$

$\Delta h_2 = h_o - h_1$ $\qquad P_2 = P_A + \Delta h_2 \rho \left\{1 + \frac{A_2}{A_1}\right\}$

ρ = density of mercury at T_R

A_1, A_2 = areas of limbs of manometer

T_B = bath temperature

$\underline{V_{CR}}$

(a) Evacuate the whole system with valves 8 and 9 closed.

(b) Close valves 2 and 3 and bleed helium into the system using valve 1.

(c) Measure the new mercury level, h_1, corresponding to the internal pressure, P_1.

(d) Open valve 3 and record the new mercury level, h_2, corresponding to the final pressure, P_2.

(e) Compute the value of V_{CR} from the following equation:

$$V_{CR} = \frac{(P_1-P_2)\ V_d\ T_B}{P_2\ T_R} + \frac{(P_1-P_2)}{P_2} V_c + \frac{(P_1\ \Delta h_1 - P_2\ \Delta h_2)\ A_2\ T_B}{P_2\ T_R}$$

$\underline{V_A}$

(a) Evacuate the whole system.

(b) Close valves 8 and 9 and bleed helium into the system using valve 1.

(c) Measure the new mercury level, h_1, corresponding to the internal pressure, P_1.

(d) Open valves 8 and 9 and record the new mercury level, h_2, corresponding to the final pressure, P_2.

(e) Compute the value of V_A from the following equation:

$$V_A = \frac{(P_1-P_2)\ V_d\ T_B}{P_2\ T_R} + \frac{(P_1-P_2)}{P_2} V_c + \frac{(P_1-P_2)\ V_{CR}}{P_2} + \frac{(P_1\ h_1 - P_2\ h_2)\ A_2\ T_B}{P_2\ T_R}$$

Repeat the above process for V_{AD} when the adsorption vessel is full of adsorbents.

(iii) Measure the absolute density of each adsorbent sample used by filling 30 cm^3 HOKE stainless steel cylinder with a known weight of activated adsorbents and measure the internal volume of the cylinder using the technique described for V_{CR}. The absolute density is obtained by dividing the mass of adsorbents used by the volume occupied by the adsorbents in the cylinder.

The various volumes within the apparatus are given in Table II.1 together with the standard deviation associated with each. The absolute density determined for each adsorbent sample is given in Table II.2 together with the standard deviation associated with it.

TABLE II.1

Uncertainties in Volume Determination

Volume Designation	Calibrated Volume cm^3	Standard Deviation cm^3
V_d	134.820	1.07
V_{CR}	745.706	0.913
V_A	665.94	1.277
Laporte 4A		
$V_{AD(T = 303.15\ K)}$	462.65	1.01
$V_{AD(T = 293.15\ K)}$	468.01	0.191
$V_{AD(T = 278.15\ K)}$	469.19	1.04
Laporte 5A		
$V_{AD(T = 303.15\ K)}$	486.011	0.819
$V_{AD(T = 293.15\ K)}$	488.867	0.844
$V_{AD(T = 278.15\ K)}$	492.147	0.841
Laporte 13X		
$V_{AD(T = 303.15\ K)}$	498.672	2.93
$V_{AD(T = 293.15\ K)}$	503.3	0.365
$V_{AD(T = 278.15\ K)}$	504.34	0.369
EKA 5A		
$V_{AD(T = 303.15\ K)}$	484.656	0.298
$V_{AD(T = 293.15\ K)}$	488.641	0.902
$V_{AD(T = 278.15\ K)}$	494.492	0.801
Na-Mordenite		
$V_{AD(T = 303.15\ K)}$	470.975	0.276
$V_{AD(T = 293.15\ K)}$	483.307	0.231
$V_{AD(T = 278.15\ K)}$	487.145	0.513

TABLE II.2

Determined Absolute Densities for Laporte's 4A, 5A and 13X, EKA 5A and Na-Mordenite at Temperature 293.15 K

Adsorbent	Absolute Density g/cm^3	Standard Deviation g/cm^3
Laporte 4A	2.552	0.168
Laporte 5A	3.18	0.034
Laporte 13X	2.845	0.174
EKA 5A	3.367	0.194
Na-Mordenite	2.711	0.100

(b) Operating procedure for the oxygen analyser

(i) Switch power on and allow 12 hours warm up, prior to calibration.

(ii) Select the 0-25 per cent oxygen range by the front panel switch.

(iii) Select the 0-10 millivolt output range by an internal switch.

(iv) Connect the output terminals to a pen recorder adjusted to read in the 10 millivolt range.

(v) Switch lamp and FEEDBACK off and adjust AMPLIFIER BALANCE until meter reads between zero and 2.5 per cent oxygen on the pen recorder. Switch lamp and FEEDBACK on again.

(vi) Plug in sample selector to zero gas (oxygen-free nitrogen is chosen) and adjust the by-pass needle valve so that the by-pass rotameter reads at least 10 per cent of scale. Allow two minutes for the analyser to reach equilibrium, then adjust the mechanical zero control. When the zero is approximately correct, open the FEEDBACK switch. This increases the sensitivity by a factor of at least 100 and permits an extremely accurate zero adjustment. Close the FEEDBACK switch.

(vii) Plug in the sample selector to span gas (oxygen gas is chosen). Check that the sample flow is normal, i.e. by-pass rotameter reads at least 10 per cent of scale. Allow ten minutes for the analyser to reach equilibrium then adjust the SPAN CONTROL to give the correct analyser reading, i.e. 100 per cent.

(viii) Adjust any discrepancy between the analyser and the pen recorder reading, with the internal SET METER control.

This should not require frequent readjustment.

(ix) Plug in the sample selector to the sample gas line.

The analyser is now ready fcr sample analysis.

B. Equipment Specifications

1. Vacuum system

Manufacturer: Edwards High Vacuum Ltd., Crawley.

Oil Diffusion Pump:	Type: E04
	Pump speed: 600 lit/s
	Ultimate vacuum: 10^{-7} torr
	Fluid charge: 175 ml
	Number of stages: 4
Backing Pump:	Type: ED200
	Displacement: 190 lit/min
	Ultimate vacuum: 10^{-4} torr
	Total oil required: 1.85 litres
Vacuum Gauges:	(a) Penning Type: 6
	Ranges: 10^{-2} to 10^{-7} torr
	(b) Pirani 11
	Ranges: 3.0 - 0.001 torr
Vacuum Valves:	½" and 1" speedivalves, diaphram type

2. Water bath

Manufacturer: Grant Instruments Ltd., Cambridge.

Type: SX50, size: 50 lit, sensitivity: $\pm$ 0.1^{o}C, uniformity: $\pm$ 0.05 C

3. Cooler unit

Manufacturer: Grant Instruments Ltd., Cambridge.

Type: CC20

For cooling water down to 0^{o}C

4. Pressure transducer

Manufacturer: Bell and Howell Ltd., Basingstoke.

Type: 4-306-0221, range: 0-150 psi

Sensitivity: 42.45 mvolts, non-linearity

and hysteresis: ± 0.06% full range

output

5. Bridge supply and balance unit

Manufacturer: Bell and Howell Ltd., Basingstoke.

Type: 8-125, output voltage: 3-12 volts

Current: 35 mAmps maximum, output

resistance: 0.2 ohms, noise and ripple

< ± 0.01 per cent output

6. Valves

Manufacturer: Hoke International Ltd., New Barnet, Herts.

(a) Type: 4600 series, 316 stainless

steel bellows sealed valves,

maximum operating pressure: 300 psig,

tube size: 1/4" o.d.

(b) Type: 4100 series, 316 stainless

steel bellows sealed valves,

maximum operating pressure: 1000 psig,

tube size: 1/4" o.d., 'Gyrolok' tube

fittings

7. Circulating pump

Manufacturer: McDonald and Dawson Ltd., Ashbourne.

Type: D/416-1E

Maximum working pressure: 60 psig,

flow-rate: 2-10 ℓ/min

8. Adsorption vessel and holding vessel

(Schematic sketch shown in Figure II.1.)

Stainless steel, maximum operating pressure: 150 psi, dimensions: 0.15 m x 0.09 m

9. Oxygen analyser

Manufacturer: Taylor Servomex Ltd., Crowborough, Sussex.

Type: O.A.137, ranges: 0-2.5, 0-5, 0-10, 0-25 and 0-100 per cent

Accuracy: $\pm$ 0.05% oxygen, sample pressure: minimum 0.74 kN/m^2, maximum 347 kN/m^2, sample flow-rate: 100 ml/min

Response time: 7 seconds, level sensitivity: < 0.01% per degree of tilt

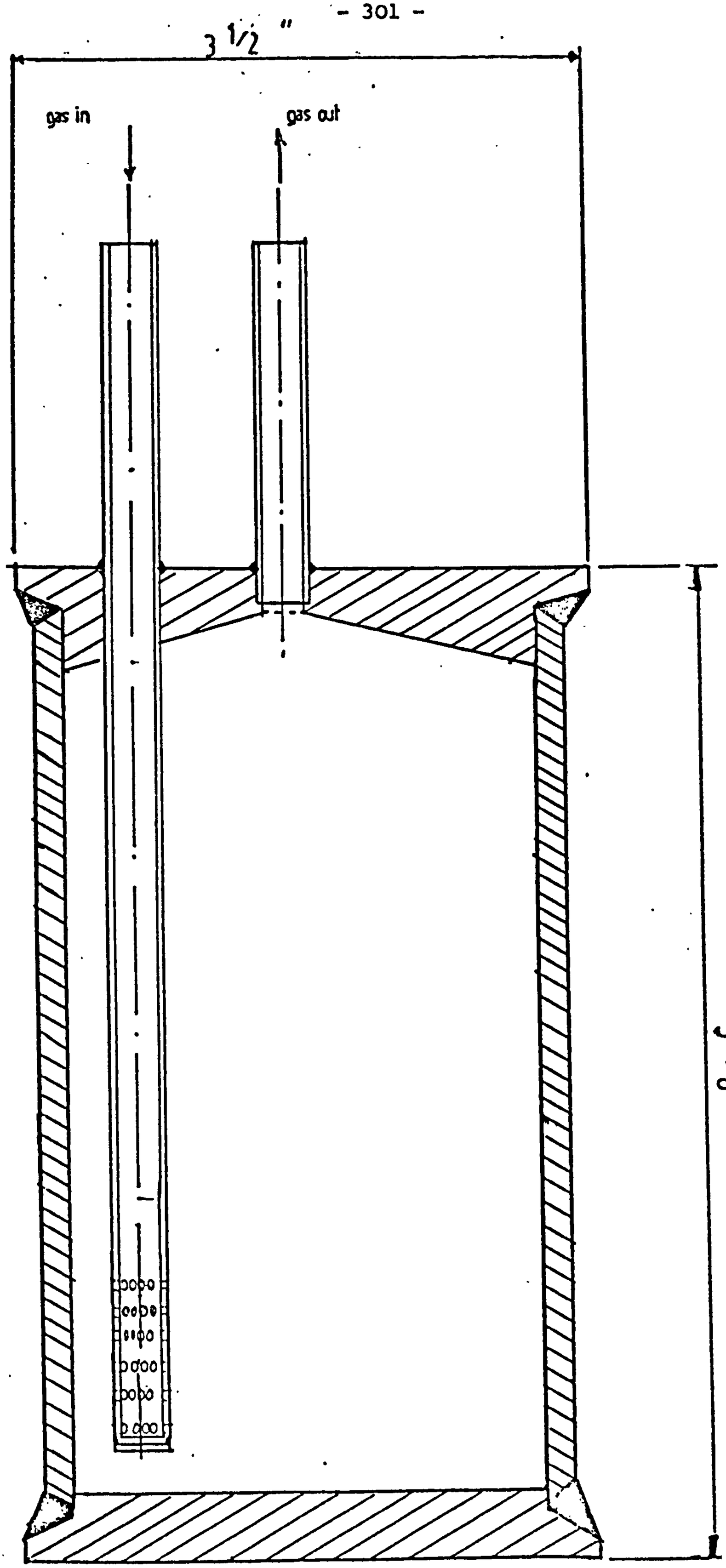

Figure II-1 Schematic Sketch of the Adsorption Vessel

APPENDIX III

COMPUTER PROGRAMMES

Programme Ruthven	Prediction of Binary Gas Adsorption by the Statistical Thermodynamic Model
Programme Cook	Prediction of Binary Gas Adsorption by Cook and Basmadjian Model
Programme IAST	Prediction of Binary Gas Adsorption by the Ideal Adsorbed Solution
Programme Vacancy	Prediction of Binary Gas Adsorption by the Vacancy Solution Model
Programme Act	Calculation of the Activity Coefficients for the Binary Experimental Data

```
      PROGRAM RUTHVEN
C
C
C     PREDICTION OF BINARY ADSORPTION
C     FROM PURE COMPONENT ISOTHERMS BY
C     THE STATISTICAL THERMODYNAMICS METHOD
C
C
C     NOMENCLATURE OF PROGRAM
C
C
C     EQUATION 2.49 IN TEXT IS USED FOR
C     EVALUATING THE AMOUNT ADSORBED OF
C     N2 . ITS' CORRESPONDING EQUATION
C     IS USED FOR O2 .
C
C
C     PRES=TOTAL PRESSURE OF MIXTURE
C     T=TEMPERATURE OF ADSORPTION
C     VPORE=PORE VOLUME OF ZEOLITE CAVITY
C     CMOL=CONVERSION FACTOR FOR CONVERTING
C          MOLECULE/CAVITY TO MOL/KG
C     M=I IN EQUATION 2.49 AND ITS CORRESPONDING EQUATION
C       ( TAKEN AS NO. OF MOLECULES OF O2 IN ZEOLITE CAVITY )
C     N=J IN EQUATION 2.49 AND ITS CORRESPONDING EQUATION
C       ( TAKEN AS NO. OF MOLECULES OF N2 IN ZEOLITE CAVITY )
C     A(I)=REGRESSION PARAMETERS OBTAINED FROM
C          THE PURE COMPONENTS ISOTHERMS
C          A(1),A(2)=HENRY'S LAW CONSTANTS FOR
C          THE STRONGLY ADSORBED COMPONENT I.E. N2
C          A(3),A(4)=HENRY'S LAW CONSTANTS FOR
C          THE LESS ADSORBED COMPONENT I.E. O2
C          A(5),A(6)=EFFECTIVE MOLECULAR VOLUME OF N2
C          A(7),A(8)=EFFECTIVE MOLECULAR VOLUME OF O2
C     Y1M=MOLE FRACTION OF 1 IN GAS PHASE (I.E. N2 )
C     Y2M=MOLE FRACTION OF 2 IN GAS PHASE (I.E. O2 )
C     P01=PARTIAL PRESSURE OF N2
C     P02=PARTIAL PRESSURE OF O2
C     BIN1= I OR J FACTORIAL IN EQUATION 2.49
C           AND ITS CORRESPONDING EQUATION FOR THE OTHER COMPONENT
C     BIN2= (I-1) OR (J-1) FACTORIAL IN EQUATION 2.49
C           AND ITS CORRESPONDING EQUATION FOR THE OTHER COMPONENT
C     SUM= SUM OF DENOMENATOR IN EQUATION 2.49 OR ITS
C          CORRESPONDING EQUATION TO MAXIMUM VALUES OF
C          M AND N ( I.E. FOR N2 OR O2 )
C     SUMA=SUM OF NUMERATOR IN EQUATION 2.49 TO MAXIMUM
C          VALUES OF M AND N
C          (FOR N2)
C     SUMB=SUM OF NUMERATOR IN EQUATION 2.49 TO MAXIMUM
C          VALUE OF N WHEN M=0
C          (FOR N2)
```

```
C       SUMC=SUM OF NUMERATOR IN THE CORRESPONDING EQUATION
C            TO EQUATION 2.49 TO MAXIMUM
C            VALUE OF M WHEN N=0
C            (FOR O2)
C       SUMD=SUM OF DENOMENATOR IN EQUATION 2.49 OR ITS
C            CORRESPONDING EQUATION TO MAXIMUM
C            VALUE OF N WHEN M=0
C            (FOR N2 OR O2)
C       SUME=SUM OF DENOMENATOR IN EQUATION 2.49 OR ITS
C            CORRESPONDING EQUATION TO MAXIMUM
C            VALUE OF M WHEN N=0
C            (FOR N2 OR O2)
C       SUMF=SUM OF NUMERATOR IN THE CORRESPONDING
C            EQUATION TO EQUATION 2.49 TO MAXIMUM
C            VALUES OF M AND N
C            (FOR O2)
C       X1=AMOUNT ADSORBED OF N2
C       X2=AMOUNT ADSORBED OF O2
C       X1M=MOLE FRACTION OF N2 IN ADSORBED PHASE
C       X2M=MOLE FRACTION OF O2 IN ADSORBED PHASE
C       RV=SEPARATION FACTOR AS DEFINED IN TEXT
C
C
C
      DIMENSION A(8),PO1(51),PO2(51),X1M(51),X2M(51),
     1Y1M(51),Y2M(51),XT(51),X1(51),X2(51),RV(51),
     2BIN1(15),BIN2(15)
      CHARACTER*80 TITLE(4)
      READ(*,3) TITLE
      WRITE(2,3) TITLE
      READ*, PRES,T
      READ*, VPORE,CMOL
      READ*, M,N
      READ*, (A(I),I=1,8)
      WRITE (2,25) PRES,T
C     CALCULATE THE INCREMENT SIZE OF MOLE FRACTION
C     IN GAS PHASE
      DYI=(1.0-0.0)/50.0
      DO 44 J=2,50
      Y1M(J)=0.0+(J-1)*DYI
      Y2M(J)=1.0-Y1M(J)
      PO1(J)=Y1M(J)*PRES
44    PO2(J)=Y2M(J)*PRES
      BIN1(1)=1.0
      DO 5 I=2,15
5     BIN1(I)=BIN1(I-1)*I
```

```
      BIN2(1)=1.0
      BIN2(2)=1.0
      DO 17 I=3,15
17    BIN2(I)=BIN2(I-1)*(I-1)
      DO 45 J=2,50
      SUM=0.0
      SUMA=0.0
      SUMB=0.0
      SUMC=0.0
      SUMD=0.0
      SUME=0.0
      SUMF=0.0
      DO 13 I=3,N+1
13    SUMB=((A(1)*EXP(A(2)/T))*PO1(J))**(I-1)*
     1(1-(I-1)*A(5)*EXP(A(6)/T)/VPORE)**(I-1)/BIN2(I-1)+SUMB
      DO 14 I=2,N
14    SUMD=((A(1)*EXP(A(2)/T))*PO1(J))**I*
     1(1-I*A(5)*EXP(A(6)/T)/VPORE)**I/BIN1(I)+SUMD
      DO 12 K=1,M
      DO 11 I=1,N
11    SUM=(A(1)*EXP(A(2)/T)*PO1(J))**I*
     1(A(3)*EXP(A(4)/T)*PO2(J))**K*
     2(1-I*A(5)*EXP(A(6)/T)/VPORE-
     3K*A(7)*EXP(A(8)/T)/VPORE)**(I+K)
     3/(BIN1(I)*BIN1(K))+SUM
12    CONTINUE
      DO 16 K=1,M
      DO 19 I=2,N+1
19    SUMA=(A(1)*EXP(A(2)/T)*PO1(J))**(I-1)*
     1(A(3)*EXP(A(4)/T)*PO2(J))**K*
     2(1-(I-1)*A(5)*EXP(A(6)/T)/VPORE-
     3K*A(7)*EXP(A(8)/T)/VPORE)**((I-1)+K)
     3/(BIN2(I-1)*BIN1(K))+SUMA
16    CONTINUE
      DO 21 I=3,M+1
21    SUMC=(A(3)*EXP(A(4)/T)*PO2(J))**(I-1)*
     1(1-(I-1)*A(7)*EXP(A(8)/T)/VPORE)**(I-1)/BIN2(I-1)+SUMC
      DO 22 I=2,M
22    SUME=(A(3)*EXP(A(4)/T)*PO2(J))**I*
     1(1-I*A(7)*EXP(A(8)/T)/VPORE)**I/BIN1(I)+SUME
      X1(J)=(A(1)*EXP(A(2)/T)*PO1(J)+SUMA+SUMB)/
     1(1+A(1)*EXP(A(2)/T)*PO1(J)+A(3)*EXP(A(4)/T)*PO2(J)+
     2SUM+SUMD+SUME)
```

```
      DO 28 K=2,M+1
      DO 29 I=1,N
29    SUMF=(A(1)*EXP(A(2)/T)*PO1(J))**I*
     1(A(3)*EXP(A(4)/T)*PO2(J))**(K-1)*
     2(1-I*A(5)*EXP(A(6)/T)/VPORE-(K-1)*A(7)*EXP(A(8)/T)/VPORE)
     3**(I+(K-1))
     4/(BIN1(I)*BIN2(K-1))+SUMF
28    CONTINUE
      X2(J)=(A(3)*EXP(A(4)/T)*PO2(J)+SUMF+SUMC)/
     1(1+A(1)*EXP(A(2)/T)*PO1(J)+A(3)*EXP(A(4)/T)*PO2(J)+
     2SUM+SUME+SUMD)
      X1(J)=X1(J)*CMOL
      X2(J)=X2(J)*CMOL
      XT(J)=X1(J)+X2(J)
      X1M(J)=X1(J)/XT(J)
      X2M(J)=1.0-X1M(J)
      RV(J)=(Y2M(J)*X1M(J))/(Y1M(J)*X2M(J))
45    CONTINUE
      WRITE(2,170)
      WRITE(2,180) (Y2M(J),X2M(J),X1(J),X2(J),XT(J),RV(J),J=2,50)
      STOP
C     .............FORMAT SECTION.........................
3     FORMAT(A)
25    FORMAT(//T6,'EQUILIBRIUM PRESSURE',F10.5,'BAR'//
     1T6,'TEMPERATURE OF ADSORPTION',F10.3,'DEGREES KELVIN'//)
170   FORMAT (////T7,'ADSORPTION EQUILIBRIA'//T6,'MOLE FRACTION',
     1T23,'MOLE FRACTION',T39,'AMOUNT ADSORBED,MOL/KG OF ADSORBENT'
     1,T81,'REL. VOL. '/
     2T6,'GAS PHASE,',T22,'ADSORBED PHASE',T39,'COMPONENT1',T52,
     3'COMPONENT 2',T69,'TOTAL'//)
180   FORMAT (T8,F9.7,T24,F9.7,T39,E12.5,T52,E12.5,T66,E12.5,T81
     1,F9.7)
      END
```

```
      PROGRAM COOK
C
C
C
C     PREDICTION OF BINARY ADSORPTION
C     FROM PURE COMPONENT ISOTHERMS BY
C     COOK AND BASMADJIAN METHOD
C
C
C     EQUATION 4.1 IN TEXT IS USED AS THE
C     CORRELATING EQUATION FOR THE PURE
C     COMPONENTS ISOTHERMS
C
C
C
C     NOMENCLATURE OF PROGRAM
C
C
C
C     PRES=PRESSURE OF MIXTURE
C     T=TEMPERATURE OF ADSORPTION
C     A1,A2=REGRESSION PARAMETERS OF EQUATION 4.1
C     FOR THE PURE COMPONENT ISOTHERMS
C     (1 FOR LESS ADSORBED ( O2 ) , 2 FOR STRONGLY ADSORBED ( N2 )
C     X1E=ASSUMED AMOUNT ADSORBED AT PRESSURE OF MIXTURE
C     W1=AMOUNT ADSORBED OF PURE 1 AT PRESSURE OF MIXTURE
C     W2=AMOUNT ADSORBED OF PURE 2 AT PRESSURE OF MIXTURE
C     FI11=INTEGRATION OF NUMERATOR OF EQUATION 2.57A IN TEXT
C     FI12=INTEGRATION OF NUMERATOR OF EQUATION 2.57B IN TEXT
C     FI21=INTEGRATION OF DENOMENATOR OF EQUATION 2.57A
C     FI22=INTEGRATION OF DENOMENATOR OF EQUATION 2.57B
C     B1=SEPARATION FACTOR AT X2=1.0
C     B2=SEPARATION FACTOR AT X1=1.0
C     PI1=P1/X1
C     PI2=P2/X2
C     X1=MOLE FRACTION OF 1 IN ADSORBED PHASE
C     X2=MOLE FRACTION OF 2 IN ADSORBED PHASE
C     P1=PARTIAL PRESSURE OF 1
C     P2=PARTIAL PRESSURE OF 2
C     XT=TOTAL AMOUNT ADSORBED
C     X1M=AMOUNT ADSORBED OF 1
C     X2M=AMOUNT ADSORBED OF 2
C     Y1=MOLE FRACTION OF 1 IN GAS PHASE
C     Y2=MOLE FRACTION OF 2 IN GAS PHASE
C     RV12=SEPARATION FACTOR ( Y1.X2 / Y2.X1 )
C
C
C
```

```
      COMMON/SEA/ A1(10),A2(10),TP,J
      DIMENSION Y1(51),Y2(51),PI1(51),PI2(51),PI11(51)
     1,PI22(51),X1(51),X2(51),X1M(51),X2M(51),XTM(51),
     2XT(51),RV12(51)
      CHARACTER*80 TITLE(4)
      READ(*,3) TITLE
      WRITE(2,3) TITLE
      READ*, PRES,T
      READ*, (A1(I),I=1,4),(A2(I),I=1,4)
      WRITE (2,25) PRES,T
C     CALCULATE THE AMOUNT ADSORBED OF EACH PURE
C     COMPONENT AT THE TOTAL PRESSURE OF MIXTURE
      TP=PRES
      X1E=0.5
      CALL SEARCH (X1E,W1,1)
      CALL SEARCH (X1E,W2,2)
C     EVALUATE THE INTEGRALS OF EQUATIONS 2.57A AND 2.57B
      CALL SPREAD (W1,FI11,1)
      CALL SPREAD (W2,FI12,1)
      CALL SPREAD (W1,FI21,2)
      CALL SPREAD (W2,FI22,2)
      B1=EXP(1/W2*(FI12-FI22))
      B2=EXP(1/W1*(FI11-FI21))
      PI1(51)=PRES*B1
      PI2(1)=PRES/B2
C     ASSUME THE BINARY ISOTHERMS ARE LINEAR
C     IN A LOG-LOG PLOT AND EVALUATE THEIR SLOPES
C     FROM THE KNOWN END POINTS
      W22=ALOG(W2)
      W11=ALOG(W1)
      PI11(51)=ALOG(PI1(51))
      PI22(1)=ALOG(PI2(1))
      PI11(1)=ALOG(PRES)
      PI22(51)=ALOG(PRES)
      SL1=(W22-W11)/(PI11(51)-PI11(1))
      SL2=(W22-W11)/(PI22(51)-PI22(1))
C     CALCULATE THE INCREMENT SIZE OF LOG OF
C     TOTAL AMOUNT ADSORBED
      DXMT=(W22-W11)/50.0
      DO 45 J=2,50
      XTM(J)=W11+(J-1)*DXMT
C     CALCULATE THE RATIOS P1/X1 AND P2/X2 FOR EACH
C     TOTAL AMOUNT ADSORBED EVALUATED IN THE PREVIOUS STEP
      PI11(J)=(SL1*PI11(1)-W11+XTM(J))/SL1
      PI22(J)=(SL2*PI22(1)-W11+XTM(J))/SL2
      PI1(J)=EXP(PI11(J))
      PI2(J)=EXP(PI22(J))
      XT(J)=EXP(XTM(J))
```

```
C       CALCULATE THE INDIVIDUAL AMOUNTS ADSORBED OF
C       EACH COMPONENT , THE COMPOSITION OF EACH COMPONENT
C       IN BOTH PHASES AND THE SEPARATION FACTOR
        X2(J)=(PI1(J)-PRES)/(PI1(J)-PI2(J))
        X1(J)=1.0-X2(J)
        X1M(J)=X1(J)*XT(J)
        X2M(J)=X2(J)*XT(J)
        Y1(J)=PI1(J)*X1(J)/PRES
        Y2(J)=1.0-Y1(J)
45      RV12(J)=(Y1(J)*X2(J))/(Y2(J)*X1(J))
        WRITE(2,170)
        WRITE(2,180) (Y1(J),X1(J),X1M(J),X2M(J),XT(J),
       1RV12(J),J=2,50)
        STOP
C       .............FORMAT SECTION.....................
3       FORMAT(A)
25      FORMAT(//T6,'EQUILIBRIUM PRESSURE',F10.5,'BAR'//
       1T6,'TEMPERATURE OF ADSORPTION',F10.3,'DEGREES KELVIN'//)
170     FORMAT (////T7,'ADSLRPTION EQUILIBRIA'//T6,'MOLE FRACTION',
       1T23,'MOLE FRACTION',T39,'AMOUNT ADSORBED,MOL/KG OF ADSORBENT'
       1,T81,'REL. VOL. '/
       2T6,'GAS PHASE,',T22,'ADSORBED PHASE',T39,'COMPONENT 1',T52,
       3'COMPONENT 2',T69,'TOTAL'//)
180     FORMAT (T8,F9.7,T24,F9.7,T39,E12.5,T52,E12.5,T66,E12.5,
       1T81,F9.7)
        END
C
C
C
        SUBROUTINE SEARCH (D1,DR,JCOMP)
C       THIS SUBROUTINE SEARCHS FOR A ROOT USING
C       NEWTON-RAPHSON METHOD
        FD=FUNCS(D1,JCOMP)
40      DELX=FD/(FDER(D1,JCOMP))
        D1=D1-DELX
        FD=FUNCS(D1,JCOMP)
        IF(ABS(DELX).LE.0.1E-08) GOTO 60
        GOTO 40
60      DR=D1
        RETURN
        END
C
C
C
```

```
C       CALCULATE THE TOTAL AMOUNT ADSORBED
        XT(J)=X1C(J)*X2O(J)/(X1M(J)*X2O(J)+X2M(J)*X1O(J))
C       CALCULATE THE SEPARATION FACTOR
        RV(J)=(Y2M(J)*X1M(J))/(Y1M(J)*X2M(J))
C       CALCULATE THE INDIVIDUAL AMOUNTS ADSORBED
        X1(J)=X1M(J)*XT(J)
45      X2(J)=X2M(J)*XT(J)
        WRITE(2,170)
        WRITE(2,180) (Y2M(J),X2M(J),X1(J),X2(J),XT(J),RV(J),J=2,50)
        STOP
C       .............FORMAT SECTION.....................
3        FORMAT(A)
25       FORMAT(//T6,'EQUILIBRIUM PRESSURE',F10.5,'BAR'//
      1T6,'TEMPERATURE OF ADSORPTION',F10.3,'DEGREES KELVIN'//)
170      FORMAT (////T7,'ADSORPTION EQUILIBRIA'//T6,'MOLE FRACTION',
      1T23,'MOLE FRACTION',T39,'AMOUNT ADSORBED,MOL/KG OF ADSORBENT'
      1,T81,'REL. VOL. '/
      2T6,'GAS PHASE,',T22,'ADSORBED PHASE',T39,'COMPONENT1',T52,
      3'COMPONENT 2',T69,'TOTAL'//)
180      FORMAT (T8,F9.7,T24,F9.7,T39,E12.5,T52,E12.5,T66,E12.5,T81
      1,F9.7)
         END
C
C
C
         SUBROUTINE SEARCH (D1,DR,JFUN,JCOMP)
C        THIS SUBROUTINE SEARCHS FOR A ROOT USING
C        NEWTON-RAPHSON METHOD
         FD=FUNCS(D1,JFUN,JCOMP)
40       DELX=FD/(FDER(D1,JFUN,JCOMP))
         D1=D1-DELX
         FD=FUNCS(D1,JFUN,JCOMP)
         IF(ABS(DELX).LE.0.1E-06) GOTO 60
         GOTO 40
60       DR=D1
         RETURN
         END
C
C
C
         SUBROUTINE SPREAD(XC,PIO,JCOMP)
         COMMON/SEA/ A1(6),A2(6)
        1,PI(51),PO1(51),PO2(51),
        2J,TP,X10(51),X20(51)
         DIMENSION Y(101),DLP(101),A(8)
C        THIS SUBROUTINE COMPUTES THE SPREADING PRESSURE FUNCTION
C        FOR A GIVEN AMOUNT ADSORBED FOR A PURE COMPONENT USING
C        TRAPEZOIDAL RULE FOR 100 INCREMENTS
         GLTL (3,4), JCOMP
```

```
      SUBROUTINE SPREAD(XO,PIO,JCOMP)
      COMMON/SEA/ A1(10),A2(10),TP,J
      DIMENSION X(101),DLP(101),A(8)
C     THIS SUBROUTINE EVALUATES THE INTEGRALS OF EQATIONS 2.57A
C     AND 2.57B USING TRAPEZOIDAL RULE FOR 100 INCREMENTS
      GOTO (3,4), JCOMP
3     DO 5 I=1,4
5     A(I)=A1(I)
      GOTO 8
4     DO 7 I=1,4
7     A(I)=A2(I)
8     DX=XO/100.0
      SUM=0.0.
      X(1)=0.0
      DO 11 I=2,101
      X(I)=X(I-1)+DX
      X11=X(I)
      DLP(I)=ALOG(((A(1)*X11)*EXP(X11/(A(3)-X11)-
     1A(4)*X11))/(A(2)-X11))
11    SUM=SUM+DLP(I)
      PIO=DX*(SUM-0.5*DLP(101))
      RETURN
      END
C
C
C

      FUNCTION FUNCS(X,JCOMP)
      COMMON/SEA/ A1(10),A2(10),TP,J
      DIMENSION A(8)
      GOTO (30,40),JCOMP
30    DO 31 I=1,4
31    A(I)=A1(I)
      GOTO 100
40    DO 41 I=1,4
41    A(I)=A2(I)
C     ISOTHERM FUNCTION
100   FUNCS=(((A(1)*X)*EXP(X/(A(3)-X)-A(4)*X))
     1/(A(2)-X))/TP-1.0
      RETURN
      END
C
C
C
      FUNCTION FDER (X,JCOMP)
C     FUNCTION FDER COMPUTES THE DERIVATIVE OF FUNCS
C     ( I.E. THE ISOTHERM FUNCTION ) FOR USE IN
C     SUBROUTINE SEARCH
      COMMON/SEA/ A1(10),A2(10),TP,J
      DIMENSION A(8)
      GOTO (30,40),JCOMP
30    DO 31 I=1,4
31    A(I)=A1(I)
      GOTO 100
40    DO 41 I=1,4
41    A(I)=A2(I)
100   Z1=EXP(X/(A(3)-X)-A(4)*X)
      Z2=A(1)*Z1+A(1)*X*((A(3)/(A(3)-X)**2)-A(4))
     1*Z1/(A(2)-X)
      Z3=Z2+A(1)*X*Z1/(A(2)-X)**2
      FDER=Z3/TP
      RETURN
      END
```

```
      PROGRAM IAST
C
C
C
C     PREDICTION OF BINARY ADSORPTION
C     FROM PURE COMPONENT ISOTHERMS BY
C     THE IDEAL ADSORBED SOLUTION THEORY
C     ( I . A . S . T . )
C
C
C     EQUATION 4.1 IN TEXT IS USED AS THE
C     CORRELATING EQUATION FOR THE PURE
C     COMPONENT ISOTHERMS
C
C
C     NOMENCLATURE OF PROGRAM
C
C
C     PRES=PRESSURE OF MIXTURE
C     TEMP=TEMPERATURE OF ADSORPTION
C     A1,A2=REGRESSION PARAMETERS FOR
C           EQUATION 4.1 FOR BOTH PURE COMPONENTS
C           ( 1 FOR STRONGLY ADSORBED COMPONENT ( N2 )
C             2 FOR LESS ADSORBED COMPONENT ( O2 ) )
C     X1E=ASSUMED AMOUNT ADSORBED AT PRESSURE OF MIXTURE
C     X10=AMOUNT ADSORBED OF PURE COMPONENT 1 AT THE
C         SPREADING PRESSURE OF MIXTURE
C     X20=AMOUNT ADSORBED OF PURE COMPONENT 2 AT THE
C         SPREADING PRESSURE OF MIXTURE
C     PI10=SPREADING PRESSURE OF PURE COMPONENT 1
C     PI20=SPREADING PRESSURE OF PURE COMPONENT 2
C     PI=SPREADING PRESSURE OF MIXTURE
C     P01=EQUILIBRIUM PRESSURE OF PURE COMPONENT 1
C         AT THE SPREADING PRESSURE OF MIXTURE
C     P02=EQUILIBRIUM PRESSURE OF PURE COMPONENT 2
C         AT THE SPREADING PRESSURE OF MIXTURE
C     X1M=MOLE FRACTION OF 1 IN ADSORBED PHASE
C     X2M=MOLE FRACTION OF 2 IN ADSORBED PHASE
C     Y1M=MOLE FRACTION OF 1 IN GAS PHASE
C     Y2M=MOLE FRACTION OF 2 IN GAS PHASE
C     XT=TOTAL AMOUNT ADSORBED
C     X1=AMOUNT ADSORBED OF COMPONENT 1
C     X2=AMOUNT ADSORBED OF COMPONENT 2
C     RV=SEPARATION FACTOR ( Y2M.X1M / Y1M.X2M )
C
C
```

```
C
      COMMON/SEA/ A1(8),A2(8)
     1,PI(51),PO1(51),PO2(51),
     2J,TP,X10(51),X20(51)
      DIMENSION X1M(51),X2M(51),Y1M(51),Y2M(51),
     1XT(51),X1(51),X2(51),Rv(51)
      CHARACTER*80 TITLE(4)
      READ(*,3) TITLE
      WRITE(2,3) TITLE
      READ*, PRES,TEMP
      READ*, (A1(I),I=1,4),(A2(I),I=1,4)
      WRITE (2,25) PRES,TEMP
C     CALCULATE THE AMOUNT ADSORBED OF BOTH
C     PURE COMPONENTS AT THE TOTAL PRESSURE OF MIXTURE
      TP=PRES
      X1E=0.5
      CALL SEARCH (X1E,X10(51),1,1)
      CALL SEARCH (X1E,X20(1),1,2)
C     CALCULATE THE SPREADING PRESSURE OF BOTH PURE
C     COMPONENTS CORRESPONDING TO THE PRESSURE OF MIXTURE
      CALL SPREAD (X10(51),PI10,1)
      CALL SPREAD (X20(1),PI20,2)
C     THE SPREADING PRESSURE OF THE BINARY MIXTURE LIES
C     BETWEEN THE PURE COMPONENTS SPREADING PRESSURES AT
C     PRESSURE OF MIXTURE I.E. PI10 AND PI20
C
C     CALCULATE THE INCREMENT SIZE OF THE SPREADING PRESSURE
C     OF THE BINARY MIXTURE
      DPI=(PI10-PI20)/50.0
      PO1(51)=PRES
      PO2(1)=PRES
      DO 45 J=2,50
      PI(J)=PI20+(J-1)*DPI
C     CALCULATE THE AMOUNT ADSORBED OF THE PURE
C     COMPONENTS AT THE SPREADING PRESSURE OF MIXTURE
      CALL SEARCH (X10(51),X10(J),2,1)
      CALL SEARCH (X20(1),X20(J),2,2)
C     CALCULATE THE EQUILIBRIUM PRESSURE OF THE PURE
C     COMPONENTS AT THE SPREADING PRESSURE OF MIXTURE
      PO1(J)=FUNCS(X10(J),3,1)
      PO2(J)=FUNCS(X20(J),3,2)
C     EVALUATE THE MOLE FRACTIONS OF BOTH COMPONENTS
C     IN THE ADSORBED PHASE
      X1M(J)=(PO2(J)-PRES)/(PO2(J)-PO1(J))
      X2M(J)=1.0-X1M(J)
C     EVALUATE THE MOLE FRACTIONS OF BOTH COMPONENTS
C     IN THE GAS PHASE
      Y1M(J)=PO1(J)*X1M(J)/PRES
      Y2M(J)=1.0-Y1M(J)
```

```
C       CALCULATE THE TOTAL AMOUNT ADSORBED
        XT(J)=X1C(J)*X20(J)/(X1M(J)*X20(J)+X2M(J)*X10(J))
C       CALCULATE THE SEPARATION FACTOR
        RV(J)=(Y2M(J)*X1M(J))/(Y1M(J)*X2M(J))
C       CALCULATE THE INDIVIDUAL AMOUNTS ADSORBED
        X1(J)=X1M(J)*XT(J)
45      X2(J)=X2M(J)*XT(J)
        WRITE(2,170)
        WRITE(2,180) (Y2M(J),X2M(J),X1(J),X2(J),XT(J),RV(J),J=2,50)
        STOP
C       .............FORMAT SECTION.....................
3        FORMAT(A)
25       FORMAT(//T6,'EQUILIBRIUM PRESSURE',F10.5,'BAR'//
      1T6,'TEMPERATURE OF ADSORPTION',F10.3,'DEGREES KELVIN'//)
170      FORMAT (////T7,'ADSORPTION EQUILIBRIA'//T6,'MOLE FRACTION',
      1T23,'MOLE FRACTION',T39,'AMOUNT ADSORBED,MOL/KG OF ADSORBENT
      1,T81,'REL. VOL. '/
      2T6,'GAS PHASE,',T22,'ADSORBED PHASE',T39,'COMPONENT1',T52,
      3'COMPONENT 2',T69,'TOTAL'//)
180      FORMAT (T8,F9.7,T24,F9.7,T39,E12.5,T52,E12.5,T66,E12.5,T81
      1,F9.7)
         END
C
C
C
         SUBROUTINE SEARCH (D1,DR,JFUN,JCOMP)
C        THIS SUBROUTINE SEARCHS FOR A ROOT USING
C        NEWTON-RAPHSON METHOD
         FD=FUNCS(D1,JFUN,JCOMP)
40       DELX=FD/(FDER(D1,JFUN,JCOMP))
         D1=D1-DELX
         FD=FUNCS(D1,JFUN,JCOMP)
         IF(ABS(DELX).LE.0.1E-08) GOTO 60
         GOTO 40
60       DR=D1
         RETURN
         END
C
C
C
         SUBROUTINE SPREAD(XO,PIO,JCOMP)
         COMMON/SEA/ A1(8),A2(8)
        1,PI(51),PO1(51),PO2(51),
        2J,TP,X10(51),X20(51)
         DIMENSION X(101),DLP(101),A(8)
C        THIS SUBROUTINE COMPUTES THE SPREADING PRESSURE FUNCTION
C        FOR A GIVEN AMOUNT ADSORBED FOR A PURE COMPONENT USING
C        TRAPEZOIDAL RULE FOR 100 INCREMENTS
         GOTO (3,4), JCOMP
```

```
3       DO 5 I=1,4
5       A(I)=A1(I)
        GOTO 8
4       DO 7 I=1,4
7       A(I)=A2(I)
8       DX=X0/100.0
        SUM=0.0
        X(1)=0.0
        DO 11 I=2,101
        X(I)=X(I-1)+DX
        X22=X(I)*X(I)
        X3=X(I)*X22
        X11=X(I)
        DLP(I)=1.0+X11*(A(3)/(A(3)-X11)**2-A(4))
       1+X11/(A(2)-X11)
11      SUM=SUM+DLP(I)
        PIO=DX*(SUM-0.5*DLP(101))
        RETURN
        END
C
C
C

        FUNCTION FUNCS(XX,JFUN,JCOMP)
        COMMON/SEA/ A1(8),A2(8)
       1,PI(51),PO1(51),PO2(51),
       2J,TP,X10(51),X20(51)
        DIMENSION A(8),DLP(101)
        GOTO (10,20,50),JFUN
10      X=XX
        GOTO (30,40),JCOMP
30      DO 31 I=1,4
31      A(I)=A1(I)
        GOTO 100
40      DO 41 I=1,4
41      A(I)=A2(I)
C       ISOTHERM FUNCTION
100     FUNCS=(((A(1)*X)*EXP(X/(A(3)-X)-A(4)*X))
       1/(A(2)-X))/TP-1.0
        RETURN
C       SPREADING PRESSURE FUNCTION
20      GOTO (3,4), JCOMP
3       DO 5 I=1,4
5       A(I)=A1(I)
        X10(J)=XX
        DX=X10(J)/100.0
        GOTO 8
4       DO 7 I=1,4
7       A(I)=A2(I)
        X20(J)=XX
        DX=X20(J)/100.0
8       SUM=0.0
        X=0.0
        DO 11 I=2,101
        X11=X+DX
        X22=X11*X11
        X3=X22*X11
        DLP(I)=1.0+X11*(A(3)/(A(3)-X11)**2-A(4))
       1+X11/(A(2)-X11)
11      SUM=SUM+DLP(I)
        X=X11
        FUNCS=DX*(SUM-0.5*DLP(101))/PI(J)-1
        RETURN
```

```
50      X=XX
        GOTO (60,70),JCOMP
60      DO 80 I=1,4
80      A(I)=A1(I)
        GOTO 90
70      DO 85 I=1,4
85      A(I)=A2(I)
C       ISOTHERM FUNCTION
90      FUNCS=((A(1)*X)*EXP(X/(A(3)-X)-
       1A(4)*X))/(A(2)-X)
        RETURN
        END
C
C
C
        FUNCTION FDER(XX,JFUN,JCOMP)
C       FUNCTION FDER COMPUTES THE DERIVATIVE OF THE FIRST
C       TWO FUNCTIONS IN FUNCS FOR USE IN SUBROUTINE SEARCH
        COMMON/SEA/ A1(8),
       1A2(8),PI(51),PO1(51),PO2(51),
       2J,TP,X10(51),X20(51)
        DIMENSION A(8),DLP(101)
        GOTO (10,20),JFUN
10      X=XX
        GOTO (30,40),JCOMP
30      DO 31 I=1,4
31      A(I)=A1(I)
        GOTO 100
40      DO 41 I=1,4
41      A(I)=A2(I)
100     Z1=EXP(X/(A(3)-X)-A(4)*X)
        Z2=A(1)*Z1+A(1)*X*((A(3)/(A(3)-X)**2)-A(4))
       1*Z1/(A(2)-X)
        Z3=Z2+A(1)*X*Z1/(A(2)-X)**2
        FDER=Z3/TP
        RETURN
20      GOTO (3,4),JCOMP
3       DO 5 I=1,4
5       A(I)=A1(I)
        X10(J)=XX
        X=X10(J)
        GOTO 6
4       DO 7 I=1,4
7       A(I)=A2(I)
        X20(J)=XX
        X=X20(J)
8       Z4=1.0+X*((A(3)/(A(3)-X)**2)-A(4))+X/(A(2)-X)
        FDER=Z4/PI(J)
        RETURN
        END
```

```
      PROGRAM VACANCY
C
C
C
C     PREDICTION OF BINARY ADSORPTION
C     FROM PURE COMPONENT ISOTHERMS
C     BY THE VACANCY SOLUTION MODEL
C
C
C     NOMENCLATURE OF PROGRAM
C
C
C     P=TOTAL PRESSURE OF MIXTURE
C     TEMP=TEMPERATURE OF ADSORPTION
C     INTER=1  ADSORBATE-ADSORBATE INTERACTIONS (Z12,Z21)
C           ARE TAKEN TO BE EQUAL TO UNITY
C          =ANY INTEGER OTHER THAN 1  ADSORBATE-ADSORBATE
C           INTERACTIONS ARE ESTIMATED FROM EQUATIONS
C           4.8-4.10 IN TEXT
C     Z=COORDINATION NUMBER ACCORDING TO
C       WILSONS EQUATION
C     QST1=INFINITE DILUTION ISOSTERIC HEAT OF
C          ADSORPTION FOR COMPONENT 1 ( O2 )
C     QST2=INFINITE DILUTION ISOSTERIC HEAT OF
C          ADSORPTION FOR COMPONENT 2 ( N2 )
C     R=UNIVERSAL GAS CONSTANT
C     B1=HENRYS LAW CONSTANT FOR COMPONENT 1
C     B2=HENRYS LAW CONSTANT FOR COMPONENT 2
C     Z13=ADSORBATE-VACANCY INTERACTION FOR COMPONENT 1
C     Z31=VACANCY-ADSORBATE INTERACTION FOR COMPONENT 1
C     Z23=ADSORBATE-VACANCY INTERACTION FOR COMPONENT 2
C     Z32=VACANCY-ADSORBATE INTERACTION FOR COMPONENT 2
C     Z12,Z21=INTERACTION PARAMETERS BETWEEN COMPONENT 1
C               AND COMPONENT 2
C     V1M=MAXIMUM NUMBER OF MOLES OF COMPONENT 1 IN
C         ADSORBED PHASE
C     V2M=MAXIMUM NUMBER OF MOLES OF COMPONENT 2 IN
C         ADSORBED PHASE
C     VTT=MAXIMUM TOTAL NUMBER OF MOLES OF MIXTURE IN
C         ADSORBED PHASE
C     VT=TOTAL NUMBER OF MOLES OF MIXTURE IN
C        ADSORBED PHASE
C     V1=NUMBER OF MOLES OF 1 IN ADSORBED PHASE
C     V2=NUMBER OF MOLES OF 2 IN ADSORBED PHASE
C     Y1=MOLE FRACTION OF 1 IN GAS PHASE
C     Y2=MOLE FRACTION OF 2 IN GAS PHASE
C     X1=MOLE FRACTION OF 1 IN ADSORBED PHASE
C     X2=MOLE FRACTION OF 2 IN ADSORBED PHASE
C     RV=SEPARATION FACTOR ( Y1.X2 / Y2.X1 )
C     X1S=MOLE FRACTION OF 1 IN ADSORBED PHASE
C         VACANCY SOLUTION
```

```
C       X2S=MOLE FRACTION OF 2 IN ADSORBED PHASE
C           VACANCY SOLUTION
C       X3S=MOLE FRACTION OF 3 (VACANCY) IN ADSORBED PHASE
C           VACANCY SOLUTION
C       PHI1=ACTIVITY COEFFICIENT OF 1 IN ADSORBED PHASE
C            VACANCY SOLUTION
C       PHI2=ACTIVITY COEFFICIENT OF 2 IN ADSORBED PHASE
C            VACANCY SOLUTION
C       PHI3=ACTIVITY COEFFICIENT OF 3 (VACANCY) IN ADSORBED
C            VACANCY SOLUTION
C       PI1=SPREADING PRESSURE OF 1 IN ADSORBED MIXTURE
C       PI2=SPREADING PRESSURE OF 2 IN ADSORBED MIXTURE
C
C
C
        COMMON/SEA/XM,P,B1,B2,Z13,Z31,Z23,Z32,V1M,
       1V2M,VTM,X1E,Z12,Z21
        DIMENSION V1(51),V2(51),VT(51),X1(51),X2(51),Y1(51),
       1Y2(51),VTT(51),RV(51)
        CHARACTER*80 TITLE(4)
        READ (*,3) TITLE
        WRITE (2,3) TITLE
        V1(1)=0.0
        V2(51)=0.0
        X1(1)=0.0
        Y1(1)=0.0
        X1(51)=1.0
        Y1(51)=1.0
        READ*, INTER
        IF(INTER.EQ.1) GOTO 4
        READ*, Z,QST1,QST2,R
4       READ *, P,TEMP
        WRITE (2,25) P,TEMP
        READ*, B1,B2,Z13,Z31,Z23,Z32,V1M,V2M
        X1E=0.5
C       CALCULATE THE AMOUNT ADSORBED OF BOTH
C       PURE COMPONENTS AT THE TOTAL PRESSURE OF MIXTURE
        CALL SEARCH (X1E,VT(1),2)
        CALL SEARCH (X1E,VT(51),1)
C       ESTIMATE THE ADSORBATE-ADSORBATE INTERACTIONS
        IF(INTER.EQ.1) THEN
        Z12=1.0
        Z21=1.0
        ELSE
        A11=-2.0/Z*(-QST1-R*TEMP)
        A22=-2.0/Z*(-QST2-R*TEMP)
        A12=(A11*A22)**0.5
        Z12=V2M/V1M*EXP((A11-A12)/(R*TEMP))
        Z21=V1M/V2M*EXP((A22-A12)/(R*TEMP))
        END IF
```

```
C       CALCULATE THE INCREMENT SIZE OF THE
C       MOLE FRACTION IN THE ADSORBED PHASE
        DXI=(1.0-0.0)/50.0
        DO 45 J=2,50
        X1(J)=0.0+(J-1)*DXI
C       CALCULATE THE MAXIMUM TOTAL NUMBER OF MOLES
C       OF MIXTURE IN ADSORBED PHASE
        VTT(J)=X1(J)*V1M+(1.0-X1(J))*V2M
        XM=X1(J)
        VTM=VTT(J)
C       EVALUATE THE TOTAL AMOUNT ADSORBED
        CALL SEARCH (X1E,VT(J),3)
C       CALCULATE THE INDIVIDUAL AMOUNTS ADSORBED
        V1(J)=VT(J)*XM
        V2(J)=VT(J)*(1.0-XM)
C       CALCULATE THE MOLE FRACTIONS OF BOTH COMPONENTS
C       IN THE GAS PHASE AND THE SEPARATION FACTORS
        Y1(J)=FUNCS(VT(J),4)
        Y2(J)=1.0-Y1(J)
        X2(J)=1.0-XM
45      RV(J)=(Y1(J)*X2(J))/(Y2(J)*XM)
        WRITE (2,170)
        WRITE (2,180) (Y1(J),X1(J),V1(J),V2(J),VT(J),RV(J),
       1J=2,50)
        STOP
C       .............FORMAT SECTION.........................
3       FORMAT(A)
25      FORMAT(//T6,'EQUILIBRIUM PRESSURE',F10.5,'BAR'//
       1T6,'TEMPERATURE OF ADSORPTION',F10.3,'DEGREES KELVIN'//)
170     FORMAT (////T7,'ADSORPTION EQUILIBRIA'//T6,'MOLE FRACTION',
       1T23,'MOLE FRACTION',T39,'AMOUNT ADSORBED,MOL/KG OF ADSORBENT'
       1,T81,'REL. VOL. '/
       2T6,'GAS PHASE,',T22,'ADSORBED PHASE',T39,'COMPONENT1',T52,
       3'COMPONENT 2',T69,'TOTAL'//)
180     FORMAT (T8,F9.7,T24,F9.7,T39,E12.5,T52,E12.5,T66,E12.5,T81
       1,F9.7)
        END
C
C
C
        SUBROUTINE SEARCH (D1,DR,JFUN)
C       THIS SUBROUTINE SEARCHS FOR A ROOT
C       USING LINEAR INTERPOLATION
        E1=FUNCS(D1,JFUN)
        IF(E1.GT.0.0) GOTO 40
C       ........E1.LT.0.0........
        D3=1.01*D1
        E3=FUNCS(D3,JFUN)
        SLO=(E1-E3)/(D1-D3)
```

```
      IF(SLO.LT.0.0) GOTO 20
C     .........TYPE (1) CURVE.........
10    IF(E3.GT.0.0) GOTO 70
      D3=1.1*D3
15    E3=FUNCS(D3,JFUN)
      IF(E3.LT.-0.99999999999) GOTO 20
      GOTO 10
C     ........TYPE (4) CURVE...........
20    D3=0.95*D1
30    E3=FUNCS(D3,JFUN)
      IF(E3.GT.0.0) GOTO 70
      IF(D3.GT.0.1E-15) GOTO 35
      D3=1.2*D1
      GOTO 15
35    D3=0.95*D3
      GOTO 30
C     ........E1.GT.0.0.......
40    D3=1.01*D1
      E3=FUNCS(D3,JFUN)
      SLO=(E1-E3)/(D1-D3)
      IF(SLO.LT.0.0) GOTO 60
C     ............TYPE (2) CURVE............
      D3=0.95*D1
50    E3=FUNCS(D3,JFUN)
      IF(E3.LT.0.0) GOTO 70
      D3=0.95*D3
      GOTO 50
C     ........TYPE (3) CURVE..........
60    IF(E3.LT.0.0) GOTO 70
      D3=1.1*D3
      E3=FUNCS(D3,JFUN)
      GOTO 60
70    D2=0.5*(D1+D3)
      E2=FUNCS(D2,JFUN)
      IF(D3.GT.D1) GOTO 80
      D1L=D1
      E1L=E1
      D1=D3
      E1=E3
      D3=D1L
      E3=E1L
80    D12=D1*D1
      D22=D2*D2
      D32=D3*D3
      DR=D2
90    DENOM=DETEM(1.0,D1,D12,1.0,D2,D22,1.0,D3,D32)
      A0=DETEM(E1,D1,D12,E2,D2,D22,E3,D3,D32)/DENOM
      A1=DETEM(1.0,E1,D12,1.0,E2,D22,1.0,E3,D32)/DENOM
      A2=DETEM(1.0,D1,E1,1.0,D2,E2,1.0,D3,E3)/DENOM
```

```
      SUMZ=A1*A1-4.0*A2*A0
      IF(SUMZ.LE.0.0) GOTO 130
      DRP=(-A1+SQRT(SUMZ))/(2.0*A2)
      DRM=(-A1-SQRT(SUMZ))/(2.0*A2)
      IF(DRP.LE.0.0) DR=DRM
      IF(DRM.LE.0.0) DR=DRP
      IF(DRP.GT.0.0.AND.DRM.GT.0.0) GOTO 100
      GOTO 110
100   DRL=DR
      DRPL=ABS(DRP-DRL)
      DRML=ABS(DRM-DRL)
      IF(DRPL.LT.DRML) DR=DRP
      IF(DRML.LT.DRPL) DR=DRM
110   CONTINUE
C     ..........CHECK FOR CONVERGENCE..............
      ER=FUNCS(DR,JFUN)
      IF(ABS(ER).LT.0.1E-07) GOTO 999
      IF(DR.LT.D1) GOTO 130
      IF(DR.GT.D3) GOTO 130
      IF(DR.LT.D2) GOTO 120
C     ..........DR.LT.D3.AND.GT.D2.................
      D1=D2
      D12=D22
      E1=E2
      D2=DR
      D22=DR*DR
      E2=ER
      GOTO 90
C     ..............DR.LT.D2.AND.GT.D1.........
120   D3=D2
      D32=D22
      E3=E2
      D2=DR
      D22=DR*DR
      E2=ER
      GOTO 90
C     ..........USE A LINEAR TECHNIQUE.............
130   SLO=(E1-E3)/(D1-D3)
      CON=0.5*(E1-SLO*D1+E3-SLO*D3)
      DR=-CON/SLO
      ER=FUNCS(DR,JFUN)
      IF(ABS(ER).LT.0.1E-07) GOTO 999
      IF(ER.GT.0.0) GOTO 140
C     ...........ER.LT.0.0.....
      D3=DR
      E3=ER
      GOTO 130
C     ........ER.GT.0.0.................
140   D1=DR
```

```
      E1=ER
      GOTO 130
999   CONTINUE
      RETURN
      END
C
C
C
      FUNCTION FUNCS (X,JFUN)
      COMMON/SEA/XM,P,B1,B2,Z13,Z31,Z23,Z32,V1M,V2M,VTM,X1E
     1,Z12,Z21
      GOTO (10,20),JFUN
      X1S=XM*X/VTM
      X2S=(1.0-XM)*X/VTM
      X3S=1.0-(X/VTM)
      PHI1=EXP(1.0-ALOG(X1S+Z12*X2S+X3S*Z13)-(X1S/(X1S+X2S*Z12+
     1X3S*Z13)+Z21*X2S/(X1S+Z21*X2S+X3S*Z23)+X3S*Z31/(X1S*Z31+
     2X2S*Z32+X3S)))
      PHI2=EXP(1.0-ALOG(X2S+Z21*X1S+X3S*Z23)-(X2S/(X2S+Z21*X1S+
     1X3S*Z23)+Z12*X1S/(X2S+Z12*X1S+X3S*Z13)+X3S*Z32/(X2S*Z32+
     2X1S*Z31+X3S)))
      PHI3=EXP(1.0-ALOG(X1S*Z31+X2S*Z32+X3S)-(X1S*Z13/(X1S+
     1Z12*X2S+X3S*Z13)+X2S*Z23/(Z21*X1S+X2S+X3S*Z23)+X3S/(X1S*Z31+
     2X2S*Z32+X3S)))
      PI1=(1.0+(VTM-V1M)/X)*ALOG(PHI3*X3S)
      PI2=(1.0+(VTM-V2M)/X)*ALOG(PHI3*X3S)
      GOTO (10,20,50,60),JFUN
C     ISOTHERM FUNCTION FOR PURE COMPONENT 1
10    FUNCS=((V1M/B1)*(X/V1M)/(1.0-X/V1M)*(Z13*(1.0-
     1(1.0-Z31)*(X/V1M))/(Z13+(1.0-Z13)*X/V1M))*EXP((
     2-Z31*(1.0-Z31)*X/V1M)/(1.0-(1.0-Z31)*(X/V1M))
     3-((1.0-Z13)*X/V1M)/(Z13+(1.0-Z13)*X/V1M)))/P-1.0
      RETURN
C     ISOTHERM FUNCTION FOR PURE COMPONENT 2
20    FUNCS=((V2M/B2)*(X/V2M)/(1.0-X/V2M)*(Z23*(1.0-
     1(1.0-Z32)*(X/V2M))/(Z23+(1.0-Z23)*X/V2M))*EXP((
     2-Z32*(1.0-Z32)*X/V2M)/(1.0-(1.0-Z32)*(X/V2M))
     3-((1.0-Z23)*X/V2M)/(Z23+(1.0-Z23)*X/V2M)))/P-1.0
      RETURN
C     SUM OF THE EQUILIBRIUM EQUATIONS FOR COMPONENTS 1
C     AND 2 IN THE BINARY MIXTURE
50    FUNCS=(PHI1*XM*X*V1M*Z13/(VTM*B1)*EXP(Z31-1.0)*
     1EXP(-PI1)+PHI2*(1.0-XM)*X*V2M*Z23/(VTM*B2)*
     2EXP(Z32-1.0)*EXP(-PI2))/P-1.0
      RETURN
C     EQUILIBRIUM EQUATION FCR COMPONENT 1 IN THE
C     BINARY MIXTURE
60    FUNCS=(PHI1*XM*X*V1M*Z13/(VTM*B1)*EXP(Z31-1.0)
     1*EXP(-PI1))/P
      RETURN
      END
```

```
C
C
C
      FUNCTION DETEM (A1,A2,A3,B1,B2,B3,C1,C2,C3)
C     FUNCTION DETEM EVALUATES A THREE DIMENSIONAL
C     DETERMINANT FOR USE IN SUBROUTINE SEARCH
      DETEM=A1*(B2*C3-B3*C2)-A2*(B1*C3-B3*C1)
     1+A3*(B1*C2-C1*B2)
      RETURN
      END
```

```
      PROGRAM ACT
C
CC
C
CC    THIS PROGRAM CALCULATES THE ACTIVITY
C     COEFFICIENTS FOR THE EXPERIMENTAL
C     BINARY SYSTEM
CC
C
C
C     NOMENCLATURE OF PROGRAM
C
C
C     N=NUMBER OF DATA POINTS
C     M1=ORDER OF POLYNOMIAL PLUS ONE
C     TP=AVERAGE EQUILIBRIUM PRESSURE
C     A1=REGRESSION PARAMETERS FOR PURE COMPONENT
C        1 ( O2 ) FOR EQUATION 4.1 IN TEXT
C     A2=REGRESSION PARAMETERS FOR PURE COMPONENT
C        2 ( N2 ) FOR EQUATION 4.1 IN TEXT
C     YO2=MOLE FRACTION OF COMPONENT 1 IN GAS PHASE
C     XO2=MOLE FRACTION OF COMPONENT 1 IN ADSORBED PHASE
C     YN2=MOLE FRACTION OF COMPONENT 2 IN GAS PHASE
C     XN2=MOLE FRACTION OF COMPONENT 2 IN ADSORBED PHASE
C     WT=TOTAL AMOUNT ADSORBED
C     PA=EXPERIMENTAL EQUILIBRIUM TOTAL PRESSURE
C     W1E=ASSUMED AMOUNT ADSORBED
C     WOO=AMOUNT ADSORBED OF COMPONENT 1 AT THE
C         TOTAL PRESSURE OF THE MIXTURE
C     WNN=AMOUNT ADSORBED OF COMPONENT 2 AT THE
C         TOTAL PRESSURE OF THE MIXTURE
C     PIO2=SPREADING PRESSURE OF PURE COMPONENT 1 AT
C          THE TOTAL PRESSURE OF THE MIXTURE
C     PIO1=SPREADING PRESSURE OF PURE COMPONENT 2 AT
C          THE TOTAL PRESSURE OF THE MIXTURE
C     PIM=SPREADING PRESSURE OF THE BINARY MIXTURE
C     WI1=AMOUNT ADSORBED OF PURE COMPONENT 1 AT
C         THE SPREADING PRESSURE OF THE MIXTURE
C     WI2=AMOUNT ADSORBED OF PURE COMPONENT 2 AT
C         THE SPREADING PRESSURE OF THE MIXTURE
C     PO1=EQUILIBRIUM PRESSURE OF PURE COMPONENT 1
C         AT THE SPREADING PRESSURE OF THE MIXTURE
C     PO2=EQUILIBRIUM PRESSURE OF PURE COMPONENT 2
C         AT THE SPREADING PRESSURE OF THE MIXTURE
C     PA1=PARTIAL PRESSURE OF 1 IN MIXTURE
C     PA2=PARTIAL PRESSURE OF 2 IN MIXTURE
C     ACT1=ACTIVITY COEFFICIENT OF 1 IN ADSORBED PHASE
C     ACT2=ACTIVITY COEFFICIENT OF 2 IN ADSORBED PHASE
C
C
C
```

```
      COMMON/SEA/ M1,W1E,PIM(35),J,WI1(35),WI2(35),YO2(35),
     1A1(8),A2(8),A(20),YN2(35),WOO,WNN,PIO1,PIO2,PIM1(35),TP
      DIMENSION XO2(35),WT(35),PA(35),X(35),
     1Y(35),PO1(35),PO2(35),PA1(35),PA2(35),
     2XN2(35),ACT1(35),ACT2(35)
      CHARACTER*80 TITLE(2)
      READ (*,2) TITLE
      WRITE(2,2) TITLE
      READ *,N,M1,TP
      READ*,(A1(I),I=1,4),(A2(I),I=1,4)
      READ*, (YO2(I),XO2(I),WT(I),PA(I),I=N,1,-1)
      DO 3 I=N,1,-1
      XN2(I)=1.0-XO2(I)
      YN2(I)=1.0-YO2(I)
C     CALCULATE THE EXPRESSION NT.(X1-Y1) / Y1.Y2 IN
C     EQUATION 4.6 IN TEXT
      Y(I)=WT(I)*(XO2(I)-YO2(I))/(YO2(I)*YN2(I))
      X(I)=YO2(I)
3     CONTINUE
C     CALCULATE THE AMOUNT ADSORBED OF BOTH PURE
C     COMPONENTS AT THE TOTAL PRESSURE OF MIXTURE
      W1E=0.5
      CALL SEARCH (W1E,WOO,1,1)
      CALL SEARCH (W1E,WNN,1,2)
C     CALCULATE THE SPREADING PRESSURE OF BOTH PURE
C     COMPONENTS AT THE TOTAL PRESSURE OF THE MIXTURE
      CALL SPREAD (WOO,PIO2,1)
      CALL SPREAD (WNN,PIO1,2)
C     CURVE-FIT THE EXPRESSION NT.(X1-Y1) / Y1.Y2 IN
C     EQUATION 4.6 IN TEXT TO A POLYNOMIAL OF DEGREE
C     (M1-1) USING NAG SUBROUTINE E02ACF
      SUM=0.0
      M=M1-1
      N1=N
      CALL E02ACF (X,Y,N1,A,M1,REF)
C     WRITE THE ORDER OF THE POLYNOMIAL
      WRITE (2,5) M
C     WRITE THE COEFFICIENTS OF THE POLYNOMIAL
      WRITE (2,6) (A(I),I=1,M1)
      WRITE (2,7)
      DO 100 J=N,1,-1
      Z=X(J)
      S=A(M+1)
      I=M
40    S=S*Z+A(I)
      IF(I-1) 80,80,60
60    I=I-1
      GOTO 40
80    T=Y(J)
```

```
      H=S-T
      W=H/T*100.0
      SUM=W*W/1.0E+04+SUM
      WRITE(2,8) Z,S,T,H,W
100   CONTINUE
C     WRITE THE MAXIMUM DEVIATION OF THE COMPUTED VALUE
C     FROM THE EXPERIMENTAL VALUE
      WRITE (2,9) REF
C     WRITE THE SUM OF SQUARES OF THE RELATIVE RESIDUAL
      WRITE (2,11) SUM
      DO 110 J=1,N
C     EVALUATE THE SPREADING PRESSURE OF THE MIXTURE
      CALL PRES (1.0,YO2(J),PIM1(J))
      PIM(J)=PIO2+PIM1(J)
C     CALCULATE THE AMOUNT ADSORBED OF BOTH PURE
C     COMPONENTS AT THE SPREADING PRESSURE OF MIXTURE
      CALL SEARCH (W1E,WI1(J),2,2)
      CALL SEARCH (W1E,WI2(J),2,1)
C     CALCULATE THE EQUILIBRIUM PRESSURE OF BOTH PURE
C     COMPONENTS AT THE SPREADING PRESSURE OF MIXTURE
      PO1(J)=FUNCS(WI1(J),3,2)
      PO2(J)=FUNCS(WI2(J),3,1)
C     CALCULATE THE PARTIAL PRESSURE OF BOTH COMPONENTS
      PA1(J)=TP*YN2(J)
      PA2(J)=TP*YO2(J)
C     CALCULATE THE ACTIVITY COEFFICIENTS OF BOTH COMPONENTS
      ACT1(J)=PA1(J)/(PO1(J)*XN2(J))
      ACT2(J)=PA2(J)/(PO2(J)*XO2(J))
110   CONTINUE
      WRITE (2,120)
      WRITE(2,130)(YO2(J),XO2(J),ACT2(J),ACT1(J),J=1,N)
      STOP
C     ..... FORMAT SECTION .....
2     FORMAT (A)
5     FORMAT (///5X,'FOR DEGREE OF ',I2,' THE ',
     1'COEFFICIENTS ARE '/)
6     FORMAT (5X,E12.4)
7     FORMAT (/5X,'X',7X,'F(X)',8X,'FIT',7X,'RESIDUALS',
     18X,'ERROR'/T52,'PERCENT'/)
8     FORMAT (1X,F7.2,3E12.4,3X,F9.4)
9     FORMAT (///5X,'NAG FINAL REFERENCE DEVIATION IS ',E12.4)
11    FORMAT (/5X,'SUM OF SQUARES OF THE ',
     1'ABSOLUTE ERRORS = ',E15.7)
120   FORMAT (////T6,'MOLE FRACTION',T23,'MOLE FRACTION',T50,
     1'ACTIVITY COEFFICIENT',T77,'ACTIVITY COEFFICIENT'/
     2T6,'OF OXYGEN',T23,'OF OXYGEN',T50,'OF OXYGEN',T77,
     3'OF NITROGEN '/T6,'GAS PHASE',T22,'ADSORBED PHASE'//)
130   FORMAT(T8,F9.7,T24,F9.7,T52,F9.7,T79,F9.7)
      END
C
C
C
```

```
      SUBROUTINE SEARCH (D1,DR,JFUN,JCOMP)
C     THIS SUBROUTINE SEARCHS FOR A ROOT
C     USING NEWTON RAPHSON METHOD
      FD=FUNCS(D1,JFUN,JCOMP)
40    DELX=FD/(FDER(D1,JFUN,JCOMP))
      D1=D1-DELX
      FD=FUNCS(D1,JFUN,JCOMP)
      IF(ABS(DELX).LE.0.1E-08) GOTO 60
      GOTO 40
60    DR=D1
      RETURN
      END
C
C
C
      FUNCTION FDER(X,JFUN,JCOMP)
      COMMON/SEA/ M1,W1E,PIM(35),J,WI1(35),WI2(35),YO2(35),
     1A1(8),A2(8),A(20),YN2(35),WOO,WNN,PIO1,PIO2,PIM1(35),TP
      DIMENSION B(20),DLP(101)
C     FUNCTION FDER EVALUATES THE DERIVATIVE OF THE
C     FIRST TWO FUNCTIONS IN FUNCS FOR USE IN SEARCH
      GOTO (10,20),JFUN
10    GOTO (30,40),JCOMP
30    DO 31 I=1,4
31    B(I)=A1(I)
      GOTO 100
40    DO 41 I=1,4
41    B(I)=A2(I)
100   Z1=EXP(X/(B(3)-X)-B(4)*X)
      Z2=B(1)*Z1+B(1)*X*((B(3)/(B(3)-X)**2)-B(4))
     1*Z1/(B(2)-X)
      Z3=Z2+B(1)*X*Z1/(B(2)-X)**2
      FDER=Z3/TP
      RETURN
20    GOTO (3,4),JCOMP
3     DO 5 I=1,4
5     B(I)=A1(I)
      GOTO 8
4     DO 7 I=1,4
7     B(I)=A2(I)
8     Z4=1.0+X*((B(3)/(B(3)-X)**2)-B(4))+X/(B(2)-X)
      FDER=Z4/PIM(J)
      RETURN
      END
C
C
C
```

```
      SUBROUTINE SPREAD(XO,PIO,JCOMP)
      COMMON/SEA/M1,W1E,PIM(35),J,WI1(35),WI2(35),YO2(35),
     1A1(8),A2(8),A(20),YN2(35),WOO,WNN,PIO1,PIO2,PIM1(35),TP
      DIMENSION Y(101),DLP(101),B(20)
C     THIS SUBROUTINE COMPUTES THE SPREADING PRESSURE FUNCTION
C     FOR A GIVEN AMOUNT ADSORBED FOR A PURE COMPONENT
      GOTO (3,4), JCOMP
3     DO 5 I=1,4
5     B(I)=A1(I)
      DX=XO/100.0
      X(1)=0.0
      GOTO 8
4     DO 7 I=1,4
7     B(I)=A2(I)
      DX=XO/100.0
      X(1)=0.0
8     SUM=0.0
      DO 11 I=2,101
      X(I)=X(I-1)+DX
      X22=X(I)*X(I)
      X3=X(I)*X22
      X11=X(I)
      DLP(I)=1.0+X11*(B(3)/(B(3)-X11)**2-B(4))
     1+X11/(B(2)-X11)
11    SUM=SUM+DLP(I)
      PIO=DX*(SUM-0.5*DLP(101))
      RETURN
      END
C
C
C
      SUBROUTINE PRES (XI,XO,PIO)
      COMMON/SEA/M1,W1E,PIM(35),J,WI1(35),WI2(35),YO2(35),
     1A1(8),A2(8),A(20),YN2(35),WOO,WNN,PIO1,PIO2,PIM1(35),TP
      DIMENSION X(101),DLP(101),B(20)
C     THIS SUBROUTINE COMPUTES THE SPREADING PRESSURE FUNCTION
C     FOR A GIVEN AMOUNT ADSORBED FOR A BINARY MIXTURE
      DO 9 I=1,M1
9     B(I)=A(I)
      DX=(XO-XI)/100.0
      X(1)=XI
      D=B(M1)
      K=M1-1
42    D=D*X(1)+B(K)
      IF(K-1) 82,82,62
62    K=K-1
      GOTO 42
82    SUM=D
      D=B(M1)
```

```
      K=M1-1
41    D=D*XO+B(K)
      IF (K-1) 81,81,61
61    K=K-1
      GOTO 41
81    SUM=SUM+D
      DO 13 I=2,100
      X(I)=X(I-1)+DX
      X11=X(I)
      D=B(M1)
      K=M1-1
40    D=D*X11+B(K)
      IF(K-1) 80,80,60
60    K=K-1
      GOTO 40
80    DLP(I)=D*2.0
13    SUM=SUM+DLP(I)
      PIO=DX/2.0*SUM
      RETURN
      END
C
C
C
      FUNCTION FUNCS(XX,JFUN,JCOMP)
      COMMON/SEA/ M1,W1E,PIM(35),J,WI1(35),WI2(35),YO2(35),
     1A1(8),A2(8),A(20),YN2(35),WOO,WNN,PIO1,PIO2,PIM1(35),TP
      DIMENSION B(20),DLP(101)
      GOTO (10,20,50),JFUN
10    X=XX
      GOTO (30,40),JCOMP
30    DO 31 I=1,4
31    B(I)=A1(I)
      GOTO 100
40    DO 41 I=1,4
41    B(I)=A2(I)
C     ISOTHERM FUNCTION
100   FUNCS=(((B(1)*X)*EXP(X/(B(3)-X)-B(4)*X))
     1/(B(2)-X))/TP-1.0
      RETURN
C     SPREADING PRESSURE FUNCTION
20    GOTO (3,4), JCOMP
3     DO 5 I=1,4
5     B(I)=A1(I)
      DX=XX/100.0
      X=0.0
      GOTO 8
4     DO 7 I=1,4
7     B(I)=A2(I)
      DX=XX/100.0
```

```
      X=0.0
 8    SUM=0.0
      DO 11 I=2,101
      X11=X+DX
      X22=X11*X11
      X3=X22*X11
      DLP(I)=1.0+X11*(B(3)/(B(3)-X11)**2-B(4))
     1+X11/(B(2)-X11)
      SUM=SUM+DLP(I)
 11   X=X11
      FUNCS=DX*(SUM-0.5*DLP(101))/PIM(J)-1
      RETURN
 50   X=XX
      GOTO (60,70),JCOMP
 60   DO 80 I=1;4
 80   B(I)=A1(I)
      GOTO 90
 70   DO 85 I=1,4
 85   B(I)=A2(I)
 C    ISOTHERM FUNCTION
 90   FUNCS=((B(1)*X)*EXP(X/(B(3)-X)-
     1B(4)*X))/(B(2)-X)
      RETURN
      END
```